AD-752 494

ENVIRONMENTAL-ACOUSTICS ATLAS OF THE CARIBBEAN SEA AND GULF OF MEXICO. VOLUME II. MARINE ENVIRONMENT

Naval Oceanographic Office
Washington, D. C.

August 1972

SP-189 II

ENVIRONMENTAL—ACOUSTICS ATLAS OF THE CARIBBEAN SEA AND GULF OF MEXICO

VOLUME II
MARINE ENVIRONMENT

AUGUST 1972

Prepared and Published by the Naval Oceanographic Office
for the Long Range Acoustic Propagation Project,
Maury Center for Ocean Science,
Office of Naval Research

U.S. NAVAL OCEANOGRAPHIC OFFICE
WASHINGTON, D. C. 20390

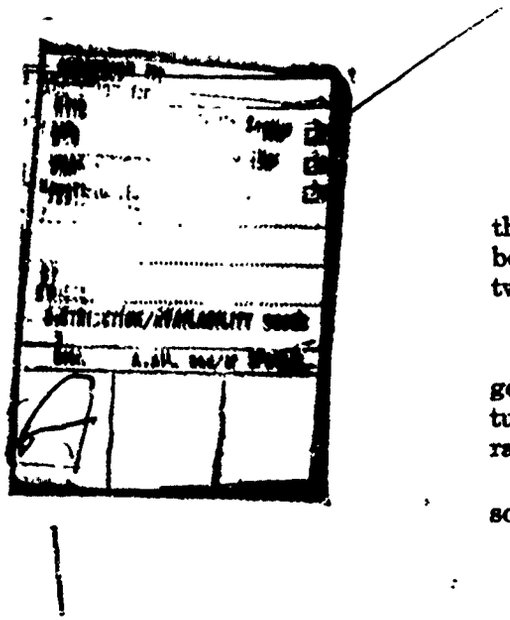

ABSTRACT

This atlas summarizes available acoustic and environmental data in the Caribbean Sea, Gulf of Mexico, and in their Atlantic Ocean approaches between 10°N and 30°N and west of approximately 56°W. It consists of two volumes and a separately bound appendix.

Volume I—Marine Acoustics and its appendix.

Volume II—Marine Environment. This volume includes data on geomagnetic background, water masses, sound velocity and thermal structure, bathymetry, bottom composition, sub-bottom structures, wind, waves, rainfall, and currents.

Bibliographies in each volume and in the appendix list the principal sources of information.

ACKNOWLEDGEMENTS

The U. S. Naval Oceanographic Office acknowledges major contributions to this atlas provided by the Long Range Acoustic Propagation Project (LRAPP), the Anti-Submarine Warfare Programs Office (CNO OP-095), the Office of Research, Development, Test and Evaluation (CNO OP-098) and the Fleet Numerical Weather Central (FNWC). LRAPP, OP-095, and the ASW Systems Project Office (PM-4) provided guidance concerning the format and content of the atlas, technical advice during its compilation, and technical reviews of the finished product.

UNCLASSIFIED
Security Classification

DOCUMENT CONTROL DATA - R & D

(Security classification of title, body of abstract and indexing annotation must be entered when the overall report is classified)

1 ORIGINATING ACTIVITY (Corporate author) U. S. Naval Oceanographic Office Washington, D. C. 20390	2a. REPORT SECURITY CLASSIFICATION UNCLASSIFIED 2b. GROUP None

3 REPORT TITLE

Environmental-Acoustics Atlas of the Caribbean Sea and Gulf of Mexico, Volume II-Marine Environment

4 DESCRIPTIVE NOTES (Type of report and inclusive dates)

Special publication

5 AUTHOR(S) (First name, middle initial, last name)

U. S. Naval Oceanographic Office

6 REPORT DATE	7a. TOTAL NO OF PAGES	7b. NO OF REFS
August 1972	190	140

8a. CONTRACT OR GRANT NO	9a. ORIGINATOR'S REPORT NUMBER(S)
None b. PROJECT NO. 714-GT	SP-189 II
c.	9b. OTHER REPORT NO(S) (Any other numbers that may be assigned this report) None
d.	

10 DISTRIBUTION STATEMENT

Approved for public release; distribution unlimited

11 SUPPLEMENTARY NOTES	12 SPONSORING MILITARY ACTIVITY
None	U.S. Naval Oceanographic Office and Office of Naval Research

13 ABSTRACT

(U) This atlas, consisting of two volumes and a separately bound appendix, summarizes available acoustic and environmental data in the Caribbean Sea, Gulf of Mexico and in their Atlantic Ocean approaches between 10°N and 30°N and west of approximately 56°W. This volume includes data on geomagnetic background, subbottom structures, wind, waves, rainfall, and currents.

Details of illustrations in this document may be better studied on microfiche

Ia

DD FORM 1 NOV 65 1473 (PAGE 1)

UNCLASSIFIED
Security Classification

14 KEY WORDS	LINK A		LINK B		LINK C	
	ROLE	WT	ROLE	WT	ROLE	WT
Caribbean Sea						
Gulf of Mexico						
Lesser Antilles						
Straits of Florida						
Geomagnetism						
Marine Environment						
Sound Velocity Structure						
Bottom Properties						
Wind						
Sea						
Swell						
Currents						
Oxygen Content						
Sediments						
Bathymetry						
Physiography						
Seismic Reflection						
Magnetic Anomaly Detection (MAD)						
Water Masses						
Thermal Structure						
Sound Channels						

I6

FOREWORD

The U. S. Naval Oceanographic Office has prepared this atlas in response to requirements laid down by the Manager, Anti-Submarine Warfare Systems Project (MASWSP ltr ser ASW-1112:HM of 17 February 1971 to COMNAVOCEANO). The atlas is intended for use by ASW planning staffs. It summarizes existing acoustic and environmental data, provides samples of the data and charts showing the temporal and spatial distribution of environmental parameters relevant to ASW. It also provides the information necessary for planning the collection of additional data.

The Long Range Acoustic Propagation Project provided a large percentage of the funds, and Dr. J. B. Hersey provided technical guidance for the preparation of this atlas.

TABLE OF CONTENTS

LIST OF FIGURES

LIST OF FIGURES (Continued)

INTRODUCTION

This atlas is designed for briefing and reference use by planning and study groups in evaluating and selecting the most effective surveillance systems to be deployed in the region. It can also be used to plan survey operations to fill data gaps.

This atlas covers the Caribbean Sea, Gulf of Mexico, and their North Atlantic approaches between 10°N and 30°N. The eastern boundary of the area is 56°W between 10°N and 20°N and is 60°W between 20°N and 30°N (Fig. 1-1). However, in some figures data are shown slightly north and east of these limits. All place names used in the atlas within these limits are located in Figs. 1-1 and 1-2. The area divides geographically into the three major regions listed above and is subdivided by ridges and island arcs into seven major basins.

Selective bibliographies are included in the marine acoustics, geomagnetics, and marine environment sections. The bibliographic references are numbered in order to relate them to the data-location charts. They also carry letter prefixes which key them to the applicable subsections of the text. Reference numbers, as well as authors and dates, are used to cite multiple sources which are keyed by numbers to data-location charts. Reference numbers alone are used in citing long series of references (usually five or more). All other references are noted by author and date alone. The bibliographies are not intended to be exhaustive or comprehensive. With a few exceptions, only those sources from which data or information were taken are cited.

More than 400 figures are included in this atlas. It is published in two volumes in order to provide the widest possible distribution and utilization consistent with the protection of classified information:

Volume I. Marine Acoustics (U) (Confidential)
Appendix to Marine Acoustics (U) (Secret)

Volume II. Marine Environment (Unclassified)

Volume I provides a brief summary of the effects of the marine environment on sound transmission. Transmission loss, bottom loss, bottom reverberation, volume reverberation, and ambient noise data are evaluated in terms of quantity, type, and temporal and spatial distribution. Samples of the data are presented in graphic or tabular form, and the data sources are identified in a bibliography. Both English and metric units of measurement are used, because it was not technically feasible to convert one to the other in the time available. The appendix to Volume I contains six secret figures, a commentary, and a bibliography.

This volume contains two sections (Geomagnetism and Marine Environment). The Marine Environment section contains eight subsections which treat sound velocity structure, bottom properties (sediments, bathymetry, seismic reflection), wind, sea, swell, currents, and oxygen content, and a selective bibliography of data sources. Charts show the temporal and spatial distribution of data and identify data deficiencies.

The data presented in this atlas have been collected by many activities over a period of 15 years or more and are reported in the many sources listed in the bibliographies.

Five of the bathymetric survey track charts (Figs. 4-101, 4-102, 4-104, 4-106, and 4-107), which are classified, are bound in Volume I to permit unrestricted distribution of Volume II in unclassified form. For a similar reason some of the references used in this volume are listed in Volume I Appendix.

3. GEOMAGNETISM

A. Introduction

This region is marked by a sparsity of detailed geomagnetic data for practically the entire Caribbean Sea and the southern Gulf of Mexico. Data for the remainder of the area generally show long-wavelength, low-amplitude magnetic features indicative of good ASW Magnetic Anomaly Detection (MAD) operational effectiveness. Except in the immediate vicinity of volcanic structures there are few areas of high-frequency, high-amplitude anomalies which would seriously affect MAD systems. The northern and western Gulf of Mexico and the western portions of the North American Basin are very "flat" magnetically. Geomagnetic data do not permit an accurate estimate of MAD effectiveness in many of the possible barrier areas. Bathymetric data show that the depth to the geologic source of magnetic anomalies exceeds 1000 fathoms in most of the Caribbean Sea, and their effect on MAD systems should be minimal.

B. Effects on Magnetic Anomaly Detection

The effects of the natural magnetic environment, particularly the geological magnetic background "noise", on MAD has been described in some detail in Brennan and Davis, 1969, and Vogt et al., 1971. Other evaluations and development of techniques, MAD equipment and filters, signal processing, and charts to aid in reducing these effects have been described in reference 32a in Volume I.

In general, MAD effectiveness decreases as the background magnetic anomaly frequency and amplitude increase. Naturally occurring magnetic anomalies with wavelengths less than one mile may mask or be mistaken for the magnetic anomalies produced by submarines. Such anomalies are almost always located in shallow water (less than 1000 fathoms) where the distance to the magnetic source material (usually basaltic lavas or magnetized intrusives) is small. Areas covered by more than 1000 fathoms of water or nonmagnetic sediments will be characterized by lower amplitude, longer wavelength anomalies. In deep ocean areas the typical magnetic anomalies are linear features parallel to the ocean ridges, or anomalies associated with seamounts and fracture zones. It is possible to make a gross prediction of MAD effectiveness based on knowledge of the bathymetry and geology in regions for which little magnetic data exist. Such predictions must be made for those parts of the area not covered by mag-

netic surveys.

C. Geomagnetic Background

A preliminary, residual-magnetic-intensity contour chart of the Gulf of Mexico, North American Basin, and the Caribbean Sea is shown in Fig. 3-1. This chart presents the anomalous features of the earth's magnetic field caused by geological structures and is based on all available data from surveys with a 20-mile track spacing or less. The location, track density, direction, and altitude of the various surveys are shown in the index chart and legend. Contours in areas where the track spacing exceeds 6 miles are questionable, but can be used to determine the general magnetic characteristics and major lineations. The geologic significance of much of these data has been described in Anderson et al., 1965; Bracey, 1968; Taylor et al., 1968; and Vogt et al., 1970 and 1971.

Because of the wide, track spacing, most of the available data are exploratory. No detailed magnetic survey data were available for the Caribbean sea or the southern Gulf of Mexico. The rest of the area is generally characterized by long-wavelength magnetic anomalies, which should normally be filtered out by the MAD system. More detailed survey work is required to define magnetic anomalies in adequate detail for MAD operations.

The northwestern Gulf of Mexico has very broad features and low gradients and should provide an optimum background for MAD operation. The only significant anomalies are produced by salt domes (less than one gamma) or possibly by oil well casings or sunken ships in the regions of very shallow water. The eastern Gulf is more anomalous, with a group of circular anomalies near 26°N and 84°30'W that could produce 1 to 2 gammas of noise through the MAD HTA filter. Most of the features in the Gulf of Mexico should create no major problems for MAD operation.

A number of high-amplitude anomalies occur on the continental shelf off the U. S. east coast, which will require a lower sensitivity setting to be used on the MAD equipment (Brennan and Davis, 1969) and will reduce its effectiveness. Magnetite and ilmenite sand lenses along the northern Florida coast may produce short-wavelength, low-amplitude anomalies not indicated on the chart.

In the Blake Basin (28°N and 78°W) the magnetic anomalies are broad features oriented northeast-southwest. This characteristically flat region is known as the "magnetic quiet zone", and MAD performance should not be affected. On the southern extension of the Bermuda rise, 30°N and 69°W, a series of parallel magnetic anomalies oriented northeast-southwest occur. These are the sea-floor-spreading anomalies; permanently magnetized ribbons of the crust, reflecting reversals of the earth's magnetic field as the basaltic sea floor was formed along the mid-ocean ridge. These features are frequently broken by transform faults which produce a rather confused anomaly pattern in some areas. Because of the deep water (2800-3200 fathoms) these anomalies have wavelengths which should not pass through the MAD filter. The anomalies, however, are at least as complex and have higher amplitudes than the anomalies occurring near the east coast of Florida, where the noise level through the MAD HTA filter is about 1 to 2 gammas. It may be necessary, therefore, to reduce the MAD sensitivity when eitner flying perpendicular to the lineations or in MAD-trapping circles.

Magnetic gradients in some parts of this region exceed 200 gammas per mile or about .03 gamma per foot. If a MAD-equipped aircraft traveling parallel to these linear anomalies has a horizontal motion transverse to the flight path of only a few feet in 10 to 25 seconds at 180 to 200 knots, the MAD sensor will be moved up and down the gradient. This will produce a low amplitude anomaly that will pass through the MAD filter. In this area the apparent anomaly probably would not exceed a few tenths of a gamma, but because of the intermittent character of the signal it might be mistaken for a submarine anomaly. In other deep ocean areas, particularly near the ocean ridges, these linear anomalies may have gradients as high as 0.1 gamma per foot, even though the depth to source is over 1000 fathoms. The reduction in MAD effectiveness, however, is undetermined. The survey-track spacing in this area is approximately 20 miles and is inadequate to produce an accurate contour chart. Therefore, the features may be even more complex or have larger amplitudes than shown.

Northeast of the Bahama Islands, the northwest-southeast trending anomalies are prominent, and MAD performance can be expected to degrade in that direction. Southwest of the Bahamas the broad circular anomalies should produce no major problems for MAD operations. The magnetic field over the Puerto Rico Trench is fairly flat, but becomes more complex with high frequency anomalies near the volcanic coastal regions of Puerto Rico and the Virgin Islands where MAD operations would be difficult.

With regard to bathymetric measurements, a few magnetic profiles reported in Heirtzler et al., 1966, and geomagnetic data in adjacent areas the magnetic characteristics in the southern Gulf of Mexico should be similar to those in the northern. The field should be particularly flat in the southern Mexico Basin. Igneous intrusions (Heirtzler et al., 1966; Lyons, 1957) create magnetic anomalies near the edge of Campeche Bank.

Low-level aeromagnetic and shipboard data for the Caribbean Sea show very smooth magnetic fields over most of the deep areas of the Venezuelan Basin, the southern part of the Colombian Basin, and the Grenada and Tobago Basins (Ewing et al., 1960). The deeper areas of the Yucatan Basin and the Cayman Trench probably also have a smooth field. The Cayman, Beata, and Aves Ridges and the Nicaraguan Rise probably are characterized by short-period, high-amplitude anomalies that are associated with volcanics or near-surface intrusives. The southern peninsula of Haiti and the coastal areas of Cuba, Jamaica, Venezuela, and the

Lesser Antilles also are magnetically disturbed areas, which will be especially difficult for MAD operations.

Methods of displaying the environmental geomagnetic characteristics in terms of MAD operational effectiveness and recommended filter and sensitivity settings are currently under development in response to fleet requirements in other ocean areas. Regional charts of MAD-detection probability or detection confidence levels might also be produced. These techniques could eventually be utilized in producing more detailed comprehensive charts of the Caribbean Region, if specific requirements are established.

D. Bibliography

1. Anderson, C. N., Vogt, P. R., Bracey, D. R., and Kontis, A. L., 1965, A magnetic survey in the eastern Gulf of Mexico and its relation to the east coast aeromagnetic survey: Trans. Amer. Geophys. Union, v. 50, p. 207.
2. Bracey, D. R., 1968, Structural implications of magnetic anomalies north of the Bahamas-Antilles Islands: Geophysics, v. 33, n. 6.
3. Brennan, J. A., and Davis, T. M., 1969, The influence of the natural environment on MAD operations: U.S. Naval Oceanographic Office, Tech. Rept. 218.
4. Ewing, J., Antoine, J., and Ewing, M., 1960, Geophysical measurements in the western Caribbean Sea and in the Gulf of Mexico: Jour. Geophys. Research, v. 65, n. 12.
5. Heirtzler, J. R., Burckle, L. H., and Peters, G., 1966, Magnetic anomalies in the Gulf of Mexico: Jour. Geophys. Research, v. 71, n. 2.
6. Lyons, P. L., 1957, Geology and geophysics of the Gulf of Mexico: Trans. Gulf Coast Assoc. Geol. Societies, v. 7, p. 1-10.
7. Taylor, P. T., Zeitz, I., and Dennis, L. S., 1968, Geologic implications of aeromagnetic data for the eastern continental margin of the United States: Geophysics, v. 33, n. 5.
8. Vogt, P. R., Anderson, C. N., Bracey, D. R., and Schneider, E. D., 1970, North Atlantic magnetic smooth zones: Jour. Geophys. Research, v. 75, n. 20.
9. Vogt, P. R., Anderson, C. N., and Bracey, D. R., 1971, Mesozoic magnetic anomalies, sea-floor spreading and geomagnetic reversals in the southwestern North Atlantic: Jour. Geophys. Research, v. 76, n. 20.
10. Vogt, P. R., Lorentzen, G. R., and Higgs, R. H., 1971, Magnetic anomalies of geologic origin: NOL/NRL MAD Symposium, October 1971 (unpublished).

4. MARINE ENVIRONMENT

A. Introduction

The marine environment in the area covered by this atlas is presented in sections that describe sound velocity structure, bottom properties, winds, sea and swell, currents, and oxygen content. The sound velocity structure is described in terms of the major water masses defined in Fig. 4-1.

Ridges and island arcs divide the area into seven major basins with flat or gently sloping floors, which are listed below with the range of depths typical of their deep areas:

REGION	TYPICAL WATER DEPTH RANGE (FATHOMS)
1. MEXICAN BASIN	1,700—2,000
2 NORTH AMERICAN BASIN	
PUERTO RICO TRENCH	4,000—4,400
HATTERAS PLAIN	2,800—3,000
NARES PLAIN	2,800—3,100
3. YUCATAN BASIN	2,300—2,400
CAYMAN TROUGH	2,600—3,700
4. COLOMBIAN BASIN	1,800—2,300
5. VENEZUELAN BASIN	2,100—2,900
MUERTOS TRENCH	2,600—2,900
6. GRENADA BASIN	1,400—1,600
7. GUIANA BASIN	2,300—2,900

These and other major physiographic features are identified and delineated in Fig. 1-1.

In addition to the seven major basins, other regions deeper than 100 fathoms consist of small basins, and ridges and rises characterized by rugged relief and steep slopes. The principal exceptions, the Blake Plateau, Basin, and Ridge, are flat or gently sloping.

This area is dominated by two weather regimes; the subtropical (Bermuda) high and the intertropical convergence zone or doldrums. The semipermanent subtropical high dominates the entire area in the summer. The weather is persistently mild and mostly fair. Seasonal variability is not pronounced, and in the south the diurnal variability can be as great as the seasonal. Mean temperatures are 80°F to 83°F in August and in February vary from 63°F in Bermuda to 70°F in the south. The doldrums dominate the southern Caribbean in summer and are characterized by warm temperatures, high humidity, considerable cloudiness, frequent intermittent showers, and light winds. Tropical storms are limited principally to the hurricane season (July-October). Winds, sea, and swell come principally from the east and northeast throughout the year and are highest in autumn and winter.

Surface currents are a part of the general clockwise circulation of the North Atlantic Ocean. Extensions of the North Equatorial Current flow west, both north and south of the Greater Antilles. The Guiana Current sets west along the coast of South America and combines with the southern part of the North Equatorial Current to form a general westward flow through the Caribbean Sea. This flow moves north through Yucatan Channel, splits into both clockwise and counterclockwise circulation in the Gulf of Mexico, exits eastward through the Straits of Florida, and combines with the Antilles Current to form the Gulf Stream.

B. Major Water Masses

The oceanographic features of the area are described in relation to five regions: the Caribbean Sea, Gulf of Mexico, Straits of Florida, North American Basin, and Guiana Basin. Temperature-salinity indices for the major water masses are shown on Fig. 4-1 (Defant, 1961; Schroeder, et al., 1959; Sturges, 1965; Sverdrup et al., 1942; Wust, 1964). The temperature-salinity index for "18° Water" (Schroeder, et al., 1959) represents a long-term average off Bermuda. Water mass characteristics are defined in the above references and by Nowlin and McLellan, 1967; Starr, 1970; and Wennekens, 1959.

The surface oceanography of the Caribbean Sea is dominated by the Caribbean Current which originates in the Guiana Basin at the confluence of the Guiana and North Equatorial Currents (Boisvert, 1967). The relatively warm, saline North Atlantic Central Water in the Caribbean Current is diluted during summer by Amazon River outflow and precipitation (Wust, 1964). This current flows westward through the south and central Caribbean Sea, becomes the Yucatan Current, and feeds the Florida Current in the Straits of Florida and the Eastern Gulf Loop Current. Off Grand Bahama Island, the Florida Current merges with the Antilles Current to form the Gulf Stream. Surface circulation in the western Gulf of Mexico is complicated and variable (Naval Oceanographic Office, 1965e) and is influenced by Mississippi River runoff, particularly during spring and summer.

The subsurface water layers of the Caribbean Sea, Gulf of Mexico, and Guiana Basin contain Subtropical Underwater, which has a characteristic salinity maximum between 50 and 150 meters. This water mass is formed in the Equatorial Atlantic Ocean by evaporation (Wust, 1936) and is transported into the Caribbean Sea through most of the Greater and Lesser Antilles passages. Subtropical Underwater enters the Straits of Florida from the Gulf of Mexico and through the Old Bahama Channel and is an important component of the Gulf Stream. The subsurface layers in the Sargasso Sea consist of "18° Water" (Worthington, 1959) that is formed by sinking along the Subtropical Convergence during winter (Istoshin, 1961). The Central Atlantic Front (Subtropical Convergence) and the Equatorial Atlantic Front influence the surface oceanography of the North American and Guiana Basins, respectively. Laevastu and LaFond, 1970 give seasonal positions for both fronts.

Antarctic Intermediate Water influences water structures at intermediate depths in the Caribbean Sea, Gulf of Mexico, and Guiana Basin. This water mass is characterized by a salinity minimum between 700 and 850 meters and enters the Caribbean through St. Lucia and St. Vincent Channels. Antarctic Intermediate Water generally is not found north of the Greater Antilles. At depths between 1200 and 1500 meters, the North American and Guiana Basins are influenced by Mediterranean Intermediate Water. A salinity maximum at its core depth characterizes this water mass, which has been markedly diluted by mixing over the Mid-Atlantic Ridge and throughout the North American Basin (Defant, 1961). Unmixed Mediterranean Intermediate Water penetrates into the Bahama Island passages and occasionally into Windward and Anegada Passages. Neither Antarctic nor Mediterranean Intermediate Water normally are present in the Straits of Florida.

Below 2000 meters the North American and Guiana Basins are occupied by North Atlantic Deep and Bottom Water. However, the shallow sills of the Antilles passages block the spread of this water mass into the Caribbean Sea. The deeper layers of the Caribbean and Gulf of Mexico are occupied by Caribbean Deep Water, which is characterized by an oxygen maximum and enters the Caribbean through Windward and Anegada/Jungfern Passages. Because Caribbean Deep Water is formed from upper North Atlantic Deep Water, it has higher temperatures and salinities than North Atlantic Deep and Bottom Water. According to Worthington, 1955 and 1966, Caribbean Deep Water is not being renewed at the present time. However, according to Sturges, 1965, deep water in the Venezuelan Basin is being renewed through the Anegada/Jungfern Passages.

Oceanographic data used in the analysis of sound velocity structure, temperature, and salinity consist of ocean station (Nansen cast), bathythermograph (BT), and sound velocimeter measurements. The distribution of ocean station and sound velocimeter measurements are shown for two six-month "seasons"; winter, November through April, (Fig. 4-2) and summer, May through October, (Fig 4-3). The distribution is shown in terms of the number of measurements per whole one-degree square. In partially water-covered squares the number shown is proportional to the water area. The amount and distribution of data for winter is sufficient for reliable definition of the upper sound velocity structure. The distribution of summer data shows some deficiencies in the deep regions of the Caribbean Sea and the central Gulf of Mexico.

Definition of the deep sound channel requires that sound velocimeter and temperature-salinity measurements extend deeper than the axis of the deep sound channel, also called deep axial depth (Fig. 4-4). Blank squares indicate no deep measurements. The western Venezuelan

and western Colombian Basins are deep water areas where more observations are needed to define deep axial depth more precisely.

Five-degree square totals of BT's (including expendable BT's) processed by the Fleet Numerical Weather Central through July 1971 are shown for winter in Figure 4-5 and for summer in Figure 4-6. Seasonal totals of BT's (19,500 in summer and 19,100 in winter) and their geographic distributions are quite similar for both seasons.

C. Sound Velocity and Thermal Structure

Sound velocity structures are shown by cross sections, profiles, and areal contour charts.

Sound Velocity Profiles

Locations of sound velocity profiles selected to show representative temporal and spatial variations in major basins and trenches of the area are shown on Figure 4-7. Where station data are available, profiles are shown for every month (Figs. 4-8 through 4-22); however, July, August, and December profiles are noticeably lacking for many regions. The smaller basins, Grenada and Barbados, have fewer profiles because of their size. Where feasible, profiles are extrapolated from the maximum observed depth to the approximate bottom depth at the profile location.

Because all profiles shown on Figures 4-8 through 4-22 are actual measurements (not averaged data), there may be small differences between characteristics shown on these profiles and those shown on the areal contour charts and sound velocity cross sections. Some of the significant features of the profiles are tabulated below:

BASIN OR TROUGH	SURFACE SOUND VELOCITY (M/SEC) MINIMUM	MAXIMUM	SURFACE DUCT PRESENT (MONTHS)	DEPTH OF DEEP SOUND CHANNEL (M) MINIMUM	MAXIMUM	PROFILE SHOWN ON FIG NO
EAST MEXICO	1536 MAR	1546 AUG-OCT	AUG-SEP, DEC-APR	700	1200	4-8
WEST MEXICO	1529 FEB	1547 SEP-OCT	NOV-MAR	700	1100	4-9
YUCATAN	1539 JAN	1546 OCT-NOV	NOV-FEB	900	1100	4-10
CAYMAN	1539 JAN MAR	1547 OCT	OCT-MAR	800	1200	4-11, 4-12
NORTH COLOMBIAN	1538 JAN MAR	1544 SEP	OCT-APR	800	1200	4-13
SOUTH COLOMBIAN	1538 FEB	1544 SEP	OCT-APR	800	1000	4-14
NORTH VENEZUELAN	1537 JAN	1543 SEP	AUG, OCT-APR	700	1100	4-15
SOUTH VENEZUELAN	1538 JAN	1543 OCT NOV	NOV-APR	600	1100	4-16
GRENADA	1539 JAN	1543 AUG-SEP	OCT-APR	600	1100	4-17
BARBADOS	1539 FEB-MAR	1543 SEP	FEB-MAR	700	750	4-17
GUIANA	1538 MAR, AUG	1544 SEP	JUN-AUG, NOV-MAR	600	900	4-18
PUERTO RICO	1536 JAN-MAR	1544 AUG-SEP	JUL-AUG, OCT-DEC, MAR	1000	1400	4-19, 4-20 4-21
NORTH AMERICAN	1528 JAN-MAR	1543 JUL-OCT	FEB-MAR, NOV-DEC	1000	1500	4-22

Several general conclusions can be drawn from the data:

The sound velocity at the surface is near 1540 m/sec for all months and all regions except in the west Mexico and North American Basins, where seasonal fluctuations are greatest (from less than 1530 m/sec during winter to nearly 1550 m/sec during summer).

A surface duct generally is present during winter throughout the area. During summer, a surface duct generally is absent except in the Guiana, north Venezuelan, and east Mexico Basins, and in the Puerto Rico Trench.

The deep, sound channel axis is shallowest in the Guiana, south Colombian, and Venezuelan Basins and deepest in the vicinity of the Puerto Rico Trench and North American Basin.

Locations of profiles for one of the winter months (November April) and one of the summer months (May-October) are shown for principal straits and passages (Fig. 4-23). All profiles (Fig. 4-24 and 4-25) are actual measurements obtained from the rather limited data within the particular strait or passage. An attempt was made to indicate seasonal changes, but no summer profiles are available for several regions. Each profile has been extended, where feasible, to the approximate bottom.

Compared to the sound velocity profiles in the basins, profiles for the straits and passages indicate much greater variability in vertical structure. This may be a result of shallow water conditions, local runoff from adjacent land masses, or mixing of different water masses within a strait. Surface sound velocities are slightly higher during summer months. The bottom depth in many of the passages is shallower than the axis of the deep sound channel.

Sound Velocity Cross Section

Figure 4-26 shows the locations of eight selected north-south and five selected east-west cross sections. These cross sections are shown in Figures 4-27 through 4-34 and 4-35 through 4-39 respectively. The cross sections represent selected sound velocity profiles within the one-degree that they transect. Deviations from a straight line by the cross sec-

tions in Figures 4-28, 4-29, and 4-32 are necessary to transit passages between islands. Figure 4-31 deviates to the west, north of Cuba, in order to follow deep water in the Straits of Florida. The sound velocity cross sections represent winter (November-April) conditions. No seasonal comparisons have been made because of inadequate summer data. Sound velocity contours are shown at intervals of 10 m/sec by thick, solid lines. Thinner, 5 m/sec contours have been added in places for better definition. When present, the following sound velocity features are shown as dashed lines on each cross section:

Deep sound channel axis (deepest sound velocity minimum and absolute minimum in this area);

Subsurface (secondary) minima (upper sound velocity minima, lying between upper mixed layer and the axis of the deep sound channel, which is also called deep axial depth);

Subsurface maxima (lying between upper minimum, if present, and deep axial depth);

Critical (limiting) depth (bottom boundary of deep sound channel).

The locations of individual sound velocity profiles used in constructing the cross sections are shown by ticks inside the bottom margin on each cross section. The generalized bottom topography on the cross sections shows only large-scale bathymetric features that influence sound velocity structures.

The sound velocity cross sections show spatial variations in sound velocity features, such as the deep sound channel axis and critical depth, and large-scale changes in sound velocity regimes. For example, Fig. 4-27 shows a deep sound channel that deepens northward and has velocities varying from less than 1485 m/sec over the Barbados Ridge to greater than 1495 m/sec at 30°N latitude in the North American Basin. These variations can be explained by the presence of Antarctic Intermediate Water in the south that disappears at about 20°N. Figure 4-27 also shows an upper maxima/minima structure north of 28°N that is caused by "18° Water", a shallow sonic layer depth south of 25°N that is caused by winter cooling, and critical depths that become shallower to the north as a result of decreasing surface temperatures. The maxima/minima structure at about 1000 meters at 20°N probably is caused by mixing of Antarctic Intermediate Water with North Atlantic Central Water.

Figure 4-30 (across Windward Passage) shows many of the same variations in sound velocity features shown on Fig. 4-27. In addition, this figure shows the marked difference between the sound velocity regimes in the Caribbean Sea and the North Atlantic Ocean below about 2000 meters. At 3000 meters the difference in sound velocity is about 5 m/sec, while at 4200 meters it is nearly 10 m/sec. This is caused by the higher temperatures and salinities of Caribbean Deep Water compared to North Atlantic Deep and Bottom Water (Fig. 4-1). Figure 4-33 (central Gulf of Mexico) shows a deep sound channel at depths (700-1000 meters) and velocities (1490 m/sec) similar to those found in the Guiana, Venezuelan, and Colombian Basins (Fig. 4-35). This indicates that Antarctic Intermediate Water still controls deep axial depth and velocity in the Gulf of Mexico. Figure 4-33 also shows low surface sound velocities (1510 m/sec) that are caused by Mississippi River runoff near the coast of Louisiana and the concave sound velocity isolines commonly found in the upper 1000 meters of the Gulf of Mexico.

Figures 4-35, 4-36, and 4-37 show the strong effects of Antarctic Intermediate Water on the deep sound channel axis throughout the Caribbean Sea and Gulf of Mexico, the differences in sound velocity regimes between the Caribbean and the North Atlantic below 2000 meters, and a persistent, shallow mixed layer during winter. Figure 4-39 (along the northern boundary of the area) shows a good example of the transitory upper maxima/minima structure in the Sargasso Sea during winter ("18° Water"). In addition, this figure shows the influence of dilute (less than 30 percent) concentrations of Mediterranean Intermediate Water on the deep sound channel axis (i.e., sound velocity maxima/minima structure found above and below deep axial depth between 65°W and 70°W). Of particular interest are the anomalously low sound velocities (1490 m/sec) near the bottom over the Blake Plateau. These low velocities may be caused by a relatively cold, low-salinity counter current below 800 meters under the Gulf Stream (Boisvert, 1967).

Sound Velocity/Temperature-Salinity Comparisons

Sound velocity/temperature-salinity (T-S) comparisons in major basins and trenches and in selected straits and passages are indexed on Figure 4-40 and shown in Figures 4-41 through 4-66. T-S profiles show temperature-salinity combinations at various depths (in meters) in the water column indicated by the adjacent numbers. Each figure shows a sound velocity and T-S profile for winter and summer conditions at the given location, with the following exceptions:

Figures 4-57 and 4-61, no summer sound velocity and T-S profiles;

Figures 4-62 and 4-64, no summer T-S profiles (sound velocimeter data used for summer sound velocity profile).

All sound velocity profiles, with the exception of the sound velocimeter profiles listed above, were computed using Wilson's equation (Wilson, 1960). Sound velocity profiles have been extended below the depth of actual data to either the maximum depth of the basin or to sill depth in the strait or passage. T-S profiles have not been extended below the depth of actual data. The percentages (concentrations) of unmixed Antarctic and/or Mediterranean Intermediate Water shown on the figures were derived using the temperature-salinity curves in Defant, 1961 shown on Figure 4-1.

Each sound velocity and T-S profile shown represents the same single observation in all cases and none are synthetic, i.e. constructed

by averaging several observations. Therefore, the profiles may not be typical of a large region, but show general trends encountered throughout the area. For example, the deep sound channel axis is formed at or slightly below the depth of the Antarctic Intermediate Water salinity minimum which occurs in winter at 735 m. in the Gulf of Mexico, 770 m. in the Colombian Basin, and 650 m. in the Guiana Basin (Figs. 4-42, 4-48, and 4-52 respectively). However, in the North American Basin and Puerto Rico Trench (in the absence of Antarctic Intermediate Water), the deep sound channel axis is formed at or slightly above the depth of the salinity maximum of the well-diluted Mediterranean Intermediate Water in winter (1200 m. on Fig. 4-41 and 1070 m. on Fig. 4-46). Mediterranean Intermediate Water is also found in the Guiana Basin below the deep sound channel axis in both summer and winter (Fig. 4-52) and can penetrate into some of the deeper passages (Mouchoir Passage, Fig. 4-58 and Anegada Passage, Fig. 4-63). The presence of Mediterranean Intermediate Water tends to broaden the deep sound channel and increase its axial depth and velocity. The winter salinity minimum directly above the Mediterranean Intermediate Water core (35.06‰ at 1107 m. on Fig. 4-41, 34.93‰ at 890 m. on Fig.4-46, and 34.96‰ at 930 m. on Fig. 4-58), represents the bottom of North Atlantic Central Water, not the Antarctic Intermediate Water core. The same applies for the salinity minimum found just above the bottom at 1300 m. on Figure 4-56 and at 1510 m. on Figure 4-57.

An upper sound channel can be formed in the Sargasso Sea (winter) in the presence of substantial quantities of unmixed "18° Water" (250 m. on Fig. 4-41). This water mass extends as far south as the Bahama passages in a diluted form, where it diminishes the negative velocity gradient below the surface mixed layer at about 300 m. (Figs. 4-55 through 4-58). There is no "18° Water" in the Straits of Florida (Figs. 4-53 and 4-54). Subtropical Underwater occurs at about 50 to 200 m. throughout the Gulf of Mexico, Caribbean Sea, Guiana Basin, Straits of Florida, Bahama Island passages, and Caribbean passages, but it is imbedded in the main thermocline. The rather persistent sonic layer depth found between 20 and 100 meters during winter and summer (less likely) on all the sound velocity/T-S comparisons is caused by winter cooling rather than the presence of Subtropical Underwater.

Upper Sound Velocity Minima and Maxima

The upper sound velocity minimum is located between the surface mixed layer and the deep sound channel axis. Upper sound velocity minima can act as effective channels for sound transmission. The subsurface sound velocity maximum lies between the upper minimum (if present) and the deep sound channel axis. Definition of the upper sound velocity minimum and the subsurface sound velocity maxima is derived solely from ocean station and sound velocimeter data whose distribution is shown on Figures 4-2 and 4-3. BT data have not been included in this particular analysis because, unlike ocean station data, salinity is not measured with each BT and use of salinity data from a different location and time may reduce the reliability of the derived sound velocity. Both features undergo considerable temporal variations. Therefore, three categories are given for each: present more than 80 percent of the time, present 20-80 percent, and present less than 20 percent of the time. In the following discussion, the first case will be referred to as Permanent, the second as Transitory. In the third case, both features effectively are Absent. Data generally are adequate for the definition of either feature except as shown on individual figures. The regions where Permanent minima form are distinguished from the regions where the minima are Absent, by a dashed boundary with the Tranistory regions and by the presence of average depth contours (Figs. 4-68, 4-69, and 4-70).

Figures 4-67 through 4-70 show the areal extent and average depth of the upper sound velocity minimum for the seasons of January-March, April-June, July-September, and October-December, respectively. Upper minima generally are formed by insolation during the warm months (May-October) of surface and near-surface layers, which are characterized by positive velocity gradients during the cold months (November-April). During January-March (Fig. 4-67), Transitory upper minima are formed in regions north of 25°N and east of Florida, south of Cuba, and east of Trinidad. Deeper minima in the first region are caused by the "18° Water" formed here during winter along the Subtropical Convergence (Istoshin, 1961). No Permanent minima occur during January-March (Fig. 4-67). During April-June (Fig. 4-68), Permanent minima are found along the northern boundary of the area (increased surface insolation), while Transitory minima are found farther south over the North American Basin (southward spread of "18° Water"). The region of Transitory minima south of Cuba is much smaller in spring than in winter because of the increased depth of surface insolation. Transitory minima also occur east of Trinidad during this season. During July-September (Fig. 4-69) both Permanent and Transitory minima extend farther south over the North American Basin. Two separate regions with Transitory minima occur west of Guadaloupe and east of Trinidad. They are related to the summer position of the Equatorial Atlantic Front (Laevastu and LaFond, 1970). Data in the southwest quadrant of the area are insufficient for evaluation, but Transitory minima probably are absent owing to intense surface insolation. The extent of Permanent and Transitory minima in fall (Fig. 4-70) closely resembles that for spring (Fig. 4-68), except that no upper minima occur east of Trinidad. The average depth of the upper sound velocity minimum can vary up to 50 meters from season to season at any location.

Figures 4-71 through 4-74 show the areal extent and average depth of seasonal subsurface sound velocity maxima. North of 20°N–25°N latitude and east of Florida, the maxima coincide with the bottom of the "18° Water" layer. Throughout the remainder of the area maxima

represent sonic layer depths. The Subtropical Underwater salinity maximum (Wust, 1964) does not cause an associated sound velocity maximum. During winter (Fig. 4-71) Permanent subsurface maxima are present in most of the area except in the east and central Gulf of Mexico. These maxima represent the maximum depth of winter cooling except in the Sargasso Sea ("18° Water"). During April-June (Fig. 4-72) shallower Transitory maxima are found in regions where Permanent maxima occur during winter except in the northeast corner of the area and over the Guiana Basin. These Transitory maxima result from the effect of increased surface insolation on winter positive velocity gradients. Maxima are Absent in most of the Gulf of Mexico and north of Panama during this season. During July-September (Fig. 4-73), Permanent maxima are found over the Bermuda Rise (due to the southward spread of "18° Water") and in a band extending from the southeast corner of the area into the Caribbean This latter region corresponds well with a low salinity surface flow shown by Wust, 1964. Data in the western Caribbean and southern Gulf of Mexico are insufficient to evaluate during summer. During fall (Fig. 4-74), Permanent maxima exist in most of the area except between Florida and Yucatan, in the western Gulf of Mexico, and in the southern Caribbean Sea. These maxima represent either the bottom of the "18° Water" layer or the maximum depth of the fall overturn. The subsurface sound velocity maximum generally is deepest during winter (Fig. 4-71) and shallowest in summer (Fig. 4-73) in response to the annual heating cooling cycle.

Upper Thermal Structure

Figures 4-75 to 4-86 show monthly variations in the upper thermal structure. The analyses were provided by FNWC (Fleet Numerical Weather Central, 1968) and are derived primarily from 1968 BT data. The four parameters shown, sea surface temperature, thermocline gradient, potential mixed layer depth, and depth to the bottom of the thermocline describe the spatial and temporal variations of the upper thermal structure.

Sea surface temperature contours are accurate to approximately 0.5°C. The potential mixed layer depth, defined by FNWC as the lower boundary of the turbulent mixed surface layer or the upper boundary of the thermocline, is subject to daily and local fluctuations; the monthy charts indicate average conditions. In the absence of any sharp inflection point the potential mixed layer depth is defined as the depth where the temperature is 2°F (1.1°C) colder than the sea surface temperature. The thermocline gradient and depth to the bottom of the thermocline also are presented in terms of average monthly conditions. Figures 4-75 to 4-86 are based primarily on 1968 data. However, the figures portray the broad, general features of the upper thermal structure that occur during typical monthly periods.

Several general conclusions can be drawn from these charts. Sea surface temperatures, throughout the year, are highest in the Caribbean Sea and Gulf of Mexico and generally lowest in the North Atlantic portion of the area. Maximum sea surface temperatures of about 30°C occur during August and September in the Gulf of Mexico and Caribbean; minimum sea surface temperatures of less than 20°C occur in February through April in the northern portion of the area. As expected, the largest sea surface temperature fluctuations occur in the northern portions of the area.

A slight seasonal variation in the thermocline gradient is evident. Gradients are strongest during summer months when they generally range between 2°C and 4°C per 100 feet. Gradients greater than 5°C per 100 feet occur in the northeast Gulf of Mexico during July and August (Figs. 4-81 and 4-82). Winter gradients (Figs. 4-75 through 4-77) generally range between 1°C and 3°C per 100 feet with the strongest gradients occurring off Honduras and Venezuela.

The potential mixed layer depth changes significantly from summer to winter, especially in the North Atlantic portion of the area. During June through October (Figs. 4-80 through 4-84) mixed layer depths are less than 200 feet over most of the area. During winter months the mixed layer depths increase to greater than 450 feet in March in the northeast corner of the area (Fig. 4-77). Layer depths less than 150 feet occur in the western or southwestern Gulf of Mexico and western Caribbean throughout the year. The remainder of the Caribbean has layer depths that vary between 200 and 300 feet during winter (November-April) and between 150 and 200 feet during summer (June-October). Potential mixed layer depths generally agree with sub-surface sound velocity maxima shown on Figures 4-71 through 4-74 for the Caribbean Sea, Gulf of Mexico, and Guiana Basin. Sub-surface sound velocity maxima in the Sargasso Sea correspond to the bottom of the "18° Water" layer, not the lower boundary of the turbulent mixed surface layer.

During winter (November-April) the depth of the bottom of the thermocline remains relatively stable through most of the area, ranging between 450 and 600 feet. During summer the bottom of the thermocline shoals to less than 300 feet in the Sargasso Sea (Figs. 4-79 through 4-81).

BT's selected from recent measurements (Fleet Numerical Weather Central, 1971 and Fuglister, 1960) are shown for winter and summer on Figures 4-87 and 4-88. Wherever possible, traces were selected from measurements located near the center of each five-degree square, except where the square is divided by land features.

Since all BT's are actual measurements (not averaged data) they may not always represent the conditions indicated in Figures 4-75 through 4-86. Local conditions may affect the BT traces significantly, especially near coastal areas. In general, however, the individual traces agree quite well with the sea surface temperatures, layer depths, and bottom depths of the thermocline shown in Figures 4-76 and 4-82 (Feb-

ruary and August, 1968). If Figures 4-87 and 4-88 are compared it is evident that the greatest seasonal changes occur in the North Atlantic portion of the area. Also, it is obvious that the layer depth and the bottom of the thermocline are deeper during winter throughout the area.

Deep Sound Channel

The deep sound channel axis is defined as the deepest sound velocity minimum (absolute minimum in this area). The average depth of the deep sound channel axis is presented in meters on an annual basis (Fig. 4-89), because in any given two-degree square, monthly and seasonal variations are often as great as annual variations. Oceanographic data generally are adequate for the definition of this parameter, except in the region south of about 17°N and west of about 70°W (Fig. 4-4). Most of the data deeper than axial depth in the Caribbean Sea are from winter months (November-April). However, throughout the rest of the area, winter and summer data are distributed more or less equally.

In the Caribbean Sea, Gulf of Mexico, and Guiana Basin deep axial depths range from 800 to somewhat greater than 1000 meters, whereas in the North American Basin deep axial depths are greater than 1000 meters (Fig. 4-89). This results from the presence of Antarctic Intermediate Water, which tends to cause a shallower and narrower deep sound channel with axial velocities less than 1490 m/sec. (Piip, 1966). Antarctic Intermediate Water generally is not found north of the Greater Antilles. Figure 4-90 shows annual average deep axial depth in fathoms and bathymetry shoaler than deep axial depth. Only three passages between the Caribbean and the Atlantic Ocean are deeper than deep axial depth: Windward Passage, Anegada Passage, and St. Lucia Channel. The Yucatan Channel also is deeper than deep axial depth. The high relief of the Nicaraguan Rise partially isolates the Yucatan Basin from the eastern Caribbean Sea. The entire Straits of Florida region is shallower than deep axial depth. Two separate figures (4-89 and 4-90), showing the same deep axial depth information, one in meters and the other in fathoms, are included because of the great difficulty in converting bathymetric contours to meters in order to show topographic interference (Fig. 4-90).

Critical (Limiting) Depth, Depth Difference, and Depth Excess

Critical depth is the depth below the deep sound channel axis, where the sound velocity is equal to the surface or near-surface maximum sound velocity. All available ocean station and sound velocimeter data were included to determine average values of critical depth for each two-degree square. Most of these data came from References 1, 2, 7, 26, 36, 50, 55, 79, 80, 91, 92, 93, 108, 120, 121, and 122. Data for winter (Fig. 4-2) are adequate throughout the area to define critical depth. Summer data (Fig. 4-3) are barely sufficient to determine critical depth in portions of the Caribbean and western Gulf of Mexico; additional data are required to verify values of critical depth in these areas.

Because critical depths vary seasonally, especially in the northern half of the area, their analysis is divided into six-month summer (May-October) and winter (November-April) presentations. The fact that April-May and October-November are transition months in this area has been considered in analyzing the data for seasonal critical depths.

Winter critical depths (Fig. 4-91) are shallower than summer critical depths (Fig. 4-92) throughout the area owing to the lower surface temperatures and corresponding sound velocities in winter. Critical depths in winter are about 100 fathoms shallower than in summer in the Caribbean and are 100 to 400 fathoms shallower in the Gulf of Mexico. In the North American Basin the most siginificant seasonal difference occurs north of 25°N, where winter critical depths are 100 to 500 fathoms shallower than summer. In the Caribbean and Gulf of Mexico summer critical depths range between 2300 and 2500 fathoms, and outside the Caribbean they average 2600 fathoms and deepen to over 2700 fathoms in the Bahamas and in the easternmost parts of the area.

Extreme gradients along the Lesser Antilles result primarily from the marked difference between sound velocity regimes in the Caribbean Sea and the North Atlantic Ocean below 2000 meters. Similar gradients in the Straits of Florida mark the merging of the Florida Current with the Antilles Current. These gradients are found in both summer and winter.

Figures 4-93 and 4-94 show depth difference and depth excess contours based on summer and winter critical depths. Depth difference is that portion of the bottom topography that extends into the deep sound channel. Depth excess is the depth of water between the bottom of the sound channel and the sea bottom. Bathymetric data were taken from Figure 4-109. The intervals between the zero and the 200-fathom depth excess contours represent those regions where convergence zone paths may be expected but are not assured. Because of variations in sound velocity, accuracy of bathymetric data, and the techniques used for averaging the sound velocity data and constructing the critical depth charts, the contours are accurate to approximately · 50 fathoms.

Most of the Caribbean Sea and the Gulf of Mexico is bottom limited (shaded regions). In the Caribbean during winter, significant depth excess occurs only in the Venezuelan Basin and the Cayman Trough. However, portions of the Colombian Basin, the Yucatan Basin, and the western Gulf of Mexico may include some regions of depth excess during winter. The North American Basin and the area east of the Lesser Antilles include extensive regions of depth excess during winter. During summer the Gulf of Mexico and the Colombian Basin appear to be entirely bottom limited. Other regions of depth excess are somewhat smaller in winter than during summer because of the greater critical depth.

D. Bottom Properties

Bathymetry

The locations and identifications (ship and year) of bathymetric survey tracks and areas of controlled surveys are shown in Figures 4-95 through 4-108. Figure 4-95 includes an index of the track charts numbered in accordance with the Naval Oceanographic Office bottom contour (BC) series. These numbers appear on the lower right corner of each figure. The only evaluation of data quality or positional accuracy is the distinction between random tracks and controlled surveys. Controlled surveys generally are more reliable than random tracks, because they consist of grid-type surveys in which the navigational positioning is highly accurate. Some of the track charts represent a selection of better data through elimination of sounding lines, whose lack of agreement with major bathymetric features indicated that the navigation was unreliable. Many of the sounding lines classified as random tracks are of questionable quality because of their age. However, included among the random tracks are high quality tracks by Navy laboratories and oceanographic institutions.

Bottom topography in the area is shown on Figure 4-109 by means of water depth contours with a basic interval of 100 fathoms. The contours represent depths uncorrected for variations from the standard speed of sound in sea water of 4800 ft/sec (800 fm/sec) for which the echo sounders were calibrated. Because of the chart scale the depth contours have been dropped in regions of steep slopes.

Depths shown on the bathymetric chart (Fig. 4-109) can be corrected for sound velocity structure using nomograms in Figure 4-110 for the three regions having significantly different depth correction values. Correction curves for meters and fathoms are included for both the 800 fm/sec (1463 m/sec) and the 820 fm/sec (1500 m/sec) standards. The depth correction nomograms have been newly computed for this atlas using recent data.

The principal sources of data used in compiling the bathymetric chart are cited on Figure 4-109. They also are listed in the bibliography as References 6, 10, 13, 54, and 110 in addition to the U.S. Naval Oceanographic Office bottom contour (BC) charts and compilation sheets (scale 1° longitude = 4 inches, i.e. approximately 1:1 million) for the areas indexed in Figure 4-95.

The basic sources for bathymetry were the BC charts. They were updated using sounding sheets recently compiled for the General Bathymetric Chart of the Oceans (GEBCO) and published bathymetric charts. The Bermuda Rise, Aves Ridge, Beata Ridge, Cayman Trough, and Cayman Ridge have not been charted precisely because of their complexity and the lack of controlled surveys.

The general outlines of the principal physiographic features in the area are shown in Fig. 1-1 and were based upon interpretations from References 6, 10, 13, 17, 19, 32, 53, 54, 88, and 110. The continental and insular shelves are delineated arbitrarily by the 100-fathom contour which does not everywhere coincide with the true shelf edge. Most of the sea floor topography in the area is characterized by steep slopes and rugged relief. The principal regions having relatively flat bottom are the Mexico, Blake, Yucatan, Colombian, Venezuelan, and Grenada Basins and the Hatteras and Nares Plains (Fig. 1-1).

Bottom Composition

The distribution of surficial sediments in the area is shown in Figure 4-111, which classifies the bottom materials as mud (clay and/or silt), mud-sand, sand, sand-gravel, and combination of bottom types (mostly coarse-grained sediments) dominated by gravel and rock. Bottom sediments are dominantly fine grained in the deep-water portions of the area. Complex patterns and mixtures of fine and coarse-grained sediments characterize the continental and island slopes and shelves.

The dominant constituent of deep-water sediments of the Gulf of Mexico is post glacial alluvial silt and clay, which overlies glacial alluvial material. Selected cores (located and described in Fig. 4-112) show the vertical variation in grain size (percent clay-silt-sand-gravel). Calcareous remains of pelagic foraminifera are mixed with the sediments. The continental shelf sediments west of Florida consist of quartz mixed with shell, coral fragments, and calcareous algae and include scattered shell beds and oyster reefs. The Yucatan-Campeche shelf (Campeche Bank) is calcite-cemented limestone covered by scattered coral reefs and by calcareous sand 3 inches to 4 feet thick. On the northern continental slope, the glacial mud and mud-sand, 2 to 13 feet thick, lie upon 20 feet or more of gray silty clay.

The deep-water sediments of the Caribbean Sea are principally calcareous mud-sands containing the skeletal remains of foraminifera (cores 33 and 38, Fig. 4-112). Where the water is deeper than about 2,500 fathoms, the clay and silt contain little calcareous material. On the continental shelves, coral algal reefs and detritus predominate, with volcanic materials added around the Lesser Antilles.

In the Atlantic Ocean approaches to the Caribbean Sea and Gulf of Mexico, the deep-water mud is reddish-brown clay-silt (cores 11, 15, 19, 20, and 28 in Fig. 4-112), which includes volcanic detritus, siliceous organisms, and meteoric dust. The clays are composed of equal portions of illite, kaolinite, and montmorillonite. The calcium carbonate content is usually 20 percent or less. The deep-water mud-sands have a calcium carbonate content of 20-60 percent which represents calcareous sands derived from pelagic foraminifera, coral detritus, and shells. The continental shelf sediments off Florida are mostly sand and gravel with the calcareous component increasing to the south to 100 percent south of 28°30'N. The shelf sediments in the Straits of Florida, Greater Antilles, and Bahamas are dominantly calcareous with admixtures of volcanic

material in the Greater Antilles. Calcareous clay-silt occupies the Tongue of the Ocean and Exuma Sound.

The distribution of bottom sediment data is shown in Figure 4-113 in terms of the number of cores and number of samples of surface sediments in each one-degree square. As indicated by the zeros and the blank squares, surface sediment data are lacking in many scattered regions, and core data are even more inadequate to describe horizontal and vertical variations in bottom composition reliably. Bottom sediment data were derived from many sources (Duncan, 1964). Compiled and published charts, showing the distribution of surface sediment types, prepared by the Naval Oceanographic Office (Naval Oceanographic Office, 1965f) was the principal source. The source charts were compiled from thousands of nautical chart notations of bottom type, which were amplified by descriptions and analyses of sediment samples reported in many references in the bibliography, most of which predate 1964. Figures 4-111 and 4-112 also use more recently reported sediment data contained in 29 papers published since 1963. These sources are all prefixed in the bibliography by (S).

Seismic Profiles

Figure 4-114 shows the location of typical seismic reflection profiles in the area. Subbottom profiles in the Gulf of Mexico and Caribbean Sea are primarily from reflection profile tracks of the R/V VEMA and ROBERT D. CONRAD, Lamont-Doherty Geological Observatory. The profiles in the southeastern Bahamas are from R/V CHAIN, Woods Hole Oceanographic Institution.

Seismic reflection profiling studies in the Caribbean have revealed two prominent subbottom reflectors (horizons) in otherwise acoustically transparent sediment (Edgar et al., 1971). These horizons, A" and B", can be traced throughout the Venezuelan Basin, most of the Colombian Basin, over both flanks of the Beata Ridge, on the eastern flank of the Nicaraguan Rise, and on the western flank of the Aves Ridge (Figs. 4-115 and 4-116). Two acoustically transparent layers, called the Carib beds, are separated by the upper reflector, Horizon A" (Fig. 4-115). The Carib beds are remarkably uniform in thickness and acoustical character. The upper layer is 0.55 seconds reflection time in thickness and generally is free of reflectors except near the Aves Ridge and in parts of the Beata Ridge. The lower layer, between A" and B", is about 0.4 second reflection time in thickness and also is acoustically transparent, but to a lesser degree. The lower reflector, B" characteristically is a smooth surface that returns a coherent reflection. Site 146 (Fig. 4-114), in the center of the Venezuelan Basin, is the location of a coring operation by the Deep Sea Drilling Project, Leg 15 (Benson et al., 1970). Here, the seismic reflectors Horizon A" and Horizon B" are identified at 0.5 second and 0.8 second reflection times, respectively. In the coring operation Horizon A" was encountered after cutting 406 meters of foraminiferal nannoplankton chalk and marl oozes, and interbedded marls and clays. The chalks pass into limestone with interbedded chert, which forms the seismic reflector Horizon A". About 35 meters of interbedded limestone, chalks, and cherts of Horizon A" were determined to be of early to late Paleocene age. A series of Cretaceous marls, siliceous clays, radiolarian limestone and chert, and volcanic ash was cored to 738 meters where the first dolerite (basalt) sill was encountered, corresponding to Horizon B". About 16 meters of dolerite was cored before the hole was terminated. An average velocity of about 1.9 km/sec has been determined for the layer above Horizon A". Reflection horizons that appear similar to A" and B" have been recorded in the North American Basin.

Site 28, on the Puerto Rico Ridge, is the location of a deep core of the Deep Sea Drilling Project—Leg IV (Benson et al., 1970). The reflection profile shows a two-way travel time thickness of the transparent and semitransparent layers of about 0.4 seconds (Fig. 4-117). This interval increases rapidly to the north before diminishing where the layers dip beneath the turbidites of the Nares Plain. The transparent layer was 176 meters thick at the drill site, which verified a sonic velocity of 2.0 to 2.3 km/sec for this layer. The semitransparent layer was penetrated to a depth of 404 meters without reaching "basement". The semitransparent layer was assigned a relatively high (4.2 km/sec) sonic velocity by Hersey and Bunce, 1964.

Seismic profiles within the southeastern Bahamas and Old Bahama Channel (Fig. 4-118) depict two units–a lower massive nonstratified to poorly stratified unit, and an upper well stratified unit (Uchupi et al., 1971). The lower unit, which forms the core of the Bahama Escarpment and underlies most of the southeastern Bahamas, is extremely rugged, with relief of more than 4 kilometers (Fig. 4-119). The upper unit consists of a well stratified sequence ranging in thickness from several hundred meters to as much as 4.5 kilometers (assuming a velocity of 2 km/sec).

The seismic reflection profiles in the Gulf of Mexico indicate some of the complexity of the salt tectonics in several areas of the Mexico Basin (Figs. 4-120 and 4-121). The east Mexican shelf and slope are composed of a series of anticlines that start from the continental rise and continue under the continental shelf. The general trend of these features is in the direction of the shelf break. Many of the series of long, linear anticlines have an average relief of 250 fathoms and a wavelength of 5 to 7 miles (Bryant et al., 1968).

Profile ABCDEA'FG (Fig. 4-114) in the Campeche Knolls and Sigsbee Knolls regions shows the extreme irregularity of the topography within the diapiric zones (Fig. 4-122). Knolls in the Campeche province attain a relief of 400 to 650 fathoms in the central area and decrease to an average relief of 75 fathoms at the eastern and western edges. The Sigsbee Knolls are isolated features with relief up to 150 fathoms and diameters up to 5 miles (Worzel et al., 1968).

Figure 4-123 is a location chart for sediment velocity determinations

in the area. Most of the velocity solutions have been derived from sonobuoy data obtained by Houtz et al., 1968. The results are fully annotated in a table (Fig. 4-124). One experimental velocity determination by Brown and Ricard, 1965, interpreted in terms of a 130-foot bottom layer at 1830 fathoms, was 2.027 km/sec.

Four sediment velocities were determined on cores taken by the Deep Sea Drilling Program–Leg IV (Benson et al., 1970):

Site 27—1.71 to 1 74 km/sec

Site 29—1.54 km/sec

Site 30—1.5 to 1.6 km/sec

Site 31—1.55 km/sec

E. Wind and Waves

Waves consist of sea and swell. Sea refers to waves generated or directly sustained by local winds. Swell designates waves that have traveled some distance from the generating area and is more regular, with longer periods and flatter crests, than sea. The direction from which swell is coming indicates the position of a center of strong winds, possibly hundreds of miles away; thus, swell may be the first indication of an approaching storm. Sea and swell are often present together, although low swell may be obscured by the sea. The modal direction given in Figures 4-125 through 4-136 is the direction most frequently observed.

The generally highly reliable sources used in this compilation (Naval Oceanographic Office, 1963b and U. S. Weather Bureau) contain all information available through 1960 and now on file at the U. S. Naval Oceanographic Office. Except for a few isolated regions far from the shipping lanes, temporal and spatial distributions of the data are adequate to describe the prevailing conditions.

The tables of wind, sea, and swell (Figs. 4-125 through 4-136) show average conditions for homogeneous regions, i.e., regions with similar distributions of speed and direction. Since seasonal changes are gradual in the trades, the data are presented only for the mid-seasonal months of February, May, August, and November, which are considered representative. Easterly and northeasterly winds, seas, and swell predominate throughout the year, except in the western Gulf of Mexico.

Wind and wave conditions in this area generally are favorable for ship operations, particularly in summer. However, winds are strongest and sea and swell are highest in fall and winter as a result of the passage of extratropical cyclones. In fall and winter the highest waves occur in the extreme northeastern part of the area. Here, the probability of seas higher than 4 feet is about 40 percent and that of swell higher than 12 feet about 10 percent. Tropical cyclones with winds in excess of 27 knots can occur in any month, but the hurricane season generally lasts from July through October. Fifty-eight years of data reveal that an annual average of one to two (statistically 1.6) hurricanes originate in the Caribbean and are accompanied by winds of at least 64 knots and high seas and swell. An annual average of about three hurricanes, which ultimately affect this area, form in the vicinity of the Cape Verde Islands.

Precipitation, an important source of underwater noise in this area, occurs mostly as showers, except along the northern coast of the Gulf of Mexico, where as much as 60 percent of the precipitation during winter is drizzle. The rainfall frequency varies from a minimum in spring to a maximum in fall. The average probability (percent of observations) of precipitation for midseasonal months over regions of homogeneous sea conditions is tabulated below and keyed to the regions shown in Figures 4-129 through 4-132. Locally, the likelihood of rainfall is as high as 15 to 20 percent over the Lesser Antilles in late summer and fall, and along the coast of Panama from late spring through mid-fall.

FREQUENCY OF PRECIPITATION (PERCENT OF OBS.)

LOCATION KEY SEA AREA*	SEASONALLY REPRESENTATIVE MONTH FEB	MAY	AUG.	NOV.
1	5	1	4	6
2	4	3	5	5
3	5	5	6	10
4	5	7	7	12
5	5	5	5	7
6	3	6	6	-
7	5	6	-	-
8	6	-	-	-

AVERAGE NUMBER OF OBSERVATIONS PER 2° SQUARE

	FEB.	MAY	AUG.	NOV.
1	200	225	350	275
2	600	600	775	575
3	425	500	425	425
4	450	425	425	250
5	325	350	550	500
6	375	525	650	--
7	525	525	---	---
8	450	---	---	---

*For Location see geographical insets of Figures 4-129, 4-130, 4-131, and 4-132, for Feb., May, Aug., and Nov., respectively.

F. Currents

Surface Currents

Prevailing seasonal current patterns are shown in Figures 4-137 through 4-140. However, variations in wind conditions will cause temporary changes in speed and direction of these prevailing current patterns. Seasonal current roses in Figures 4-141 through 4-148 provide a measure of variability by indicating the frequency with which currents set in different directions within specified speed ranges in the regions indicated by each inset location chart. Presentations of current speeds

and directions are based mainly on seasonal data summarized by one-degree square.

A westward flow from the North Equatorial and Guiana Currents enters the Caribbean Sea through the channels between the Lesser Antilles and eventually flows northward through Yucatan Channel. This flow is known as the Caribbean Current. Countercurrents occur along the shores, particularly those of Colombia, Panama, and Cuba. Currents are strongest off the northeast coast of Venezuela in spring and summer and the region north of Panama in summer.

The Yucatan Current transports water northward through Yucatan Channel from the Caribbean Sea into the Gulf of Mexico and Straits of Florida. Speeds increase from about 1.0 knot near the eastern edge of the channel to over 1.5 knots 20 to 30 nautical miles east of the tip of Yucatan. The currents are strongest in the western part of the channel in spring when the mean speeds are 1.5 to 1.8 knots. Clockwise eddies occur about 60 nautical miles north and south of the western end of Cuba.

The north-setting current from Yucatan Channel flows into the Gulf of Mexico with branches turning eastward and westward to form clockwise and counterclockwise circulation patterns. In winter strong northerly winds may cause south-setting currents throughout the Gulf of Mexico. The currents are usually stronger during April through September than during October through March. Currents are strongest north of Yucatan Channel and off St. Petersburg, Florida in spring when mean speeds are 1.5 to 1.7 knots.

The Florida Current sets eastward off the Florida keys and swings northeastward, then northward around Florida where it is joined by the northwest-setting Antilles Current to form the Gulf Stream. The mean position of the axis of the Florida Current generally follows the 100-fathom contour off the southeast coast of Florida. The speeds fluctuate daily due to astronomical forces; maximum speeds are attained about 9 hours before upper and lower lunar transit of the local meridian. Currents are strongest off the southeast coast of Florida in summer when the mean speed is about 3.0 knots. The maximum speed is about 6.6 knots. A countercurrent often flows along the east coast of Florida.

Subsurface Currents

Figure 4-149 locates available subsurface current measurements made where water depths equal or exceed 100 meters and the depth of the measurements equal or exceed 50 meters. Representative profiles are shown for portions of the Straits of Florida and for the Tongue of the Ocean where large numbers of measurements are available. The actual depth of measurement, average and maximum speed and direction of current (where observed), water depth, month or months of measurements, and type of current instrument are included for each profile shown in Figures 4-150 through 4-157. Current speed is given in knots and direction in one of the eight major compass directions.

Very few subsurface current measurements have been made in the Caribbean Sea. Most measurements are concentrated in the straits and passages, in the Bahamas, and in the North American Basin. Therefore, no attempt has been made to determine subsurface current patterns or seasonal fluctuations of subsurface currents based on direct measurements. Indirect current measurements, that is dynamic height calculations derived from ocean station data, may provide a generalized version of current direction and speed at selected depths. However, profiles derived from indirect measurements are not included in this report. The surface and subsurface current information presented in this atlas was derived principally from data filed in the Naval Oceanographic Office supplemented by other reports (Boisvert, 1967; Cochrane, 1963; Fuglister, 1963; Parr, 1937).

In 1970 the R/V ATLANTIS II (cruise number 56) made 175 current meter and 37 free-fall instrument observations in the Grenada, St. Vincent, and St. Lucia Passages. One thousand drift bottles were also released. The data in Stalcup et al., 1971 were received too late for inclusion in this atlas.

G. Oxygen

Another oceanographic parameter used to identify water masses is oxygen content. As previously noted, water mass identification is prerequisite to understanding sound velocity structures. Locations of selected oxygen profiles for the major basins and trenches are shown in Figure 4-158. Summer and winter profiles are included for each location (Figs. 4-159, 4-160, and 4-161).

An intermediate oxygen minimum is present on all profiles above 1000 meters. This minimum separates the warm and cold water spheres throughout the area (Wust, 1964) and corresponds to the upper boundary of Antarctic Intermediate Water in the Caribbean Sea, Gulf of Mexico, and Guiana Basin. The oxygen minimum is shallowest in the Caribbean and the Gulf of Mexico (500 to 800 meters) and deepest in the North Atlantic portion of the area (900 to 1000 meters). This indicates that the cold sphere extends deeper in the North Atlantic portion of of the area.

An oxygen maximum of greater than 6.0 ml/l occurs only in the North Atlantic (profiles A-winter, F-summer, and G-winter), inside the Jungfern Passage (profile E-both seasons), and in the Cayman Trough (profile J-summer). The depth of this maximum varies between 1500 and 2500 meters. This maximum probably is caused by Upper North Atlantic Deep Water (Wust, 1964), which enters the Caribbean through the Anegada and Windward Passages to form Caribbean Bottom Water.

H. Bibliography

The principal sources, such as technical reports, books, papers in technical journals, and serial publications used in preparation of the Marine Environment section of this atlas are listed alphabetically by author. They are referred to in the text by author and date or by the reference number when a long series is cited. The references are identified with sub-sections of the text by parenthetical letters before each reference as shown below:

(B) Bathymetry and Physiography
(BR) Bottom Reflectivity
(C) Currents
(S) Sediments
(SV) Sound Velocity Structure
(T) Temperature
(Wa) Waves
(Wi) Winds

1. (SV) Alpine Geophysical Associates, 1967a, Marine Geophysical Survey Program 65-67, western North Atlantic and eastern and central North Pacific Oceans—Area HH, Vol. 3, Catalog of data: U. S. Naval Oceanographic Office, SP-96-HH-3.
2. (SV) (S) ____, 1967b, Marine Geophysical Survey Program 65-67, western North Atlantic and eastern and central North Pacific Oceans—Area II Volumes 8 and 8A, core, sound velocimeter, hydrographic, and bottom photographic stations: U. S. Naval Oceanographic Office, SP-96-11-8 and SP-96-11-8A.
3. American Meteorological Society, 1970, Bibliography on meteorology, climatology, and physical/chemical oceanography: CICAR (Cooperative Investigation of the Caribbean and Adjacent Regions), v. 1, U.S. National Oceanographic Data Center, Wash., D. C.
4. (S) Athearn, W. D., 1962, Bathymetric and sediment survey of the Tongue of the Ocean, Bahamas, Part I—Bathymetry and sediments: ref. n. 62-65, Part II—Bottom photographs: ref. n. 62-67, Woods Hole Oceanographic Institution, Woods Hole, Mass.
5. (S) ____, 1965, Sediment cores from the Cariaco Trench, Venezuela: Woods Hole Oceanographic Institution Tech. Rept., ref. n. 65-37 (unpublished) also in Marine Geology, v. 31, n. 12, p. 32-59.
6. (B) Banks, M. G., and Richards, M. L., 1969, Structure and bathymetry of the western end of Bartlett Trough, Caribbean Sea: Am. Assoc. Petroleum Geologists Mem., n. 11, p. 221-228.
7. (SV) Beckerle, J. C., 1968, A report on ATLANTIS II cruise 22-June, July and August 1966—Part II: Sound velocity profiles: Woods Hole Oceanographic Institution ref. n. 68-67 (unpublished).
8. (S) Bell Telephone Company, 1960, Submarine telephone and telegraph cable interruptions 1914-1960, date, location, depth, cause and type of bottom: (unpublished listing).
9. (BR) (B) Benson, W. E. et al., 1970, Initial reports of the Deep Sea Drilling Project: v. IV, p. 662-673.
10. (B) Bergantino, R. N., 1971, Submarine regional geomorphology of the Gulf of Mexico: Geol. Soc. Am. Bull., v. 82, p. 741-752.
11. (C) Boisvert, W. E., 1967, Major currents in the North and South Atlantic Oceans between 64°N and 60°S: U. S. Naval Oceanographic Office Tech. Rept. 193, p. 91.
12. (S) Bowin, C., 1966, Narrative of CHAIN cruise No. 41: Woods Hole Oceanographic Institution, Tech. Rept., ref. n. 66-62, (unpublished).
13. (B) ____, 1968, Geophysical study of the Cayman Trough: Jour. Geophys. Research, v. 73, p. 5159-5173.
14. (S) British Admiralty, , List of oceanic depths and serial temperature observations received at the Admiralty during the years 1888–1919, 1924–1930, 1932, 1933, 1935–1952 from HM surveying ships, Indian Marine Survey and British Submarine Telegraph Companies: Hydrographic Department, Admiralty, London.
15. (S) ____, 1963, H.M.S. OWEN, cruise 1960–61, North and South Atlantic: Marine Sciences Pub. n. 1, Hydrographic Department, Admiralty, London.
16. (BR) Brown, M. V., and Ricard, J. H., 1965, Interference pattern observed in reflections from the ocean bottom: Jour. Acoust. Soc. Am., v. 37, n. 6, p. 1033-1036.
17. (BR) (B) Bryant, W. R., Antoine, J. W., Ewing, M., and Jones, B. R., 1968, Structure of the Mexican continental shelf and slope, Gulf of Mexico: Am. Assoc. Petroleum Geologists Bull., v. 52, n. 7, p. 1204-1228.
18. (S) Bullis, H. R., Jr., and Thompson, J. R., 1965, Collection by the exploratory fishing vessels OREGON, SILVER BAY, COMBAT and PELICAN made during 1959–60 in the southwestern North Atlantic: U.S. Bureau of Fisheries, Special Scientific Rept. Fisheries, n. 510, p. 130.

19. (B) Chase, R. L. and Hersey, J. B., 1968, Geology of the north slope of the Puerto Rico Trench: Deep-Sea Research, v. 15, p. 297-317.

20. (C) Cochrane, J. D., 1963, Yucatan current: Oceanography and Meteorology of the Gulf of Mexico, Annual Rept., 1 May 1962–30 April 1963, A & M Project 286, ref. 63-18A, Texas A & M Univ., College Station, Texas.

21. (S) Columbia University, , Alamedas cruise 4—piston cores in the Gulf of Mexico: Lamont Geological Observatory, NODC ref. 00528 (unpublished).

22. (S) Correns, C. W., 1937, Die sedimente des aquatorialen atlantischen ozeans "Meteor": 1925-27: Deutsche Atlantische Expedition, Band III, Dritter Teil.

23. (SV) Defant, A., 1961, Physical Oceanography: v. 1, New York, Pergamon Press, 729 p.

24. (S) Duncan, J. K., 1964, Submarine sediment data collection and management at the U. S. Naval Oceanographic Office: U.S. Naval Oceanographic Office, Tech. Rept. TR-150, 62 p.

25. (BR) (B) Edgar, N. T., Ewing, J. I., and Hennion, J., 1971, Seismic refraction and reflection in Caribbean Sea: Am. Assoc. Petroleum Geologists Bull., v. 55, n. 6, p. 833-870.

26. (SV) Environmental Science Services Administration, 1969, BOMEX preliminary data, salinity-temperature depth observations: v. 3, parts 1 and 2 (unvalidated teletype messages).

27. (S) Ericson, D. B., Ewing, M., and Heezen, B. C., 1952, Turbidity currents and sediments in North Atlantic: Am. Assoc. Petroleum Geologists Bull., v. 36, n. 3, p. 489-511.

28. (S) Ewing, J., Hollister, C., et al., 1970, Deep sea drilling project Leg 11: Geotimes, v. 15, n. 7, p. 14-16.

29. (BR) (S) Ewing, J., Talwani, M., Ewing, M., and Edgar, T., 1967, Sediments of the Caribbean: in Studies in Tropical Oceanography, Univ. of Miami, v. 5, p. 88-102.

30. (S) Ewing, J., and Wollin, G., 1956, Correlation of six cores from the equatorial Atlantic and the Caribbean: Deep-Sea Research, v. 3, p. 104-125.

31. (S) Ewing, J., Ewing, M., Wollin, G., and Heezen, B. C., 1961, Atlantic deep-sea sediment cores: Geol. Soc. Am. Bull., v. 72, n. 2, p. 193-285.

32. (B) (S) Fahlquist, D. A., and Davies, D. K., 1971, Fault-block origin of the western Cayman Ridge, Caribbean Sea: Deep-Sea Research, v. 18, p. 243-253.

33. (S) Fish Commission, 1886, Report of the U.S. Fish Commission Steamer ALBATROSS for the year ending December 31, 1886: U.S. Commission of Fish and Fisheries, Rept. of the Commissioner for 1886, App. D, p. 605-685.

34. (T) Fleet Numerical Weather Central, 1968, Thermal structure maps—Caribbean area for 1968: (unpublished tabulations).

35. (T)_____, 1971, Bathythermograph data processed through July 1971 and historical maps for 1968: (unpublished).

36. (SV) Fuglister, F. C., 1960, Atlantic Ocean atlas of temperature and salinity profiles and data from the International Geophysical Year of 1957-1958: Woods Hole Oceanographic Institution Atlas Series, v. 1, 209 p.

37. (C)_____, 1963, Gulf Stream: Trans. Am. Geophys. Union, v. 44, n. 2.

38. (S) Gallagher, J. J., and Nacci, V. A., 1965, Investigations of sediment properties in sonar bottom reflectivity studies: Proceedings, Second U.S. Navy Symposium on Military Oceanography 5-7 May 1965, U.S. Naval Ordnance Lab., v. 1.

39. (S) Greenman, N. N., and LeBlanc, R. J., 1956, Recent marine sediments of the northwest Gulf of Mexico: Am. Assoc. Petroleum Geologists Bull., v. 40, n. 5, p. 815-847.

40. (S) Griffin, J. J., and Goldberg, E. D., 1969, Recent sediments of Caribbean Sea: Am. Assoc. Petroleum Geologists, Mem. II, The Collegiate Press, George Banta Co. Inc., Menasha, Wisc., p. 258-268.

41. (S) Griffiths, J. C., 1951, Size versus sorting in some Caribbean sediments: Jour. Geology, v. 59, n. 3, p. 211-243.

42. (S) Heezen, B. C., Johnson, G. L., and Allen, R. C., 1963, Oceanographic information for the study of the Florida-Jamaica and Jamaica-Curacao cable routes: Bell Telephone Laboratories, Murray Hill, New Jersey.

43. (S) Heezen, B. C., and Sheridan, R. E., 1966, Lower Cretaceous rocks (Neocomian-Albian) dredged from Blake Escarpment: Science, v. 154, n. 3757.

44. (S) Hersey, J. B., and Bunce, E. T., 1964, Narrative of CHAIN cruise No. 34-Woods Hole to Puerto Rico Trench, north wall, and Outer Ridge and return, 21 October–13 December 1962: Woods Hole Oceanographic Institution, ref. n. 64-35.

45. (B) (S) Hersey, J. B., and Rustein, M. S., 1958, Reconnaissance survey of Oriente Deep, Caribbean Sea, with a precision echo sounder: Geol. Soc. Am. Bull., v. 69, p. 1297-1304.

46. (S) Hollister, C. D., 1965, Bermuda-Tortola cable route survey: (unpublished).

47. (BR) Houtz, R., Ewing, J., and LePichon, X., 1968, Velocity of deep-sea sediments from sonobuoy data: Jour. Geophys. Research, v. 73, n. 8, p. 2618-2641.

48. (SV) Istoshin, Y. V., 1961, Formative area of "eighteen-degree" water in the Sargasso Sea: Okeanologiya, v. 1, n. 4, p. 600-607 (translated from Russian in Deep-Sea Research, v. 9, p. 384-390, 1962).

49. (S) Jordan, G. F. 1951, Continental slope off Apalachicola River, Florida: Am. Assoc. Petroleum Geologists Bull., v. 35, n. 9, p. 1978-1993.

50. (SV) LaCasce, E. O., Woodring, C. M., and Beckerle, J. C., 1969, Sound velocity characteristics in the Sargasso Sea based on observations on cruise 89 of R/V CHAIN: Woods Hole Oceanographic Institution, ref. n. 69-38 (unpublished).

51. (S) Lackie, K. W., 1971, Project NAVADO, an international oceanographic survey of the North Atlantic Ocean: U.S. Naval Oceanographic Office, Washington, D. C., (in preparation).

52. (SV) Laevastu, T., and LaFond, E. C., Oct. 1970, Oceanic fronts and their seasonal positions in the surface: Naval Undersea Research and Development Center Tech. Pub. 204.

53. (B) Lidz, L. et al., 1969, Marine basins off the coast of Venezuela: Bull. Marine Science, v. 19, p. 1-17.

54. (B) Malloy, R. J., and Hurley, R. J., 1970, Geomorphology and geologic structure: Geol. Soc. Am. Bull., v. 81, p. 1947-1972.

55. (SV) Metcalf, W. G., Stalcup, M. C., and Zemanovic, M. E., 1971, Hydrographic station data from ATLANTIS II cruise 56 to the southeastern approaches to the Caribbean Sea, Feb-Apr 1970: Woods Hole Oceanographic Institution, ref. n. 71-13, (unpublished).

56. (S) Milligan, D. B., 1962, Marine geology of the Florida Straits: M.S. Thesis, Florida State University, 120 p.

57. (S) Moore, J. E., and Gorsline, D. S., 1960, Physical and chemical data for bottom sediments South Atlantic Coast of the United States, M/V THEODORE N. GILL cruises 1-9: U.S. Fish and Wildlife Service, Spec. Scient. Rept. Fisheries, n. 366, 84 p.

58. (S) Murray, H. M., and Harrison, J. L., 1956, Clay mineral composition of recent sediments from Sigsbee Deep: Jour. *Sed. Petrology, v. 26, n. 4, p. 363-368.*

59. (S) *Murray, J., 1885, Report on the results of dredging under the* supervision of Alexander Agassiz in the Gulf of Mexico (1877-78) in the Caribbean (1877-78), and along the coast of the U.S. during the summer of 1880 by the U.S. Coast Steamer BLAKE XXVII, Report on the bottom deposits: Bull. Museum Comp. Zoology at Harvard College, v. 12, n. 2.

60. (S) Murray, J., and Chumley, J., 1924, The deep-sea deposits of the Atlantic Ocean: Trans. Royal Soc. Edinburgh, v. 54, pt. I-Session 1923-1924, R. Grant & Son, Edinburgh, Scotland, p. 1-252.

61. (S) Murray, J., and Renard, A. F., 1891, Report on deep-sea deposits based on the specimens collected in the years 1872 to 1876 in Report on the scientific results of the voyage of HMS CHALLENGER during the years 1873-1876: v. 2, Longmans and Co., London, England, 523 p.

62. (S) Naval Oceanographic Office, 1962a, Bottom sediment summary sheets SAN PABLO (AGS-30) June 1962: U.S. Naval Oceanographic Office, Geological Lab. Item 166 (unpublished).

63. (S)_____, 1962b, Oceanographic survey operations in West Indies waters, Spring 1962: U.S. Naval Oceanographic Office, Informal Manuscript Rept., n. 0-27-63, 99 p. (unpublished).

64. (S)_____, 1963a, Laboratory analyses of sediment samples AUTEC-TOTO: Projects 0-156, U.S. Naval Oceanographic Office, Geological Lab. Items 136, 141 (unpublished).

65. (WA)___, 1963b, Oceanographic atlas of the North Atlantic Ocean, section IV, sea and swell: U.S. Naval Oceanographic Office, H.O. Pub. 700, 227 p.

66. (S)_____, 1964, Summary of engineering properties of S.E. Hatteras Abyssal plain Area B: U.S. Naval Oceanographic Office, Geological Lab. Item n. 218 (unpublished).

67. (S)_____, 1965a, A summary of engineering properties, size and composition of cores from Exuma Sound, May 1965: U.S. Naval Oceanographic Office, Geological Lab. Item 262 (unpublished).

68. (S)_____, 1965b, A summary of engineering properties, size and composition of cores from submarine soil mechanics (Project SUBSOME): U.S. Naval Oceanographic Office, Geological Lab. Items n. 253, 254, 264 (unpublished).

69. (S)_____, 1965c, A summary of sediment size and composition analyses of a core from western Yucatan Basin, May 1965: Geological Lab. Item n. 255 (unpublished).

70. *(S)_____, 1965d, A summary of sediment size and composition analyses of grab samples from Area* LIMA TANNER 1965. *U.S. Naval Oceanographic Office (unpublished).*

71. (C)_____, 1965e, Oceanographic atlas of the north Atlantic Ocean, section I, tides and currents: U.S. Naval Oceanographic Office, H.O. Pub. 700, 75 p.

72. (S)_____, 1965f, Oceanographic atlas of the north Atlantic Ocean, section V, Marine Geology: U.S. Naval Oceanographic Office, H.O. Pub. 700, 71 p.

73. (S)_____, 1965g, Sediment analysis sheets. Operation NAVADO IV HMS SNELLIUS, January-June 1965: U.S. Naval Oceanographic Office (unpublished).

74. (S)_____, 1967a, A summary of sound velocities, engineering properties, sediment size and composition analyses of cores and grabs for ASW/USW, April 1967 (USS LYNCH): U.S. Naval Oceanographic Office, Geological Lab. Item 309 (unpublished).

75. (S)_____, 1967b, A summary of sound velocities, engineering properties, sediment size and composition of cores for ASW/USW, 1968 Gulf of Mexico (USS SAN PABLO): U.S. Naval Oceanographic Office, Geological Lab. Items 336 and 332 (unpublished).

76. (S)_____, 1967c, Environmental atlas of the Tongue of the Ocean Bahamas: U.S. Naval Oceanographic Office, Special Publication, SP-94, 82 p.

77. (S)_____, 1968a, A summary of sediment size, composition and specific gravity of grabs from USNS LYNCH cruise 37608, Jan 1968: U.S. Naval Oceanographic Office, Sedimentology Lab. Item 327 (unpublished).

78. (S)_____, 1968b, KANE 9: Global Ocean Floor Analysis and Research Data Series, v. 1, U.S. Government Printing Office, Washington, D. C., 973 p.

79. (SV)____, 1969, Sound velocimeter profiles and Nansen casts from USN KANE cruise Sept-Dec 1969 in North Atlantic Task Area 18: U.S. Naval Oceanographic Office (unpublished data).

80. (SV)____, 1970, Oceanographic station Nansen cast data processed as of January 1970: U.S. Naval Oceanographic Office, National Oceanographic Data Center (unpublished tabulations).

81. (S) Navy Hydrographic Office, 1958a, Bottom sediments, North Atlantic Ocean and adjacent seas 1949-53: U.S. Navy Hydrographic Office, H.O. TR-36, 246 p. (unpublished).

82. (S)_____, 1958b, Bottom sediment analyses. Supplement No. 1 to oceanographic observations U.S. F & W.S. M/V THEODORE N. GILL cruises I-IX 1953-54: U.S. Navy Hydrographic Office, H O. Misc. 15610, 119 p.

83. (S)_____, , Analyses of sediment samples taken along submarine cable routes by Bell Telephone Laboratories and analyzed by the Navy Hydrographic Office: U.S. Navy Hydrographic Office (unpublished).

84. (S) National Science Foundation, 1963, Biological collecting stations R/V ANTON BRUUN cruise 4-B: World Data Center "A" 139.1 E5 (unpublished).

85. (SV) Nowlin, W. D., and McLellan, H. J., 1967, A characterization of the Gulf of Mexico waters during winter: Jour. Marine Research, v. 25, n. 1, p. 29-59.

86. (S) Ostericher, C., 1967, Oceanographic cruise summary Atlantic Fleet Tactical Underwater Range, southeast Puerto Rico—1967: U.S. Naval Oceanographic Office, Informal Rept., IR n. 67-76, 44 p. (unpublished).

87. (C) Parr, A. E., 1937, On the longitudinal variations in the dynamic elevation of the surface of the Caribbean Current: Bull. Bingham Oceanographic Collection, v. 6, pt. 2, New Haven, Conn.

88. (B) Perry, R. L., 1971, Bathymetric chart around Puerto Rico: National Ocean Survey (unpublished).

89. (S) Peterson, M. N., McLerran, A. R., Gealy, E. L., and Davies, T. A., 1969, Voyage of discovery, the GLOMAR CHALLENGER completes Atlantic track: Ocean Industry, v. 4, n. 5, p. 55-67.

90. (S) Piggot, C. S., and Urry, W. D., 1942, Radioactivity of ocean sediments, IV, The radium content of sediments of the Cayman Trough: Am. Jour. Science, v. 240, n. 1, p. 1-12.

91. (SV) Piip, A. T., 1966, Precision sound velocity profiles in the ocean, v. 1, The sound channel in the Bermuda-Barbados region (November-December 1963): Lamont Geol. Observ. Tech. Rept., n. 3 (CU-3-66).

92. (SV)____, 1967, Precision sound velocity profiles in the ocean, v. II, The sound channel in the Bermuda-Barbados region (April-July 1964): Lamont Geol. Observ. Tech. Rept., n. 4 (CU-4-67).

93. (SV)____, 1970, Precision sound velocity profiles in the ocean, v. VI, sound speeds and temperatures in and near the deep passages of the eastern Caribbean (November 1966-July 1967): Lamont-Doherty Geol. Observ. Tech. Rept. n. 1 (CU-1-70) (contract N-00014-67-A-018-0020).

94. (S) Riedel, W. R., 1959, Siliceous organic remains in pelagic sediments, in Silica in sediments: Pub. Soc. Econ. Paleontologists and Mineralogists, p. 80-91.

95. (S) Rosholt, J. N., Emiliani, C., Geiss, J., Koczy, F. F., and

Wangersky, P. J., 1961, Absolute dating of deep-sea cores by the PA 231/TH 230 method: Jour. Geology, v. 69, n. 2, p. 162-185.

96. (S) Rusnak, G. A., 1964, Modern turbidites-terrigenous abyssal plains versus bioclastic basin: Papers in Marine Geology, p. 23, Macmillan, N. York.

97. (S) Schott, W., and Zobel, B., 1966a, Stratigraphy of deep-sea sediments in the Caribbean: Results of the Caribbean Sea Expedition "CARIB 1960" of the Marine Laboratory, Miami, Florida.

98. (SV) Schroeder, E., Stommel, H., Menzel, D., and Sutcliffe, W., Jr., 1959, Climatic stability of eighteen degree water at Bermuda: Jour Geophys. Research, v. 64, n. 3, p. 363-366.

99. (C) Stalcup, M., Metcalfe, G., and Zemanovic, M., 1971, Current measurements in the Lesser Antilles: Woods Hole Oceanographic Institution, ref. n. 71-51, 14 p., 63 tables and figs.

100. (SV) Starr, R. B., 1970, An oceanographic investigation adjacent to Cay Sal Bank, Bahama Islands: ESSA Tech. Rept. ERL 167-AOML 2.

101. (S) Stetson, H. C., and Trask, P. D., 1933, Part I. The Continental terrace of the western Gulf of Mexico. Its surface sediments, origin and development. Part II. Chemical studies of sediments of the Western Gulf of Mexico: Papers in Physical Oceanography and Meteorology, Massachusetts Institute of Technology and Woods Hole Oceanographic Institution, v. XII, n. 4, p. 3-119.

102. (S) Stewart, H. B., 1360, Oceanographic cruise report USC & GSS EXPLORER. Seattle Wash. to Norfolk, Virginia, 2 Feb-27 Apr 1960: Coast and Geodetic Survey, Government Printing Office, Wash. D. C., p. 100-120.

103. (S) Stewart, H. B., Raff, A. D., and Jones, E. L., 1961, Explorer Bank-a new discovery in the Caribbean: Geological Soc. Am. Bull., v. 72, n. 8, p. 1271-1274.

104. (S) Stiles, N. T., 1967, Mass property relationships of sediments from the Hatteras Abyssal Plain: U.S. Naval Oceanographic Office, Informal Manuscript, IM n. 67-8 (unpublished).

105. (SV) Sturges, W., 1965, Water characteristics of the Caribbean Sea: Jour. Marine Research, v. 23, n. 2, p. 147-161.

106. (SV)____, 1970, Observations of deep-water renewal in the Caribbean Sea, Jour. Geophys. Research, v. 75, n. 36, p. 7602-7610.

107. (SV) Sverdrup, H., Johnson, M. W., and Fleming, R. H., 1942, The oceans, their physics, chemistry, and general biology: Englewood Cliffs, Prentice Hall, 1087 p.

108. (SV) Texas Instruments Inc., 1969, Marine Geophysical Survey Program 1965-1967, North Atlantic Ocean, Norwegian Sea and Mediterranean Sea—data validation cruise, Alpine Areas 1 and 2.

109. (S) Thorp, E. M., 1931, Description of deep-sea bottom samples from the western North Atlantic and the Caribbean Sea: Scripps Institution of Oceanography, Bull., Tech. Series, v. 3, n. 1. p. 1-31.

110. (B) Uchupi, E., and Emery, K. O., 1968, Structure of the continental margin off gulf coast of United States: Am. Assoc. Petroleum Geologists Bull., v. 52, n. 7, p. 1162-1193.

111. (BR) Uchupi, E., Milliman, J. D., Luyendyk. B. P., Bowin, C. O., and Emery, K. O., 1971, Structure and origin of southeastern Bahamas: Am. Assoc. Petroleum Geologists Bull., v. 55, n. 5, p. 687-704.

112. (S) Underwood, J. W., 1967, Oceanographic Cruise Salvops Vieques, USS HOIST: U.S. Naval Oceanographic Office, Informal Rept., n. IR 67-16 (unpublished).

113. (S) USSR Institute of Oceanology, 1961, Bottom sediment table third cruise SEDOV, Atlantic Ocean: U.S.S.R. Akad. Nauk, Institut Okeanologii, World Data Center "A" 137.5 D3 (unpublished).

114. (S)____, 1962, Bottom sediment tables fourth cruise SEDOV, Atlantic Ocean: U.S.S.R. Akad. Nauk, Institut Okeanologii, World Data Center "A" 137.5 D4 (unpublished).

115. (Wa) (Wi) U. S. Weather Bureau, , Wind, sea, and swell data tabulated from H1-9 current report and from marine decks 110, 115, 192, 193, 194, 195, 196, 197 and 281 (unpublished).

116. (S) Wangersky, P. J., 1962, Sedimentation in three carbonate cores: Jour. Geology, v. 70, n. 3, p. 364-374.

117. (S) Wangersky, P. J., and Hutchinson, G. E., 1958, Manganese deposition and deep water movements in the Caribbean: Nature, v. 181, n. 4602, p. 108-109.

118. (SV) Wennekens, M. P., 1959, Water mass properties of the Straits of Florida and related waters: Bull. Marine Science Gulf and Caribbean, v. 9, n. 1, p. 1-52.

119. (SV) Wilson, W. D., 1960, Equation for the speed of sound in sea water: Jour. Acoust. Soc. Am., v. 32, n. 10, p. 1357.

120. (SV) Woods Hole Oceanographic Institution, 1962, Sound velocimeter profiles from R/V ATLANTIS, cruise 282 July-Aug 1962: (unpublished data).

121. (SV)____, 1964, Sound velocimeter profiles from R/V ATLANTIS II, cruise 11, June-July 1964: (unpublished data).

122. (SV)____, 1965, Sound velocimeter profiles from R/V CHAIN, cruise 47 Apr-May 1965: (unpublished data).

123. (S)_____, 1966, Summary of stations 2334-2399 taken by R/V GOSNOLD cruise 74, 16-30 August 1965: (unpublished).

124. (SV) Worthington, L. V., 1955, A new theory of Caribbean bottom-water formation: Deep-Sea Research, v. 3, p. 82-87.

125. (SV)____, 1959, The 18° water in the Sargasso Sea: Deep-Sea Research, v. 5, p. 297-305.

126. (SV)____, 1966, Recent oceanographic measurements in the Sargasso Sea: Deep-Sea Research, v. 13, p. 731-739.

127. (S) Worzel, J. L., Bryant, W. et al., 1970, Deep sea drilling project Leg 10: Geotimes, v. 15, n. 6, p. 11-13.

128. (BR) Worzel, J. L., Leyden, R., and Ewing, M., 1968, Newly discovered diapirs in the Gulf of Mexico: Am. Assoc. Petroleum Geologists Bull., v. 52, n. 7, p. 1194-1203.

129. (SV) Wust, G., 1936, Schichtung und zirculation des Atlantishchen Ozeans, die stratosphere, wissenschafliche ergebnisse der Deutsche Atlantischen expedition auf dem METEOR 1925-27: v. 6, n. 1, Walter de Gruyter, Berlin, 288 p.

130. (SV)____, 1964, Stratification and circulation in the Antillean-Caribbean Basins, part I, spreading and mixing of water types, with an oceanographic atlas: Columbia Univ. Press, New York, 201 p.

131, 132, 133 See appendix to Volume I.

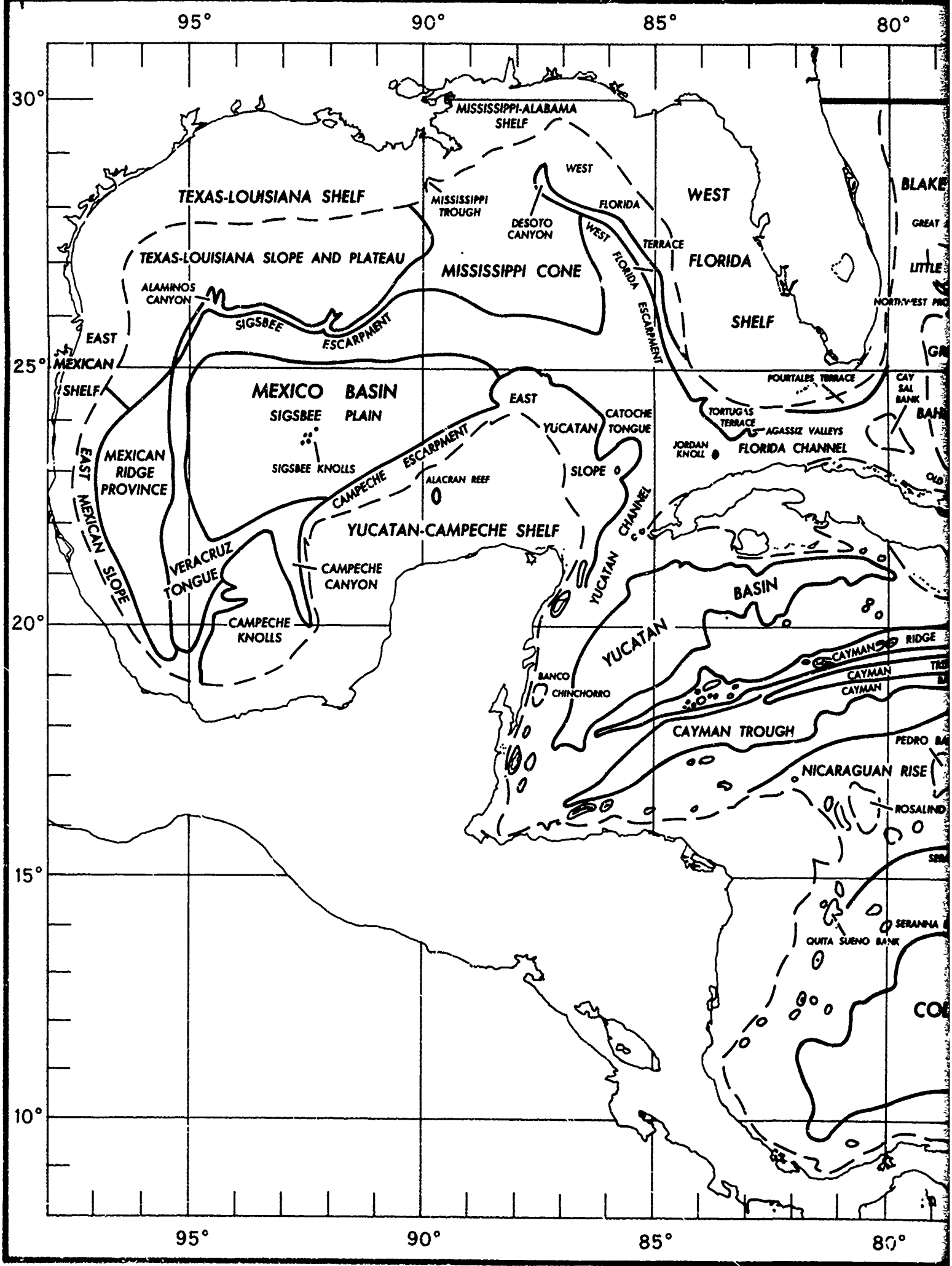
95°
90°
85°
80°
30°
25°
20°
15°
10°
MISSISSIPPI-ALABAMA SHELF
TEXAS-LOUISIANA SHELF
TEXAS-LOUISIANA SLOPE AND PLATEAU
MISSISSIPPI TROUGH
DESOTO CANYON
WEST FLORIDA TERRACE
WEST FLORIDA ESCARPMENT
MISSISSIPPI CONE
FLORIDA SHELF
BLAKE
GREAT
LITTLE
ALAMINOS CANYON
SIGSBEE ESCARPMENT
EAST MEXICAN SHELF
MEXICO BASIN
SIGSBEE PLAIN
SIGSBEE KNOLLS
MEXICAN RIDGE PROVINCE
EAST MEXICAN SLOPE
CAMPECHE ESCARPMENT
ALACRAN REEF
EAST YUCATAN SLOPE
CATOCHE TONGUE
YUCATAN-CAMPECHE SHELF
YUCATAN CHANNEL
VERACRUZ TONGUE
CAMPECHE CANYON
CAMPECHE KNOLLS
FOURTALES TERRACE
TORTUGAS TERRACE
AGASSIZ VALLEYS
JORDAN KNOLL
FLORIDA CHANNEL
CAY SAL BANK
YUCATAN BASIN
BANCO CHINCHORRO
CAYMAN RIDGE
CAYMAN TROUGH
NICARAGUAN RISE
ROSALIND
SERANILLA
QUITA SUENO BANK

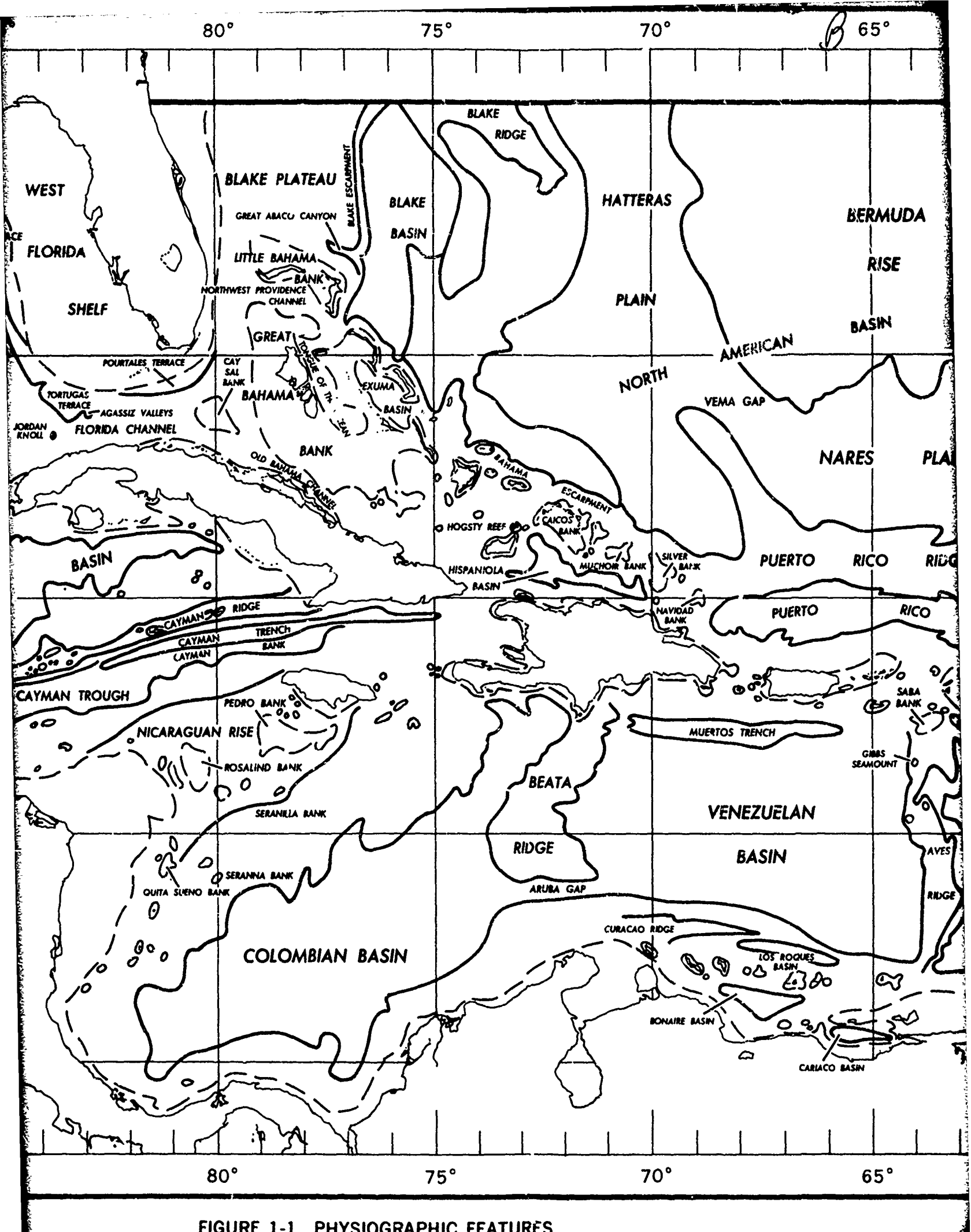

FIGURE 1-1 PHYSIOGRAPHIC FEATURES

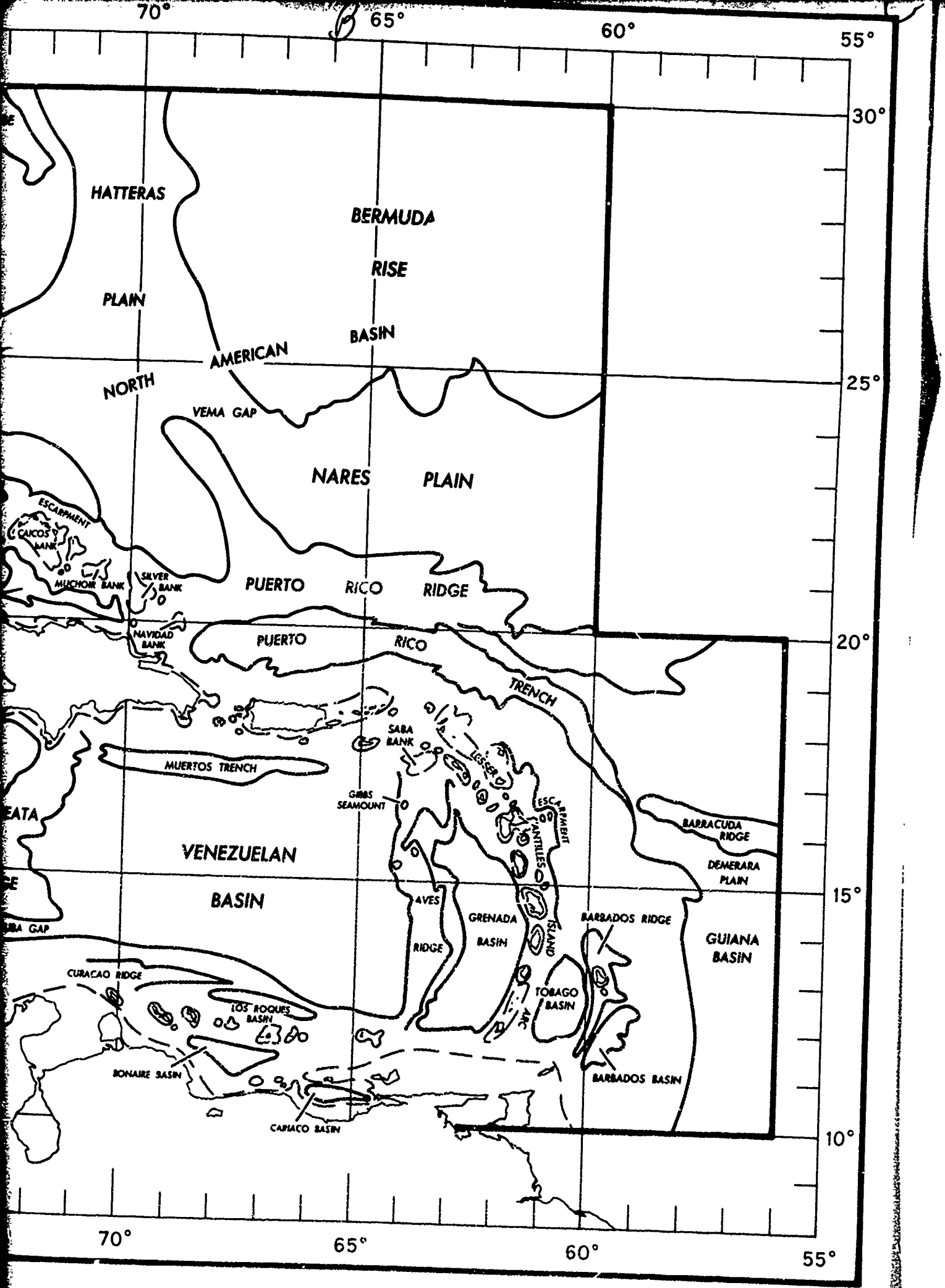
70°
65°
60°
55°
30°
25°
20°
15°
10°
HATTERAS
PLAIN
BERMUDA
RISE
BASIN
AMERICAN
NORTH
VEMA GAP
NARES PLAIN
ESCARPMENT
CAICOS BANK
MUCHOIR BANK
SILVER BANK
PUERTO RICO RIDGE
NAVIDAD BANK
PUERTO RICO TRENCH
SABA BANK
LESSER ANTILLES
MUERTOS TRENCH
GIBBS SEAMOUNT
ESCARPMENT
BARRACUDA RIDGE
DEMERARA PLAIN
VENEZUELAN BASIN
AVES RIDGE
GRENADA BASIN
ISLAND
BARBADOS RIDGE
GUIANA BASIN
CURACAO RIDGE
LOS ROQUES BASIN
TOBAGO BASIN
BONAIRE BASIN
BARBADOS BASIN
CARIACO BASIN

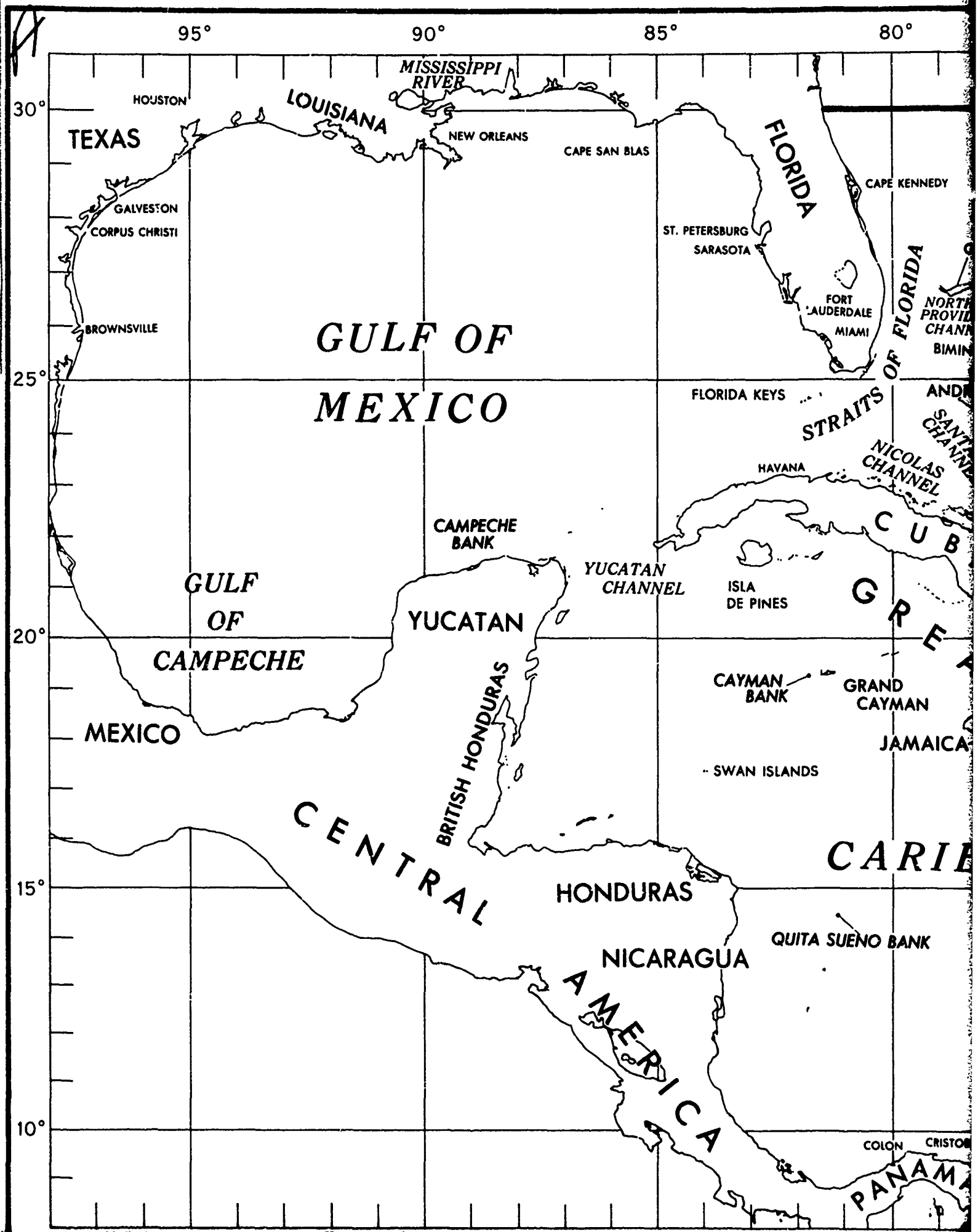
95°
90°
85°
80°
30°
25°
20°
15°
10°
MISSISSIPPI RIVER
HOUSTON
LOUISIANA
TEXAS
NEW ORLEANS
CAPE SAN BLAS
FLORIDA
CAPE KENNEDY
GALVESTON
CORPUS CHRISTI
ST. PETERSBURG
SARASOTA
FORT LAUDERDALE
MIAMI
BROWNSVILLE
GULF OF MEXICO
STRAITS OF FLORIDA
FLORIDA KEYS
HAVANA
NICOLAS CHANNEL
CAMPECHE BANK
YUCATAN CHANNEL
ISLA DE PINES
GULF OF CAMPECHE
YUCATAN
CAYMAN BANK
GRAND CAYMAN
JAMAICA
MEXICO
BRITISH HONDURAS
SWAN ISLANDS
CENTRAL AMERICA
HONDURAS
QUITA SUENO BANK
NICARAGUA
COLON
PANAMA


B
85°
80°
75°
70°
65°
SARGASSO SEA
FLORIDA
BLAS
CAPE KENNEDY
ST. PETERSBURG
SARASOTA
FORT LAUDERDALE
MIAMI
STRAITS OF FLORIDA
GRAND BAHAMA ISLAND
NORTHWEST PROVIDENCE CHANNEL
NORTHEAST PROVIDENCE CHANNEL
BIMINI
BAHAMA ISLANDS
ELEUTHERA
FLORIDA KEYS
ANDROS ISLAND
CAT ISLAND
SAN SALVADOR
SANTAREN CHANNEL
EXUMA SOUND
GREAT EXUMA
RUM CAY
SAMANA CAY
NICOLAS CHANNEL
HAVANA
LONG ISLAND
MAYAGUANA PASSAGE
DIANA BANK
COLUMBUS BANK
BROWN BANK
TURKS AND CAICOS ISLANDS
HOGSTY REEF
GRAND TURK
CUBA
OLD BAHAMA CHANNEL
GREAT INAGUA ISLAND
MOUCHOIR PASSAGE
ISLA DE PINES
GREATER ANTILLES
WINDWARD PASSAGE
MONA PASSAGE
CAYMAN BANK
GRAND CAYMAN
HAITI
DOMINICAN REPUBLIC
RAMEY
SAN JUAN
HISPANIOLA
PUERTO RICO
JAMAICA
KINGSTON
MUERTOS (DOMINICAN) TRENCH
SWAN ISLANDS
ST. CROIX
JUNGFERN PASSAGE
CARIBBEAN SEA
QUITA SUENO BANK
ARUBA
CURACAO
BONAIRE
PT. GALLINAS
LA TORTUGA
COLOMBIA
VENEZUELA
COLON
CRISTOBAL
PANAMA
SOUTH AMERICA
85°
80°
75°
70°
65°

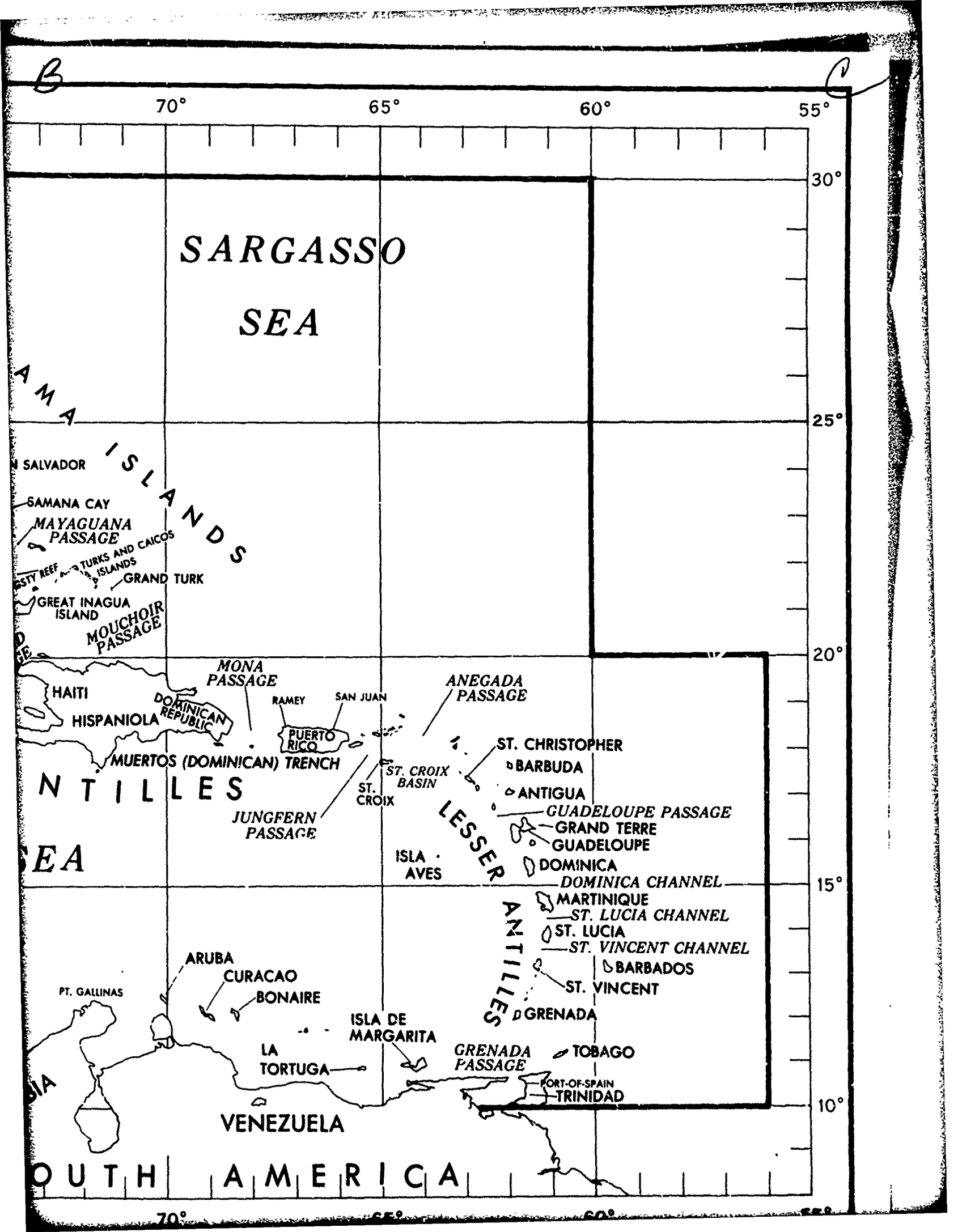
B
C
70°
65°
60°
55°
30°
25°
20°
15°
10°
SARGASSO
SEA
AMA ISLANDS
SALVADOR
SAMANA CAY
MAYAGUANA PASSAGE
TURKS AND CAICOS ISLANDS
GRAND TURK
GREAT INAGUA ISLAND
MOUCHOIR PASSAGE
MONA PASSAGE
HAITI
HISPANIOLA
DOMINICAN REPUBLIC
RAMEY
SAN JUAN
PUERTO RICO
ANEGADA PASSAGE
MUERTOS (DOMINICAN) TRENCH
NTILLES
EA
ST. CROIX BASIN
ST. CROIX
JUNGFERN PASSAGE
ST. CHRISTOPHER
BARBUDA
ANTIGUA
GUADELOUPE PASSAGE
GRAND TERRE
GUADELOUPE
LESSER ANTILLES
ISLA AVES
DOMINICA
DOMINICA CHANNEL
MARTINIQUE
ST. LUCIA CHANNEL
ST. LUCIA
ST. VINCENT CHANNEL
BARBADOS
ST. VINCENT
GRENADA
ARUBA
CURACAO
BONAIRE
PT. GALLINAS
ISLA DE MARGARITA
LA TORTUGA
GRENADA PASSAGE
TOBAGO
PORT-OF-SPAIN
TRINIDAD
VENEZUELA
OUTH AMERICA

Preceding page blank

FIGURE 1-2 GEO

2 GEOGRAPHIC NAMES EXCLUSIVE OF PHYSIOGRAPHIC FEATURES

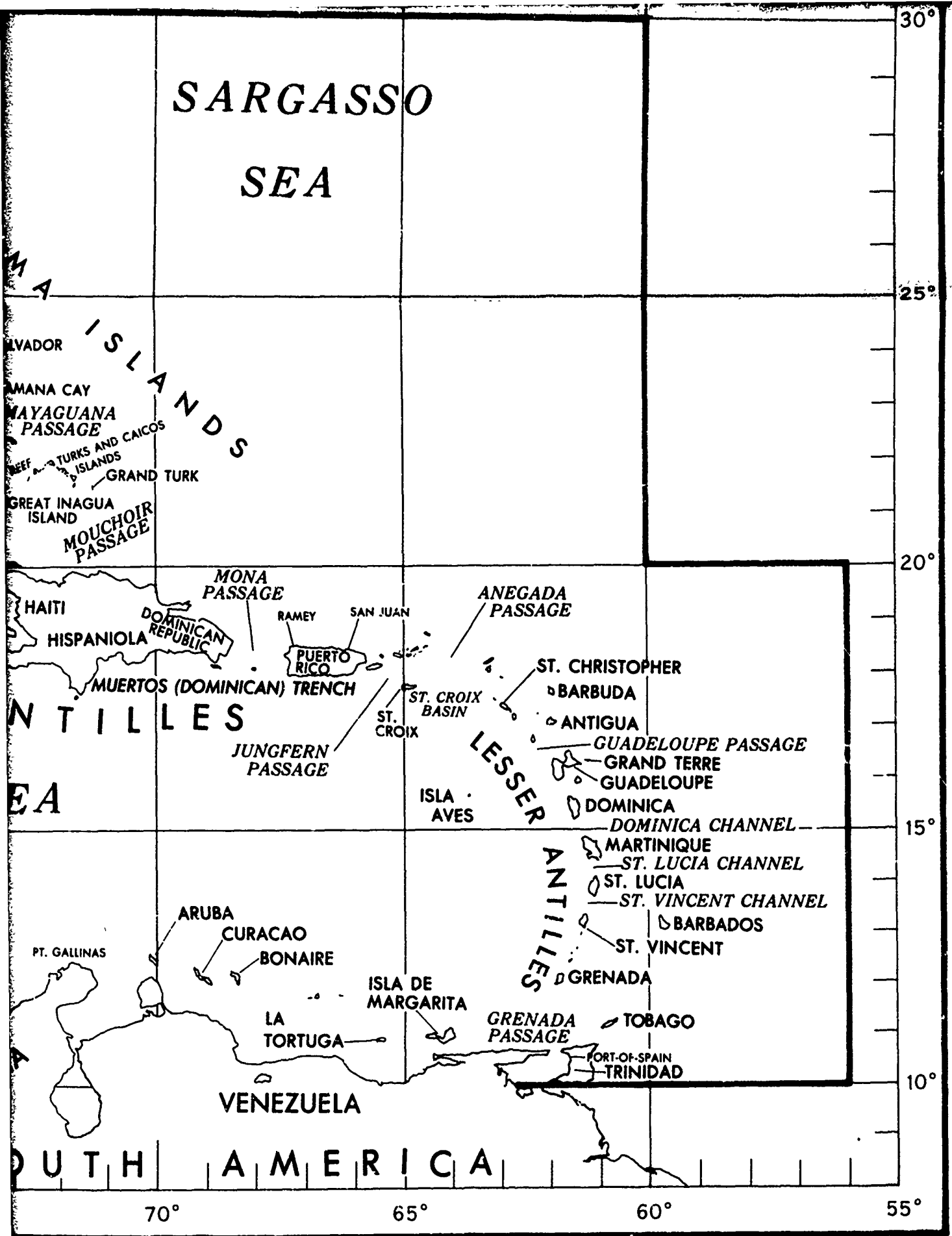

SIOGRAPHIC FEATURES

6

1

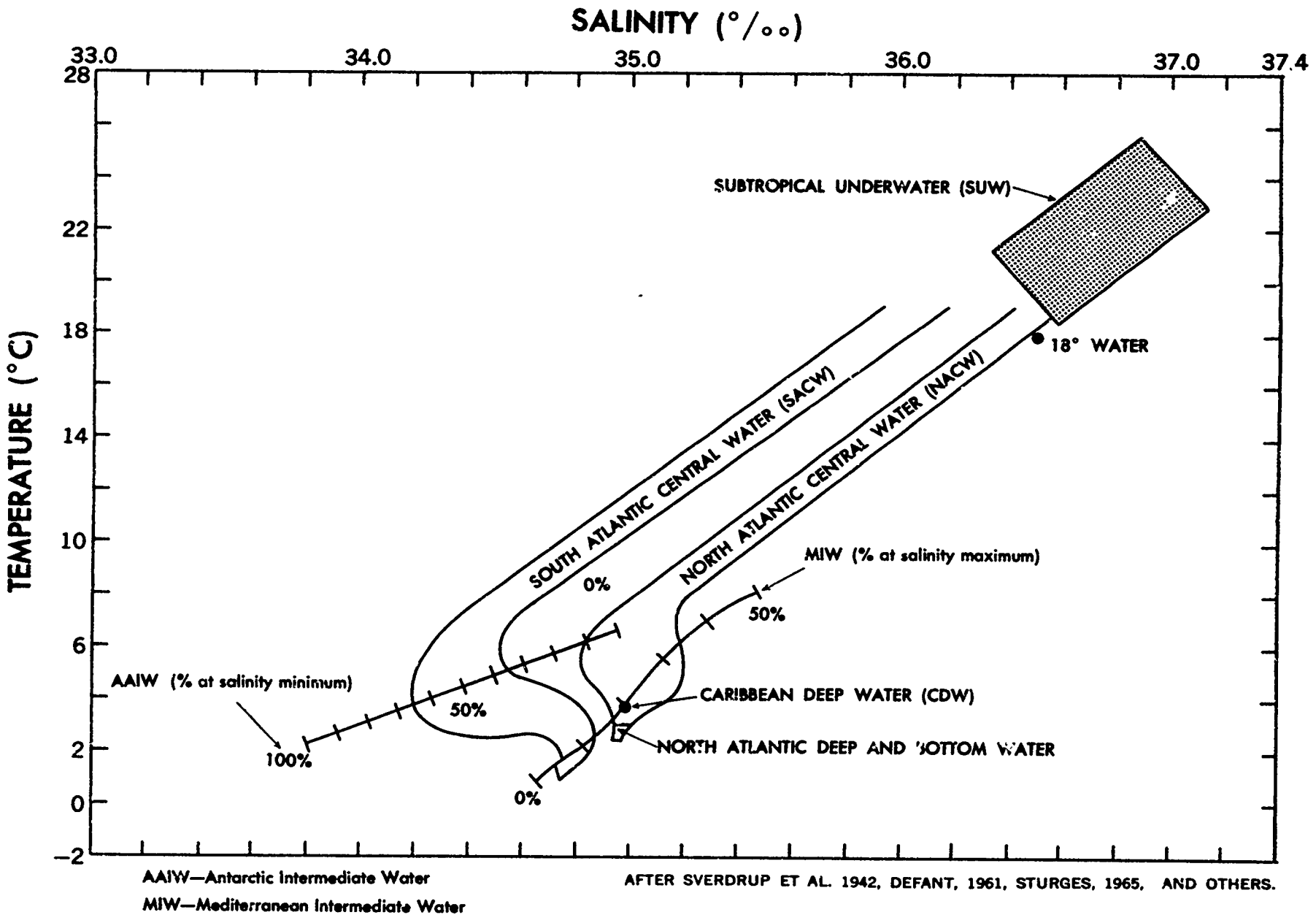

FIGURE 4-1 TEMPERATURE-SALINITY DIAGRAMS OF MAJOR WATER MASSES

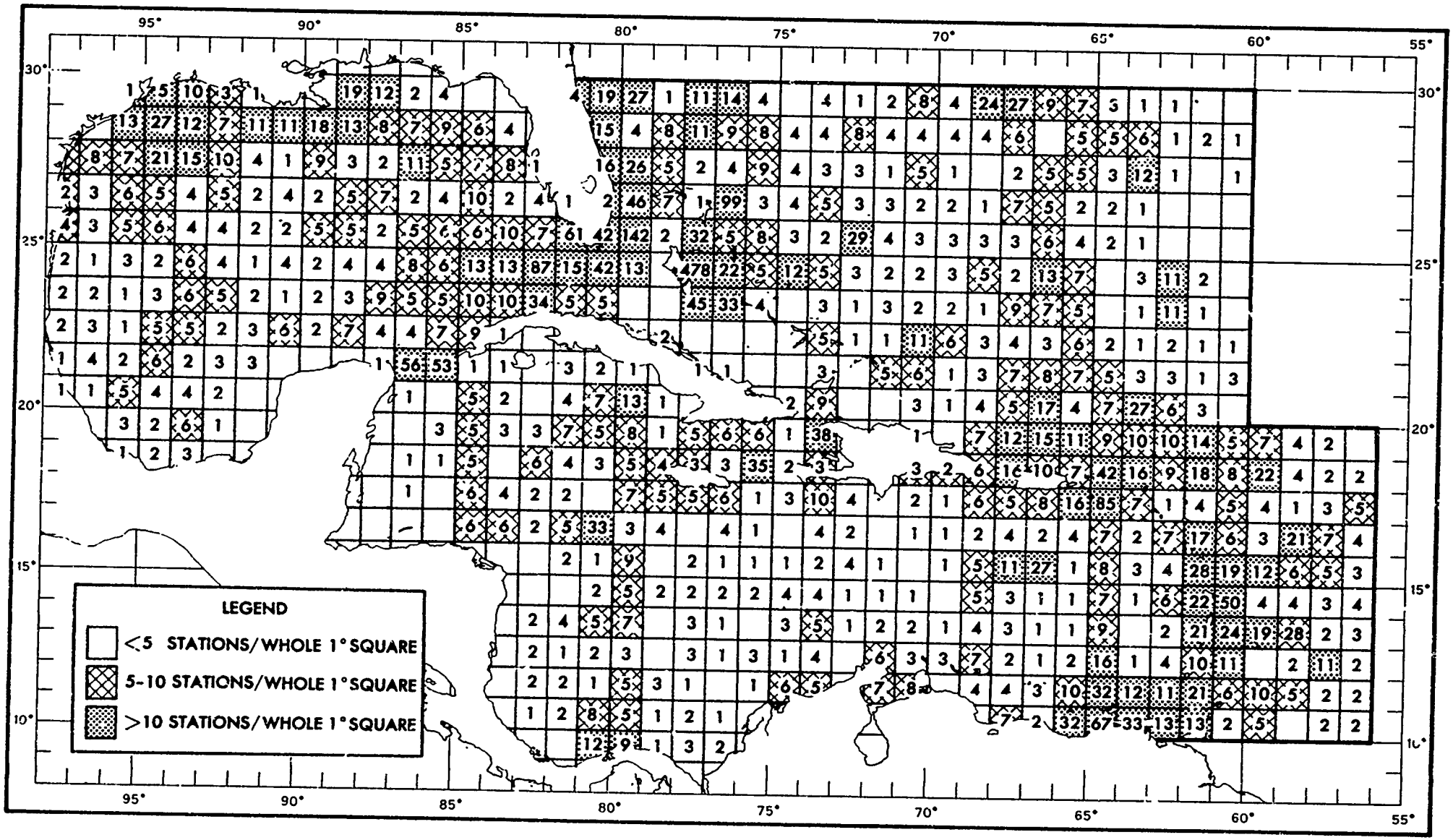

FIGURE 4-2 DISTRIBUTION OF OCEAN STATIONS AND SOUND VELOCIMETER MEASUREMENTS (WINTER, NOVEMBER-APRIL)

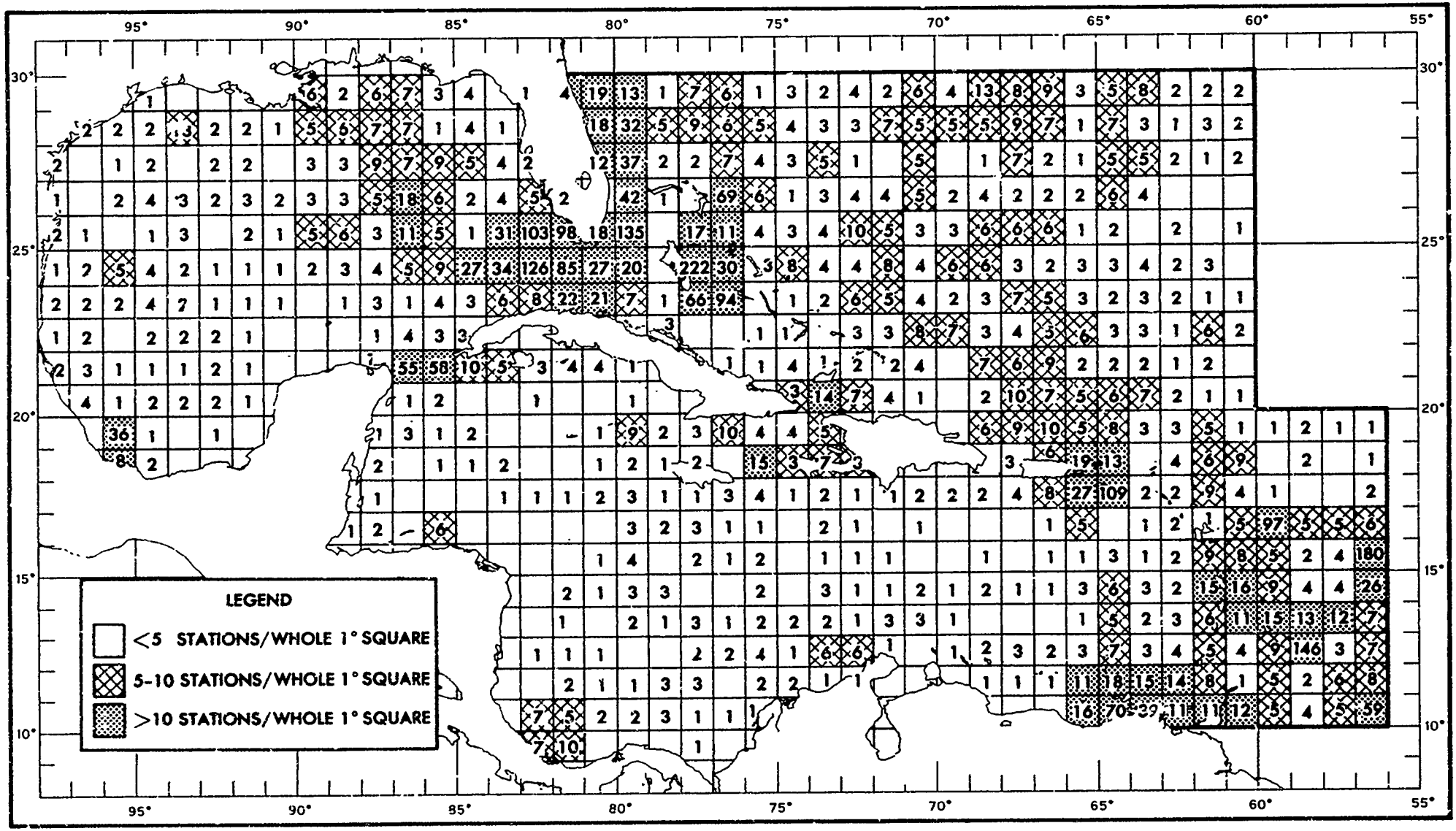

FIGURE 4-3 DISTRIBUTION OF OCEAN STATIONS AND SOUND VELOCIMETER MEASUREMENTS (SUMMER, MAY-OCTOBER)

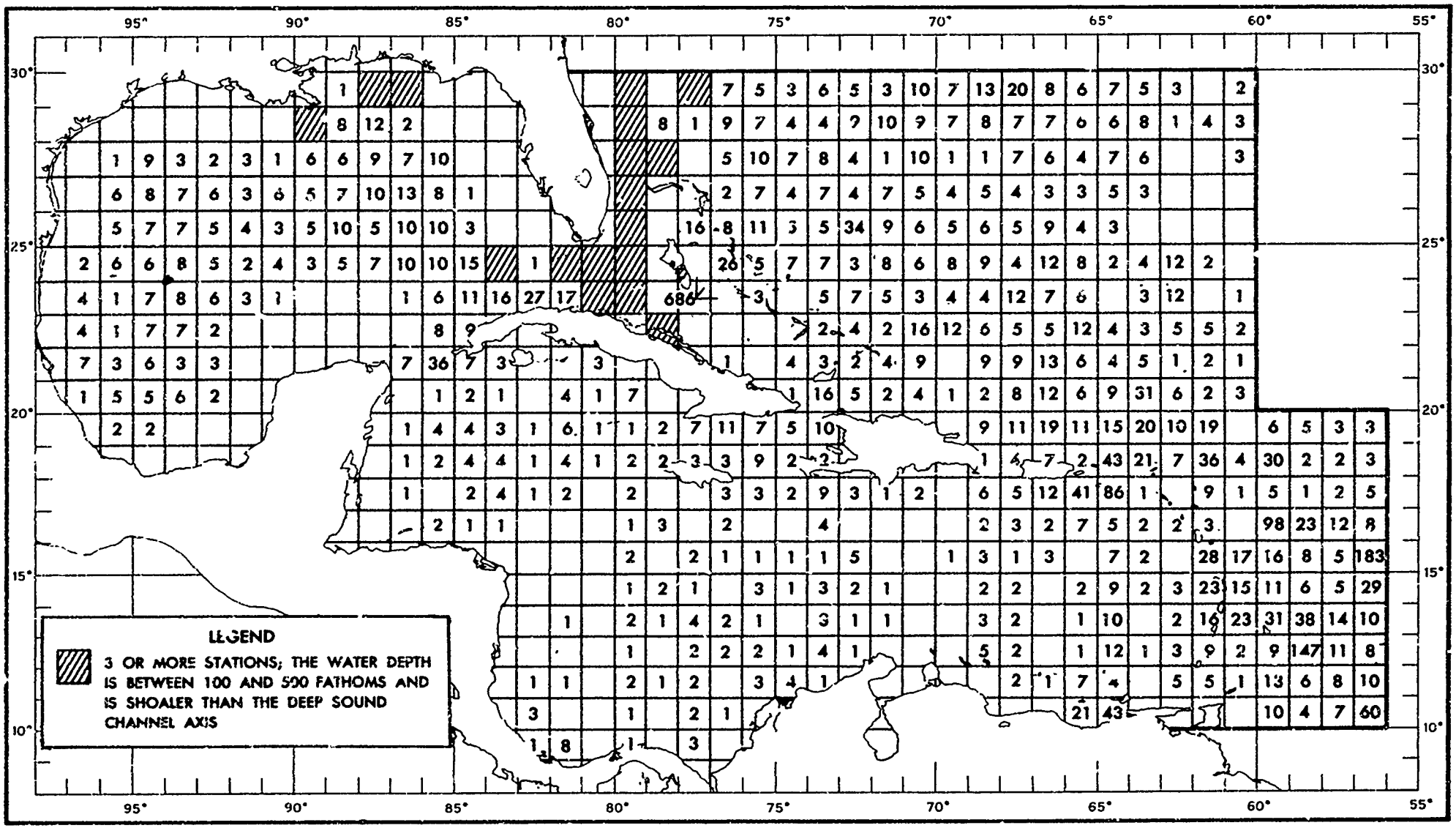

FIGURE 4-4 DISTRIBUTION OF OCEAN STATIONS AND SOUND VELOCIMETER MEASUREMENTS DEEPER THAN AXIAL DEPTH

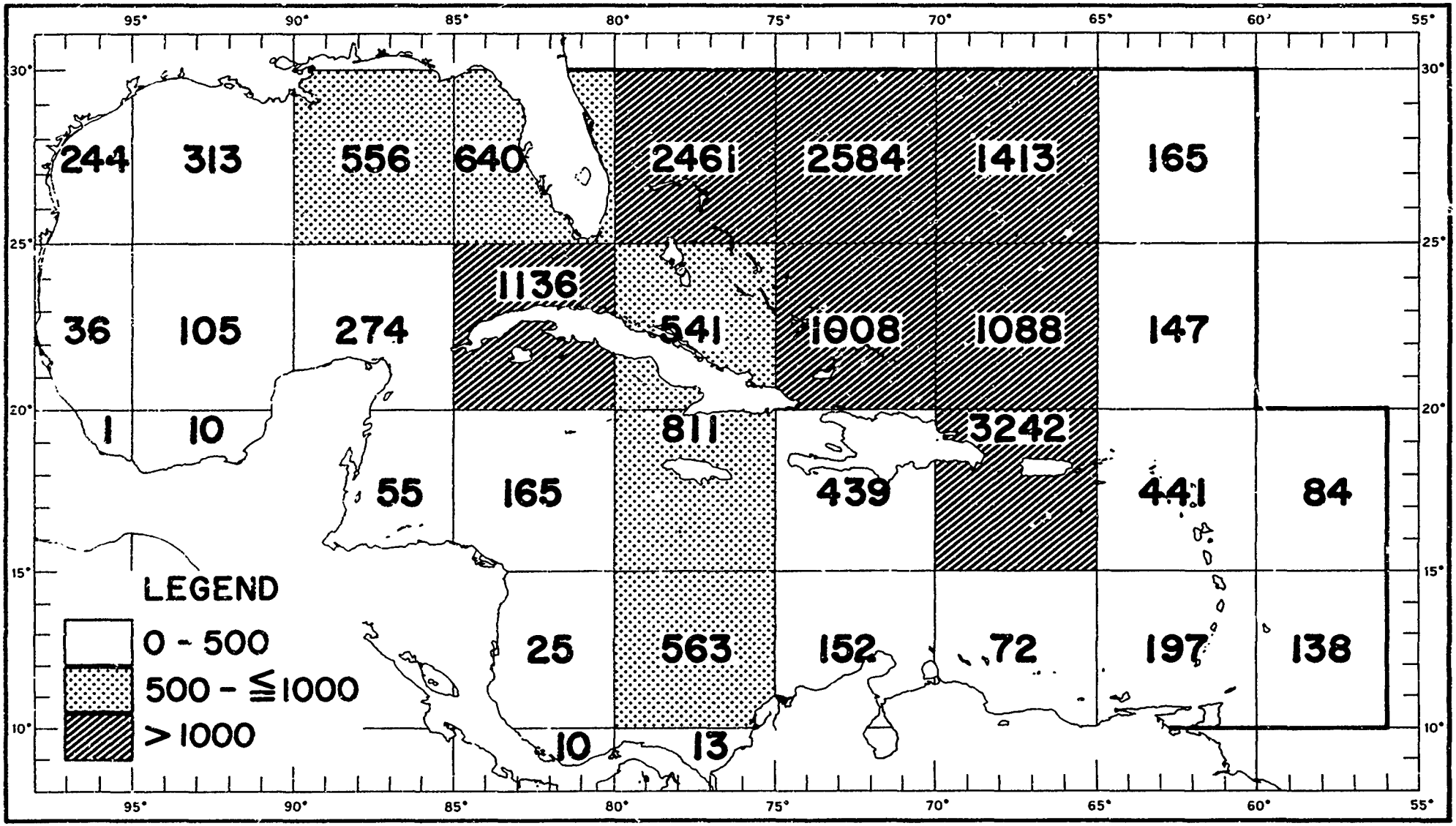

FIGURE 4-5 DISTRIBUTION OF BATHYTHERMOGRAPHS (WINTER)

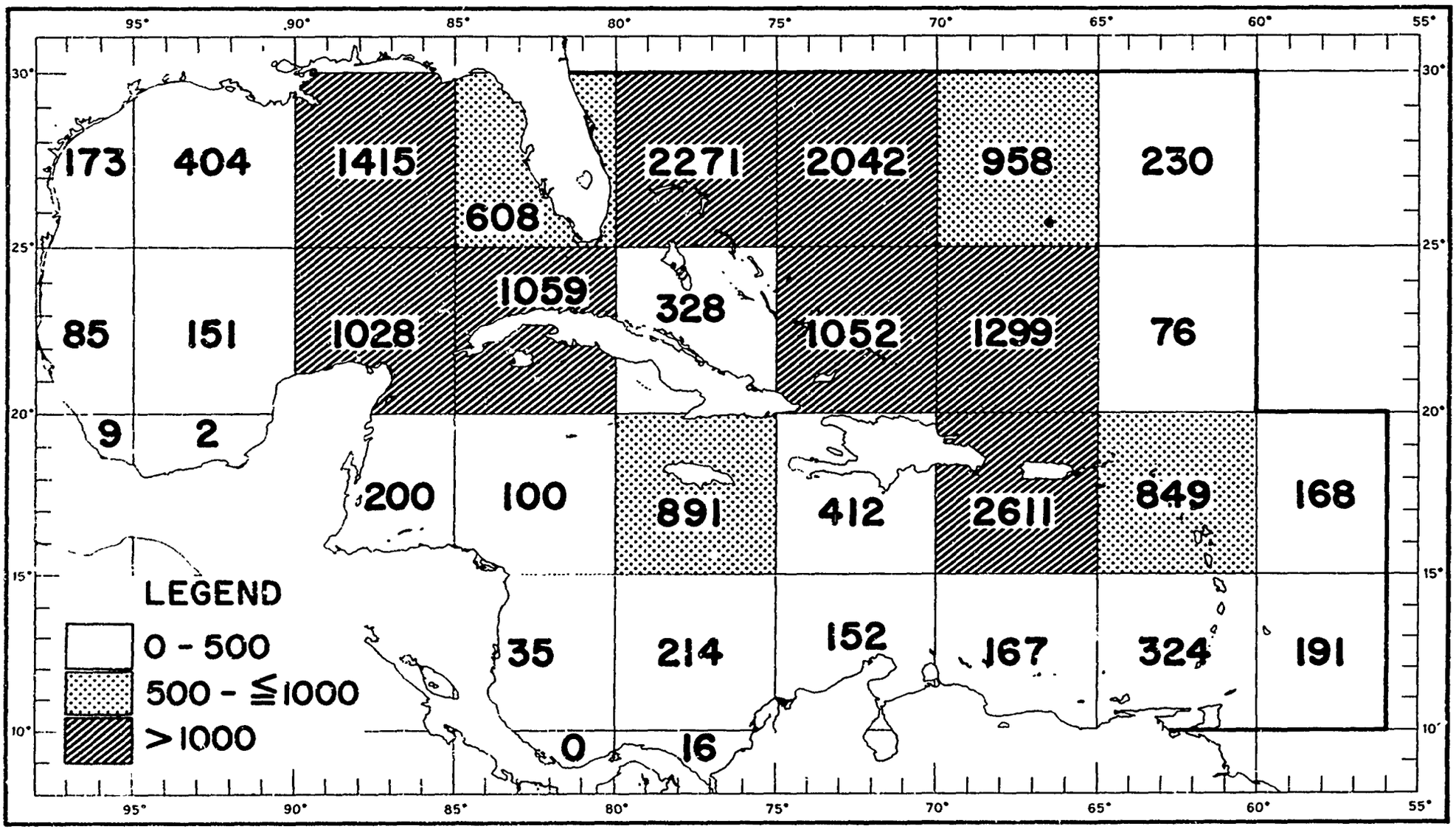

FIGURE 4-6 DISTRIBUTION OF BATHYTHERMOGRAPHS (SUMMER)

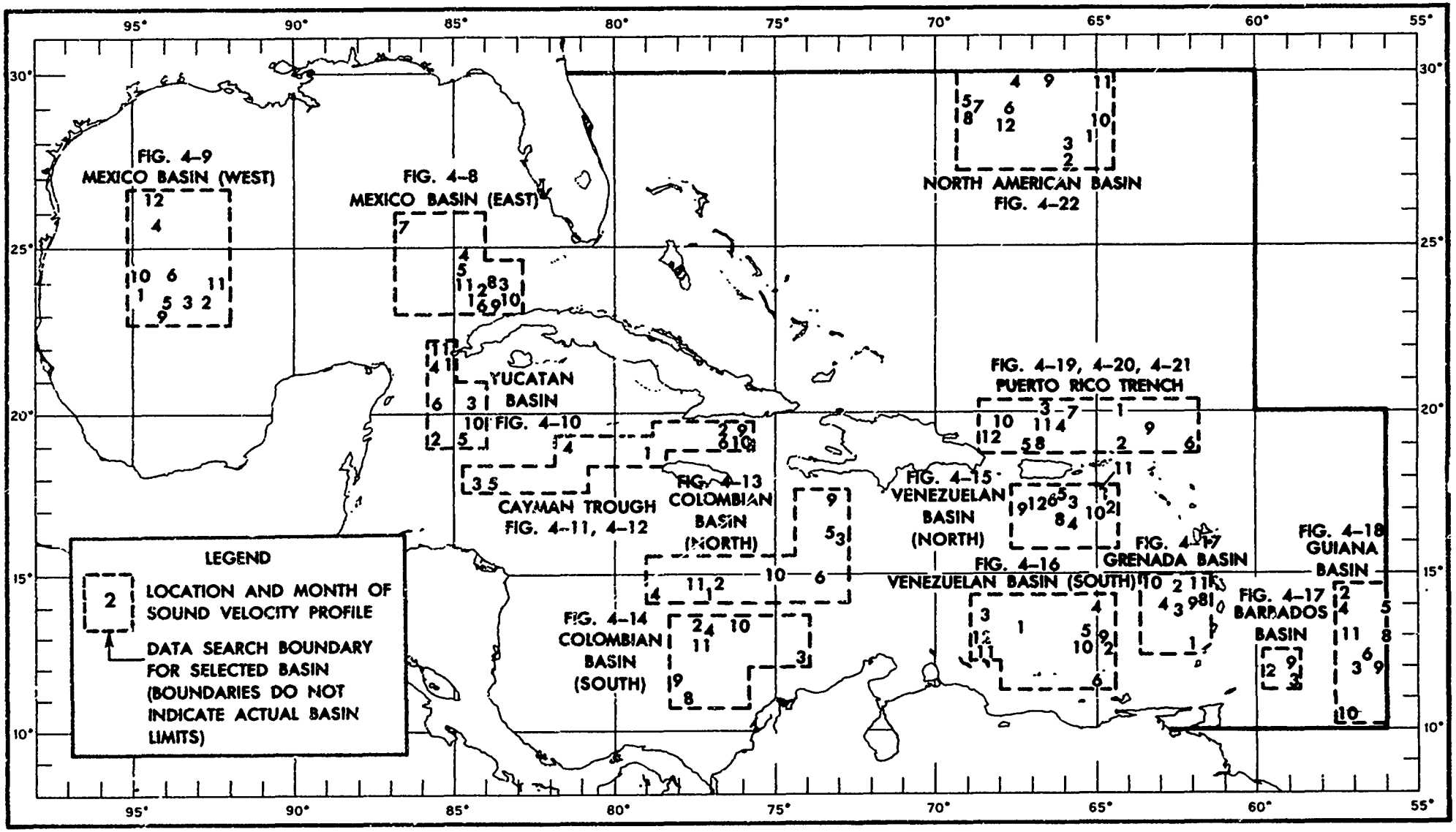

FIGURE 4-7 LOCATIONS OF SOUND VELOCITY PROFILES IN DEEP BASINS AND TRENCHES

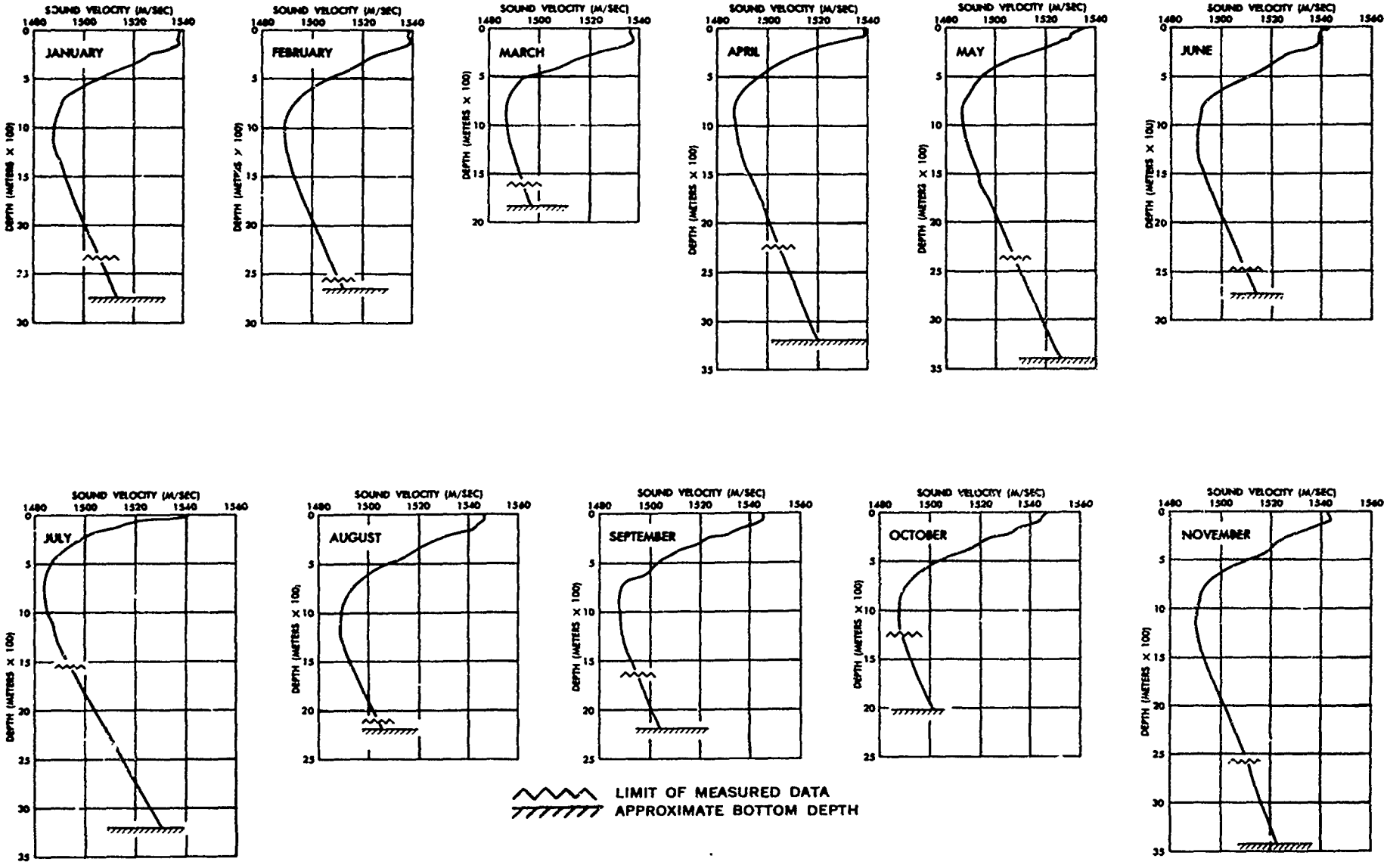

FIGURE 4-8 SOUND VELOCITY PROFILES–EAST MEXICO BASIN

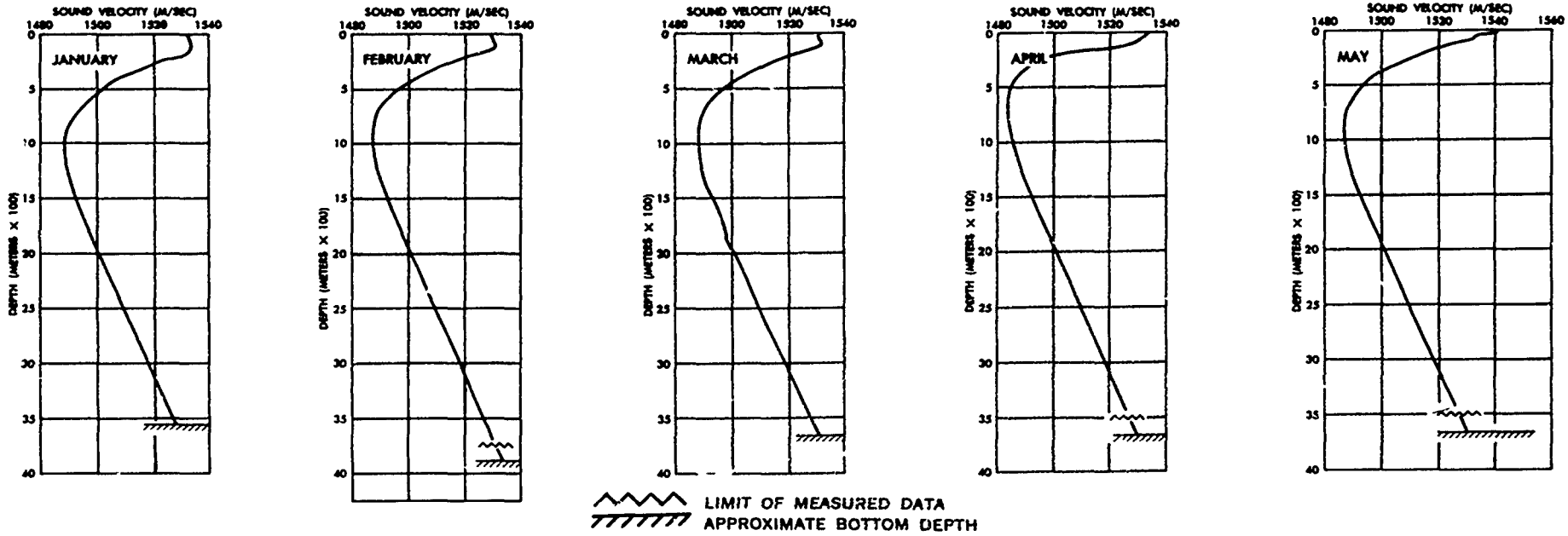

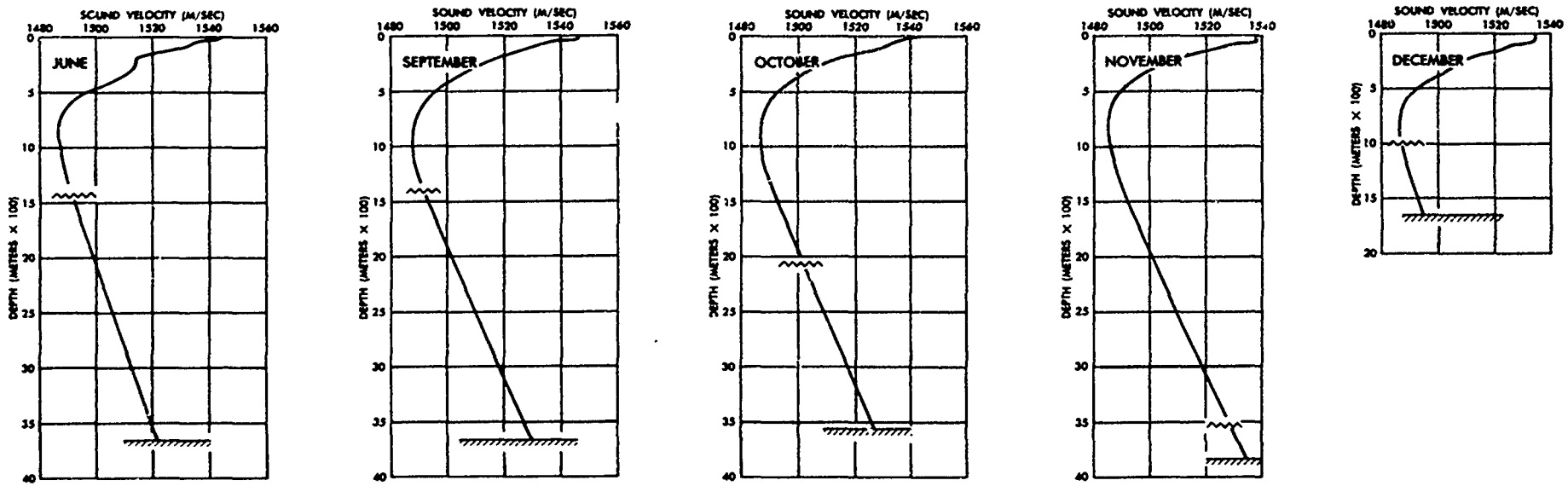

FIGURE 4-9 SOUND VELOCITY PROFILES–WEST MEXICO BASIN

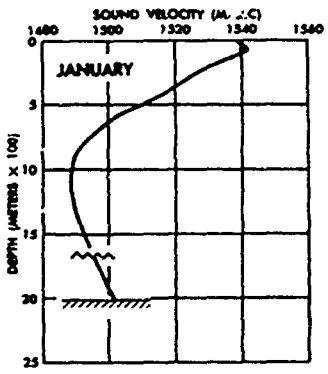

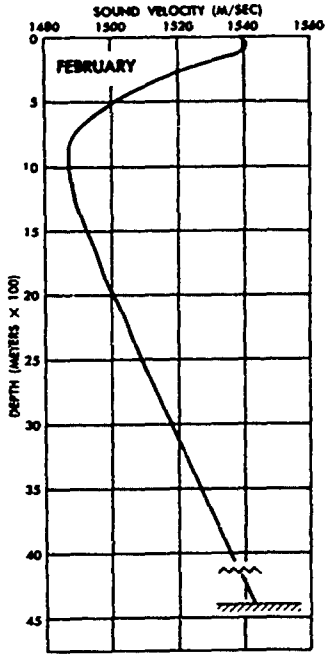

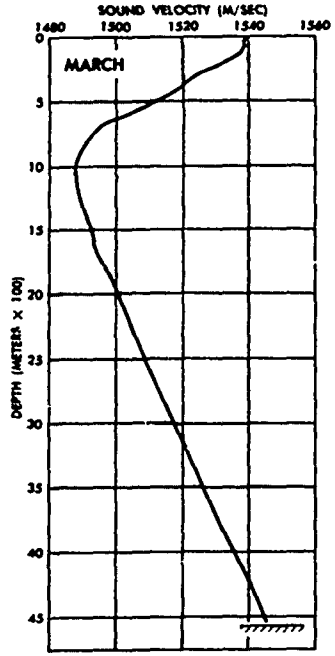

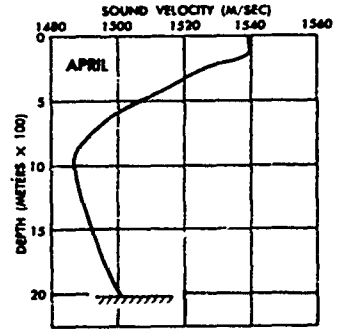

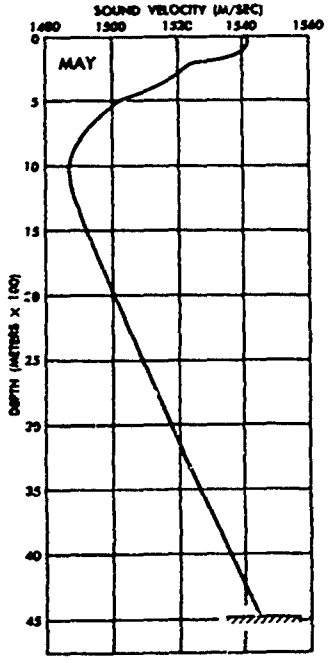

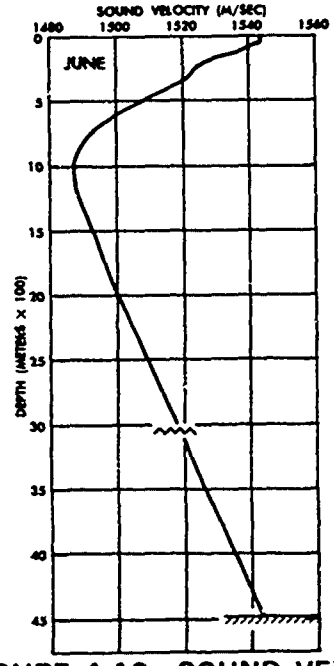

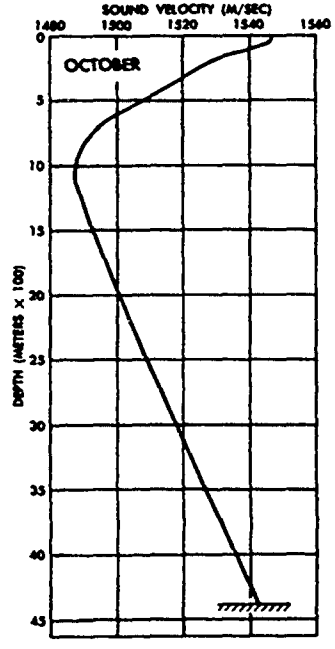

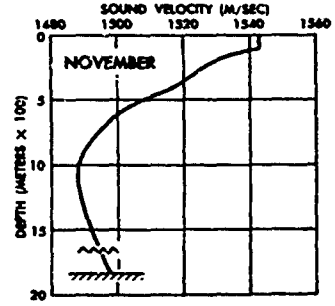

FIGURE 4-10 SOUND VELOCITY PROFILES–YUCATAN BASIN

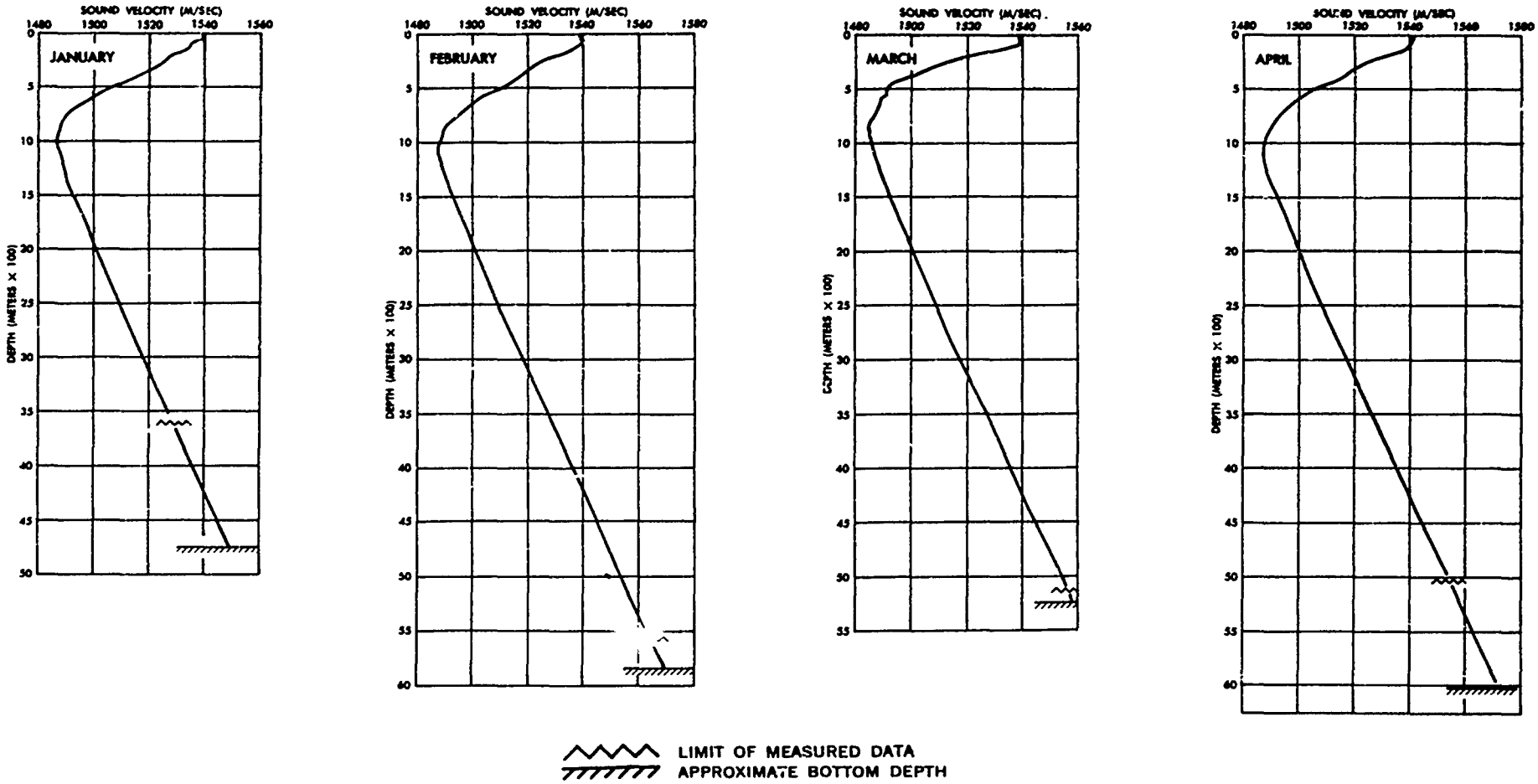

FIGURE 4-11 SOUND VELOCITY PROFILES–CAYMAN TROUGH

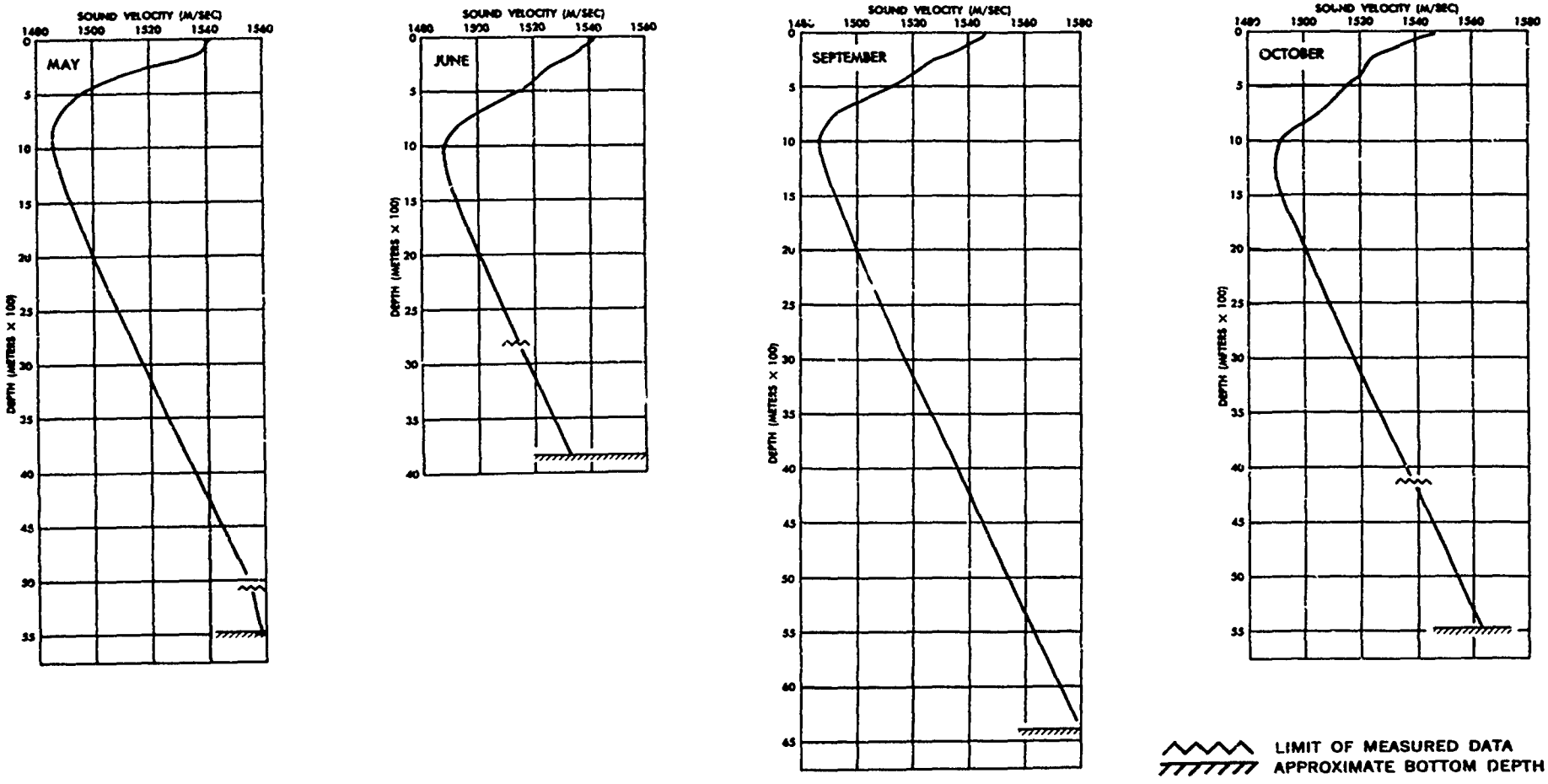

FIGURE 4-12 SOUND VELOCITY PROFILES–CAYMAN TROUGH (CONT.)

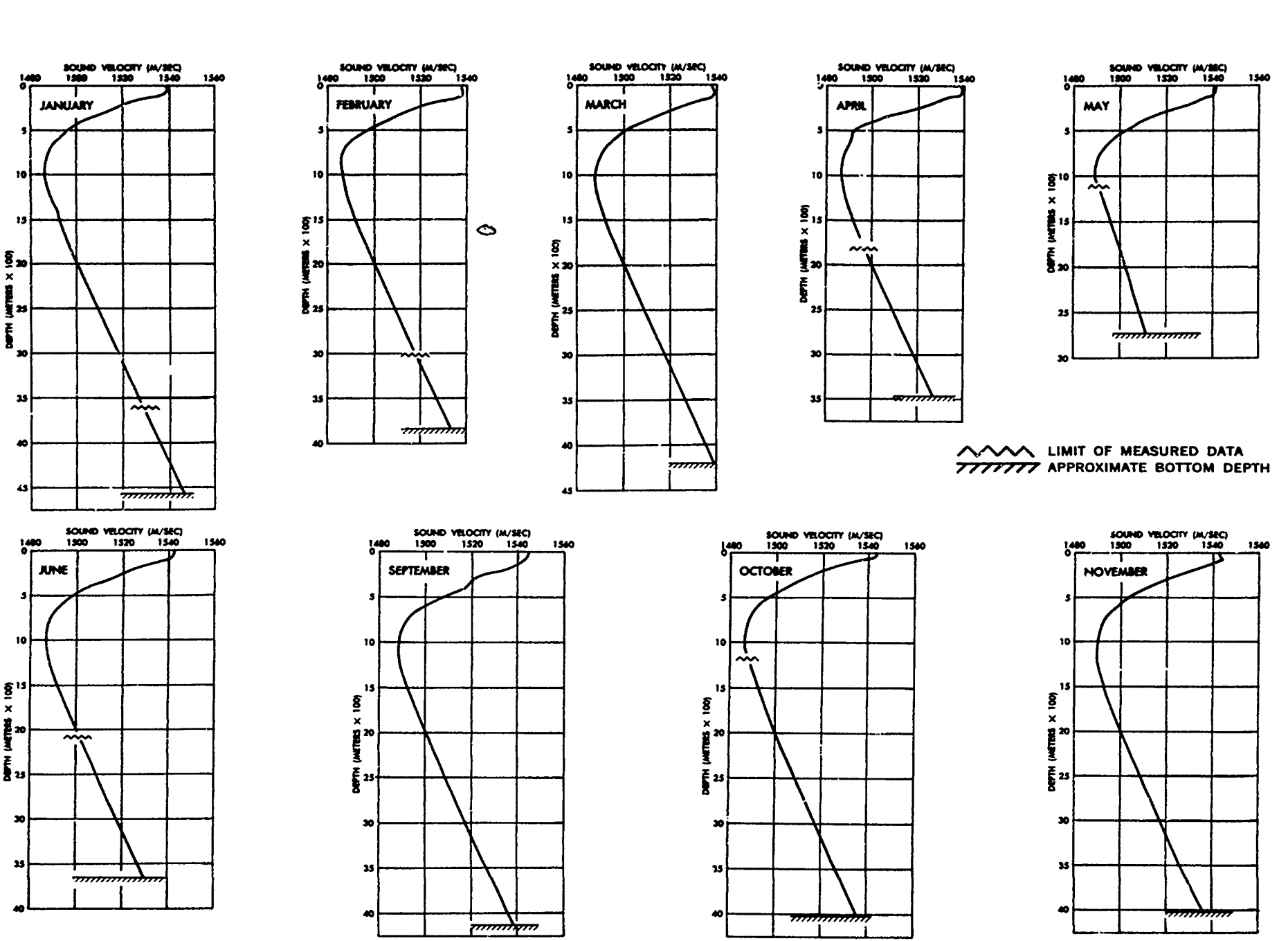

FIGURE 4-13 SOUND VELOCITY PROFILES–NORTH COLOMBIAN BASIN

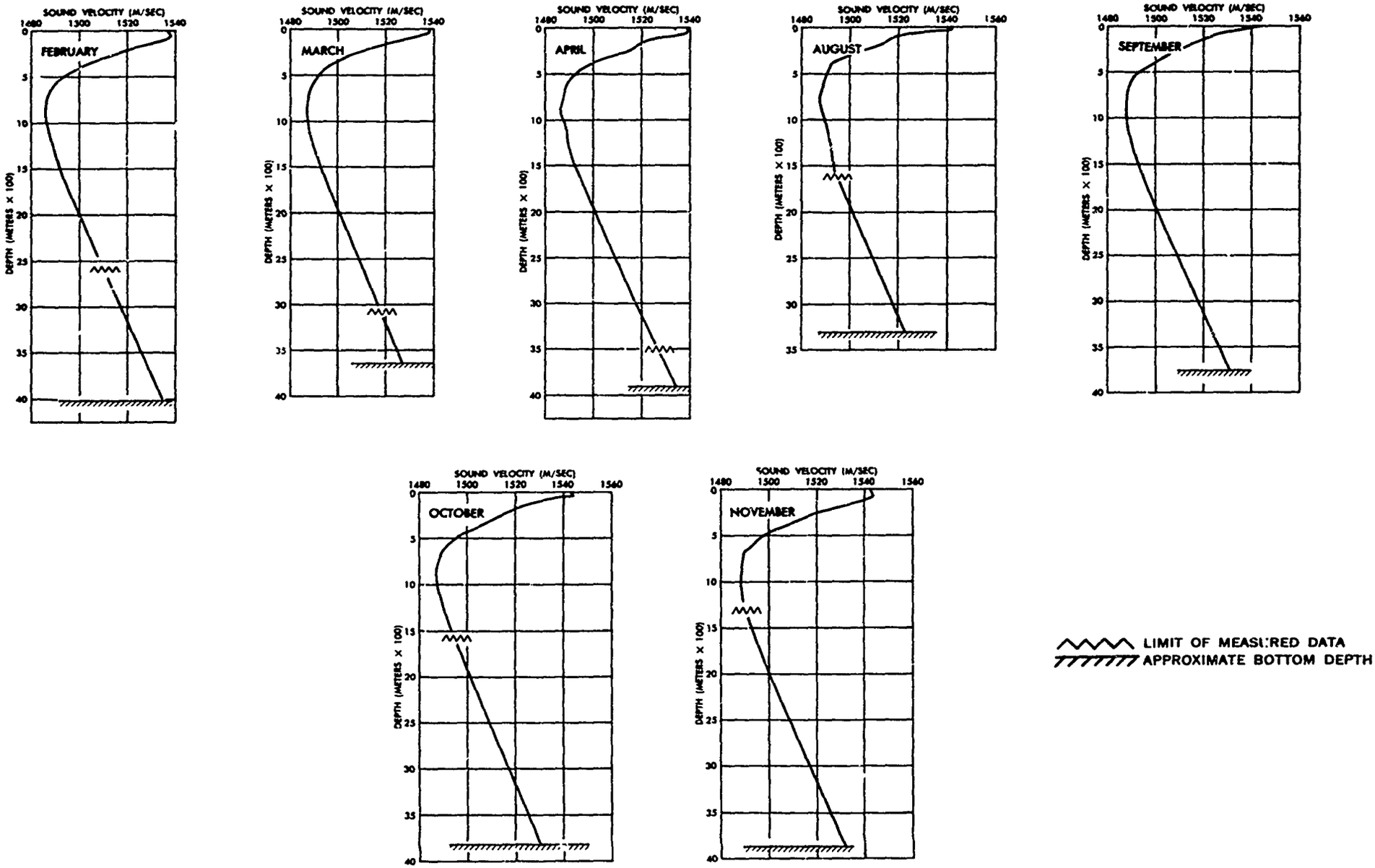

FIGURE 4-14 SOUND VELOCITY PROFILES–SOUTH COLOMBIAN BASIN

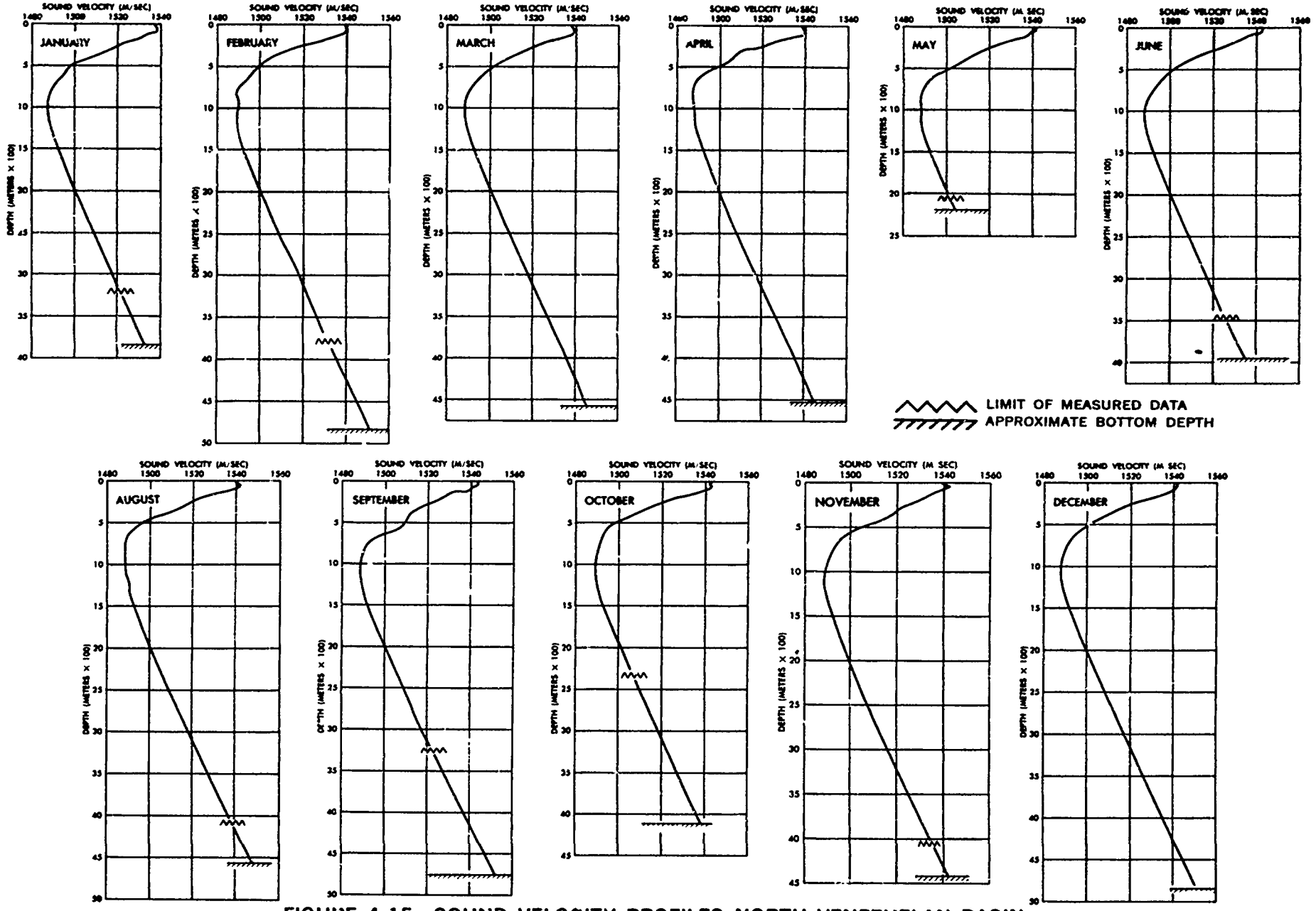

FIGURE 4-15 SOUND VELOCITY PROFILES–NORTH VENEZUELAN BASIN

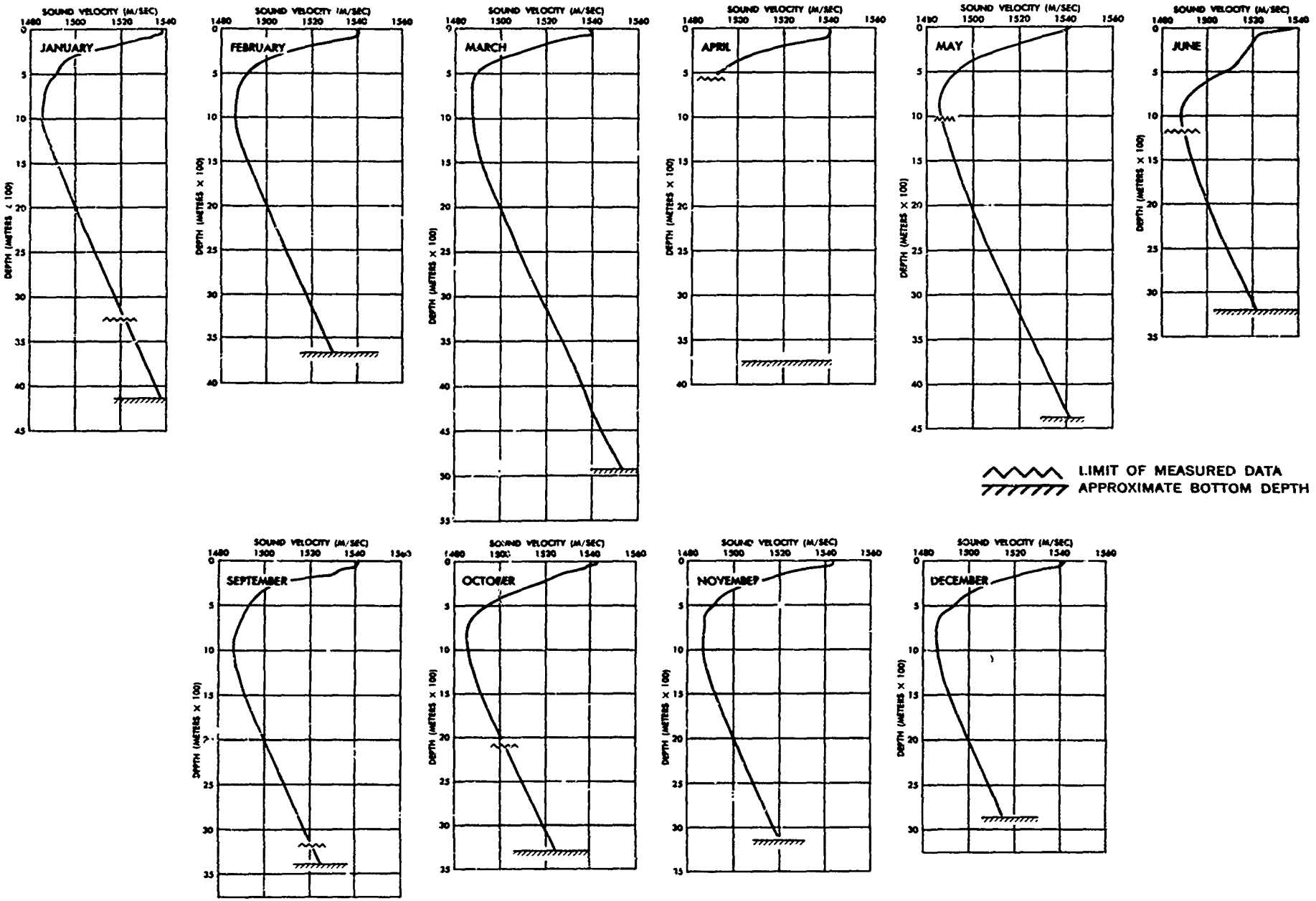

FIGURE 4-16 SOUND VELOCITY PROFILES–SOUTH VENEZUELAN BASIN

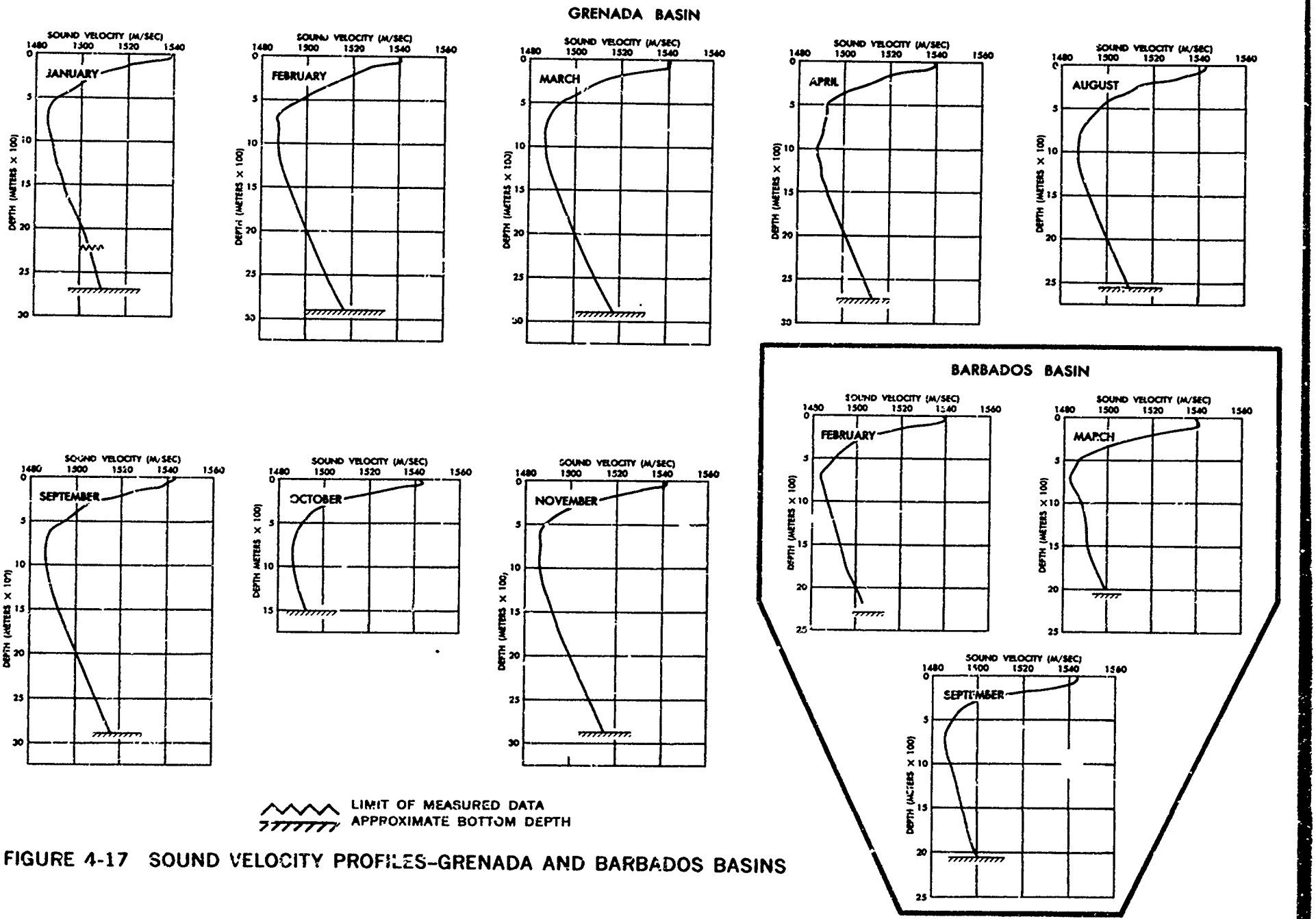

FIGURE 4-17 SOUND VELOCITY PROFILES-GRENADA AND BARBADOS BASINS

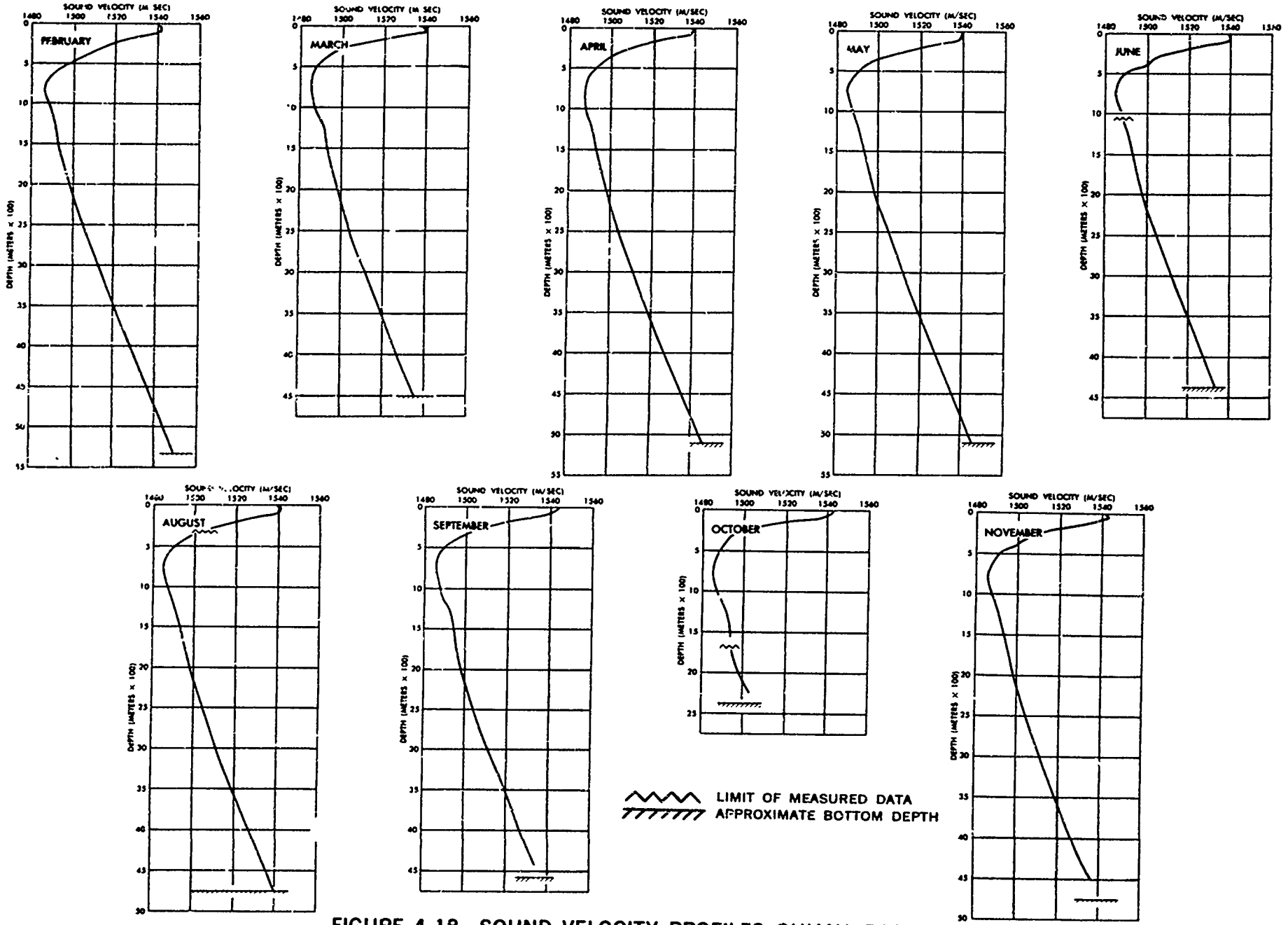

FIGURE 4-18 SOUND VELOCITY PROFILES-GUIANA BASIN

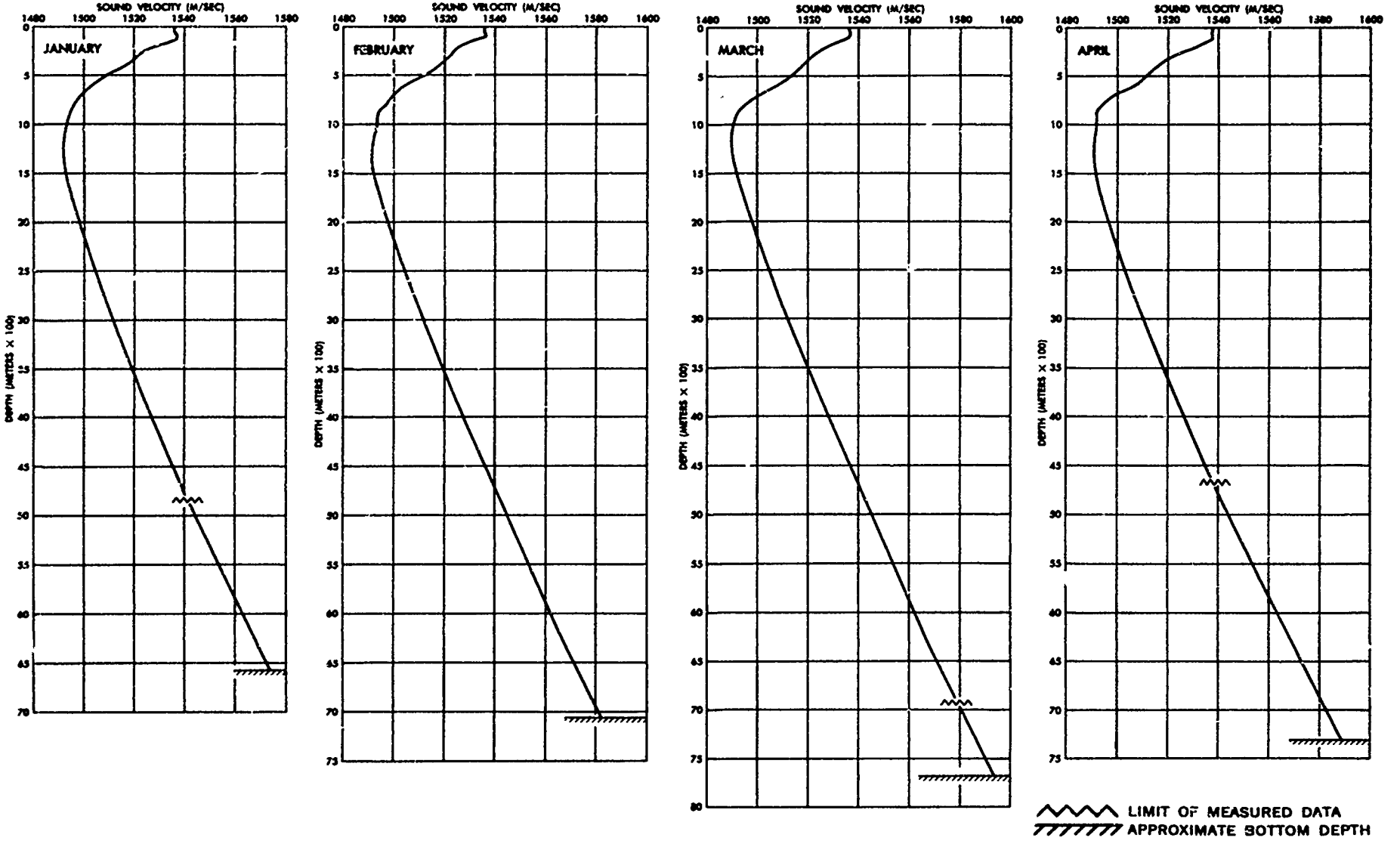

FIGURE 4-19 SOUND VELOCITY PROFILES–PUERTO RICO TRENCH

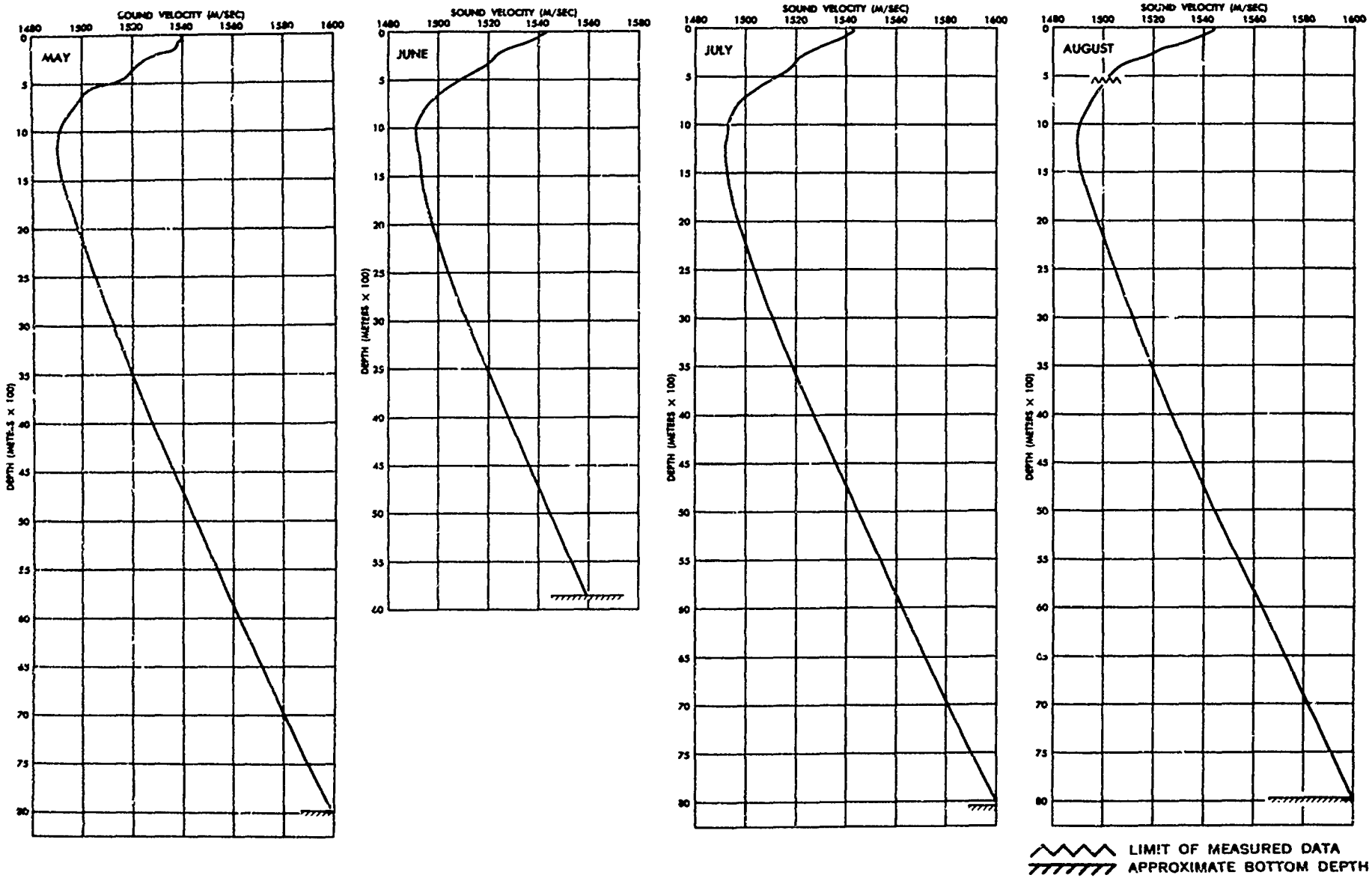

FIGURE 4-20 SOUND VELOCITY PROFILES–PUERTO RICO TRENCH (CONT.)

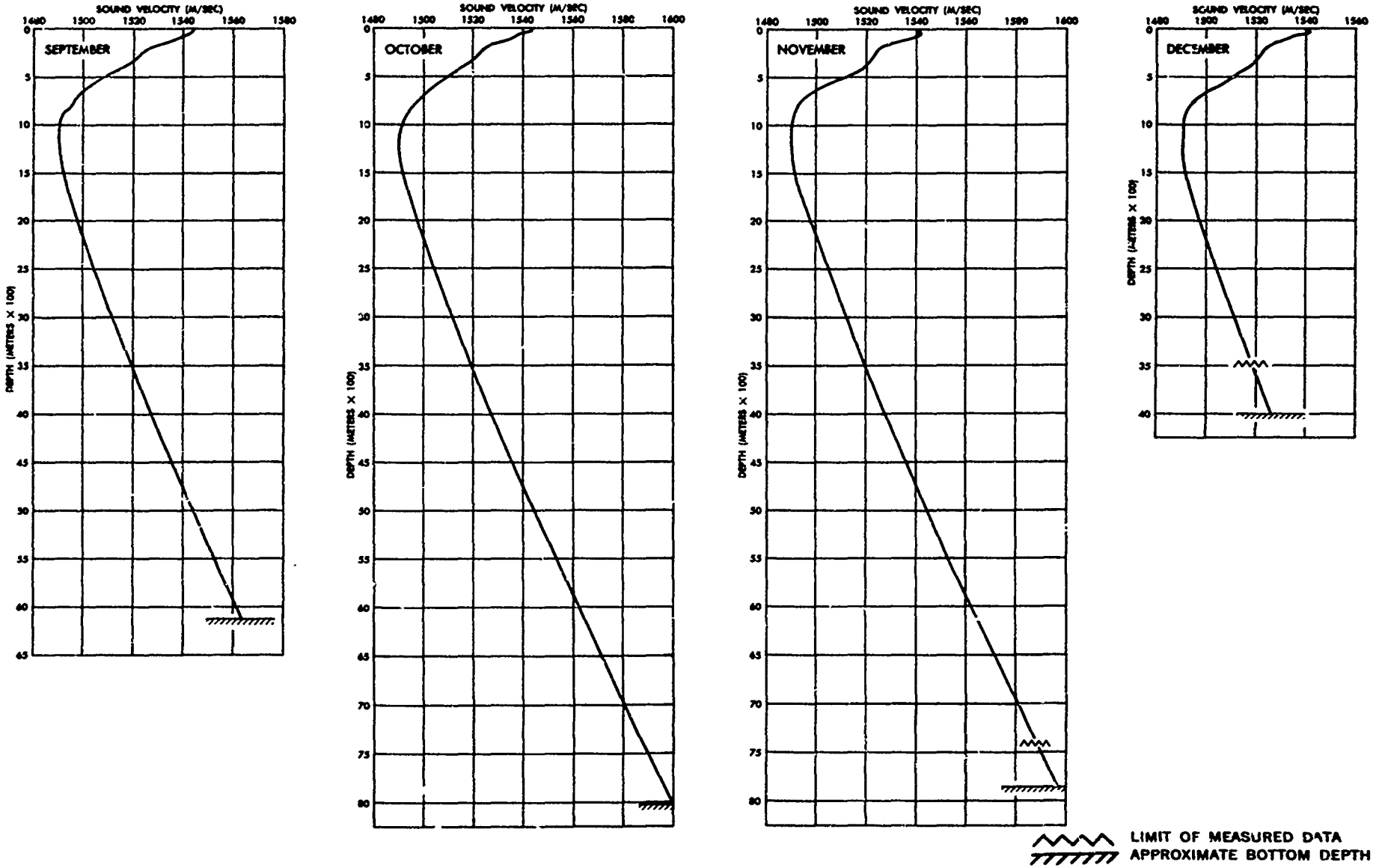

FIGURE 4-21 SOUND VELOCITY PROFILES–PUERTO RICO TRENCH (CONT.)

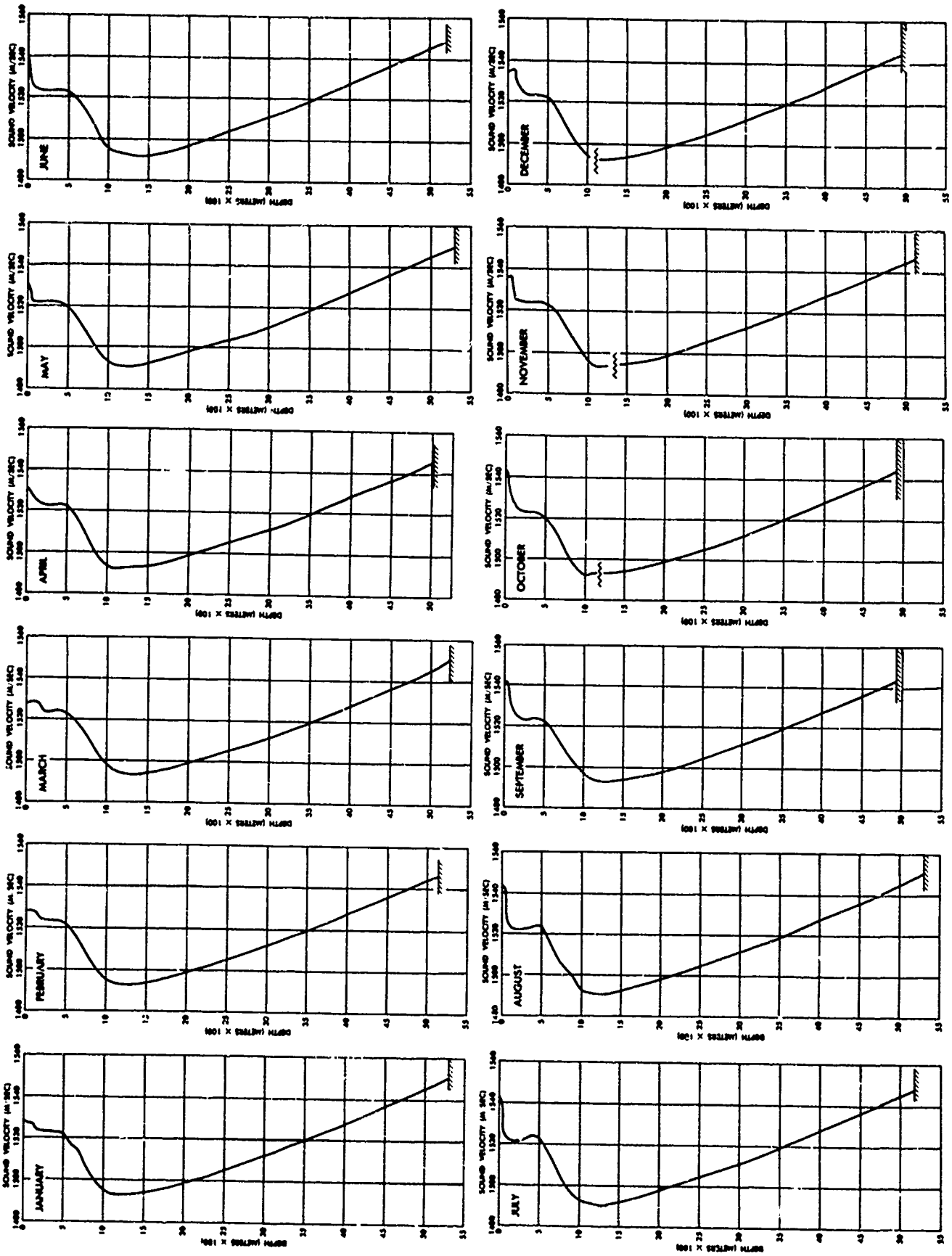

FIGURE 4-22 SOUND VELOCITY PROFILES–NORTH AMERICAN BASIN

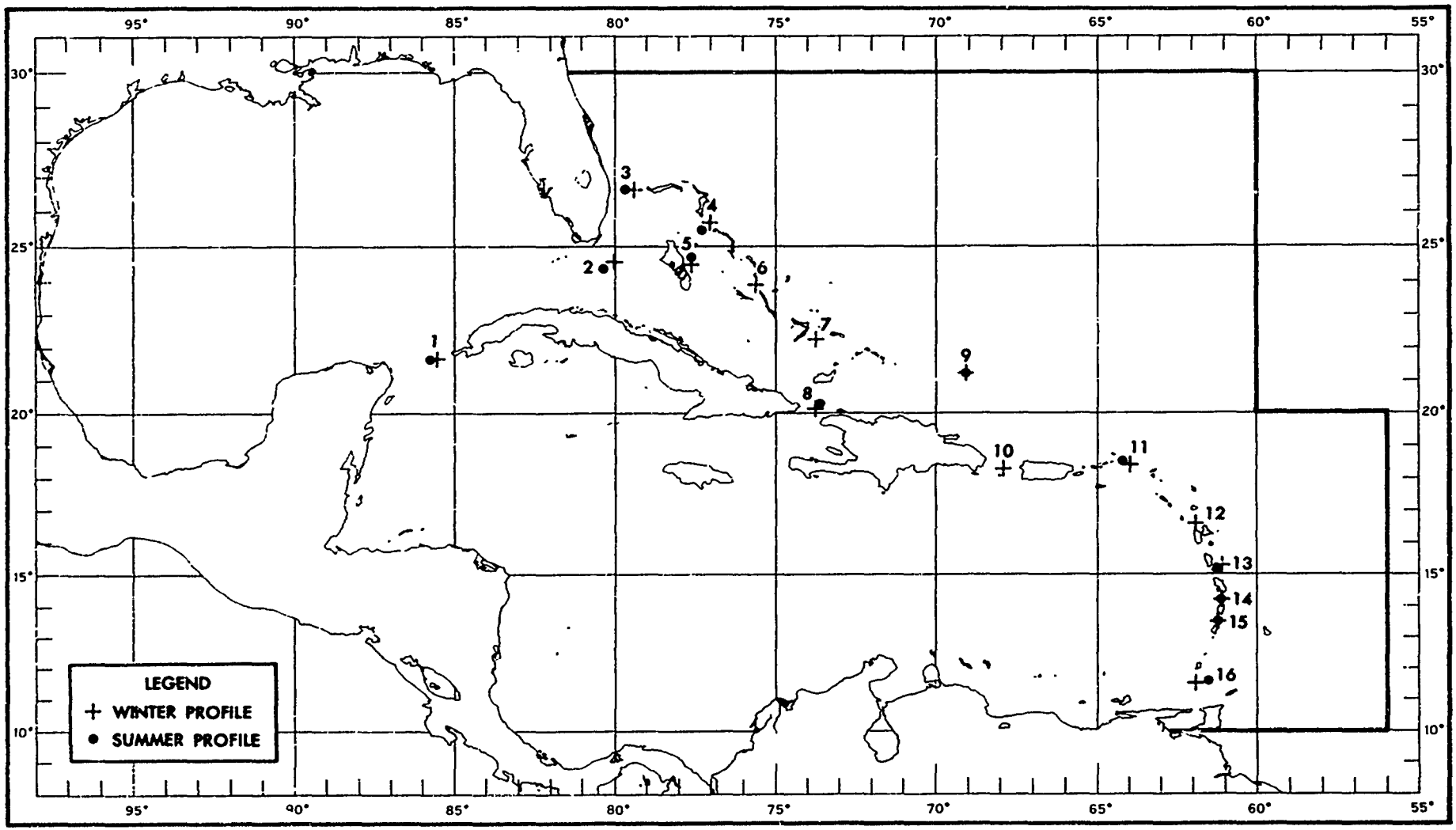

FIGURE 4-23 LOCATIONS OF SOUND VELOCITY PROFILES IN PRINCIPAL STRAITS

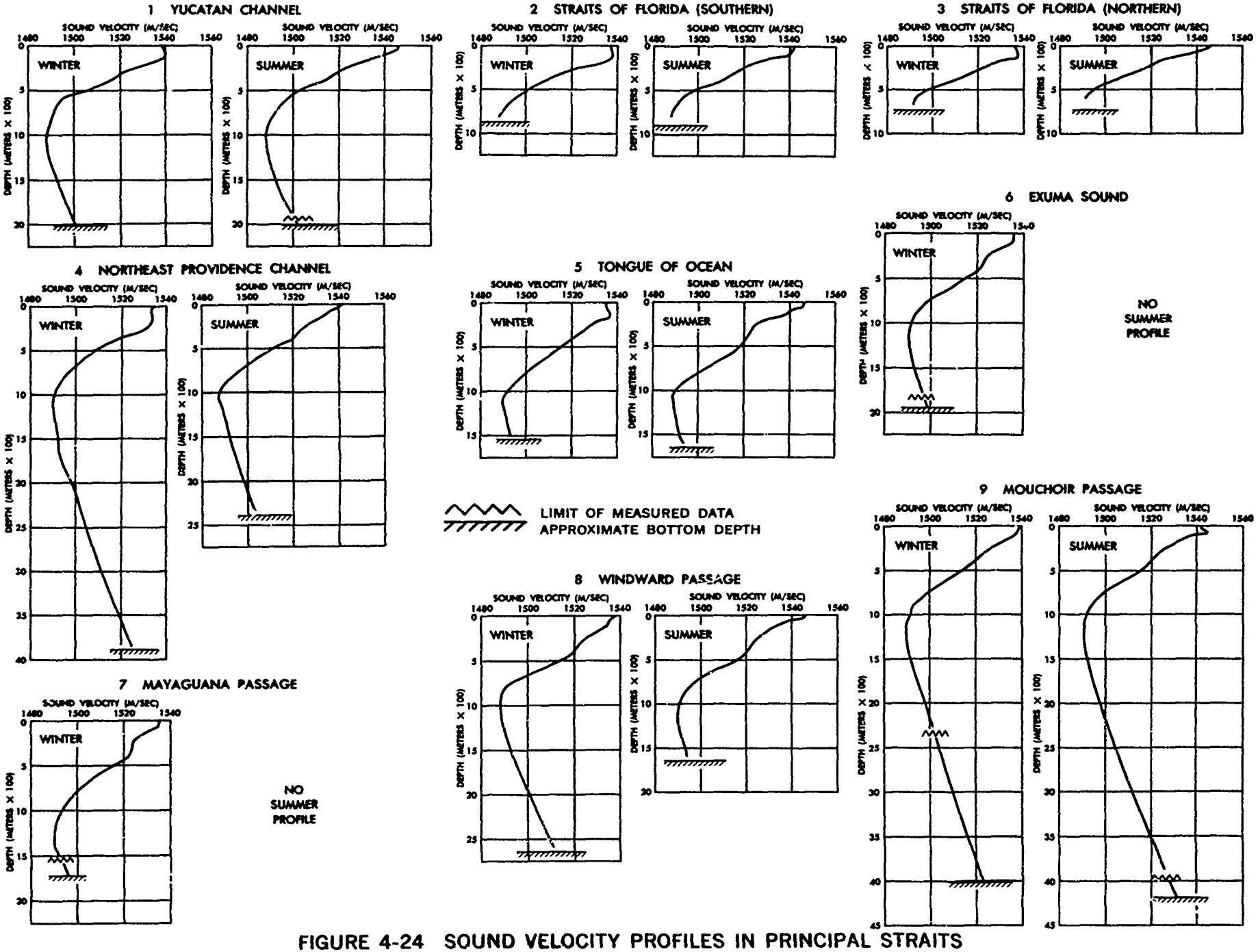

FIGURE 4-24 SOUND VELOCITY PROFILES IN PRINCIPAL STRAITS

10 MONA PASSAGE

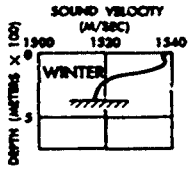

NO SUMMER PROFILE

11 ANEGADA PASSAGE

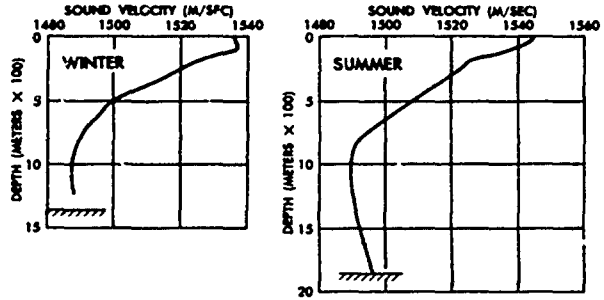

12 GUADELOUPE PASSAGE

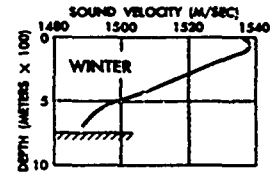

NO SUMMER PROFILE

13 DOMINICA CHANNEL

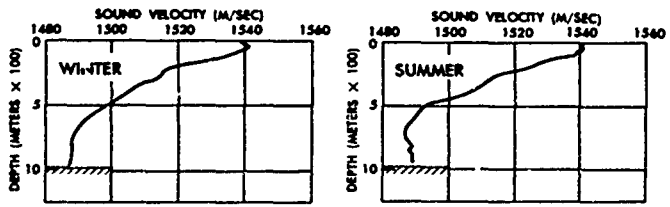

14 ST. LUCIA CHANNEL

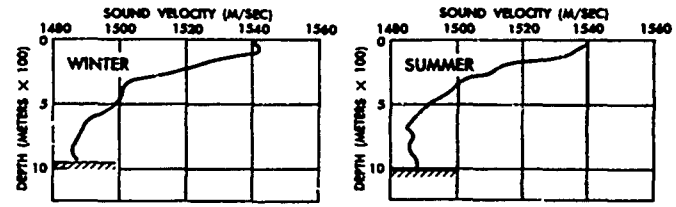

LIMIT OF MEASURED DATA
APPROXIMATE BOTTOM DEPTH

15 ST. VINCENT CHANNEL

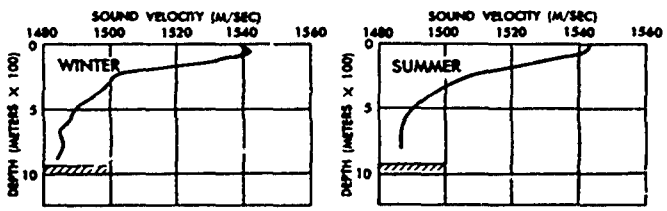

16 GRENADA PASSAGE

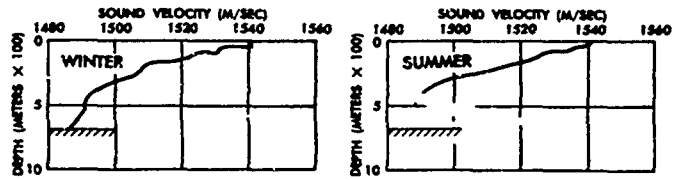

FIGURE 4-25 SOUND VELOCITY PROFILES IN PRINCIPAL STRAITS (CONT.)

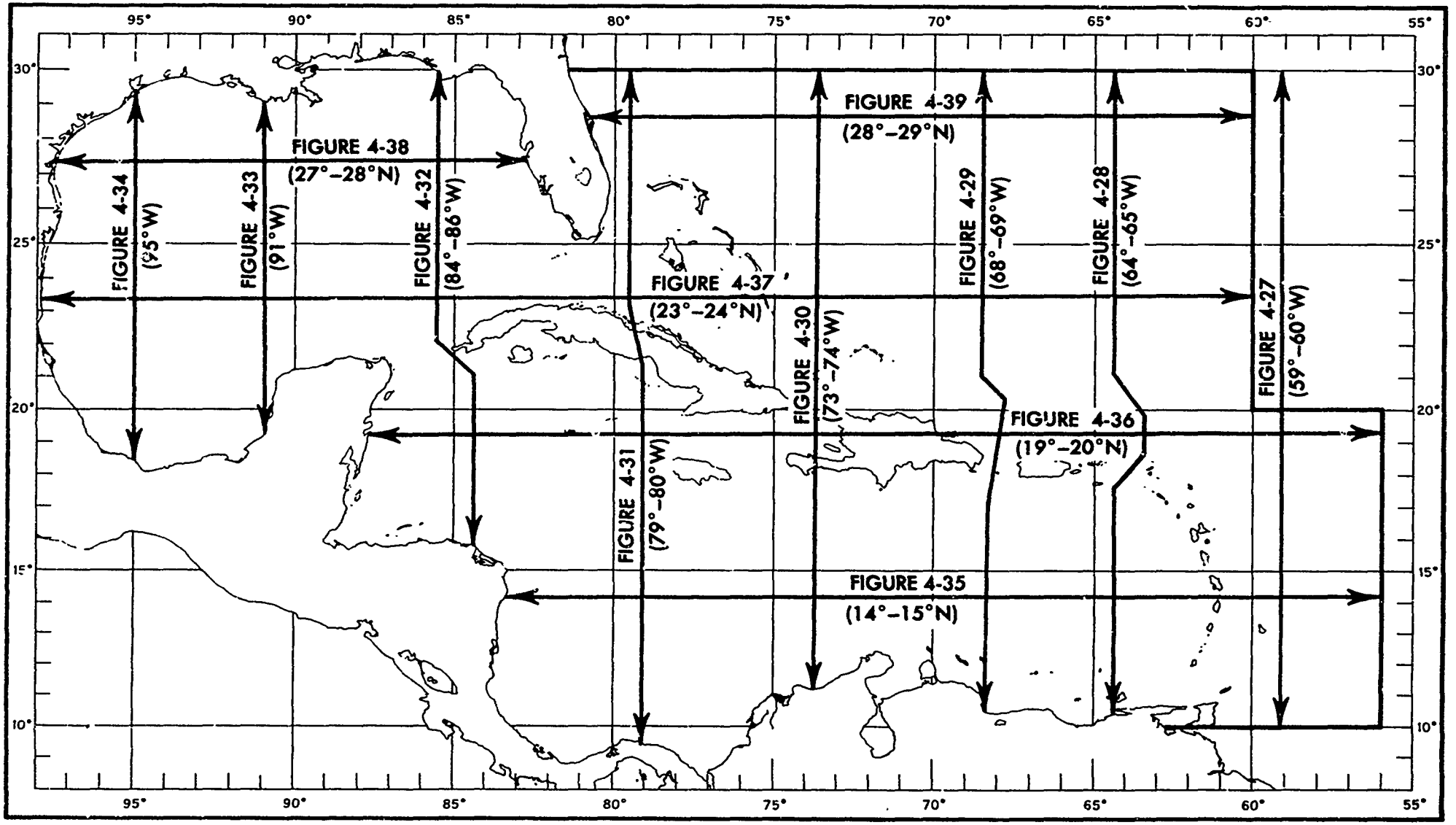

FIGURE 4-26 LOCATIONS OF SOUND VELOCITY CROSS-SECTIONS

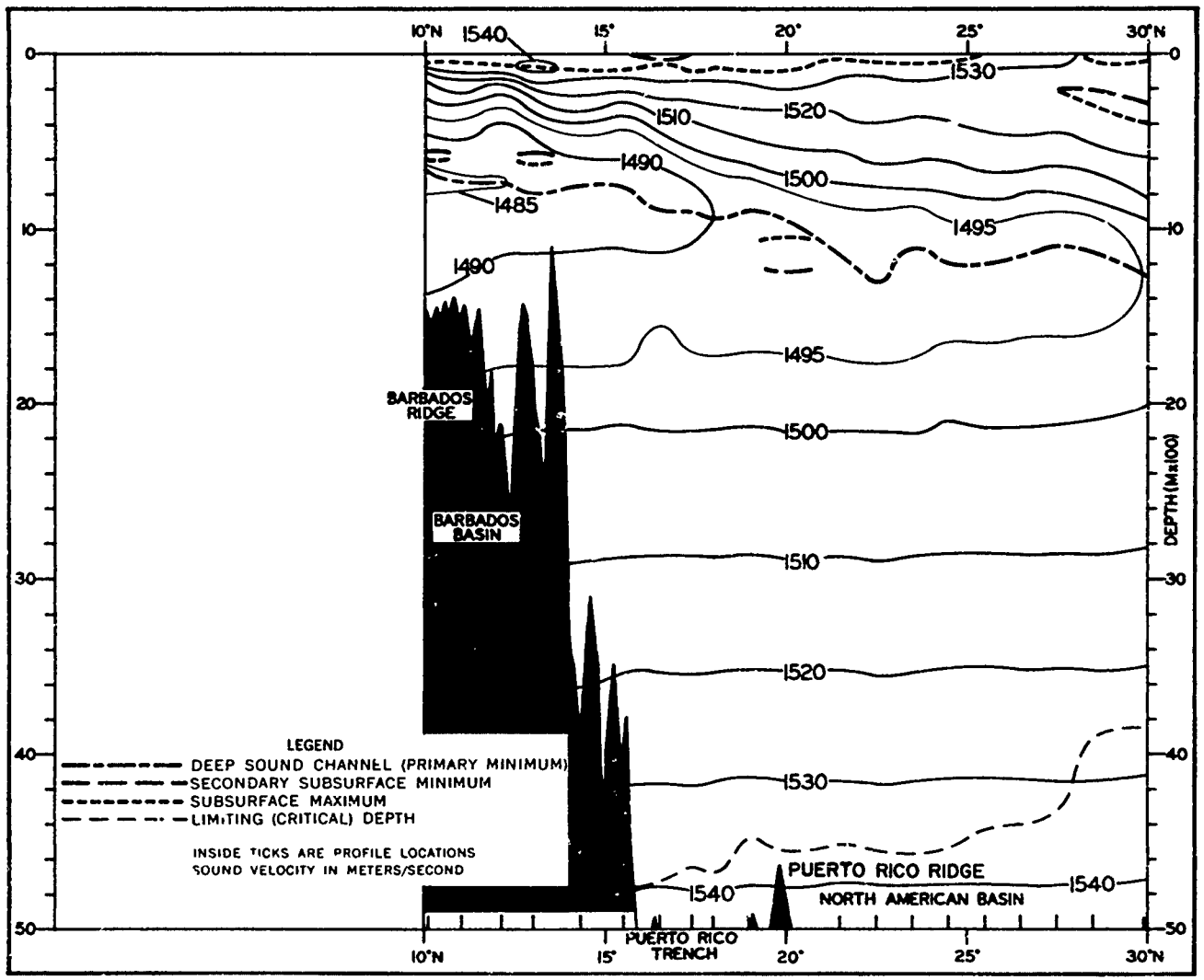

FIGURE 4-27 NORTH-SOUTH SOUND VELOCITY CROSS-SECTION BETWEEN 59° AND 60° WEST LONGITUDE (JANUARY-MARCH)

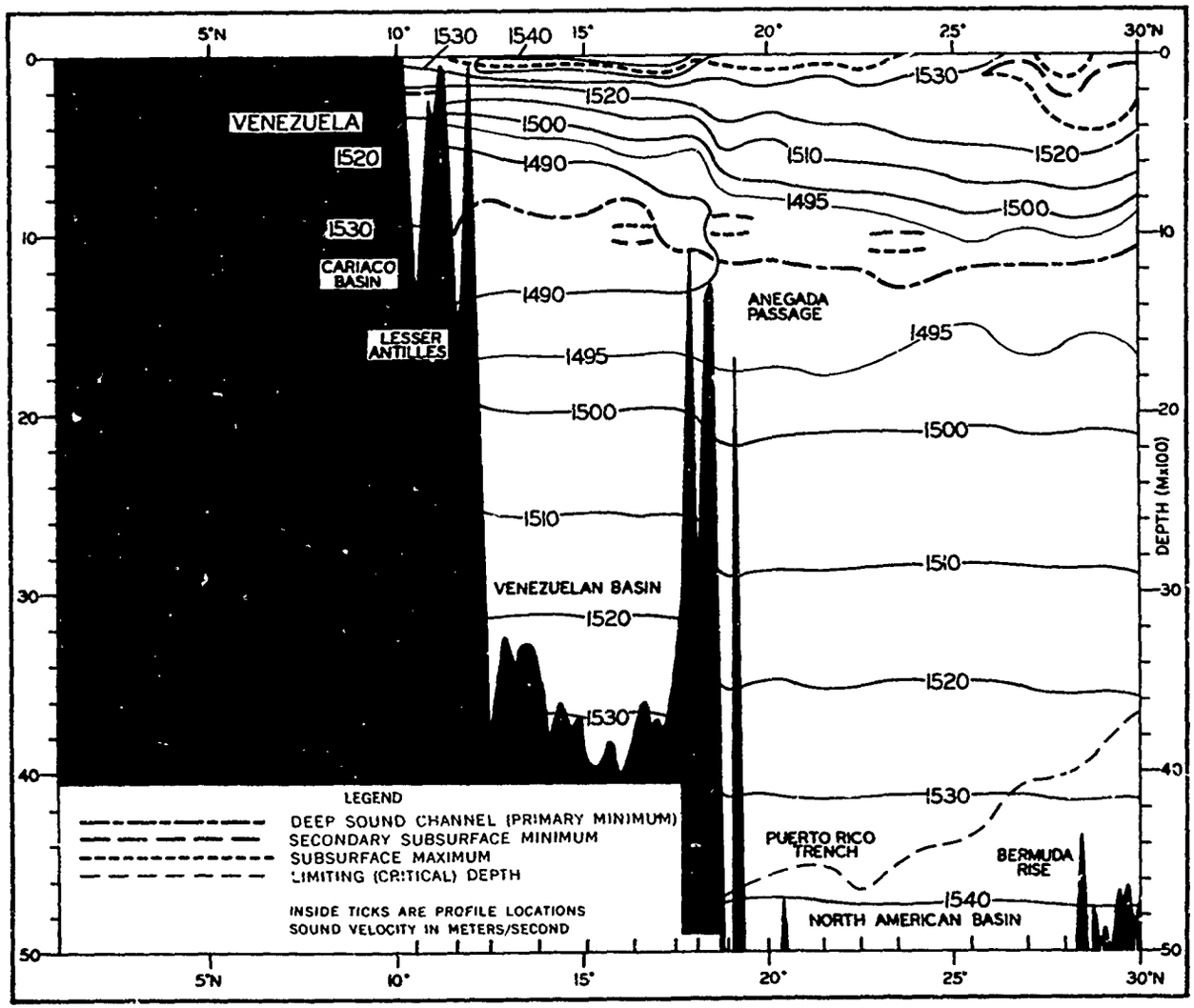

FIGURE 4-28 NORTH-SOUTH SOUND VELOCITY CROSS-SECTION BETWEEN 64° AND 65° WEST LONGITUDE (FEBRUARY-MARCH)

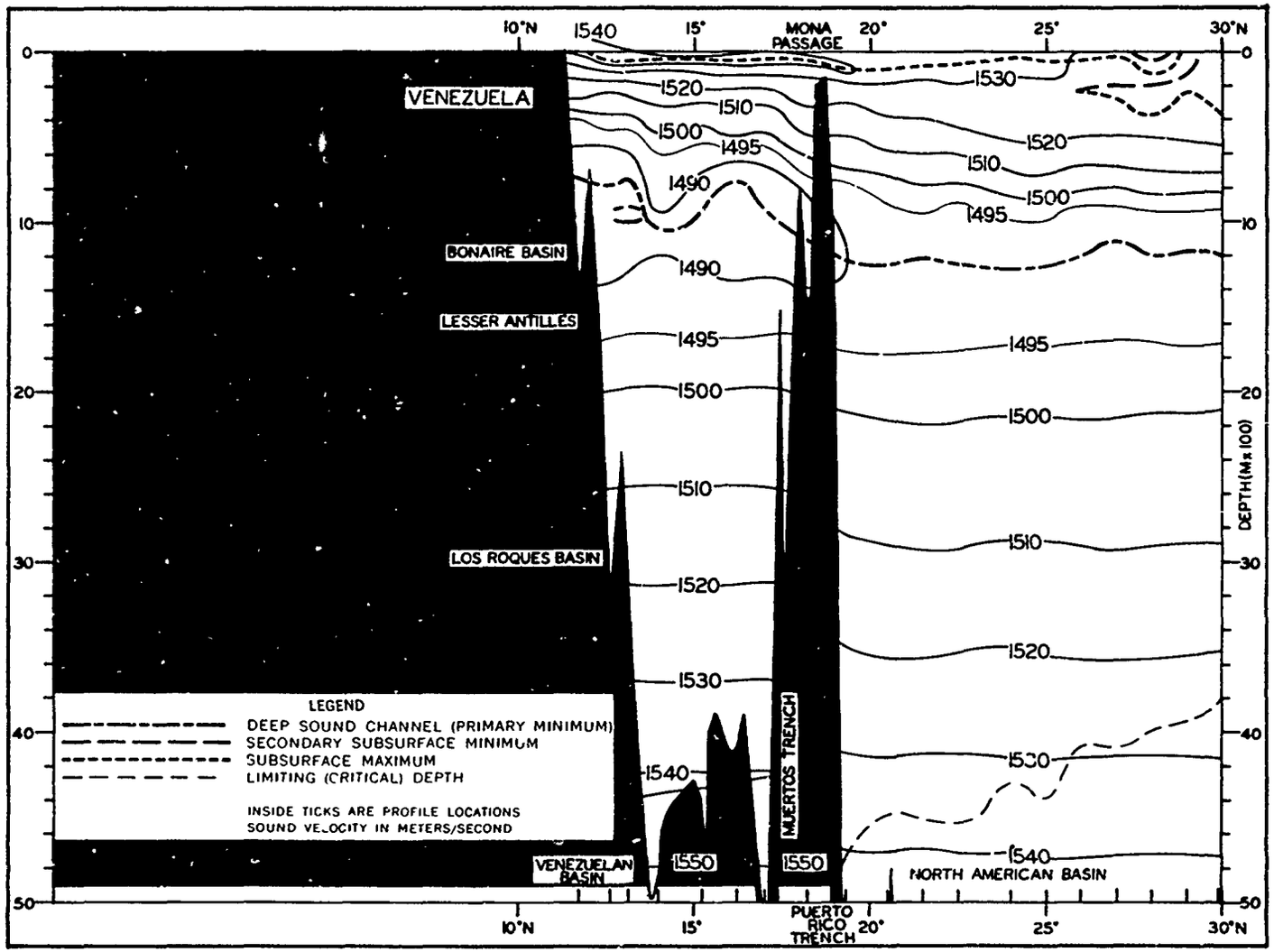

FIGURE 4-29 NORTH-SOUTH SOUND VELOCITY CROSS-SECTION BETWEEN 68° AND 69° WEST LONGITUDE (DECEMBER-APRIL)

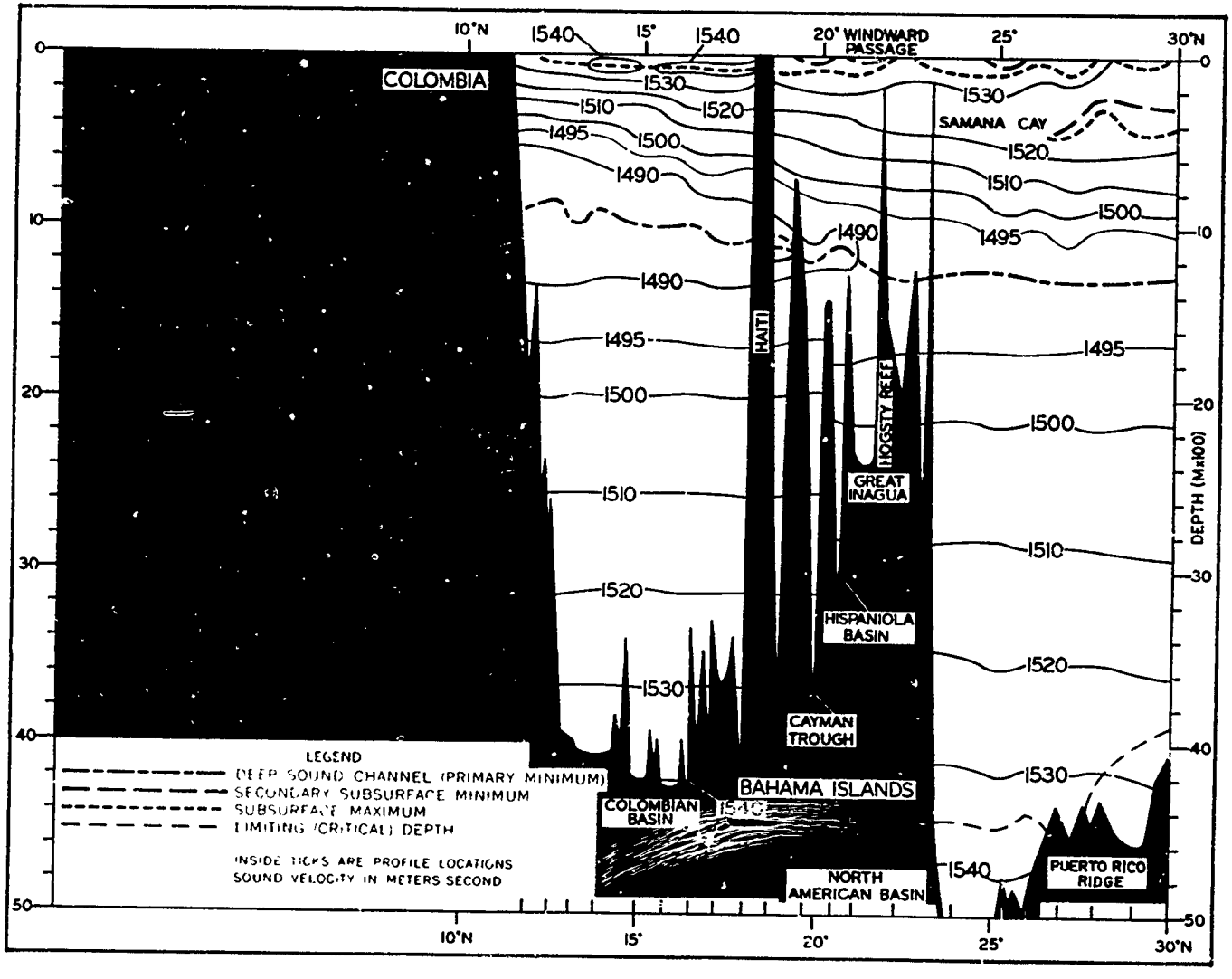

FIGURE 4-30 NORTH-SOUTH SOUND VELOCITY CROSS-SECTION BETWEEN 73° AND 74° WEST LONGITUDE (JANUARY-MARCH)

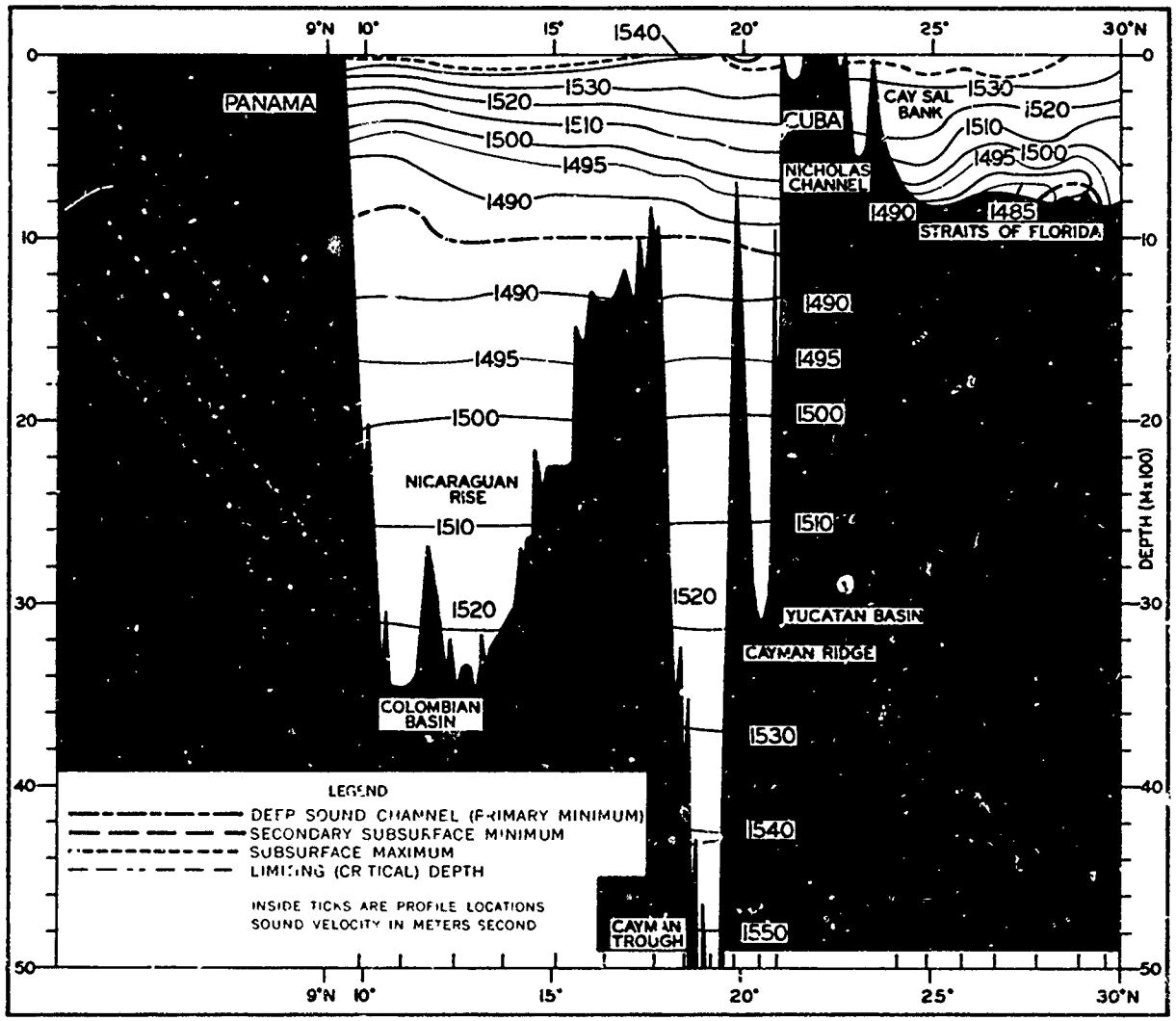

FIGURE 4-31 NORTH-SOUTH SOUND VELOCITY CROSS SECTION BETWEEN 79° AND 80° WEST LONGITUDE (FEBRUARY-MARCH)

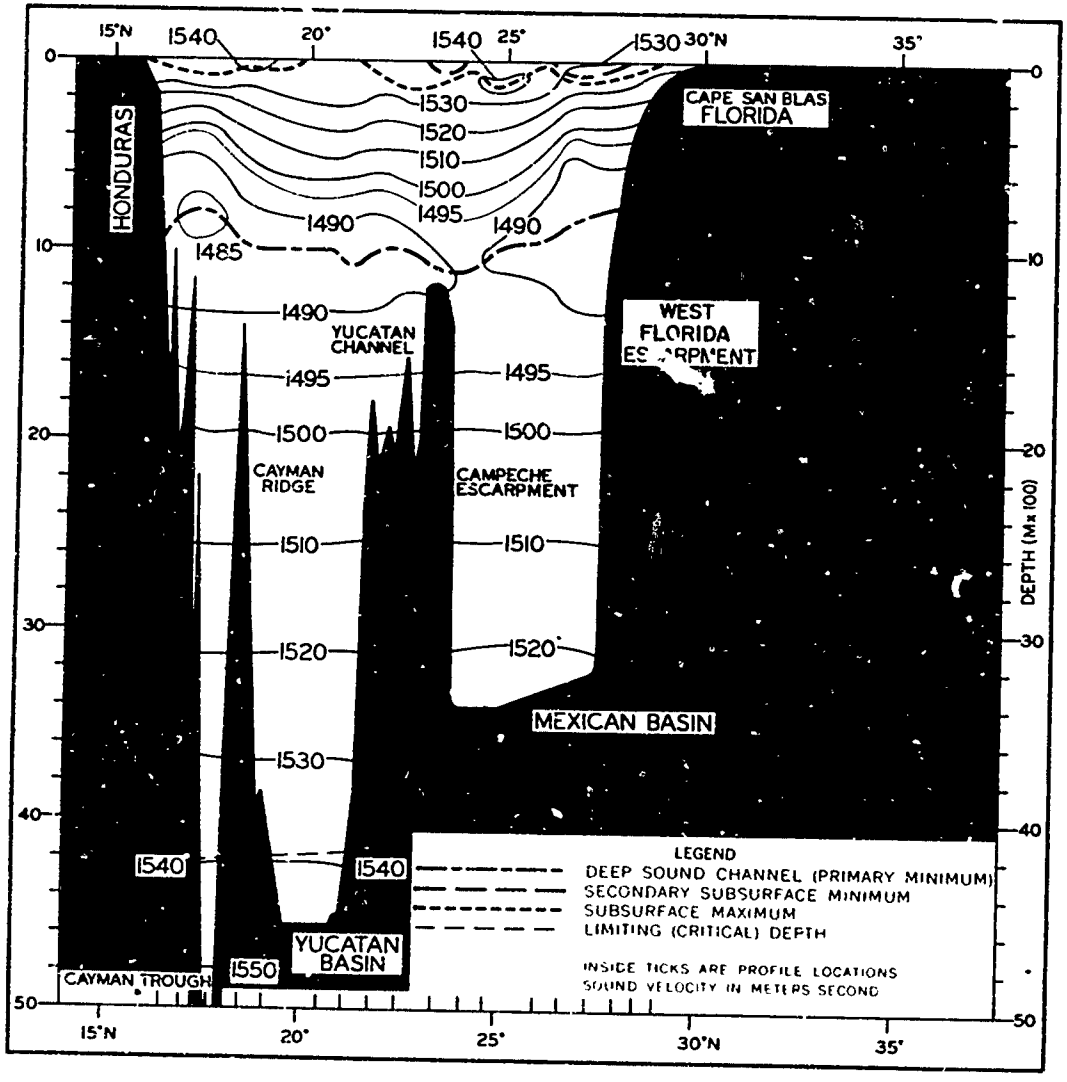

FIGURE 4-32 NORTH-SOUTH SOUND VELOCITY CROSS-SECTION BETWEEN 84° AND 86° WEST LONGITUDE (FEBRUARY-MARCH)

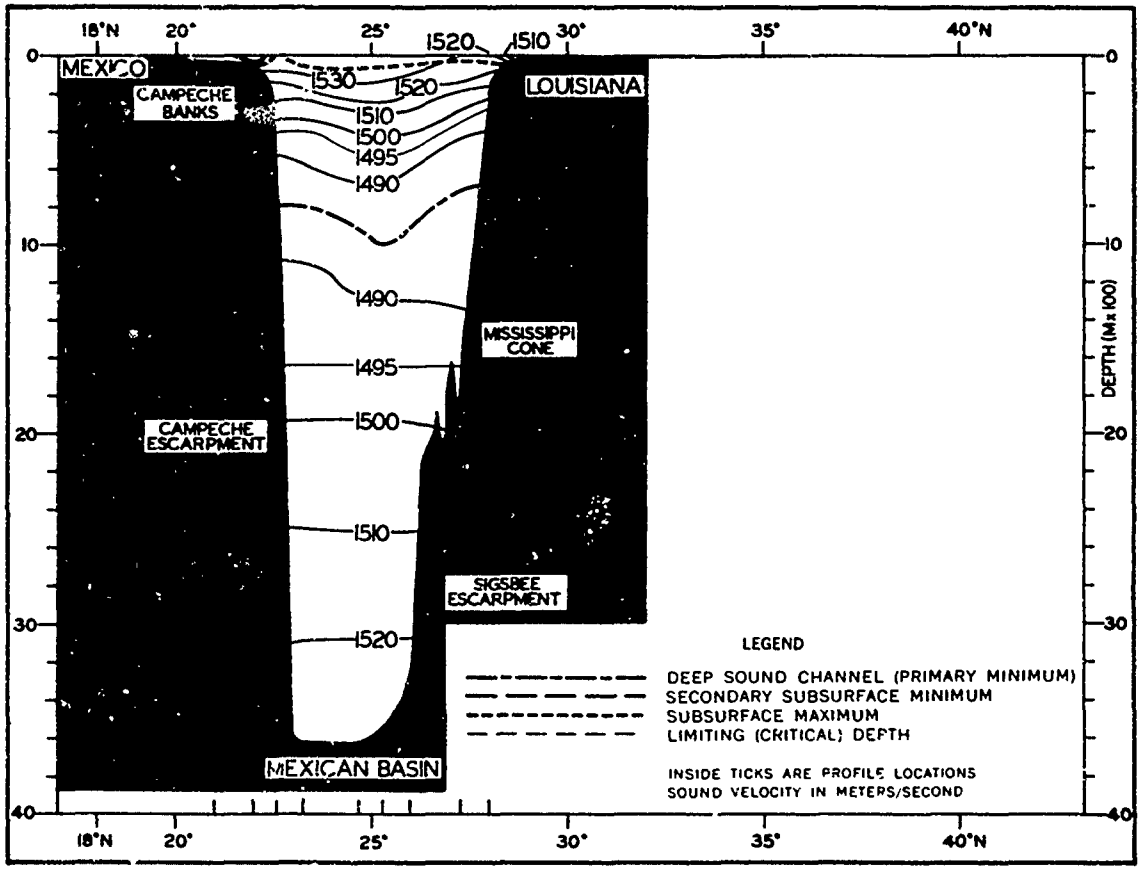

FIGURE 4-33 NORTH-SOUTH SOUND VELOCITY CROSS-SECTION ALONG 91° WEST LONGITUDE (MARCH)

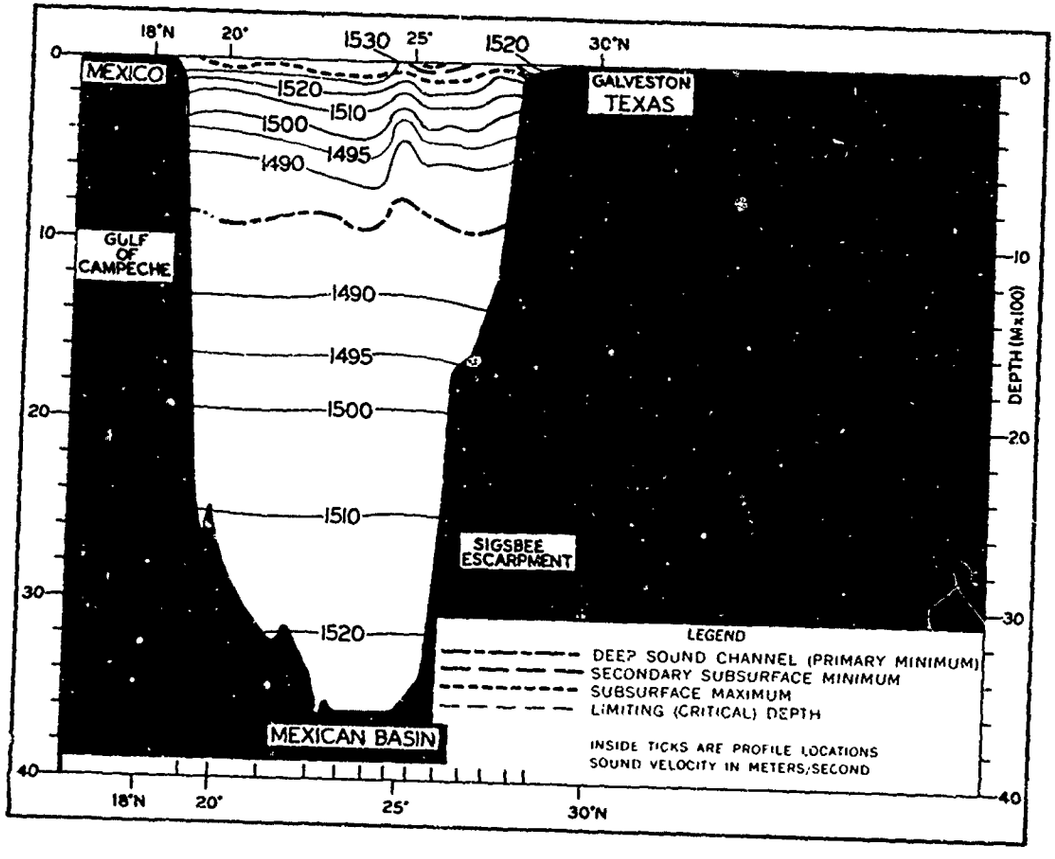

FIGURE 4-34 NORTH-SOUTH SOUND VELOCITY CROSS-SECTION ALONG 95° WEST LONGITUDE (MARCH)

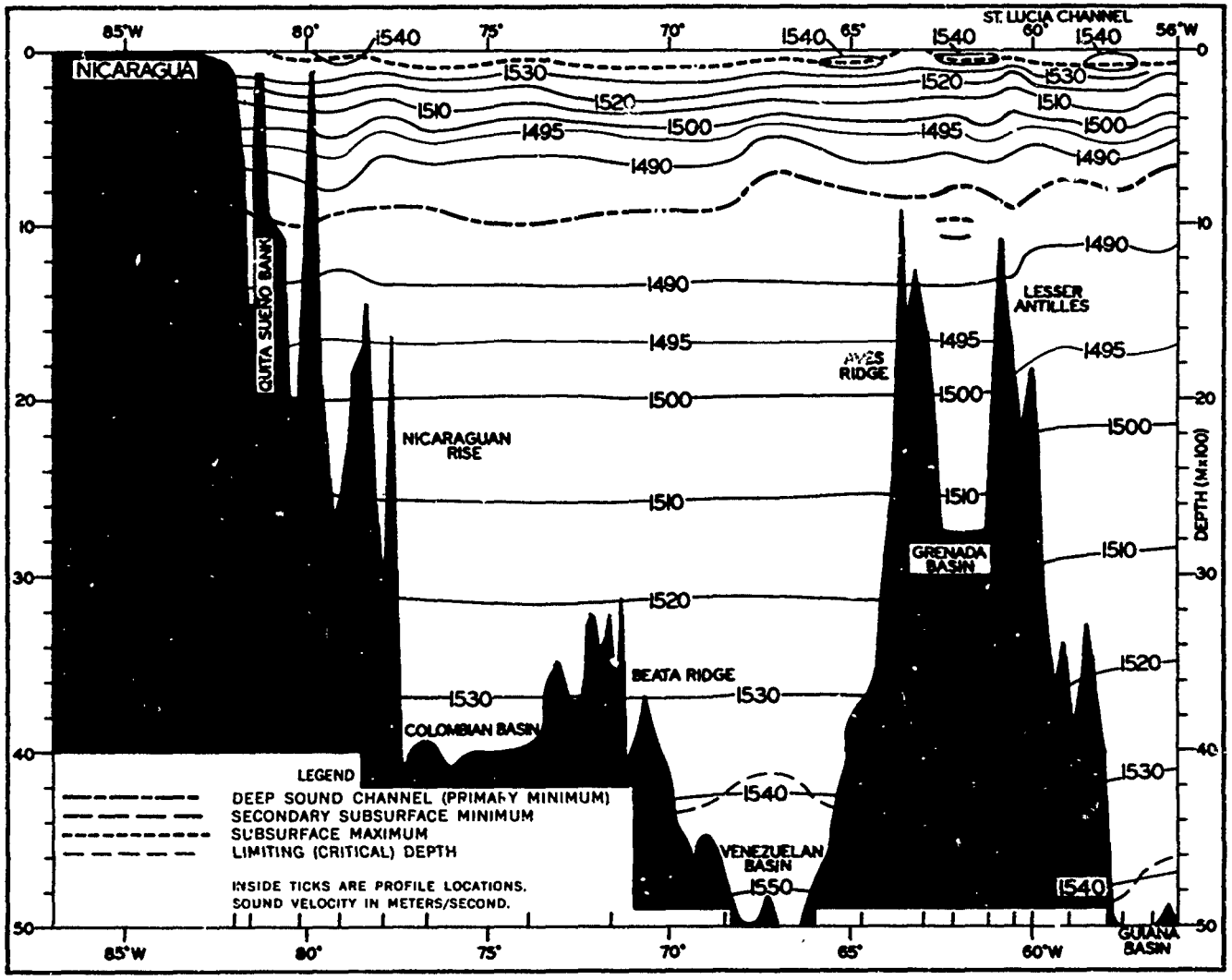

FIGURE 4-35 EAST-WEST SOUND VELOCITY CROSS-SECTION BETWEEN 14° AND 15° NORTH LATITUDE (JANUARY-MARCH)

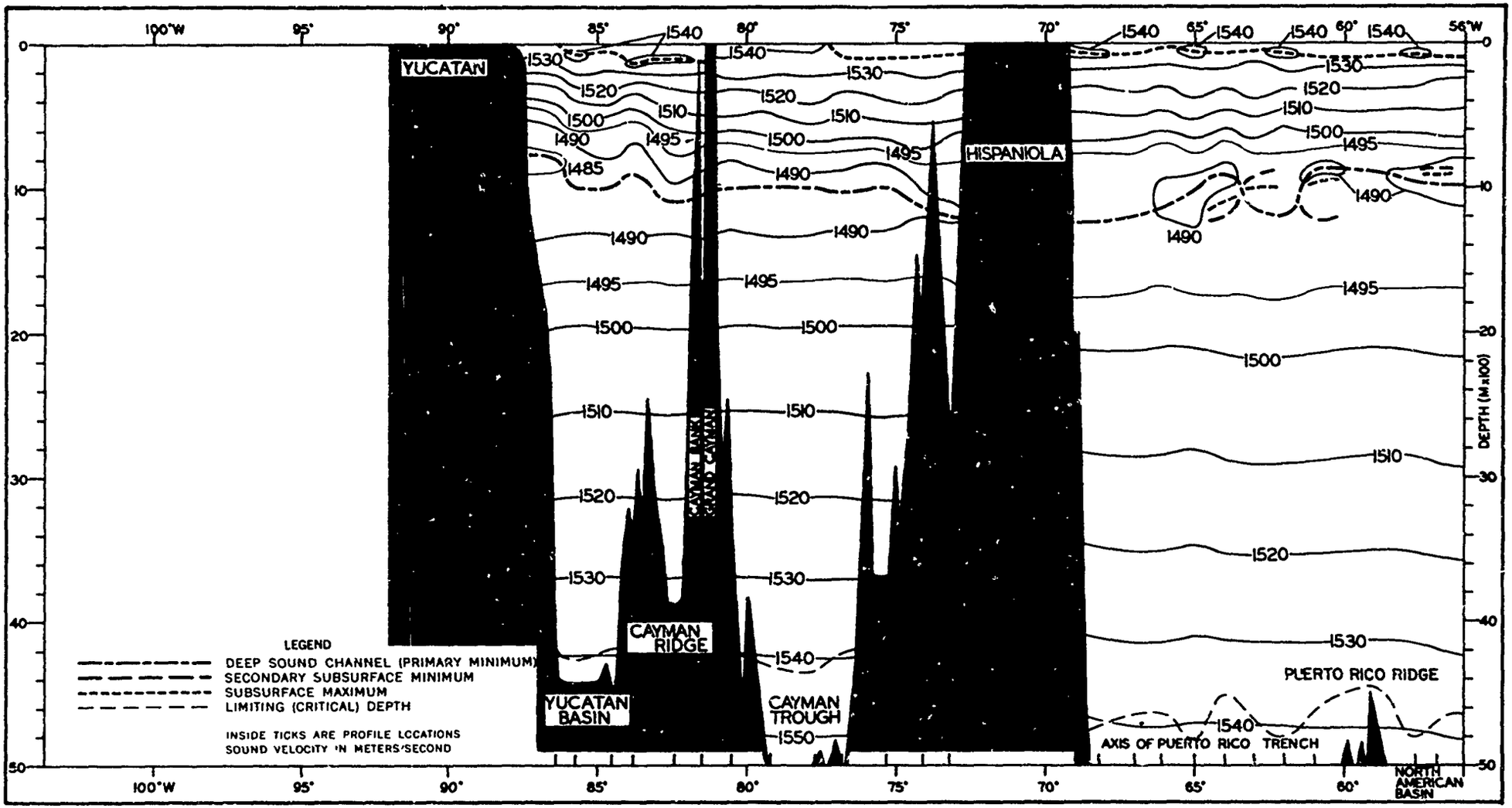

FIGURE 4-36 EAST-WEST SOUND VELOCITY CROSS-SECTION BETWEEN 19° AND 20° NORTH LATITUDE (FEBRUARY-MARCH)

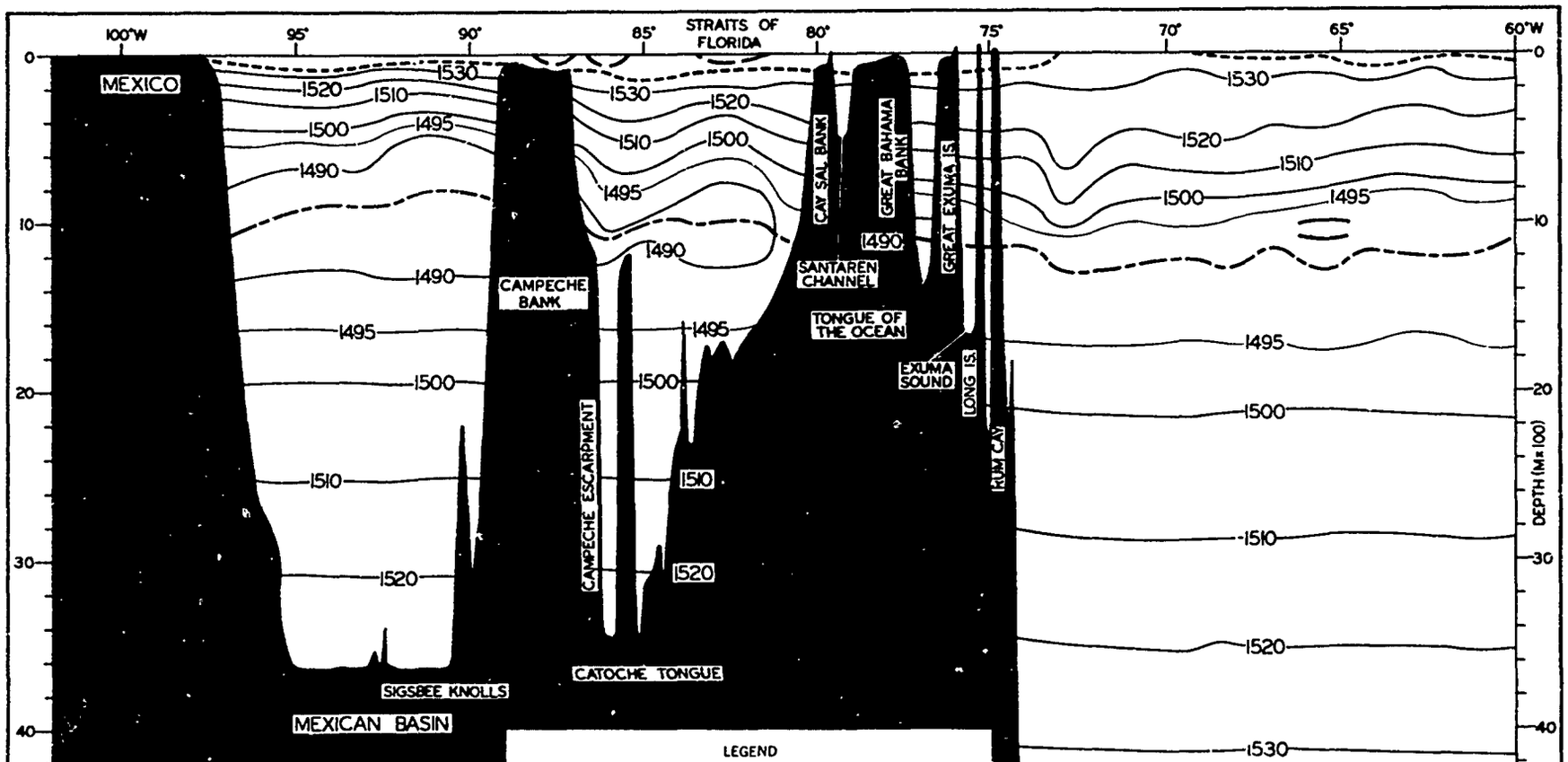

FIGURE 4-37 EAST-WEST SOUND VELOCITY CROSS-SECTION BETWEEN 23° AND 24° NORTH LATITUDE (FEBRUARY-APRIL)

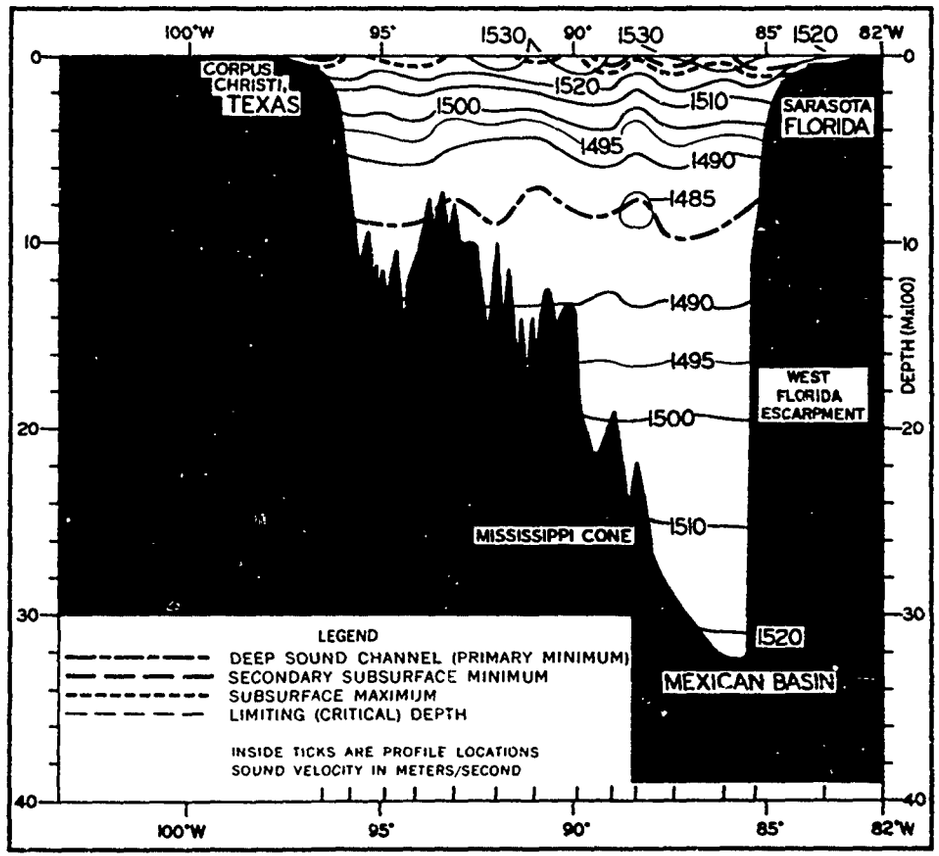

FIGURE 4-38 EAST-WEST SOUND VELOCITY CROSS-SECTION IN THE GULF OF MEXICO BETWEEN 27° AND 28° NORTH LATITUDE (FEBRUARY-MARCH)

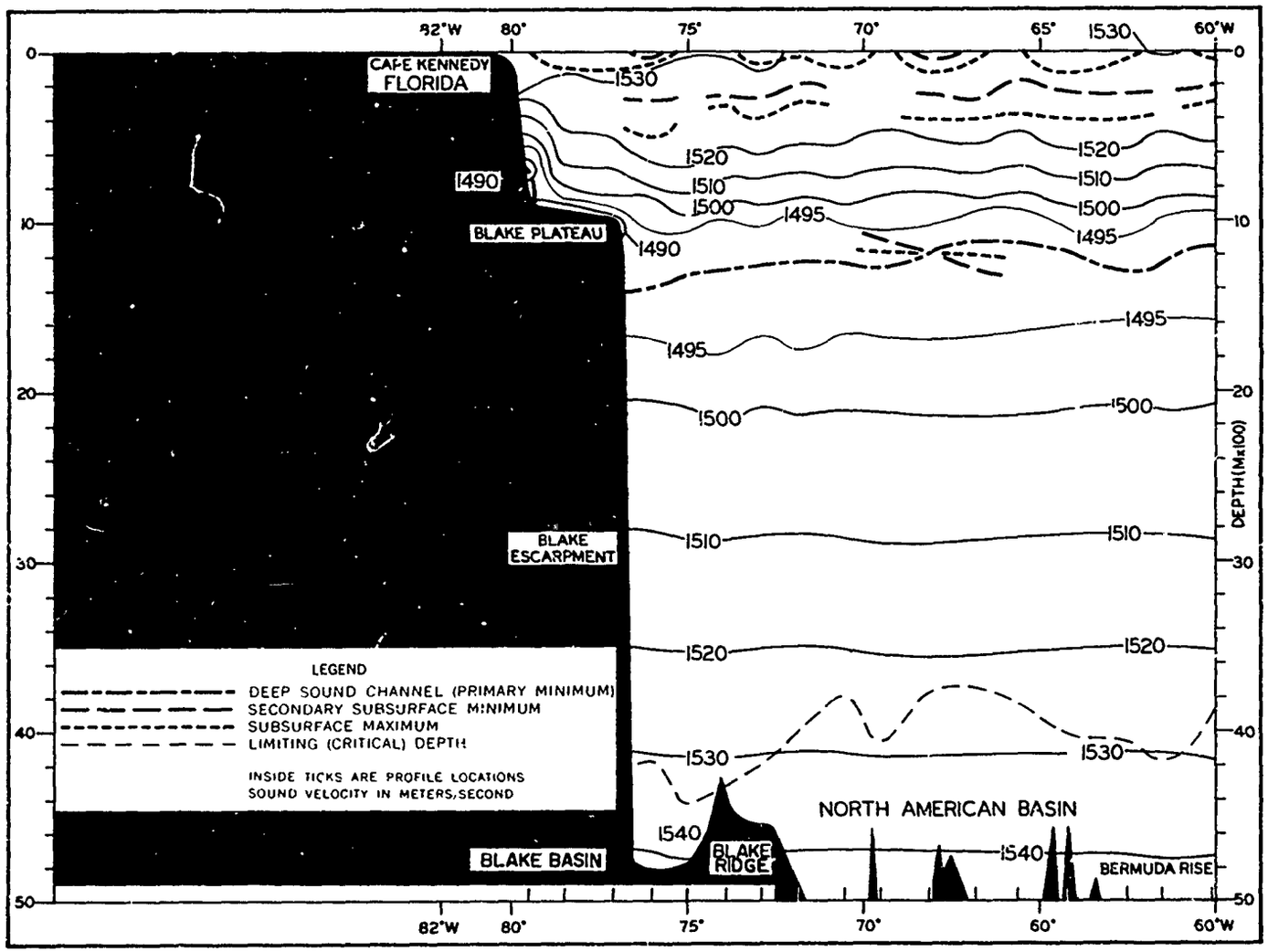

FIGURE 4-39 EAST-WEST SOUND VELOCITY CROSS-SECTION BETWEEN 28° AND 29° NORTH LATITUDE (FEBRUARY-APRIL)

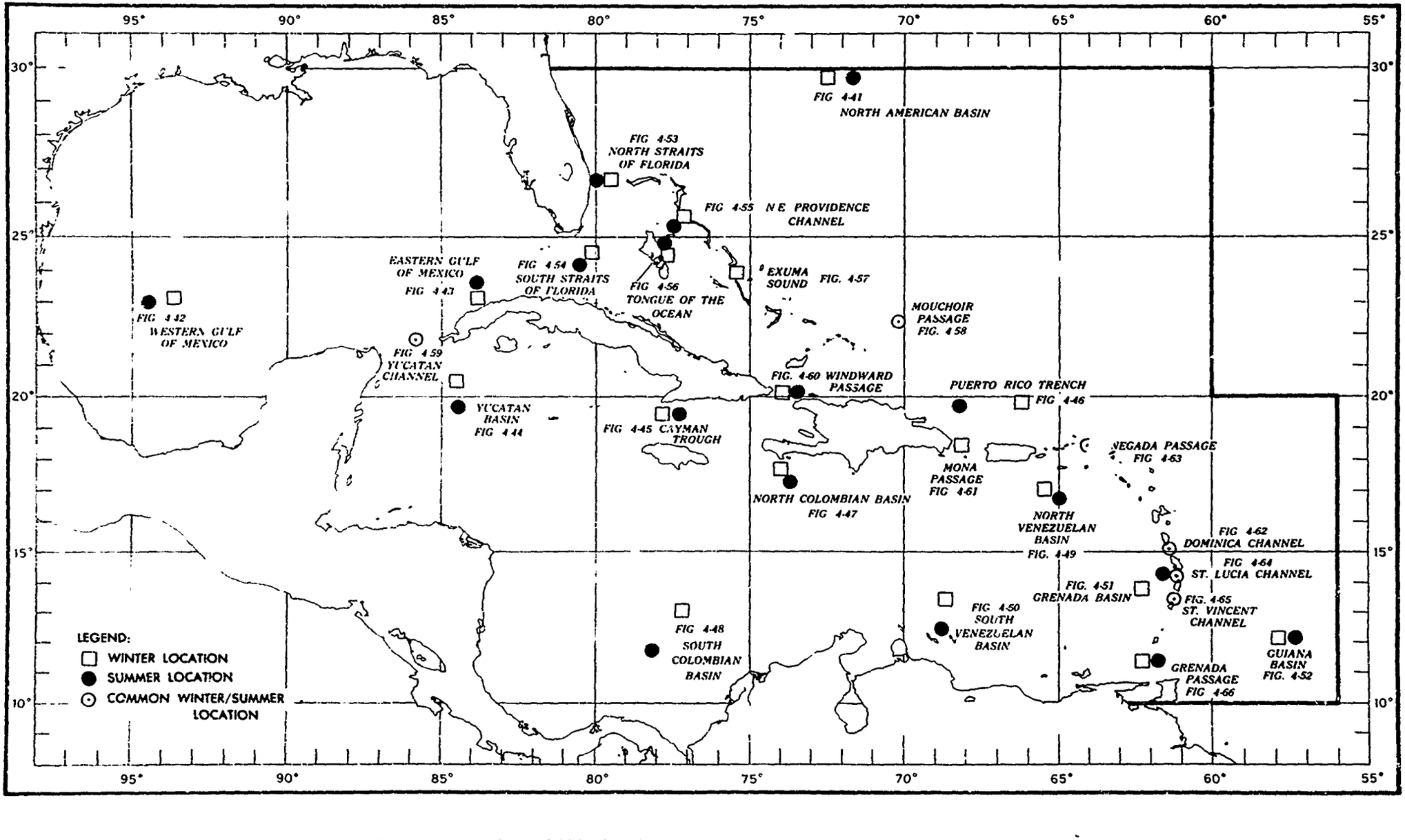

FIGURE 4-40 LOCATIONS OF SOUND VELOCITY/TEMPERATURE-SALINITY COMPARISONS

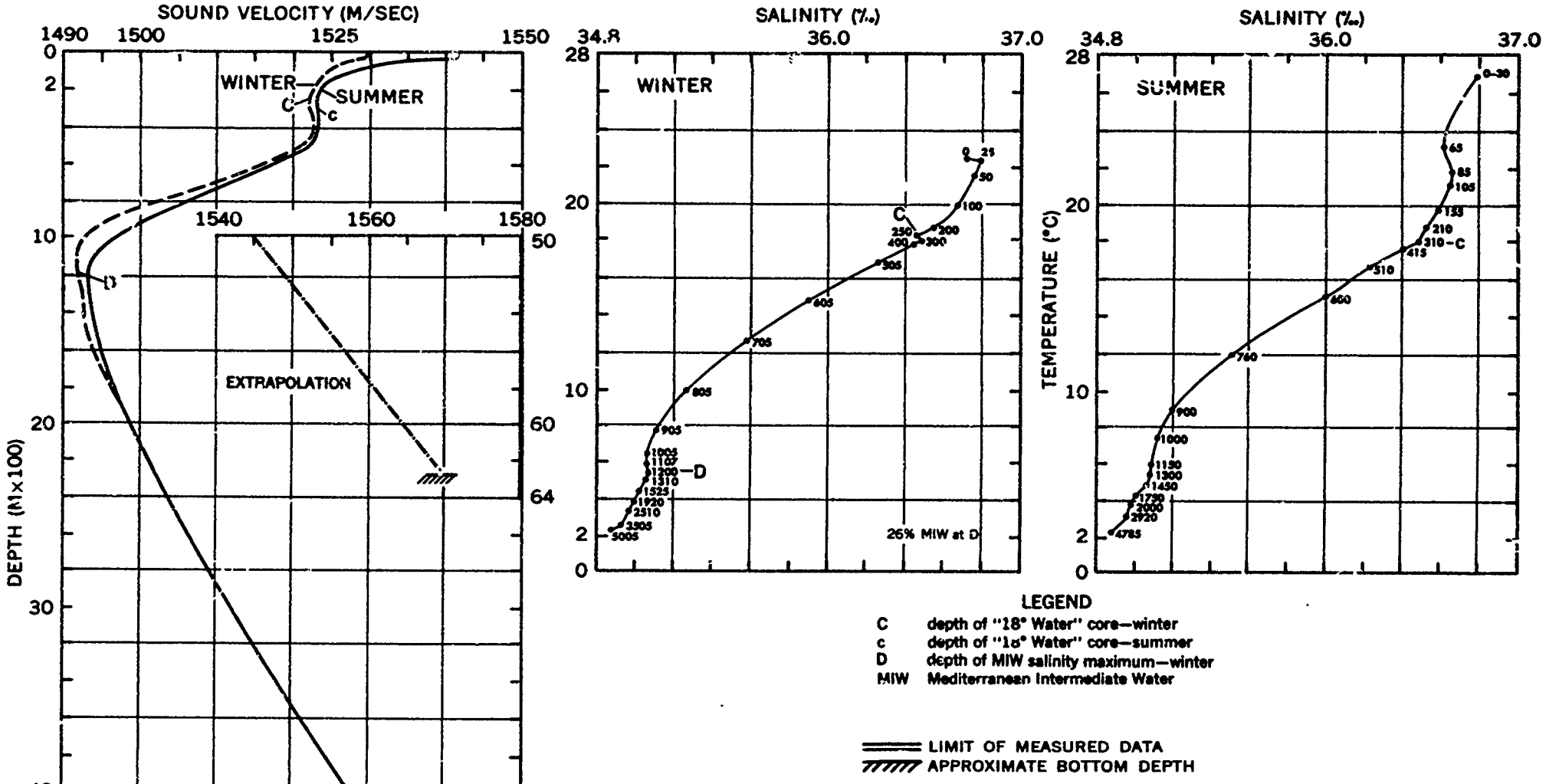

FIGURE 4-41 SOUND VELOCITY/TEMPERATURE-SALINITY COMPARISONS–NORTH AMERICAN BASIN

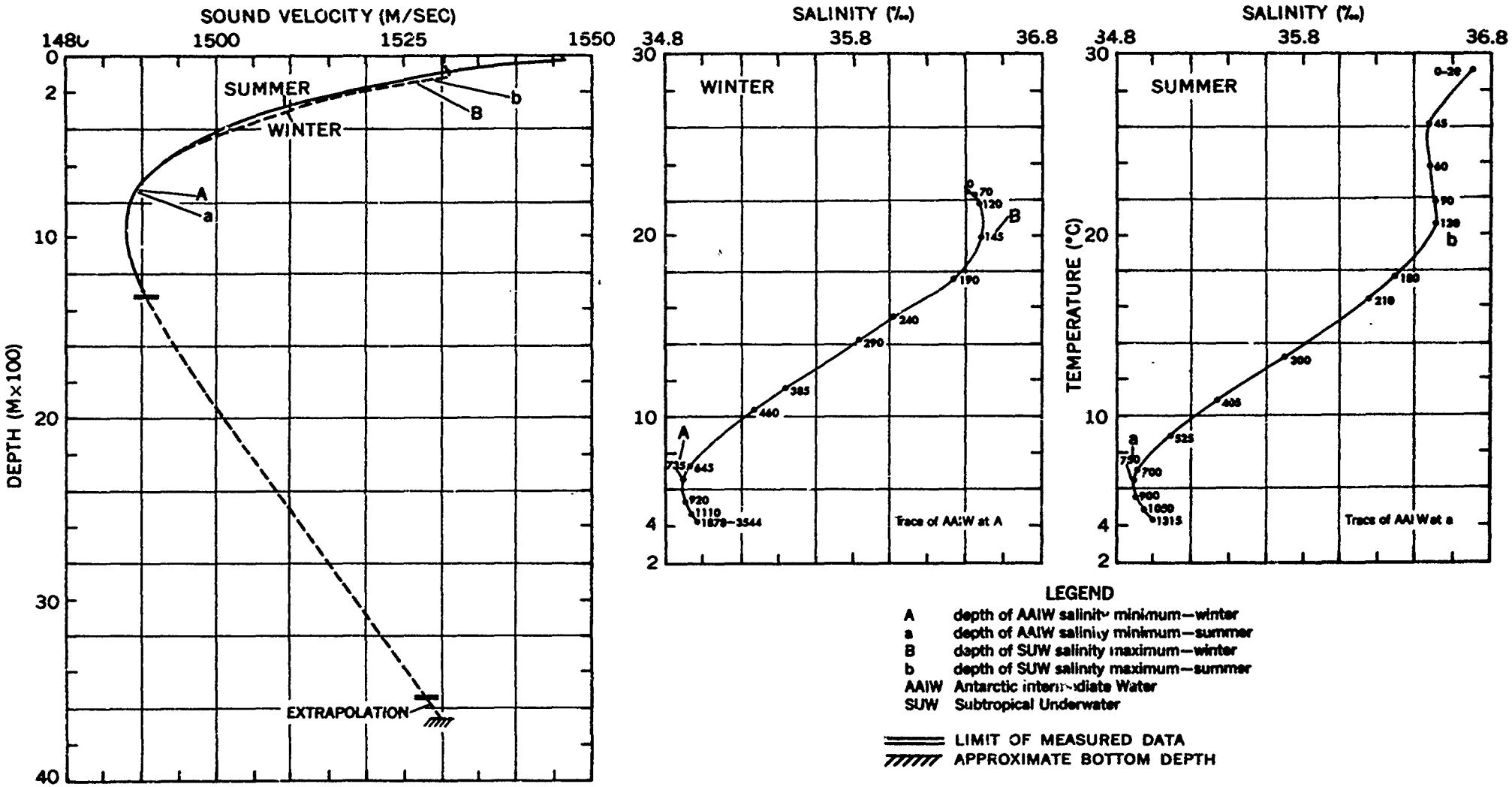

FIGURE 4-42 SOUND VELOCITY/TEMPERATURE-SALINITY COMPARISONS–WEST GULF OF MEXICO

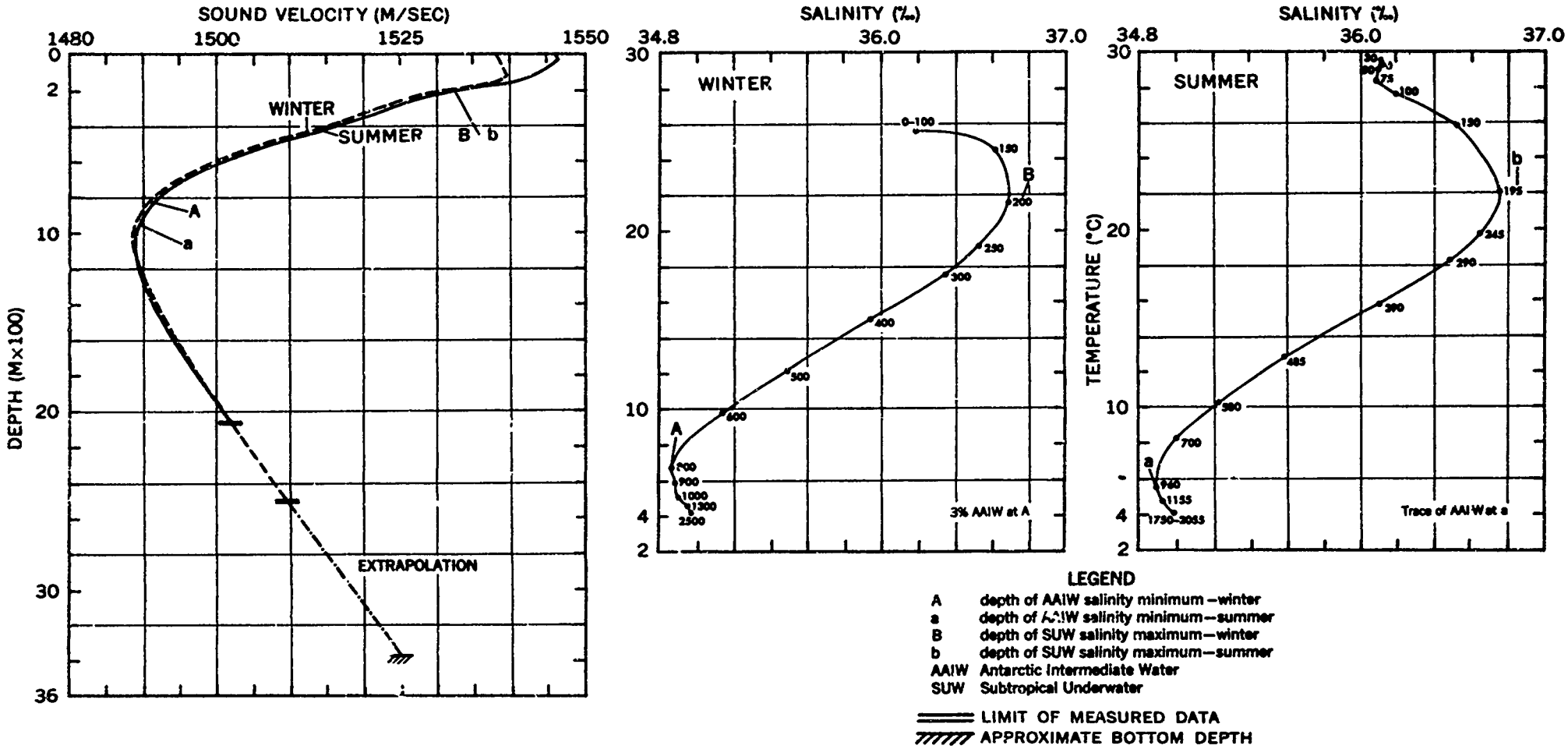

FIGURE 4-43 SOUND VELOCITY/TEMPERATURE-SALINITY COMPARISONS–EAST GULF OF MEXICO

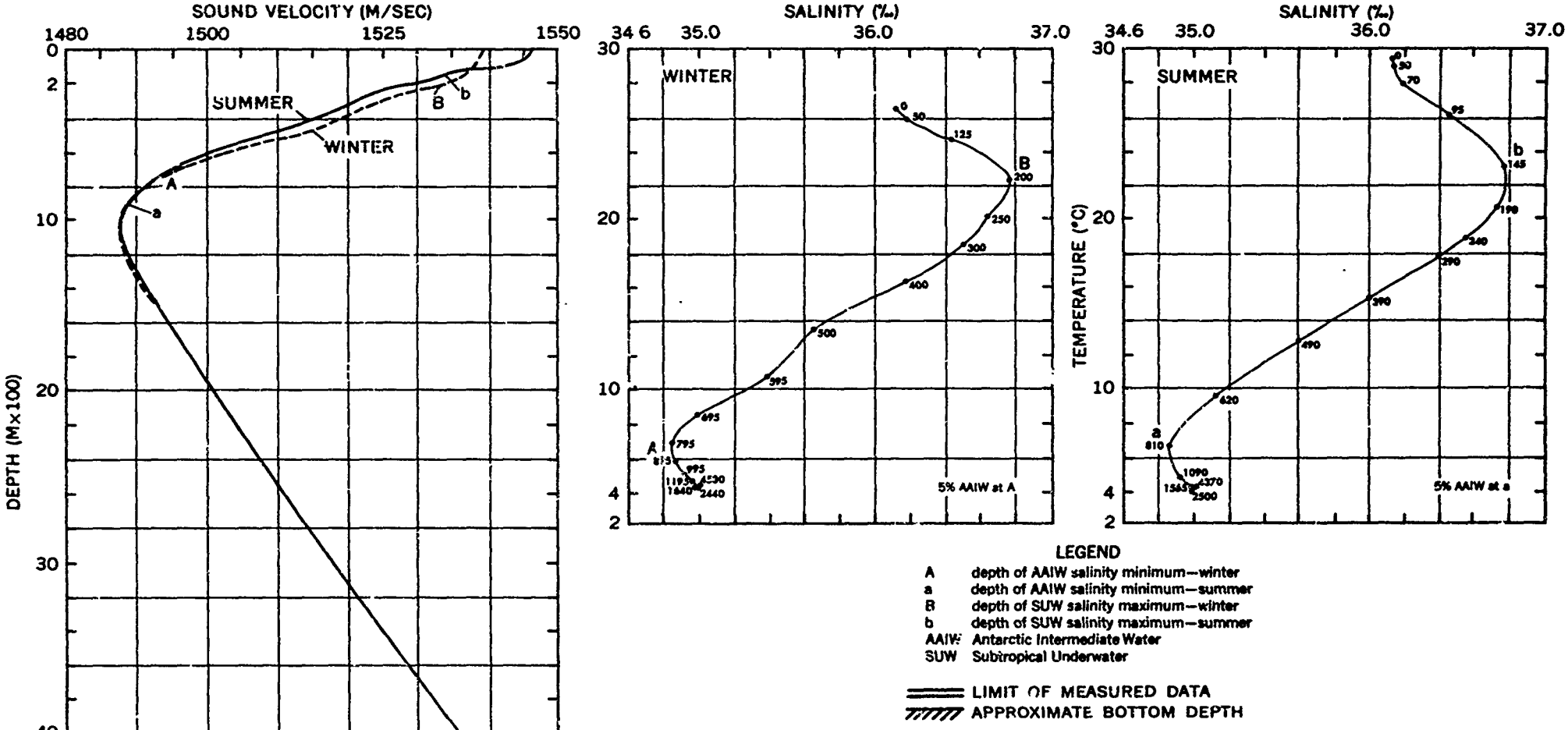

FIGURE 4-44 SOUND VELOCITY/TEMPERATURE-SALINITY COMPARISONS–YUCATAN BASIN

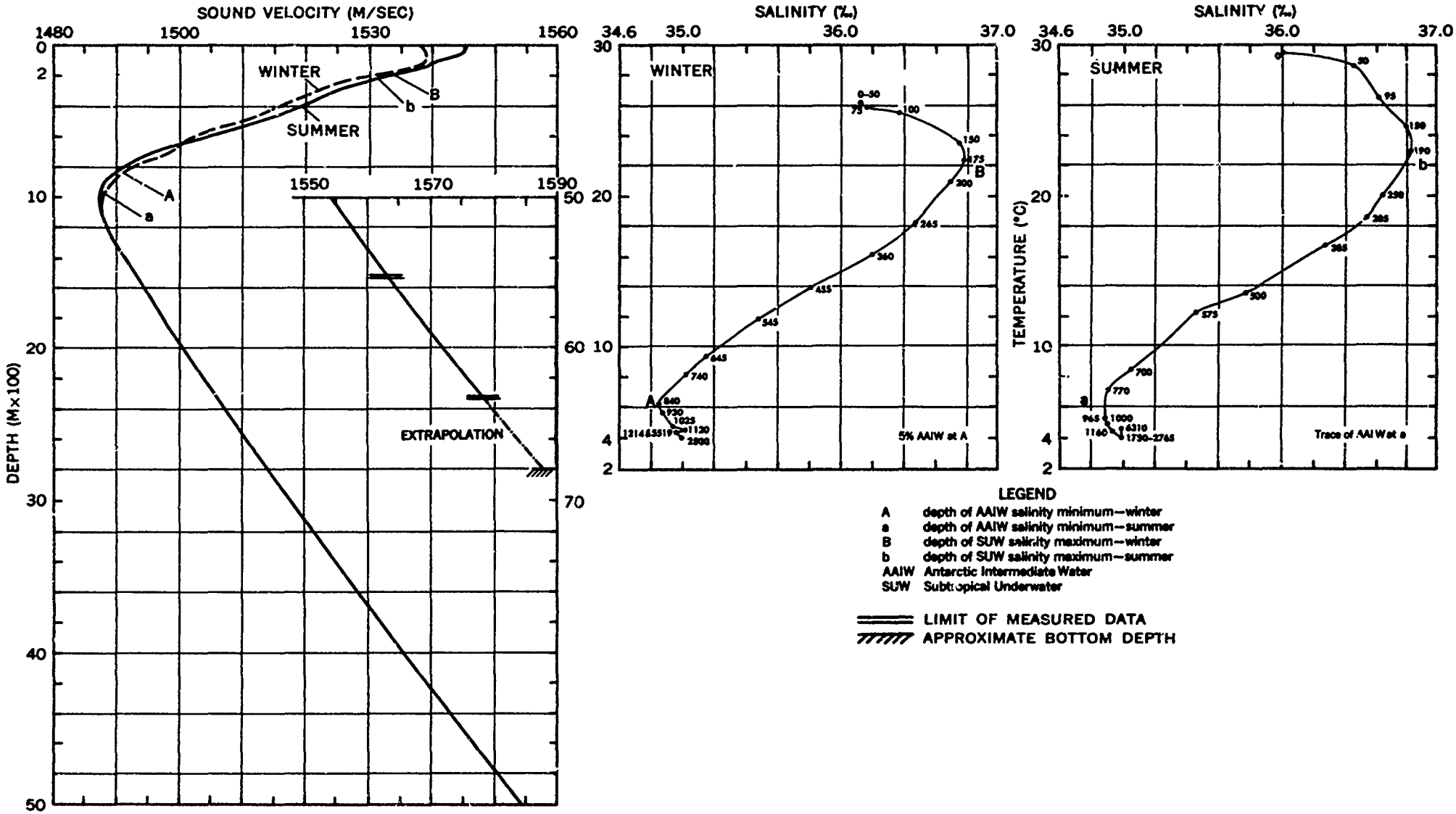

FIGURE 4-45 SOUND VELOCITY/TEMPERATURE-SALINITY COMPARISONS CAYMAN TROUGH

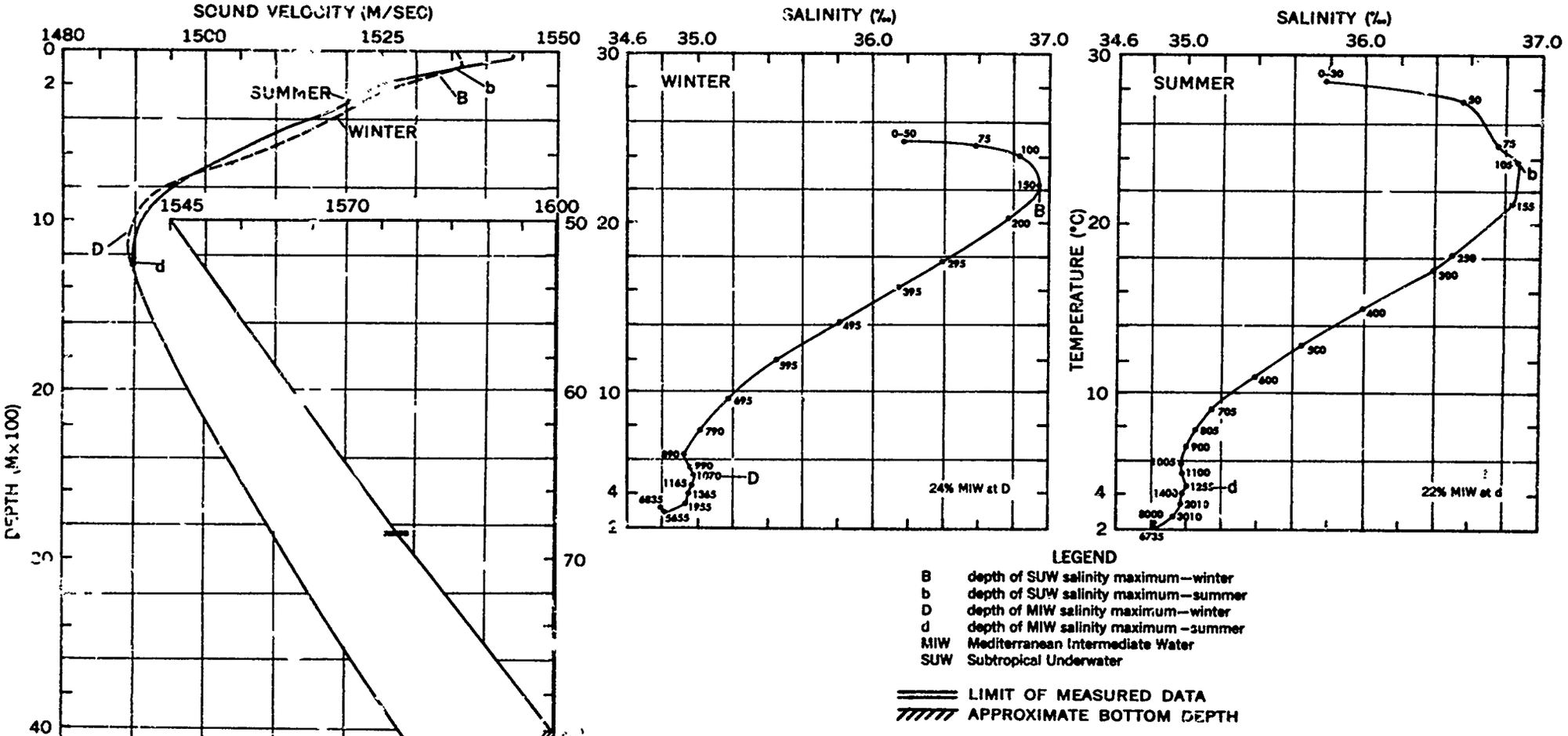

FIGURE 4-46 SOUND VELOCITY/TEMPERATURE-SALINITY COMPARISONS–PUERTO RICO TRENCH

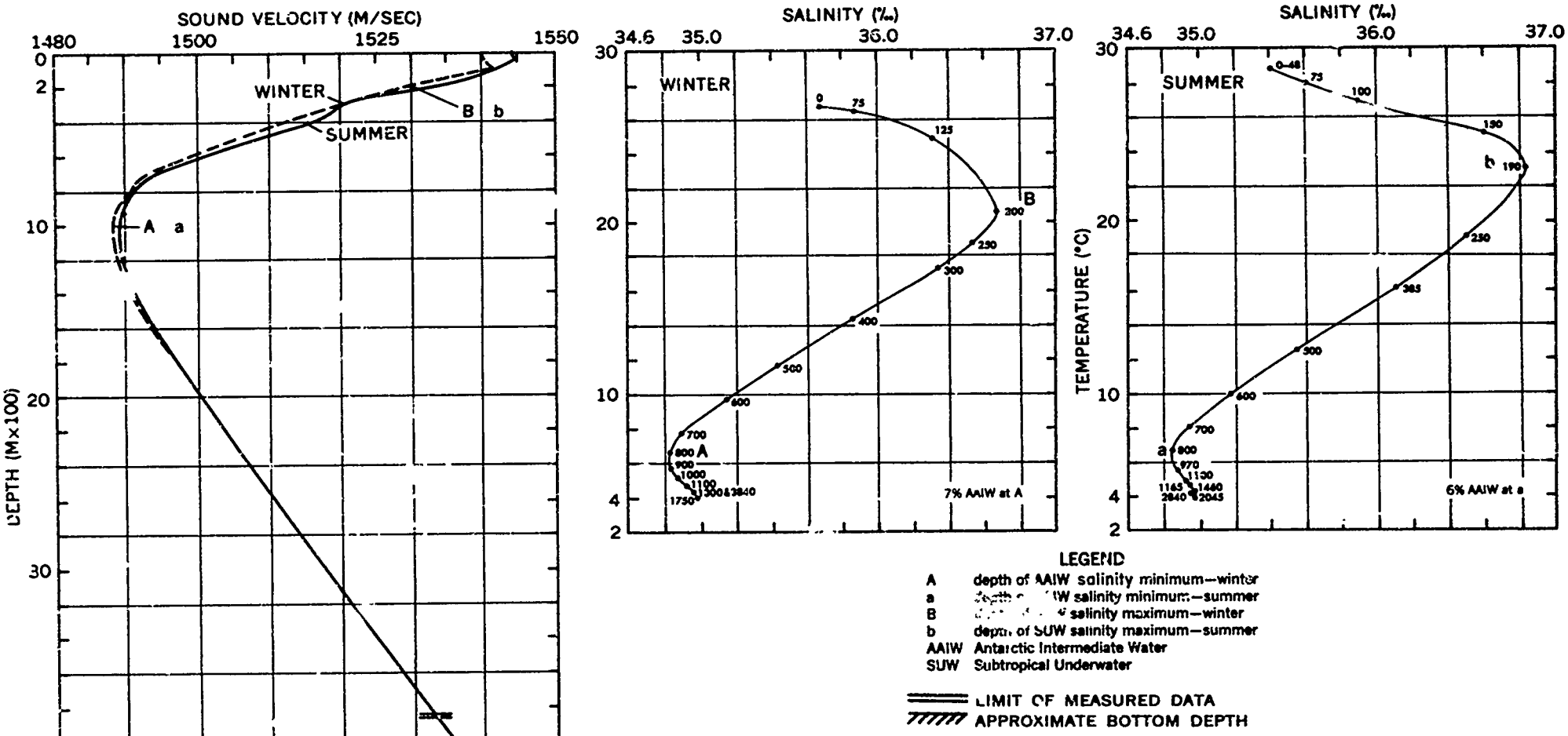

FIGURE 4-47 SOUND VELOCITY/TEMPERATURE-SALINITY COMPARISONS–NORTH COLOMBIAN BASIN

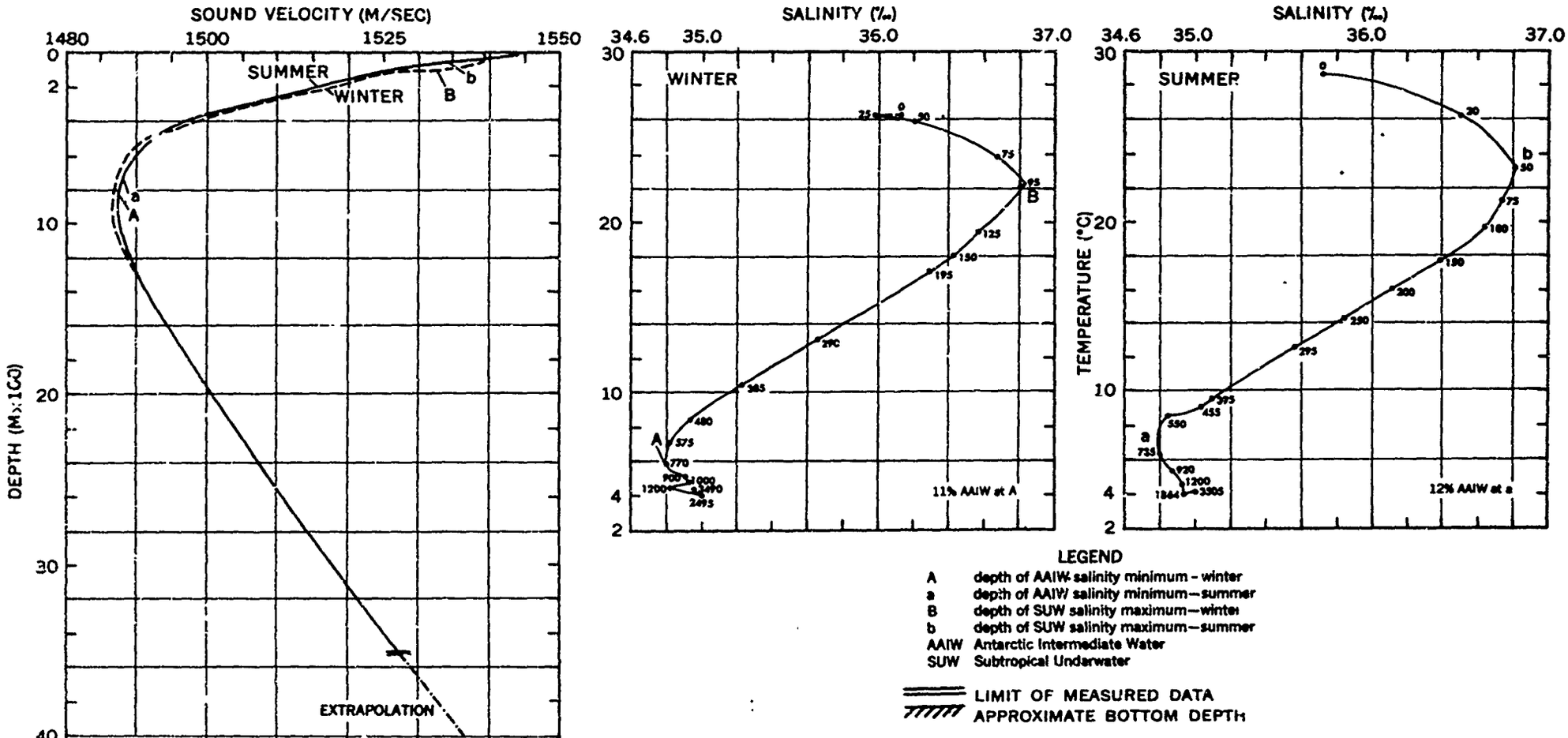

FIGURE 4-48 SOUND VELOCITY/TEMPERATURE-SALINITY COMPARISONS–SOUTH COLOMBIAN BASIN

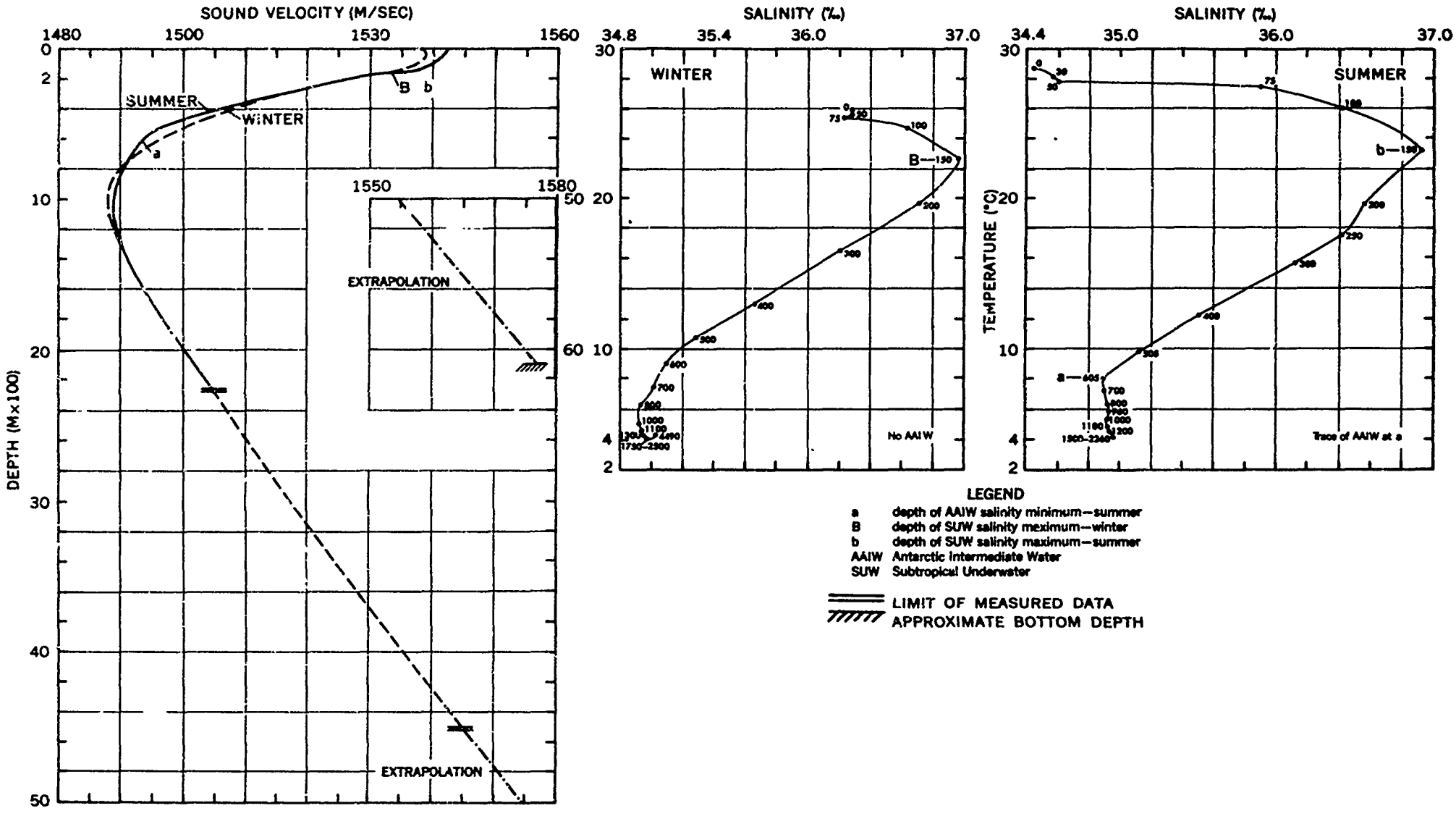

FIGURE 4-49 SOUND VELOCITY/TEMPERATURE-SALINITY COMPARISONS–NORTH VENEZUELAN BASIN

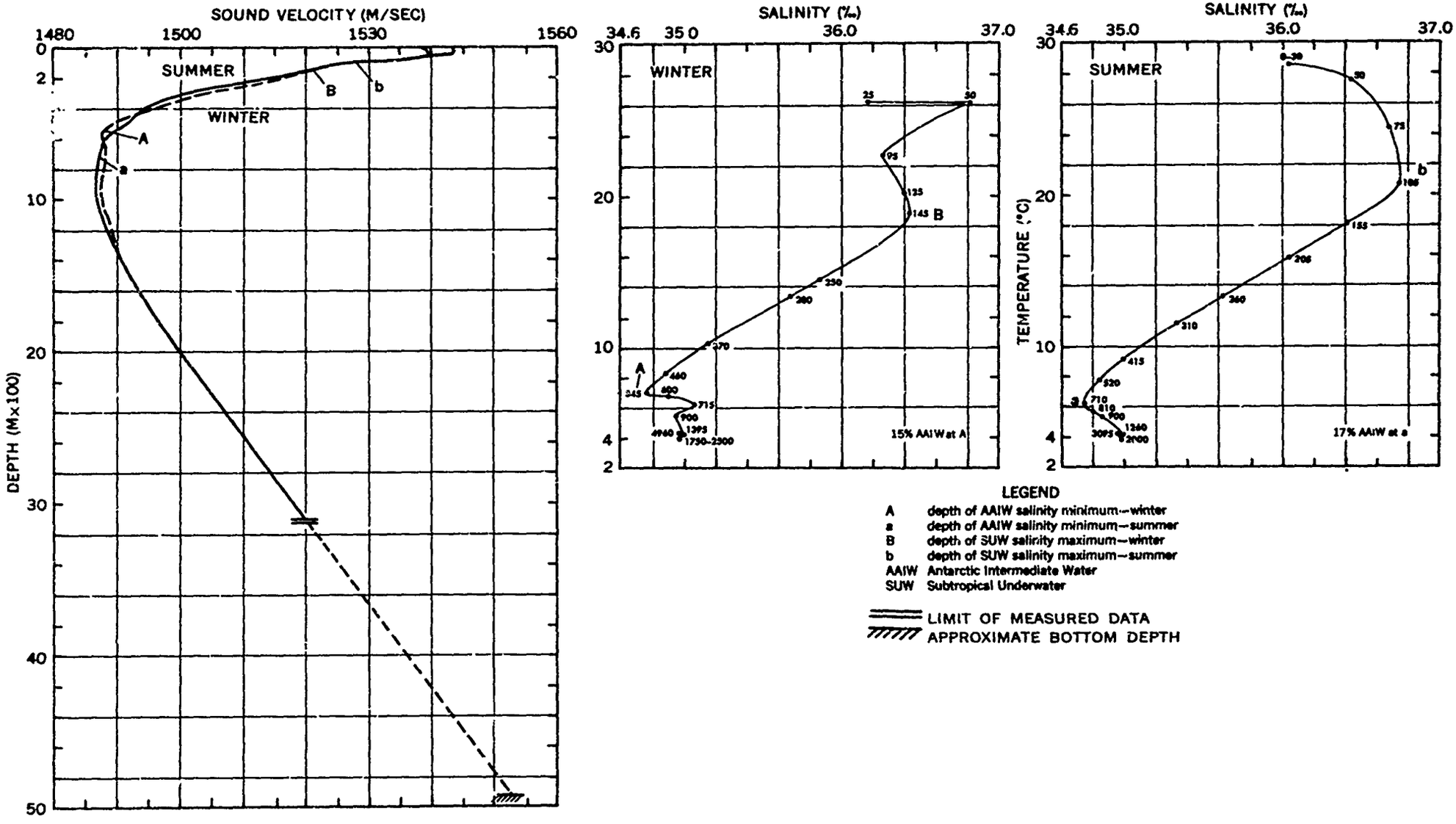

FIGURE 4-50 SOUND VELOCITY/TEMPERATURE-SALINITY COMPARISONS–SOUTH VENEZUELAN BASIN

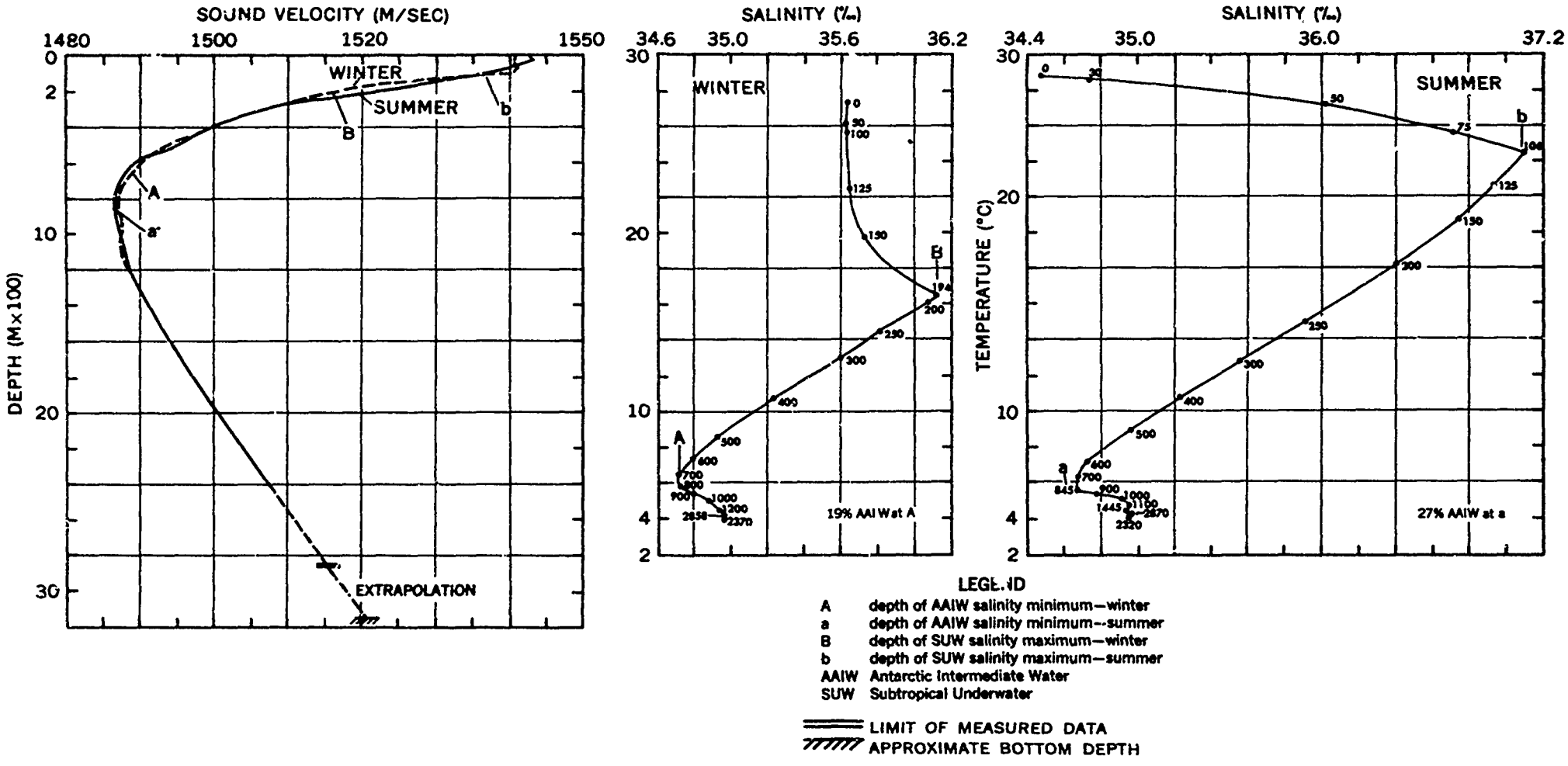

FIGURE 4-51 SOUND VELOCITY/TEMPERATURE-SALINITY COMPARISONS-GRENADA BASIN

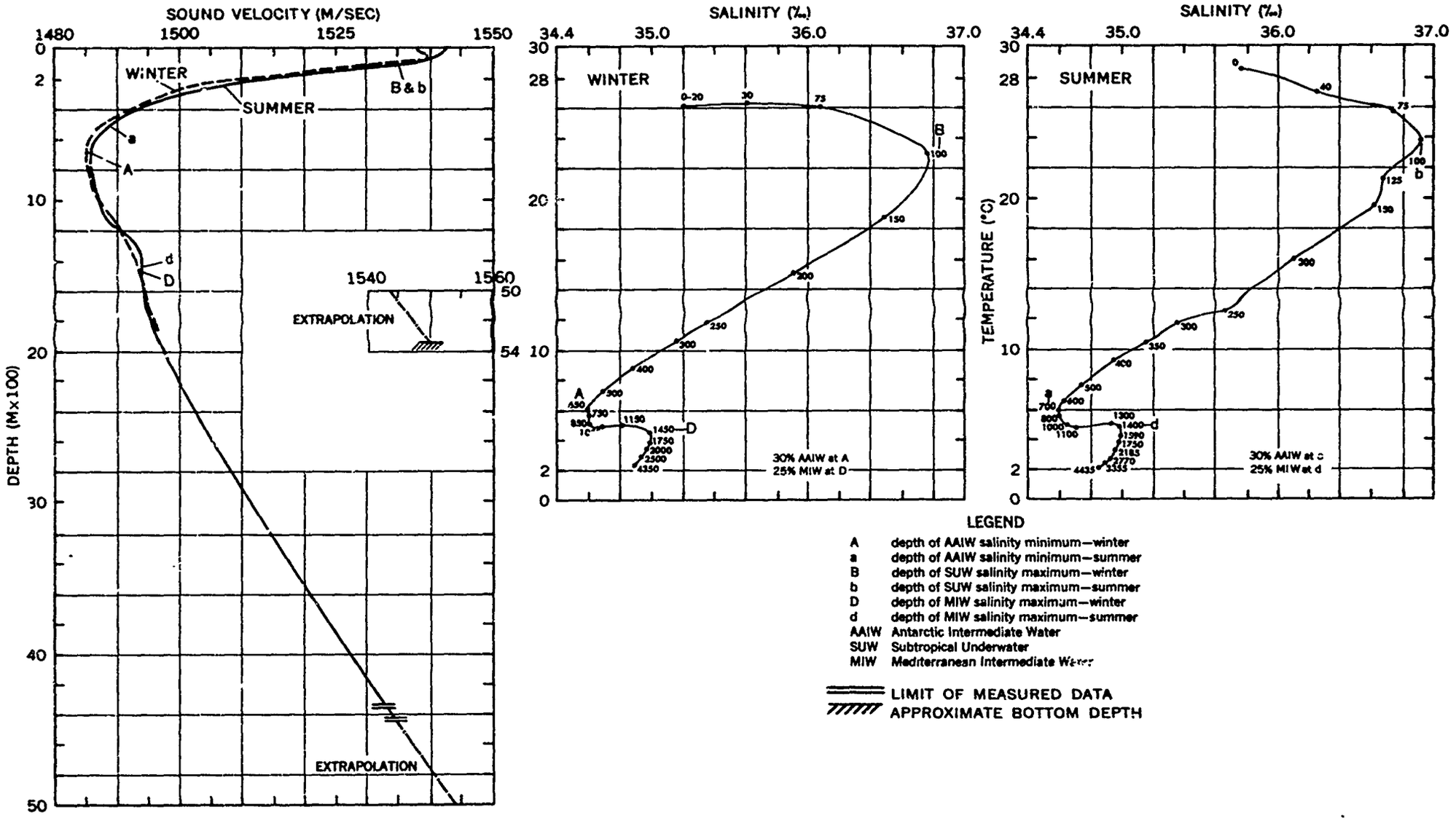

FIGURE 4-52 SOUND VELOCITY/TEMPERATURE-SALINITY COMPARISONS-GUIANA BASIN

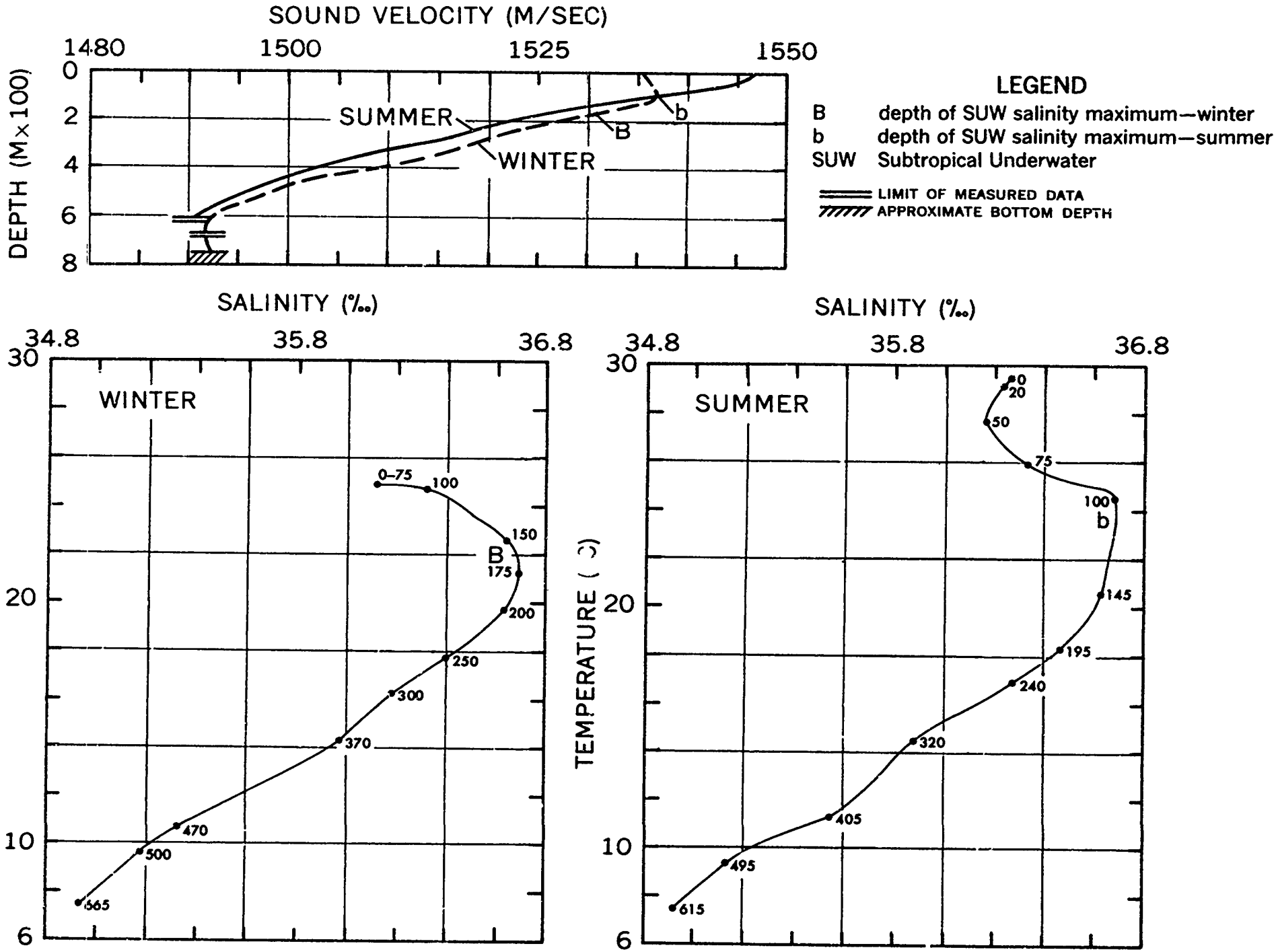

FIGURE 4-53 SOUND VELOCITY/TEMPERATURE-SALINITY COMPARISONS–FLORIDA STRAITS (NORTH)

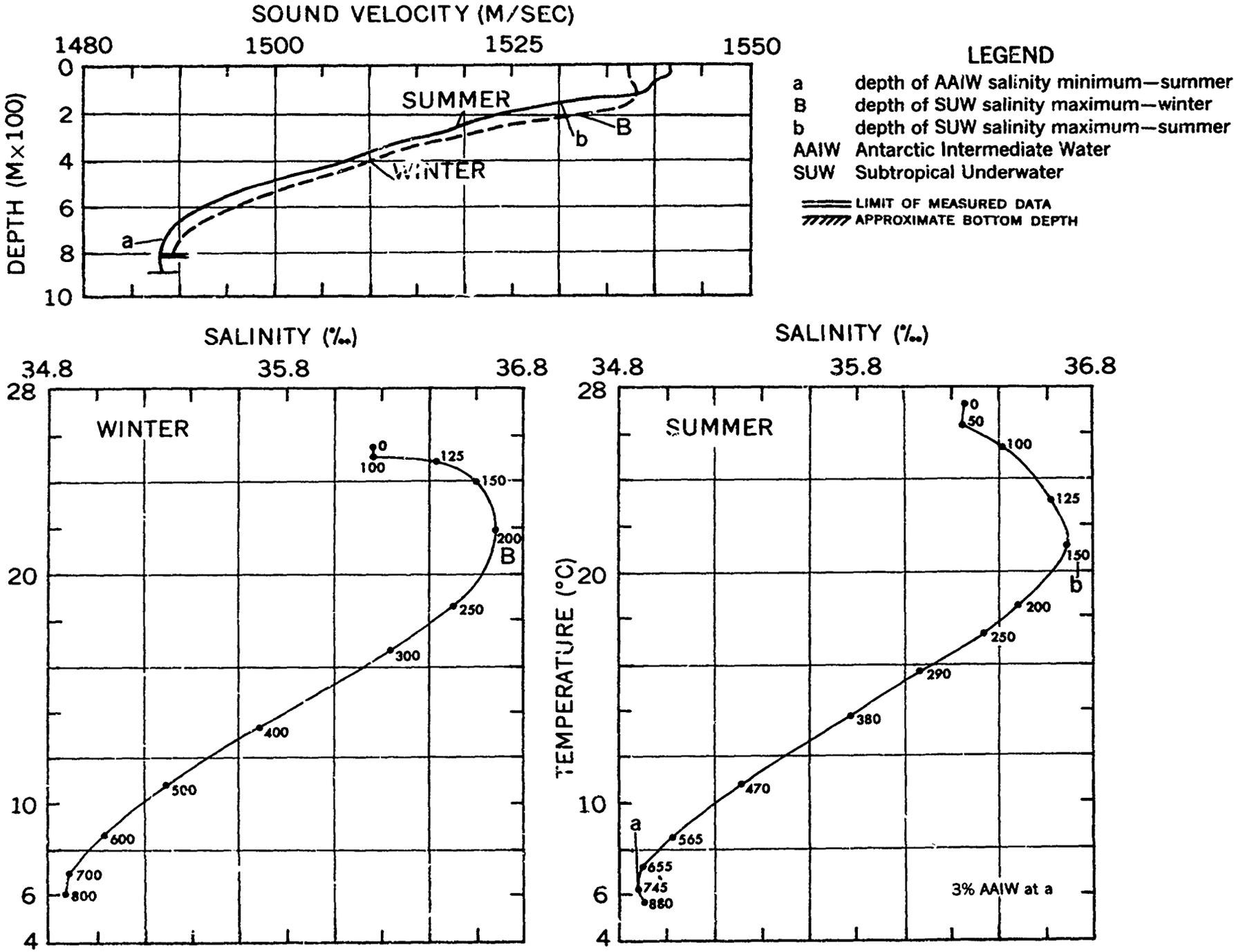

FIGURE 4-54 SOUND VELOCITY/TEMPERATURE-SALINITY COMPARISONS-FLORIDA STRAITS (SOUTH)

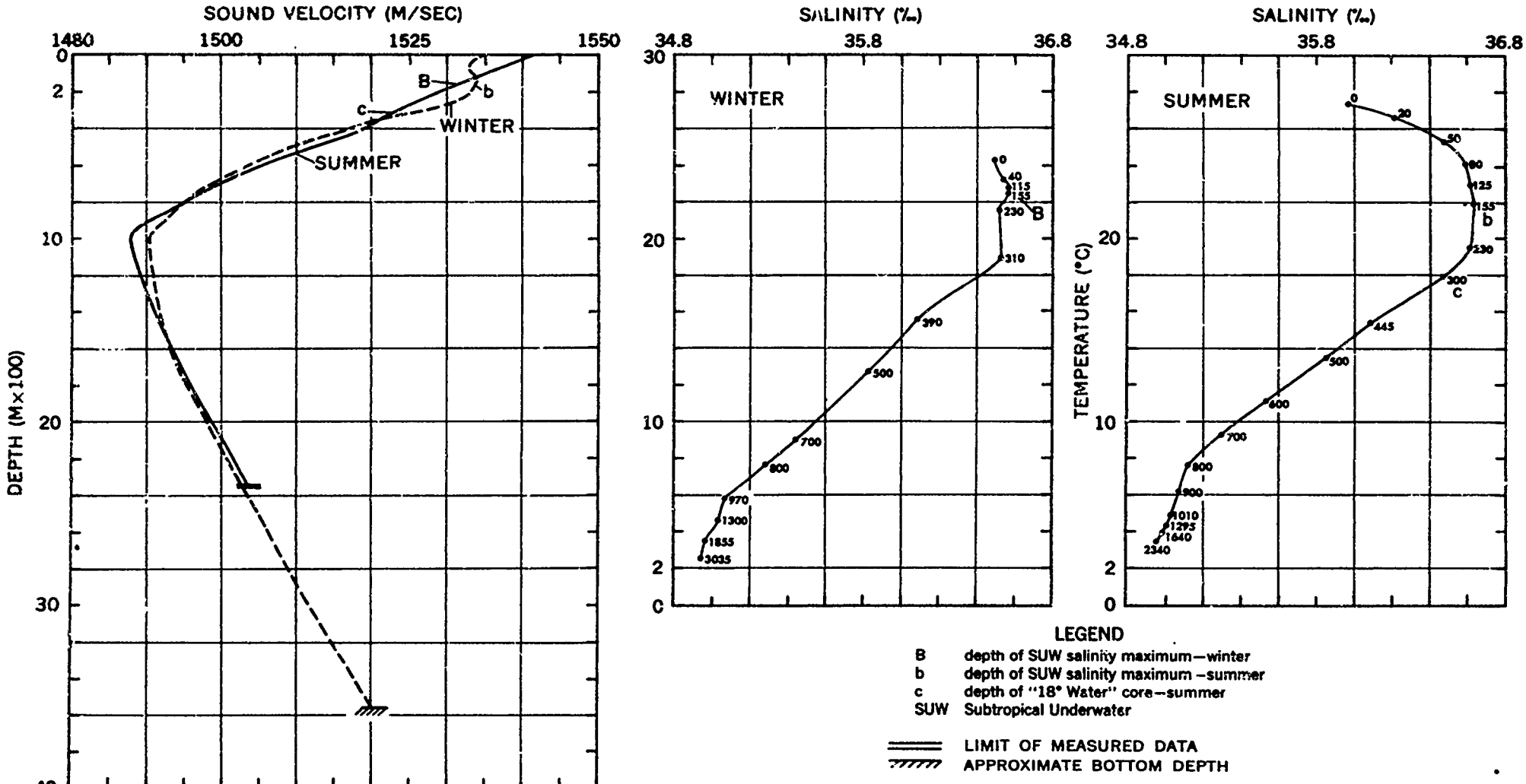

FIGURE 4-55 SOUND VELOCITY/TEMPERATURE-SALINITY COMPARISONS–NORTH EAST PROVIDENCE CHANNEL

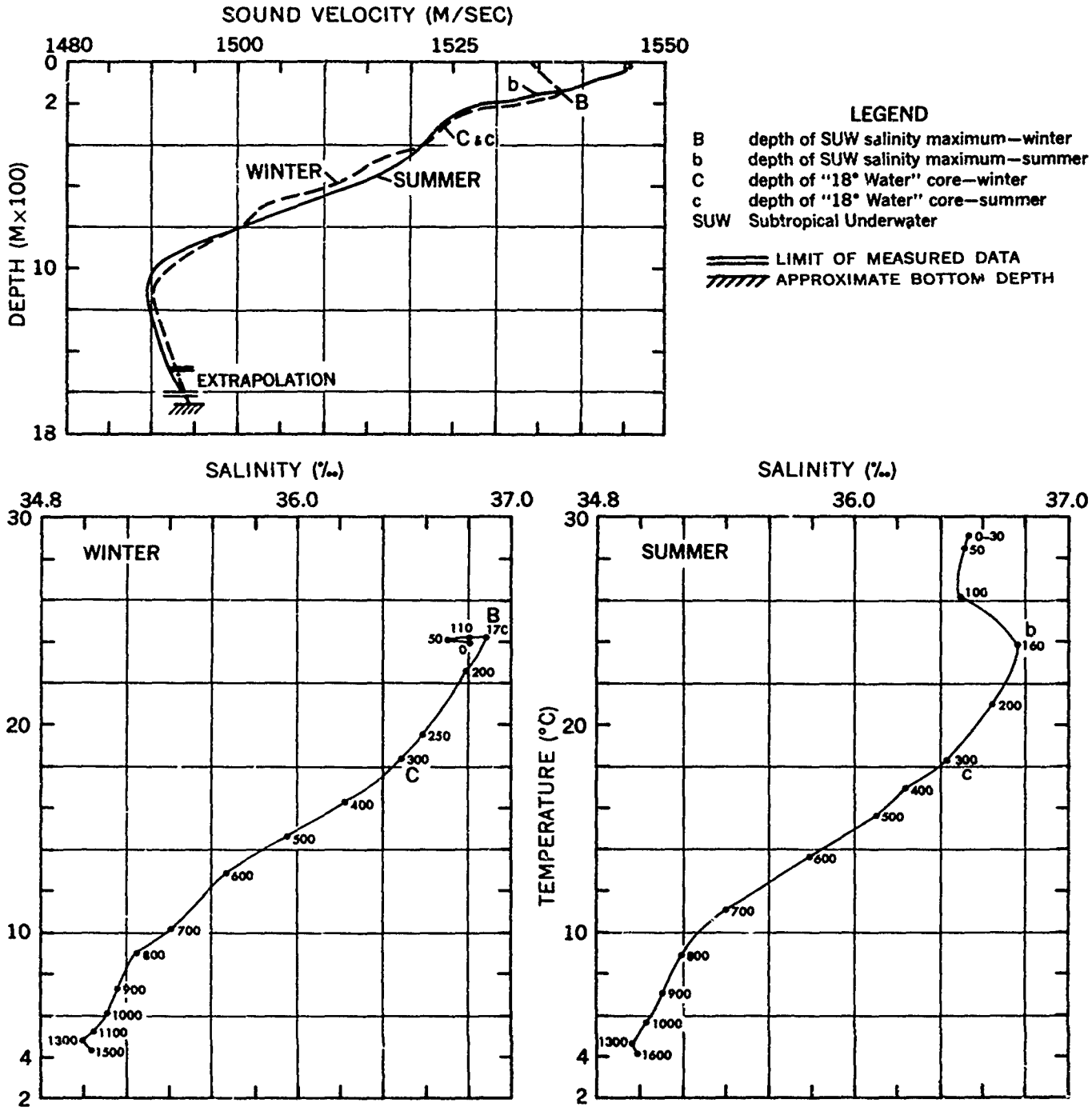

FIGURE 4-56 SOUND VELOCITY/TEMPERATURE-SALINITY COMPARISONS–TONGUE OF THE OCEAN, BAHAMAS

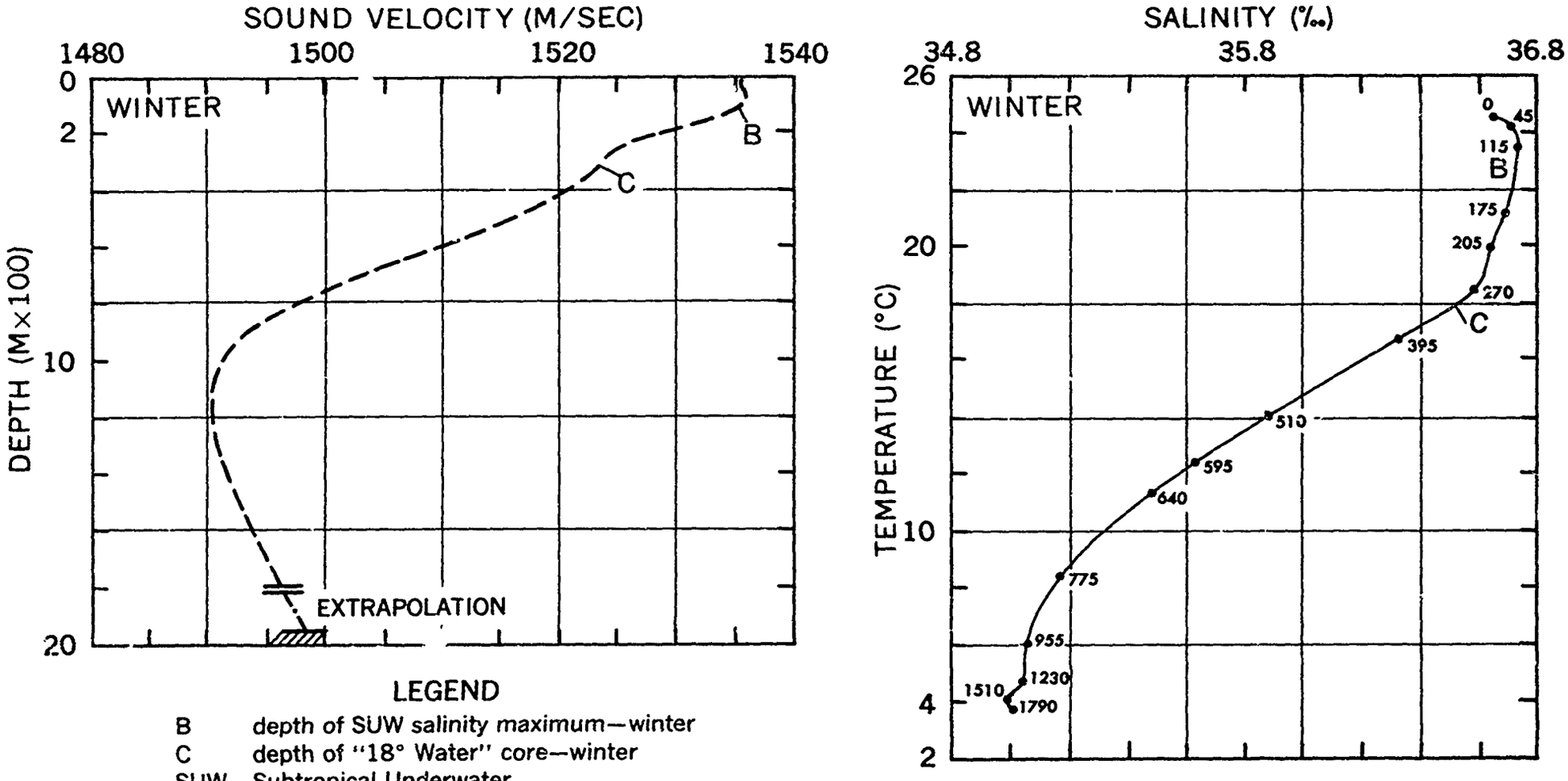

LEGEND

B depth of SUW salinity maximum—winter
C depth of "18° Water" core—winter
SUW Subtropical Underwater

NOTE: No summer observation available

LIMIT OF MEASURED DATA
APPROXIMATE BOTTOM DEPTH

FIGURE 4-57 SOUND VELOCITY/TEMPERATURE-SALINITY COMPARISONS–EXUMA SOUND, BAHAMAS

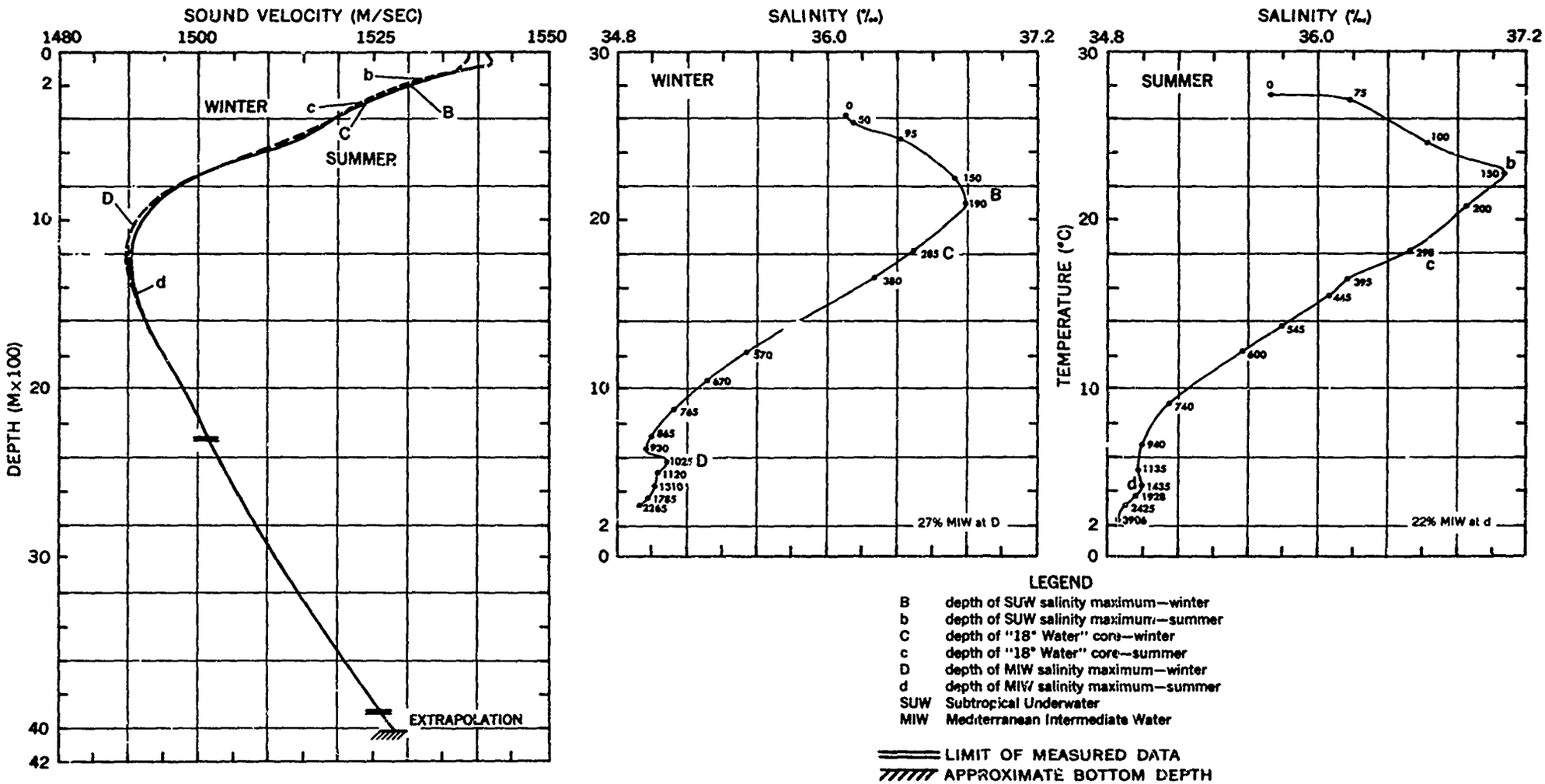

FIGURE 4-58 SOUND VELOCITY/TEMPERATURE-SALINITY COMPARISONS–MOUCHOIR PASSAGE

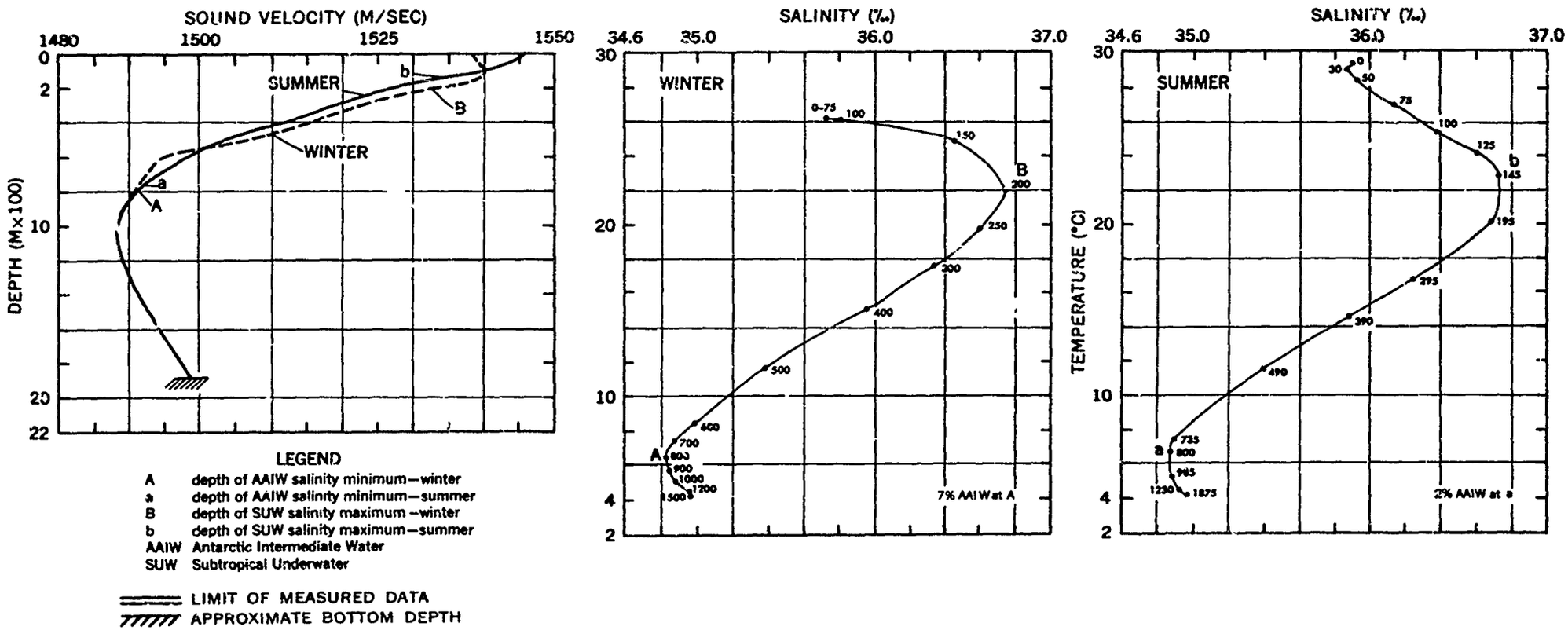

FIGURE 4-59 SOUND VELOCITY/TEMPERATURE-SALINITY COMPARISONS–YUCATAN CHANNEL

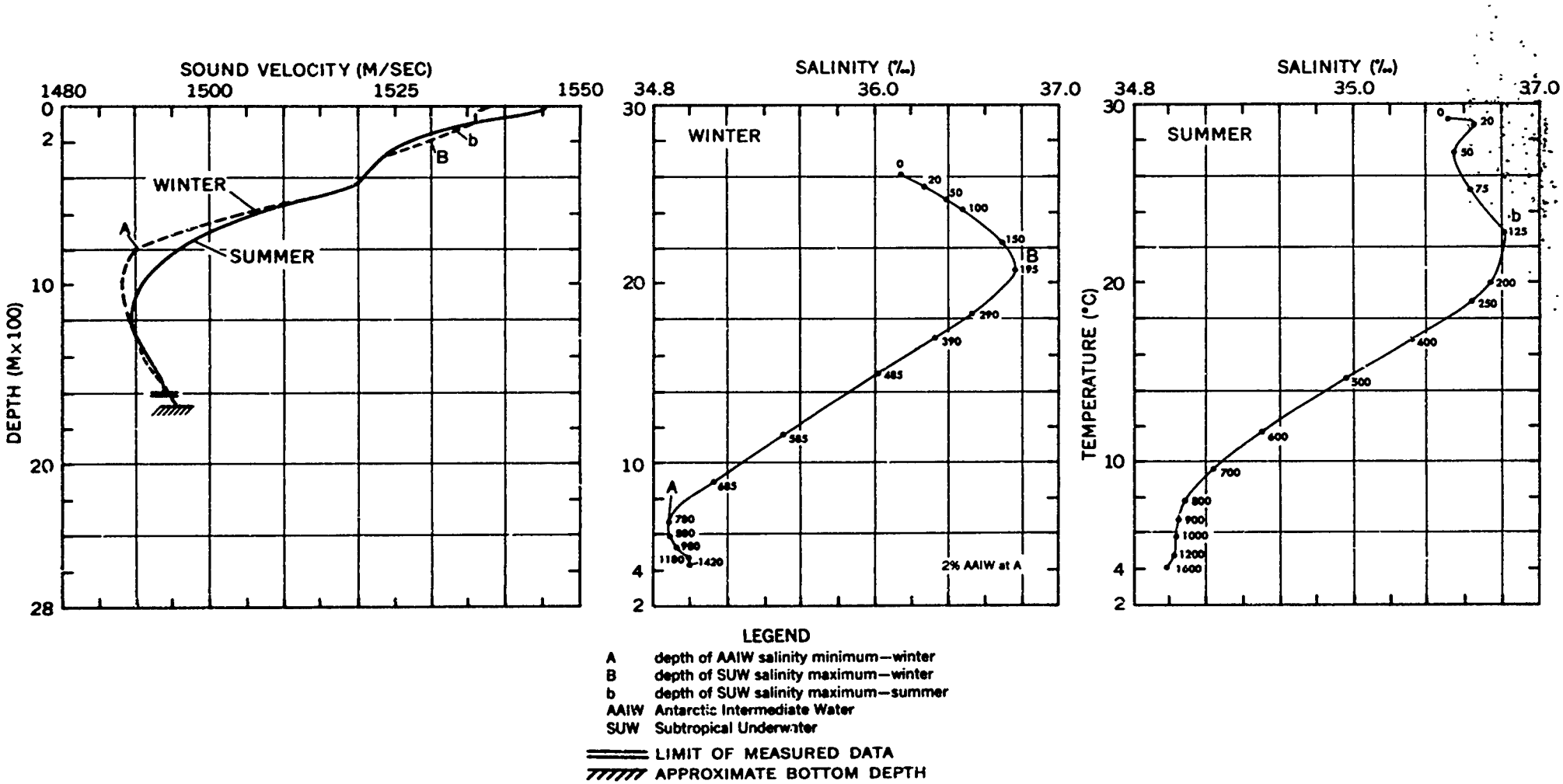

FIGURE 4-60 SOUND VELOCITY/TEMPERATURE-SALINITY COMPARISONS–WINDWARD PASSAGE

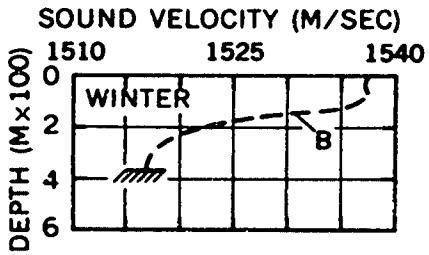

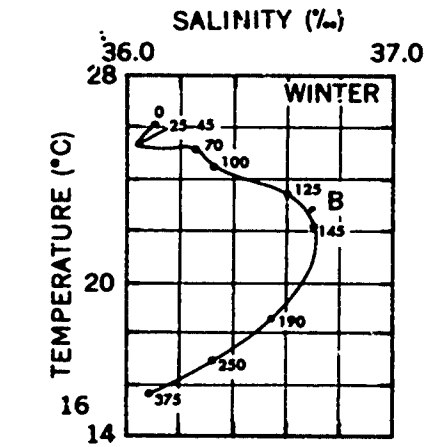

LEGEND

B depth of SUW salinity—winter
SUW Subtropical Underwater

NOTE: No summer observation available

FIGURE 4-61 SOUND VELOCITY/TEMPERATURE-SALINITY COMPARISONS–MONA PASSAGE

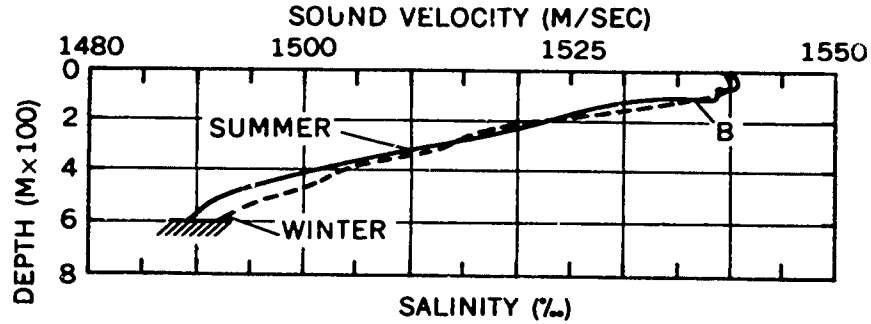

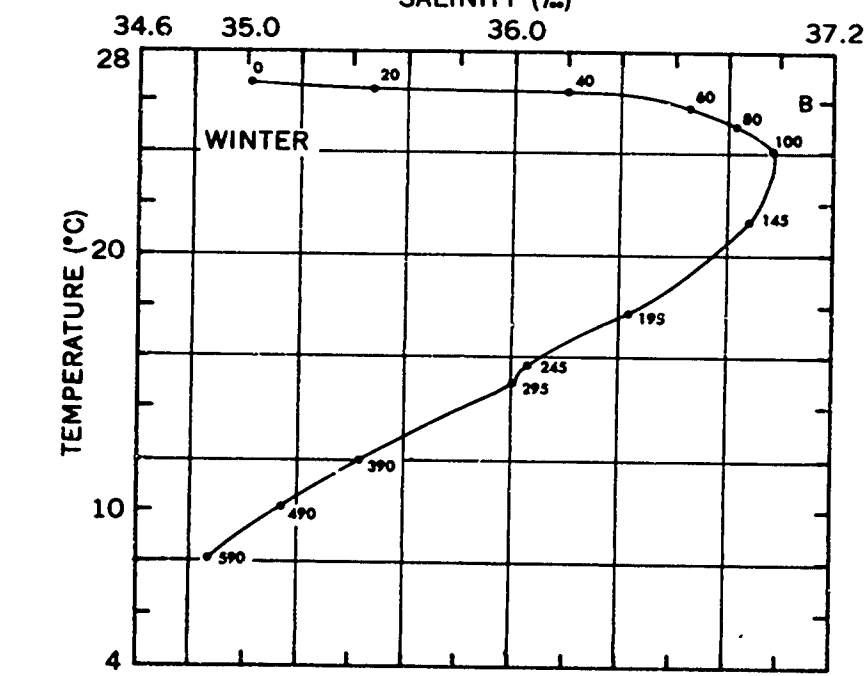

LEGEND

A depth of AAIW salinity minimum—winter
a depth of AAIW salinity minimum—summer
B depth of SUW salinity maximum—winter
b depth of SUW salinity maximum—summer
D depth of MIW salinity maximum—winter
d depth of MIW salinity maximum—summer
AAIW Antarctic Intermediate Water
SUW Subtropical Underwater
MIW Mediterranean Intermediate Water

FIGURE 4-62 SOUND VELOCITY/TEMPERATURE-SALINITY COMPARISONS–DOMINICA CHANNEL

LIMIT OF MEASURED DATA
APPROXIMATE BOTTOM DEPTH

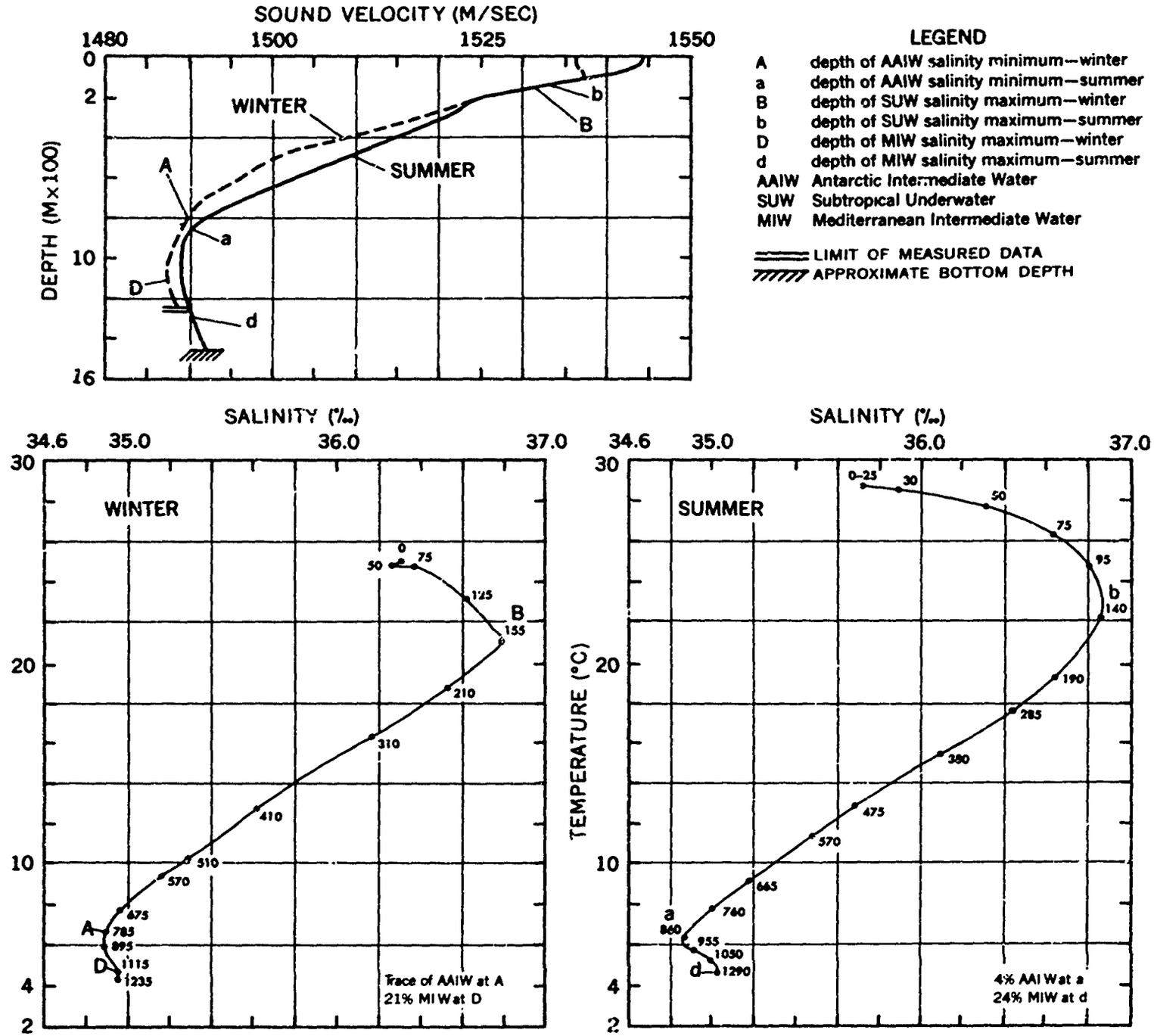

FIGURE 4-63 SOUND VELOCITY/TEMPERTURE-SALINITY COMPARISONS-ANEGADA PASSAGE

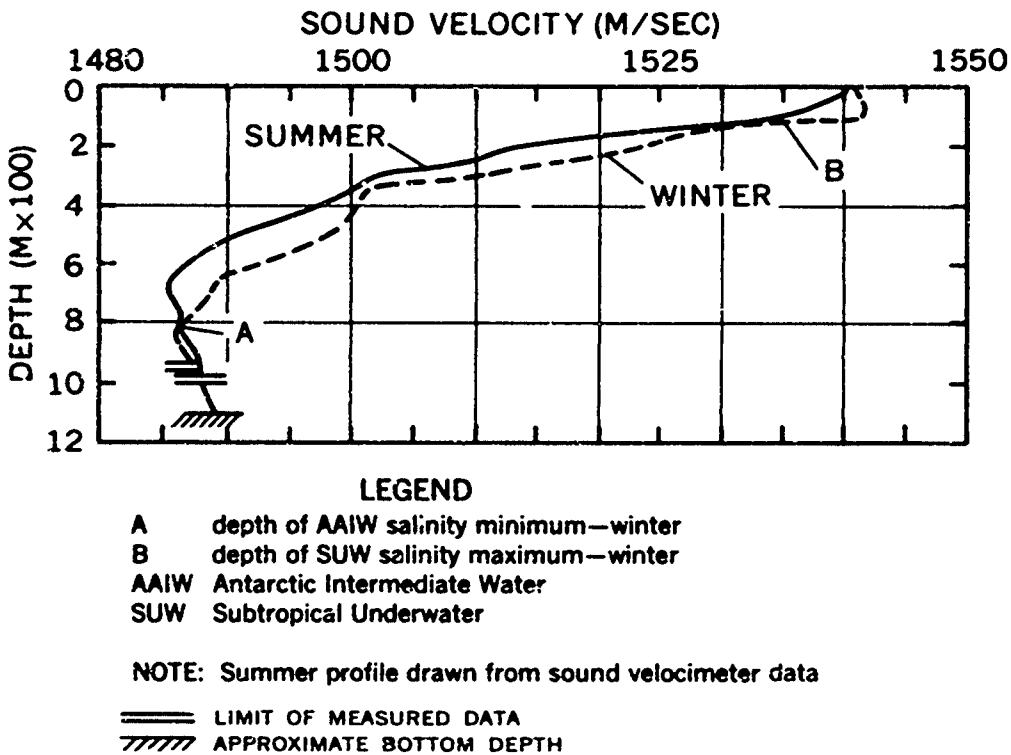

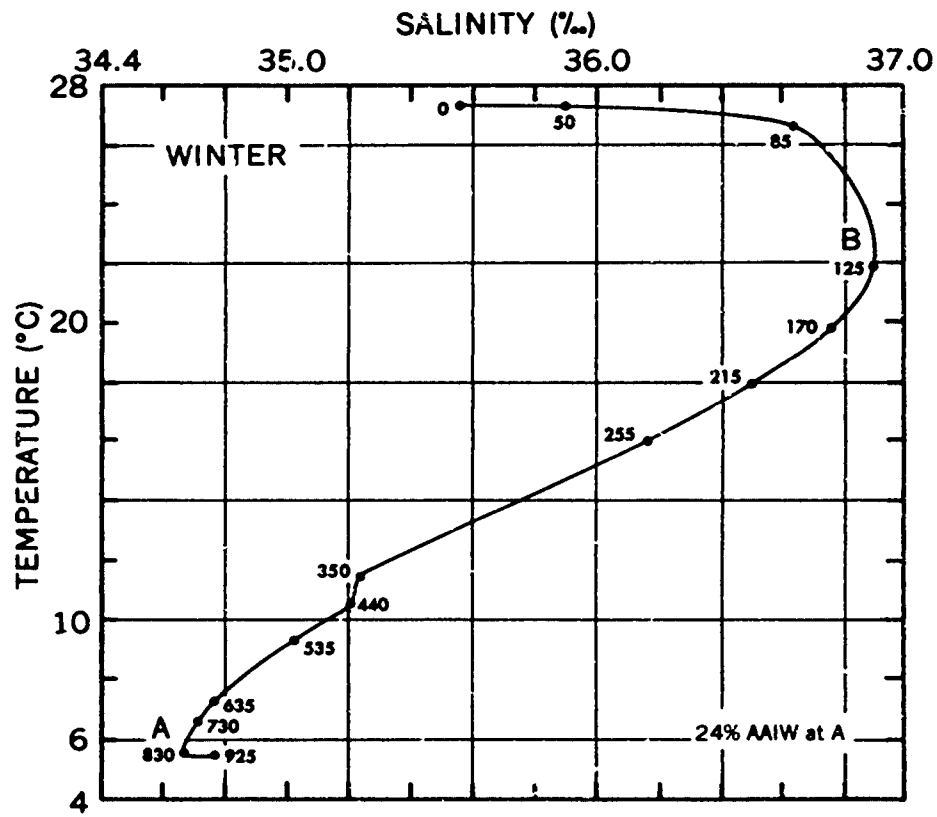

FIGURE 4-64 SOUND VELOCITY/TEMPERATURE-SALINITY COMPARISONS–ST. LUCIA CHANNEL

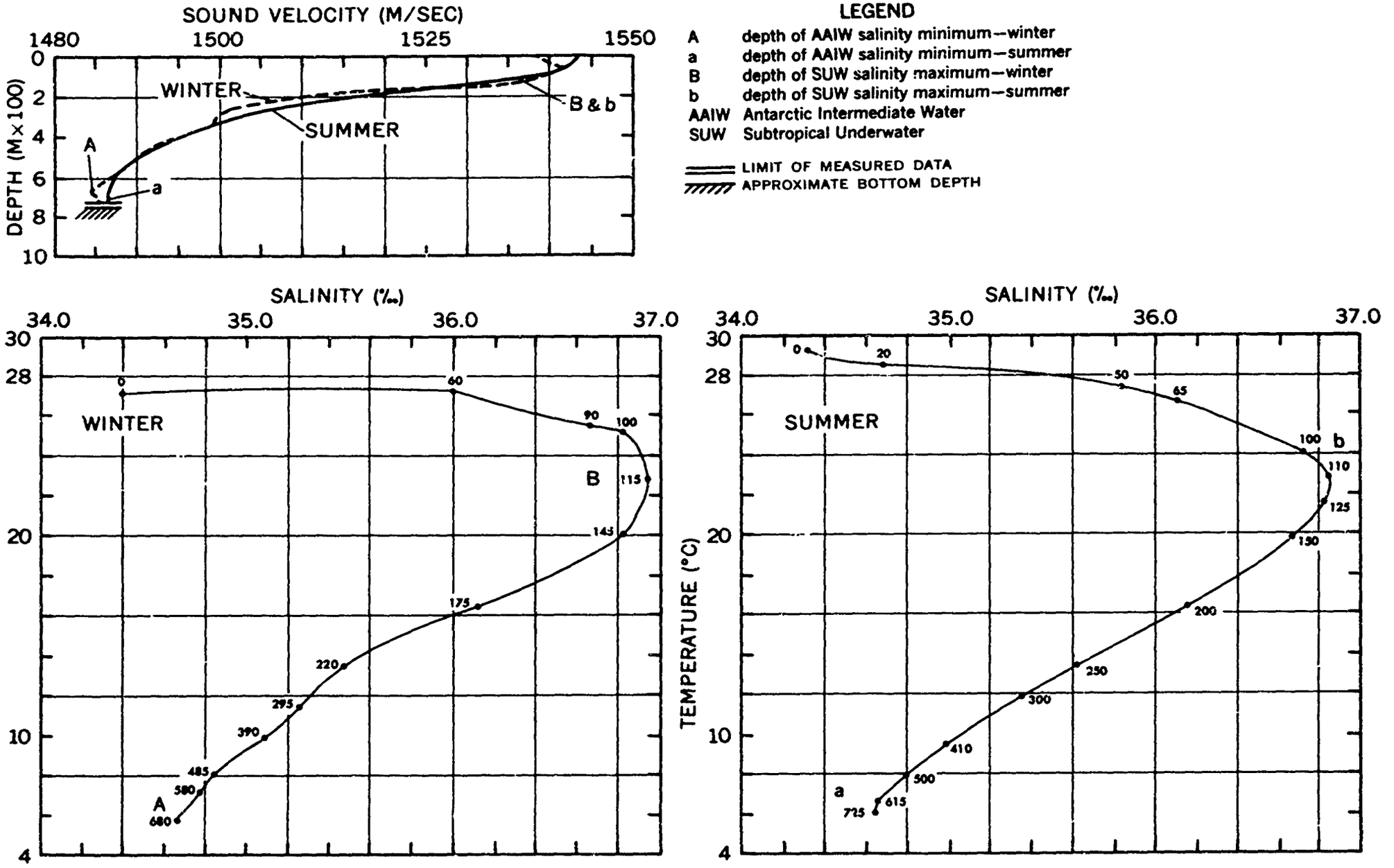

FIGURE 4-65 SOUND VELOCITY/TEMPERATURE-SALINITY COMPARISONS-ST. VINCENT CHANNEL

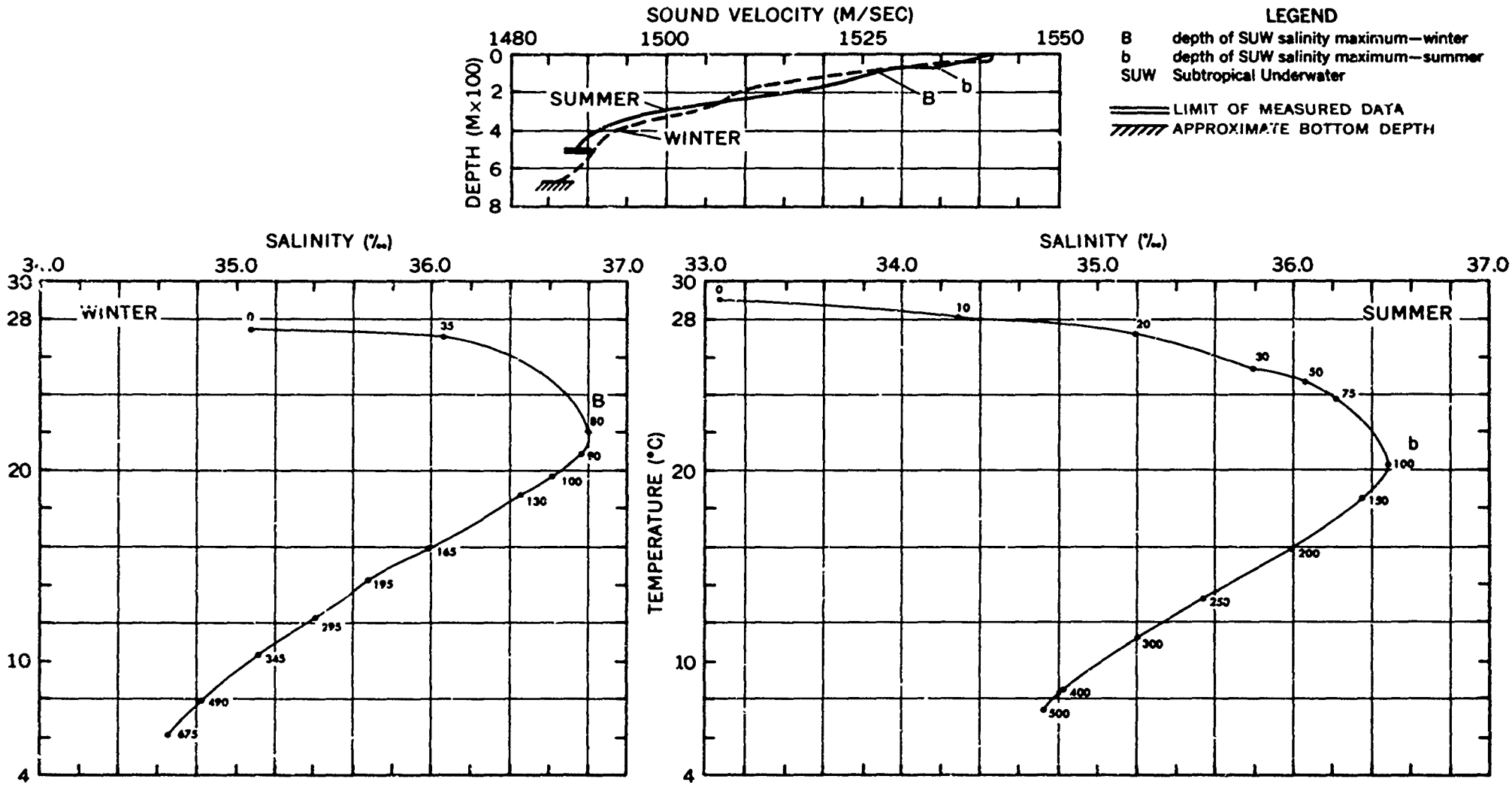

FIGURE 4-66 SOUND VELOCITY/TEMPERATURE-SALINITY COMPARISONS-GRENADA PASSAGE

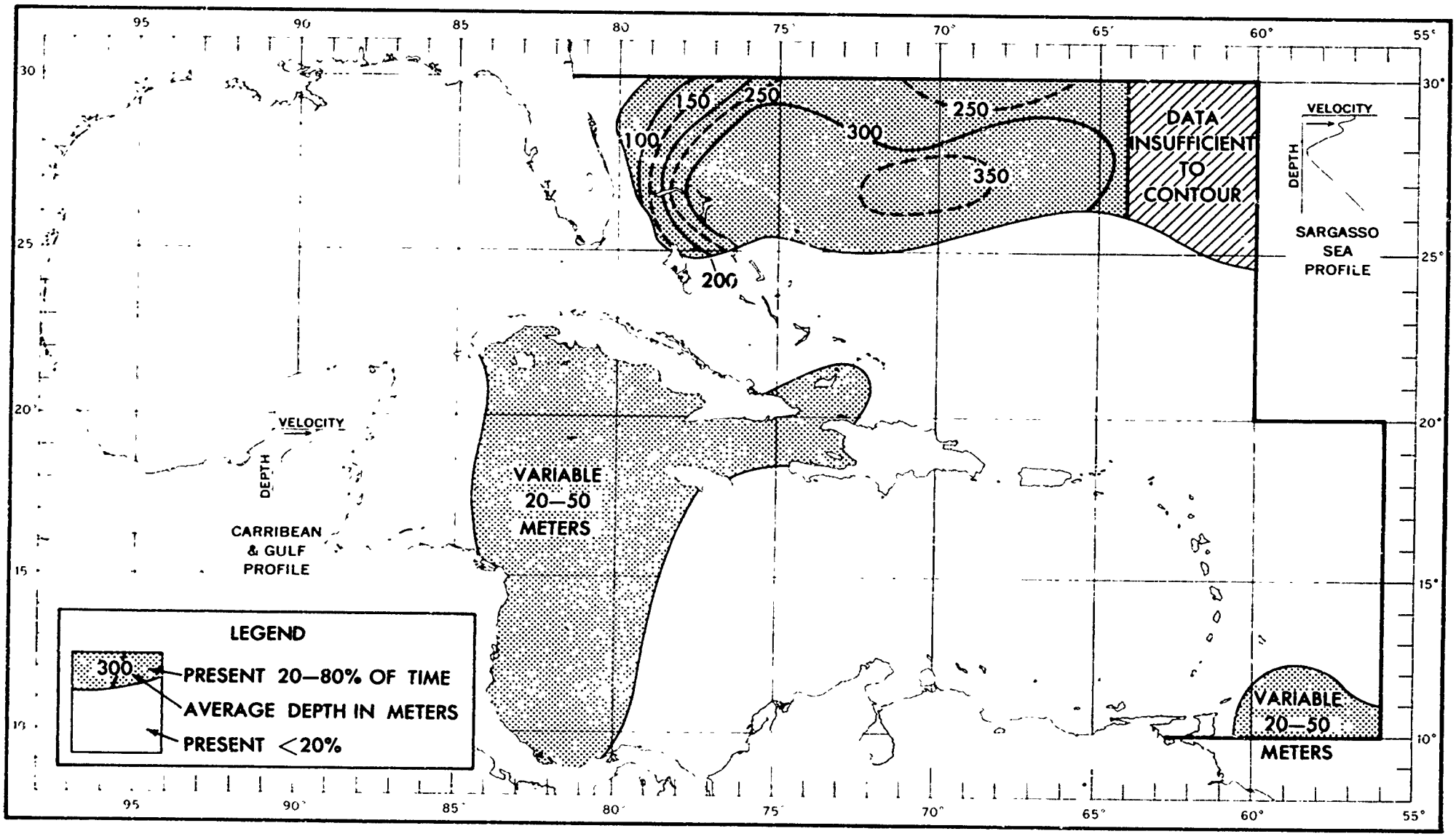

FIGURE 4-67 EXTENT AND AVERAGE DEPTH OF THE SUBSURFACE (SECONDARY) SOUND VELOCITY MINIMUM (JANUARY-MARCH)

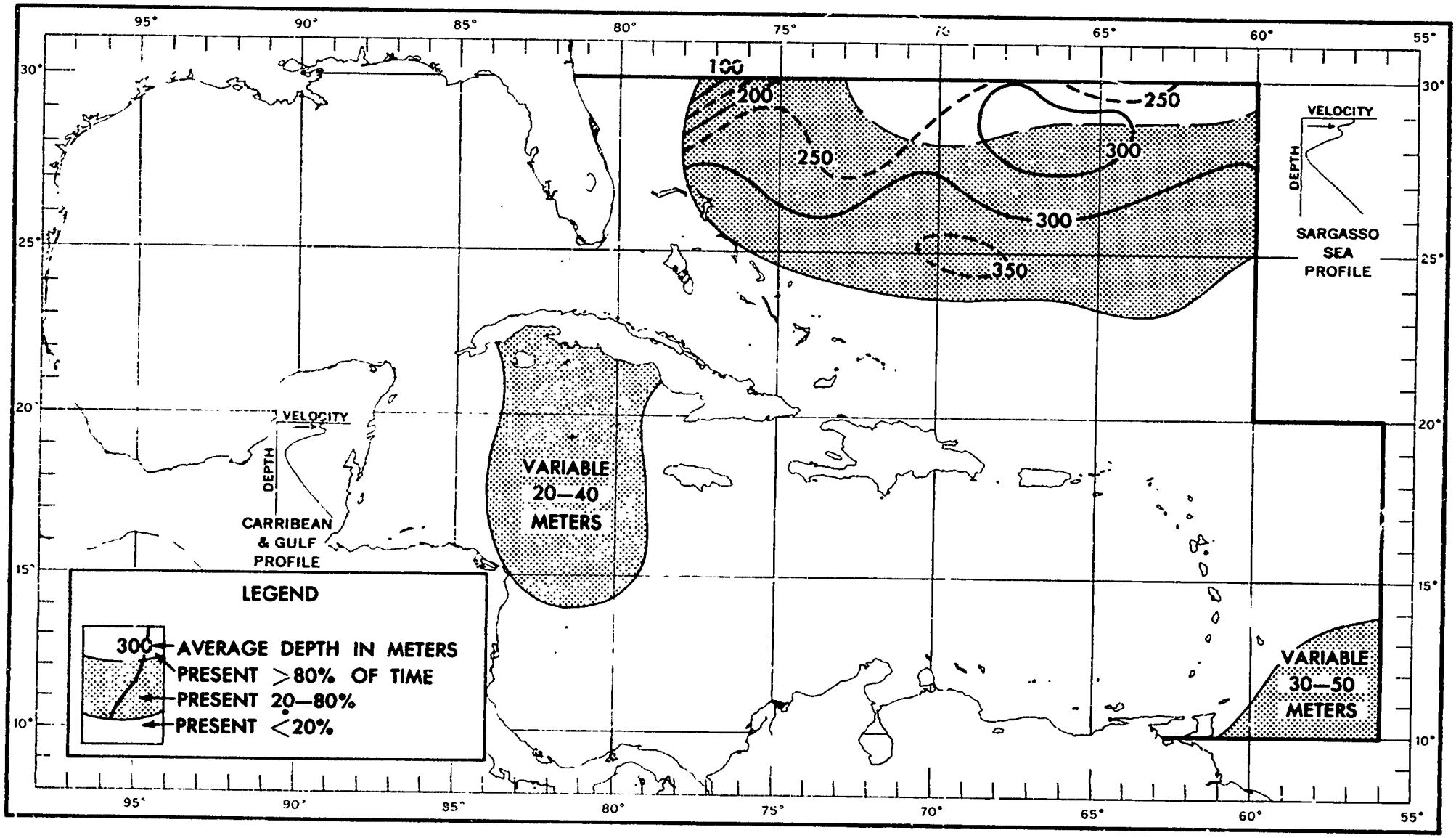

FIGURE 4-68 EXTENT AND AVERAGE DEPTH OF THE SUBSURFACE (SECONDARY) SOUND VELOCITY MINIMUM (APRIL-JUNE)

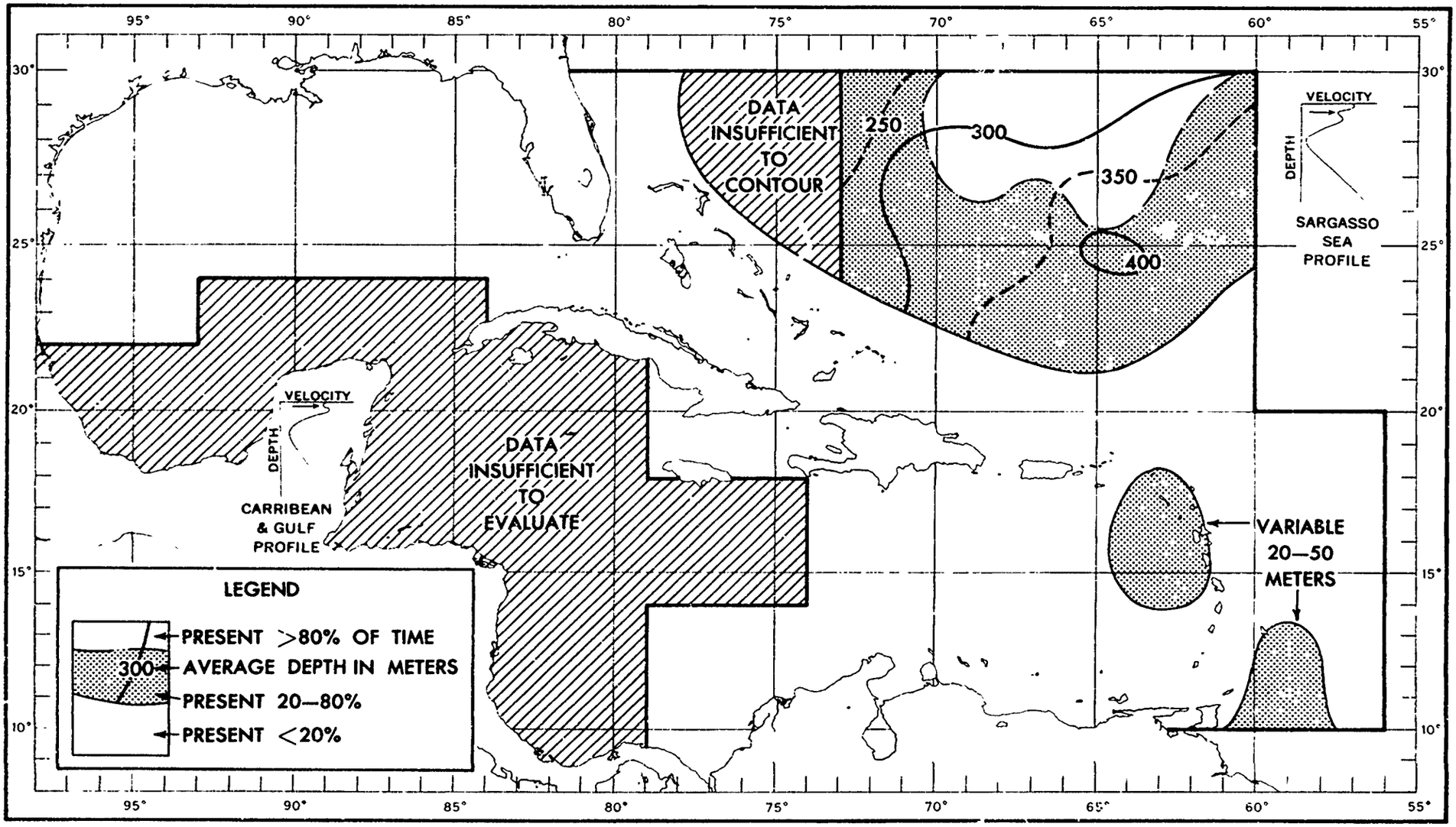

FIGURE 4-69 EXTENT AND AVERAGE DEPTH OF THE SUBSURFACE (SECONDARY) SOUND VELOCITY MINIMUM (JULY-SEPTEMBER)

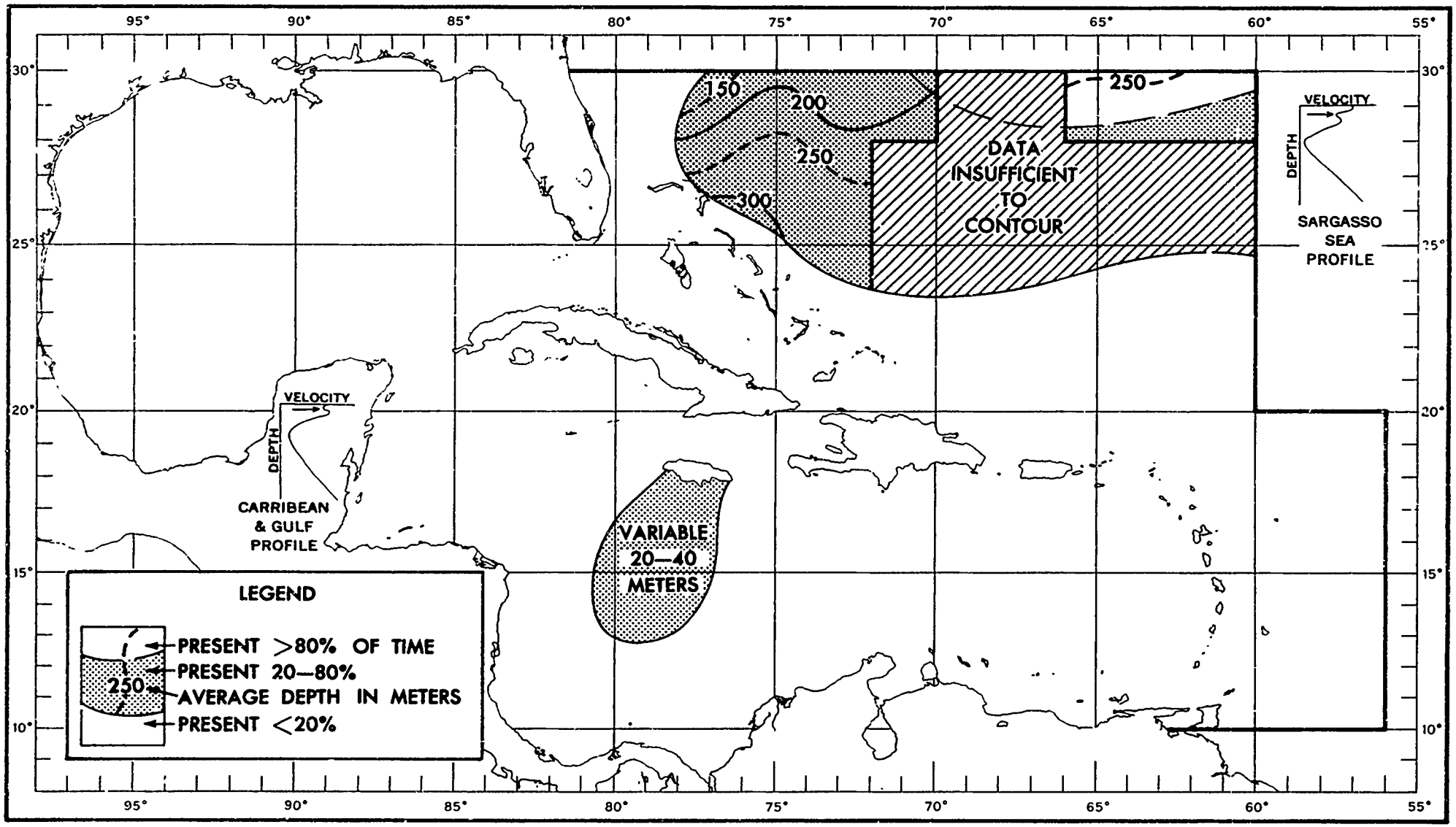

FIGURE 4-70 EXTENT AND AVERAGE DEPTH OF THE SUBSURFACE (SECONDARY) SOUND VELOCITY MINIMUM (OCTOBER-DECEMBER)

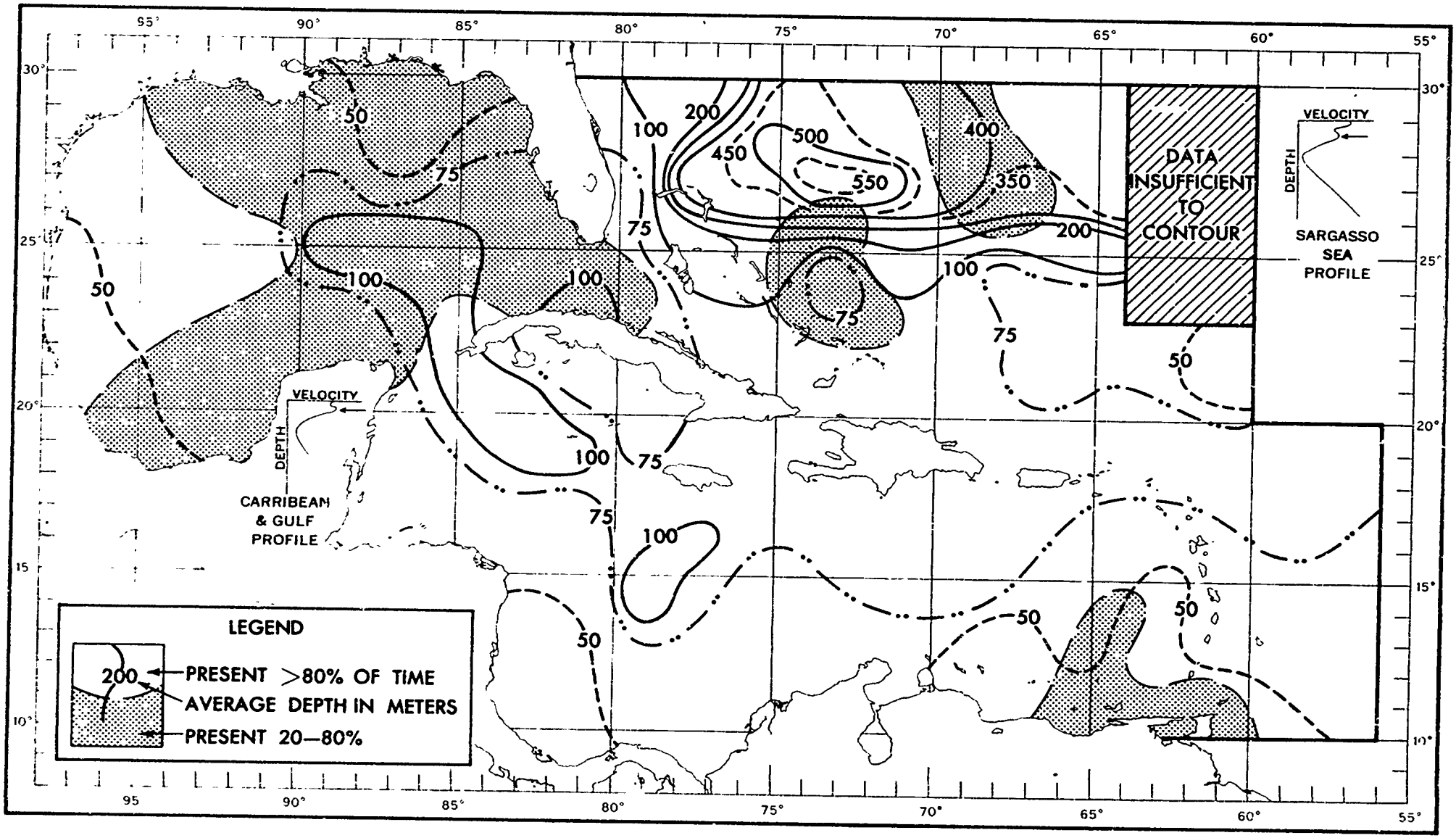

FIGURE 4-71 EXTENT AND AVERAGE DEPTH OF THE SUBSURFACE SOUND VELOCITY MAXIMUM (JANUARY-MARCH)

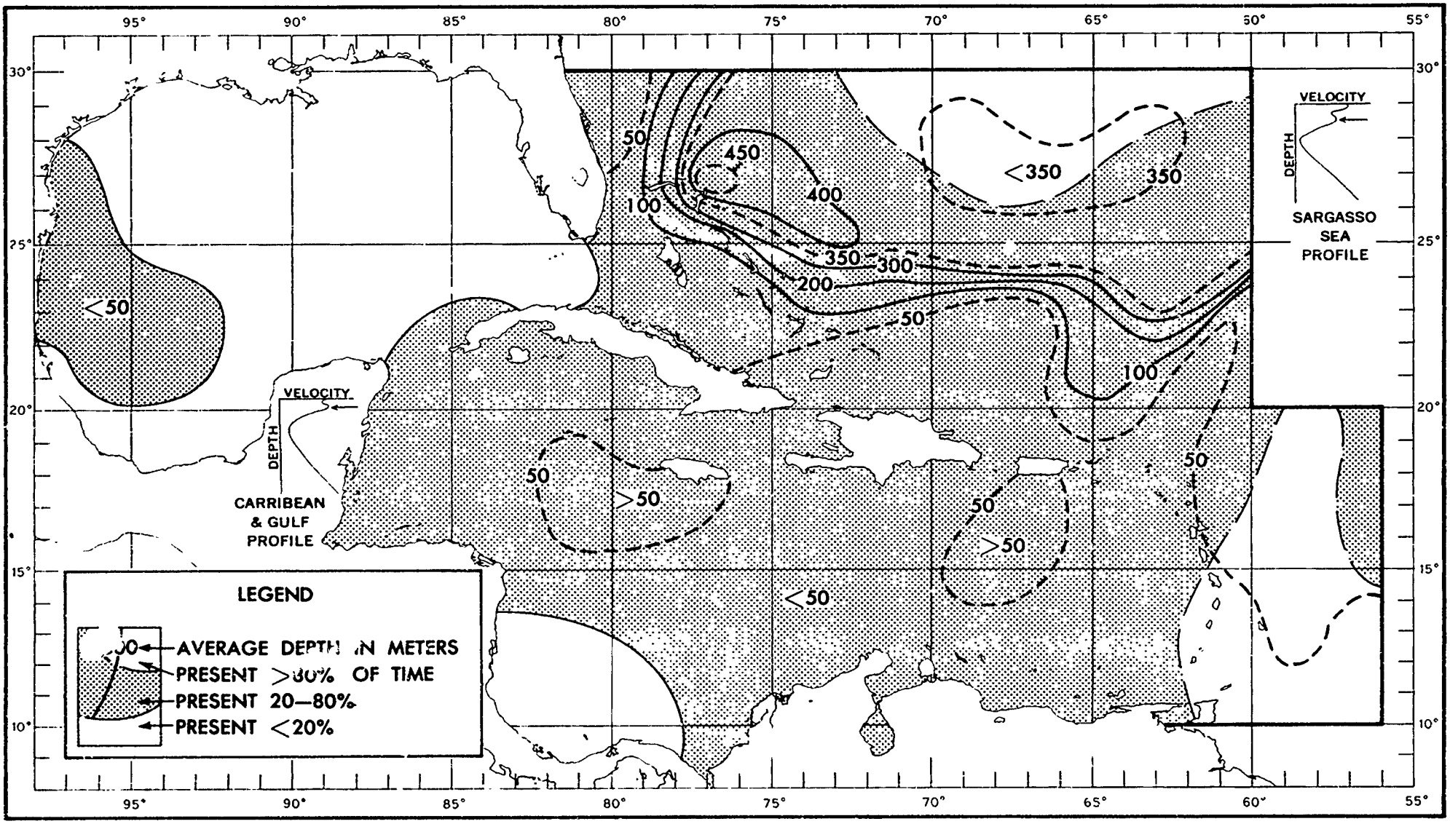

FIGURE 4-72 EXTENT AND AVERAGE DEPTH OF THE SUBSURFACE SOUND VELOCITY MAXIMUM (APRIL-JUNE)

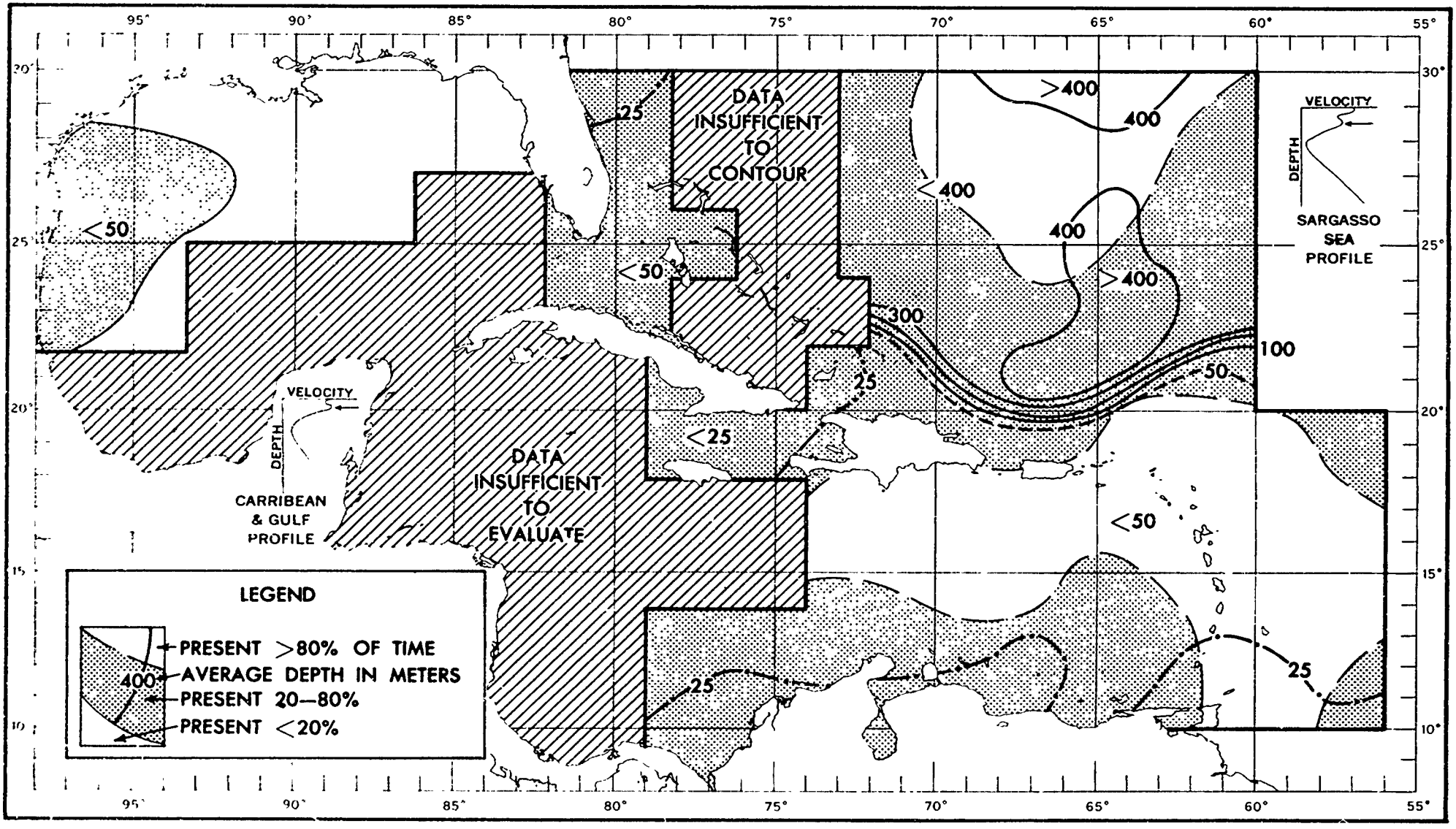

FIGURE 4-73 EXTENT AND AVERAGE DEPTH OF THE SUBSURFACE SOUND VELOCITY MAXIMUM (JULY-SEPTEMBER)

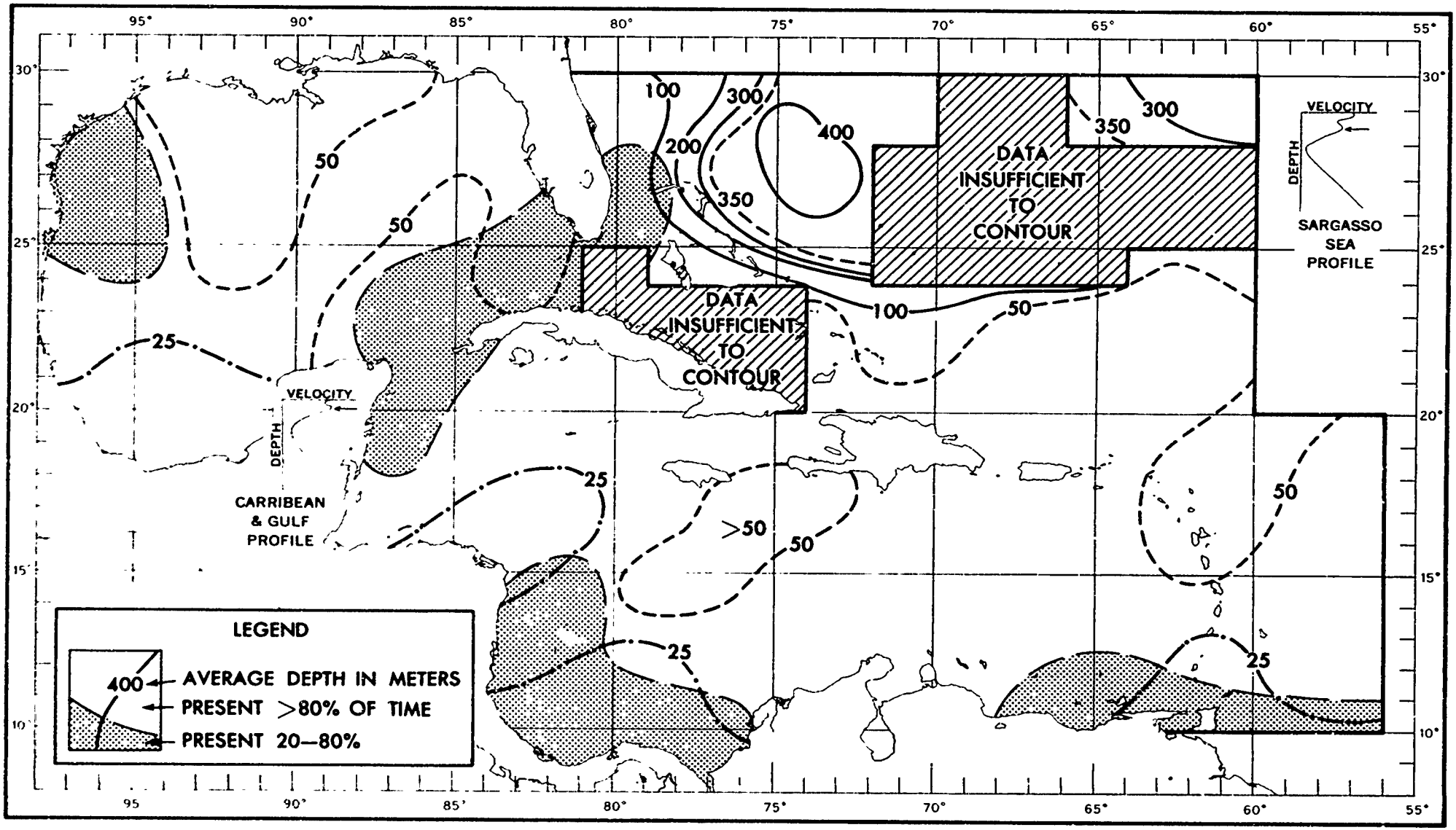

FIGURE 4-74 EXTENT AND AVERAGE DEPTH OF THE SUBSURFACE SOUND VELOCITY MAXIMUM (OCTOBER-DECEMBER)

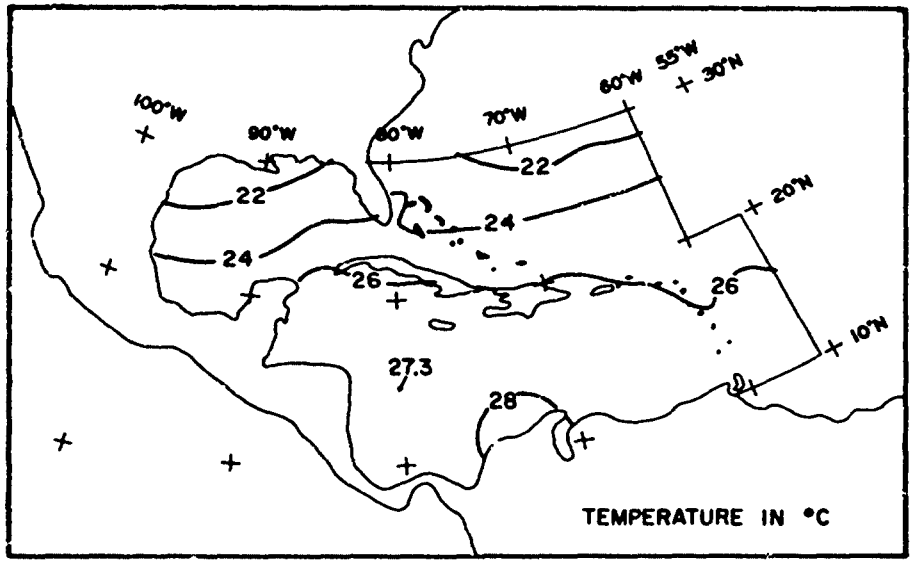

SEA SURFACE TEMPERATURE

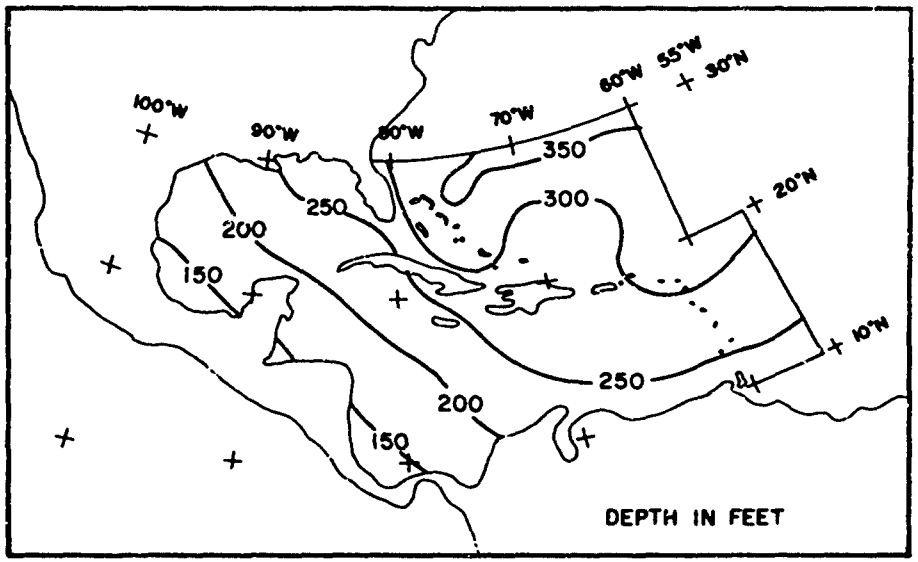

POTENTIAL MIXED LAYER DEPTH

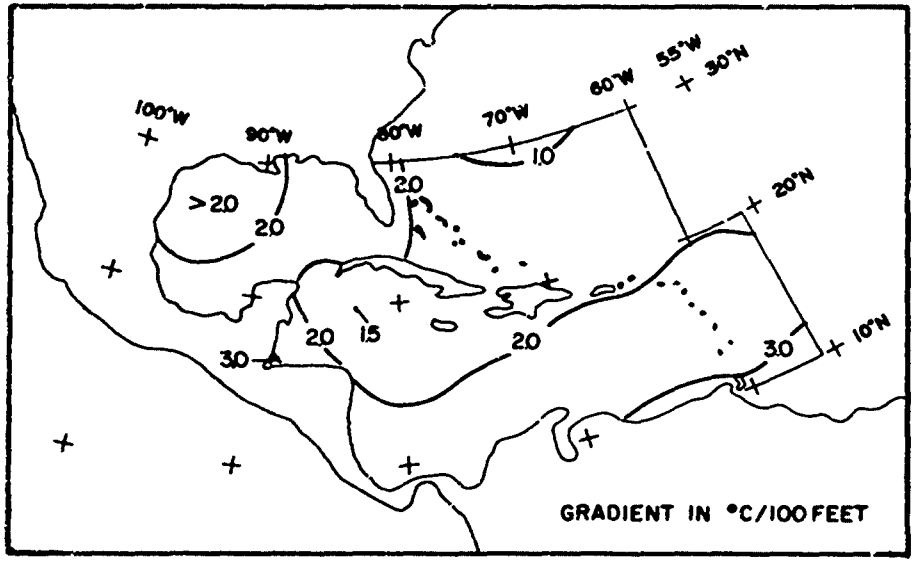

THERMOCLINE GRADIENT

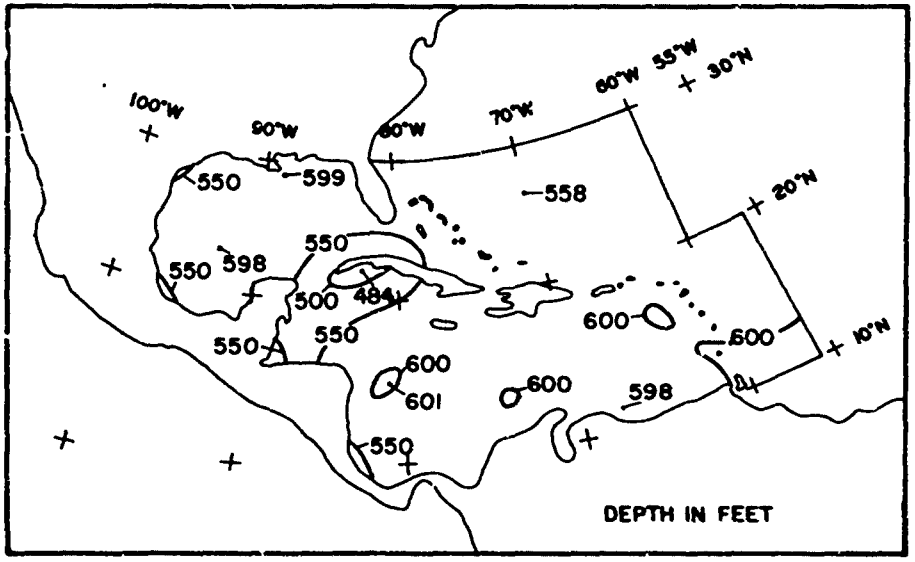

BOTTOM OF THERMOCLINE

FIGURE 4-75 UPPER THERMAL STRUCTURE (JANUARY, 1968)

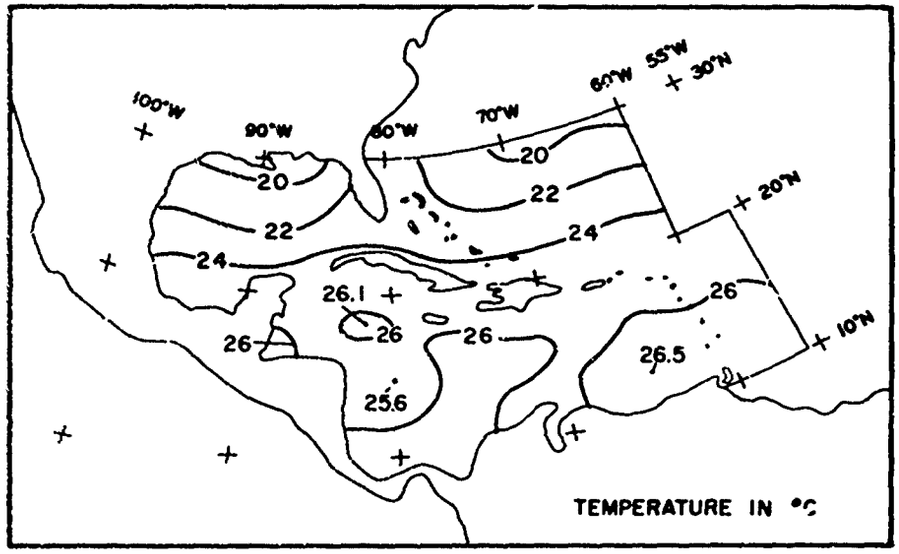

SEA SURFACE TEMPERATURE

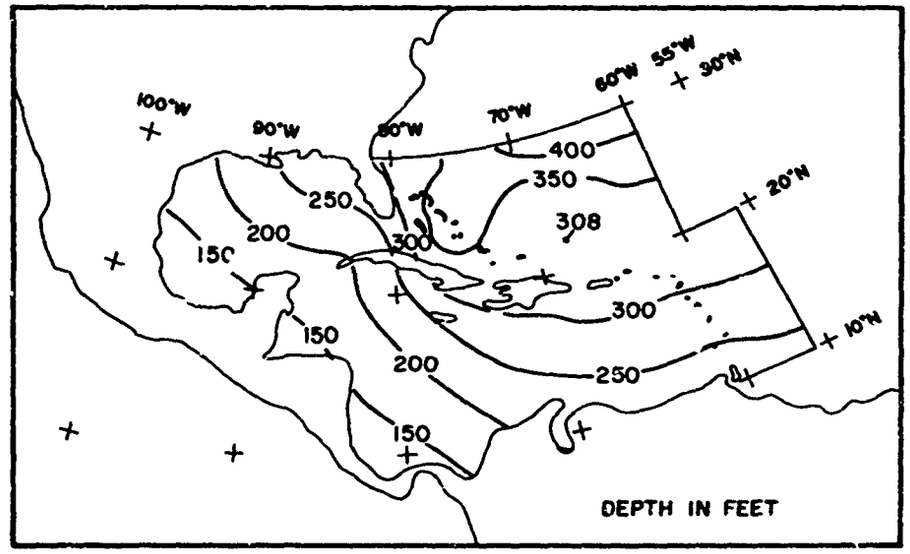

POTENTIAL MIXED LAYER DEPTH

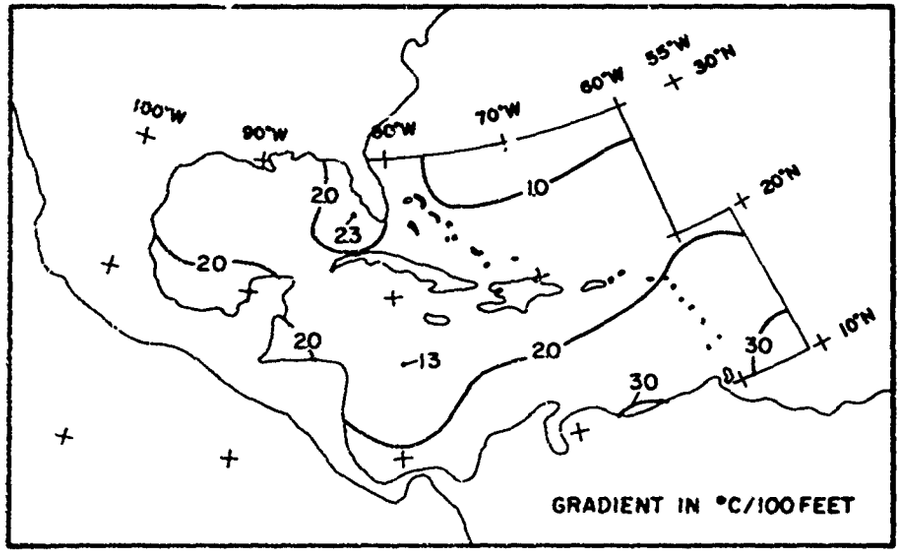

THERMOCLINE GRADIENT

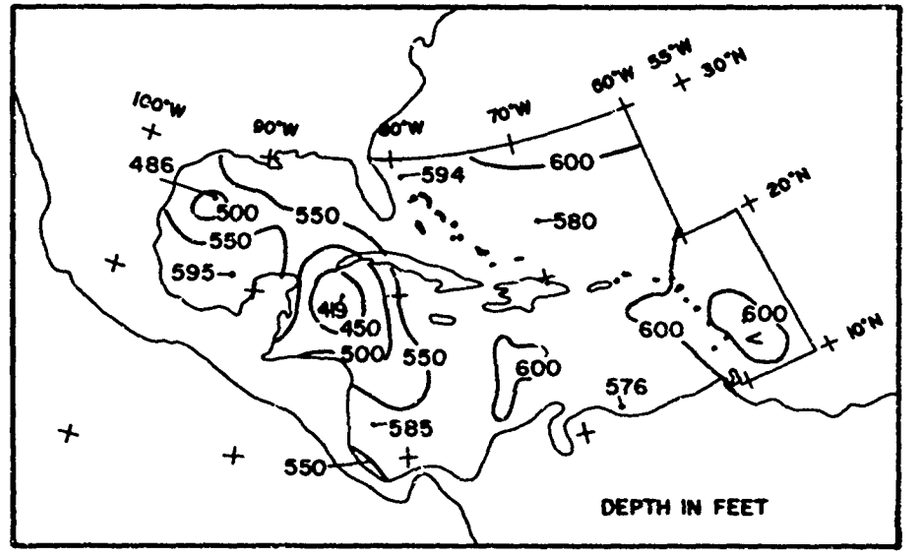

BOTTOM OF THERMOCLINE

FIGURE 4-76 UPPER THERMAL STRUCTURE (FEBRUARY, 1968)

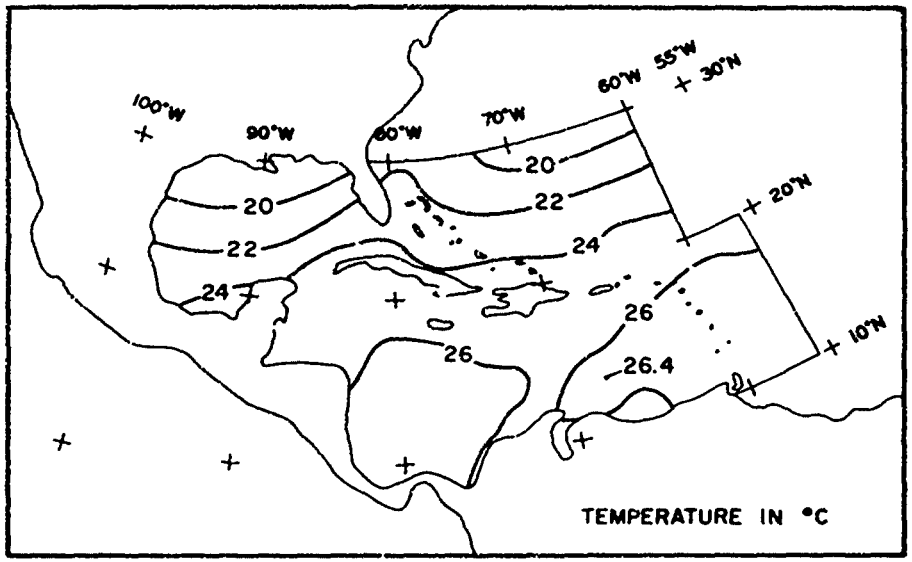

SEA SURFACE TEMPERATURE

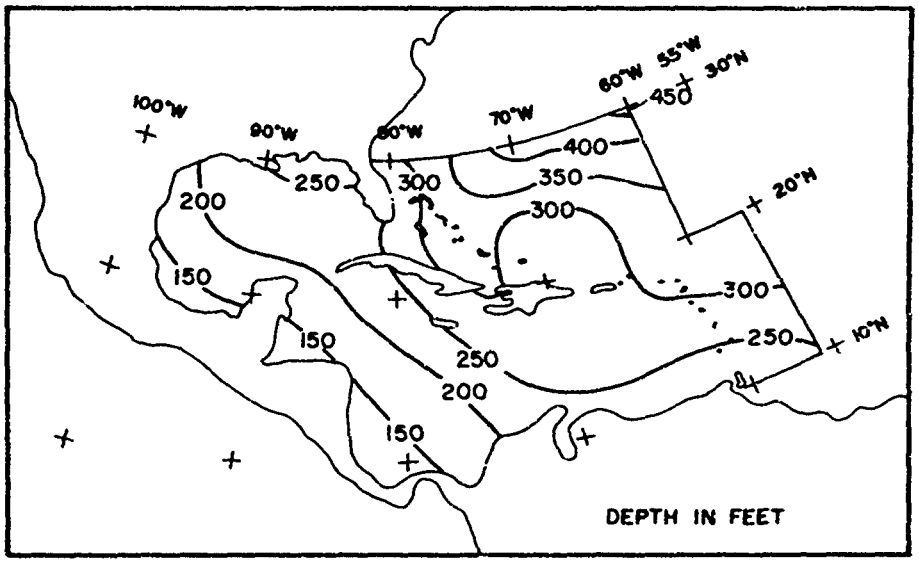

POTENTIAL MIXED LAYER DEPTH

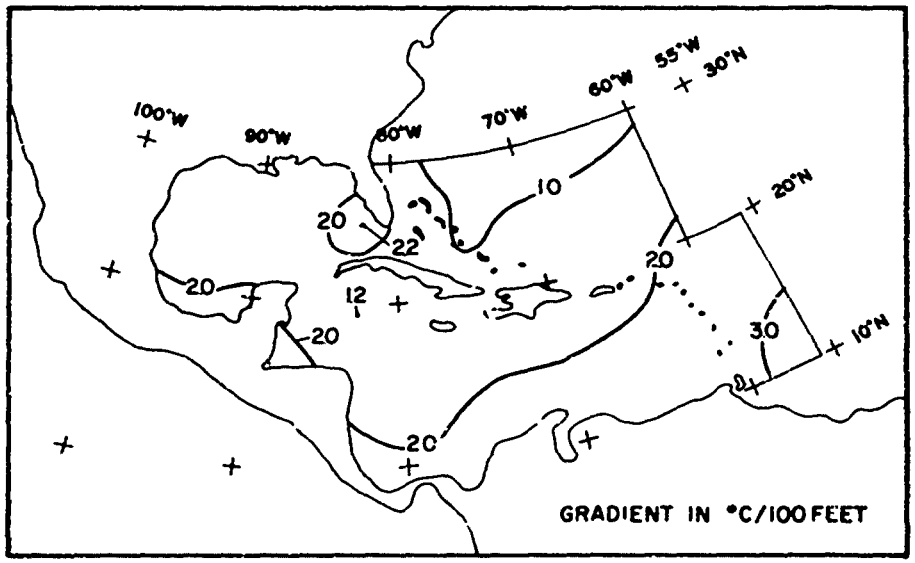

THERMOCLINE GRADIENT

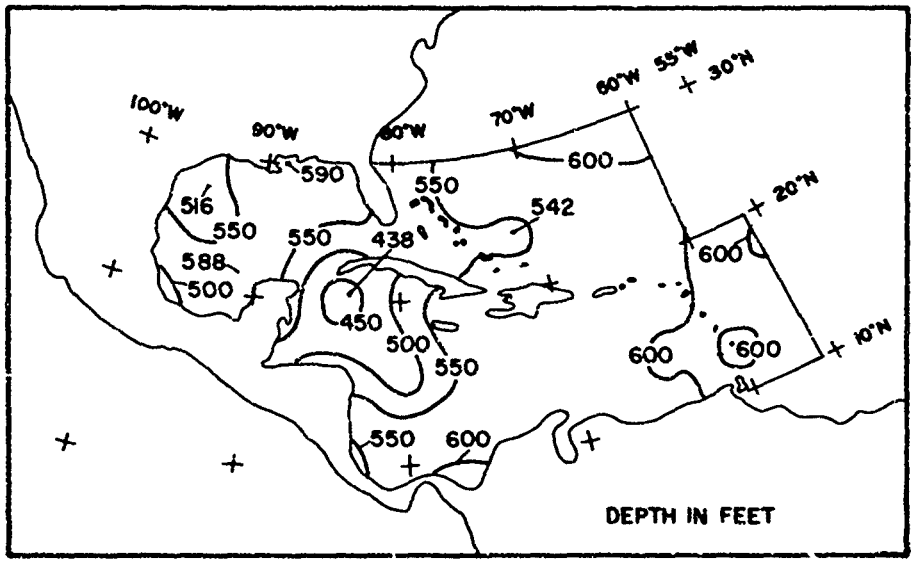

BOTTOM OF THERMOCLINE

FIGURE 4-77 UPPER THERMAL STRUCTURE (MARCH, 1968)

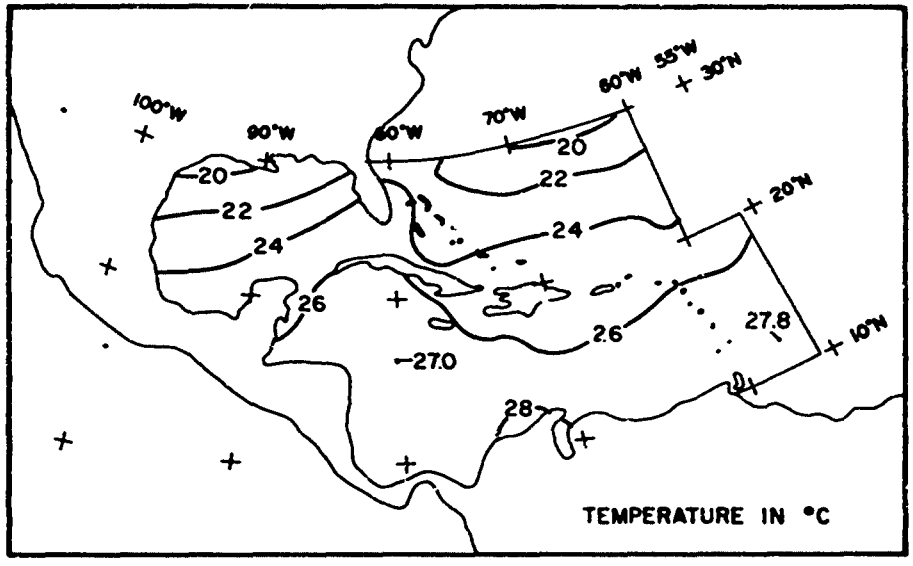

SEA SURFACE TEMPERATURE

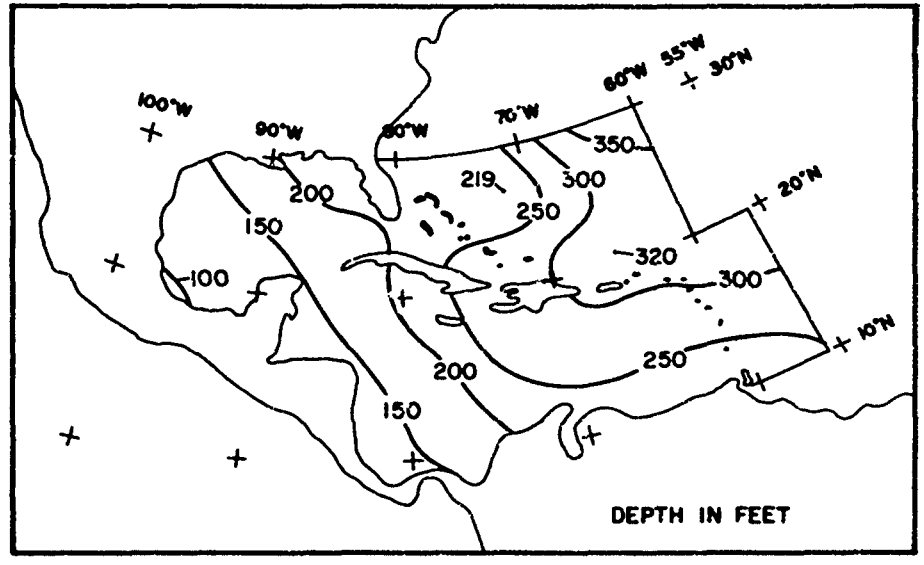

POTENTIAL MIXED LAYER DEPTH

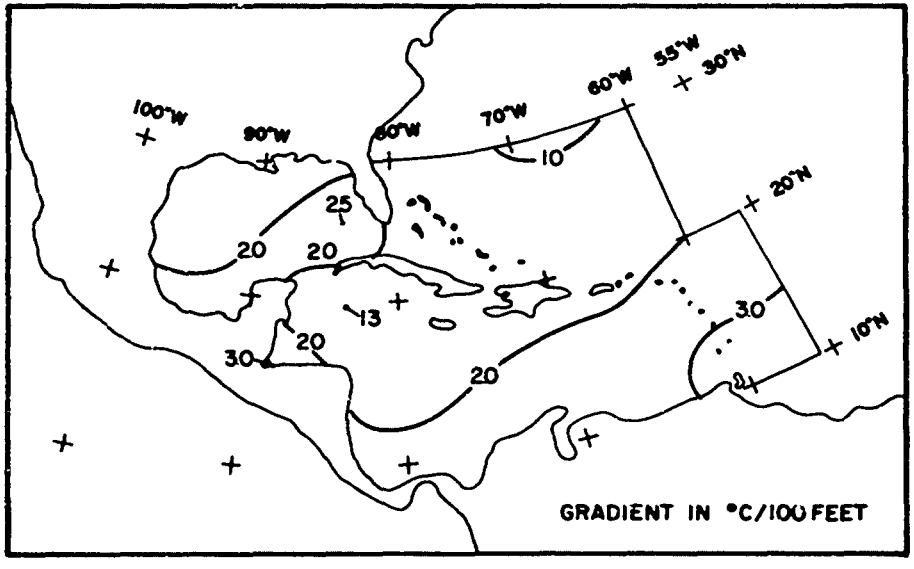

THERMOCLINE GRADIENT

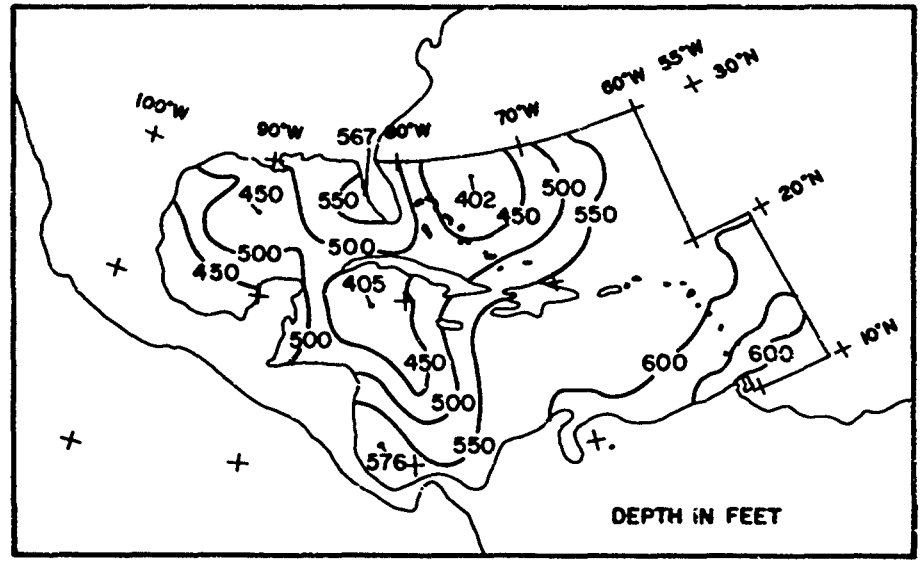

BOTTOM OF THERMOCLINE

FIGURE 4-78 UPPER THERMAL STRUCTURE (APRIL, 1968)

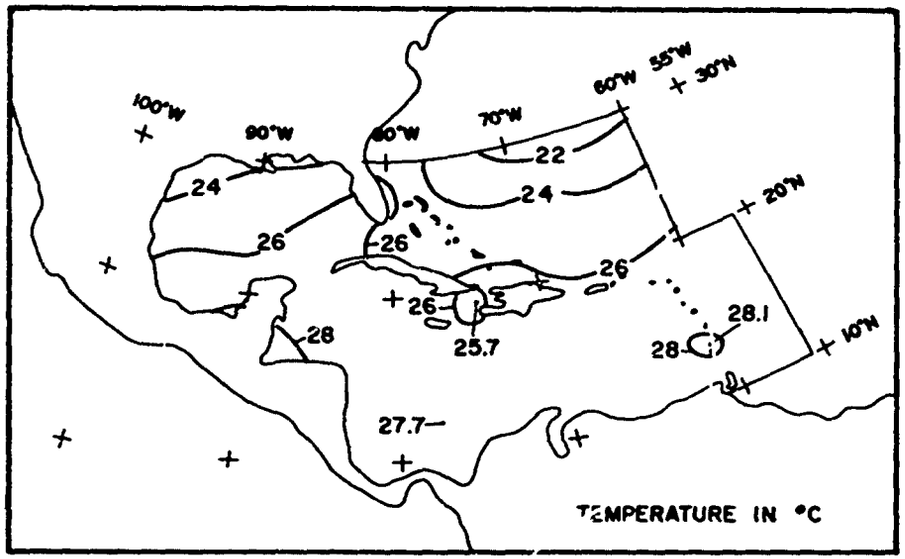

SEA SURFACE TEMPERATURE

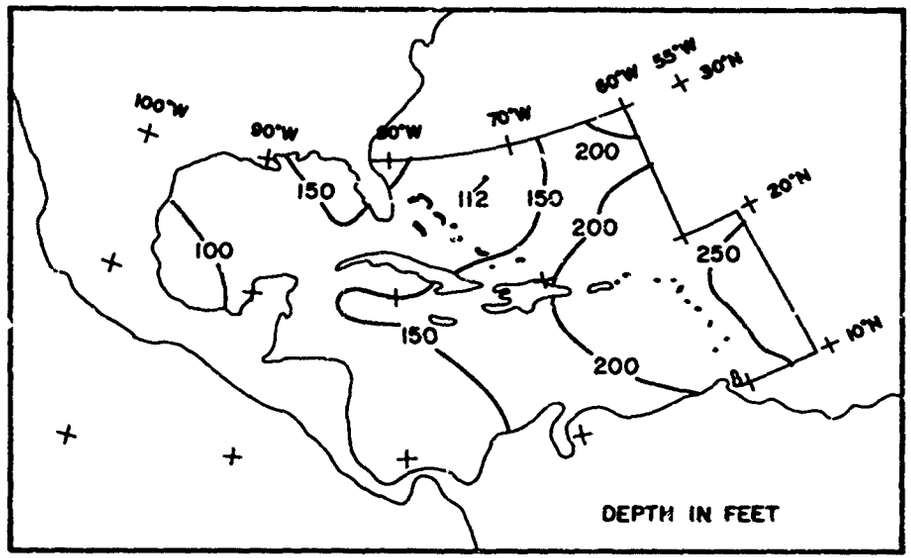

POTENTIAL MIXED LAYER DEPTH

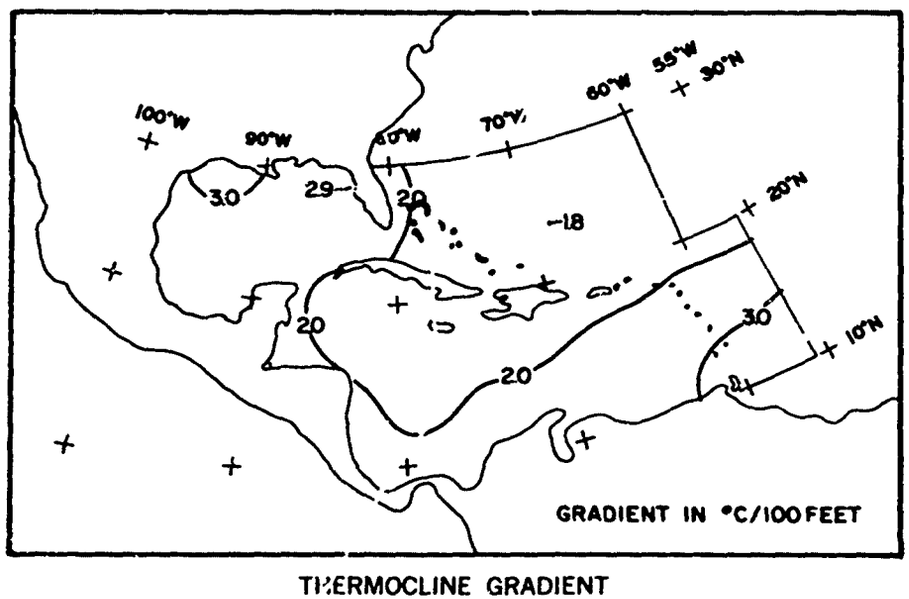

THERMOCLINE GRADIENT

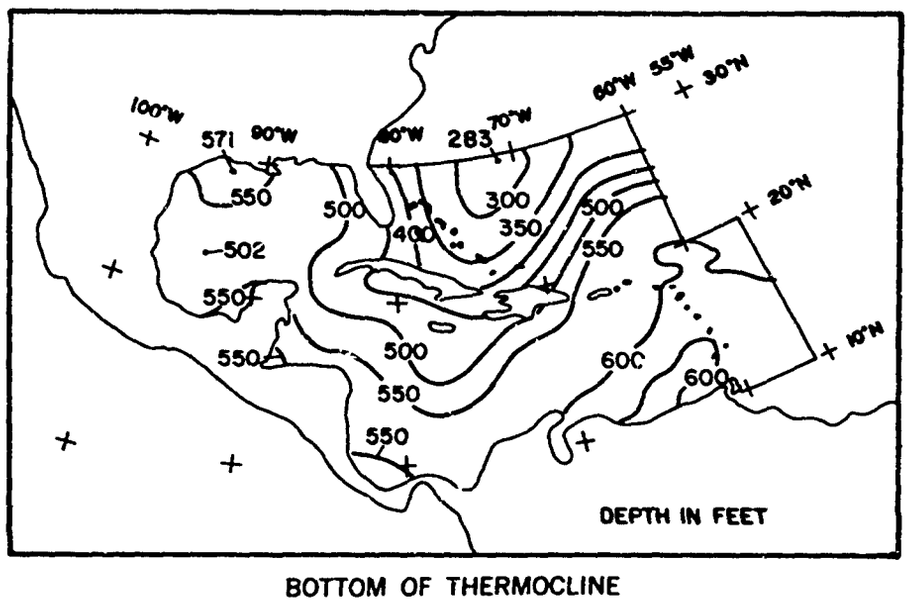

BOTTOM OF THERMOCLINE

FIGURE 4-79 UPPER THERMAL STRUCTURE (MAY, 1968)

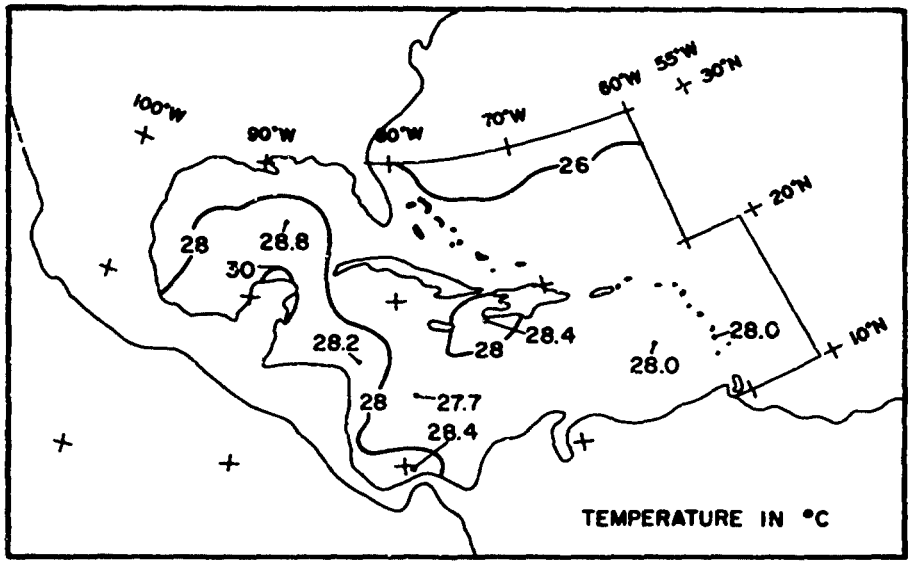

SEA SURFACE TEMPERATURE

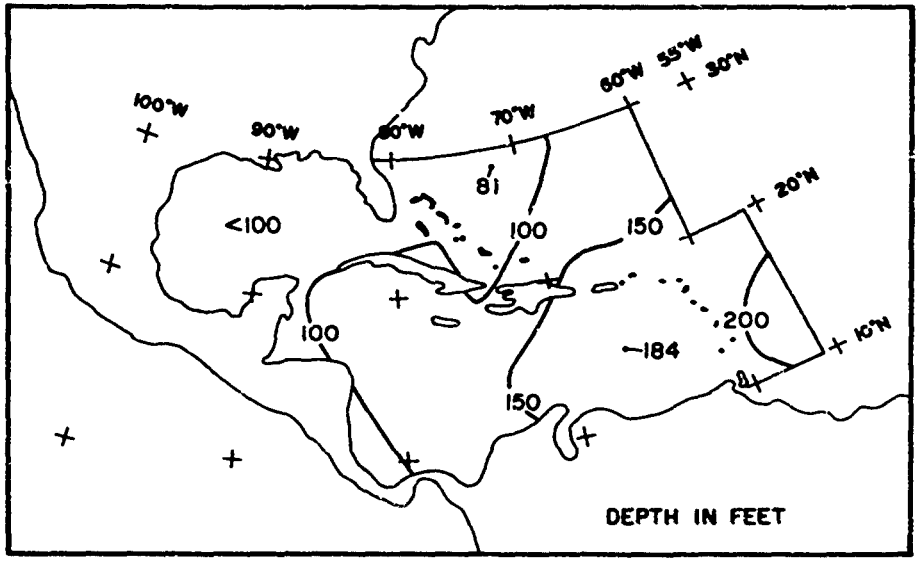

POTENTIAL MIXED LAYER DEPTH

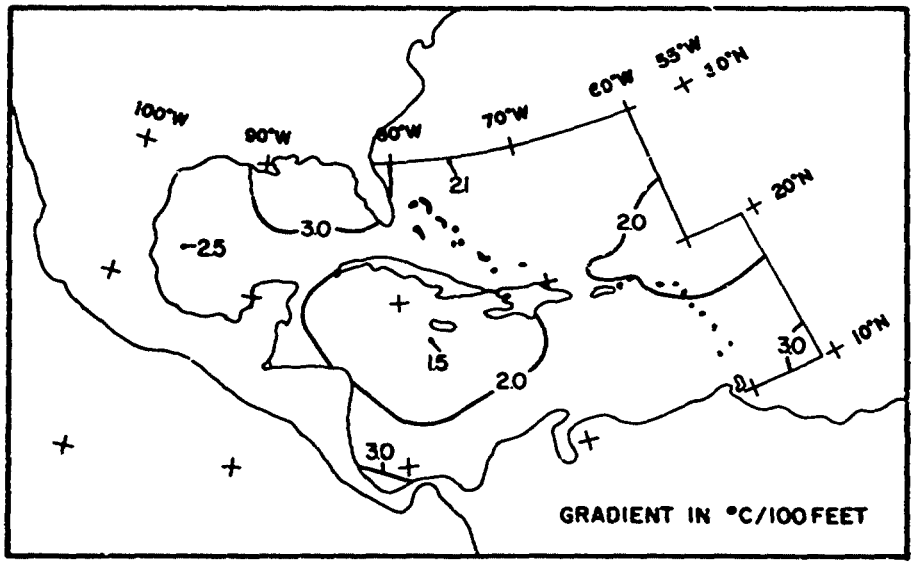

THERMOCLINE GRADIENT

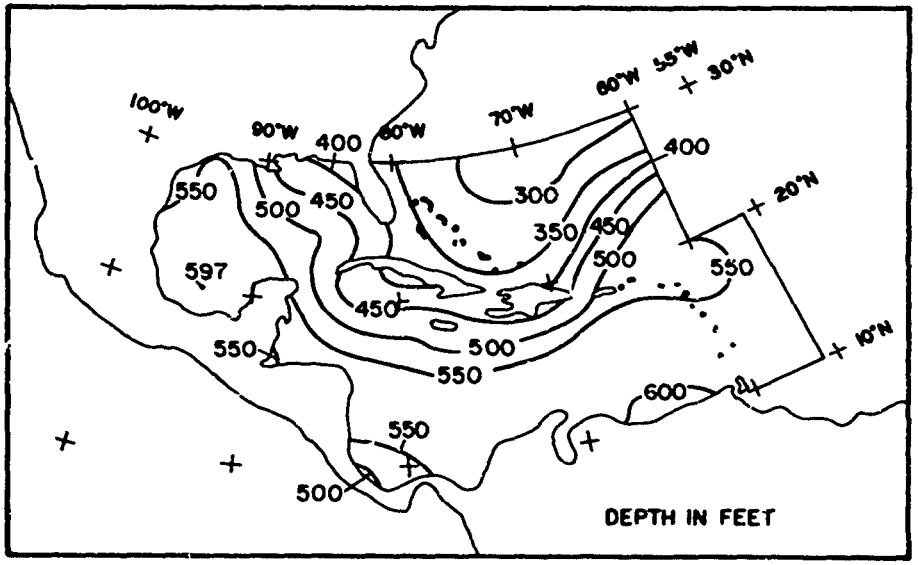

BOTTOM OF THERMOCLINE

FIGURE 4-80 UPPER THERMAL STRUCTURE (JUNE, 1968)

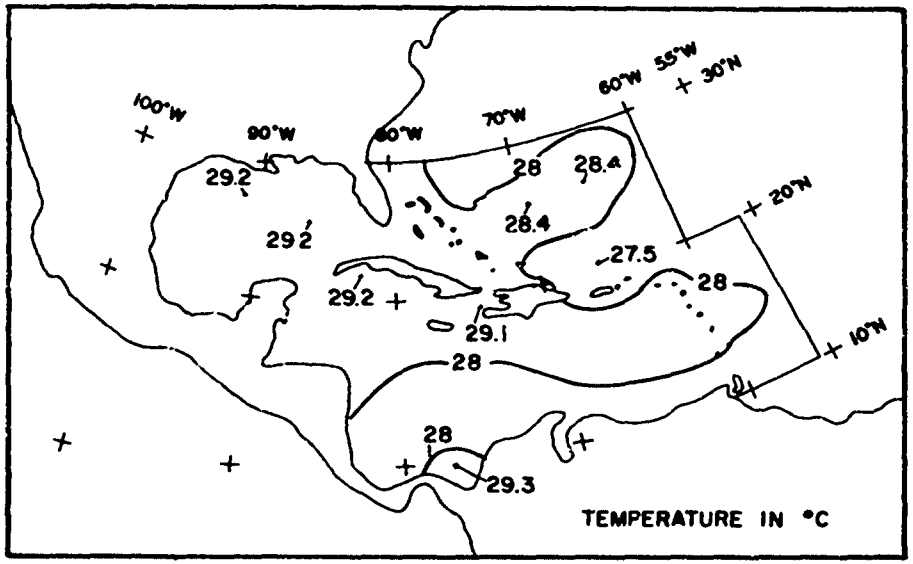

SEA SURFACE TEMPERATURE

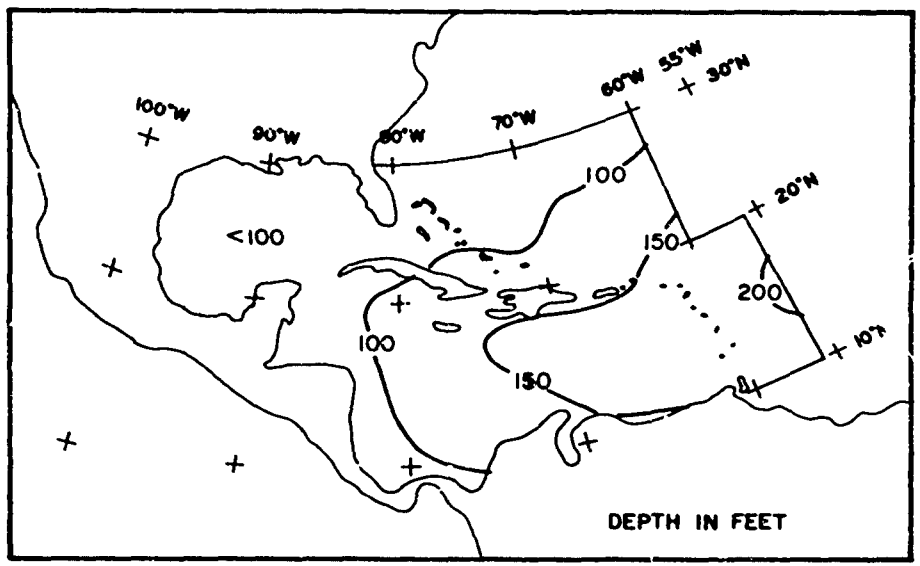

POTENTIAL MIXED LAYER DEPTH

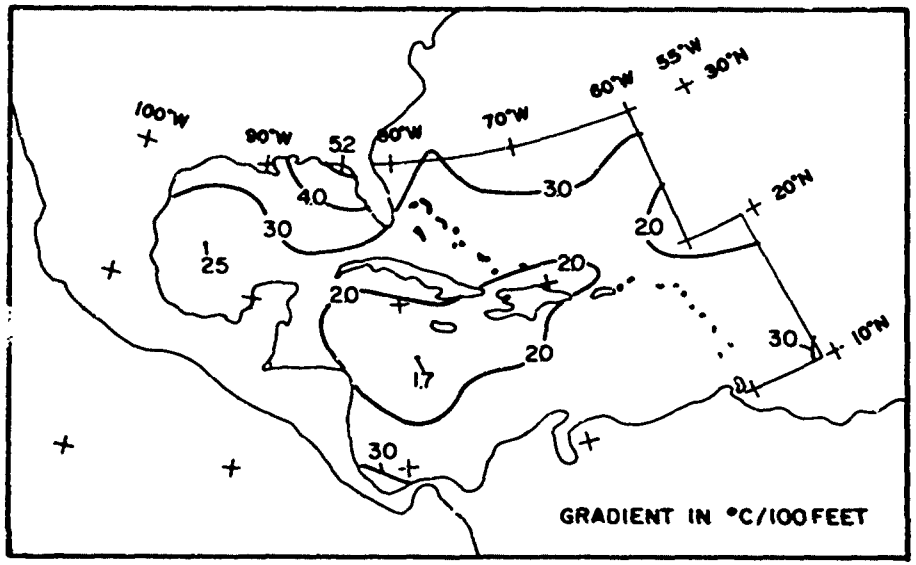

THERMOCLINE GRADIENT

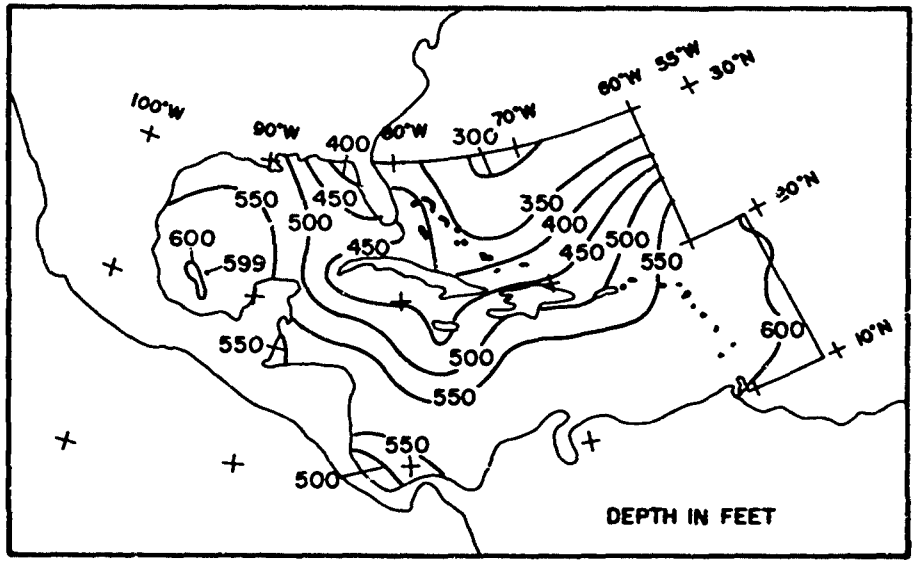

BOTTOM OF THERMOCLINE

FIGURE 4-81 UPPER THERMAL STRUCTURE (JULY, 1968)

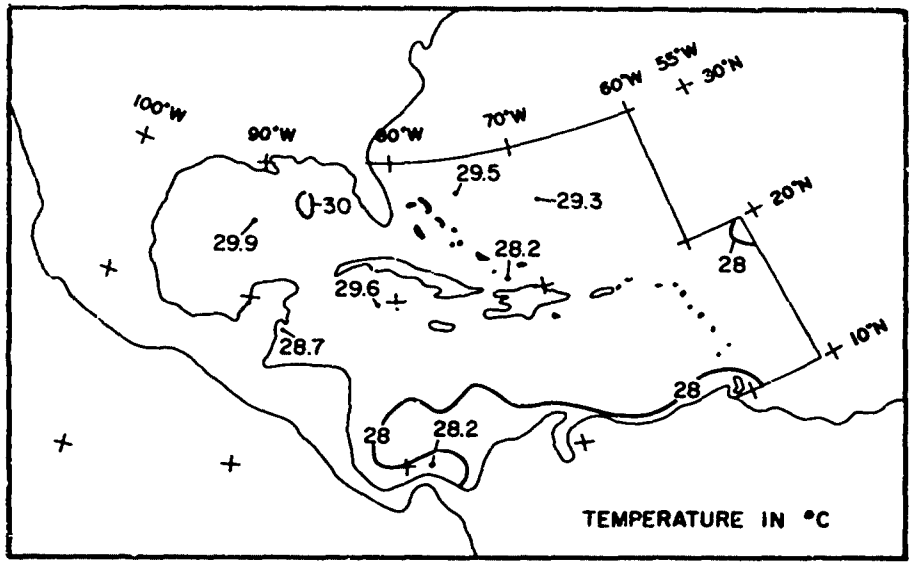

SEA SURFACE TEMPERATURE

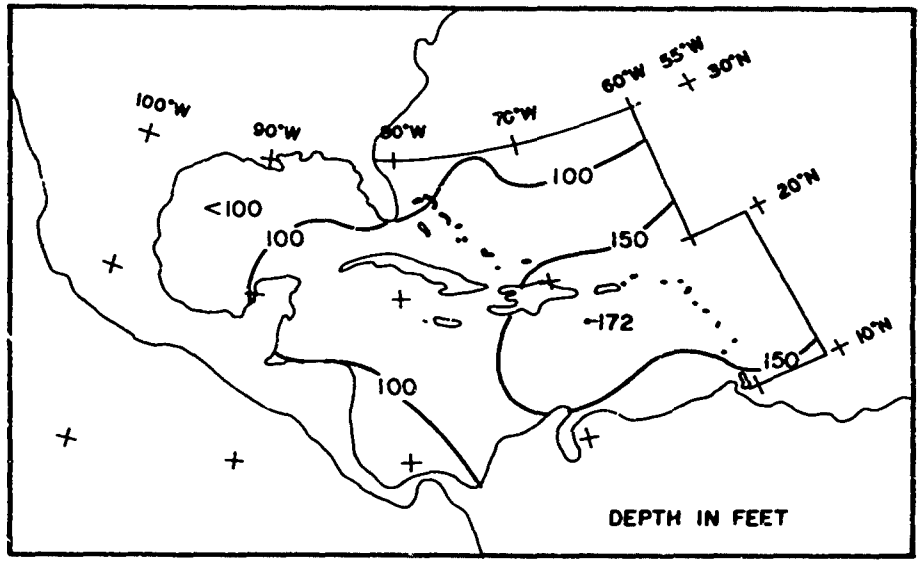

POTENTIAL MIXED LAYER DEPTH

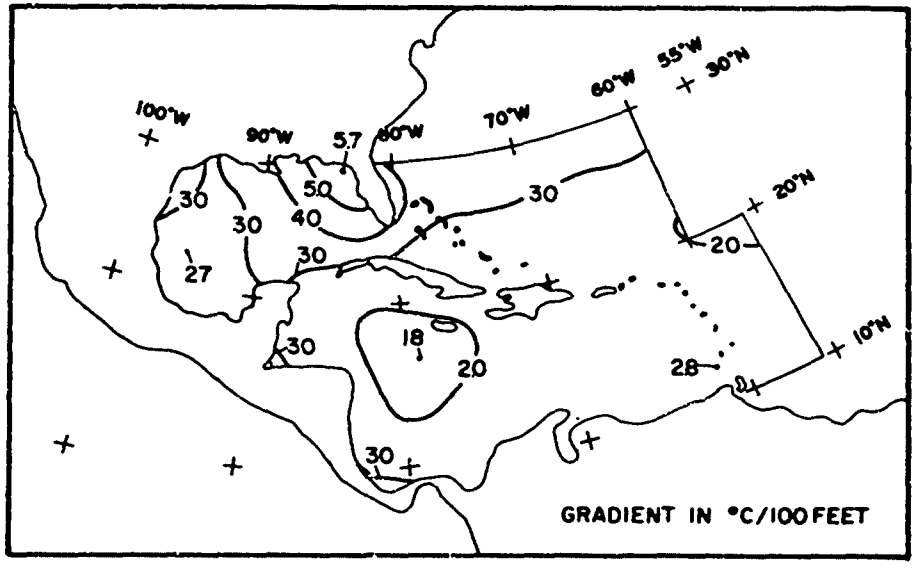

THERMOCLINE GRADIENT

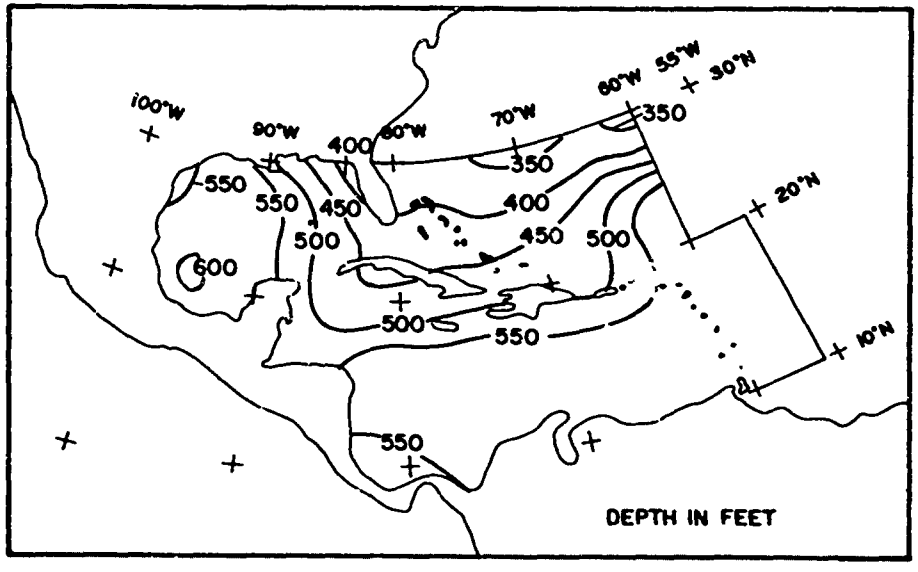

BOTTOM OF THERMOCLINE

FIGURE 4-82 UPPER THERMAL STRUCTURE (AUGUST, 1968)

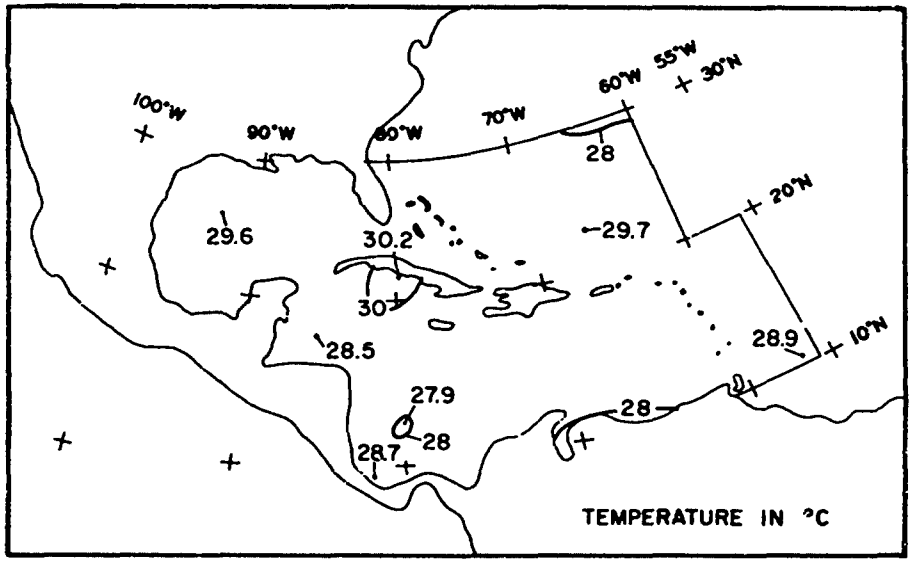

SEA SURFACE TEMPERATURE

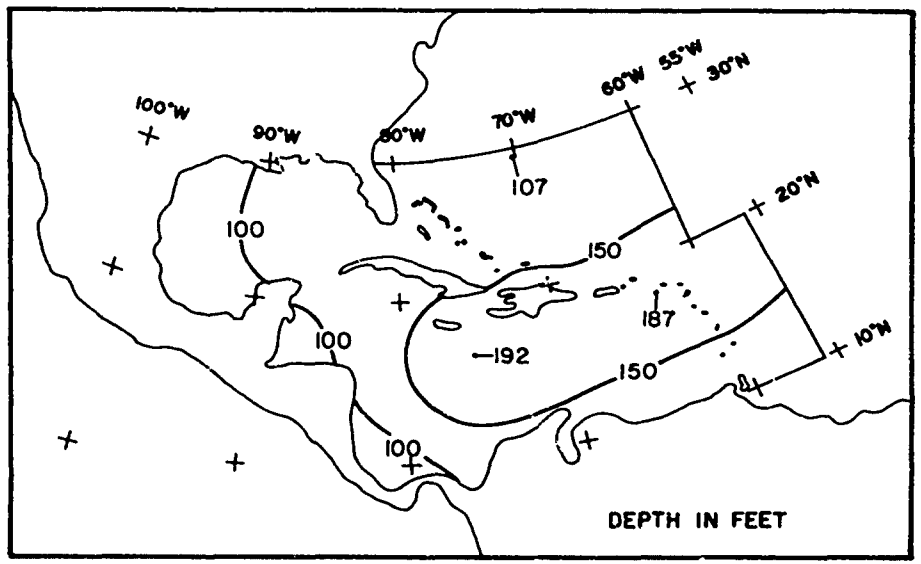

POTENTIAL MIXED LAYER DEPTH

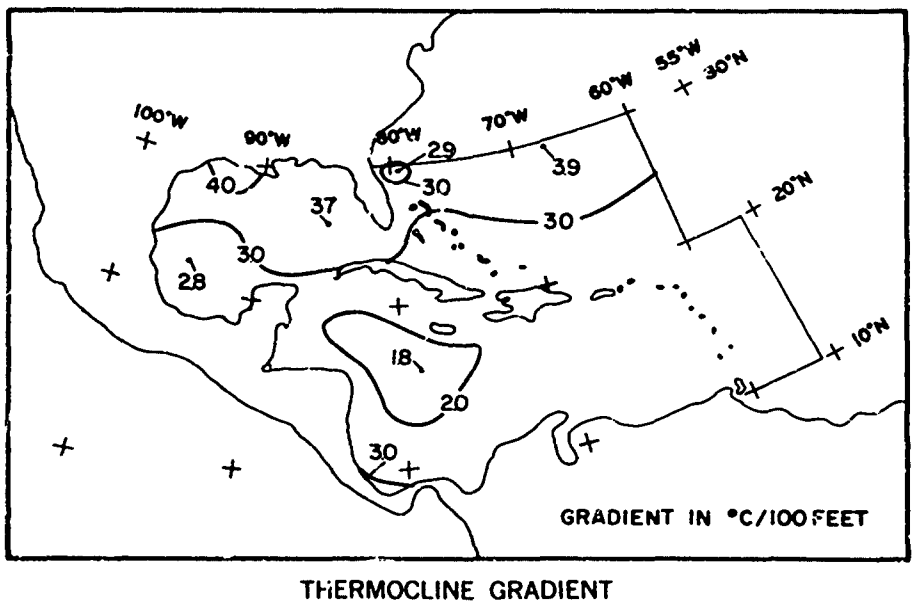

THERMOCLINE GRADIENT

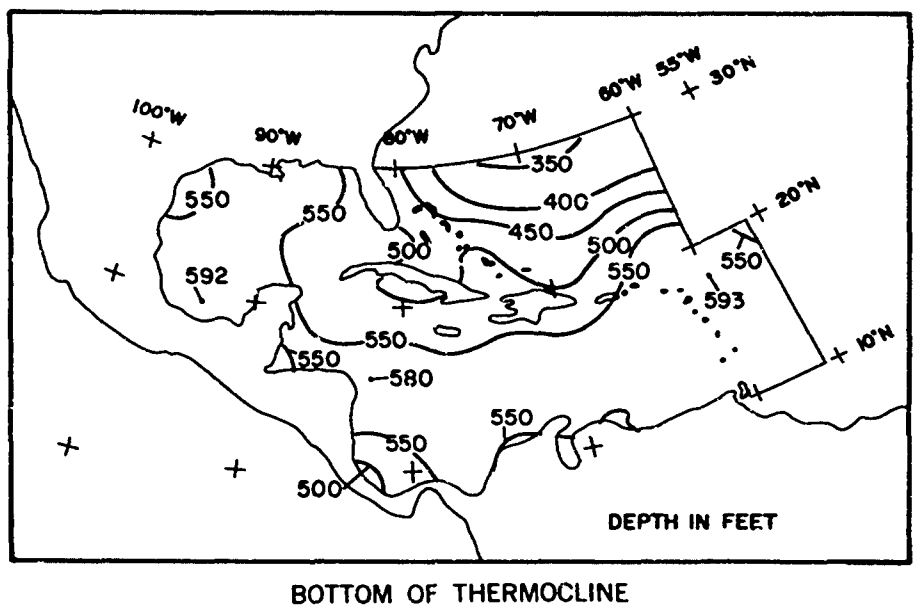

BOTTOM OF THERMOCLINE

FIGURE 4-83 UPPER THERMAL STRUCTURE (SEPTEMBER, 1968)

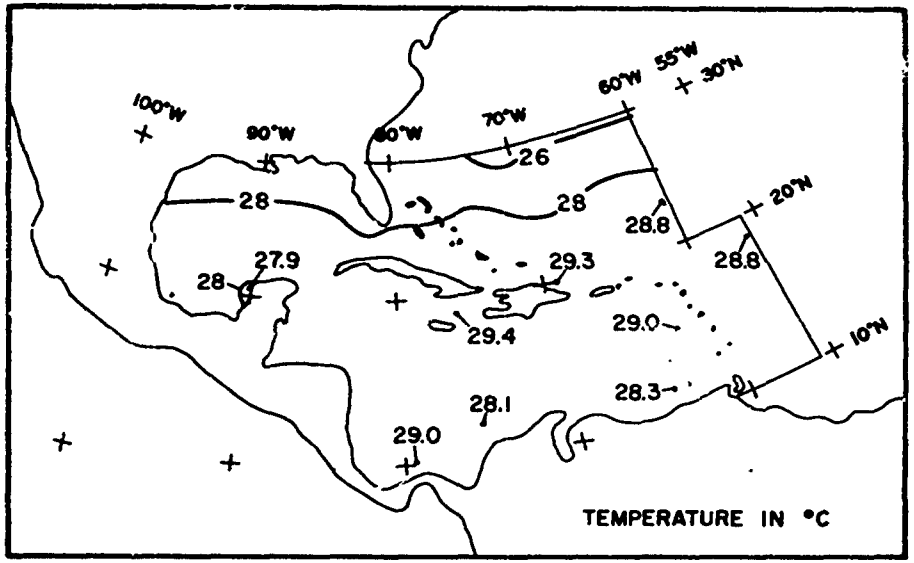

SEA SURFACE TEMPERATURE

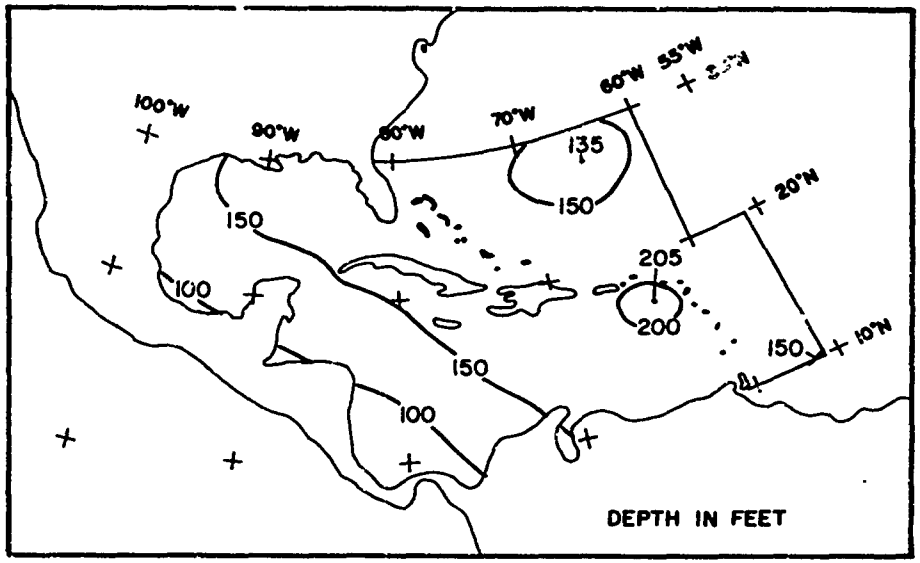

POTENTIAL MIXED LAYER DEPTH

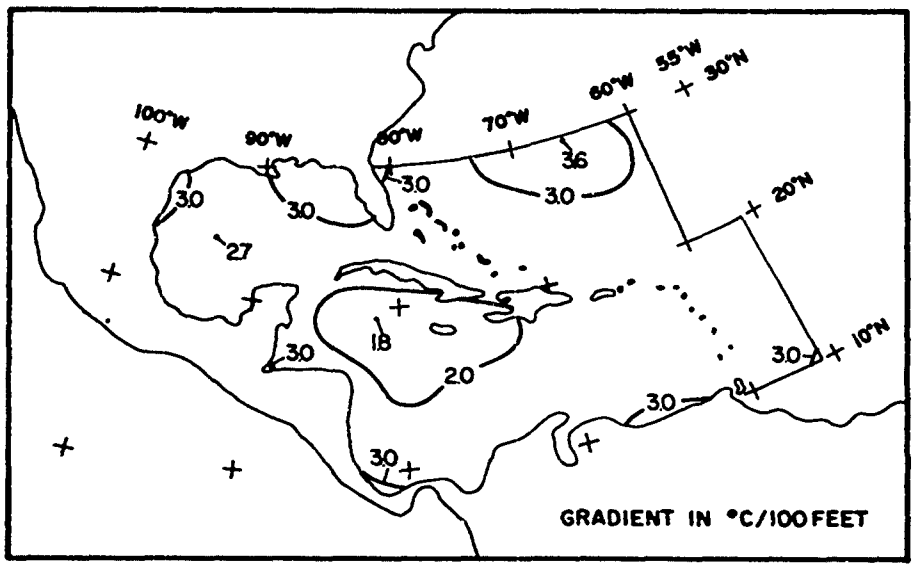

THERMOCLINE GRADIENT

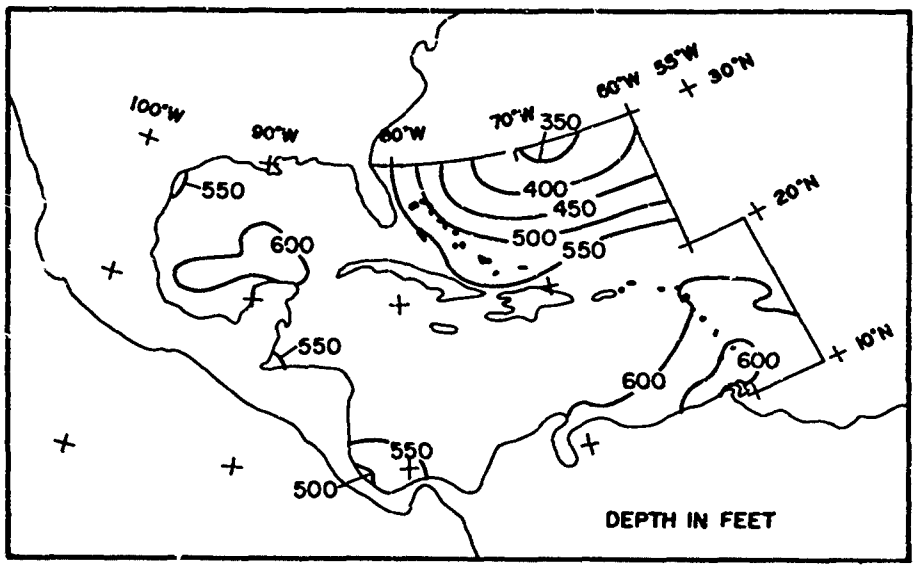

BOTTOM OF THERMOCLINE

FIGURE 4-84 UPPER THERMAL STRUCTURE (OCTOBER, 1968)

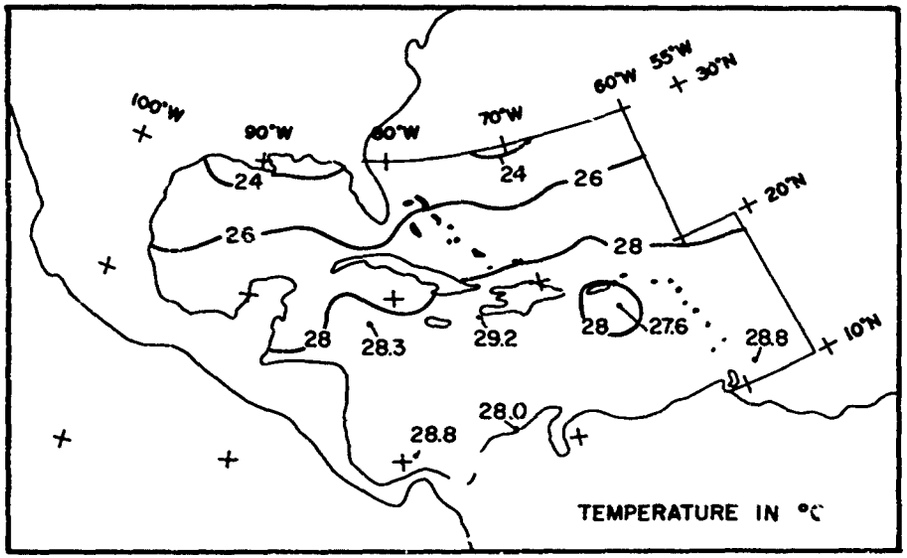

SEA SURFACE TEMPERATURE

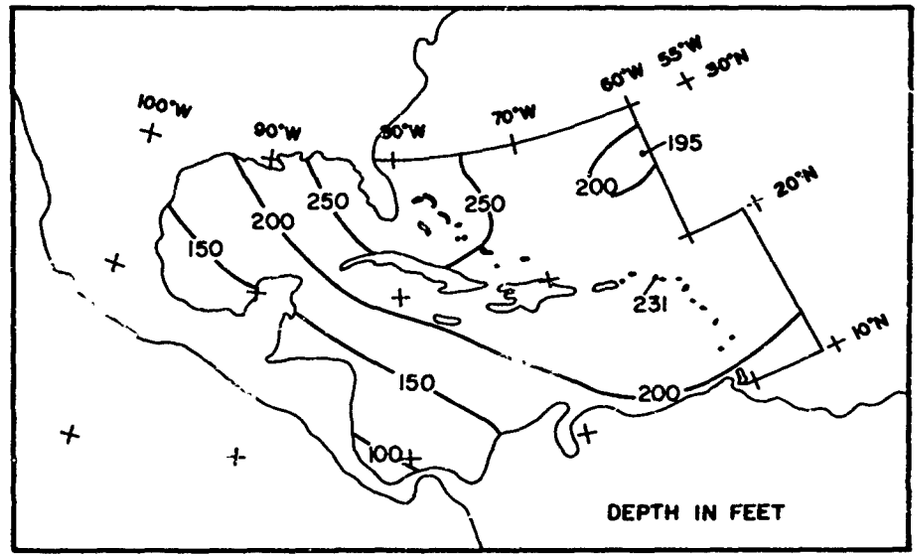

POTENTIAL MIXED LAYER DEPTH

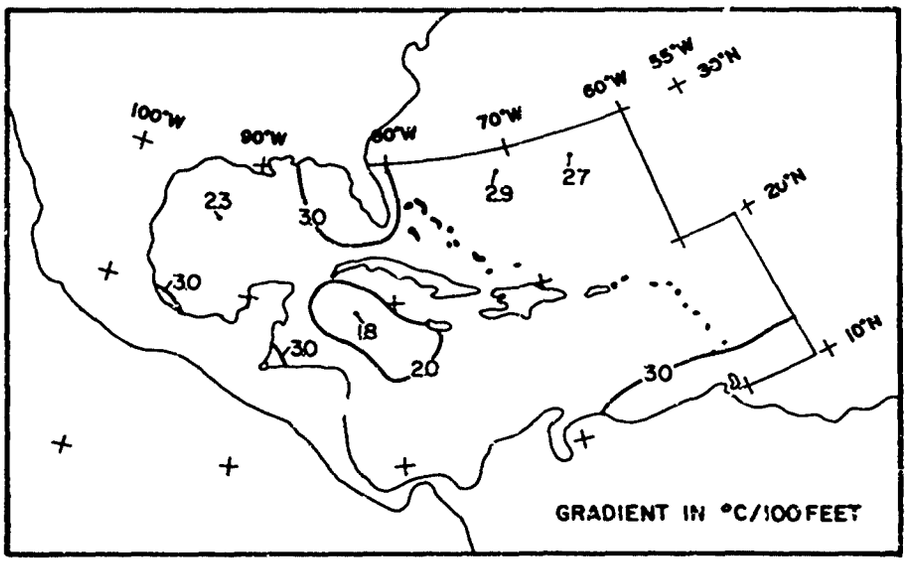

THERMOCLINE GRADIENT

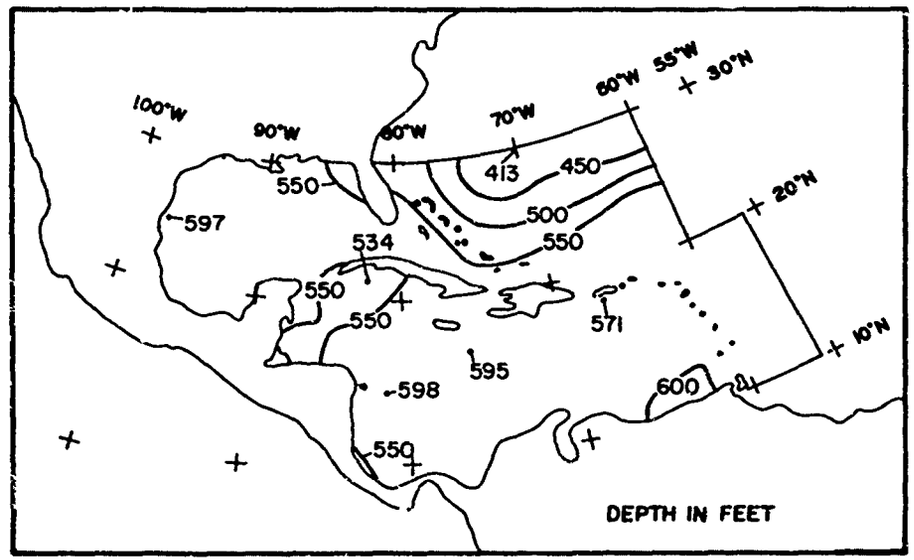

BOTTOM OF THERMOCLINE

FIGURE 4-85 UPPER THERMAL STRUCTURE (NOVEMBER, 1968)

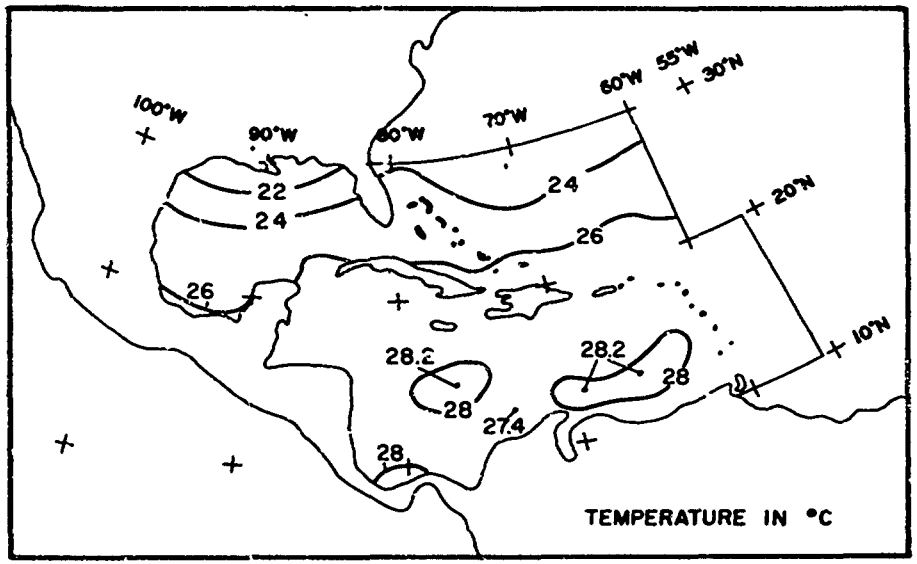

SEA SURFACE TEMPERATURE

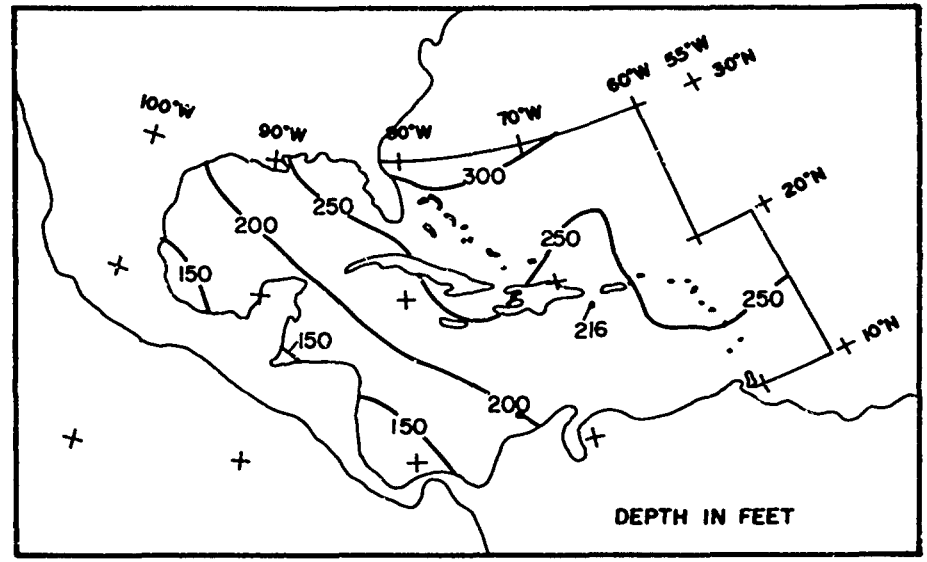

POTENTIAL MIXED LAYER DEPTH

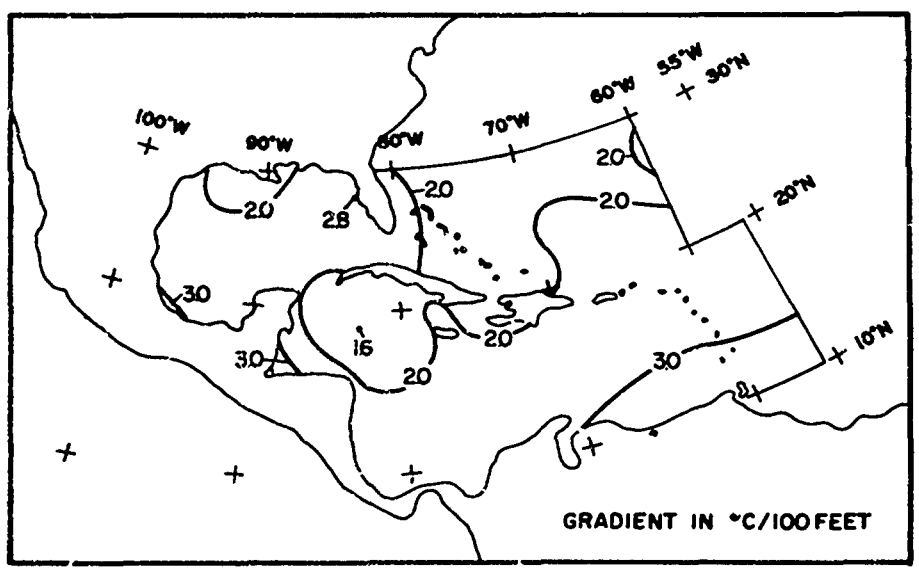

THERMOCLINE GRADIENT

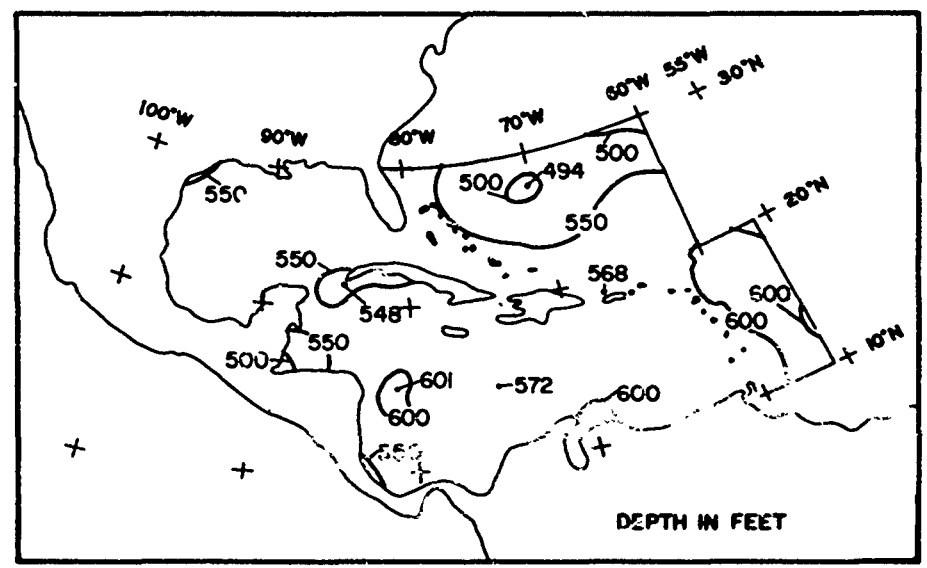

BOTTOM OF THERMOCLINE

FIGURE 4-86 UPPER THERMAL STRUCTURE (DECEMBER, 1968)

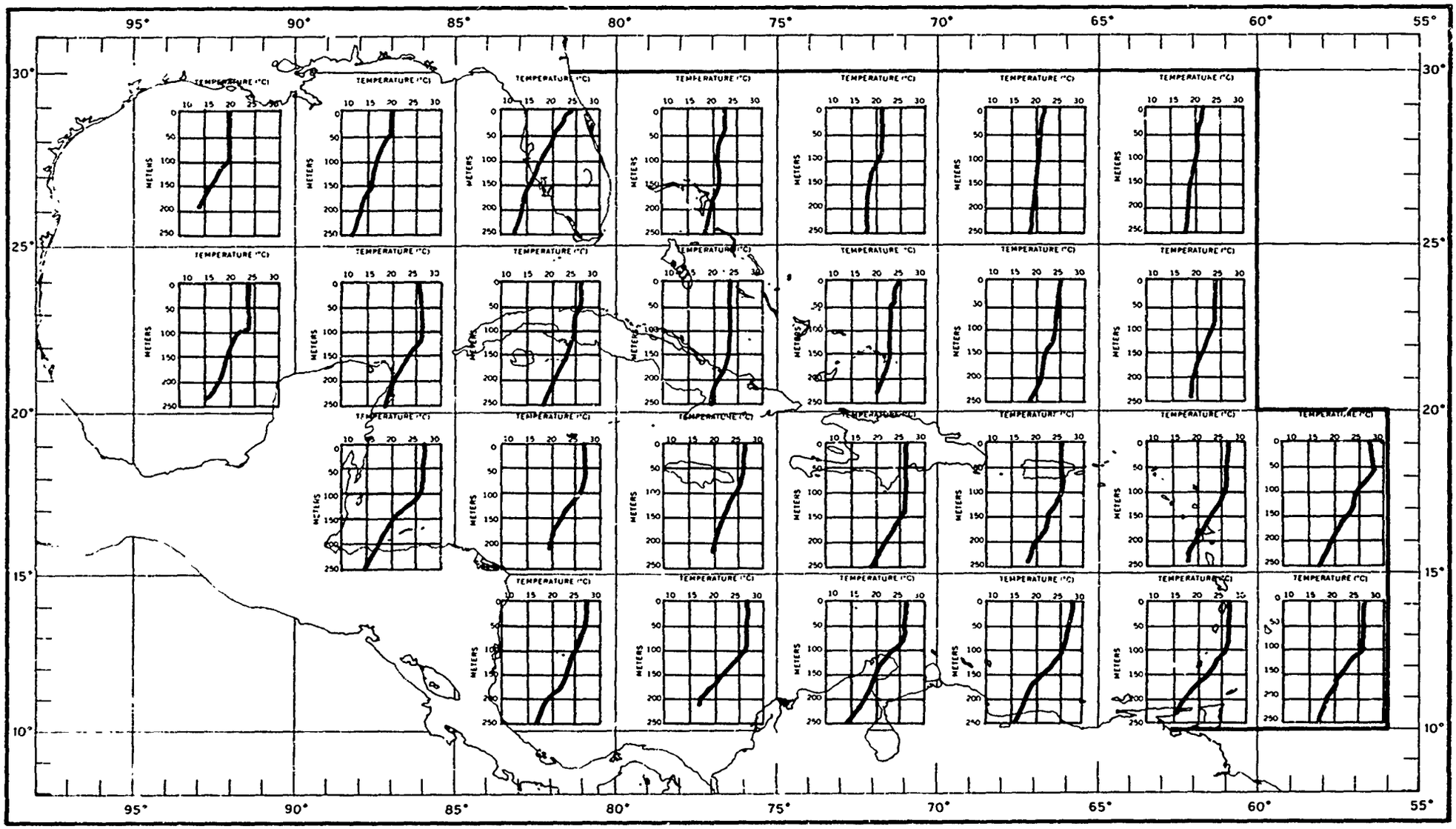

FIGURE 4-87 TYPICAL BATHYTHERMOGRAPHS IN 5-DEGREE SQUARES (WINTER, NOVEMBER-APRIL)

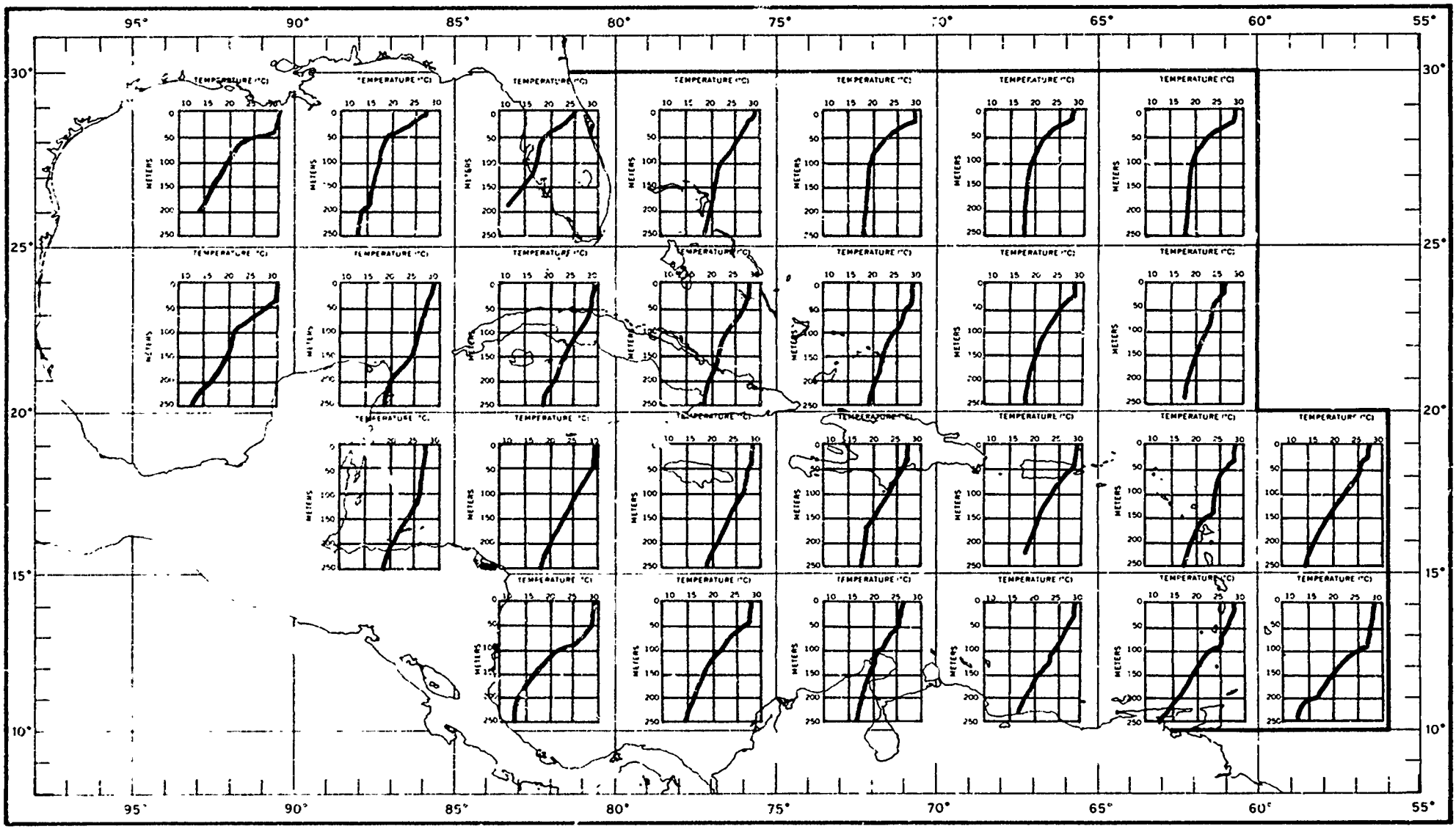

FIGURE 4-88 TYPICAL BATHYTHERMOGRAPHS IN 5-DEGREE SQUARES (SUMMER, MAY-OCTOBER)

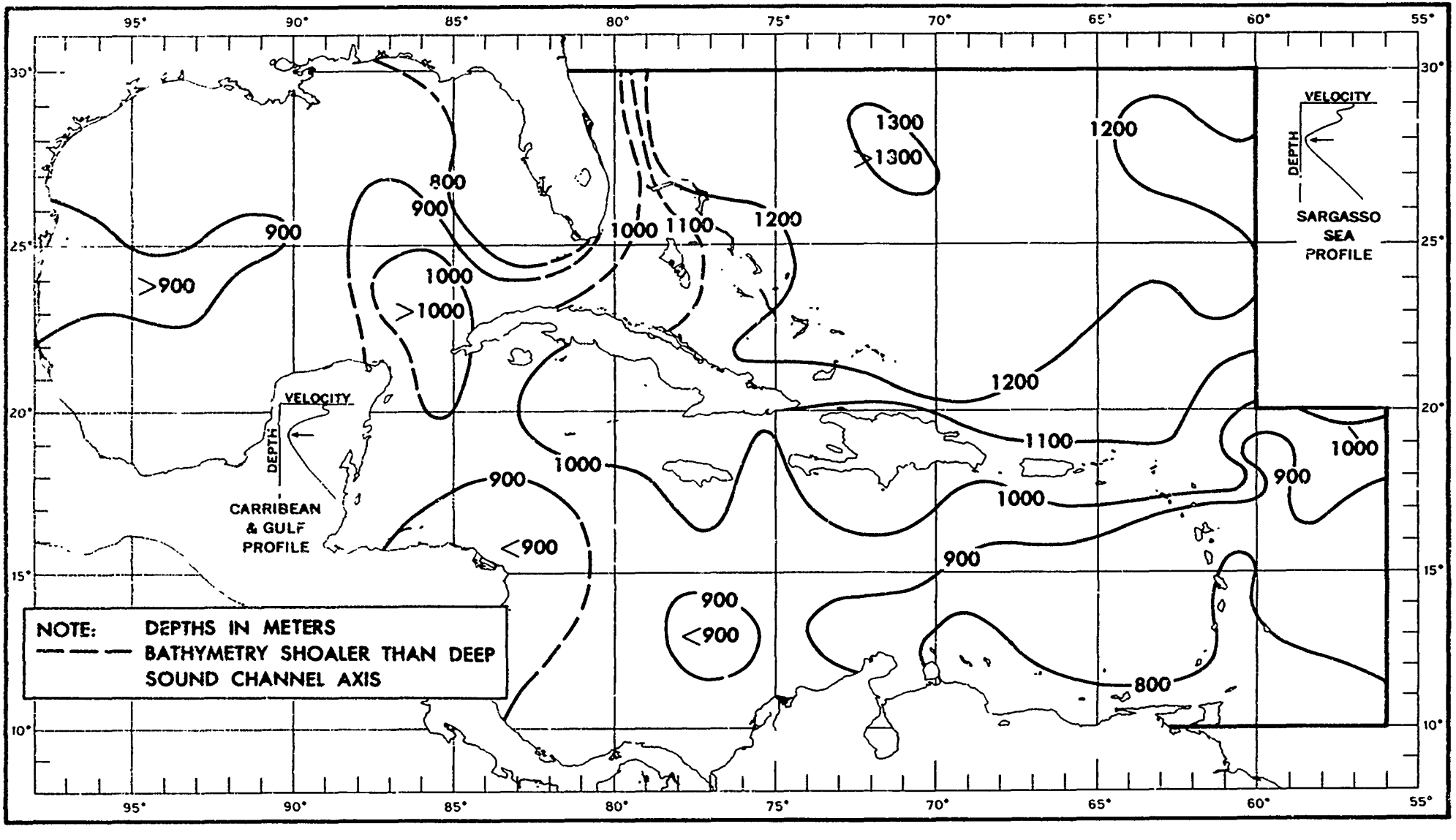

FIGURE 4-89 ANNUAL AVERAGE DEPTH OF THE DEEP SOUND CHANNEL AXIS

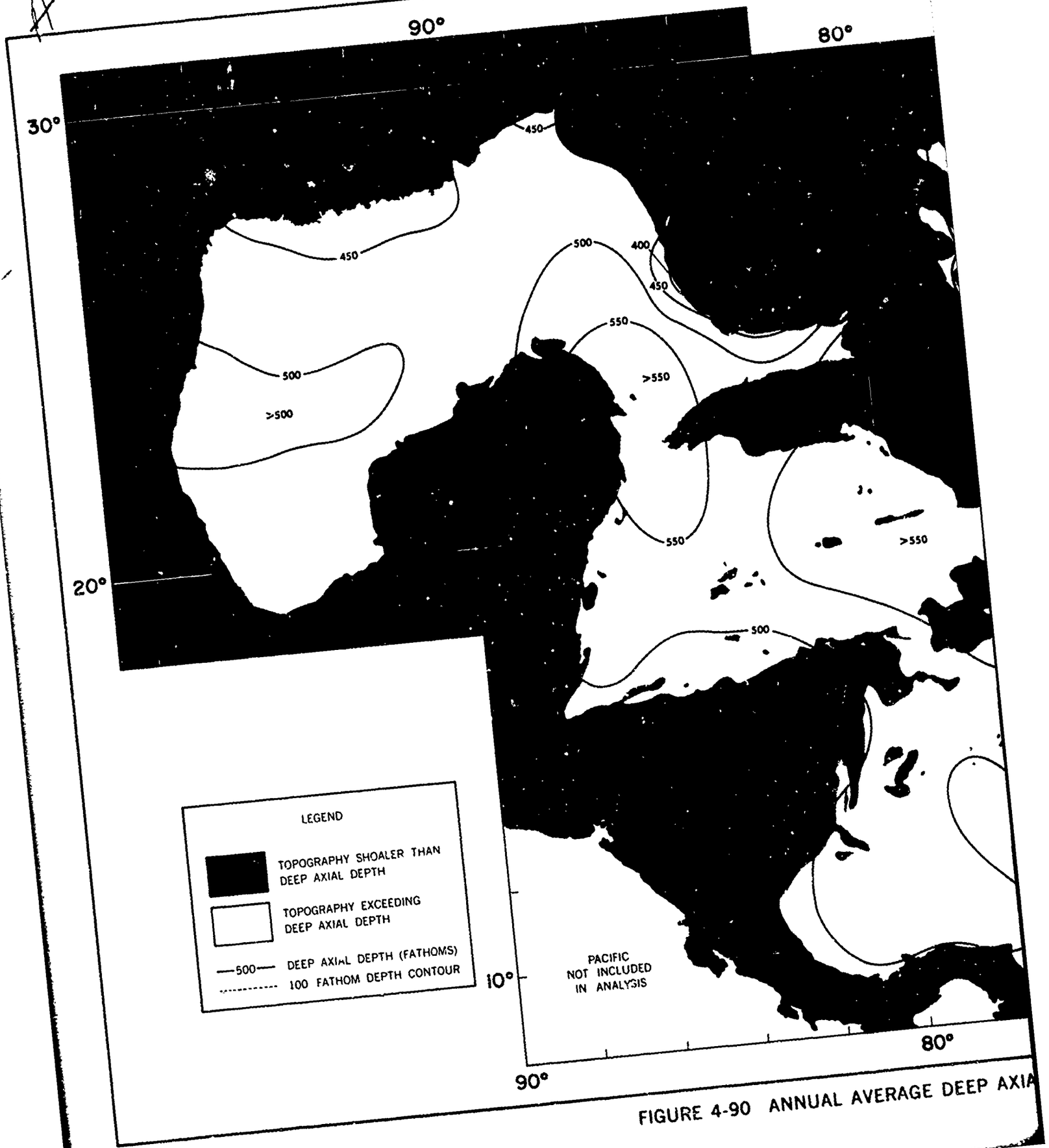

FIGURE 4-90 ANNUAL AVERAGE DEEP AXIA

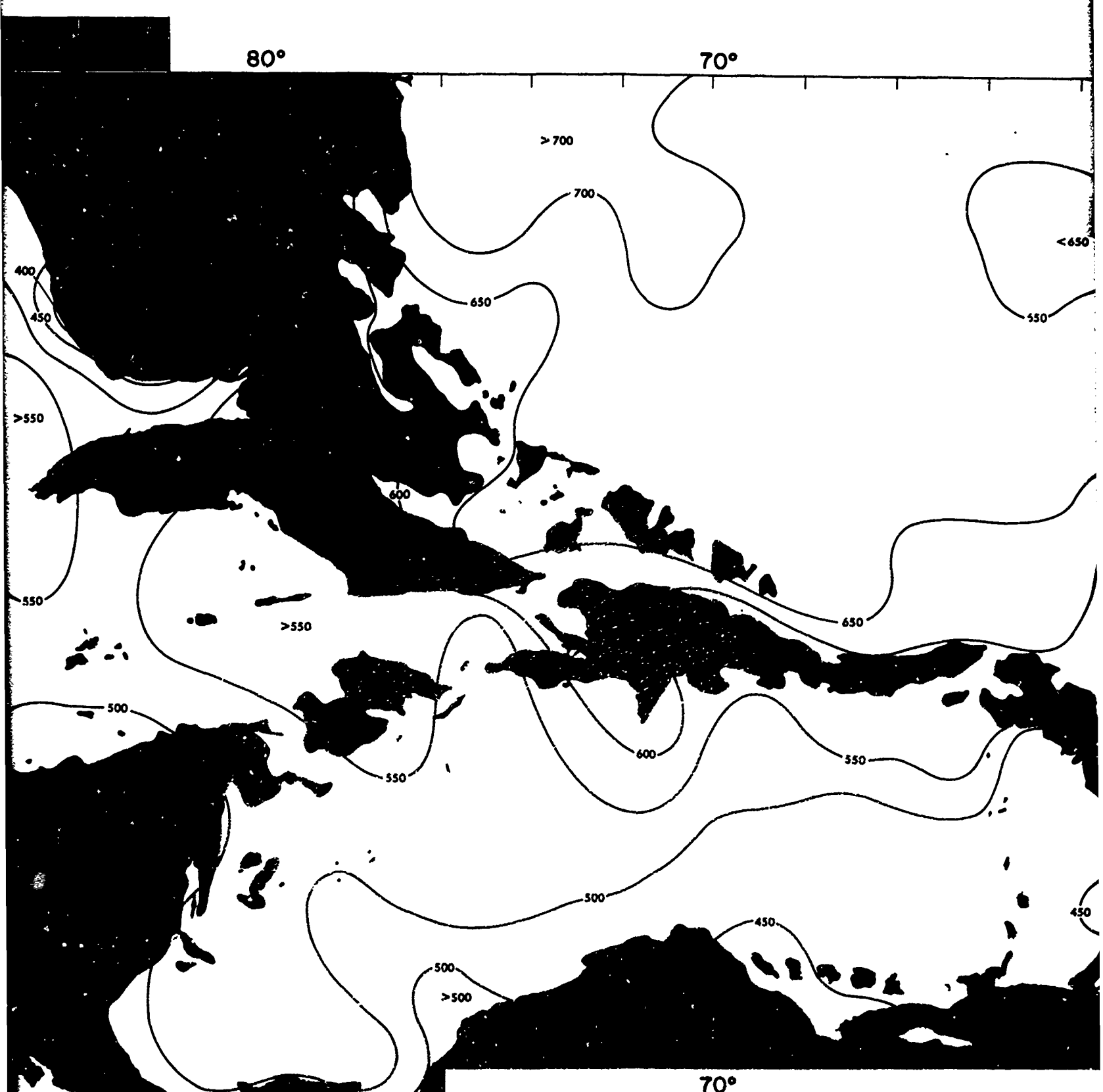

90 ANNUAL AVERAGE DEEP AXIAL DEPTH AND TOPOGRAPHIC INTERFERENCE

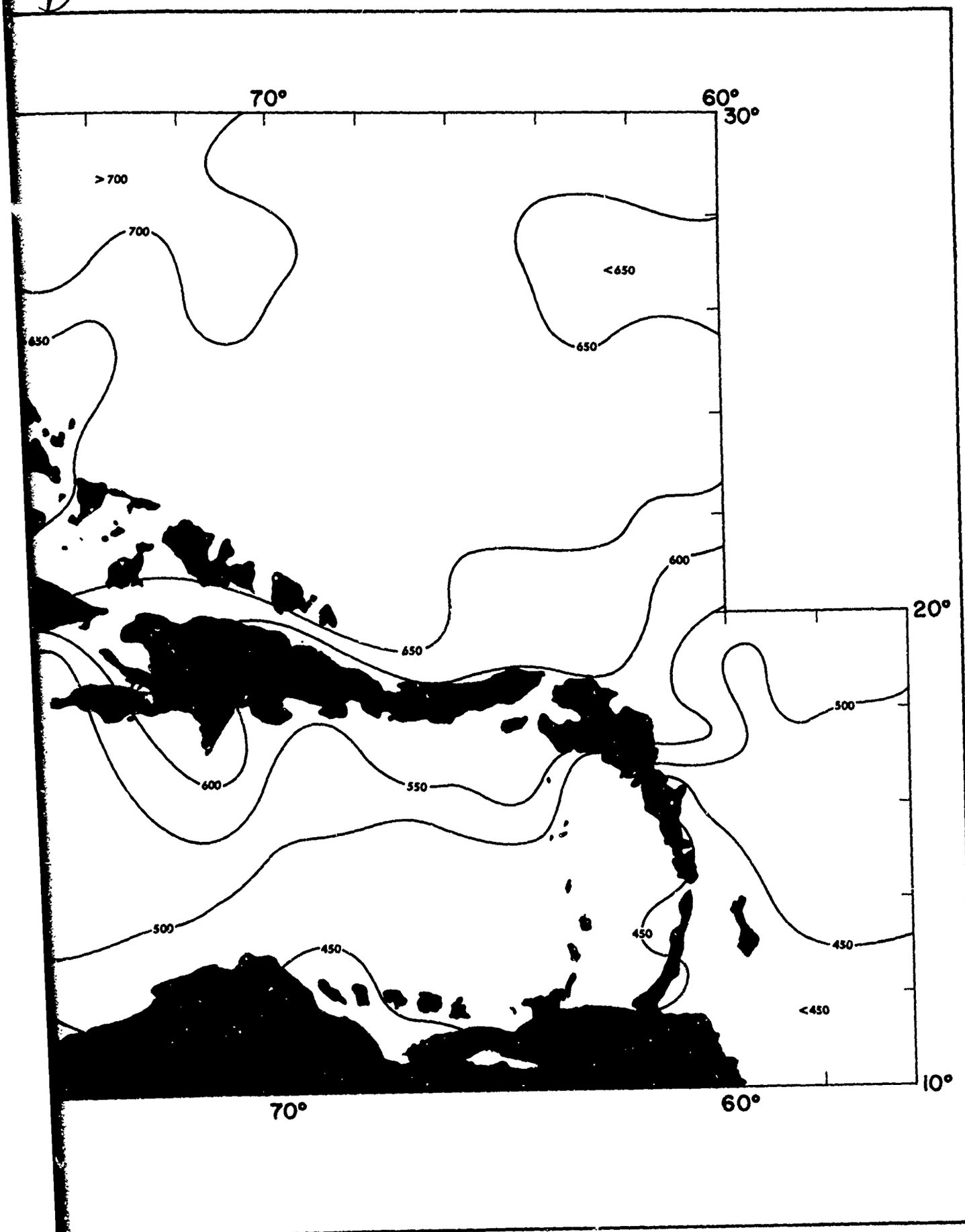

D TOPOGRAPHIC INTERFERENCE

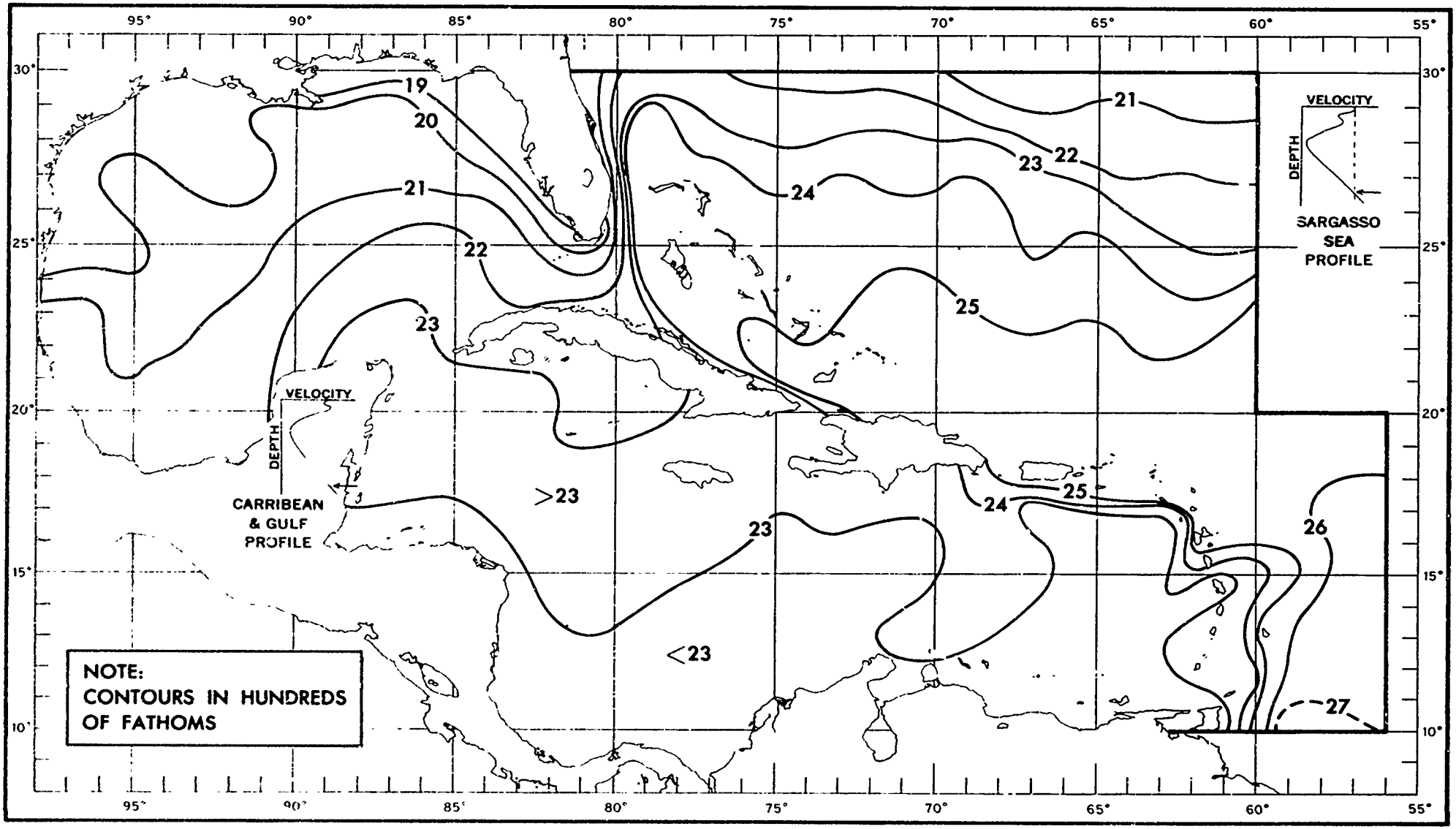

FIGURE 4-91 AVERAGE CRITICAL DEPTH (WINTER, NOVEMBER-APRIL)

Preceding page blank

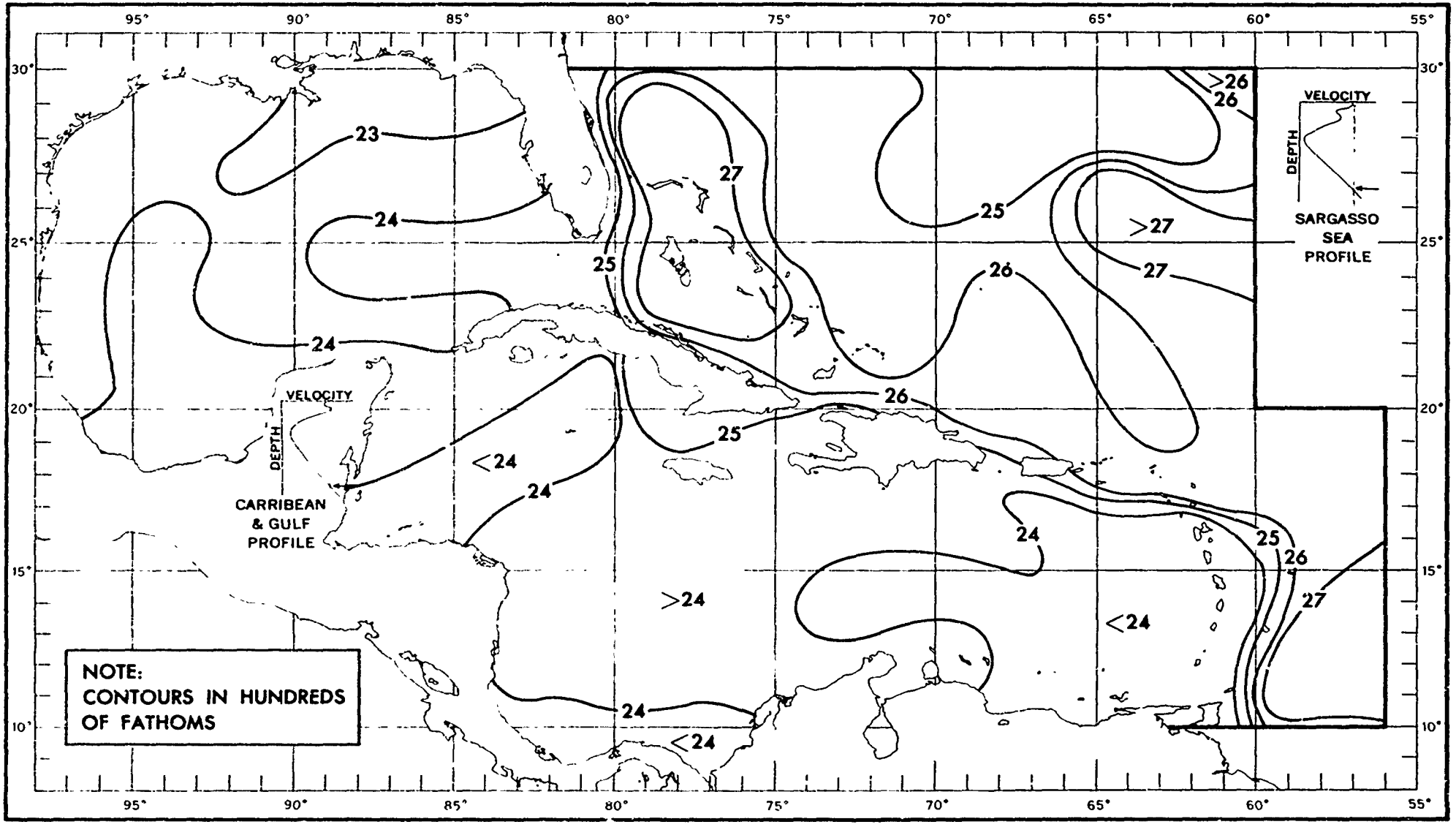

FIGURE 4-92 AVERAGE CRITICAL DEPTH (SUMMER, MAY-OCTOBER)

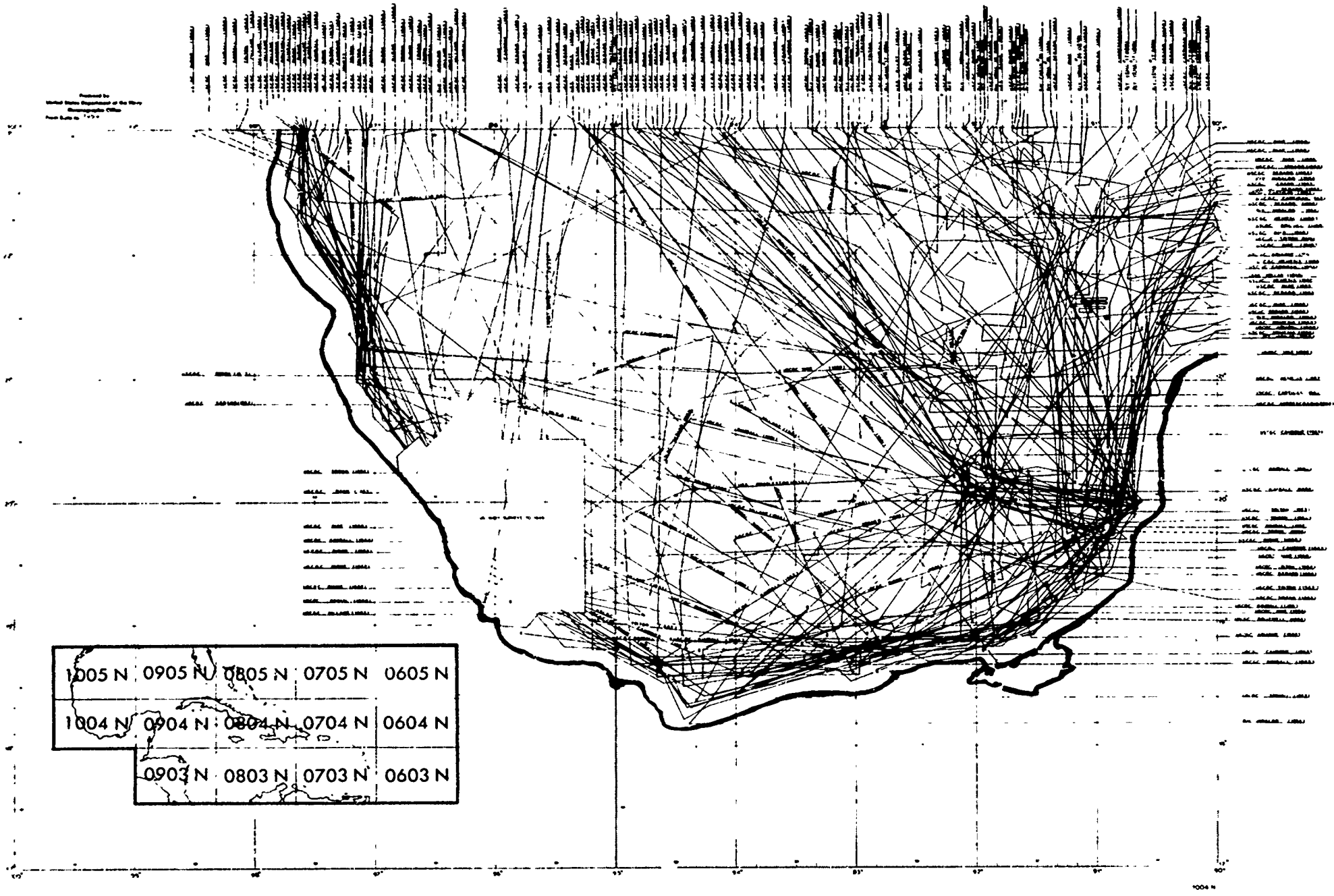

FIGURE 4-95 BATHYMETRIC TRACKS

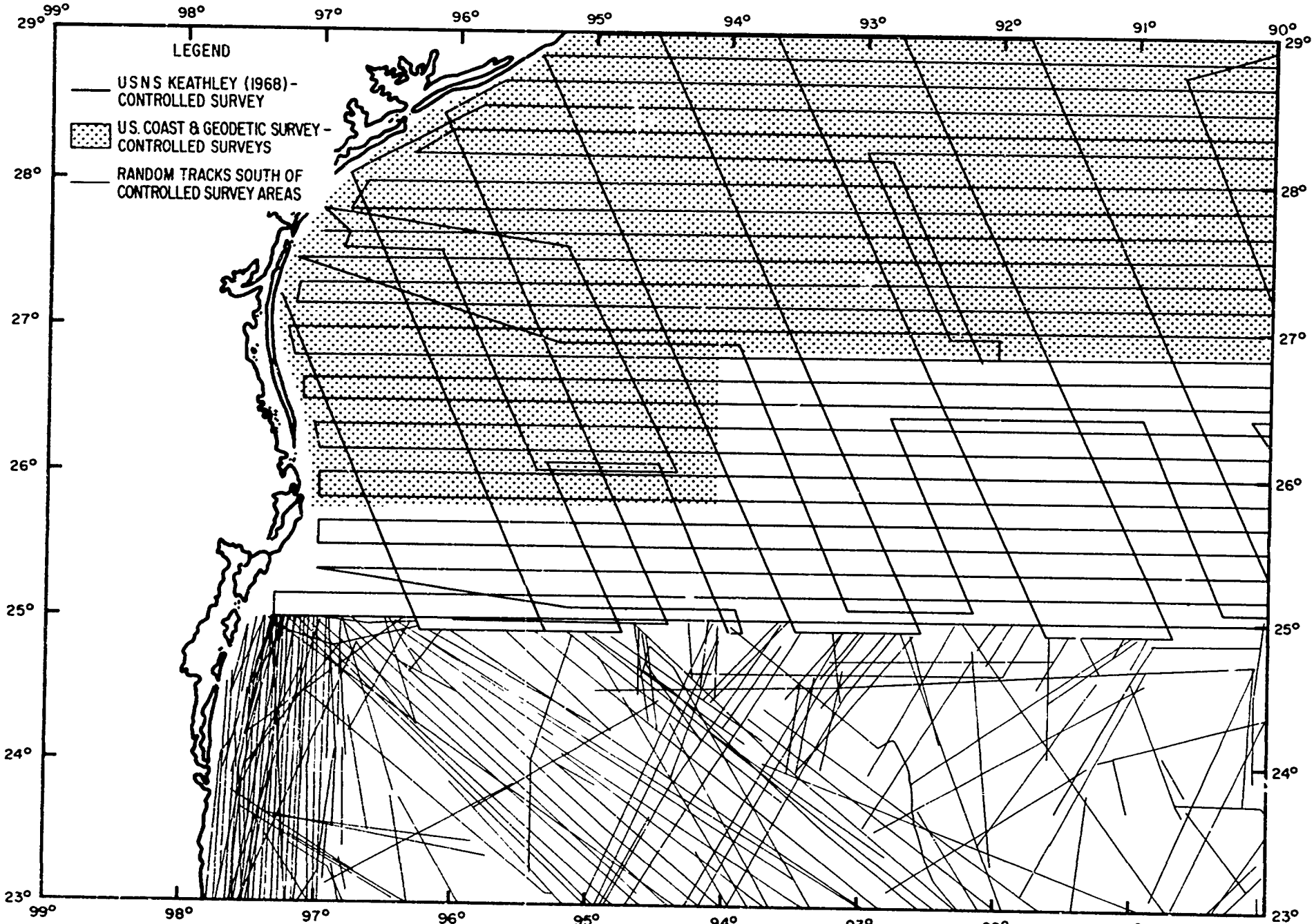

FIGURE 4-96 BATHYMETRIC TRACKS AND SURVEYED AREAS

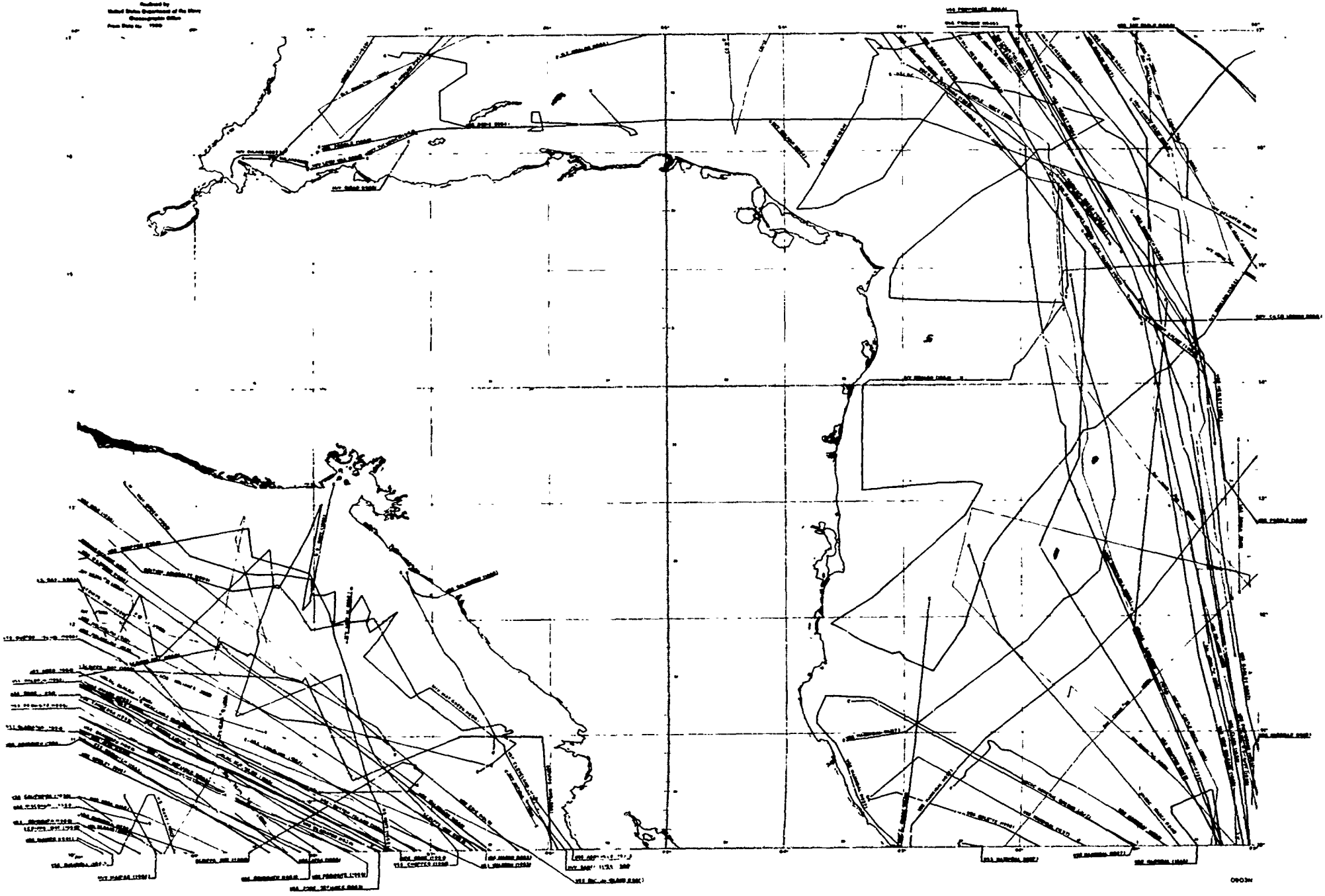

FIGURE 4-97 BATHYMETRIC TRACKS

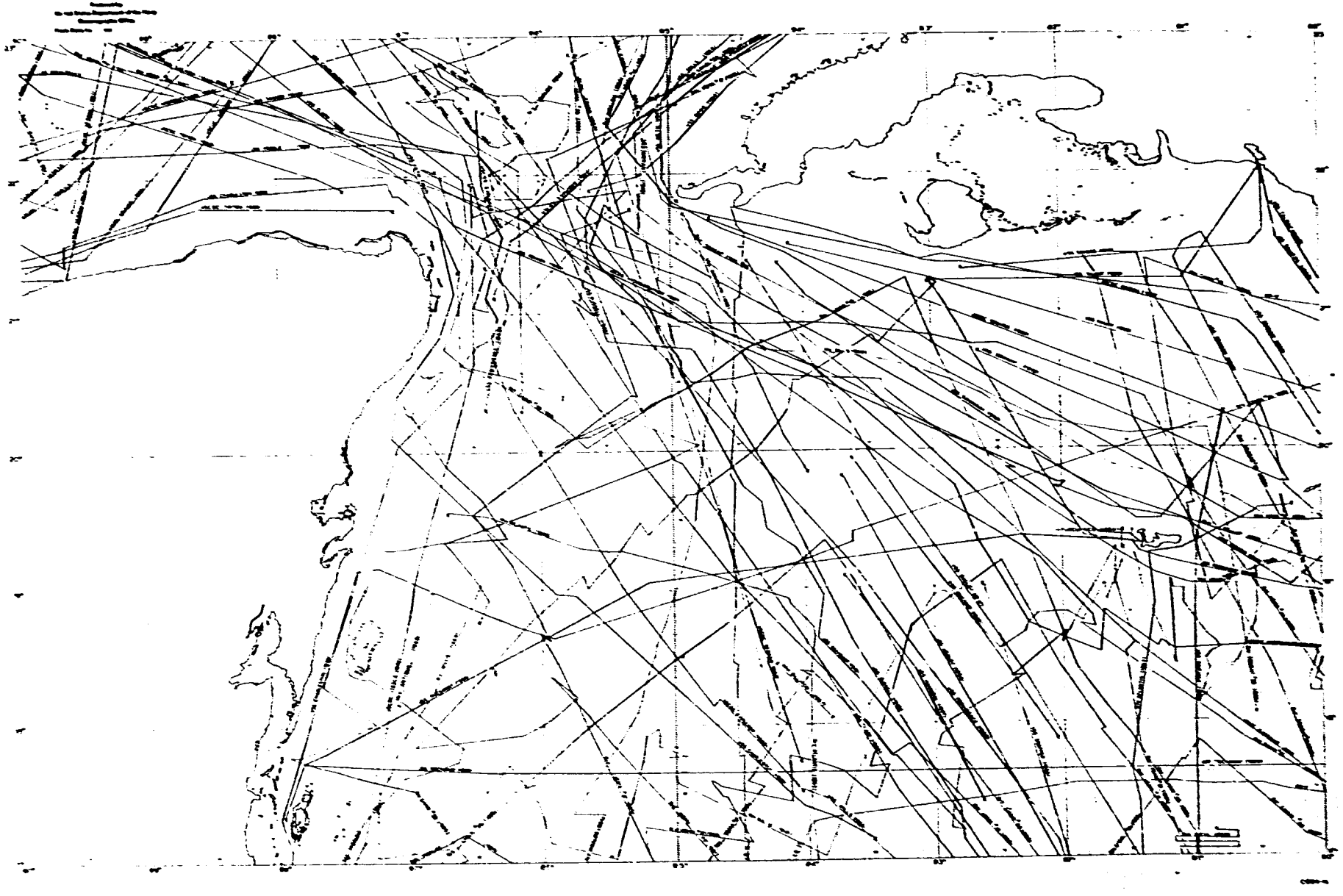

FIGURE 4-98 BATHYMETRIC TRACKS

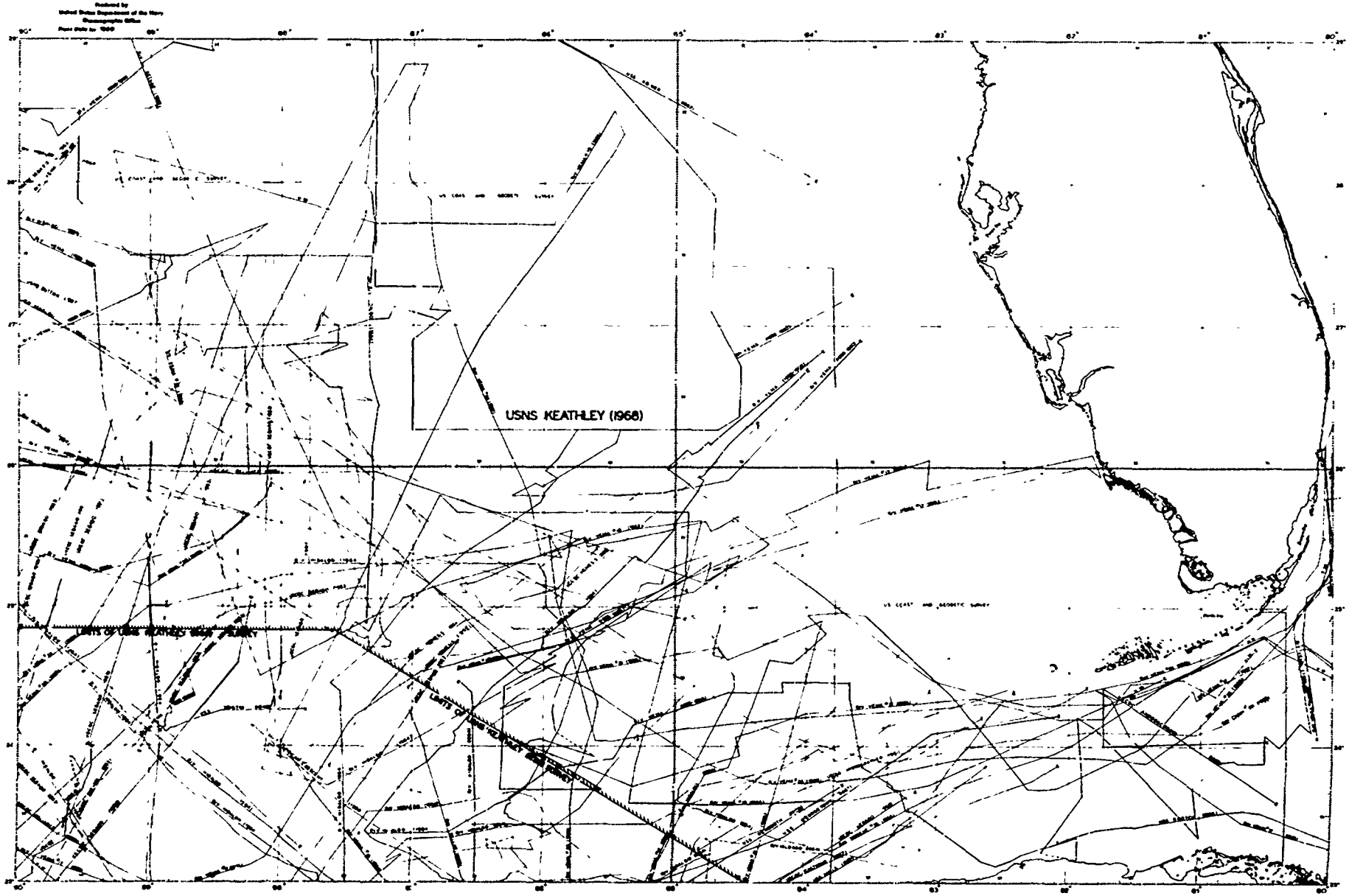

FIGURE 4-99 BATHYMETRIC TRACKS AND SURVEYED AREAS

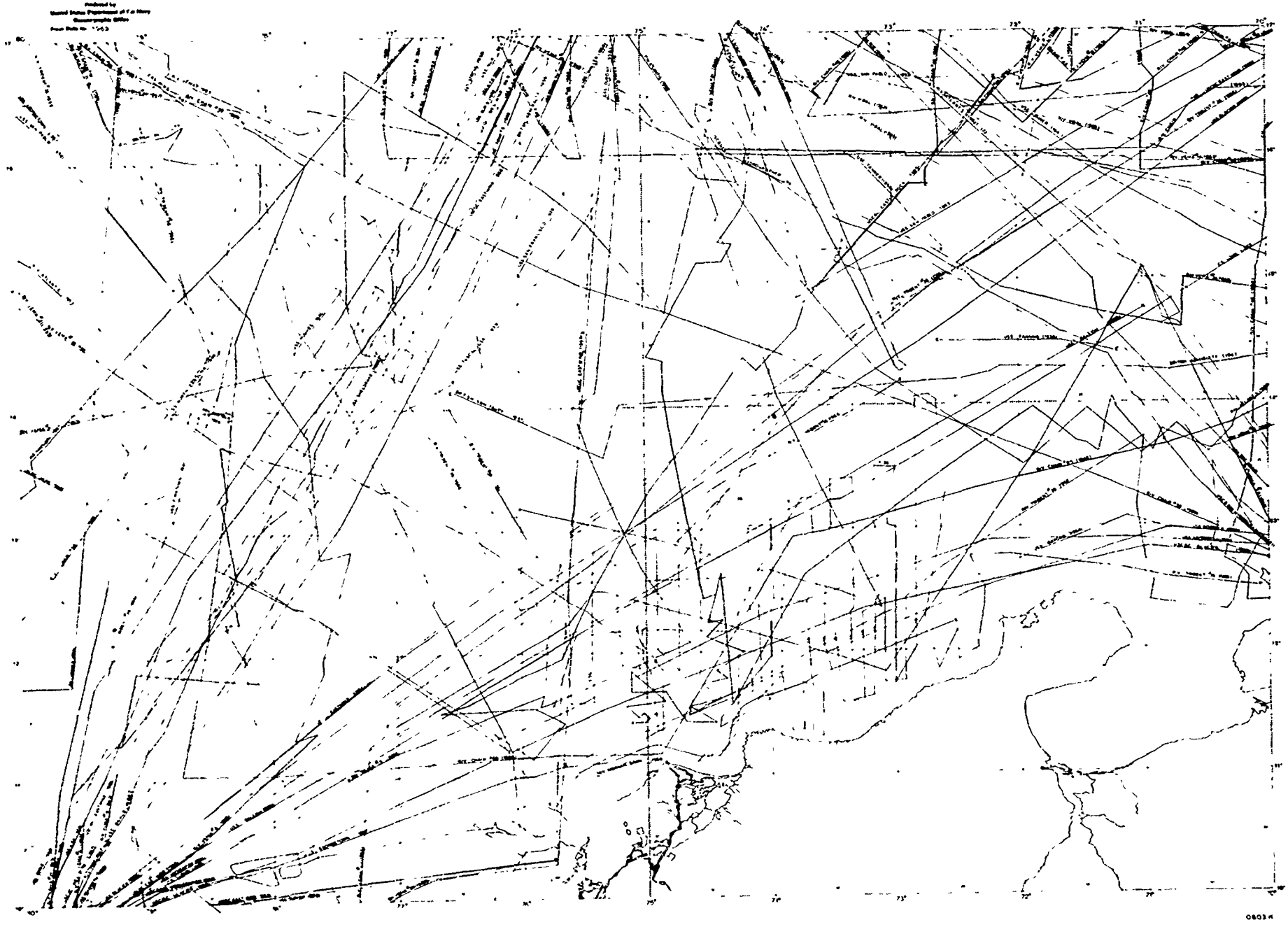

FIGURE 4-100 BATHYMETRIC TRACKS

SEE VOLUME I MARINE ACOUSTICS

FIGURE 4-101 BATHYMETRIC TRACKS AND SURVEYED AREAS

SEE VOLUME I MARINE ACOUSTICS

FIGURE 4-102 BATHYMETRIC TRACKS AND SURVEYED AREAS

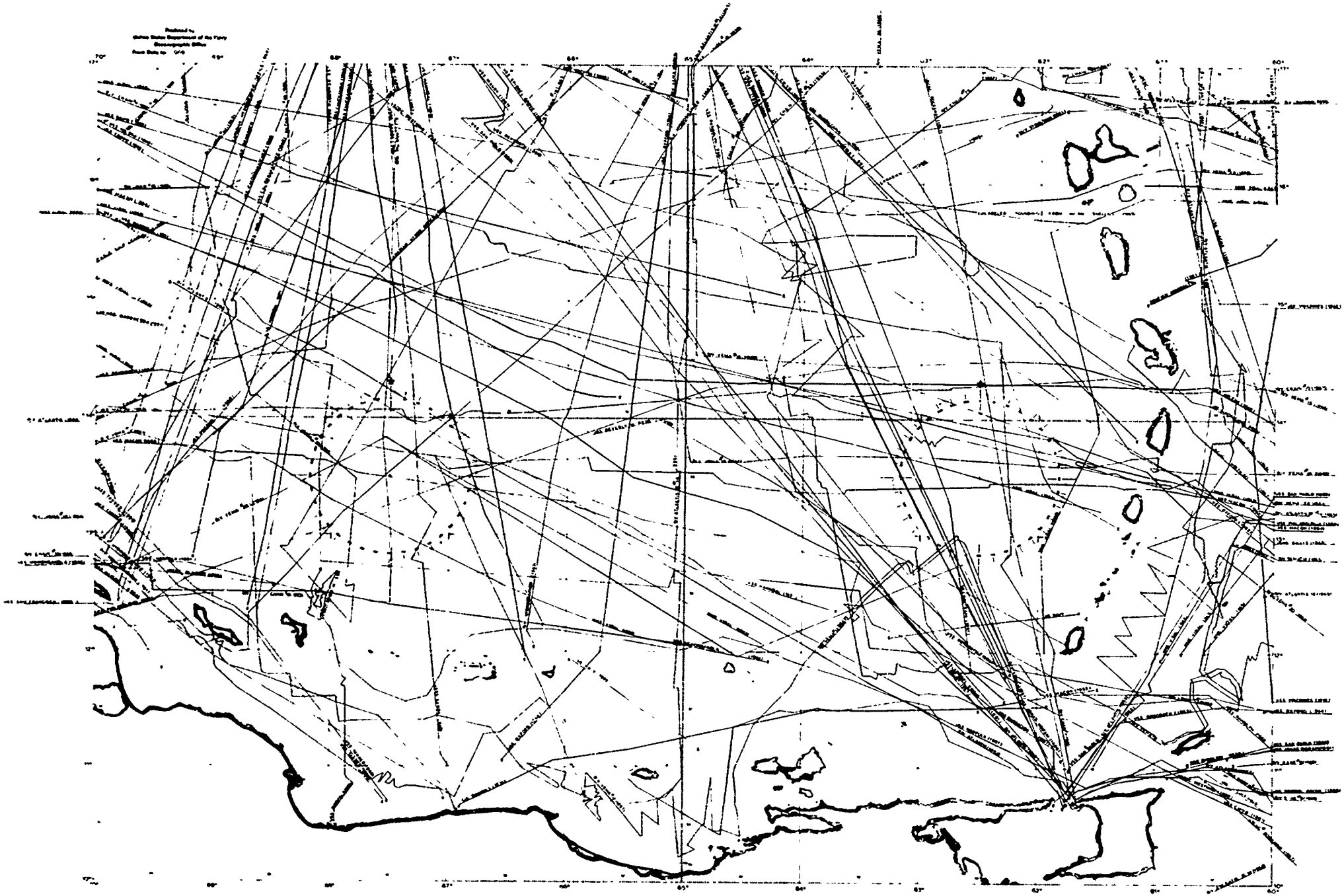

FIGURE 4-103 BATHYMETRIC TRACKS

SEE VOLUME I MARINE ACOUSTICS

FIGURE 4-104 BATHYMETRIC TRACKS AND SURVEYED AREAS

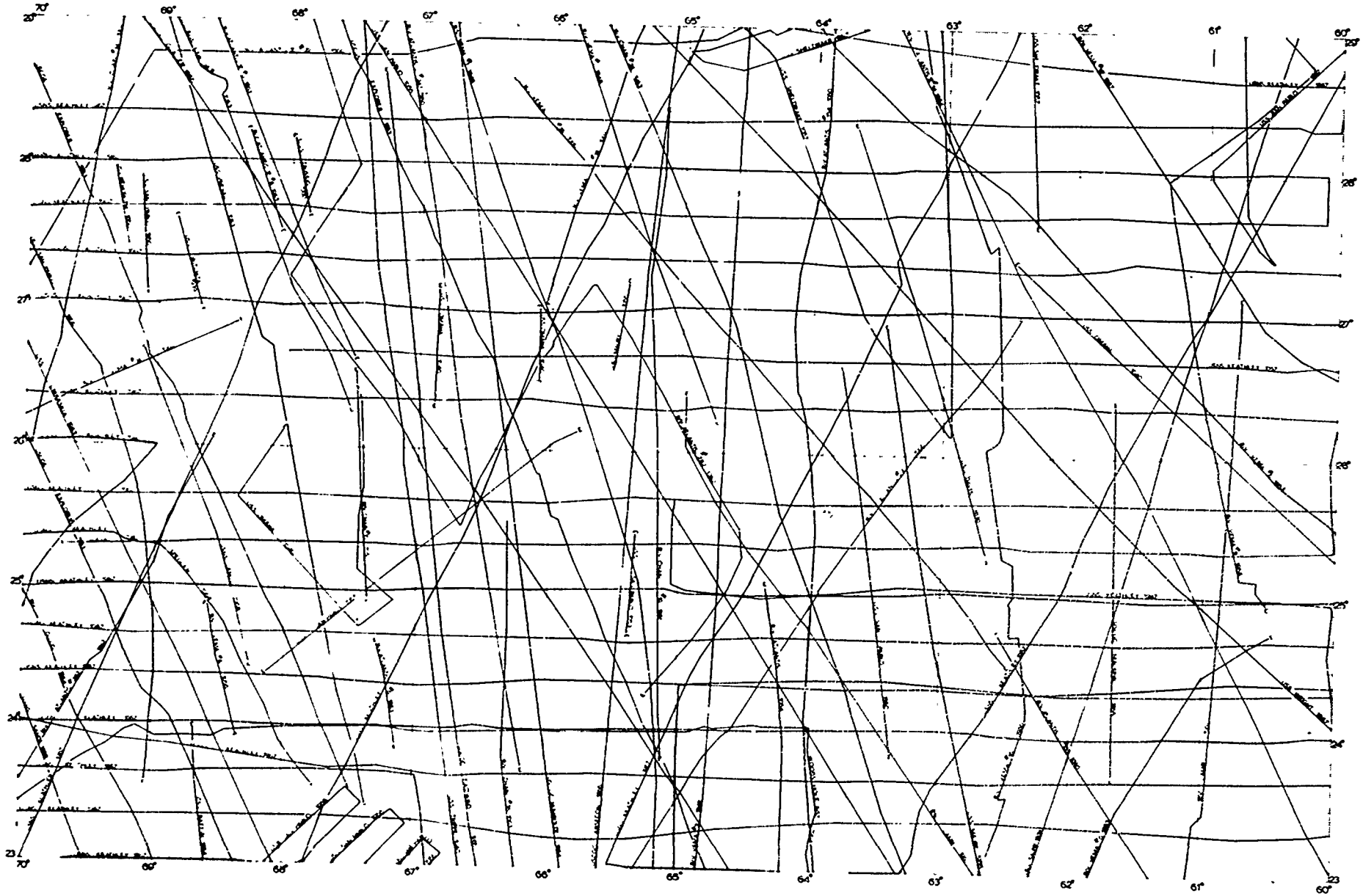

FIGURE 4-105 BATHYMETRIC TRACKS

0705

SEE VOLUME I MARINE ACOUSTICS

FIGURE 4-106 BATHYMETRIC TRACKS AND SURVEYED AREAS

SEE VOLUME I MARINE ACOUSTICS

FIGURE 4-107 BATHYMETRIC TRACKS AND SURVEYED AREAS

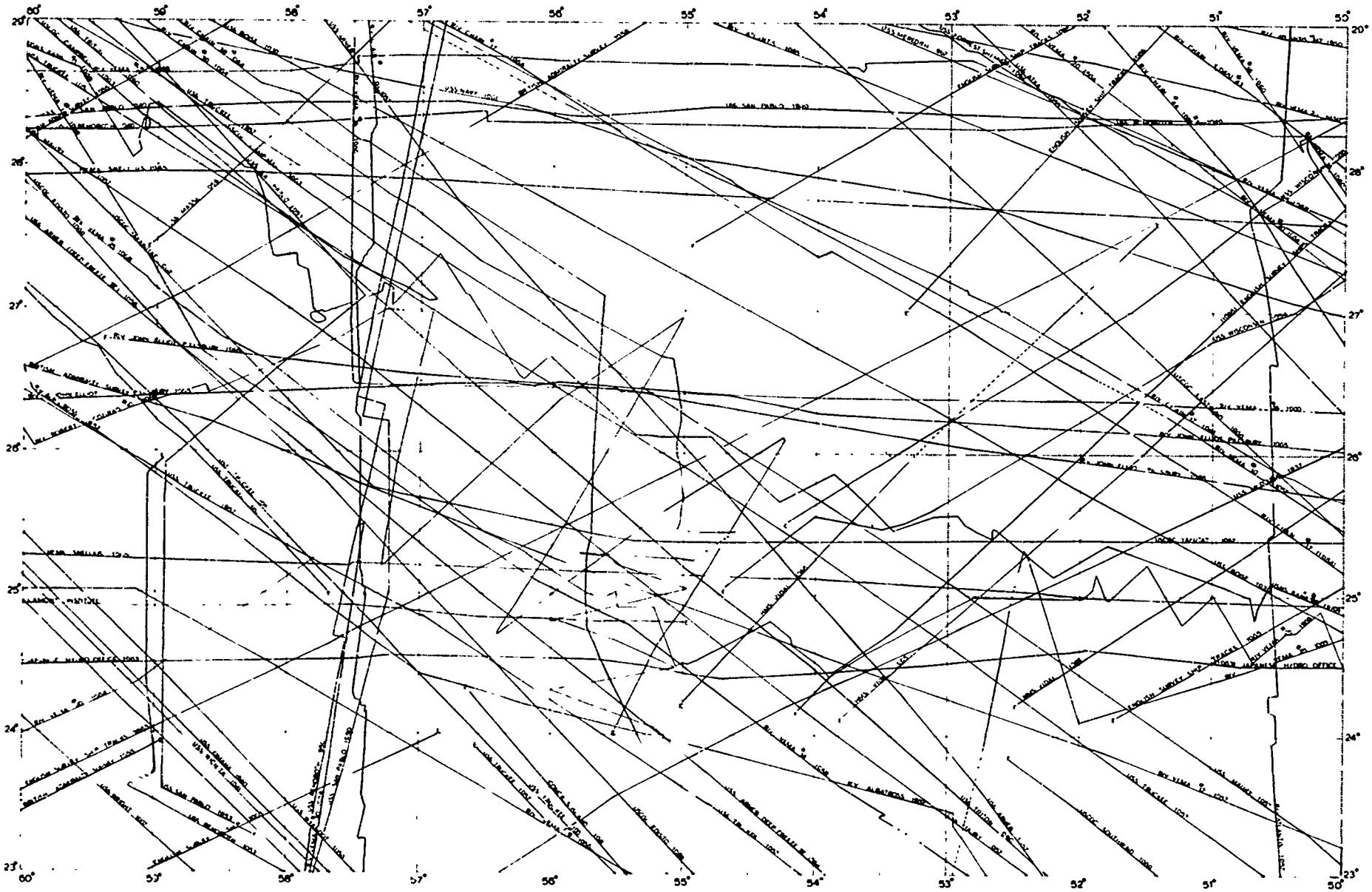

FIGURE 4-108 BATHYMETRIC TRACKS

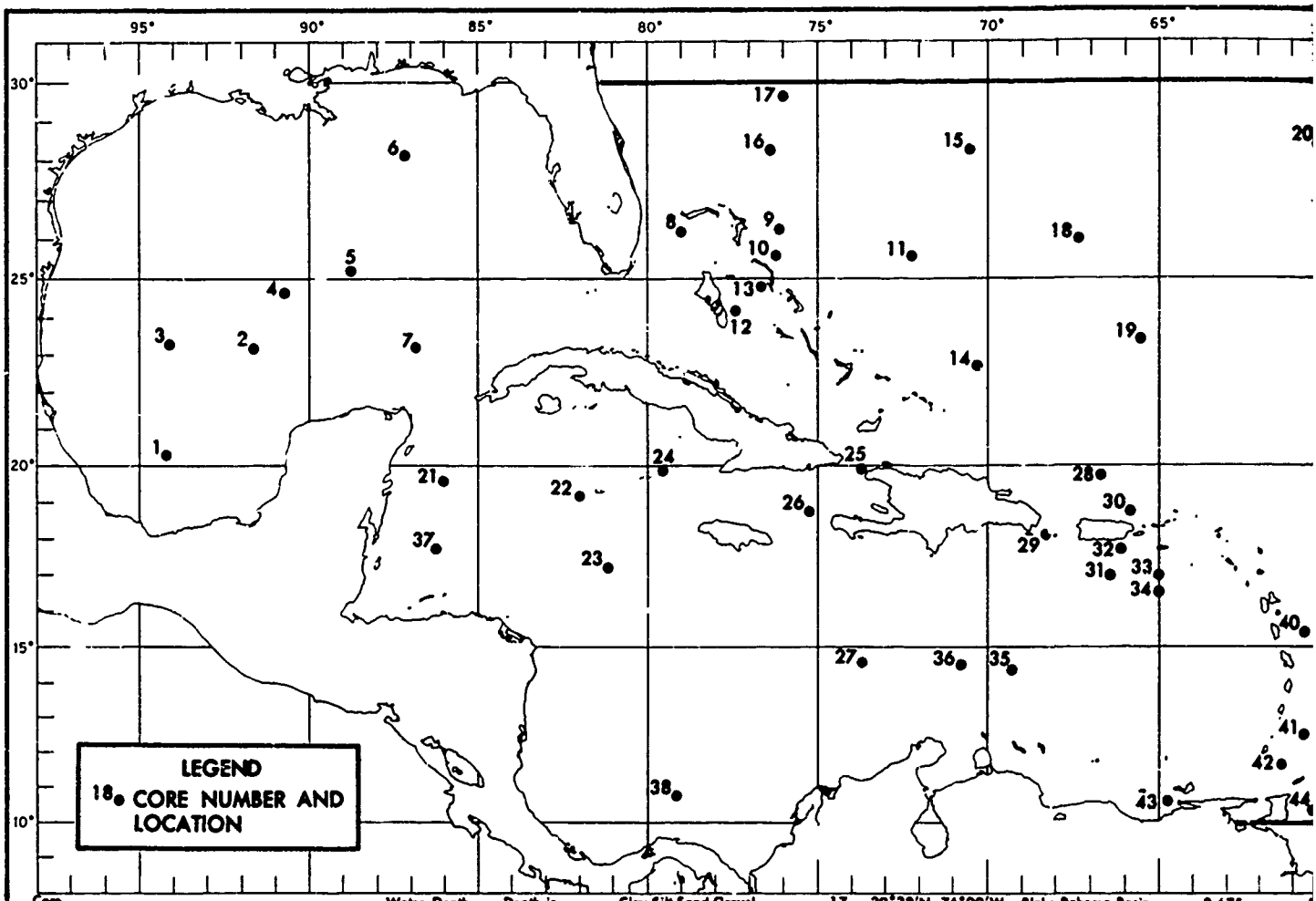

Core No	Location	Region	Water Depth (fms)	Depth in Core (cm)	Clay-Silt-Sand-Gravel Ratio (T=trace)
1	20°20'N, 94°13'W	Continental Rise Gulf of Mexico	1,203	0-89	8-1-1-T
				89-119	7-1-1-1
				119-239	7-2-1-T
2	23°03'N, 91°42'W	Mexican Basin Gulf of Mexico	2,050	0-1007	5-3-2-T
3	23°11'N, 94°10'W	Mexican Basin Gulf of Mexico	2,045	0-776	5-3-2-T
4	24°42'N, 90°46'W	Mississippi Cone Gulf of Mexico	1,055	0-13	5-3-2-0
				13-21	5-4-1-0
				21-51	8-3-1-0
				51-61	3-5-1-1
				61-135	7-2-1-0
				135-150	3-6-1-0
				150-271	6-3-1-0
5	25°09'N, 88°50'W	Mississippi Cone Gulf of Mexico	1,854	0-88	7-2-1-0
				88-103	6-3-1-0
				103-108	2-7-1-0
				108-113	1-6-3-0
				113-152	7-2-1-0
				152-307	8-1-1-0
6	28°02'N, 87°08'W	Northern Continental Slope-Gulf of Mexico	1,328	0-10	7-1-2-0
				10-76	8-2-1-0
				76-156	7-2-1-0
7	23°06'N, 86°53'W	Campeche Bank Gulf of Mexico	236	0-20	2-5-3-0
				20-32	1-4-5-0
8	26°16'N, 79°00'W		2,775	0-5	1-4-5-0
				5-13	1-6-3-0
				13-19	2-4-3-1
				19-25	1-4-5-0
9	26°20'N, 76°03'W		2,775	0-20	6-3-1-0
				20-30	3-6-1-0
				30-38	5-4-1-0
10	25°34'N, 76°12'W	Blake Ridge	2,630	0-5	5-3-2-0
				5-99	2-1-7-0
				99-160	0-1-9-0
				160-175	4-4-2-0
				175-399	0-1-7-2
11	25°43'N, 72°16'W	Hatteras Abyssal	3,800	0-10	6-4-0-0
17	29°39'N, 76°00'W	Blake-Bahama Basin	2,675		
18	26°00'N, 67°27'W	Bermuda Rise	2,920		
19	23°19'N, 65°36'W	Nares Abyssal Plain	3,200		
20	28°25'N, 60°09'W	Abyssal Hills	3,050		
21	19°38'N, 86°01'W	Yucatan Basin	2,410		
22	19°05'N, 82°00'W	Cayman Ridge	—		
23	17°13'N, 81°05'W	Nicaraguan Rise	—		
24	19°58'N, 79°34'W	Cayman Ridge	1,200		
25	19°55'N, 73°32'W	Windward Passage	1,148		

FIGURE 4 112 BOTTOM SEDIMENT CORES

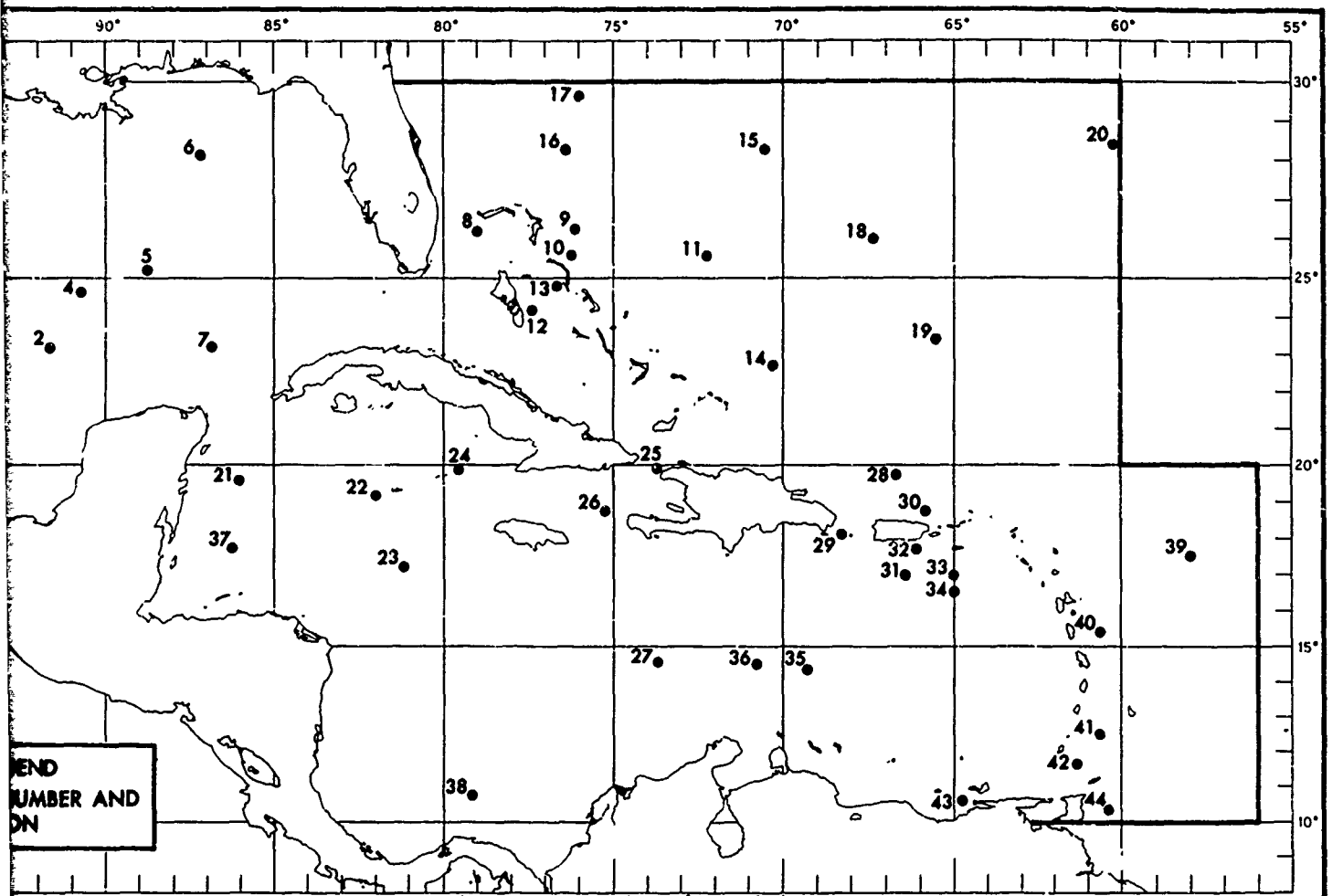

Region	Water Depth (fms)	Depth in Core (cm)	Clay-Silt-Sand-Gravel Ratio (T=trace)
Continental Rise Gulf of Mexico	1,203	0-89	8-1-1-T
		89-119	7-1-1-1
		119-239	7-2-1-T
Mexican Basin Gulf of Mexico	2,050	0-1007	5-3-2-T
Mexican Basin Gulf of Mexico	2,045	0-776	5-3-2-T
Mississippi Cone Gulf of Mexico	1,055	0-13	5-3-2-0
		13-21	5-4-1-0
		21-51	8-3-1-0
		51-61	3-5-1-1
		61-135	7-2-1-0
		135-150	3-6-1-0
		150-271	6-3-1-0
Mississippi Cone Gulf of Mexico	1,854	0-88	7-2-1-0
		88-103	6-3-1-0
		103-108	2-7-1-0
		108-113	1-6-3-0
		113-152	7-2-1-0
		152-307	8-1-1-0
Northern Continental Slope-Gulf of Mexico	1,328	0-10	7-1-2-0
		10-76	8-2-1-0
		76-156	7-2-1-0
Campeche Bank Gulf of Mexico	236	0-20	2-5-3-0
		20-32	1-4-5-0
	2,775	0-5	1-4-5-0
		5-13	1-6-3-0
		13-19	2-4-3-1
		19-25	1-4-5-0
	2,775	0-20	6-3-1-0
		20-30	3-6-1-0
		30-38	5-4-1-0
Blake Ridge	2,630	0-5	5-3-2-0
		5-99	2-1-7-0
		99-160	0-1-9-0
		160-175	4-4-2-0
		175-599	0-1-7-2
Hatteras Abyssal Plain	2,800	0-10	6-4-0-0
		10-20	4-6-0-0
		20-47	7-3-0-0
		47-95	5-5-0-0
		95-100	3-6-1-0
		100-140	7-2-1-0
		140-240	5-5-0-0
		240-360	6-4-0-0
		360-380	5-3-0-0

17	29°39'N, 76°00'W	Blake-Bahama Basin	2,675	0-73	Sand-Mud		
				73-117	Mud		
				117-143	Sand-Mud-Gravel		
				143-1120	Mud-Silt		
18	26°00'N, 67°27'W	Bermuda Rise	2,920	0-24		7-2-1-0	
19	23°19'N, 65°36'W	Nares Abyssal Plain	3,200	0-24		8-1-1-0	
20	28°25'N, 60°09'W	Abyssal Hills	3,050	0-85	Clay		
21	19°38'N, 86°01'W	Yucatan Basin	2,410	0-37		6-3-1-0	
				37-57		1-7-2-0	
				57-85		6-2-1-1	
				85-88		2-6-1-1	
				88-136		6-2-1-1	
				136-139		2-6-1-1	
				139-211		7-2-1-0	
				211-266		8-1-1-0	
				266-291		6-3-1-0	
				291-311		4-3-3-0	
				311-351		7-2-1-0	
				351-400		5-4-1-0	
				400-417		6-3-1-0	
				417-420		3-5-1-0	
22	19°05'N, 82°00'W	Cayman Ridge	—	0-290	Clay-Silt		
				290-300	Gravel		
				300-555	Sand		
23	17°13'N, 81°05'W	Nicaraguan Rise	—	0-80	Mud		
				80-85	Sand		
				85-230	Mud		
				230-235	Sand		
				235-255	Mud		
				255-270	Sand		
				270-332	Mud		
				332-338	Sand		
				338-405	Mud		
				405-500	Sand		
				500-545	Mud		
24	19°58'N, 79°34'W	Cayman Ridge	1,200	0-30		4-3-2-1	
				30-138		1-6-2-1	
25	19°55'N, 73°32'W	Windward Passage	1,148	0-17			
				17-30		4-5-1-0	
				30-45		4-5-1-0	
				45-56		2-3-4-1	
26	18°50'N, 75°09'W	Cayman Trough (East)	1,250	0-60		1-6-2-1	
				60-120		4-5-0-1	
				120-180		5-4-0-1	
				180-350		4-3-2-1	
27	14°33'N, 73°47'W	Beata Ridge	1,650	0-10		0-6-3-1	
				10-20		1-5-3-1	
				20-30		1-7-1-1	

Core No	Location	Region	Water Depth (fms)	Depth in Core (cm)	Clay-Silt-Sand-Gravel Ratio (T=trace)
1	20°20'N, 94°13'W	Continental Rise Gulf of Mexico	1,203	0-89	8-1-1-T
				89-119	7-1-1-1
				119-239	7-2-1-T
2	23°03'N, 91°42'W	Mexican Basin Gulf of Mexico	2,050	0-1007	5-3-2-T
3	23°11'N, 94°10'W	Mexican Basin Gulf of Mexico	2,045	0-776	5-3-2-T
4	24°42'N, 90°46'W	Mississippi Cone Gulf of Mexico	1,055	0-13	5-3-2-0
				13-21	5-4-1-0
				21-51	8-1-1-0
				51-61	3-5-1-1
				61-135	7-2-1-0
				135-150	3-6-1-0
				150-271	6-3-1-0
5	25°09'N, 88°50'W	Mississippi Cone Gulf of Mexico	1,854	0-88	7-2-1-0
				88-103	6-3-1-0
				103-108	2-7-1-0
				108-113	1-6-3-0
				113-152	7-2-1-0
				152-307	8-1-1-0
6	28°02'N, 87°08'W	Northern Continental Slope-Gulf of Mexico	1,328	0-10	7-1-2-0
				10-76	8-2-1-0
				76-156	7-2-1-0
7	23°06'N, 86°53'W	Campeche Bank Gulf of Mexico	236	0-20	2-5-3-0
				20-32	1-4-5-0
8	26°16'N, 79°00'W		2,775	0-5	1-4-5-0
				5-13	1-6-3-0
				13-19	2-4-3-1
				19-25	1-4-5-0
9	26°20'N, 76°03'W		2,775	0-20	6-3-1-0
				20-30	3-6-1-0
				30-38	5-4-1-0
10	25°34'N, 76°12'W	Blake Ridge	2,630	0-5	5-3-2-0
				5-99	2-1-7-0
				99-160	0-1-9-0
				160-175	4-4-2-0
				175-599	0-1-7-2
11	25°43'N, 72°16'W	Hatteras Abyssal Plain	2,800	0-10	6-4-0-0
				10-20	4-6-0-0
				20-47	7-3-0-0
				47-95	5-5-0-0
				95-100	3-6-1-0
				100-140	7-2-1-0
				140-240	5-5-0-0
				240-360	6-4-0-0
				360-380	5-5-0-0
				380-580	6-4-0-0
				580-620	8-2-0-0
				620-640	5-5-0-0
				640-660	9-1-0-0
				660-720	7-3-0-0
				720-760	9-1-0-0
				760-860	6-4-0-0
				860-880	4-6-0-0
				880-920	6-4-0-0
				920-1000	9-1-0-0
				1000-1032	7-3-0-0
				1032-1040	2-8-0-0
				1040-1100	8-2-0-0
12	24°10'N, 77°22'W	Tongue of the Ocean, Bahamas	751	0-13	4-4-2-0
				13-26	4-5-1-0
				26-39	3-6-1-0
13	24°47'N, 76°31'W	Exuma Sound, Bahamas	847	0-22	3-6-1-0
				22-30	4-4-1-1
				30-42	3-6-1-0
				42-70	4-4-1-1
				70-78	1-2-5-1
				78-86	0-1-7-2
				89-90	0-1-3-6
14	22°46'N, 70°15'W	Hatteras Abyssal Plain	2,872	0-150	Mud
				150-173	Sand-Silt
				173-387	Mud-Ferro manganese nodules
				387-415	Silt-Sand
				415-505	Mud-Ferro manganese nodules
				505-520	Silt-Sand
				520-540	Mud
15	28°19'N, 70°30'W	Hatteras Abyssal Plain	1,569	0-23	6-3-1-0
				23-30	8-1-1-0
				30-40	5-4-1-0
				40-45	9-1-0-0
				45-50	2-7-1-0
				50-84	7-2-1-0
16	28°14'N, 76°20'W	Blake-Bahama Basin	2,717	0-56	Sand
				56-122	Sand-Clay
				122-258	Silt-Clay
				258-295	Silt
17	29°39'N, 76°00'W	Blake-Bahama Basin	2,6
18	26°03'N, 67°27'W	Bermuda Rise	2,9
19	23°19'N, 65°36'W	Nares Abyssal Plain	3,2
20	28°25'N, 60°09'W	Abyssal Hills	3,0
21	19°38'N, 86°01'W	Yucatan Basin	2,4
22	19°05'N, 82°00'W	Cayman Ridge	—
23	17°13'N, 81°05'W	Nicaraguan Rise	—
24	19°58'N, 79°34'W	Cayman Ridge	1,20
25	19°55'N, 73°32'W	Windward Passage	1,14
26	18°50'N, 75°09'W	Cayman Trough (East)	1,25
27	14°33'N, 73°47'W	Beata Ridge	1,65
28	19°45'N, 66°37'W	Puerto Rico Trench	4,15
29	18°06'N, 68°11'W	Mona Passage	1,21
30	18°48'N, 65°58'W	Island Slope Puerto Rico Trench	1,20
31	17°00'N, 66°30'W	Muertos Trench	2,47
32	17°46'N, 66°01'W	Island Slope Puerto Rico	69
33	17°00'N, 65°00'W	Venezuelan Basin	2,40
34	16°40'N, 65°00'W	Venezuelan Basin	2,17
35	14°26'N, 69°22'W	Venezuelan Basin	2,45
36	14°39'N, 70°49'W	Venezuelan Basin	2,10
37	17°45'N, 86°17'W	Cayman Ridge	1,96
38	10°50'N, 79°03'W	Colombian Basin	1,85
39	17°35'N, 58°00'W	Abyssal Hills	2,90
40	15°34'N, 60°38'W	Eastern Slope off Dominica	1,60
41	12°36'N, 60°37'W	Eastern Slope off Grenada	1,35
42	11°42'N, 61°25'W	Grenada-Trinidad Passage	1,28
43	10°41'N, 64°40'W	Cariaco Trench	73
44	10°19'N, 60°24'W	Continental Slope off Trinidad	43

FIGURE 4-112 BOTTOM SEDIMENT CORES

		88-119		7-1-1-1
		119-239		7-2-1-T
Mexican Basin Gulf of Mexico	2,050	0-1007		5-3-2-T
Mexican Basin Gulf of Mexico	2,045	0-776		5-3-2-T
Mississippi Cone Gulf of Mexico	1,055	0-13		5-3-2-0
		13-21		5-4-1-0
		21-51		8-3-1-0
		51-61		3-5-1-1
		61-135		7-2-1-0
		135-150		3-6-1-0
		150-271		6-3-1-0
Mississippi Cone Gulf of Mexico	1,854	0-88		7-2-1-0
		88-103		6-3-1-0
		103-108		2-7-1-0
		108-113		1-6-3-0
		113-152		7-2-1-0
		152-307		8-1-1-0
Northern Continental Slope-Gulf of Mexico	1,328	0-10		7-1-2-0
		10-76		8-2-1-0
		76-156		7-2-1-0
Campeche Bank Gulf of Mexico	236	0-20		2-5-3-0
		20-32		1-4-5-0
	2,775	0-5		1-4-5-0
		5-13		1-6-3-0
		13-19		2-4-3-1
		19-25		1-4-5-0
	2,775	0-20		6-3-1-0
		20-30		3-6-1-0
		30-38		5-4-1-0
Blake Ridge	2,630	0-5		5-3-2-0
		5-99		2-1-7-0
		99-160		0-1-9-0
		160-175		4-4-2-0
		175-599		0-1-7-2
Hatteras Abyssal Basin	2,800	0-10		6-4-0-0
		10-20		4-6-0-0
		20-47		7-3-0-0
		47-95		5-5-0-0
		95-100		3-6-1-0
		100-140		7-2-1-0
		140-240		5-5-0-0
		240-360		6-4-0-0
		360-380		5-5-0-0
		380-580		6-4-0-0
		580-620		8-2-0-0
		620-640		5-5-0-0
		640-660		9-1-0-0
		660-720		7-3-0-0
		720-760		9-1-0-0
		760-860		6-4-0-0
		860-880		4-6-0-0
		880-920		6-4-0-0
		920-1000		9-1-0-0
		1000-1032		7-3-0-0
		1032-1040		2-8-0-0
		1040-1100		8-2-0-0
Tongue of the Ocean, Bahamas	751	0-13		4-4-2-0
		13-26		4-5-1-0
		26-39		3-6-1-0
Exuma Sound, Bahamas	847	0-22		3-6-1-0
		22-30		4-4-1-1
		30-42		3-6-1-0
		42-70		4-4-1-1
		70-78		1-2-5-1
		78-86		0-1-7-2
		89-90		0-1-3-6
Hatteras Abyssal Basin	2,872	0-150	Mud	
		150-173	Sand-Silt	
		173-387	Mud-Ferro manganese modules	
		387-415	Silt-Sand	
		415-505	Mud-Ferro manganese modules	
		505-520	Silt-Sand	
		520-540	Mud	
Barbados Abyssal Plain	1,569	0-23		6-3-1-0
		23-30		8-1-1-0
		30-40		5-4-1-0
		40-45		9-1-0-0
		45-50		2-7-1-0
		50-84		7-2-1-0
Northern Bahama Basin	2,717	0-56	Sand	
		56-122	Sand-Clay	
		122-258	Silt-Clay	
		258-295	Silt	

					117-143	Sand-Mud-Gravel	
					143-1120	Mud-Silt	
18	26°00'N, 67°27'W	Bermuda Rise	2,920	0-24			7-2-1-0
19	23°19'N, 65°36'W	Nares Abyssal Plain	3,200	0-24			8-1-1-0
20	28°25'N, 60°09'W	Abyssal Hills	3,050	0-85	Clay		
21	19°38'N, 86°01'W	Yucatan Basin	2,410	0-37			6-3-1-0
				37-57			1-7-2-0
				57-85			6-2-1-1
				85-88			2-6-1-1
				88-136			6-2-1-1
				136-139			2-6-1-1
				139-211			7-2-1-0
				211-266			8-1-1-0
				266-291			6-3-1-0
				291-311			4-3-3-0
				311-351			7-2-1-0
				351-400			5-4-1-0
				400-417			6-3-1-0
				417-420			3-5-1-0
22	19°05'N, 82°00'W	Cayman Ridge	—	0-290	Clay-Silt		
				290-300	Gravel		
				300-555	Sand		
23	17°13'N, 81°05'W	Nicaraguan Rise	—	0-80	Mud		
				80-85	Sand		
				85-230	Mud		
				230-235	Sand		
				235-255	Mud		
				255-270	Sand		
				270-332	Mud		
				332-338	Sand		
				338-405	Mud		
				405-500	Sand		
				500-545	Mud		
24	19°58'N, 79°34'W	Cayman Ridge	1,200	0-30			4-3-2-1
				30-138			1-6-2-1
25	19°55'N, 73°32'W	Windward Passage	1,148	0-17			
				17-30			4-5-1-0
				30-45			4-5-1-0
				45-56			2-3-4-1
26	18°50'N, 75°09'W	Cayman Trough (East)	1,250	0-60			1-6-2-1
				60-120			4-5-0-1
				120-180			5-4-0-1
				180-350			4-3-2-1
27	14°33'N, 73°47'W	Beata Ridge	1,650	0-10			0-6-3-1
				10-20			1-5-3-1
				20-39			1-7-1-1
28	19°45'N, 66°37'W	Puerto Rico Trench	4,350	0-272	Clay		
				272-397	Clay-Sand		
29	18°06'N, 68°11'W	Mona Passage	1,215	0-205	Sand		
				205-215	Clay		
				215-300	Sand		
30	18°48'N, 65°58'W	Island Slope Puerto Rico Trench	1,200	0-28	Silt-Clay		
				28-340	Clay		
31	17°00'N, 66°30'W	Muertos Trench	2,471	0-80			4-2-3-1
				80-104			5-3-2-0
32	17°46'N, 66°01'W	Island Slope Puerto Rico	698	0-9			3-3-3-1
				9-21			3-4-2-1
				21-32			1-1-6-2
				32-39			2-3-4-1
				39-113			5-2-3-1
33	17°00'N, 65°00'W	Venezuelan Basin	2,406	0-155			5-3-1-1
				155-195			7-2-1-0
				195-265			6-1-3-0
34	16°40'N, 65°00'W	Venezuelan Basin	2,171	0-132			5-3-1-1
35	14°26'N, 69°22'W	Venezuelan Basin	2,450	0-260	Clay		
36	14°39'N, 70°49'W	Venezuelan Basin	2,100	0-845	Mud-Sand		
37	17°45'N, 86°17'W	Cayman Ridge	1,969	0-350	Clay-Silt-Sand		
				350-355	Sand-Silt		
38	10°50'N, 79°03'W	Colombian Basin	1,850	0-350			1-3-6-0
				350-450			2-2-3-3
39	17°35'N, 58°00'W	Abyssal Hills	2,900	0-600			3-4-3-0
				600-800			7-2-1-0
40	15°34'N 60°38'W	Eastern Slope off Dominica	1,600	0-52	Clay-Silt		
41	12°36'N, 60°37'W	Eastern Slope off Grenada	1,350	0-28	Clay-Silt		
42	11°42'N, 61°25'W	Grenada-Trinidad Passage	1,280	0-335	Clay		
43	10°43'N, 64°40'W	Cariaco Trench	735	0-209	Silt-Clay		
44	10°19'N, 60°24'W	Continental Slope off Trinidad	436	0-50			5-4-1-0

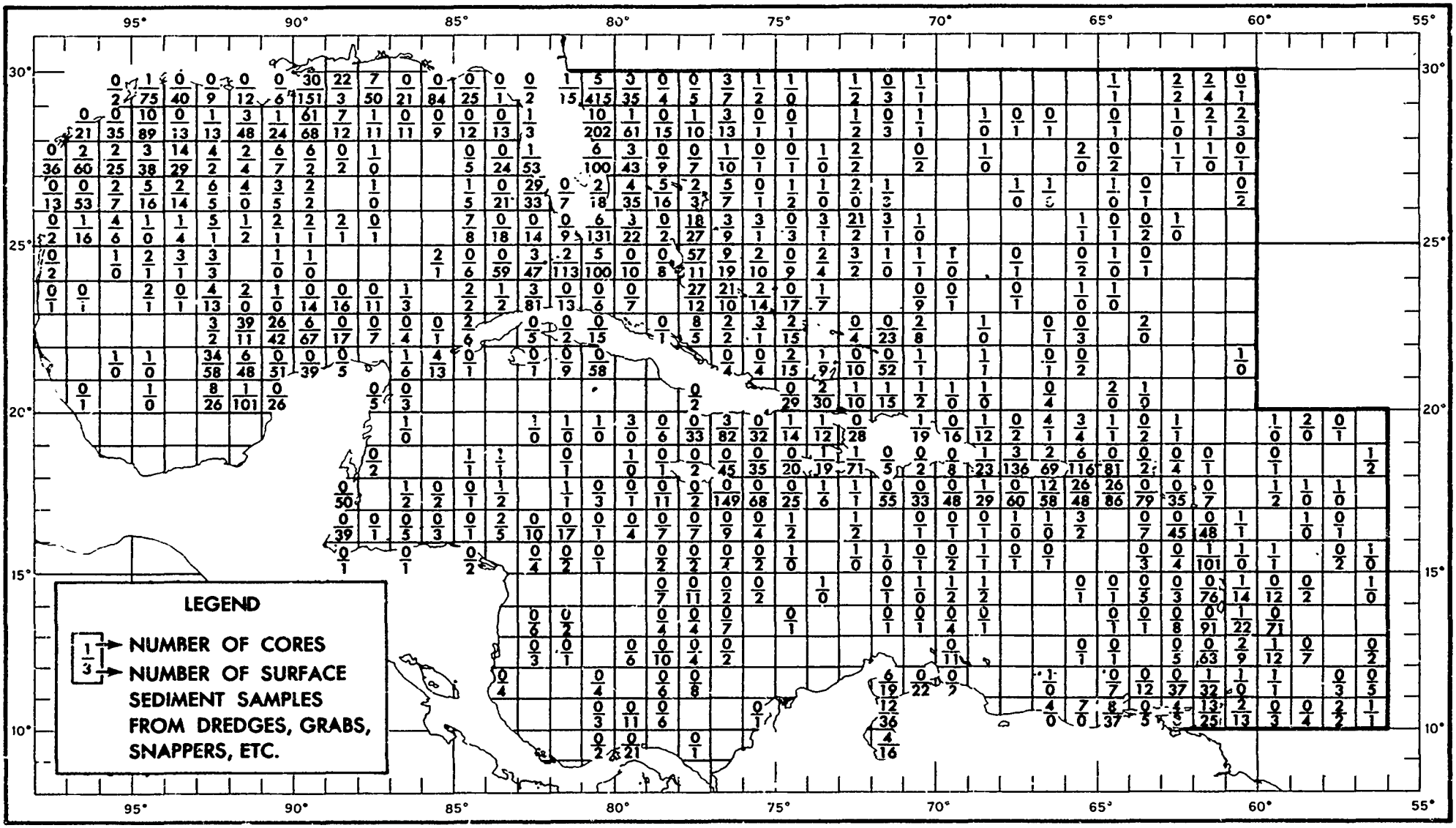

FIGURE 4-113 NUMBER OF BOTTOM SEDIMENT SAMPLES PER ONE-DEGREE SQUARE

Preceding page blank

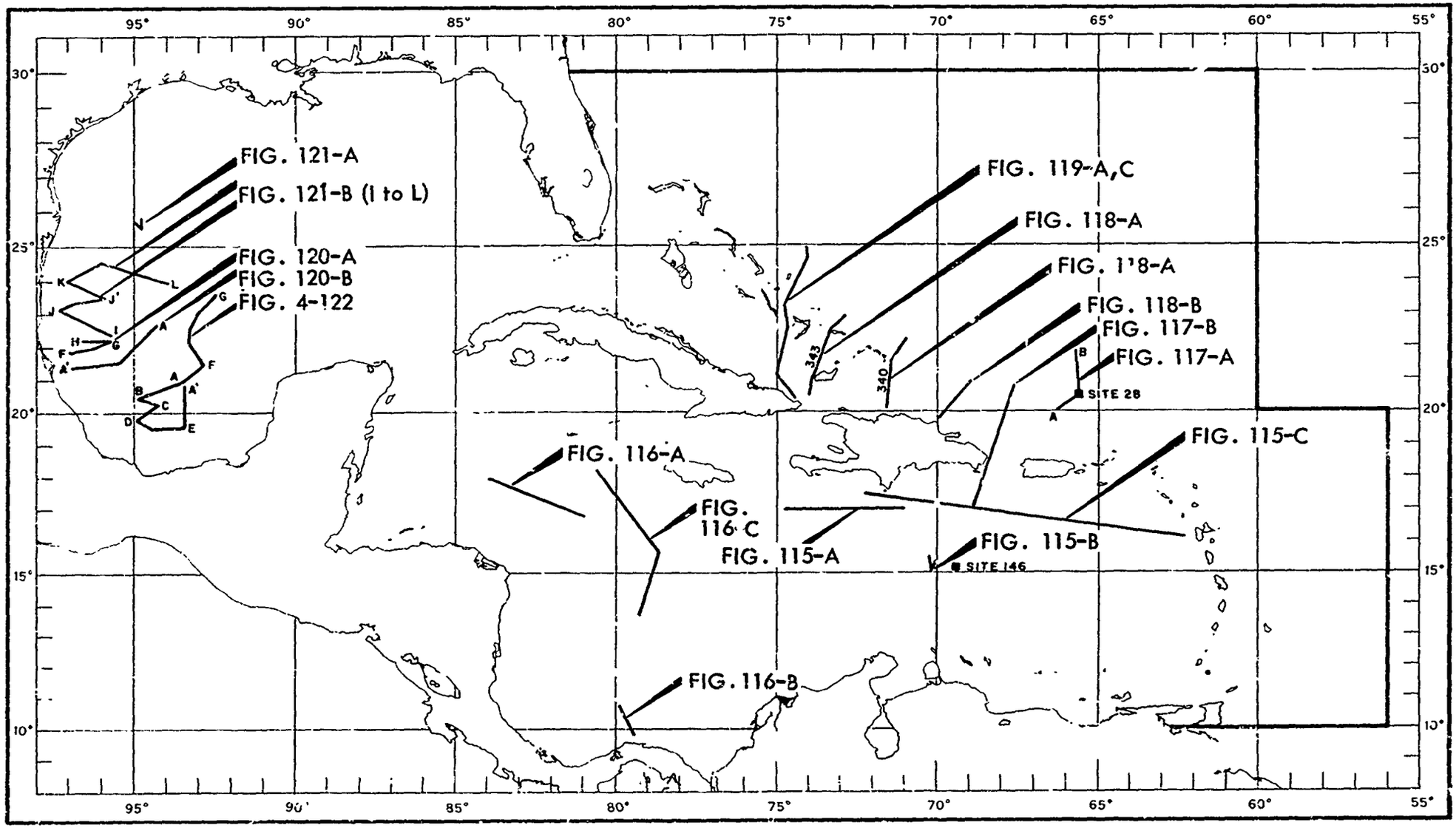

FIGURE 4-114 LOCATIONS OF SEISMIC REFLECTION PROFILES

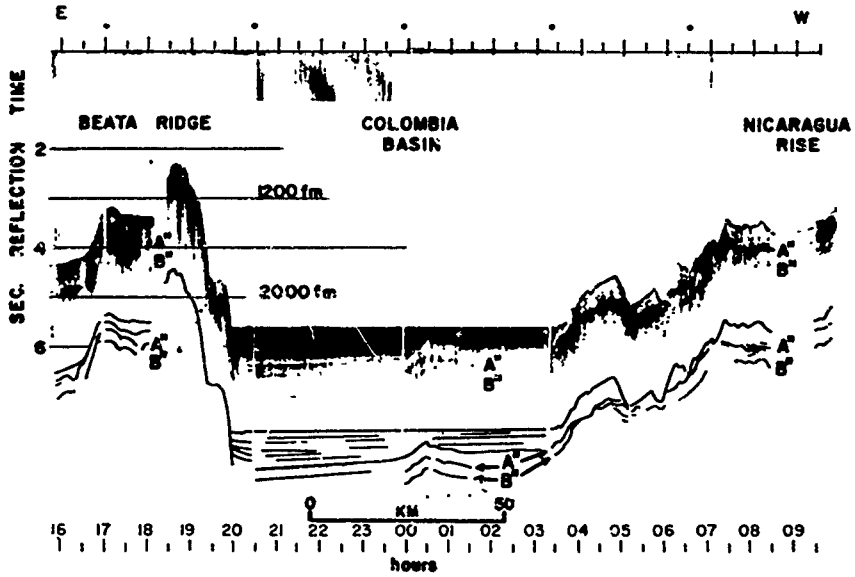

A. Profiler record across northern Colombia Basin showing presence of A" and B" on Beata Ridge, Nicaragua Rise, and beneath flat, stratified turbidites of abyssal plain (airgun, C40).

ILLUSTRATIONS FROM: SEISMIC REFRACTION AND REFLECTION IN CARIBBEAN SEA N. TERENCE EDGAR, JOHN I. EWING, AND JOHN HENNION

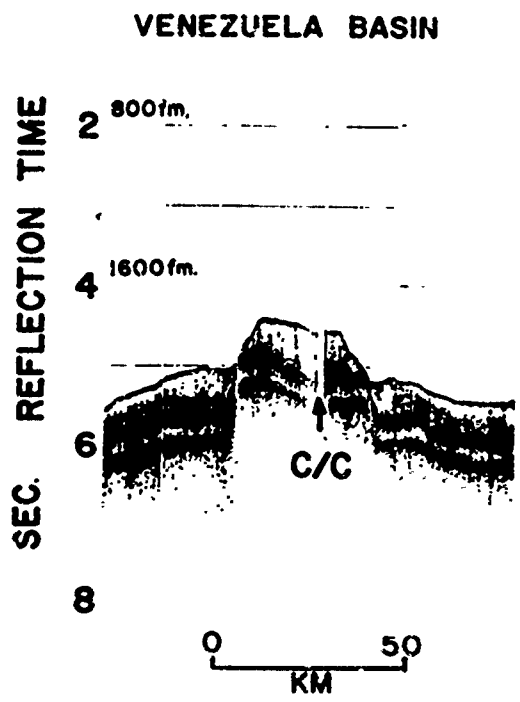

B. Profiler record showing details of acoustical properties of sediments and outcrop of A" (TNT).

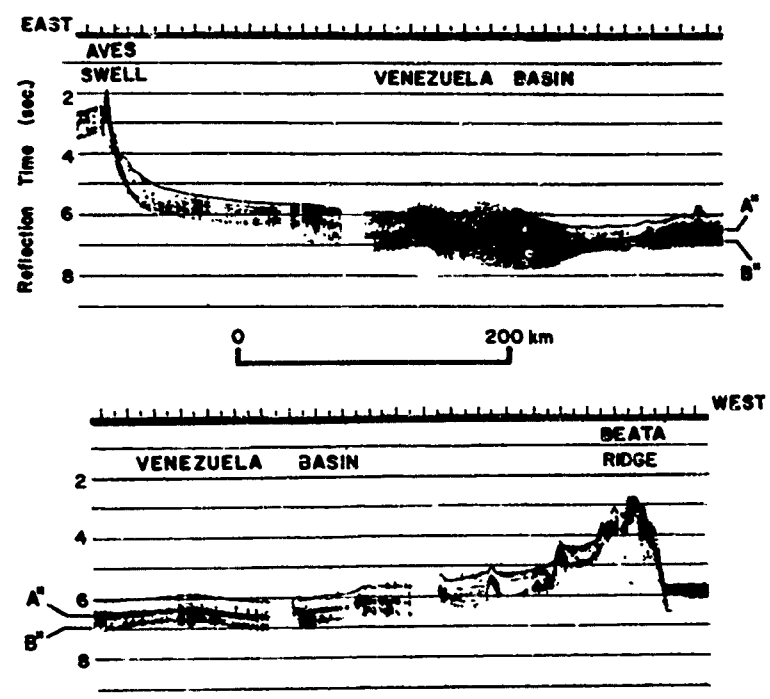

C. Profiler record across Venezuela Basin showing two strong subbottom reflectors A" and B" and acoustically transparent Carib beds above and below A" (airgun HMS Vidal, leg Charlie).

FIGURE 4-115 REFLECTION PROFILES–COLOMBIAN AND VENEZUELAN BASINS

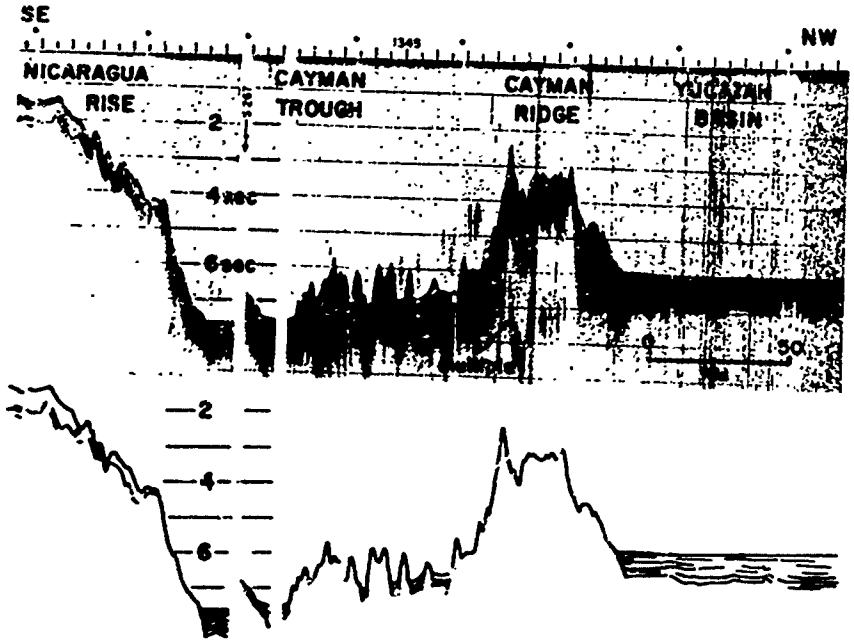

A. Profiler record across Yucatan Basin from Nicaragua Rise (airgun, C-10).

ILLUSTRATIONS FROM:
SEISMIC REFRACTION AND REFLECTION IN CARIBBEAN SEA
N. TERENCE EDGAR, JOHN I. EWING, AND JOHN HENNION

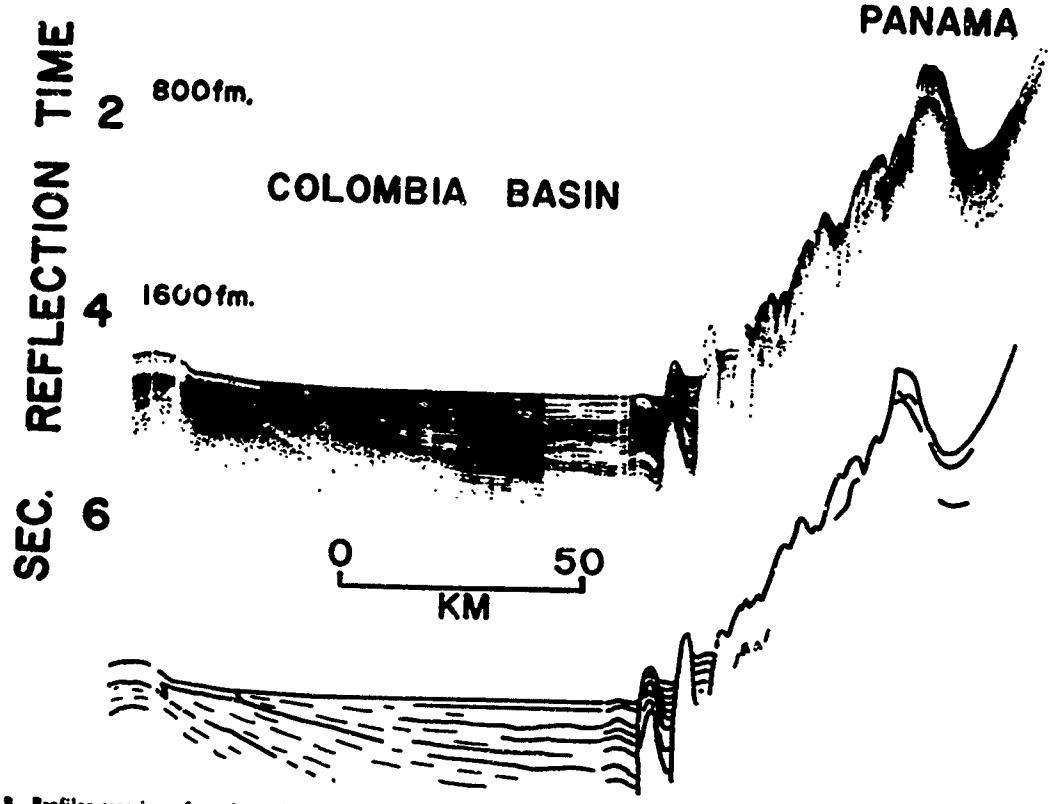

B. Profiler crossing of continental margin north of Panama. Change in sediment facies occurs between stratified turbidites and acoustically transparent sediments coincident with change in slope of ocean floor. Rough topography on slope from Panama to abyssal plain may be the result of folding of basin strata, similar to turbidites that presently are being deformed and uplifted.

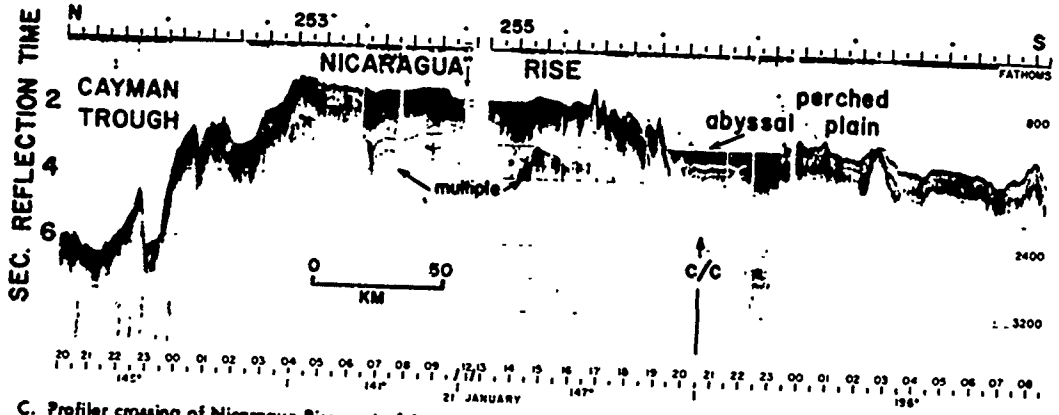

C. Profiler crossing of Nicaragua Rise west of Jamaica. Large accumulations of sediment are recorded on crust, but little is found in adjacent Cayman Trough (airgun C-10). (J. Ewing et al., 1967).

FIGURE 4-116 REFLECTION PROFILES–YUCATAN AND COLOMBIAN BASINS, AND NICARAGUAN RISE

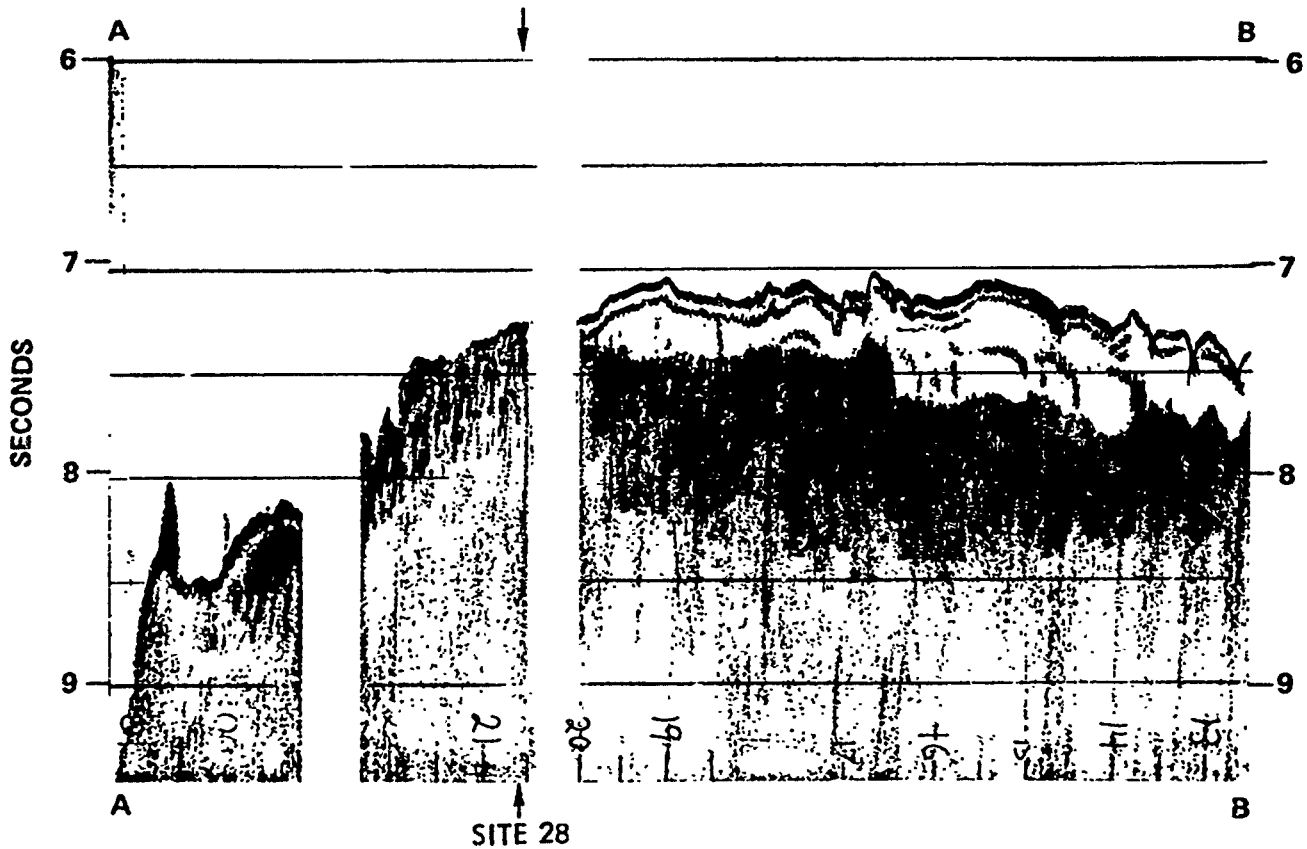

A. Reflection profiler record across the Outer Ridge obtained on cruise of the R/V ROBERT D. CONRAD 19, December, 1965. Note the thick mantle of "transparent" sediment above a rough basement over the ridge.

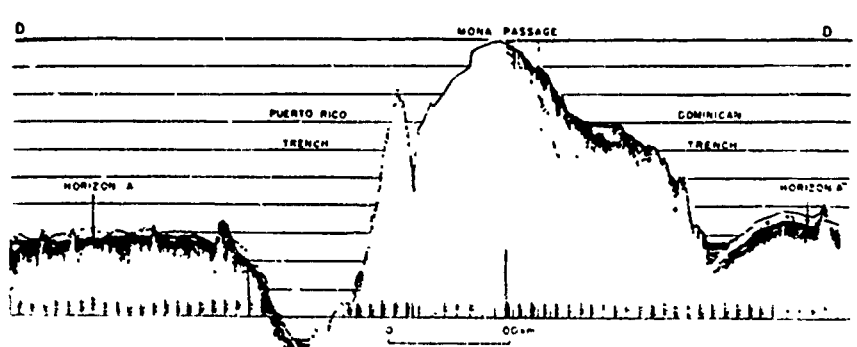

B. Seismic profiler record across the Greater Antilles and Puerto Rico trench between Hispaniola and Puerto Rico. Note the symmetry in structure but the difference in the character of the sediments on each side of the Antilles ridge. Vertical exaggeration is X 25. (Ewing et al., 1967).

FIGURE 4-117 REFLECTION PROFILES–PUERTO RICO AND MUERTOS TRENCHES, AND MONA PASSAGE

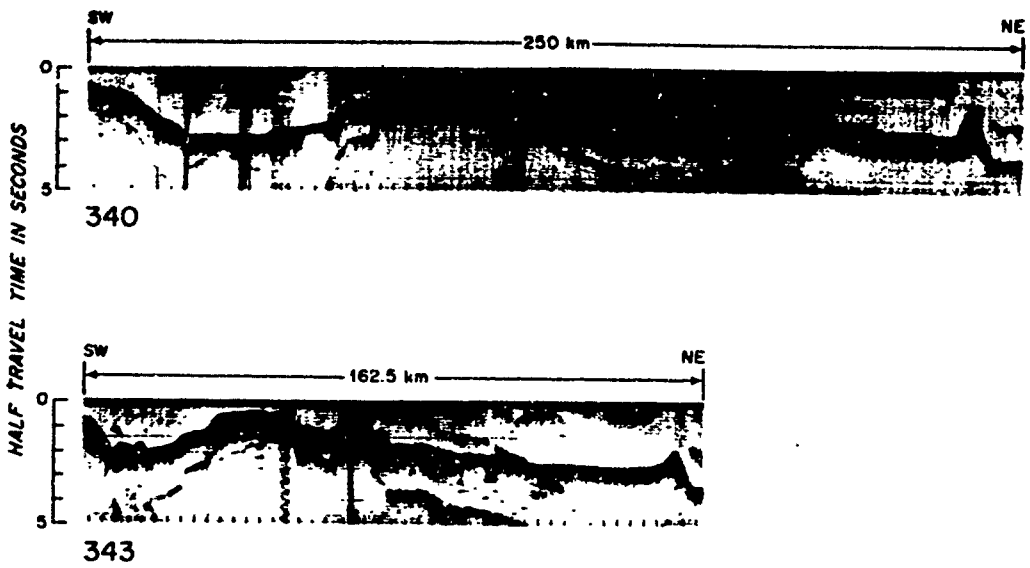

A. Reflection profiles across southeastern Bahamas. Sediments within Old Bahama Channel (profile 340, left side) are disrupted by faulting. In both profiles Bahamas Escarpment has form of ridge. If depression between bank and escarpment (profile 340) were filled with sediment, southeastern Bahamas would look like Blake Plateau.

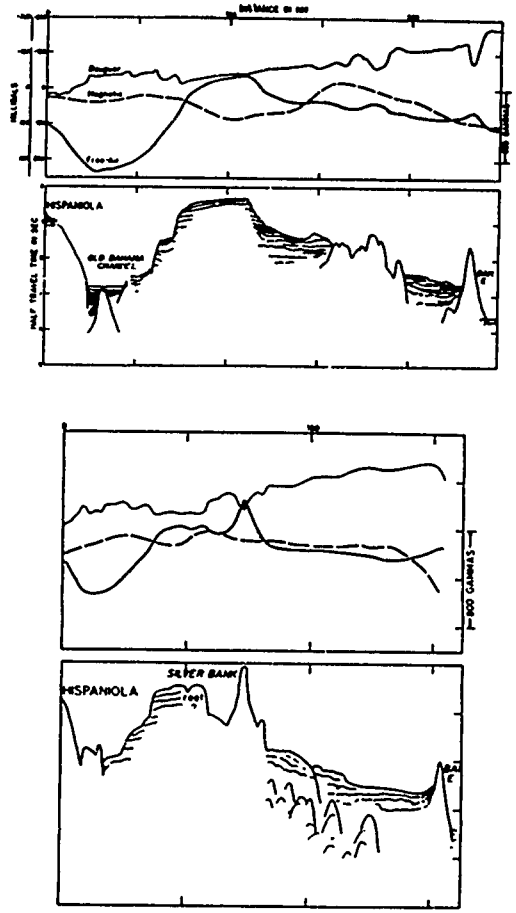

B. Reflection profiles north of Hispaniola.

ILLUSTRATIONS FROM:
STRUCTURE AND ORIGIN OF SOUTHEASTERN BAHAMAS
UCHUPI, MILLIMAN, LUYENDYK, BOWIN, AND EMERY

FIGURE 4-118 REFLECTION PROFILES–HISPANIOLA BASIN AND SOUTHEASTERN BAHAMAS

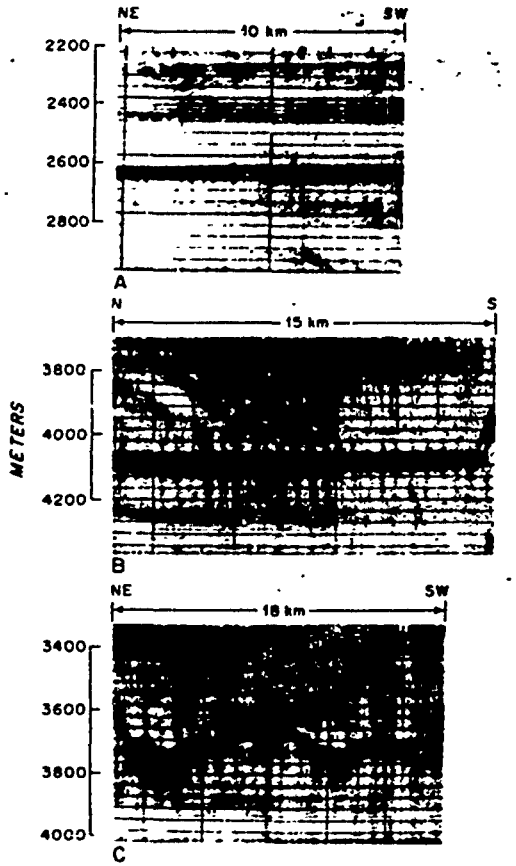

A. Typical 3.5 kHz echo-sounding traces displaying different types of sea bottom in southeastern Bahamas. A. Smooth, flat-bottom, no penetration; lack of penetration is probably due to coarse sediments. B. Smooth bottom with penetration. Strata probably consist of turbidites and pelagic sediments. This type of record is typical of most deeper sections of region. C. Irreguar bottom made up of strongly reflecting material, possibly limestone, no penetration. For positions of records see B.

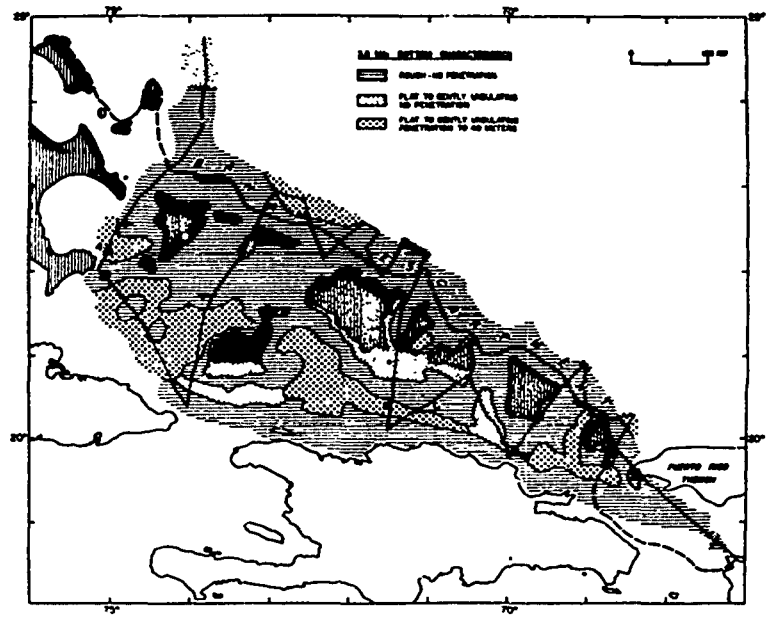

B. 3.5 kHz bottom characteristics of sea floor of southeastern Bahamas, based on recordings obtained during present investigation. Lines A, B, and C show positions of 3.5 kHz echograms in A.

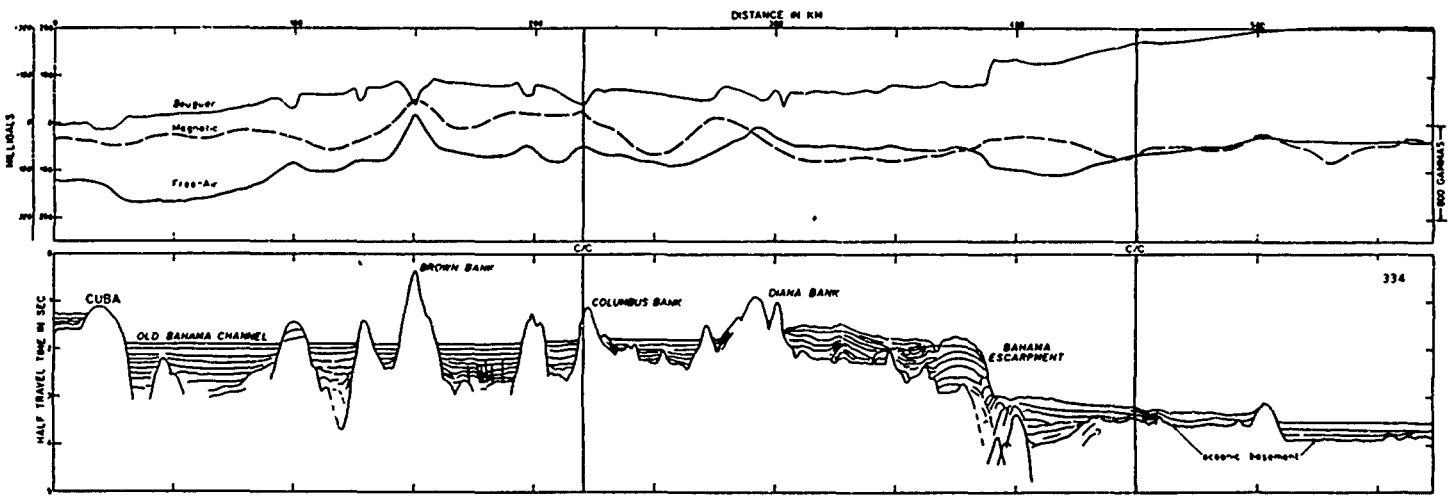

C. South-north profile 334 off eastern tip of Cuba (Fig. 2) extending across southeastern Bahamas to deep-sea floor. Top panel: total intensity magnetic anomaly (dashed line), free-air gravity anomaly (wide continuous line), and Bouguer gravity anomaly (narrow continuous line). Scale on righ shows relative amplitude of magnetic anomalies in gammas. Free-air gravity scale on left is from +200 to −200 mgal, and Bouguer (slanted numbers) +320 to −320 mgal. Bottom panel: continuous seismic profile. Oceanic basement and acoustic basement beneath Bahamas are wide lines.

ILLUSTRATIONS FROM: STRUCTURE AND ORIGIN OF SOUTHEASTERN BAHAMAS
UCHUPI, MILLIMAN, LUYENDYK, BOWIN, AND EMERY

FIGURE 4-119 REFLECTION PROFILES–SOUTHEASTERN BAHAMAS

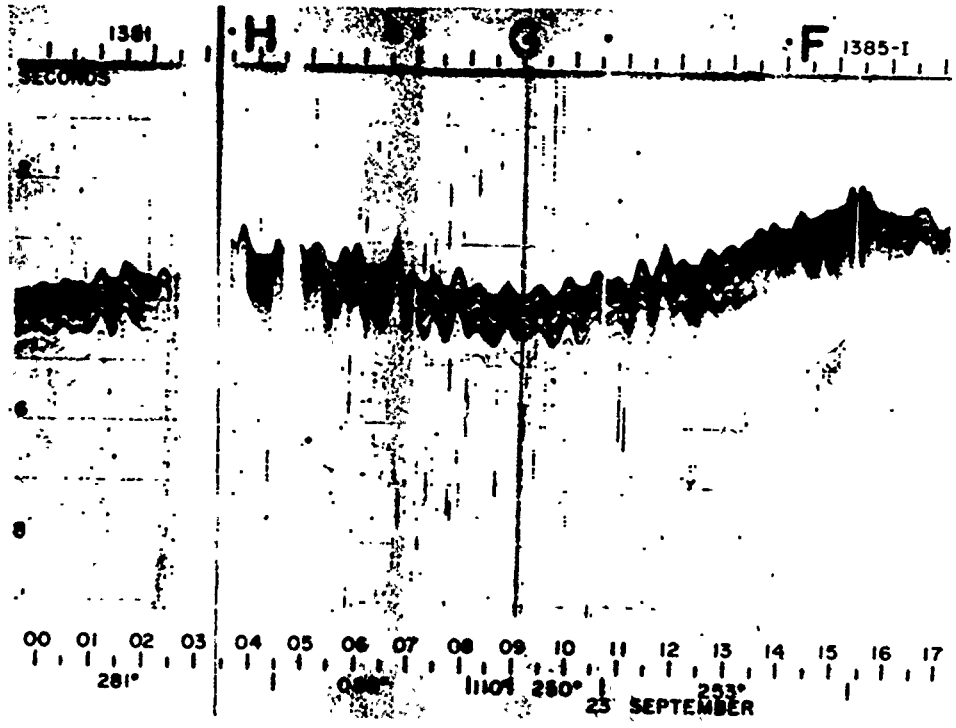

ILLUSTRATIONS FROM:
MEXICAN CONTINENTAL SHELF AND SLOPE, GULF OF MEXICO. WILLIAM R. BRYANT, JOHN ANTOINE, MAURICE EWING, AND BILL JONES

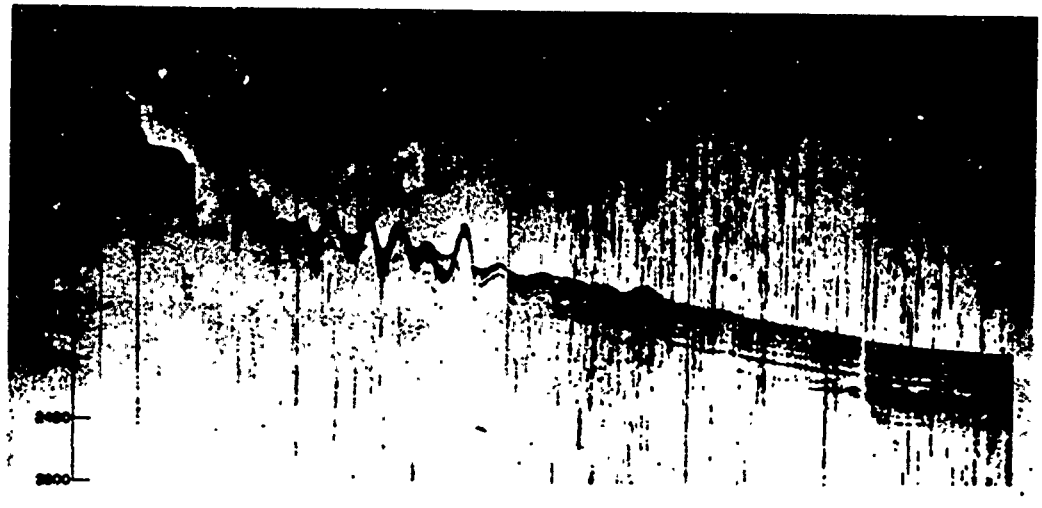

FIGURE 4-120 REFLECTION PROFILES–WESTERN GULF OF MEXICO

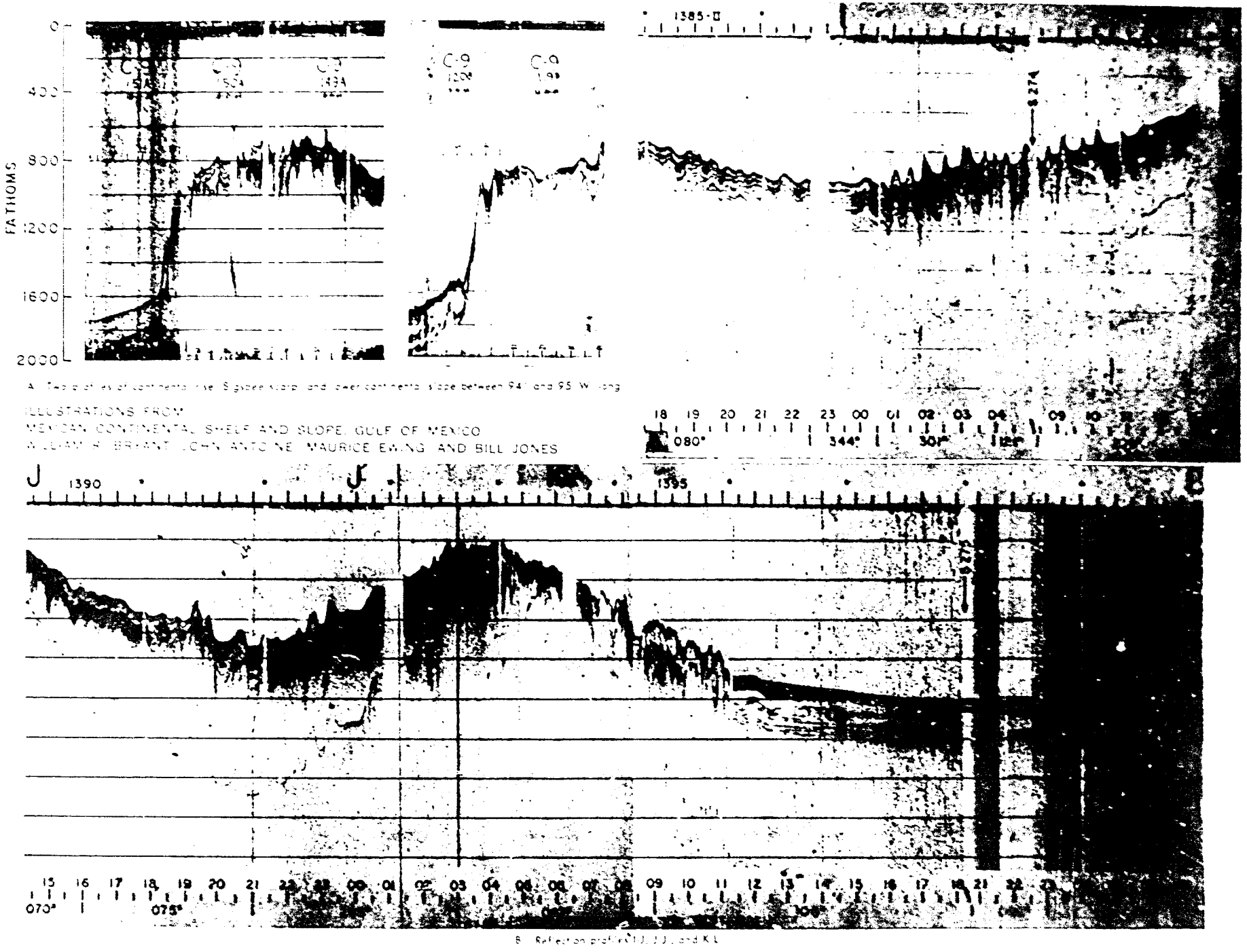

ILLUSTRATIONS FROM
MEXICAN CONTINENTAL SHELF AND SLOPE, GULF OF MEXICO
A. JEAN H. BRYANT, JOHN ANTOINE, MAURICE EWING, AND BILL JONES

FIGURE 4-121 REFLECTION PROFILES-WESTERN GULF OF MEXICO (CONT'

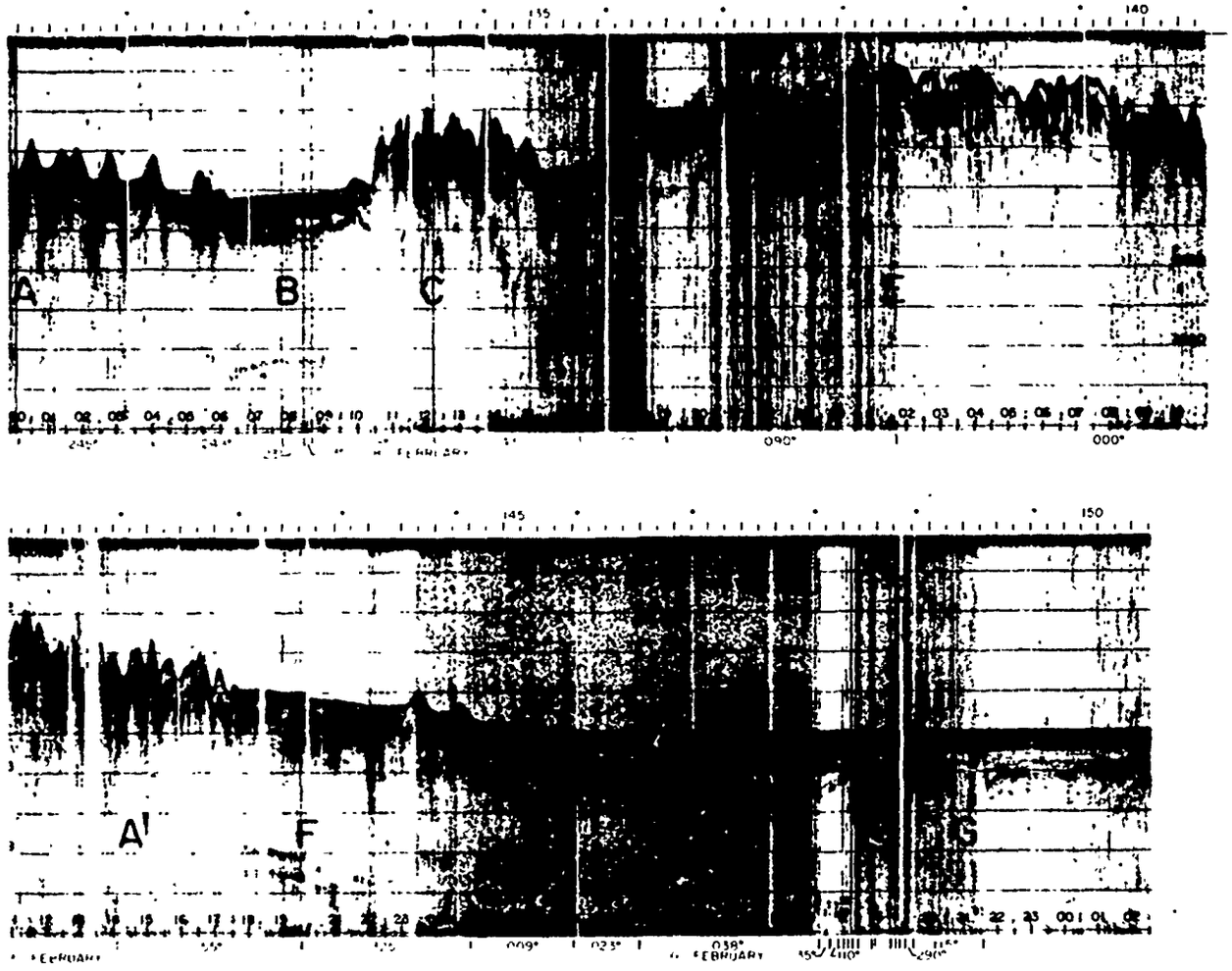

Vema-24 reflection records shown here are continuous traverse from A to G. Ship's speed was approximately 9 knots Time is in hours at bottom of records where course changes also are indicated Note abrupt boundaries of zone at B, D, and F. Transition from knolls to domes is illustrated from A'-F-G (Worzel, et al, 1968).

FIGURE 4-122 REFLECTION PROFILES–WESTERN GULF OF MEXICO (CONT.)

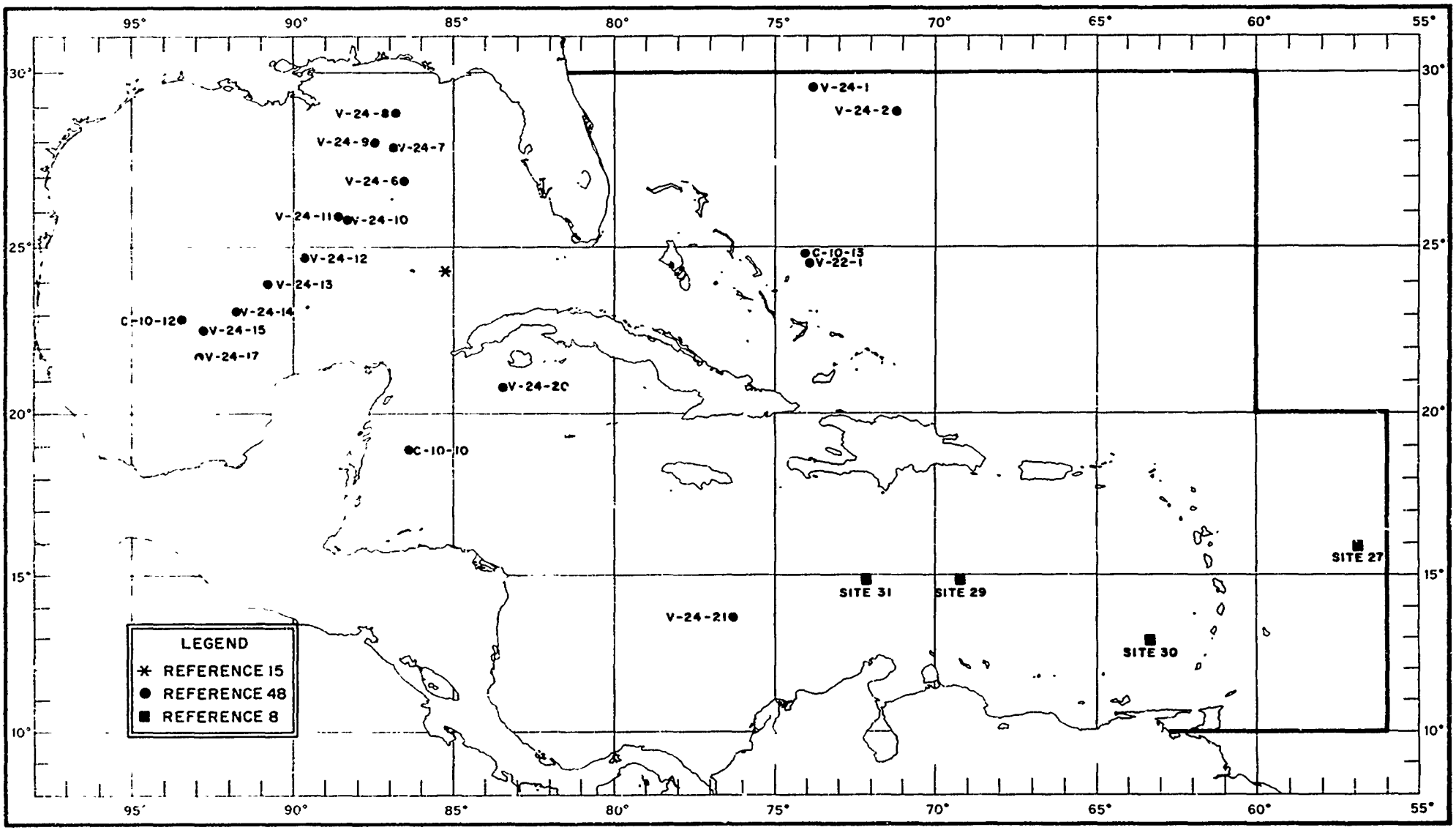

FIGURE 4-123 LOCATIONS OF SEDIMENT VELOCITY STATIONS

BUOY	CRUISE	LAYER	UPPER REFLECTION TIME (SEC)	LOWER REFLECTION TIME (SEC)	VELOCITY (KM/SEC)	STANDARD DEVIATION (KM/SEC)	REFRACTION INTERCEPT (SEC)	WATER DEPTH (SEC)	LATITUDE (N)	LONGITUDE (W)	IDENTIFICATION	BASEMENT REFLECTOR	APPARENT VELOCITY (KM/SEC)	SLOPE
						NORTH ATLANTIC								
1	V22	1	7.025	7.543	2.595	.439		7.025	24°34'	73°49'	2	1		
13A	C10	1	7.018	7.342	1.682	.086		7.018	24°49'	73°31'	1			
13A	C10	2	7.342	7.623	3.470	.159		7.018	24°49'	73°31'	3	1		
13A	C10	3			5.610		7.47	7.018	24°49'	73°31'				
13B	C10	1	6.939	7.264	1.834	.271		6.989	24°47'	73°27'	1			
13B	C10	2	7.264	7.568	2.906	.226		6.989	24°47'	73°27'	3	1		
1	V24	1	6.112	6.646	1.630	.052		6.112	29°31'	73°52'				
1	V24	2	6.646	7.735	2.151	.031		6.112	29°31'	73°52'				
1	V24	3	7.735	8.261	2.913	.251		6.112	29°31'	73°52'	1			
1	V24	4	8.261		3.600		7.40	6.112	29°31'	73°52'	3			
1	V24	5			5.510		8.00	6.112	29°31'	73°52'				
2	V24	1	7.141	7.879	1.769	.048		7.141	28°54'	71°03'				
2	V24	2	7.879	8.339	2.166	.125		7.141	28°54'	71°03'	1			
2	V24	3	8.339	8.604	3.747	.147		7.141	28°54'	71°03'	3	1		
2	V24	4	8.604		4.910		8.07	7.141	28°54'	71°03'				
						GULF OF MEXICO								
12	C10	1	4.985	5.669	1.740	.042		4.985	22°52'	93°31'				
12	C10	2	5.669	6.823	2.208	.039		4.985	22°52'	93°31'				
12	C10	3	6.823	7.237	2.791	.206		4.985	22°52'	93°31'				
12	C10	4	7.237	8.682	3.025	.062		4.985	22°52'	93 31'				
6	V24	1	4.087	5.184	1.821	.039		4.087	26°55'	86°39'			1.97	
6	V24	2	5.184	5.903	2.401	.036		4.087	26°55'	86°39'			2.13	
6	V24	3	5.903	7.075	2.809	.153		4.087	26°55'	86°39'				
6	V24	4	7.075		3.900		6.10	4.087	26°55'	86°39'				
7	V24	1	3.970	4.691	1.928	.220		3.970	26°53'	86°53'			2.21	1
7	V24	2	4.691	5.794	2.473	.065		3.970	26°53'	86°53'				1
8	V24	1	.870					.870	28°51'	86°54'				
8	V24	2			4.000		1.71	.870	28°51'	86°54'				
8	V24	3			5.450		2.15	.870	28°51'	86°54'				
9	V24	1	3.627	4.354	1.898	.060		3.627	27°59'	87°34'				1
9	V24	2	4.354	6.272	2.530	.172		3.627	27°59'	87°34'				1
10	V24	1	3.479	4.461	2.027	.185		3.479	25°42'	88°16'				
10	V24	2	4.461	5.048	2.154	.120		3.479	25°42'	88°16'				
10	V24	3	5.048	5.719	2.476	.066		3.479	25°42'	88°16'				
10	V24	4	5.719	6.199	2 923	.168		3.479	25°42'	88°16'				
10	V24	5	6.199	6.698	2 991	.304		3.479	25°42'	88°16'				
11	V24	1	4.295	5.314	1.803	.098		4.295	25°44'	88°48'			2.04	1
11	V24	2	5.314	6.382	2.449	.030		4.295	25°44'	88°48'				1
12	V24	1	4.724	5.458	2.057	.179	4.724	24°42'	89°39'					1
12	V24	2	5.458	6.414	2.672	.348		4.724	24°42'	89°39'				1
12	V24	3	6.414	7.282	2.941	.359		4.724	24°42'	89°39'				1
13	V24	1	4.922	5.699	2.048	.178		4.922	23°56'	90°42'				
13	V24	2	5.699	6.325	2.118	.067		4.922	23°56'	90°42'				
13	V24	3	6.325	6.894	2.710	.196		4.922	23°56'	90°42'				
14	V24	1	4.971	5.920	1.760	086		4.971	23°09'	91°46'				
14	V24	2	5.920	7.170	2.743	.131		4.971	23°09'	91°46'				
15	V24	1	.750					4.750	22°29'	92°48'				
15	V24	2			3.850		5.79	4.750	22°29'	92°48'				
16	V24	1	4 064	4.868	2.009	.126		4.064	20°22'	94°42'				
16	V24	2	4.868	5.709	3.960		5.73	4.064	20°22'	94°42'				
16	V24	3	5.700	6.770				4.064	20°22'	94°42'				
17	V24	1	4.315	5.004	2.150	.092		4.315	21°45'	93°02'				
17	V24	2	5.004	5.848	2.556	.083		4.315	21°45'	93°02'				
17	V24	3	5.848	6.567	3.509	.087		4.315	21°45'	93°02'				
						OTHER								
10	C10	1	5.984	6.718	1.782	.048		5.984	18°53'	86°22'				
10	C10	2	6.718	6.349	2.196	.203		5.984	18°53'	86°22'				
20	V24	1	5.958	6.928	2.360	.065		5.958	20°52'	83°25'				
21	V24	1	5.245	5.815	2.102	.101		5.245	13°07'	76°58'				

NOTES

CRUISE: V INDICATES R.V. VEMA; C, R.V. CONRAD; S,

LAYER LABELED "1" INDICATES THE FIRST SUB-BOTTOM LAYER; "2", THE SECOND; ETC.

UPPER REFLECTION TIME IS THE REFLECTION TIME TO THE UPPER INTERFACE OF LAYER.

LOWER REFLECTION TIME IS THE REFLECTION TIME TO THE LOWER INTERFACE OF LAYER.

VELOCITY IN THE LAYER IS DEFINED BY THE UPPER AND LOWER REFLECTION TIMES GIVEN IN THE PRECEDING COLUMNS.

STANDARD DEVIATION REFERS TO THE COMPUTED DEVIATION OF VELOCITY IN THE PRECEDING COLUMN.

REFRACTION INTERCEPT IS THE INTERCEPT TIME OF REFRACTED ARRIVALS. THIS COLUMN IDENTIFIES REFRACTION VELOCITIES, WHICH APPEAR IN THE SAME COLUMN AS THE INTERVAL VELOCITIES. NOTE THAT A REFRACTION VELOCITY IS USUALLY LISTED WITHOUT A LOWER INTERFACE REFLECTION TIME. REFRACTION LINES ARE BASED ON DATA POINTS THAT ARE NOT CORRECTED FOR TOPOGRAPHY; HENCE, SOLUTIONS BASED ON THE LISTED VALUES CAN ONLY BE APPROXIMATE.

IDENTIFICATION OF THE LAYER IS INDICATED AS FOLLOWS: BLANK INDICATES UNCONSOLIDATE; 1, LAYER A (ALL SEDIMENTS BELOW HORIZON A AND ABOVE HORIZON β); 2, COMBINATIONS OF VELOCITIES FROM TWO TYPES OF LAYER; 3, LAYER β.

BASEMENT REFLECTOR: THE NUMERAL "1" IN THIS COLUMN INDICATES THAT THE LOWER REFLECTION IS FROM BASEMENT.

APPARENT VELOCITY IS DETERMINED BY MEASURING THE SLOPE OF WIDE-ANGLE REFLECTIONS AT LARGE DISTANCES FROM THE SOURCE.

SLOPE: THE NUMBERAL "1" IN THIS COLUMN INDICATES THAT THE LAYERS ARE SLOPING. THIS ALSO IMPLIES THAT THE REFRACTION VELOCITIES AT THIS STATION ARE NOT LIKELY TO BE ACCURATE. REFRACTION VELOCITIES AT OTHER STATIONS MAY ALSO BE INACCURATE BECAUSE OF EXCESSIVE TOPOGRAPHY.

HOUTZ, ET AL., 1968

FIGURE 4-124 SEDIMENT VELOCITIES

1

DIR	4-10 knots	11-16 knots	17-27 knots	≥28 knots	TOTAL
N	6	4	5	2	17
NE	5	3	3		11
E	7	4	1		12
SE	12	7	6		25
S	8	5	5		18
SW	2				2
W	2	1			3
NW	2	2	3	1	8
TOTAL	44	26	23	3	96

≤ 3 KNOTS 4 OBS 494

2

DIR	4-10 knots	11-16 knots	17-27 knots	≥28 knots	TOTAL
N	6	4	4	1	15
NE	10	5	3		18
E	16	10	3		29
SE	9	8	5		22
S	2	1			3
SW	2				2
W	2				2
NW	2	1	1		4
TOTAL	49	29	16	1	95

≤ 3 KNOTS 5 OBS 1,230

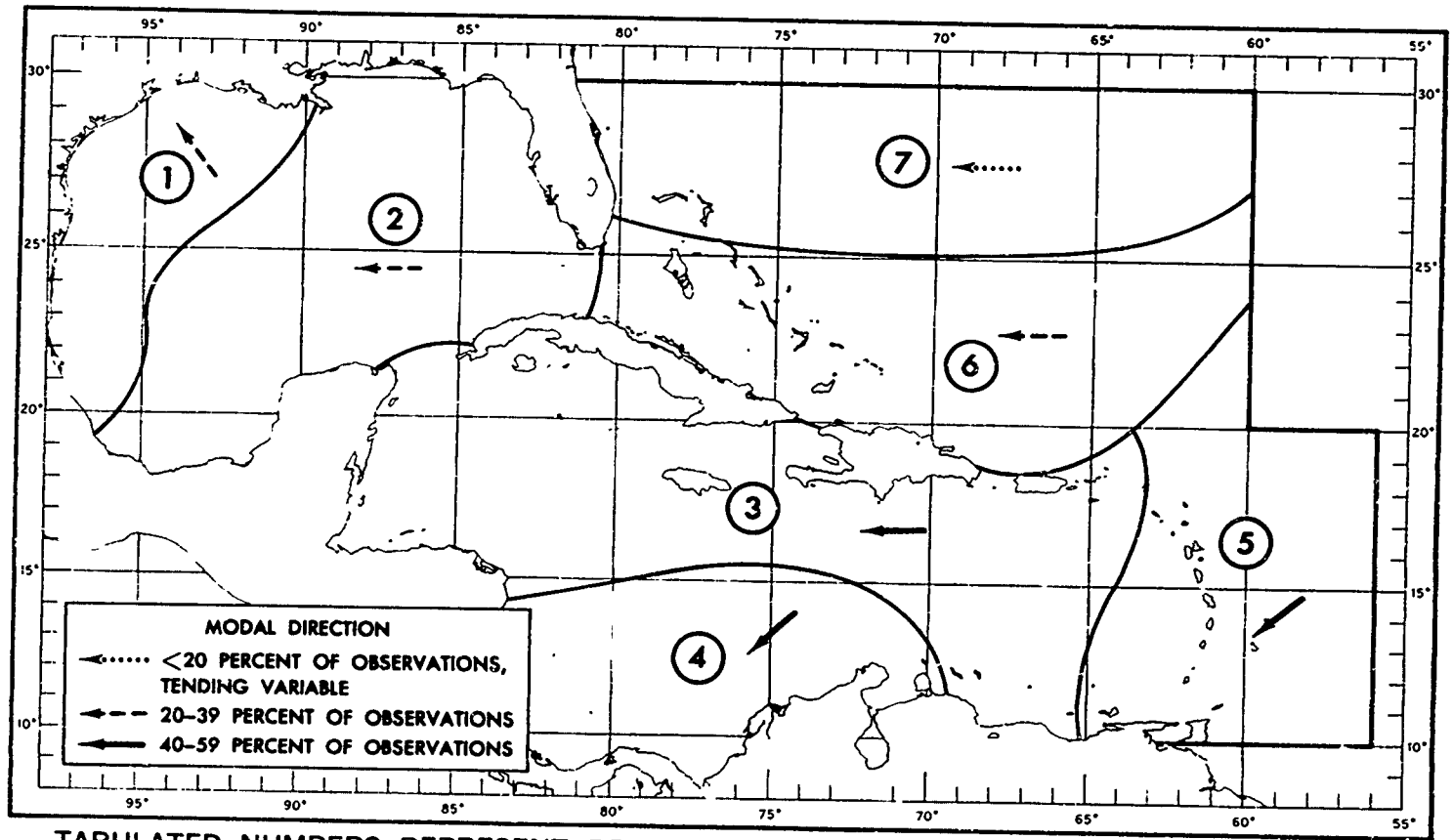

TABULATED NUMBERS REPRESENT PERCENT OF TOTAL OBSERVATIONS IN EACH REGION

3

DIR	4-10 knots	11-16 knots	17-27 knots	≥28 knots	TOTAL
N	4	2	3		9
NE	9	11	9	1	30
E	11	14	18		43
SE	4	2	3		9
S	1	1	1		3
SW					
W	1				1
NW	1	1			2
TOTAL	31	31	34	1	97

≤ 3 KNOTS 3 OBS 2,451

4

DIR	4-10 knots	11-16 knots	17-27 knots	≥28 knots	TOTAL
N	4	5	5	1	15
NE	13	14	17	1	45
E	10	9	14	1	34
SE	2	1			3
S					
SW					
W					
NW	1				1
TOTAL	30	29	36	3	98

≤ 3 KNOTS 2 OBS 1,612

5

DIR	4-10 knots	11-16 knots	17-27 knots	≥28 knots	TOTAL
N	1	1	1		3
NE	16	21	15	1	53
E	11	18	11		40
SE	1	1			2
S					
SW					
W					
NW					
TOTAL	29	41	27	1	98

≤ 3 KNOTS 2 OBS 1,408

6

DIR	4-10 knots	11-16 knots	17-27 knots	≥28 knots	TOTAL
N	5	3	2		10
NE	11	8	6		25
E	13	12	8		33
SE	5	3	1		9
S	3	1	1		5
SW	2				2
W	2	1			3
NW	3	1	1		5
TOTAL	44	29	19		92

≤ 3 KNOTS 8 OBS 4,495

7

DIR	4-10 knots	11-16 knots	17-27 knots	≥28 knots	TOTAL
N	5	4	4		13
NE	5	4	4		13
E	7	4	3		14
SE	5	3	2		10
S	5	4	3		12
SW	4	2	2		8
W	5	3	3		11
NW	3	3	4	1	11
TOTAL	39	27	25	1	92

≤ 3 KNOTS 8 OBS 3,530

FIGURE 4-125 SUMMARIES OF OBSERVED WIND SPEED AND DIRECTION–WINTER (FEBRUARY)

1

DIR	4-10 knots	11-16 knots	17-27 knots	≥28 knots	TOTAL
N	5	2	1		8
NE	5	2	1		8
E	11	7	2		20
SE	14	10	5		29
S	9	5	1		15
SW	2				2
W	2	1			3
NW	2	1			3
TOTAL	50	28	10		88

≤ 3 KNOTS 12 OBS 5,051

2

DIR	4-10 knots	11-16 knots	17-27 knots	≥28 knots	TOTAL
N	5	2	2	1	10
NE	12	7	3		22
E	14	12	5		31
SE	9	7	5		21
S	2	1			3
SW	1				1
W	1				1
NW	2	1	1		4
TOTAL	46	30	16	1	93

≤ 3 KNOTS 7 OBS 1,312

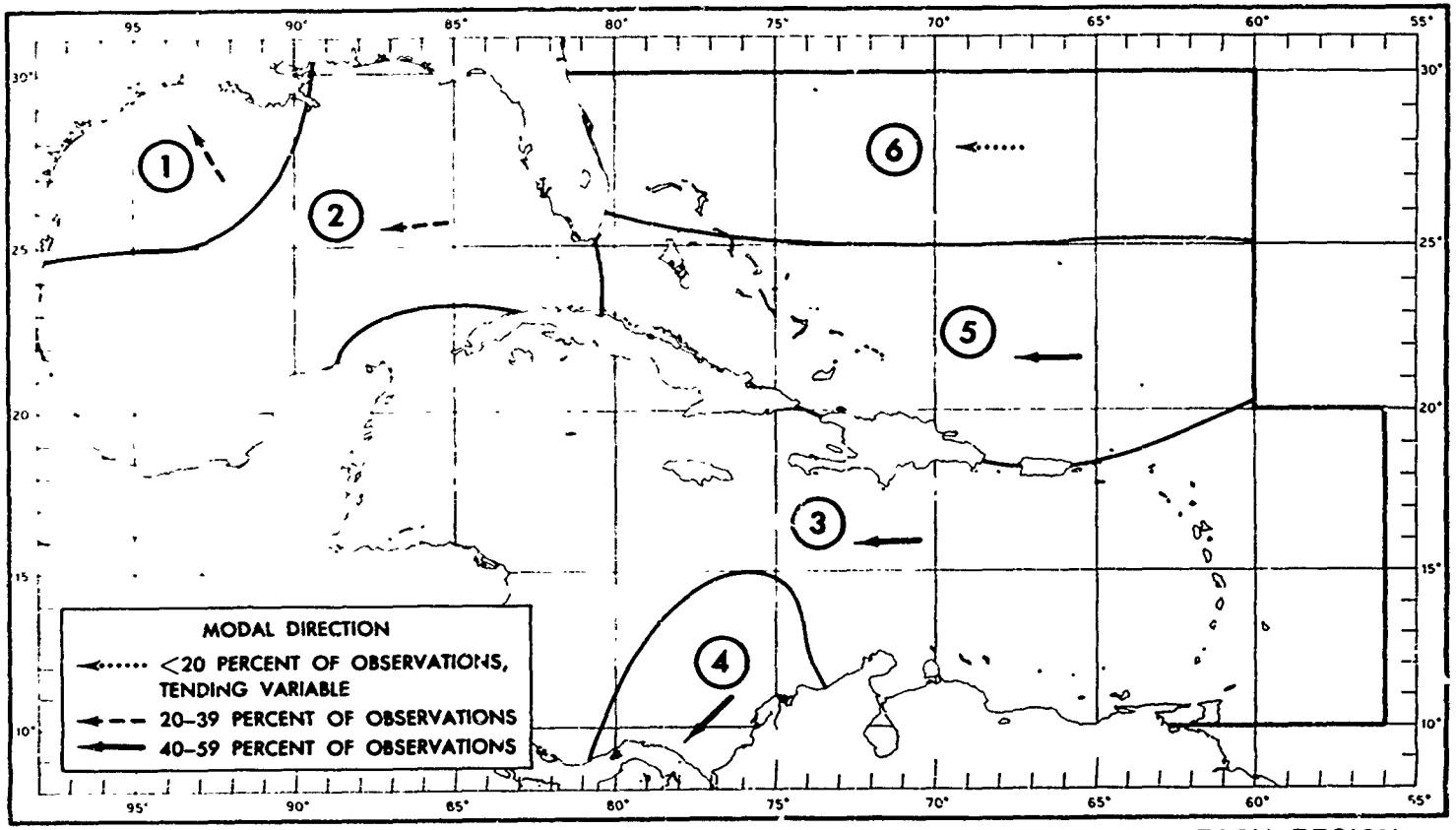

TABULATED NUMBERS REPRESENT PERCENT OF TOTAL OBSERVATIONS IN EACH REGION

3

DIR	4-10 knots	11-16 knots	17-27 knots	≥28 knots	TOTAL
N	3	1			4
NE	9	7	4		20
E	22	18	11		51
SE	6	4	2		12
S	2	1			3
SW	1				1
W	1				1
NW					
TOTAL	44	31	17		92

≤ 3 KNOTS 8 OBS 3,868

4

DIR	4-10 knots	11-16 knots	17-27 knots	≥28 knots	TOTAL
N	5	2	1		8
NE	17	16	14	1	48
E	10	10	9		29
SE	2	1			3
S	2				2
SW	1				1
W	1				1
NW	1				1
TOTAL	39	29	24	1	93

≤ 3 KNOTS 7 OBS 4,911

5

DIR	4-10 knots	11-16 knots	17-27 knots	≥28 knots	TOTAL
N	1				1
NE	10	6	1		17
E	21	16	5		42
SE	15	7	2		24
S	3	1			4
SW	1	1			2
W	1				1
NW	1				1
TOTAL	53	31	8		92

≤ 3 KNOTS 8 OBS 2,755

6

DIR	4-10 knots	11-16 knots	17-27 knots	≥28 knots	TOTAL
N	4	1	1		6
NE	6	4	2		12
E	12	5	2		19
SE	10	4	1		15
S	11	4	1		16
SW	5	2	1		8
W	4	2			6
NW	3	1			4
TOTAL	55	23	8		86

≤ 3 KNOTS 14 OBS 7,366

FIGURE 4-126 SUMMARIES OF OBSERVED WIND SPEED AND DIRECTION-SPRING (MAY)

1

DIR	4-10 knots	11-16 knots	17-27 knots	≥28 knots	TOTAL
N	4	1			5
NE	5	2			7
E	12	4	2		18
SE	11	3	1		15
S	12	3	1		16
SW	6	1			7
W	6	1			7
NW	4	1			5
TOTAL	60	16	4		80

≤ 3 KNOTS 20 OBS 6,889

2

DIR	4-10 knots	11-16 knots	17-27 knots	≥28 knots	TOTAL
N	3	1			4
NE	11	3			14
E	23	8	3		34
SE	10	3	1		14
S	5	1			6
SW	3				3
W	2	1			3
NW	2				2
TOTAL	59	17	4		80

≤ 3 KNOTS 20 OBS 9,366

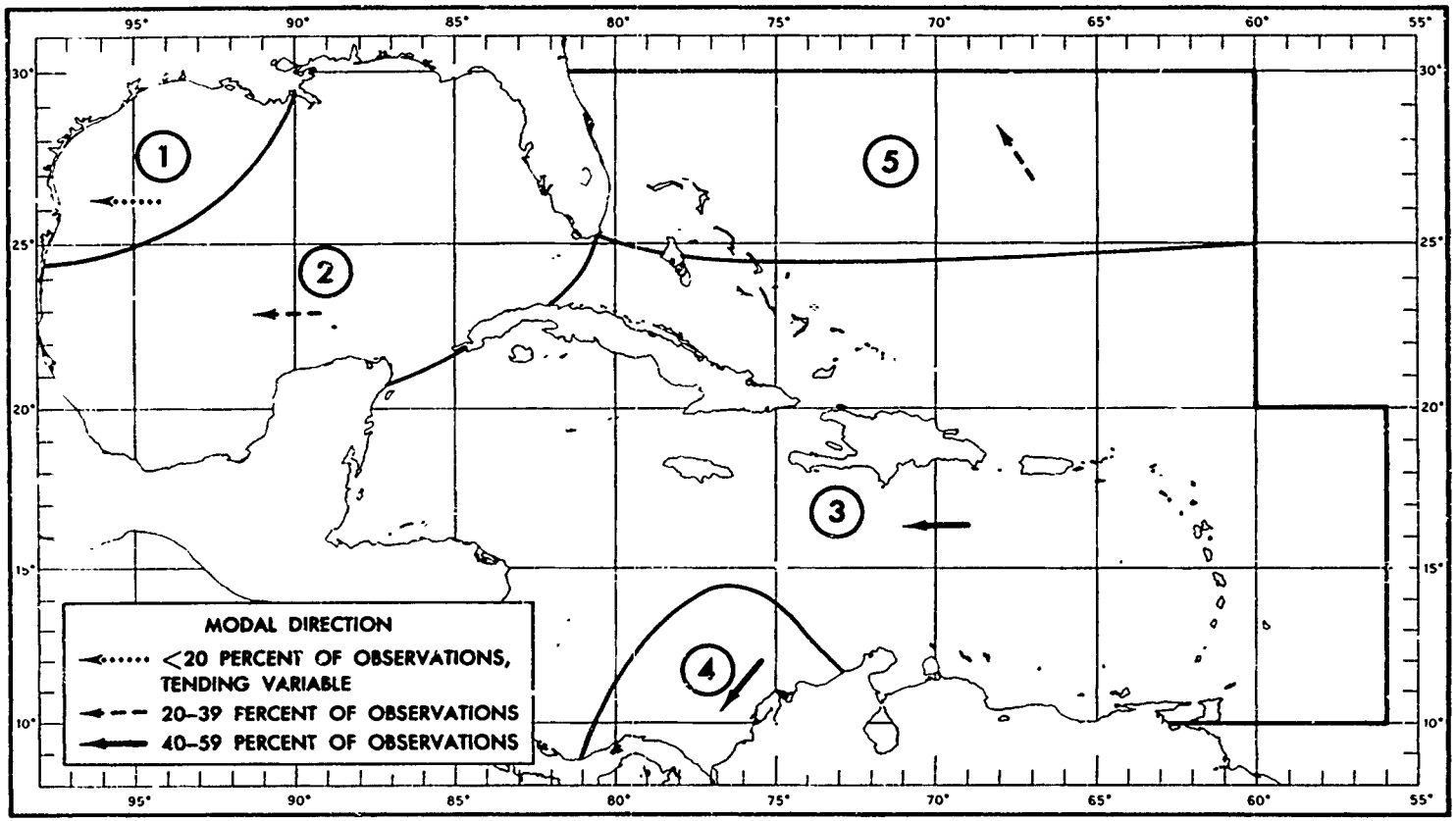

TABULATED NUMBERS REPRESENT PERCENT OF TOTAL OBSERVATIONS IN EACH REGION

3

DIR	4-10 knots	11-16 knots	17-27 knots	≥28 knots	TOTAL
N	2	1			3
NE	8	8	5		21
E	22	20	12		54
SE	5	2	1		8
S	2				2
SW	1				1
W	1				1
NW	1				1
TOTAL	42	31	18		91

≤ 3 KNOTS 9 OBS 3,733

4

DIR	4-10 knots	11-16 knots	17-27 knots	≥28 knots	TOTAL
N	4	1	1		6
NE	15	18	17	?	52
E	9	10	9	1	29
SE	2				2
S	1				1
SW	1				1
W	1				1
NW	1				1
TOTAL	34	29	27	3	93

≤ 3 KNOTS 7 OBS 4,912

5

DIR	4-10 knots	11-16 knots	17-27 knots	≥28 knots	TOTAL
N	2				2
NE	4	2			6
E	13	6	2	1	22
SE	15	6	2	1	24
S	10	5	2		17
SW	5	2	1		8
W	3	1			4
NW	2				2
TOTAL	54	22	7	2	85

< [illegible] KNOTS 15 OBS 3,469

FIGURE 4-127 SUMMARIES OF OBSERVED WIND SPEED AND DIRECTION–SUMMER (AUGUST)

1

DIR	4-10 knots	11-16 knots	17-27 knots	≥28 knots	TOTAL
N	6	5	9	2	22
NE	7	2	3		12
E	9	4	2	1	16
SE	6	5	5		16
S	6	4	6		16
SW	2	1			3
W	1	1			2
NW	2	3	2		7
TOTAL	39	25	27	3	94

≤ 3 KNOTS 6 OBS 590

2

DIR	4-10 knots	11-16 knots	17-27 knots	≥28 knots	TOTAL
N	7	6	6	1	20
NE	8	6	4		18
E	11	8	4		23
SE	6	4	2		12
S	4	2	1		7
SW	2	1			3
W	2	1	1		4
NW	3	2	3		8
TOTAL	43	30	21	1	95

≤ 3 KNOTS 5 OBS 10,514

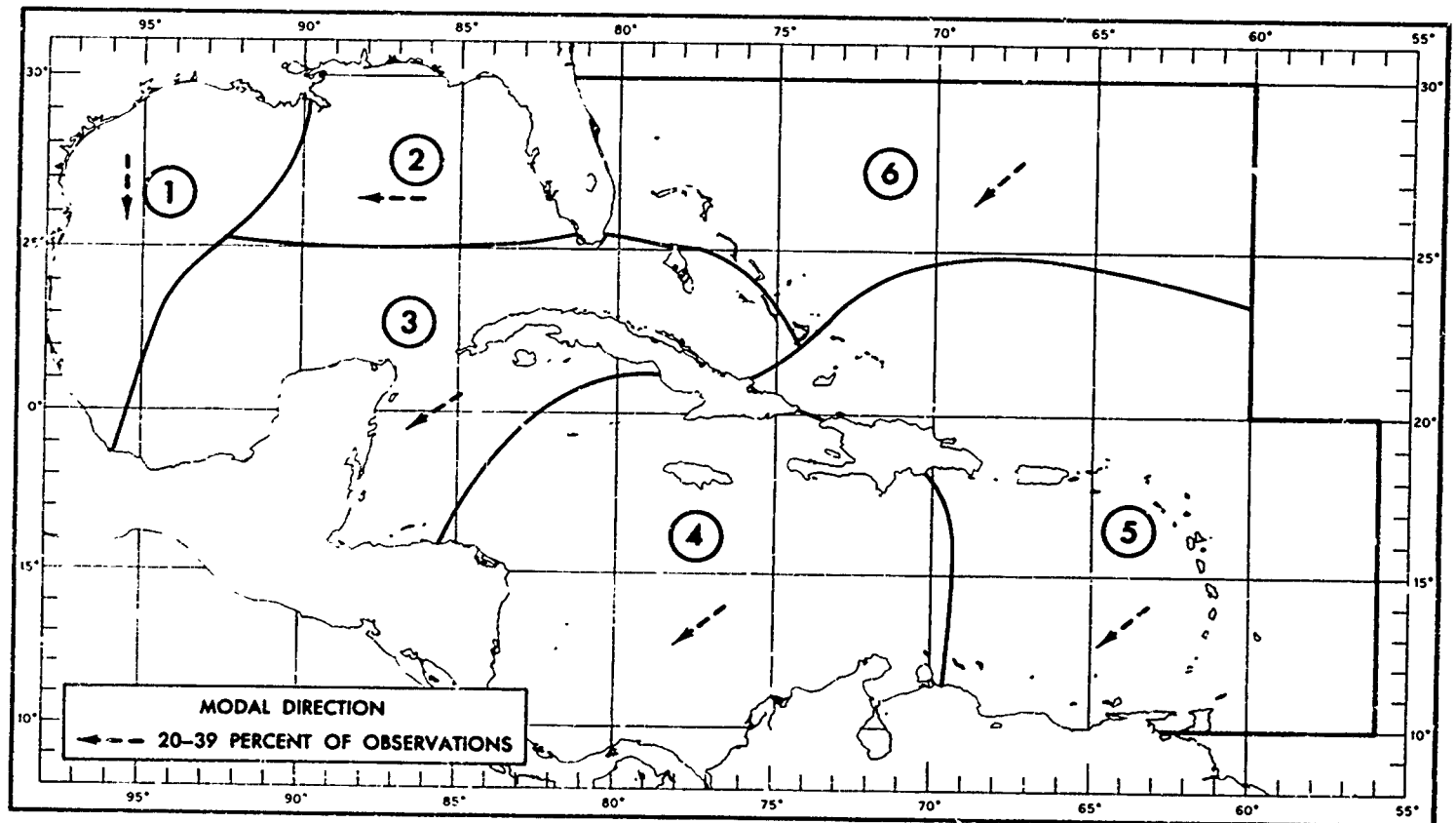

TABULATED NUMBERS REPRESENT PERCENT OF TOTAL OBSERVATIONS IN EACH REGION

3

DIR	4-10 knots	11-16 knots	17-27 knots	≥28 knots	TOTAL
N	7	6	6	1	20
NE	12	10	6	1	29
E	13	10	4		27
SE	5	2	1		8
S	2	1			3
SW	1				1
W	1	1			2
NW	3	1	1		5
TOTAL	44	31	18	2	95

≤ 3 KNOTS 5 OBS 4,081

4

DIR	4-10 knots	11-16 knots	17-27 knots	≥28 knots	TOTAL
N	5	6	6	1	18
NE	10	13	15	1	39
E	8	10	12	1	31
SE	2	1	1		4
S	1				1
SW					
W	1				1
NW	1	1	1		3
TOTAL	28	31	35	3	97

≤ 3 KNOTS 3 OBS 2,561

5

DIR	4-10 knots	11-16 knots	17-27 knots	≥28 knots	TOTAL
N	2		1		3
NE	16	12	8		36
E	17	13	7		37
SE	7	2	1		10
S	2	1			3
SW	1				1
W	1				1
NW	1				1
TOTAL	47	28	17		92

≤ 3 KNOTS 8 OBS 2,388

6

DIR	4-10 knots	11-16 knots	17-27 knots	≥28 knots	TOTAL
N	6	5	4		15
NE	8	6	7	1	22
E	9	7	6	1	23
SE	5	2	1		8
S	4	2	1		7
SW	3	1	1		5
W	3	2	1		6
NW	3	2	1		6
TOTAL	41	27	22	2	92

≤ 3 KNOTS 8 OBS 7,070

FIGURE 4-128 SUMMARIES OF OBSERVED WIND SPEED AND DIRECTION–FALL (NOVEMBER)

1

	<3'	3'-5'	3'-8'	8'-12'	≥12'	TOTAL
N	4	4	4	1		13
NE	7	3	4			14
E	6	5				11
SE	13	7	4			24
S	5	5	3			13
SW	3	1				4
W		1				1
NW	2	4	2			8
TOTAL	40	30	17	1		88

CALM 12 NO. OBS. 304

2

	<3'	3'-5'	5'-8'	8'-12'	≥12'	TOTAL
N	5	4	3	1		13
NE	7	7	2			16
E	8	7	3			18
SE	7	6	3			16
S	4	3	1			8
SW	1	1	1			3
W	1	1	1	1		4
NW	3	4	3			10
TOTAL	36	33	17	2		88

CALM 12 NO. OBS. 5,865

3

	<3'	3'-5'	5'-8'	8'-12'	≥12'	TOTAL
N	6	6	3			15
NE	14	13	4	1		32
E	11	10	3	1		25
SE	5	3	1			9
S	1	1				2
SW						
W						
NW	2	1	1			4
TOTAL	39	34	12	2		87

CALM 13 NO. OBS. 1,404

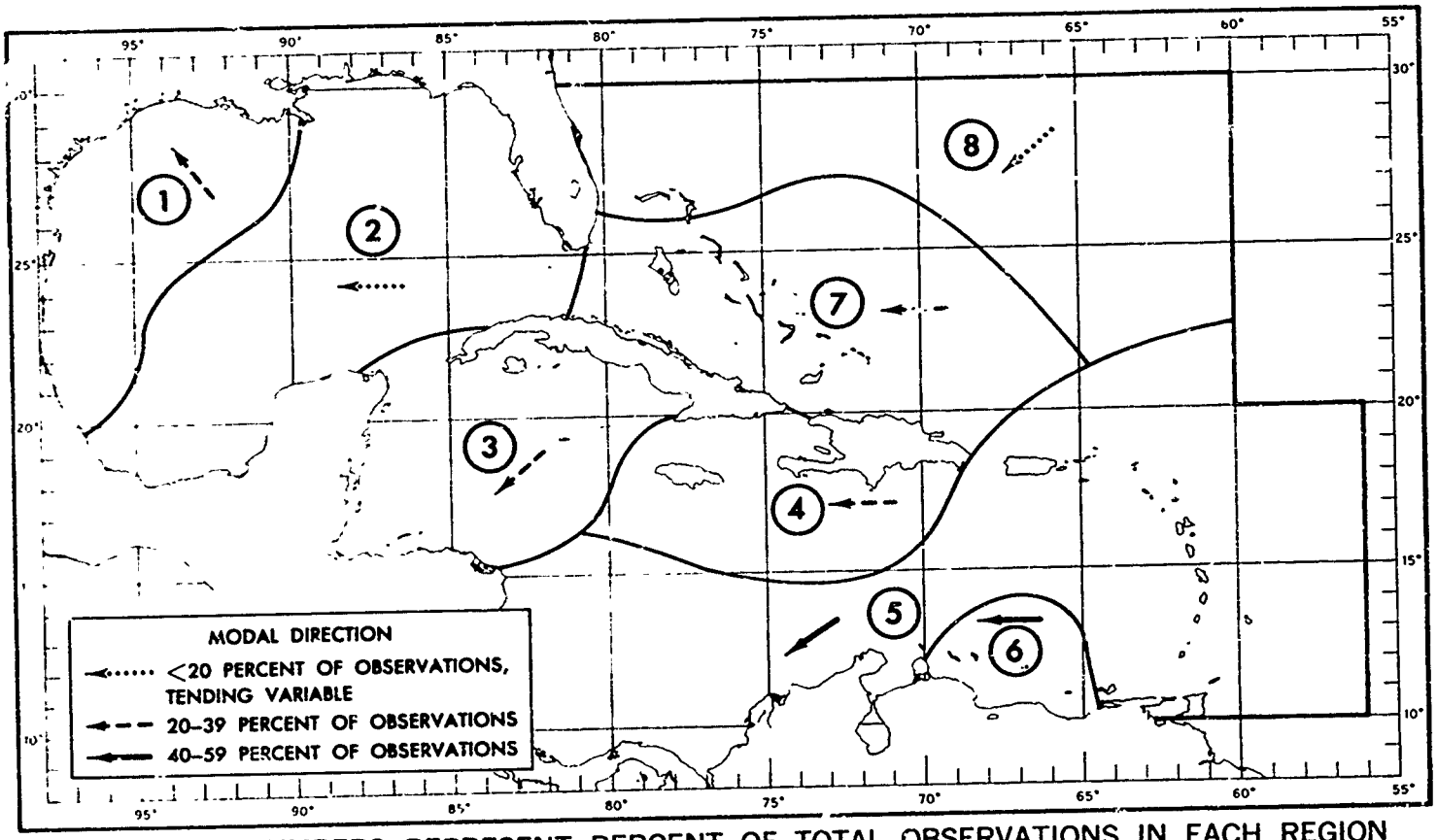

TABULATED NUMBERS REPRESENT PERCENT OF TOTAL OBSERVATIONS IN EACH REGION

4

	<3'	3'-5'	5'-8'	8'-12'	≥12'	TOTAL
N	2	2	1			5
NE	11	13	7	2		33
E	14	13	7	2		36
SE	3	2	1			6
S	1					1
SW	1					1
W	1					1
NW	1					1
TOTAL	34	30	16	4		84

CALM 16 NO. OBS. 2,483

5

	<3'	3'-5'	5'-8'	8'-12'	>12'	TOTAL
N	2	1				3
NE	18	16	9	1		44
E	14	11	4	1		30
SE	1	1				2
S						
SW						
W						
NW	1					1
TOTAL	36	29	13	2		80

CALM 20 NO. OBS. 1,875

6

	<3'	3'-5'	5'-8'	8'-12'	≥12'	TOTAL
N	1					1
NE	13	16	7	1		37
E	17	21	10	1		49
SE	1	1	1			3
S	1					1
SW						
W						
NW						
TOTAL	33	38	18	2		91

CALM 9 NO. OBS. 2,415

7

	<3'	3'-5'	5'-8'	8'-12'	≥12'	TOTAL
N	4	3	1			8
NE	11	9	4	1		25
E	12	10	4			26
SE	5	2	1			8
S	2	1				3
SW	2	1				3
W	2	1				3
NW	2	2	1			5
TOTAL	40	29	11	1		81

CALM 19 NO. OBS. 4,213

8

	<3'	3'-5'	5'-8'	8'-12'	≥12'	TOTAL
N	4	4	3			11
NE	6	4	3	1		14
E	6	3	2	1		12
SE	6	3	2			11
S	5	3	1			9
SW	3	3	1	1		8
W	3	3	1	1		8
NW	3	4	3	1	1	12
TOTAL	36	27	16	5	1	85

CALM 15 NO. OBS. 2,343

FIGURE 4-129 SUMMARIES OF OBSERVED SEA HEIGHT AND DIRECTION-WINTER (FEBRUARY)

1

	<3'	3'-5'	5'-8'	8'-12'	≥12'	TOTAL
N	5	1				6
NE	6	2	1			9
E	12	6	2	1		21
SE	18	10	3	1		32
S	7	2				9
SW	2					2
W	2					2
NW	2	1				3
TOTAL	54	22	6	2		84

CALM 16 NO OBS. 4,307

2

	<3'	3'-5'	5'-8'	8'-12'	≥12'	TOTAL
N	6	2	1			9
NE	14	6	2			22
E	16	12	3			31
SE	9	4	2			15
S	2					2
SW	1					1
W	1					1
NW	1	1	1			3
TOTAL	50	25	9			84

CALM 16 NO OBS. 1,020

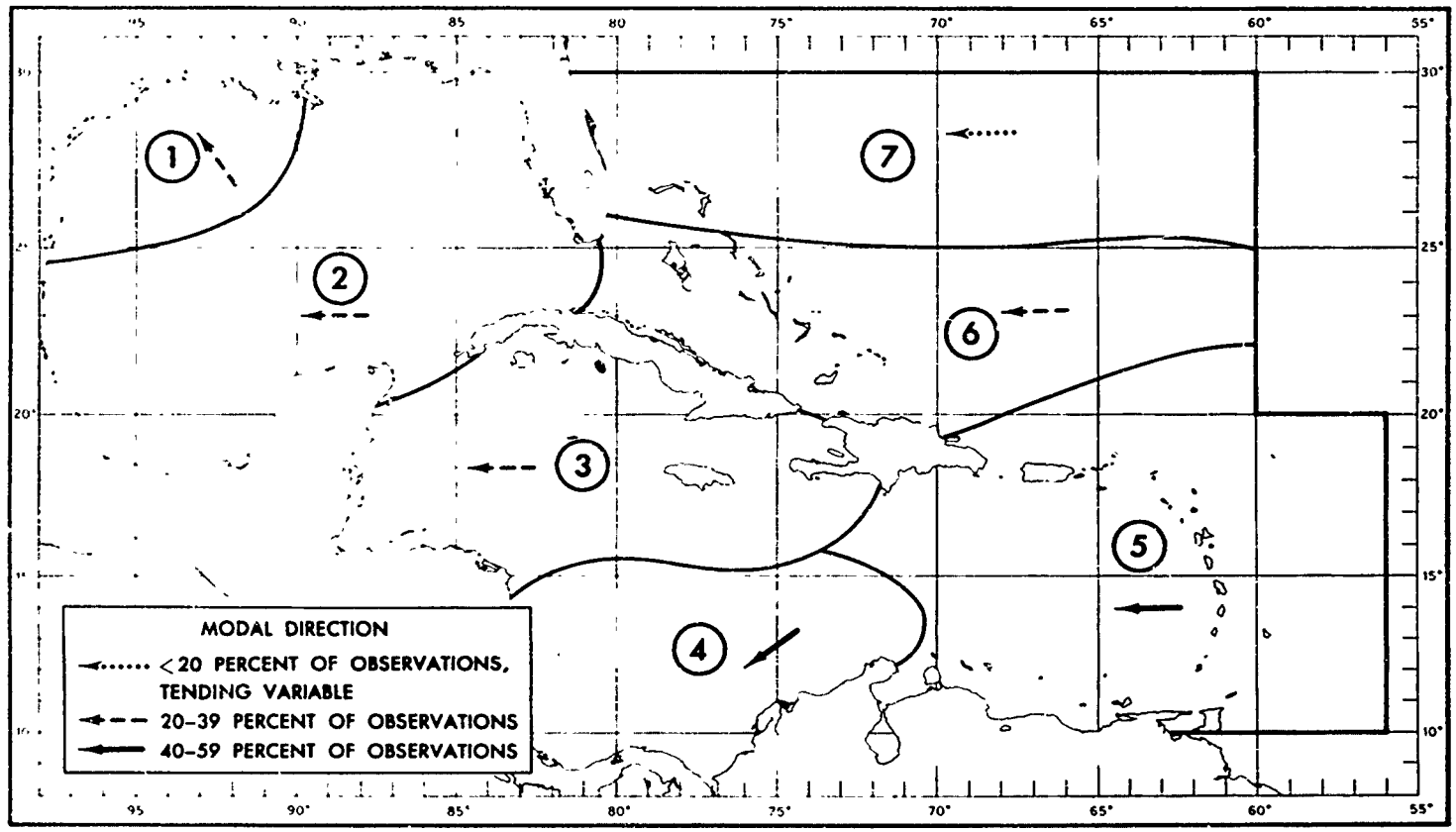

TABULATED NUMBERS REPRESENT PERCENT OF TOTAL OBSERVATIONS IN EACH REGION

3

	<3'	3'-5'	5'-8'	8'-12'	≥12'	TOTAL
N	3	1				4
NE	14	8	2			24
E	22	11	2			35
SE	7	6	2			15
S	1					1
SW						
W	1					1
NW	1					1
TOTAL	49	26	6			81

CALM 19 NO OBS. 1,420

4

	<3'	3'-5'	5'-8'	8'-12'	≥12'	TOTAL
N	5	2				7
NE	21	15	5			41
E	16	9	2			27
SE	3	1				4
S						
SW						
W	1					1
NW	1					1
TOTAL	47	27	7			81

CALM 19 NO. OBS. 1,155

5

	<3'	3'-5'	5'-8'	8'-12'	≥12'	TOTAL
N	1					1
NE	9	7	3			19
E	26	20	6			52
SE	9	6	2			17
S	1					1
SW	1					1
W						
NW						
TOTAL	47	33	11			91

CALM 9 NO. OBS. 3,571

6

	<3'	3'-5'	5'-8'	8'-12'	≥12'	TOTAL
N	1	1				2
NE	7	6	3			16
E	18	12	3			33
SE	11	9	1			21
S	3	2	1			6
SW	1	1				2
W	1					1
NW	1					1
TOTAL	43	31	8			82

CALM 18 NO OBS. 2,024

7

	<3'	3'-5'	5'-8'	8'-12'	≥12'	TOTAL
N	3	2	1			6
NE	7	6	2	1		16
E	10	6	1			17
SE	8	4				12
S	7	3	1			11
SW	5	2				7
W	2	1				3
NW	2	1				3
TOTAL	44	25	5	1		75

CALM 25 NO. OBS. 4,713

FIGURE 4-130 SUMMARIES OF OBSERVED SEA HEIGHT AND DIRECTION–SPRING (MAY)

1

	<3'	3'-5'	5'-8'	8'-12'	≥12'	TOTAL
N	3	1				4
NE	6	2				8
E	12	4				16
SE	11	5	2			18
S	8	2	1			11
SW	6	1				7
W	4	1				5
NW	3					3
TOTAL	53	16	3			72

CALM 28 NO. OBS. 5,211

2

	<3'	3'-5'	5'-8'	8'-12'	≥12'	TOTAL
N	3	1				4
NE	7	2				9
E	13	5	1			19
SE	8	3	1			12
S	4	1	1			6
SW	4	1				5
W	3	1				4
NW	2					2
TOTAL	44	14	3			61

CALM 39 NO. OBS. 9,046

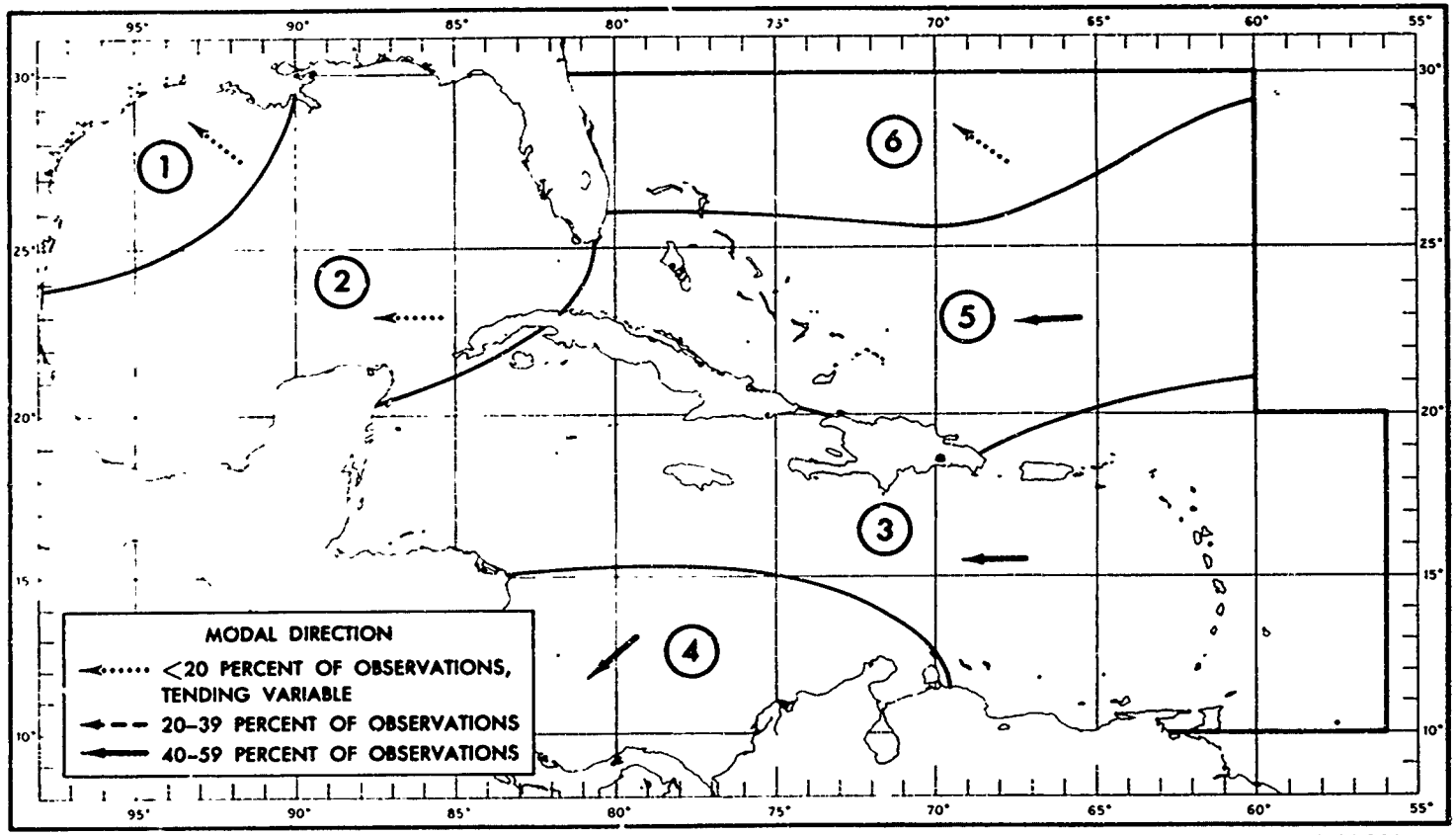

TABULATED NUMBERS REPRESENT PERCENT OF TOTAL OBSERVATIONS IN EACH REGION

3

	<3'	3'-5'	5'-8'	8'-12'	≥12'	TOTAL
N	2					2
NE	12	11	4	1		28
E	15	20	9	2		46
SE	3	2	1			6
S	1					1
SW						
W	1					1
NW						
TOTAL	34	33	14	3		84

CALM 16 NO. OBS. 3,124

4

	<3'	3'-5'	5'-8'	8'-12'	≥12'	TOTAL
N	4	3				7
NE	16	25	8	1		50
E	9	12	6			27
SE	2					2
S	1					1
SW	1					1
W						
NW						
TOTAL	33	40	14	1		88

CALM 12 NO. OBS. 1,213

5

	<3'	3'-5'	5'-8'	8'-12'	≥12'	TOTAL
N	1					1
NE	9	6	3			18
E	22	18	4	1		45
SE	9	4	1			14
S	1					1
SW	1					1
W	1					1
NW	1					1
TOTAL	45	28	8	1		82

CALM 18 NO. OBS. 4,699

6

	<3'	3'-5'	5'-8'	8'-12'	≥12'	TOTAL
N	1					1
NE	4	2	1			7
E	11	6	1			18
SE	11	6	2			19
S	9	3				12
SW	4	2	1			7
W	2	1				3
NW	1					1
TOTAL	43	20	5			68

CALM 32 NO. OBS. 5,180

FIGURE 4-131 SUMMARIES OF OBSERVED SEA HEIGHT AND DIRECTION-SUMMER (AUGUST)

1

	<3'	3'-5'	5'-8'	8'-12'	≥12'	TOTAL
N	7	4	2	2	1	16
NE	8	3	1			12
E	10	4	1			15
SE	12	6	2			20
S	2	1				3
SW	1					1
W	2	2	1			5
NW	6	2	2	2	1	13
TOTAL	48	22	9	4	2	85

CALM 15 NO. OBS. 456

2

	<3'	3'-5'	5'-8'	8'-12'	≥12'	TOTAL
N	7	7	3	1		18
NE	15	12	3	1		31
E	13	7	2			22
SE	4	3	1			8
S	1	1				2
SW						
W						
NW	2	1	1		1	5
TOTAL	42	31	10	2	1	86

CALM 14 NO. OBS. 1,013

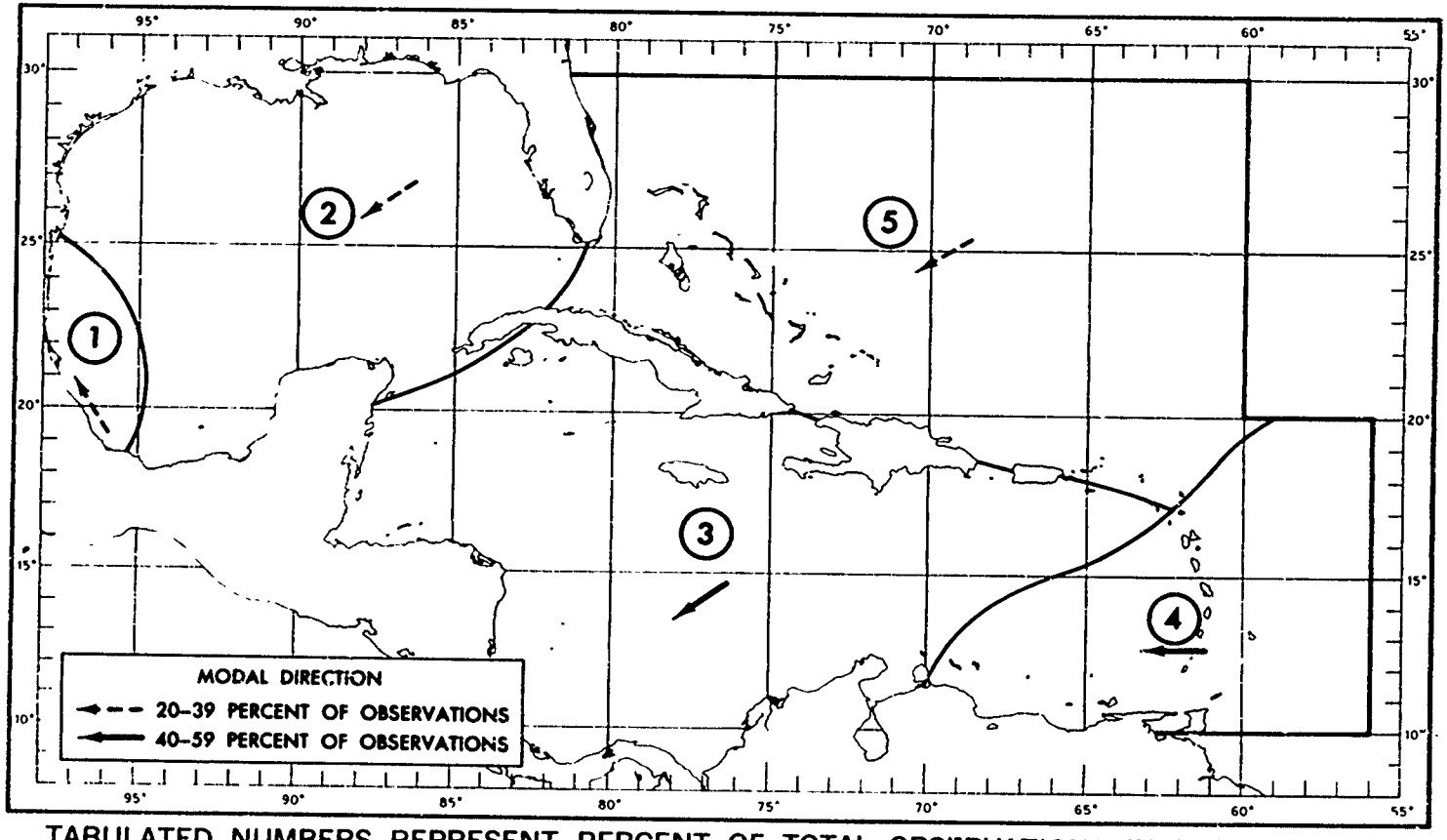

TABULATED NUMBERS REPRESENT PERCENT OF TOTAL OBSERVATIONS IN EACH REGION

3

	<3'	3'-5'	5'-8'	8'-12'	≥12'	TOTAL
N	3	3	1			7
NE	17	16	7	1		41
E	11	9	3	1		24
SE	3	1				4
S	1					1
SW	1					1
W	1					1
NW	1					1
TOTAL	38	29	11	2		80

CALM 20 NO OBS. 2,384

4

	<3'	3'-5'	5'-8'	8'-12'	≥12'	TOTAL
N	1	1				2
NE	15	11	6	1	1	34
E	19	16	7	2		44
SE	4	2				6
S	1					1
SW						
W						
NW						
TOTAL	40	30	13	3	1	87

CALM 13 NO. OBS. 1,316

5

	<3'	3'-5'	5'-8'	8'-12'	≥12'	TOTAL
N	5	5	4	1		15
NE	7	10	7	2	1	27
E	7	7	3	1		18
SE	4	2	1			7
S	2	1				3
SW	2	1				3
W	2	1	1			4
NW	4	4	2	1		11
TOTAL	33	31	18	5	1	88

CALM 12 NO. OBS. 7,530

FIGURE 4-132 SUMMARIES OF OBSERVED SEA HEIGHT AND DIRECTION–FALL (NOVEMBER)

1

	1'-6'	6'-12'	>12'	TOTAL
N	7	5	1	13
NE	8	6		14
E	10	4		14
SE	10	8		18
S	7	3	1	11
SW	2	1		3
W	2	2		4
NW	4	5		9
TOTAL	50	34	2	86

CALM 14 NO OBS. 2,136

2

	1'-6'	6'-12'	>12'	TOTAL
N	5	7	2	14
NE	11	8	1	20
E	11	7		13
SE	8	5		13
S	2	2		4
SW	1	1		2
W	1			1
NW	3	5	2	10
TOTAL	42	35	5	82

CALM 18 NO. OBS. 1,738

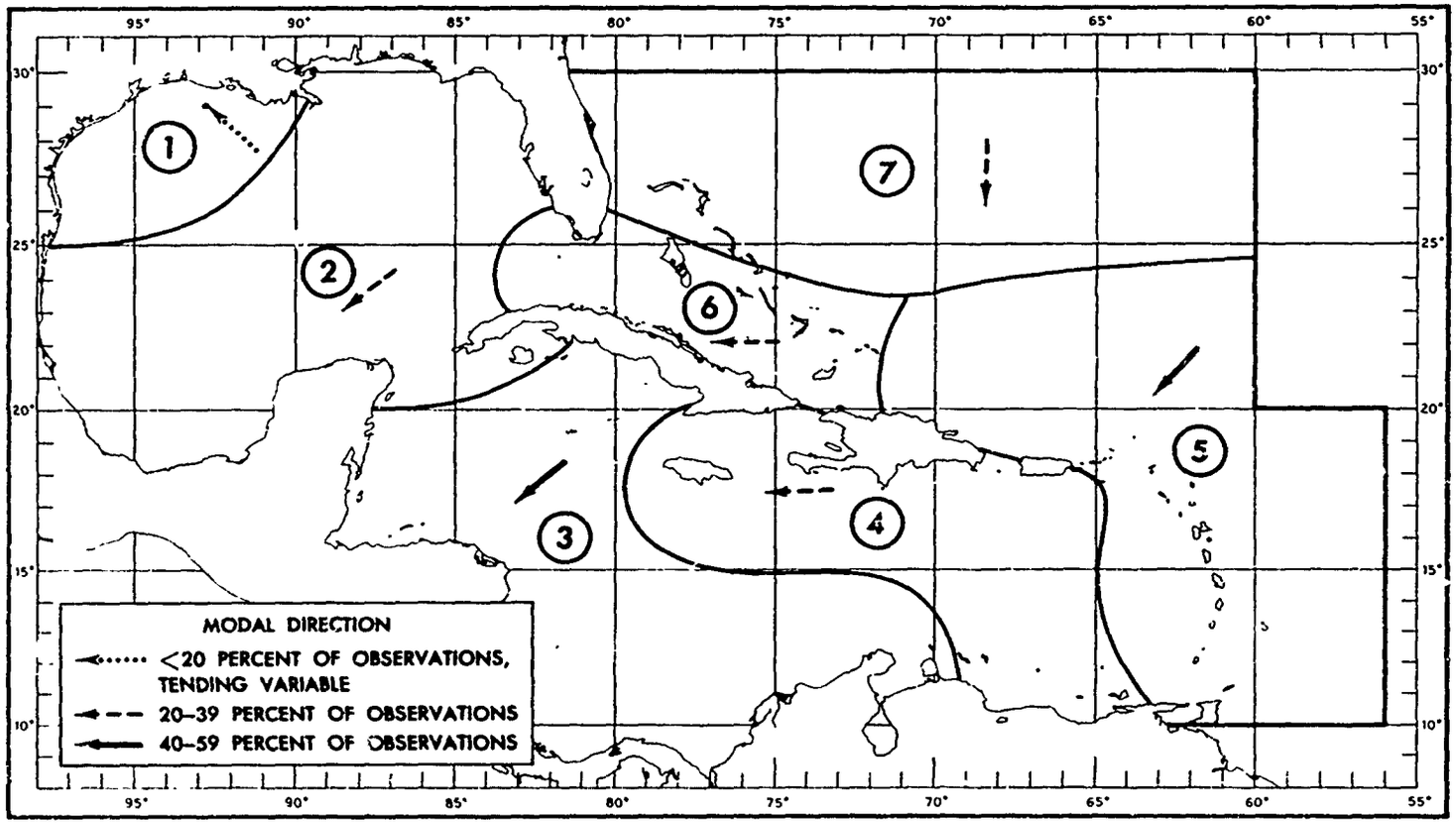

TABULATED NUMBERS REPRESENT PERCENT OF TOTAL OBSERVATIONS IN EACH REGION

3

	1'-6'	6'-12'	>12'	TOTAL
N	5	6	1	12
NE	14	26	4	44
E	13	16	2	31
SE	2	1		3
S				
SW				
W				
NW	1			1
TOTAL	35	49	7	91

CALM 9 NO. OBS 893

4

	1'-6'	6'-12'	>12'	TOTAL
N	3	2		5
NE	12	12	2	26
E	18	18	2	38
SE	6	2	1	9
S	1			1
SW				
W	1			1
NW	1			1
TOTAL	42	34	5	81

CALM 19 NO OBS. 2,071

5

	1'-6'	6'-12'	>12'	TOTAL
N	9	4		13
NE	14	23	3	40
E	18	11	1	30
SE	3	2		5
S	1			1
SW				
W				
NW	3	2		5
TOTAL	48	42	4	94

CALM 6 NO. OBS. 810

6

	1'-6'	6'-12'	>12'	TOTAL
N	4	3		7
NE	9	5		14
E	18	6	1	25
SE	8	2		10
S	1			1
SW	1			1
W	2	1		3
NW	2	1		3
TOTAL	45	18	1	64

CALM 36 NO. OBS. 394

7

	1'-6'	6'-12'	>12'	TOTAL
N	9	9	2	20
NE	7	8	2	17
E	6	4		10
SE	5	3		8
S	3	2		5
SW	3	2	1	6
W	2	4	1	7
NW	5	9	4	18
TOTAL	40	41	10	91

CALM 9 NO. OBS. 1,806

FIGURE 4-133 SUMMARIES OF OBSERVED SWELL HEIGHT AND DIRECTION–WINTER (FEBRUARY)

1

	1'-6'	6'-12'	>12'	TOTAL
N	2			2
NE	12	5		17
E	20	10	1	31
SE	10	5		15
S	3	1		4
SW	1			1
W				
NW	1			1
TOTAL	49	21	1	71

CALM 29 NO. OBS. 2,090

2

	1'-6'	6'-12'	>12'	TOTAL
N	1			1
NE	11	12	1	24
E	20	21	2	43
SE	10	5		15
S	2			2
SW	1			1
W	1			1
NW				
TOTAL	46	38	3	87

CALM 13 NO OBS. 1,870

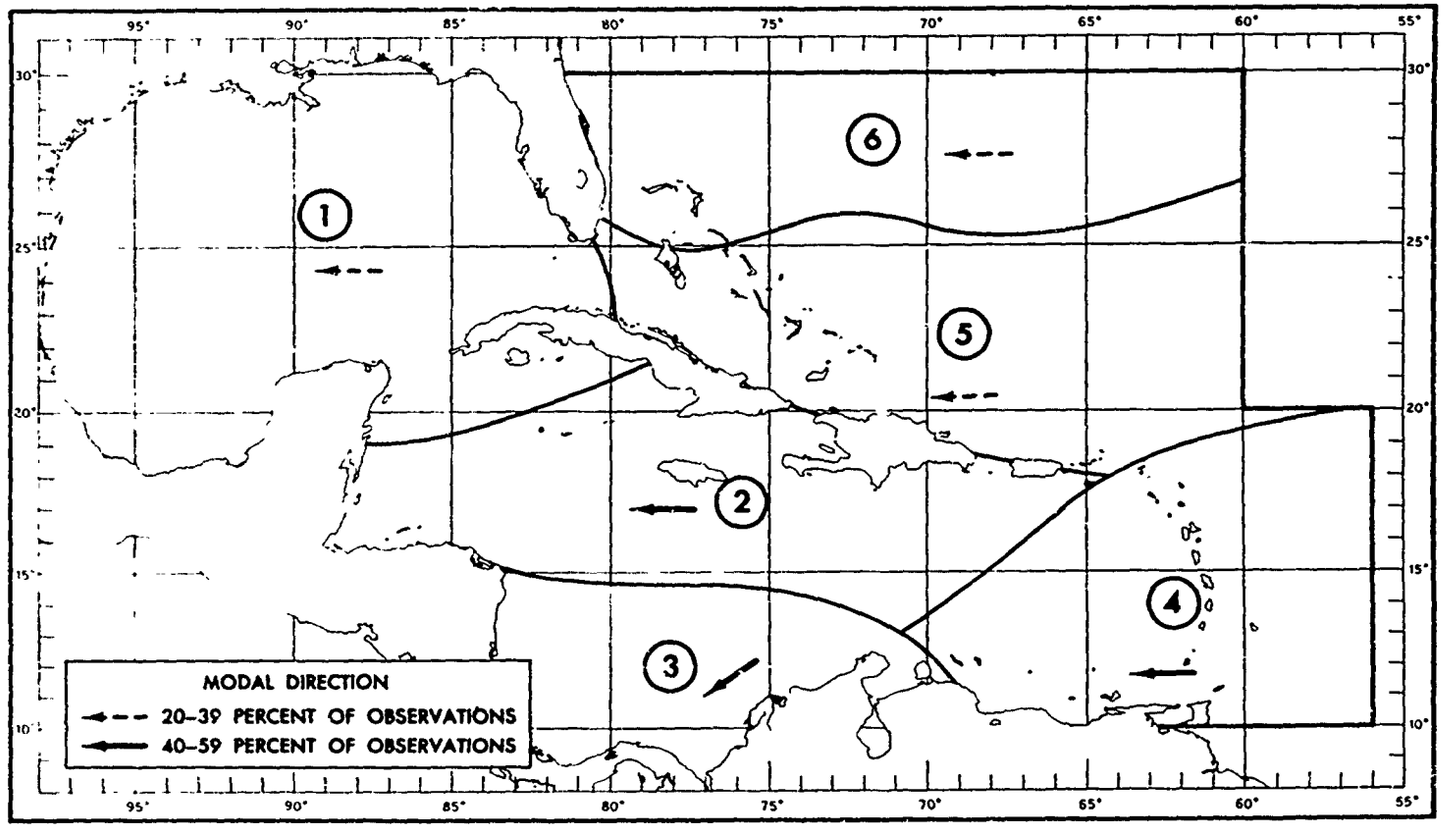

TABULATED NUMBERS REPRESENT PERCENT OF TOTAL OBSERVATIONS IN EACH REGION

3

	1'-6'	6'-12'	>12'	TOTAL
N	1			1
NE	18	23	2	43
E	17	18	2	37
SE	3	1		4
S				
SW	1			1
W				
NW				
TOTAL	40	42	4	86

CALM 14 NO OBS. 1,752

4

	1'-6'	6'-12'	>12'	TOTAL
N				
NE	9	9		18
E	29	26	1	56
SE	6	3		9
S				
SW				
W				
NW				
TOTAL	44	38	1	83

CALM 17 NO. OBS. 1,679

5

	1'-6'	6'-12'	>12'	TOTAL
N	2	2		4
NE	9	7		16
E	20	14	1	35
SE	17	8		25
S	3	2		5
SW	1			1
W	1			1
NW	1	1		2
TOTAL	54	34	1	89

CALM 11 NO OBS. 1,623

6

	1'-6'	6'-12'	>12'	TOTAL
N	4	3		7
NE	11	6	1	18
E	14	7		21
SE	14	5		19
S	5	2		7
SW	4	1		5
W	2	1		3
NW	3	1		4
TOTAL	57	26	1	84

CALM 16 NO. OBS. 3,163

FIGURE 4-134 SUMMARIES OF OBSERVED SWELL HEIGHT AND DIRECTION-SPRING (MAY)

1

	1'-6'	6'-12'	>12'	TOTAL
N	3			3
NE	5	1		6
E	10	3		13
SE	15	5	1	21
S	10	3	1	14
SW	5	2		7
W	2			2
NW	2			2
TOTAL	52	14	2	68

CALM 32 NO. OBS. 3,401

2

	1'-6'	6'-12'	>12'	TOTAL
N	1			1
NE	11	2		13
E	22	4		26
SE	10	4		14
S	3			3
SW	1			1
W	1			1
NW	1			1
TOTAL	50	10		60

CALM 40 NO. OBS. 2,357

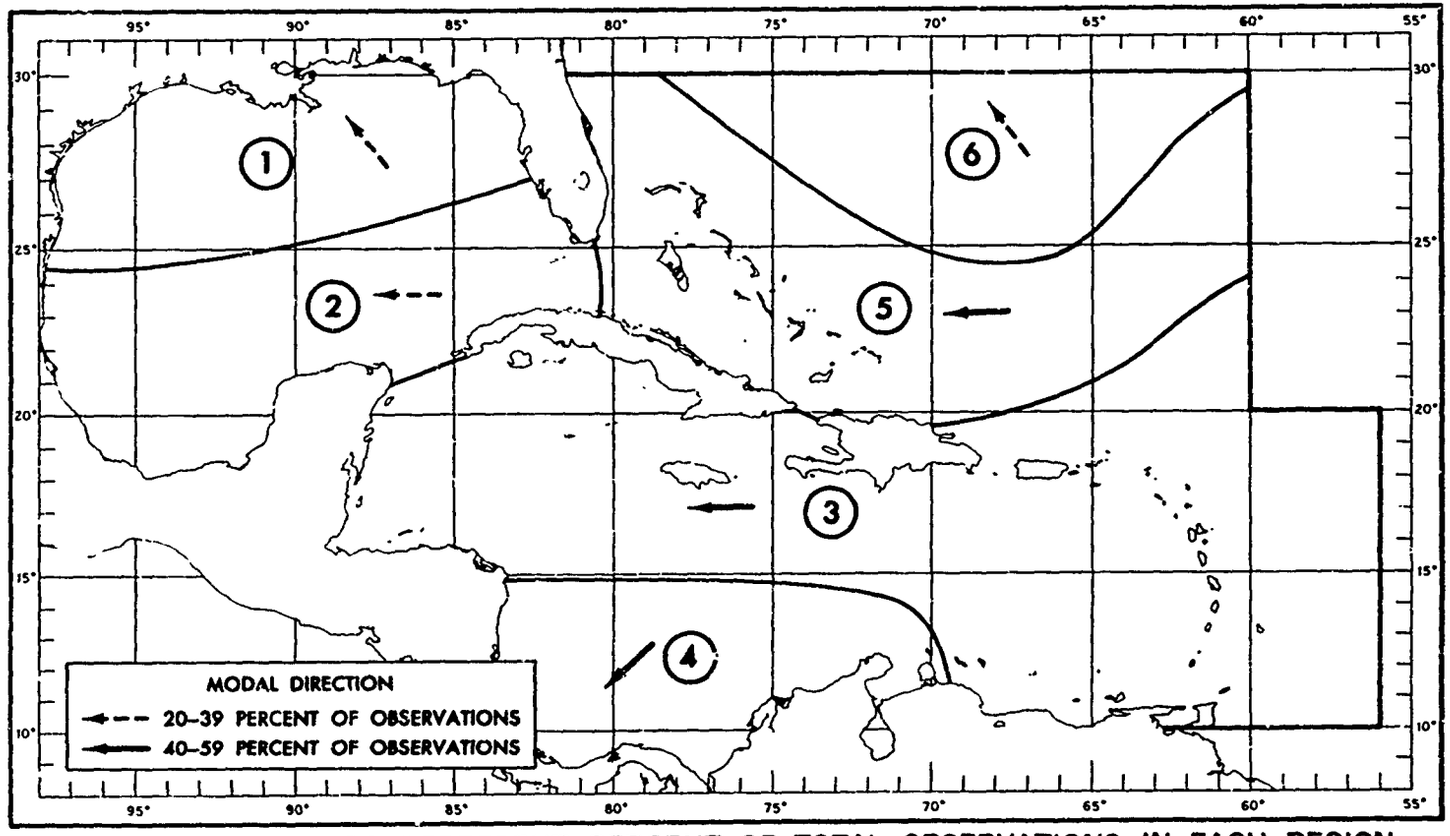

TABULATED NUMBERS REPRESENT PERCENT OF TOTAL OBSERVATIONS IN EACH REGION

3

	1'-6'	6'-12'	>12'	TOTAL
N	2			2
NE	12	10		22
E	22	22	2	46
SE	7	6		13
S	2			2
SW				
W				
NW				
TOTAL	45	38	2	85

CALM 15 NO. OBS. 2,171

4

	1'-6'	6'-12'	>12'	TOTAL
N	1	1		2
NE	16	28	4	48
E	15	21	2	38
SE	2	1		3
S				
SW				
W				
NW				
TOTAL	34	51	6	91

CALM 9 NO. OBS. 1,931

5

	1'-6'	6'-12'	>12'	TOTAL
N	1			1
NE	10	6		16
E	28	14	1	43
SE	14	4		18
S	2			2
SW				
W				
NW				
TOTAL	55	24	1	80

CALM 20 NO. OBS. 3,533

6

	1'-6'	6'-12'	>12'	TOTAL
N	2	1		3
NE	5	3		8
E	16	6		22
SE	23	8	1	32
S	7	1	1	9
SW	4	2		6
W	2			2
NW	2			2
TOTAL	61	21	2	84

CALM 16 NO. OBS. 3,920

FIGURE 4-135 SUMMARIES OF OBSERVED SWELL HEIGHT AND DIRECTION–SUMMER (AUGUST)

1

	1'-6'	6'-12'	>12'	TOTAL
N	6	7	1	14
NE	12	7	1	20
E	9	6		15
SE	7	6		13
S	4	3		7
SW	1	1		2
W	1	1		2
NW	4	5	1	10
TOTAL	44	36	3	83

CALM 17 NO. OBS. 2,756

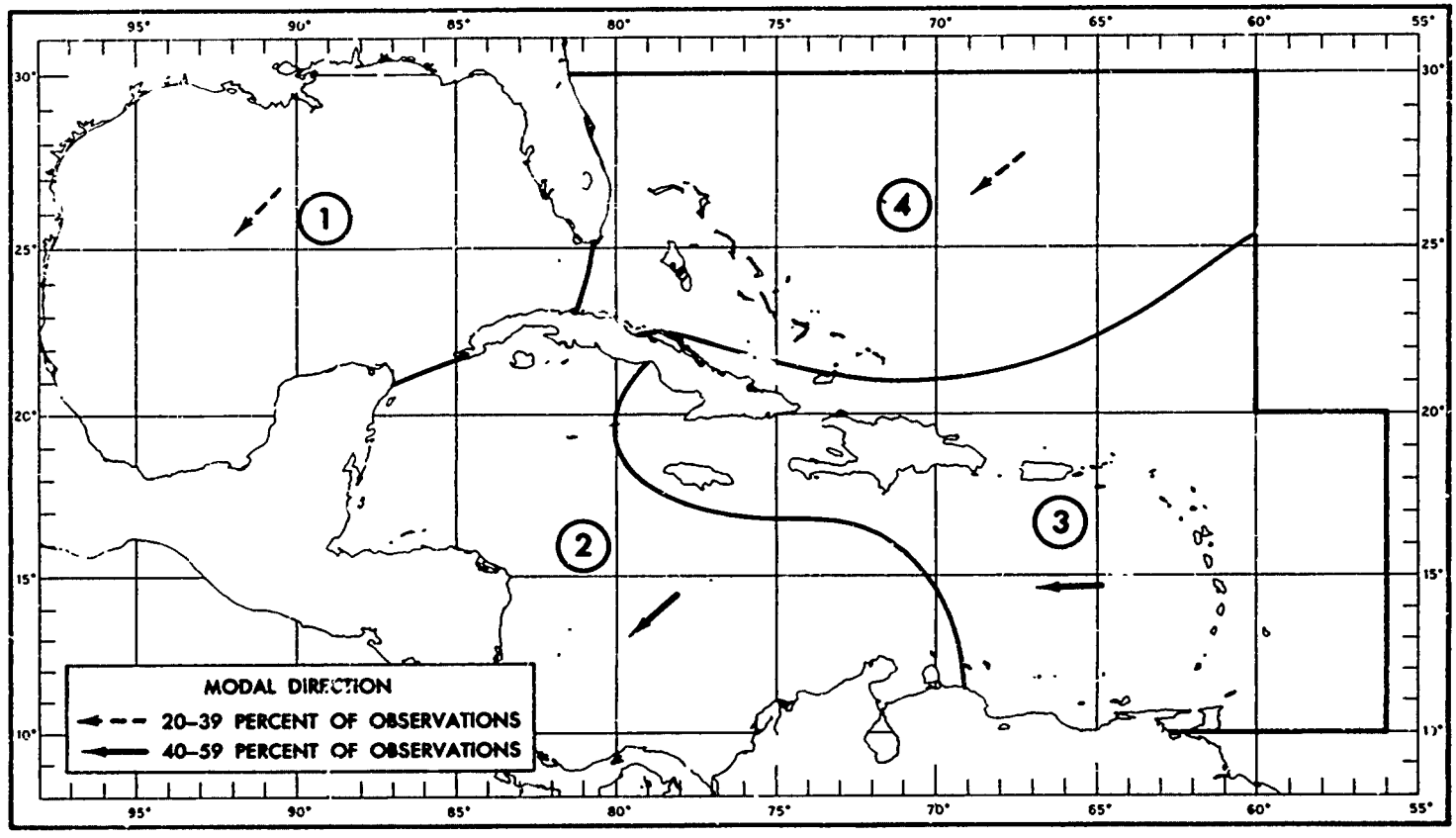

TABULATED NUMBERS REPRESENT PERCENT OF TOTAL OBSERVATIONS IN EACH REGION

2

	1'-6'	6'-12'	>12'	TOTAL
N	5	6	2	13
NE	20	19	2	41
E	14	10	1	25
SE	3	2		5
S				
SW				
W	1			1
NW	1	1		2
TOTAL	44	38	5	87

CALM 13 NO. OBS. 1,057

3

	1'-6'	6'-12'	>12'	TOTAL
N	3	4	1	8
NE	11	17	2	30
E	20	22		42
SE	5	3		8
S		1		1
SW				
W		1		1
NW	3	1		4
TOTAL	42	49	3	94

CALM 5 CONFUSED 1 NO. OBS. 800

4

	1'-6'	6'-12'	>12'	TOTAL
N	4	5	1	10
NE	8	16	5	29
E	9	13	3	25
SE	7	4	1	12
S	2	1		3
SW	1	2		3
W	2	2		4
NW	3	3	1	7
TOTAL	36	46	11	93

CALM 7 NO. OBS. 3,563

FIGURE 4-136 SUMMARIES OF OBSERVED SWELL HEIGHT AND DIRECTION–FALL (NOVEMBER)

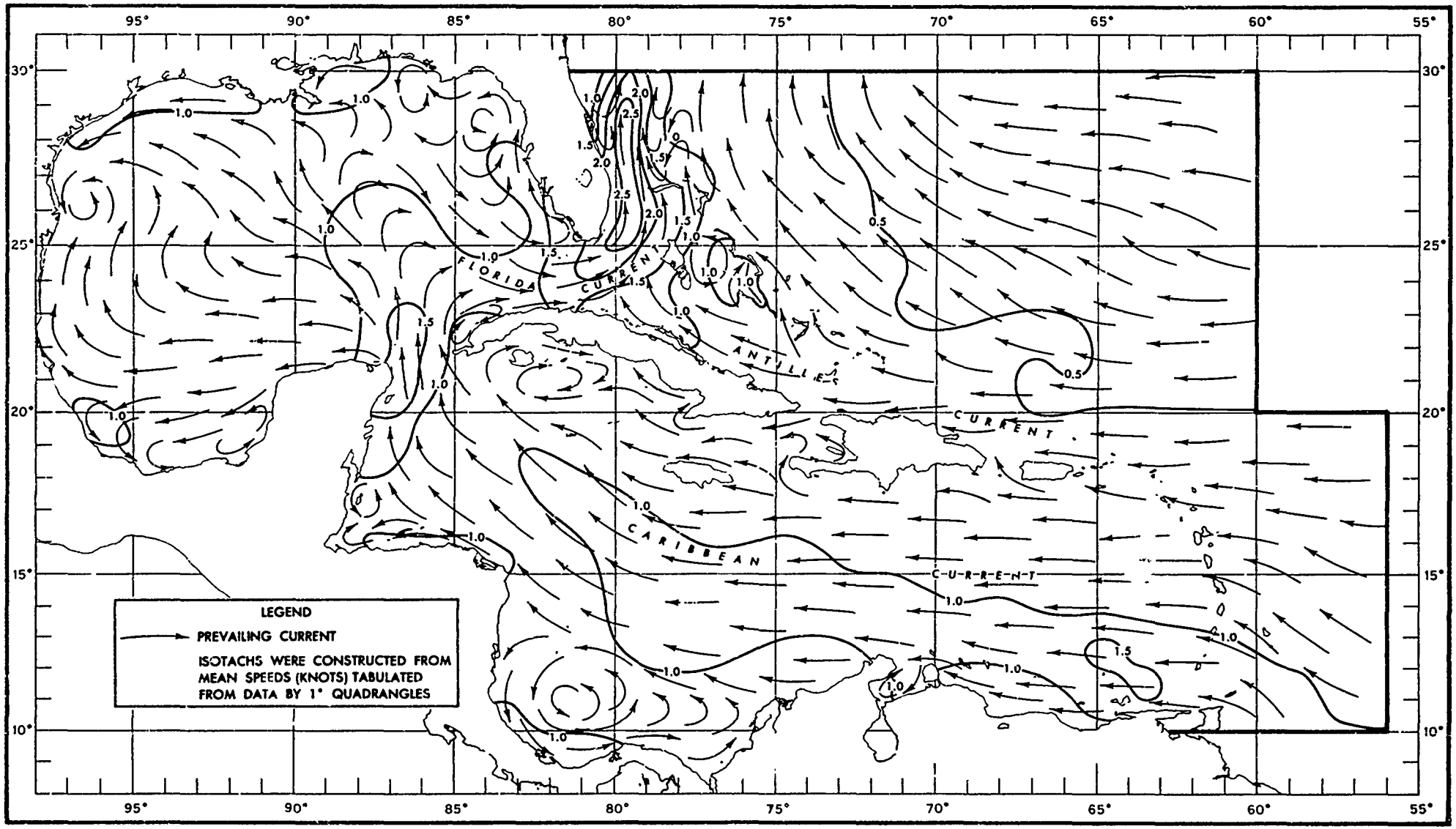

FIGURE 4-137 PREVAILING SURFACE CURRENT PATTERNS–WINTER (JANUARY-MARCH)

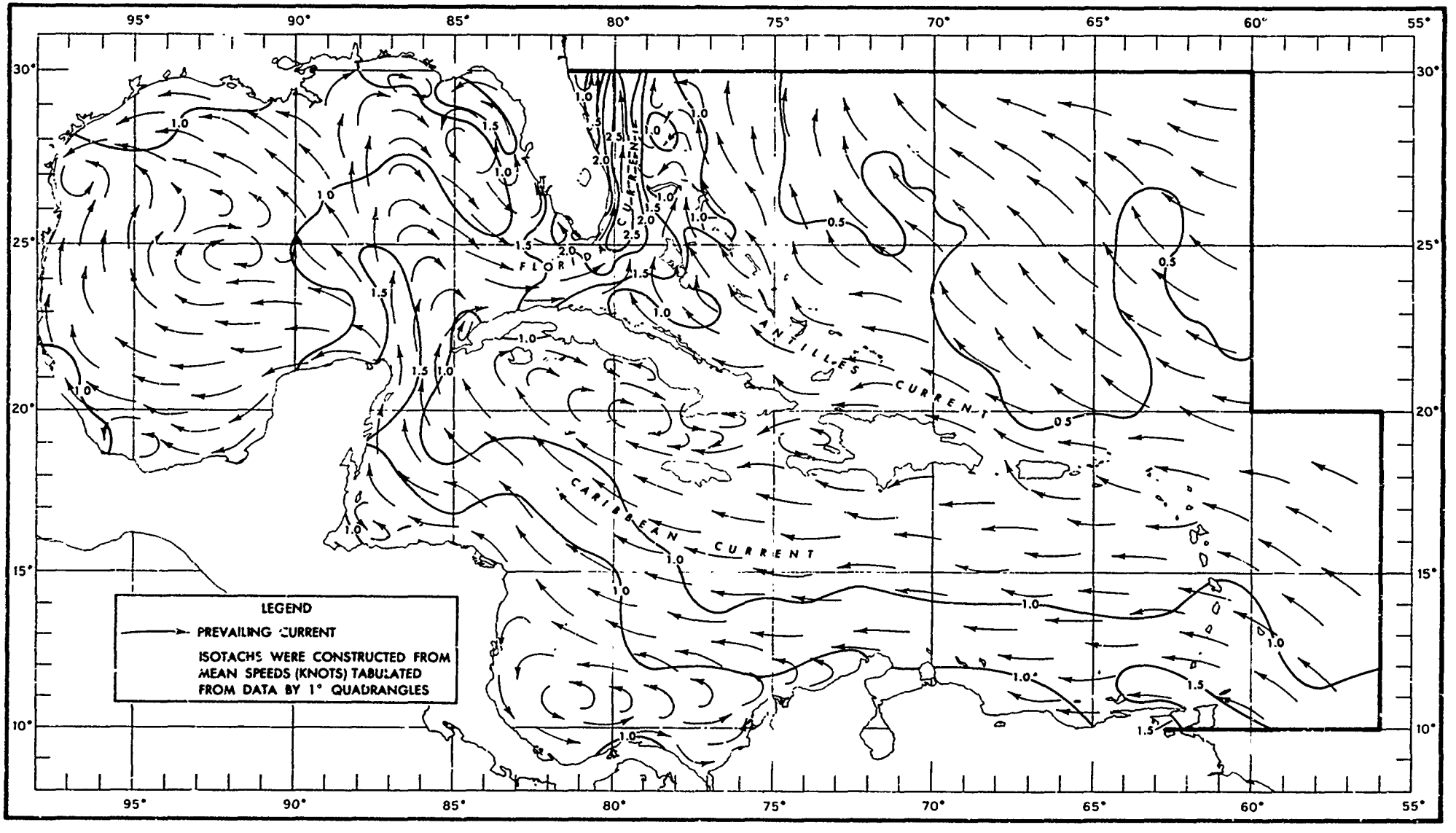

FIGURE 4-138 PREVAILING SURFACE CURRENT PATTERNS-SPRING (APRIL-JUNE)

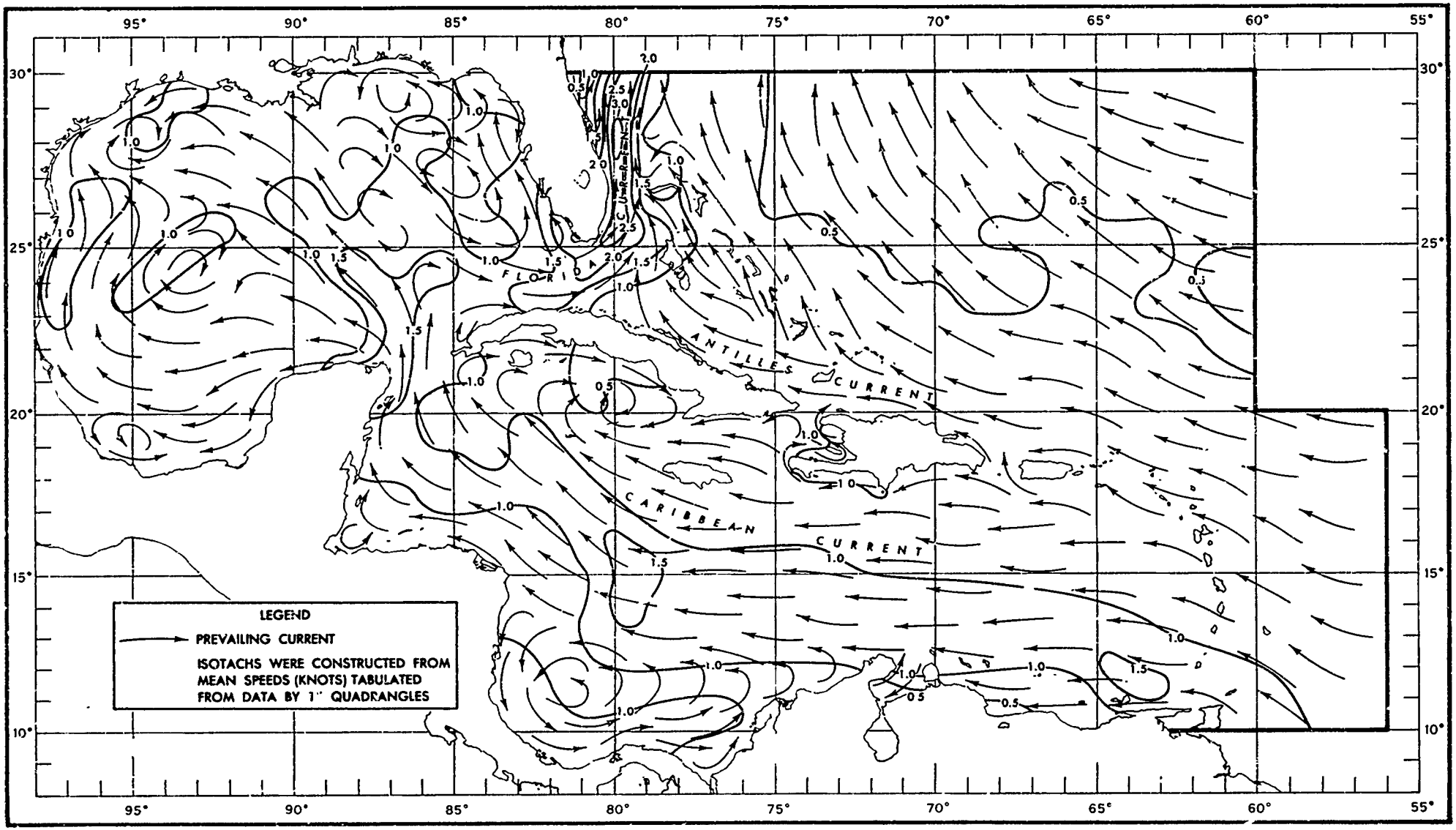

FIGURE 4-139 PREVAILING SURFACE CURRENT PATTERNS-SUMMER (JULY-SEPTEMBER)

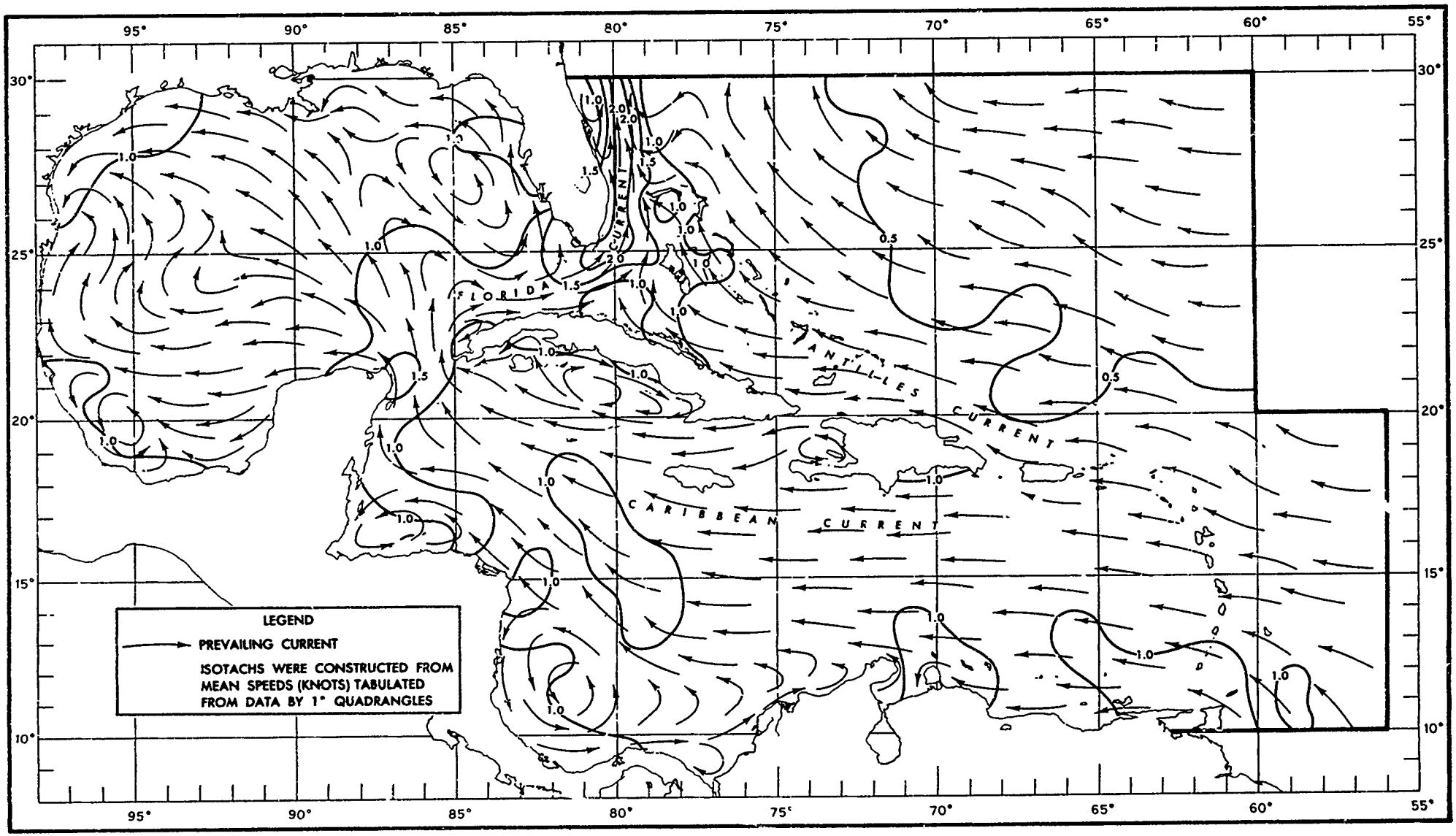

FIGURE 4-140 PREVAILING SURFACE CURRENT PATTERNS-FALL (OCTOBER-DECEMBER)

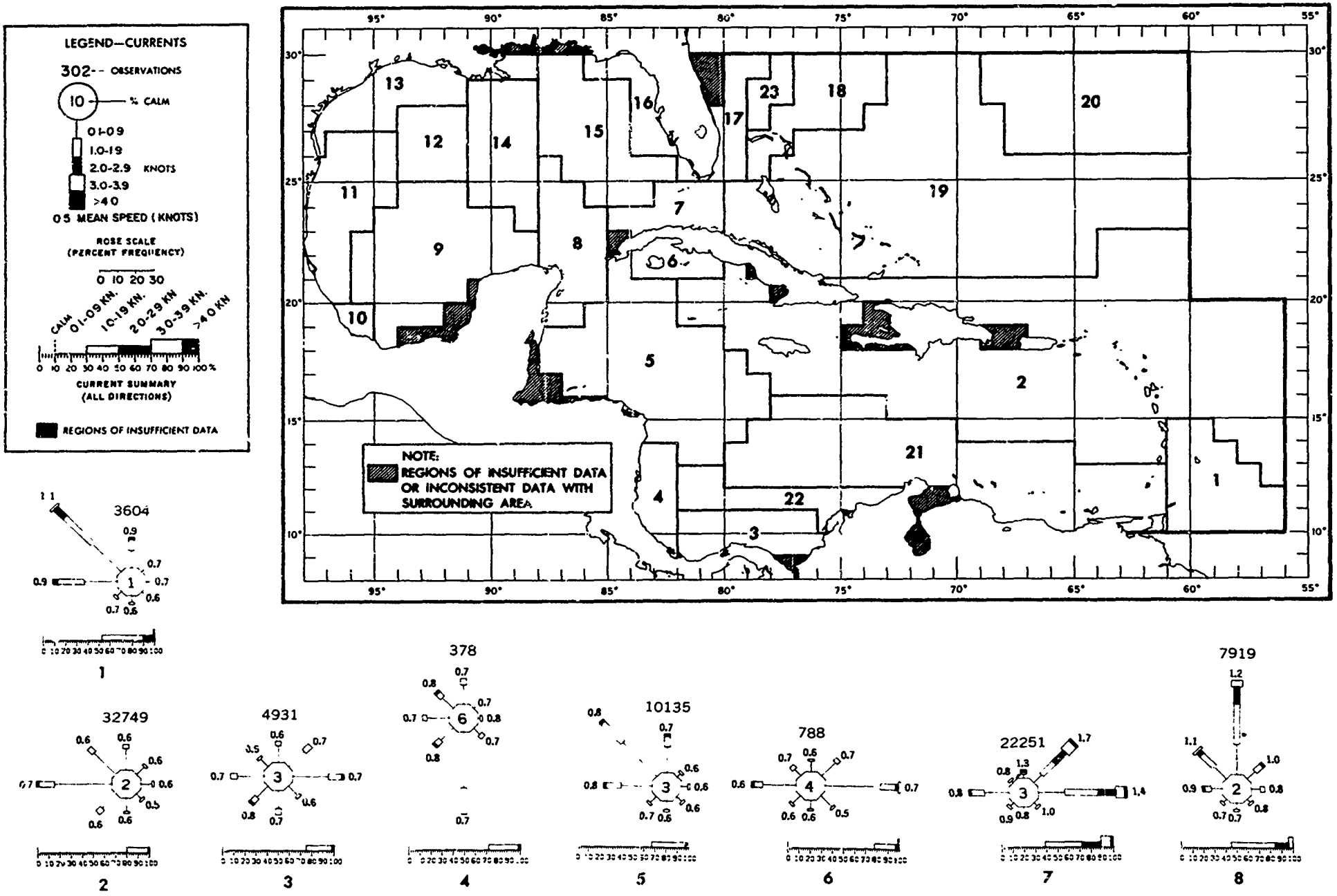

FIGURE 4-141 SURFACE CURRENTS–WINTER (JANUARY–MARCH)

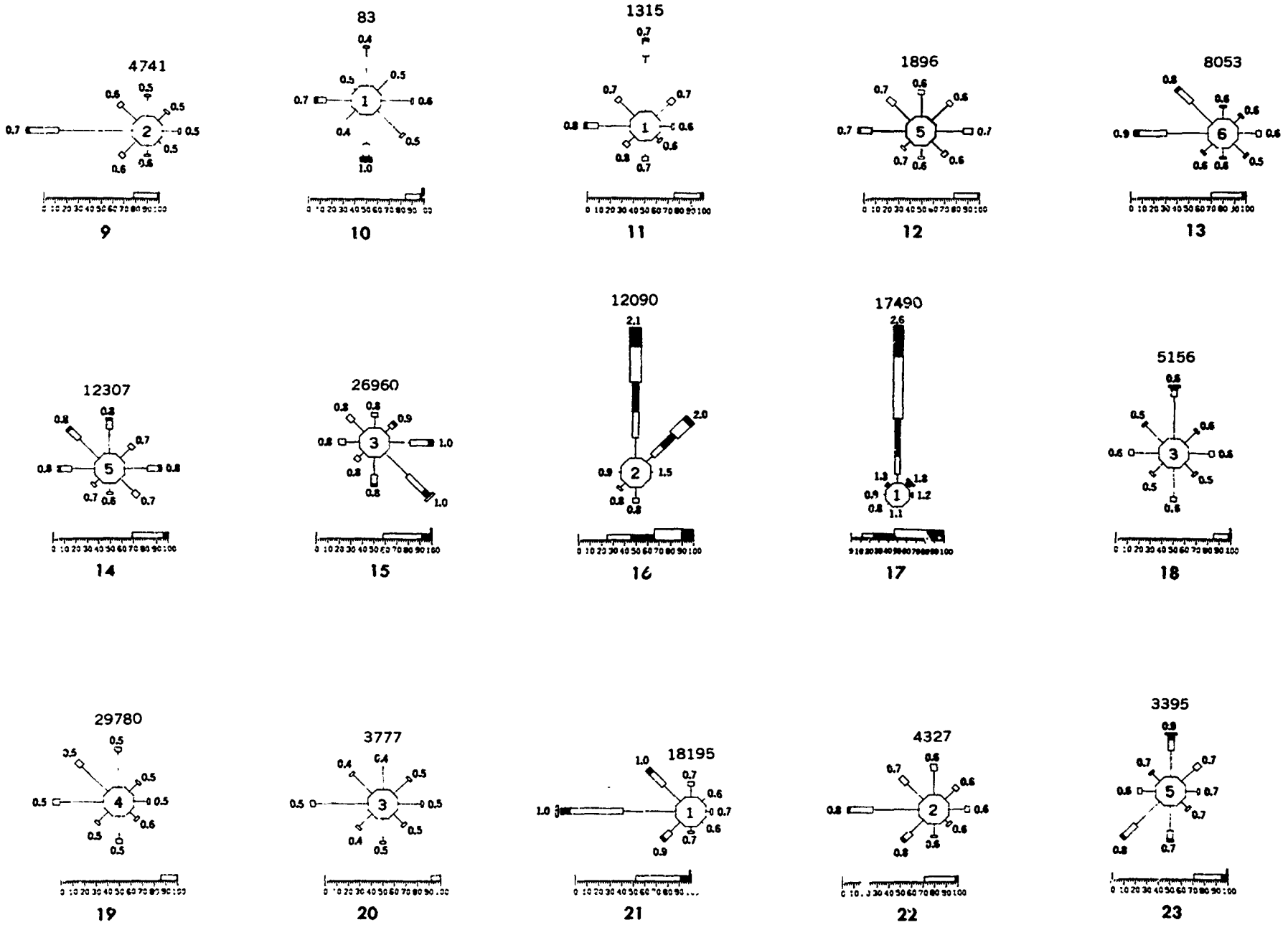

FIGURE 4-142 SURFACE CURRENTS–WINTER (JANUARY-MARCH) (CONT.)

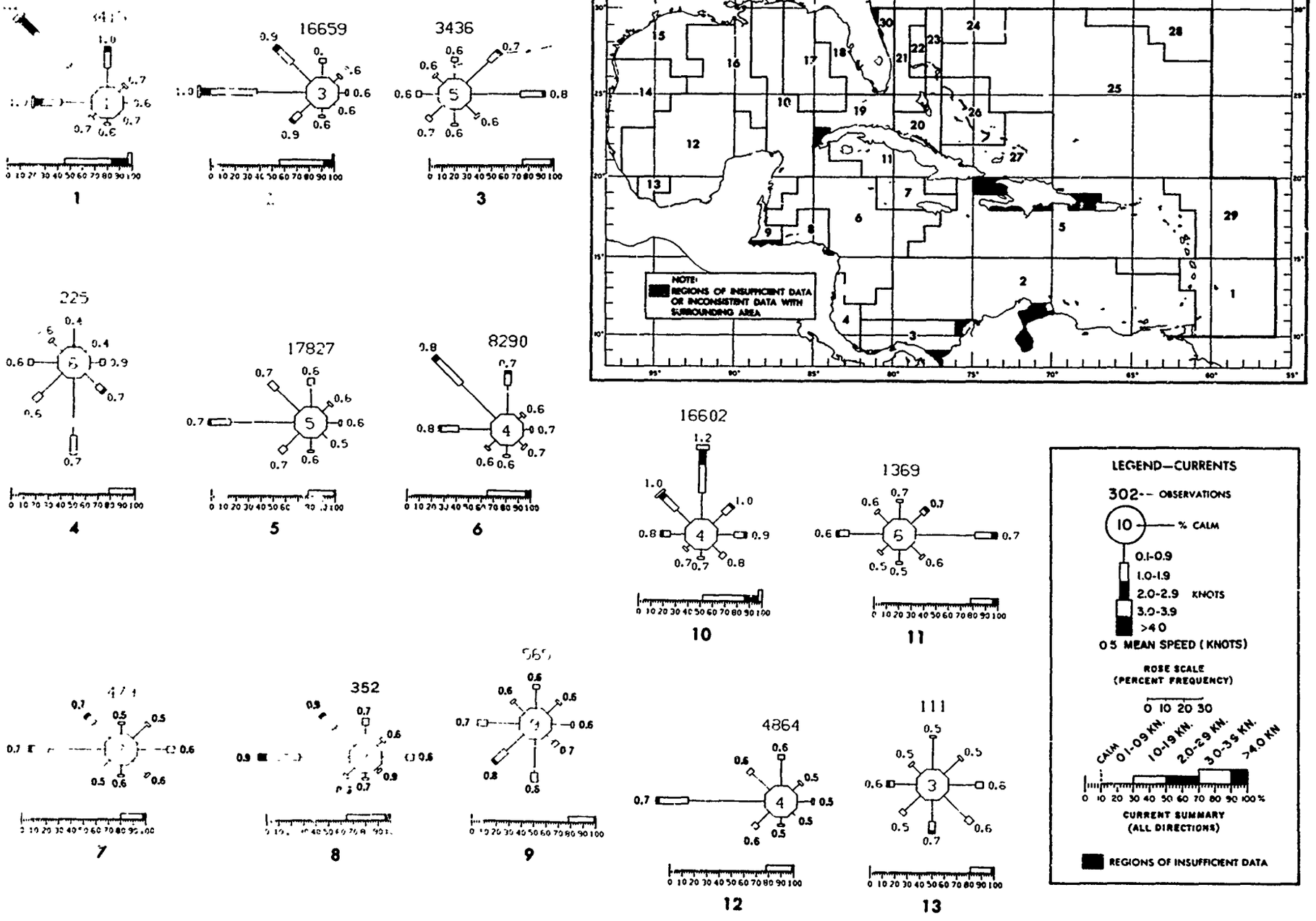

FIGURE 4-143 SURFACE CURRENTS–SPRING (APRIL-JUNE)

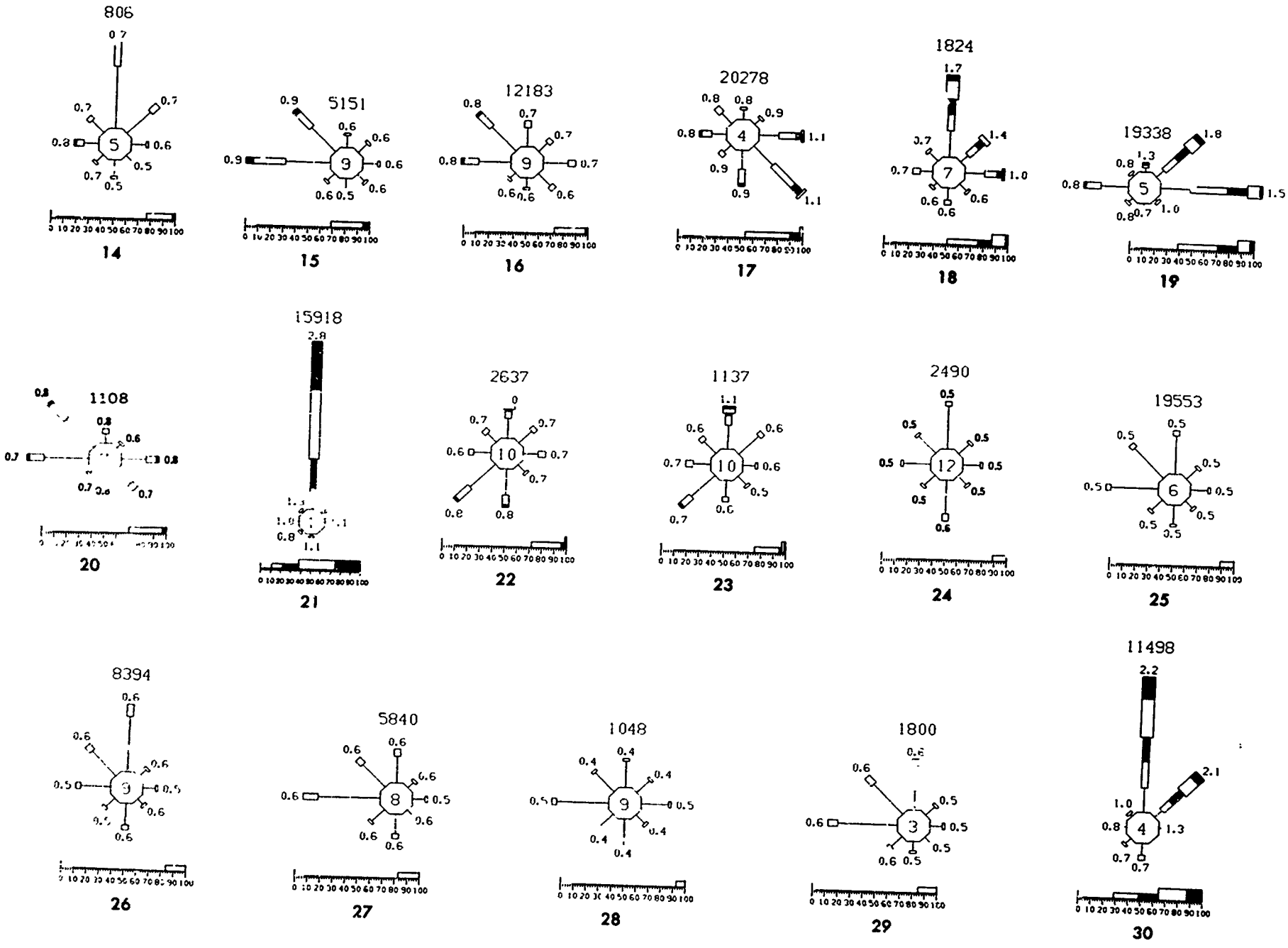

FIGURE 4-144 SURFACE CURRENTS–SPRING (APRIL-JUNE) (CONT.)

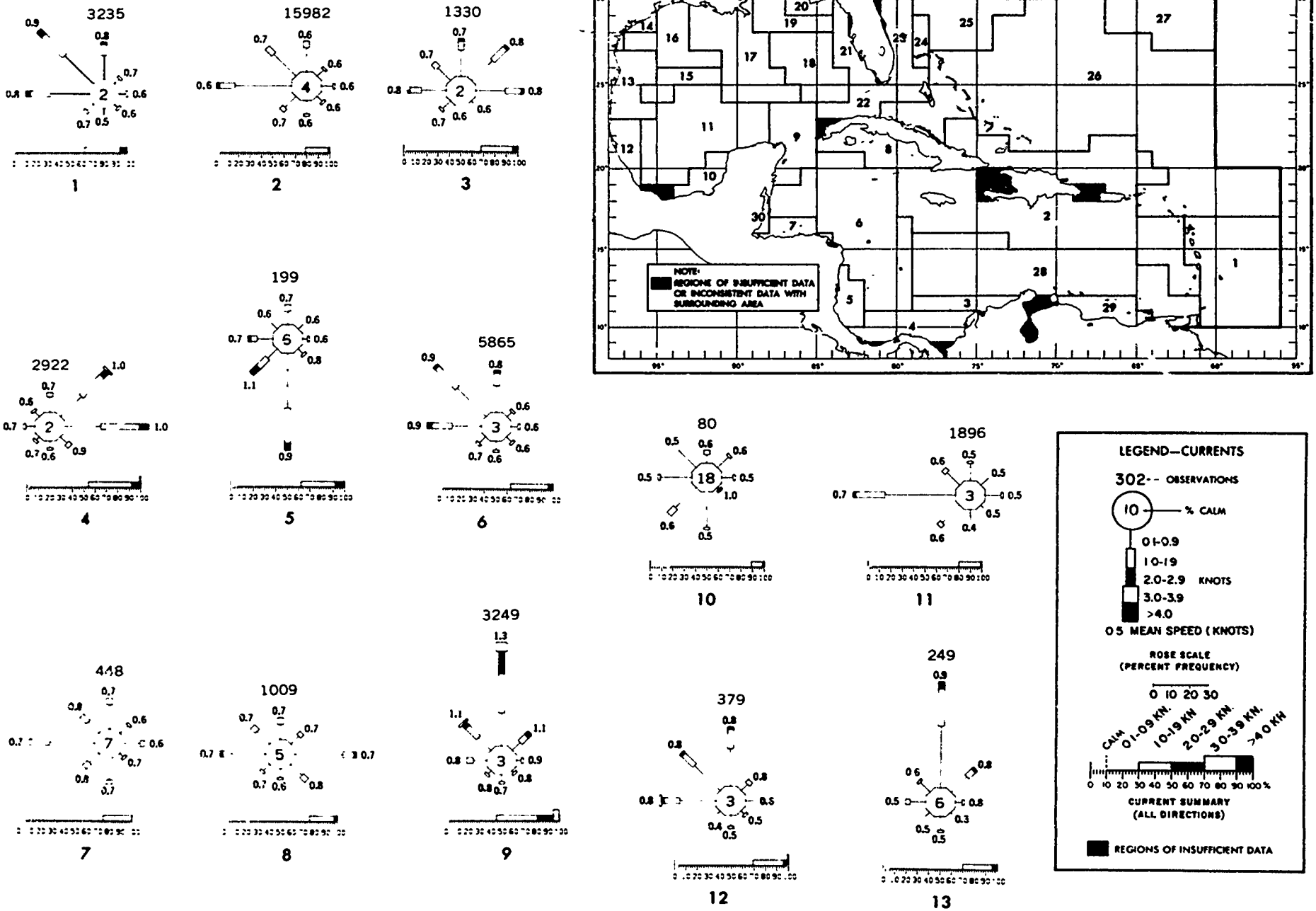

FIGURE 4-145 SURFACE CURRENTS–SUMMER (JULY-SEPTEMBER)

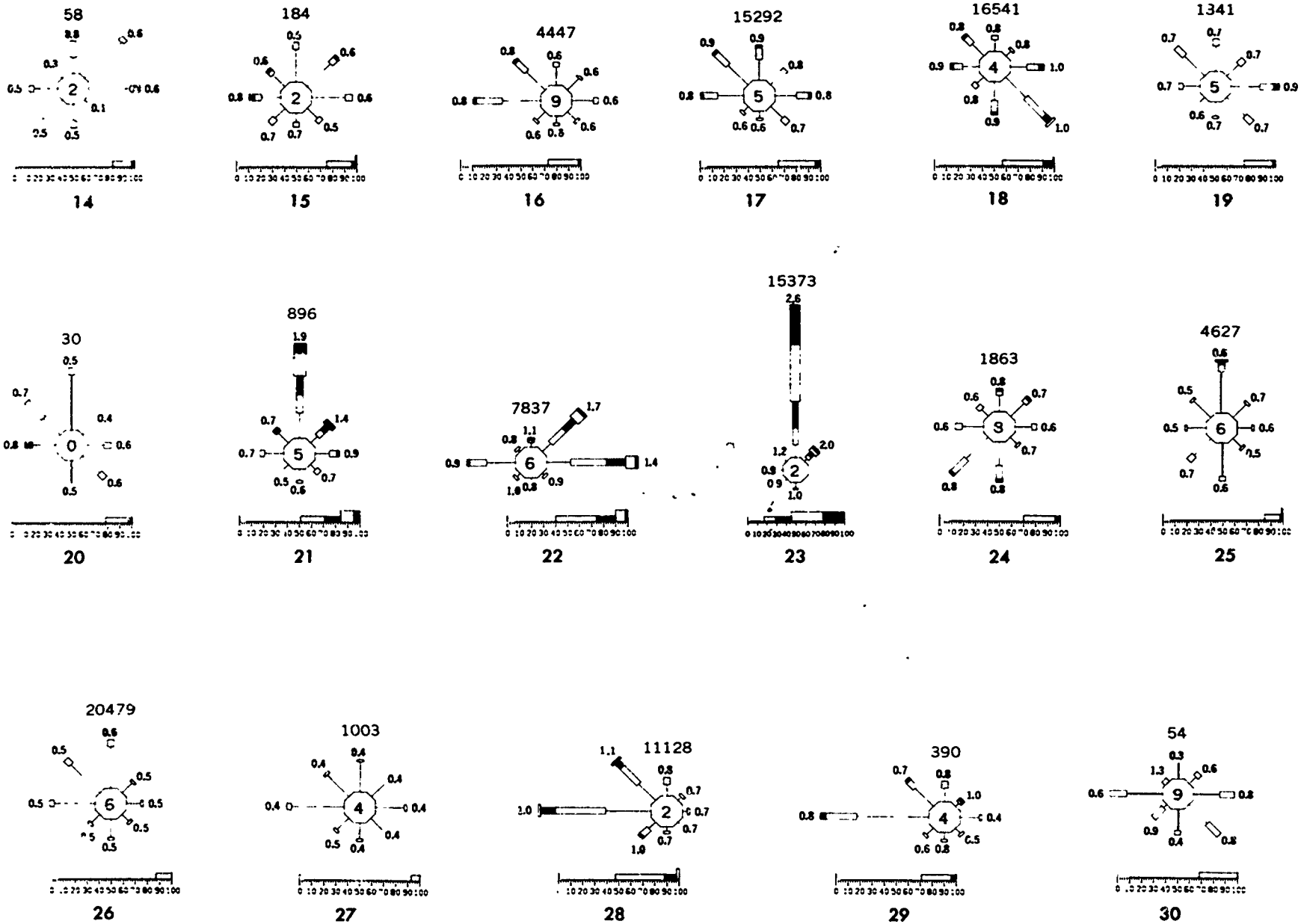

FIGURE 4-146 SURFACE CURRENTS–SUMMER (JULY-SEPTEMBER) (CONT.)

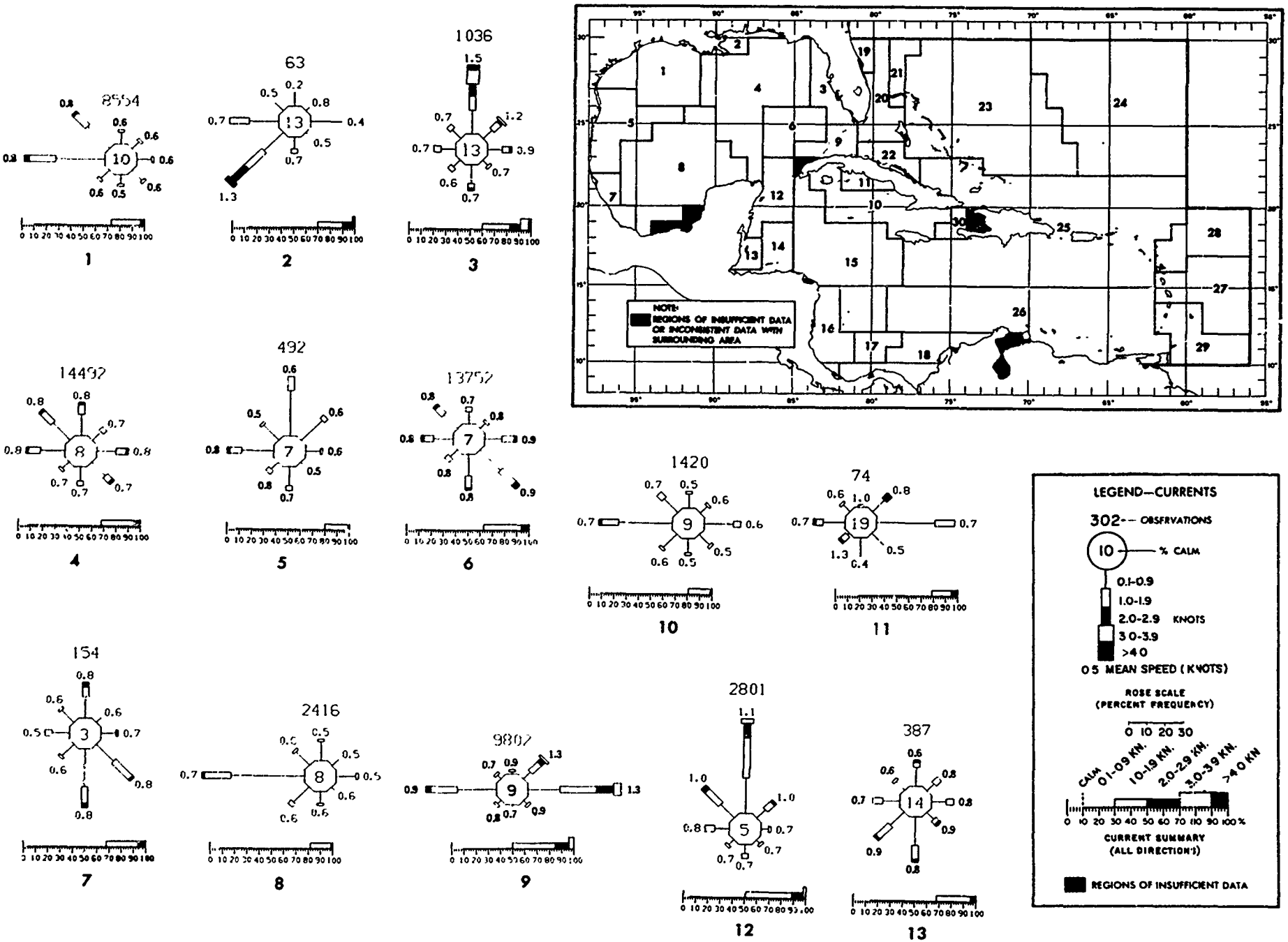

FIGURE 4-147 SURFACE CURRENTS–FALL (OCTOBER-DECEMBER)

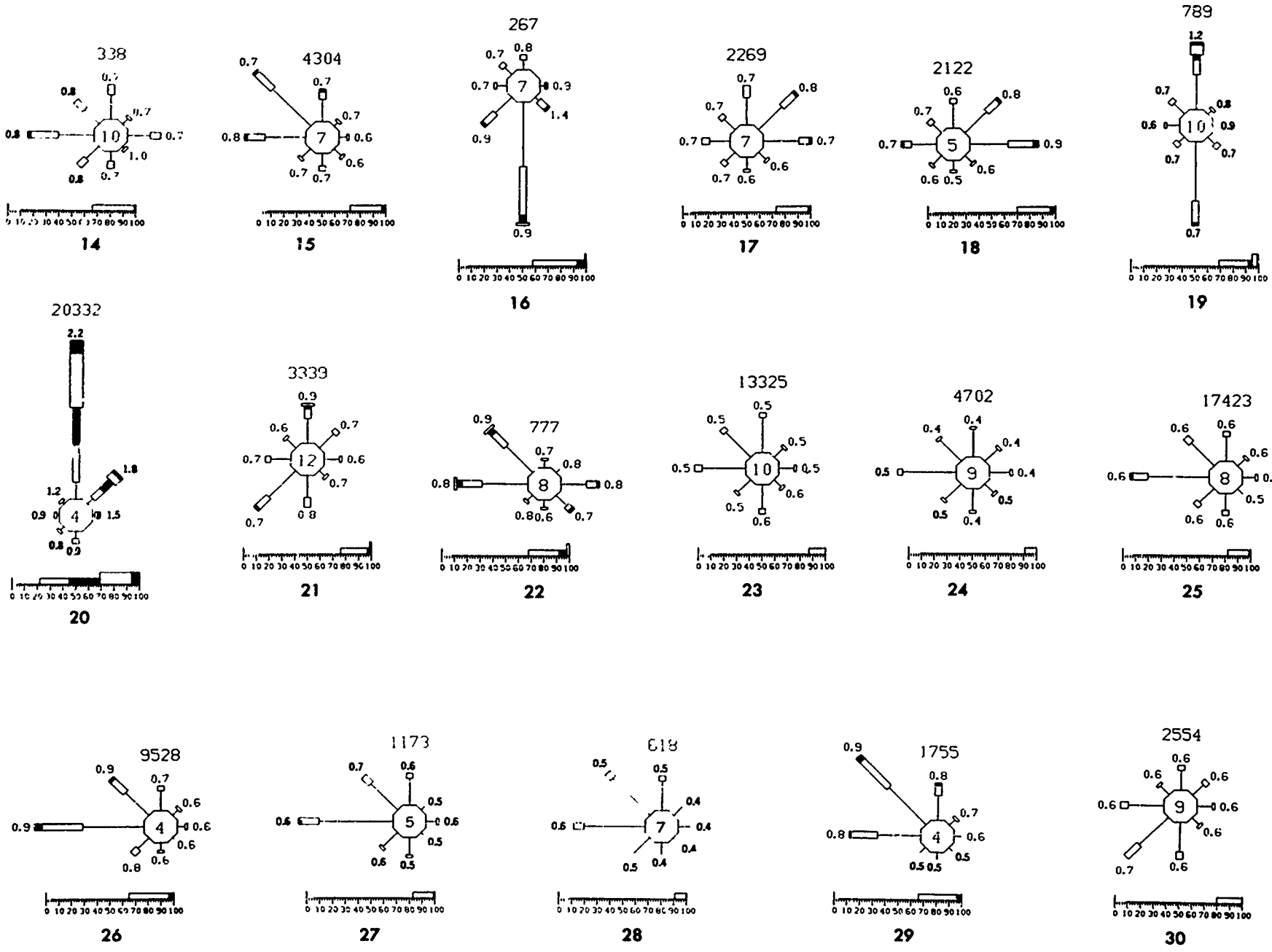

FIGURE 4-148 SURFACE CURRENTS–FALL (OCTOBER-DECEMBER) (CONT.)

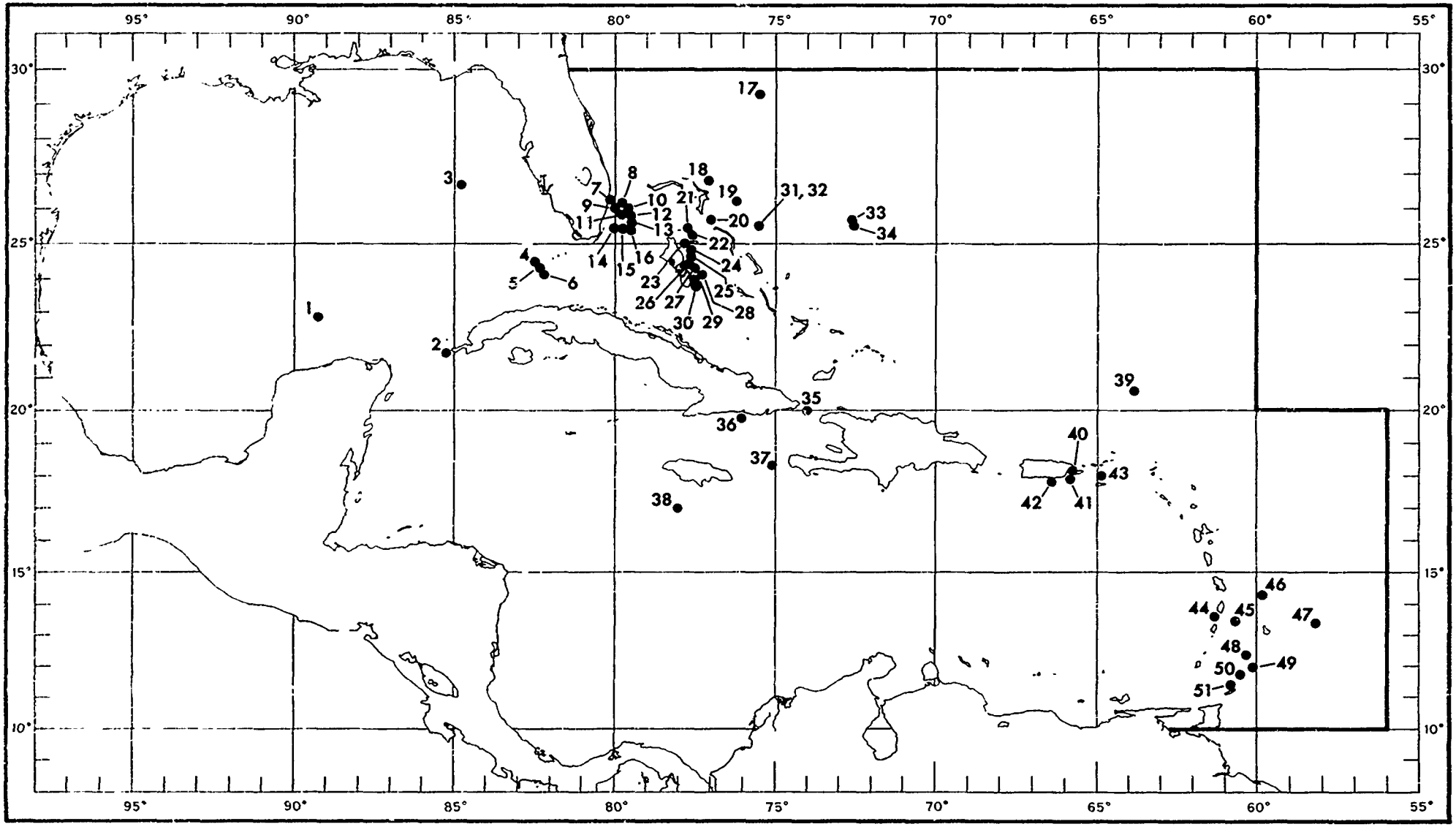

FIGURE 4-149 LOCATIONS OF SUBSURFACE CURRENT PROFILES

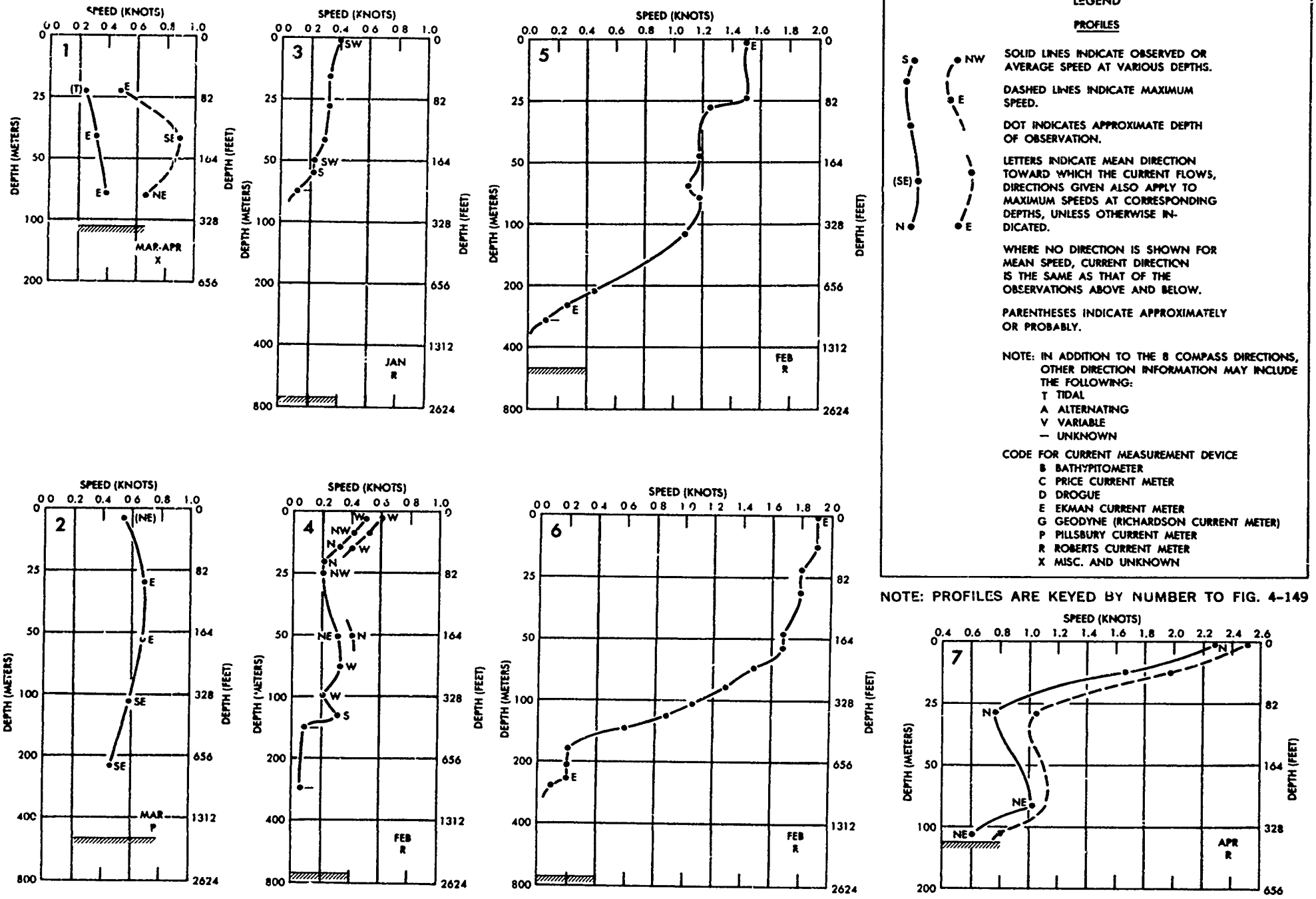

NOTE: PROFILES ARE KEYED BY NUMBER TO FIG. 4-149

FIGURE 4-150 SUBSURFACE CURRENT PROFILES (CONT.)

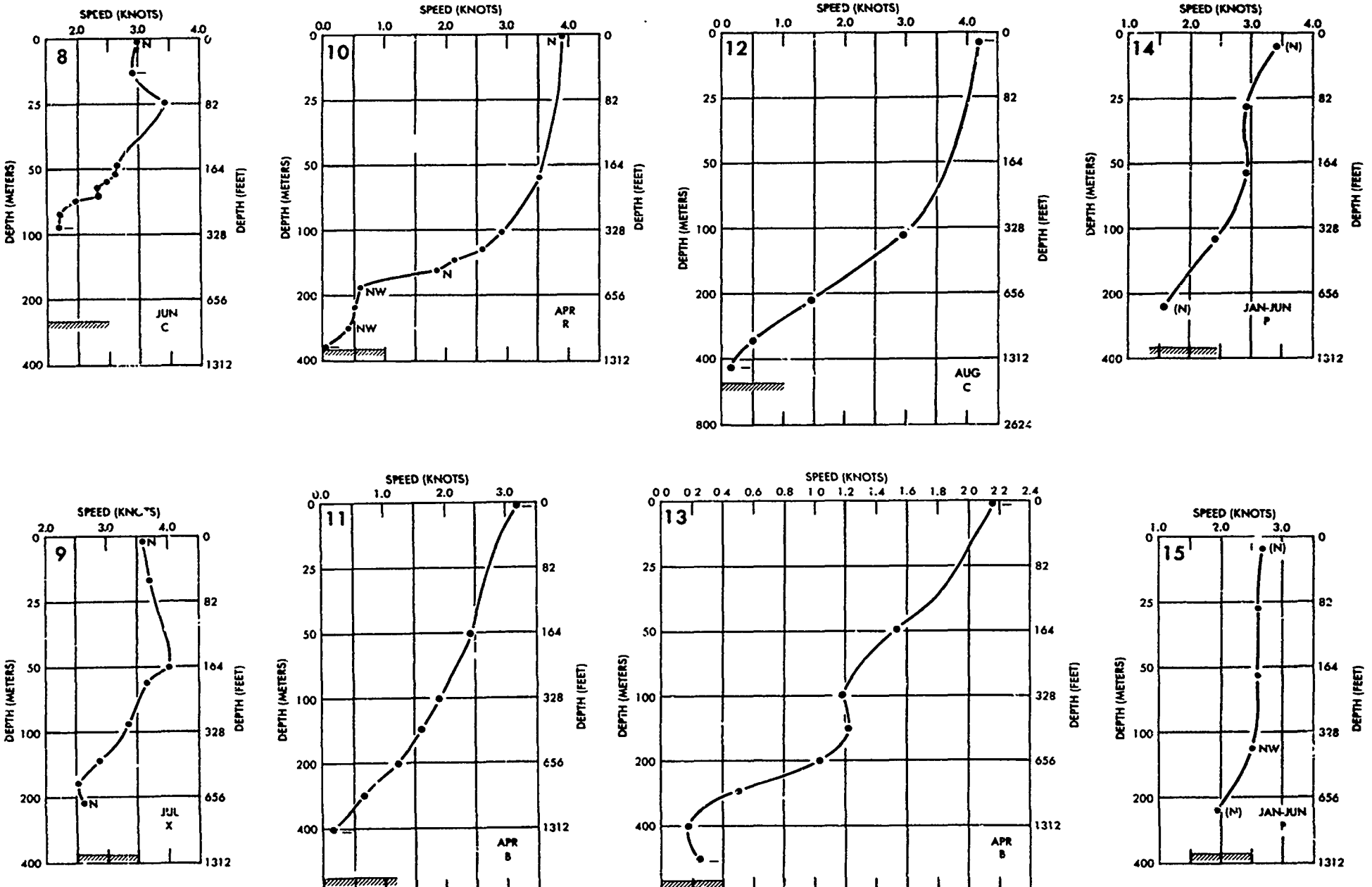

SEE LEGEND, FIG. 4-150

FIGURE 4-151 SUBSURFACE CURRENT PROFILES (CONT.)

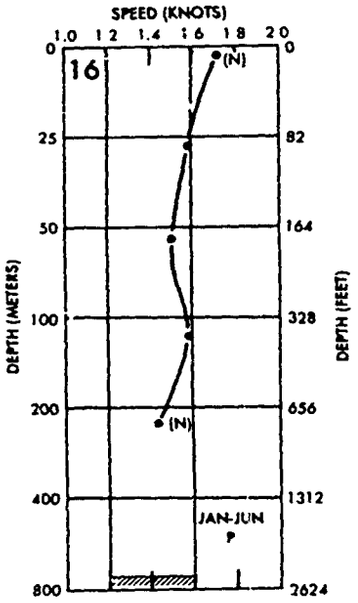

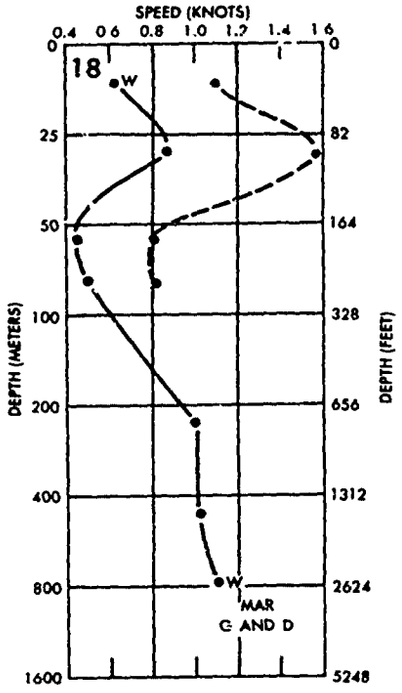

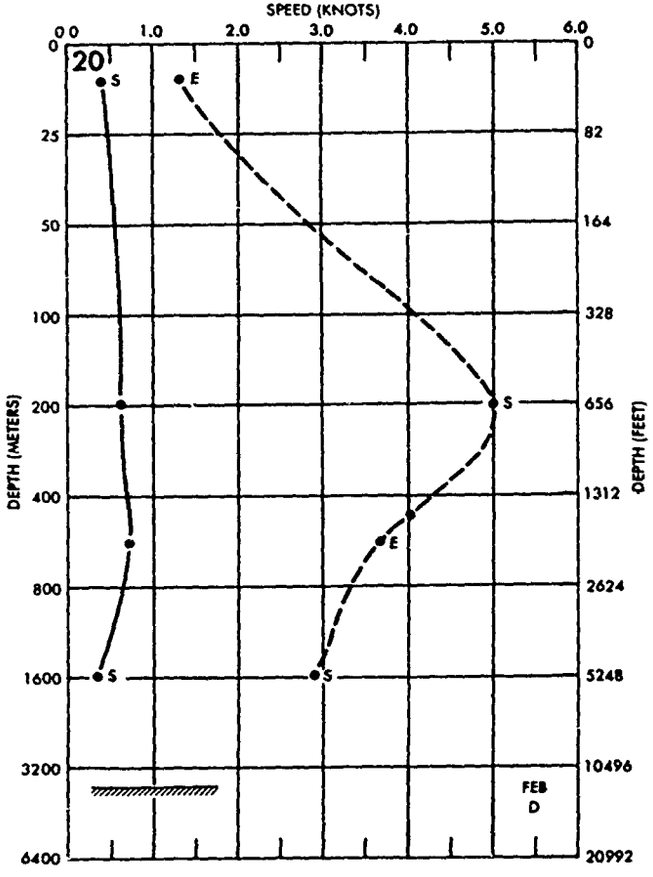

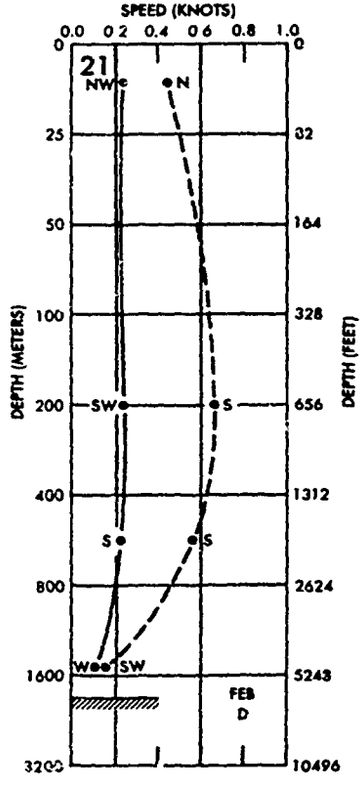

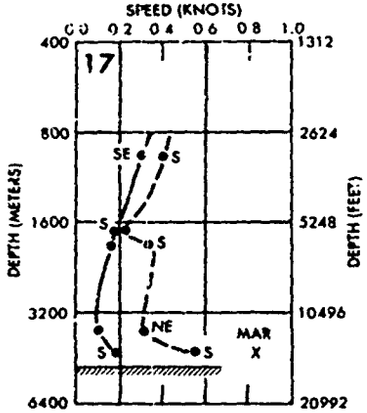

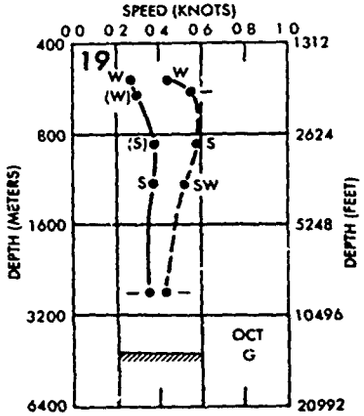

SEE LEGEND, FIG. 4-150

FIGURE 4-152 SUBSURFACE CURRENT PROFILES (CONT.)

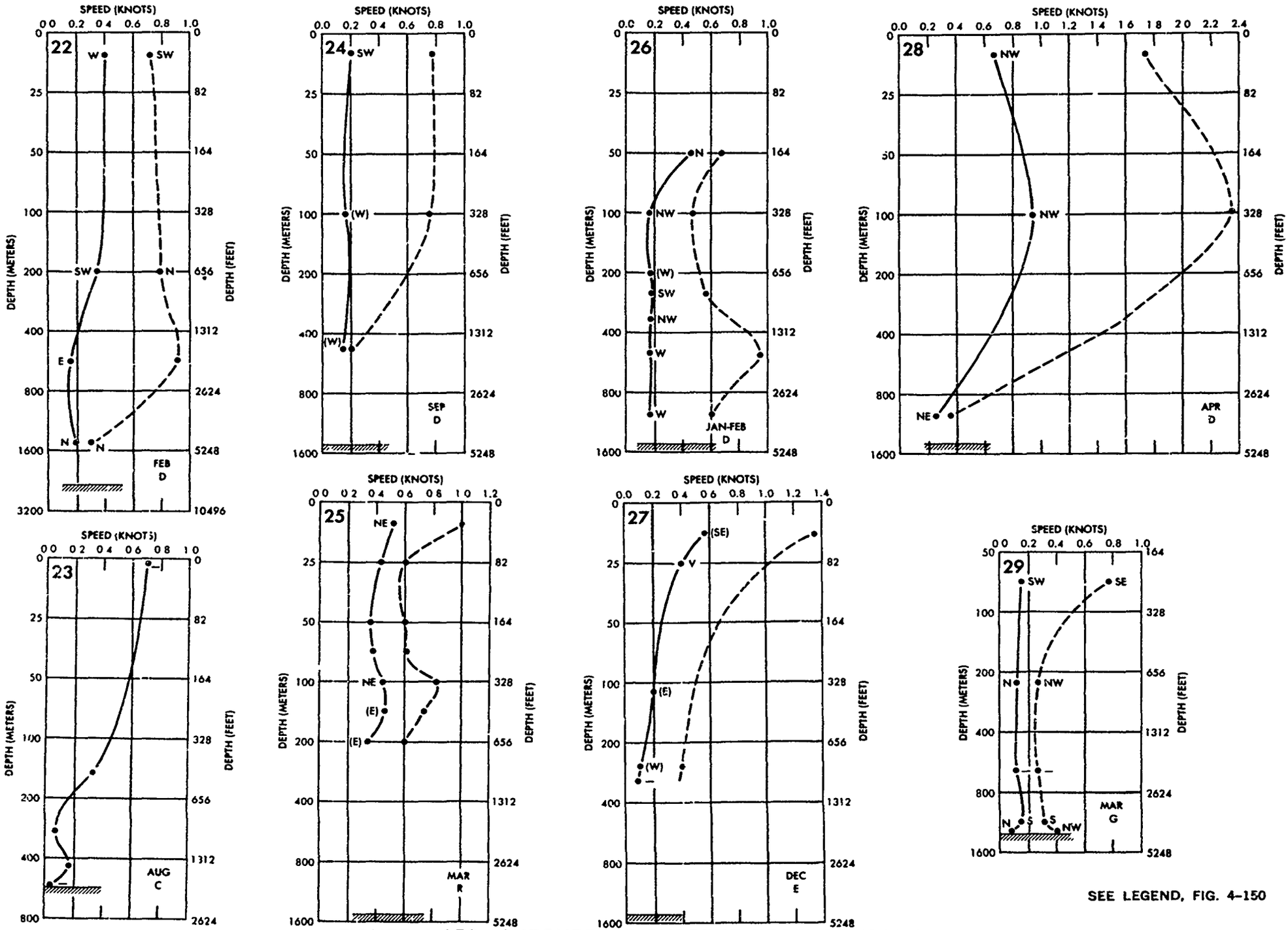

SEE LEGEND, FIG. 4-150

FIGURE 4-153 SUBSURFACE CURRENT PROFILES (CONT.)

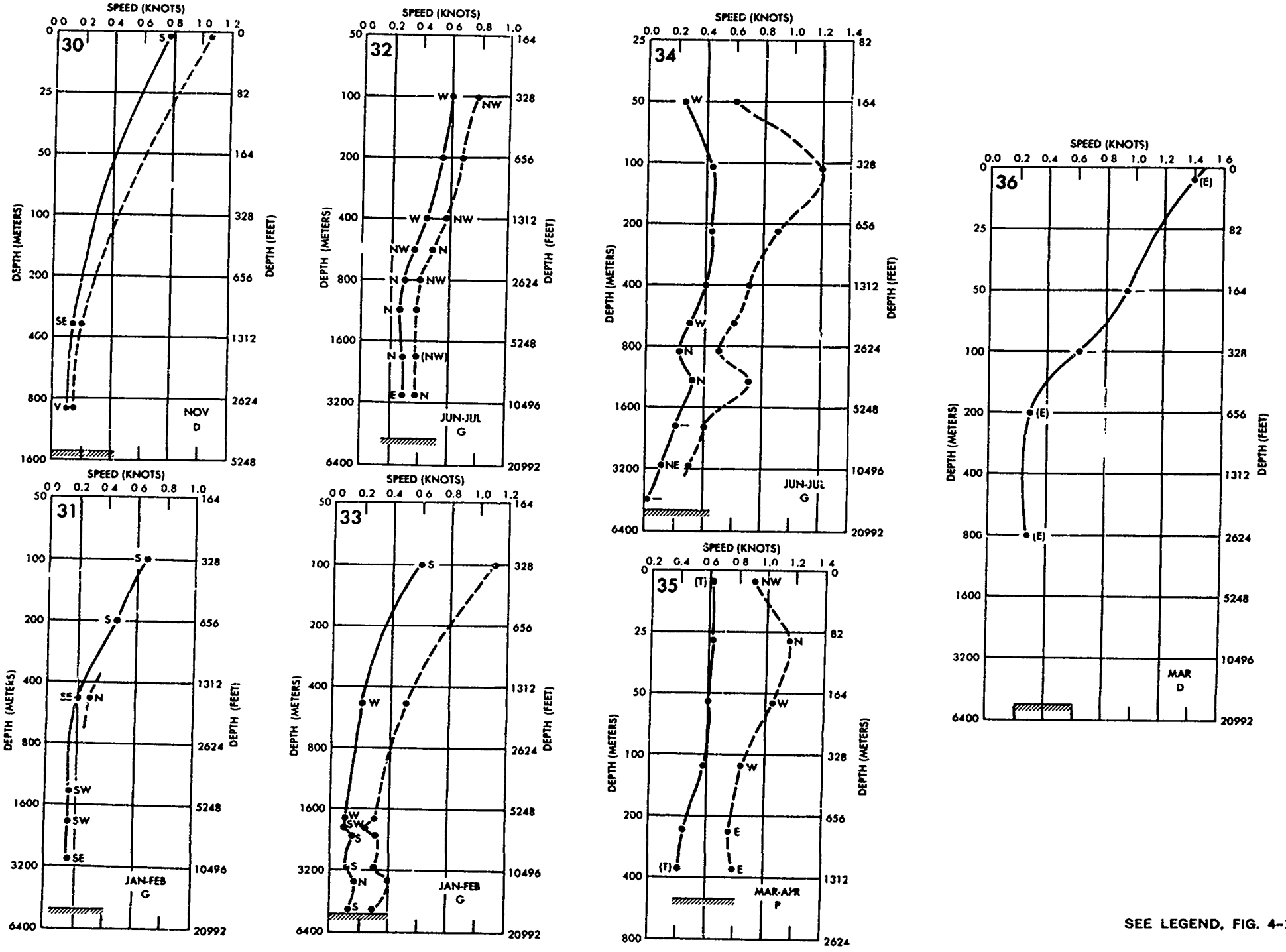

SEE LEGEND, FIG. 4-150

FIGURE 4-154 SUBSURFACE CURRENT PROFILES (CONT.)

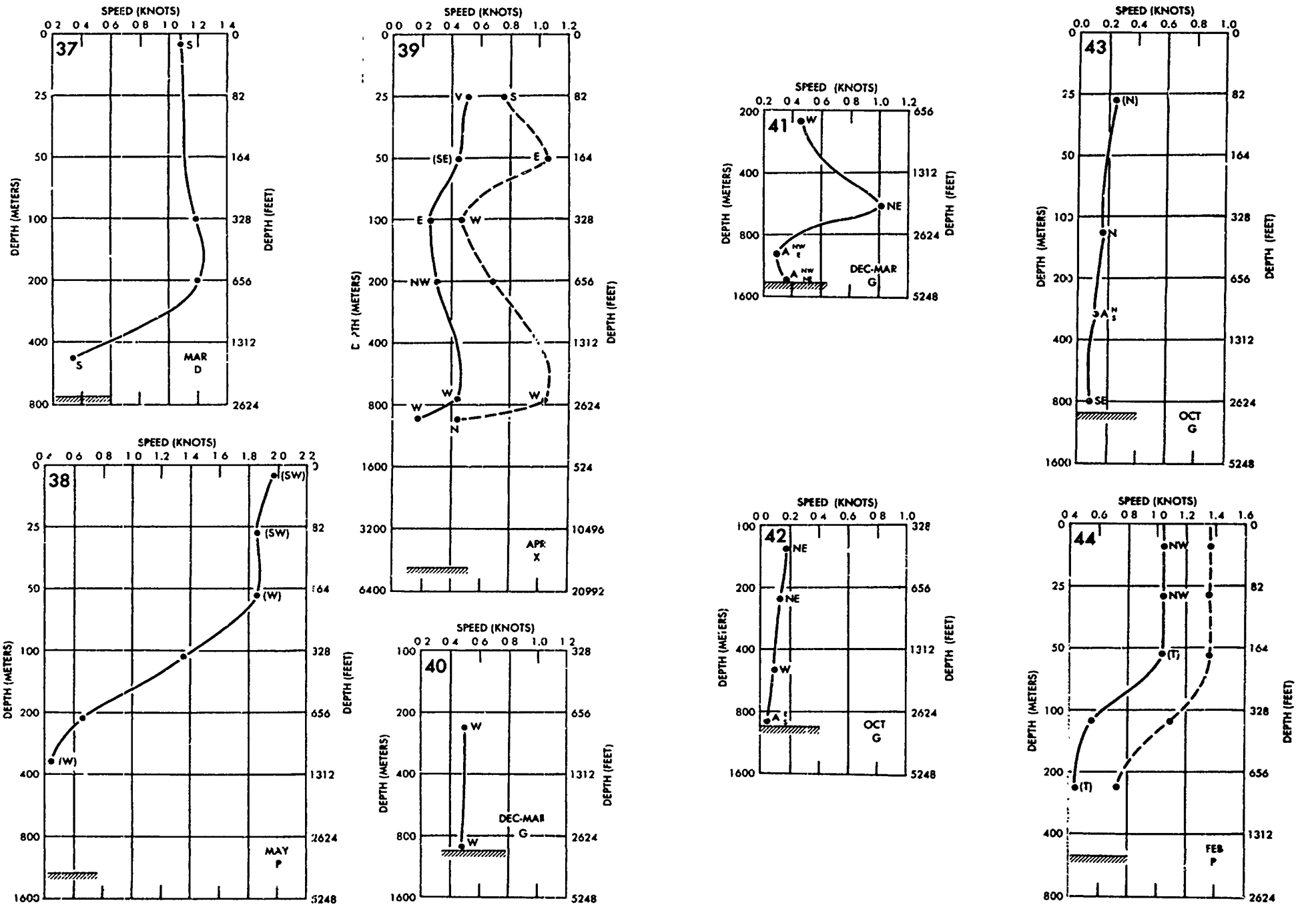

SEE LEGEND, FIG. 4-150

FIGURE 4-155 SUBSURFACE CURRENT PROFILES (CONT.)

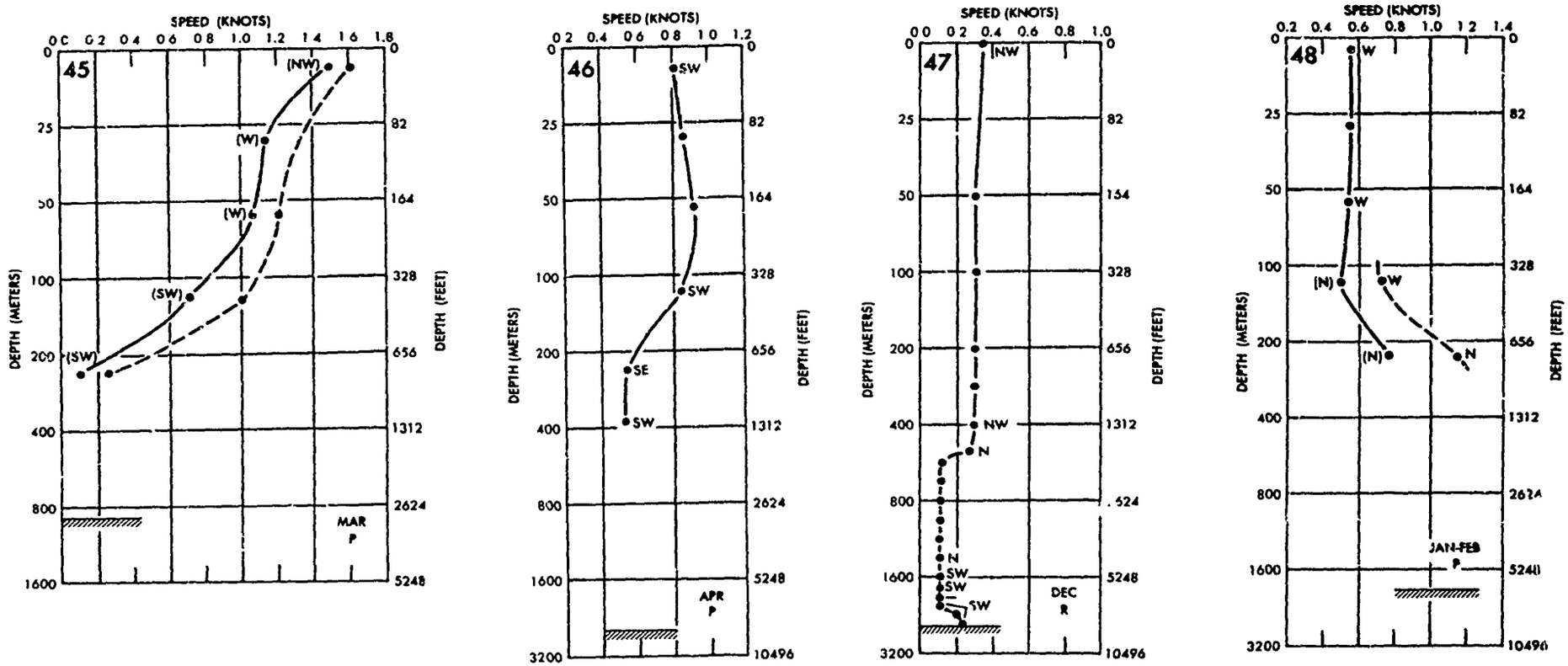

SEE LEGEND, FIG. 4-150

FIGURE 4-156 SUBSURFACE CURRENT PROFILES (CONT.)

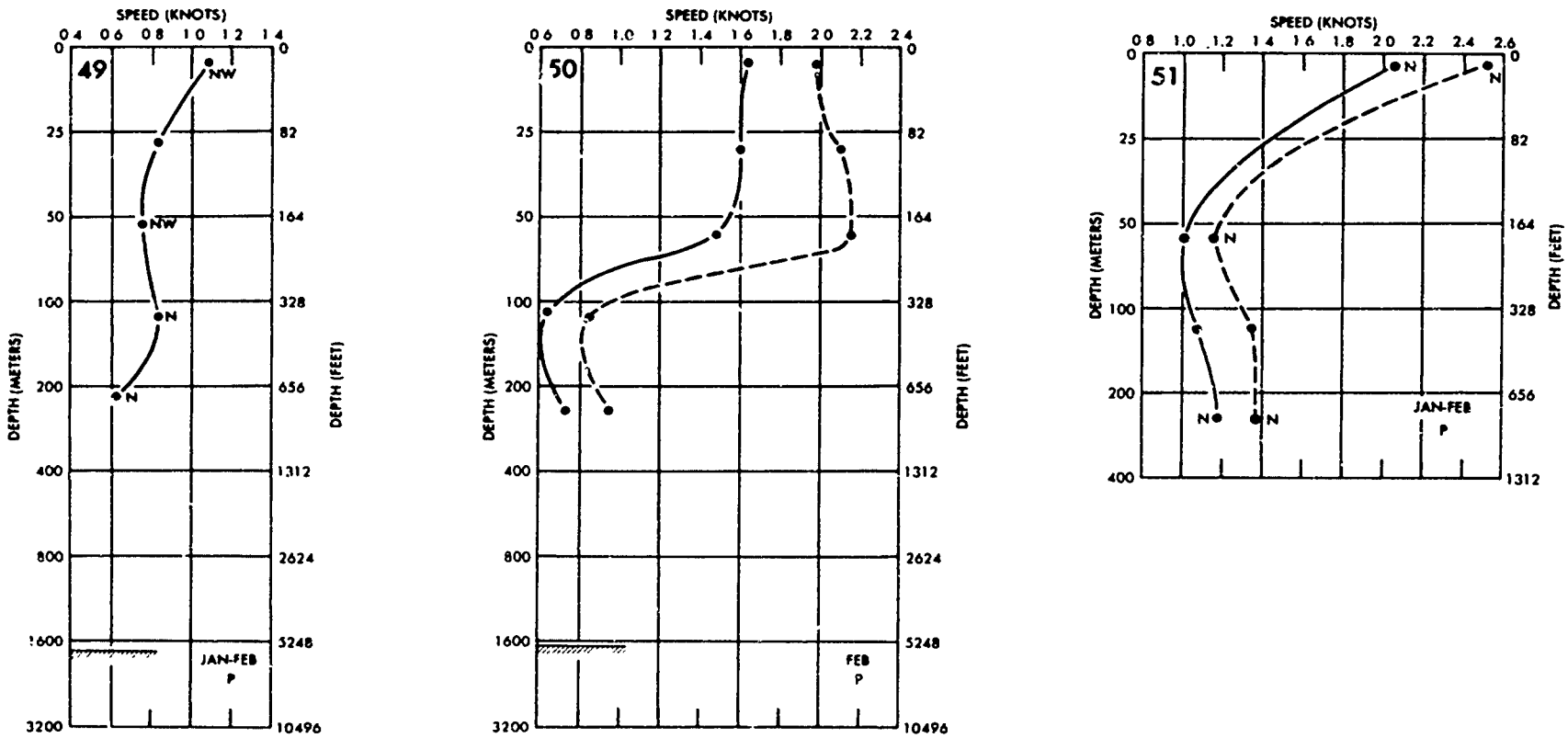

FIGURE 4-157 SUBSURFACE CURRENT PROFILES (CONT.)

SEE LEGEND, FIG. 4-150

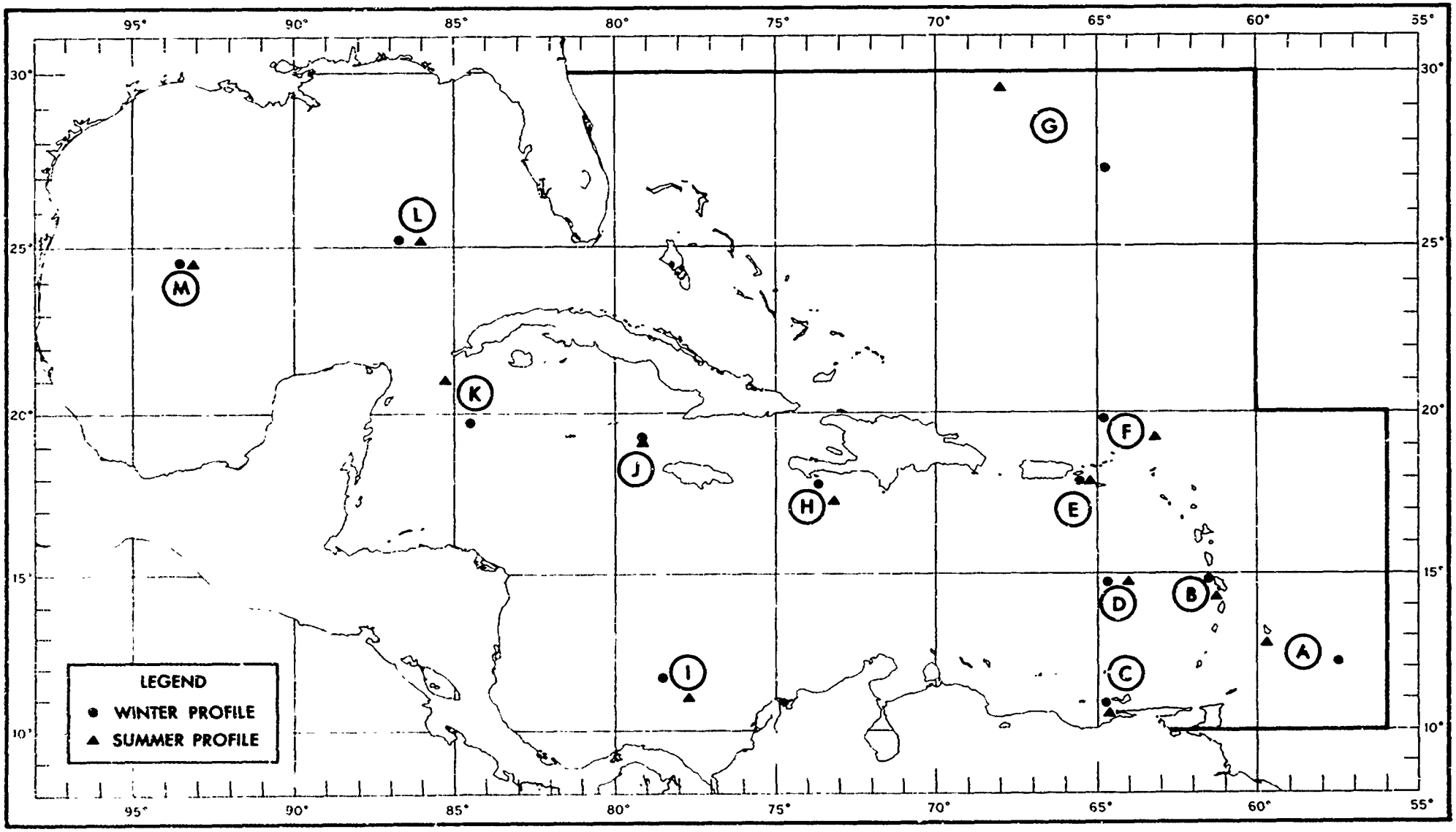

FIGURE 4-158 LOCATIONS OF REPRESENTATIVE OXYGEN PROFILES

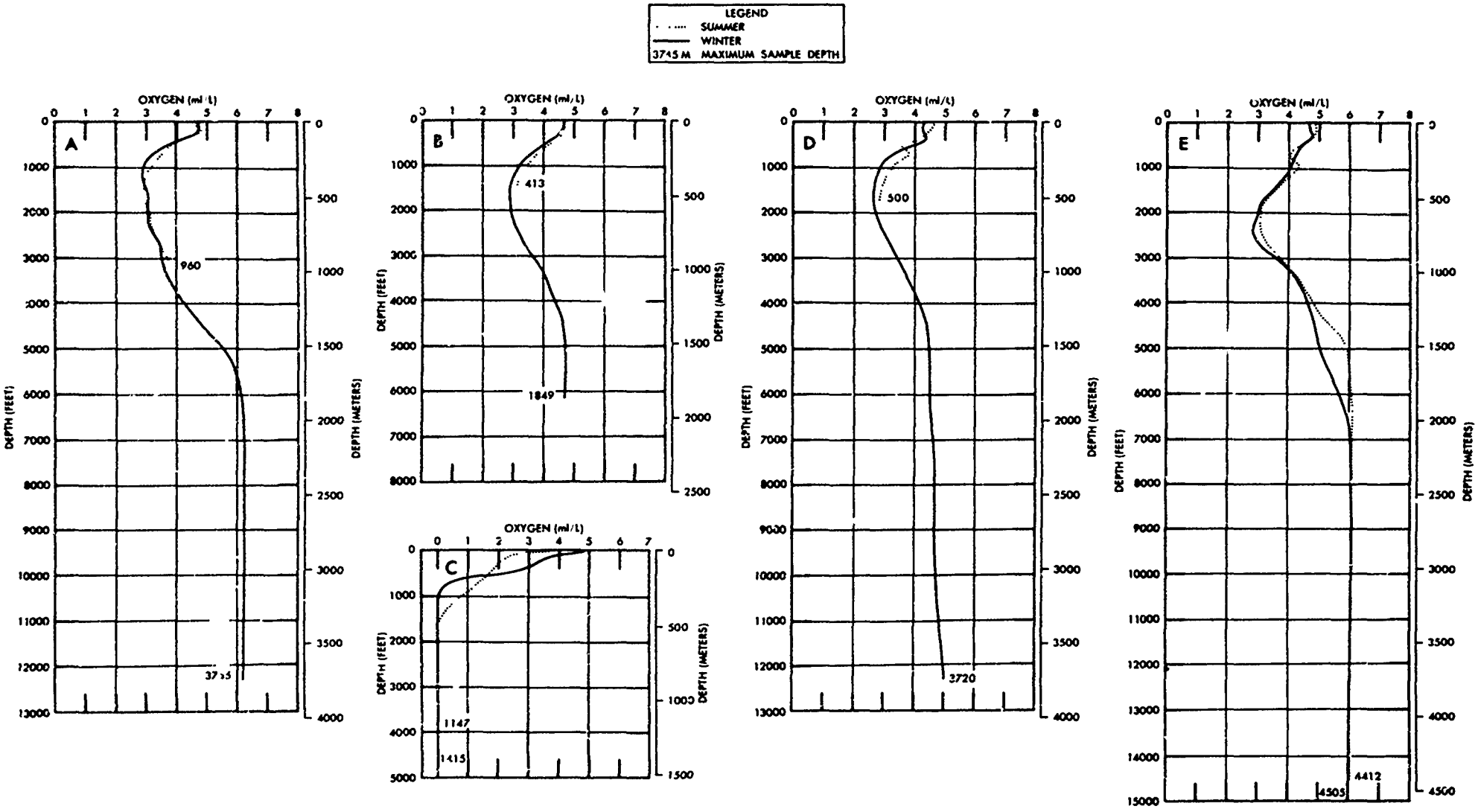

FIGURE 4-159 OXYGEN PROFILES

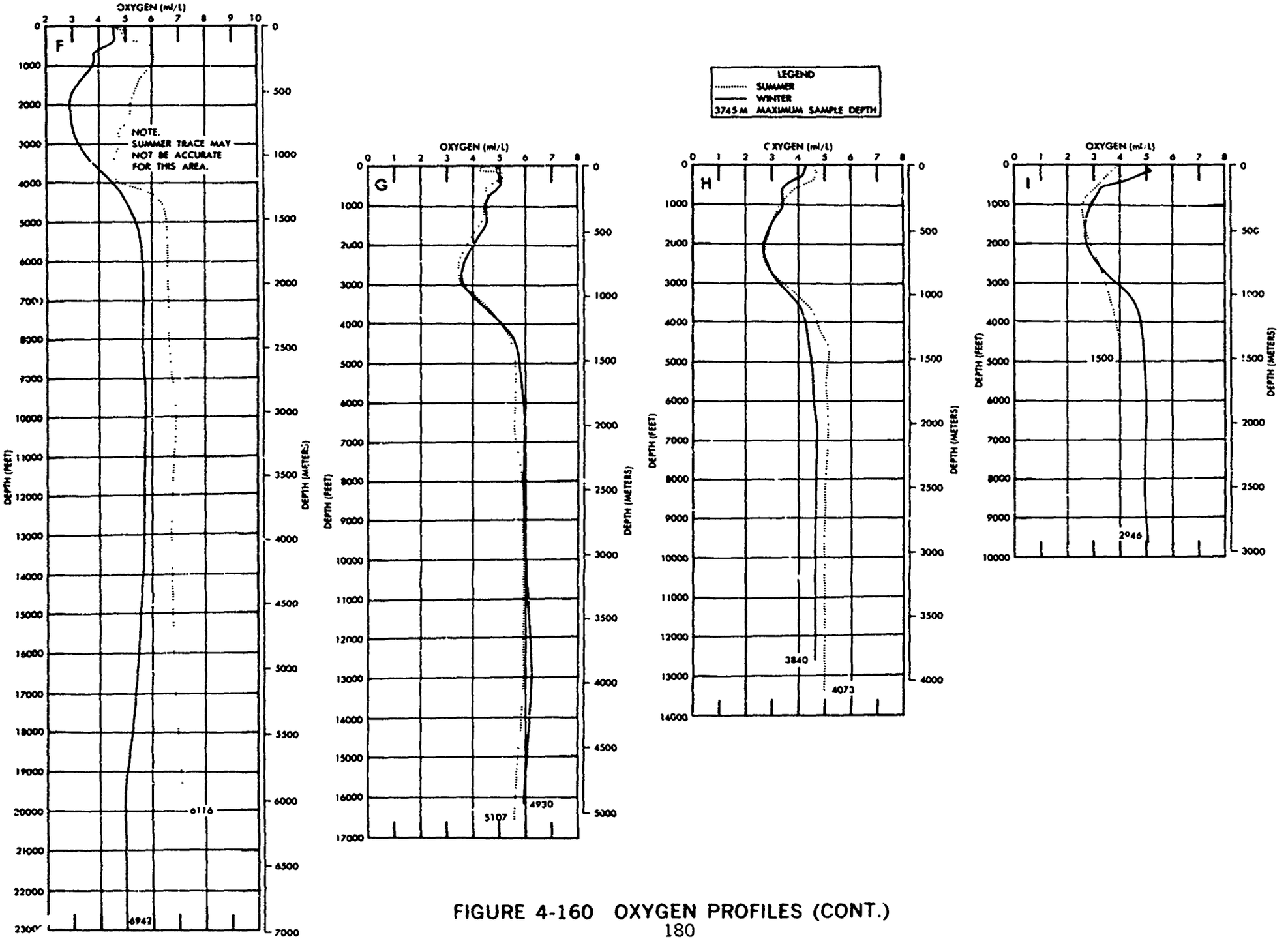

FIGURE 4-160 OXYGEN PROFILES (CONT.)

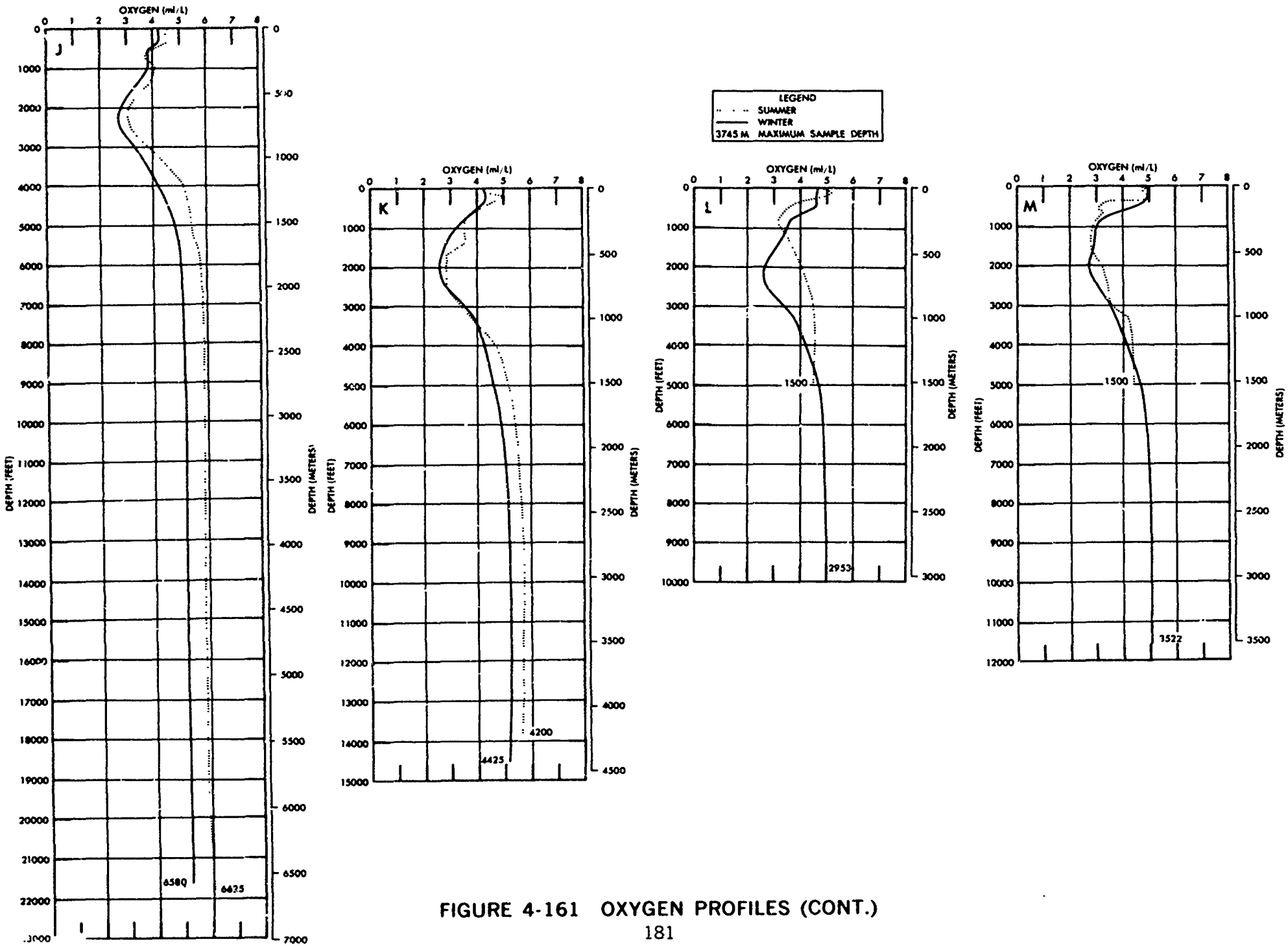

FIGURE 4-161 OXYGEN PROFILES (CONT.)

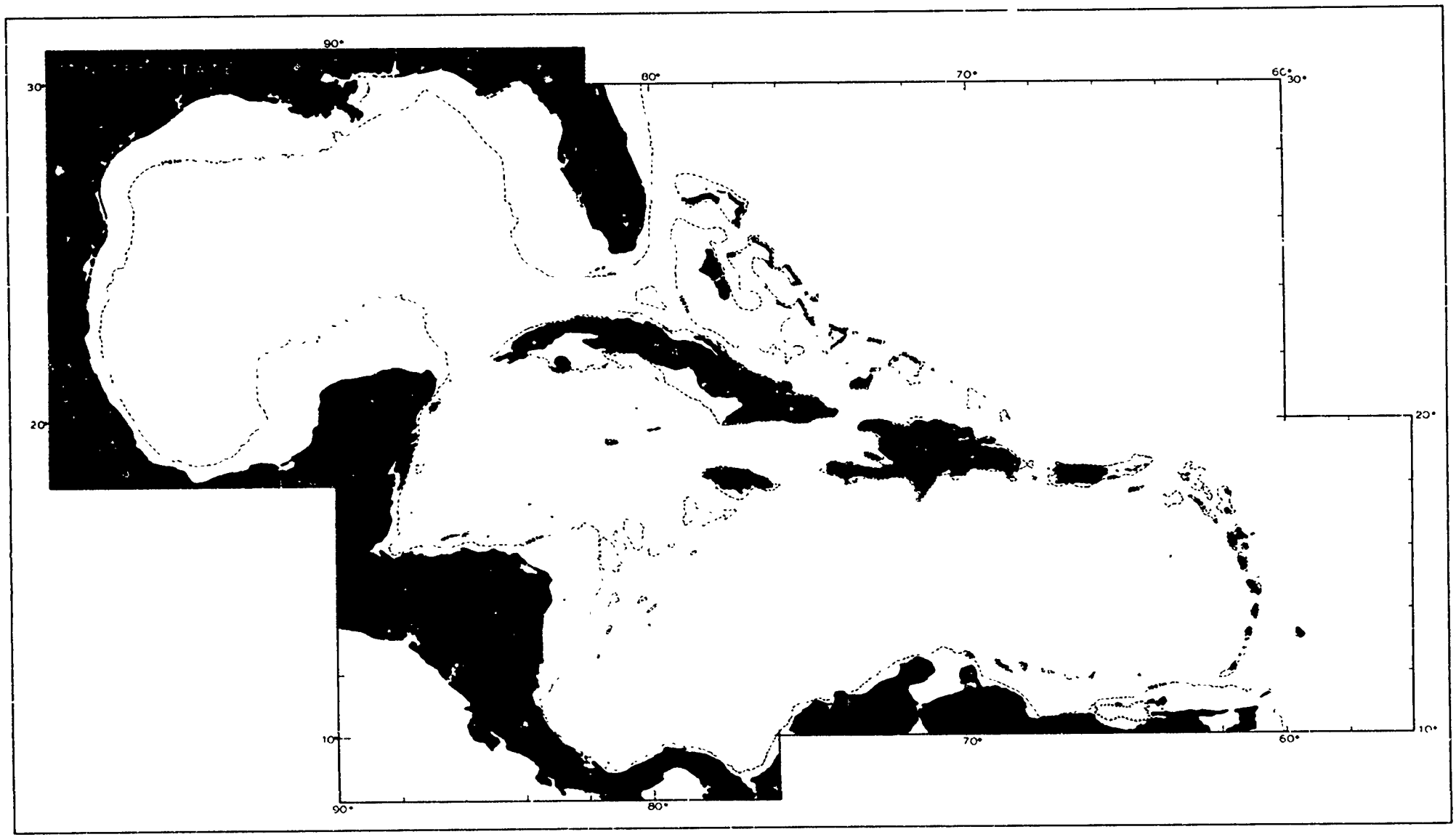
90°
80°
70°
60°
30°
20°
10°

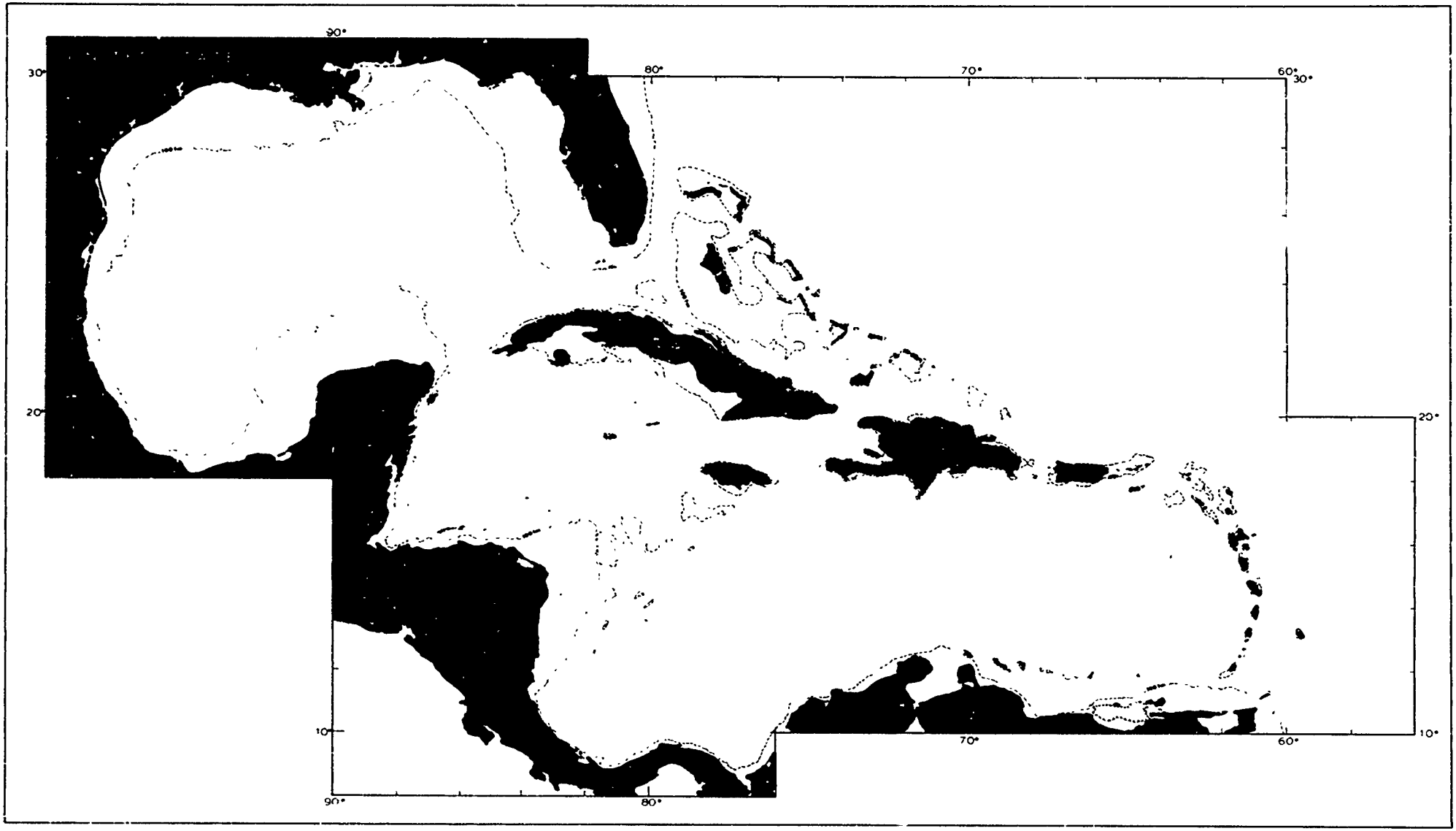
90°
80°
70°
60°
30°
20°
10°

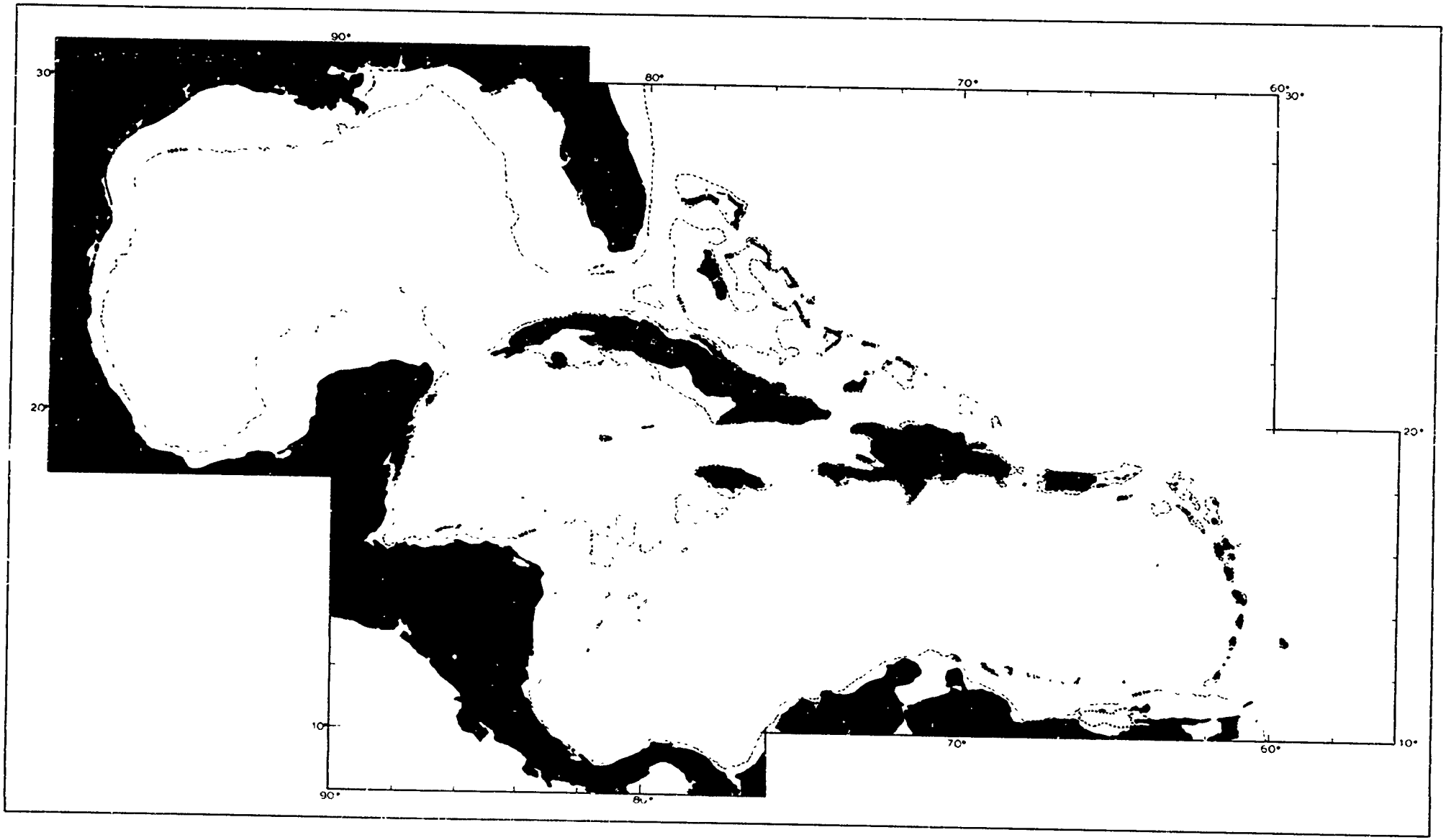
90°
80°
70°
60°
30°
20°
10°

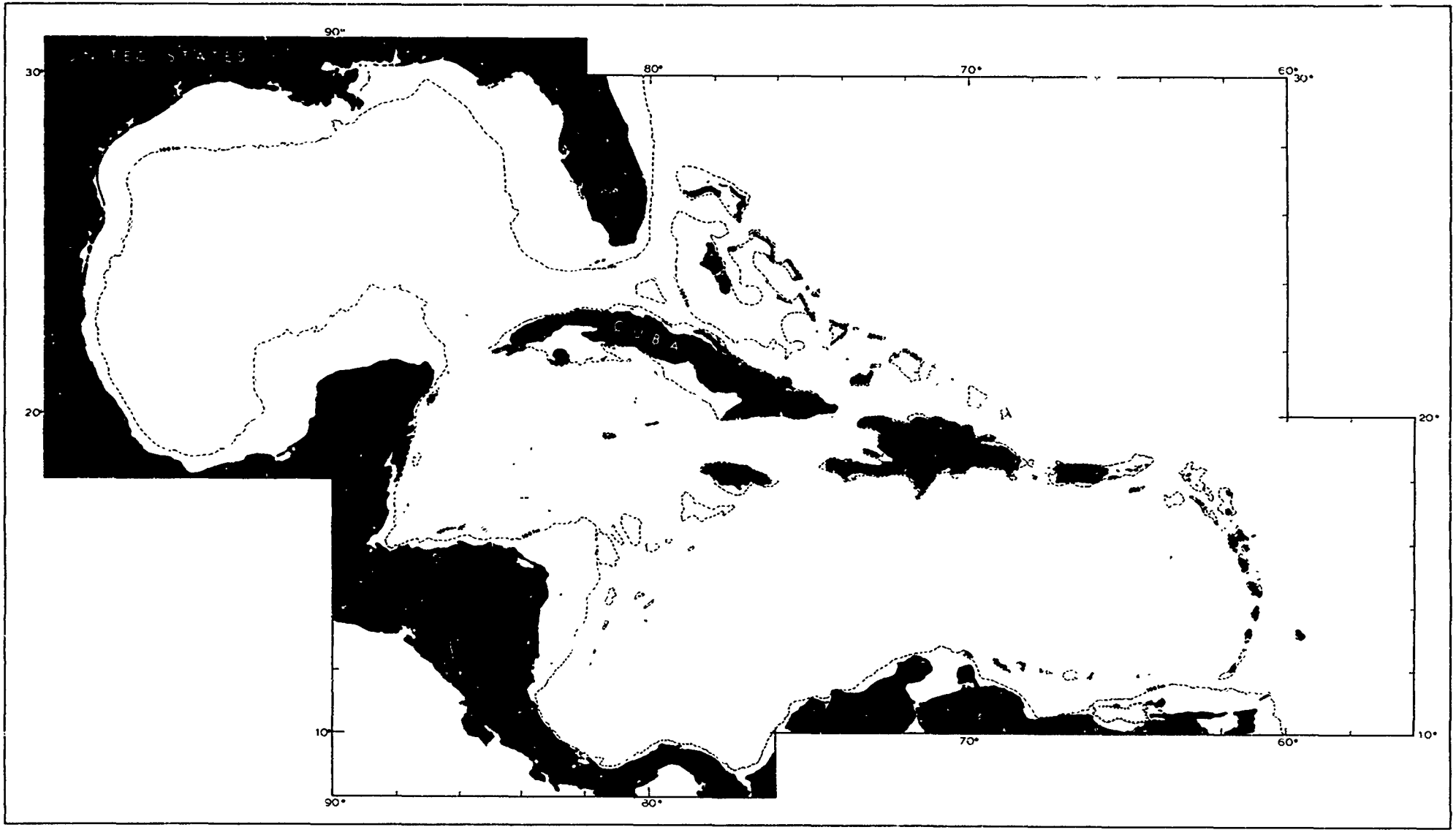
90°
80°
70°
60°
30°
20°
10°
CUBA

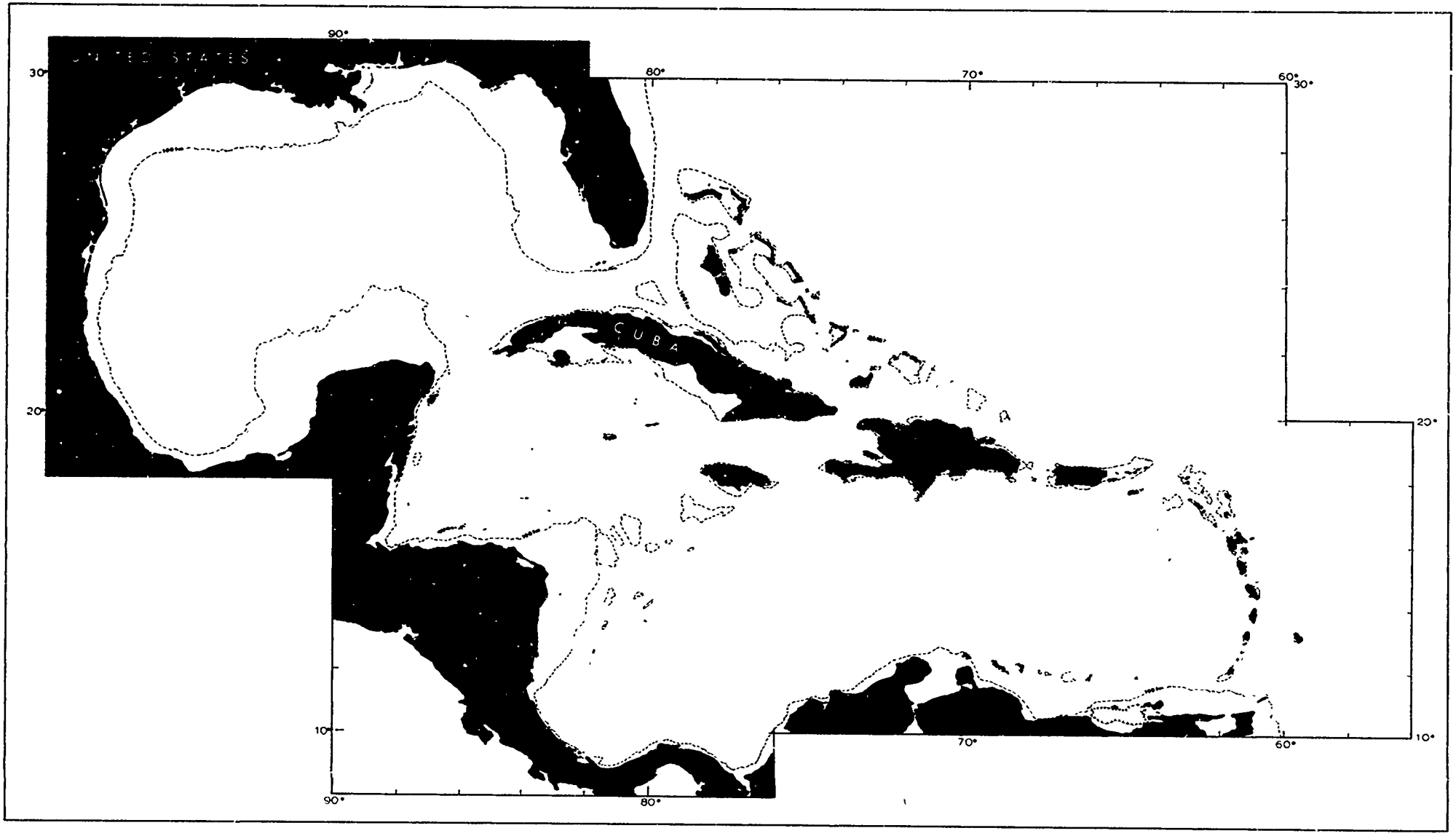
90°
30°
80°
70°
60°
30°
20°
CUBA
20°
10°
70°
60°
10°
90°
80°

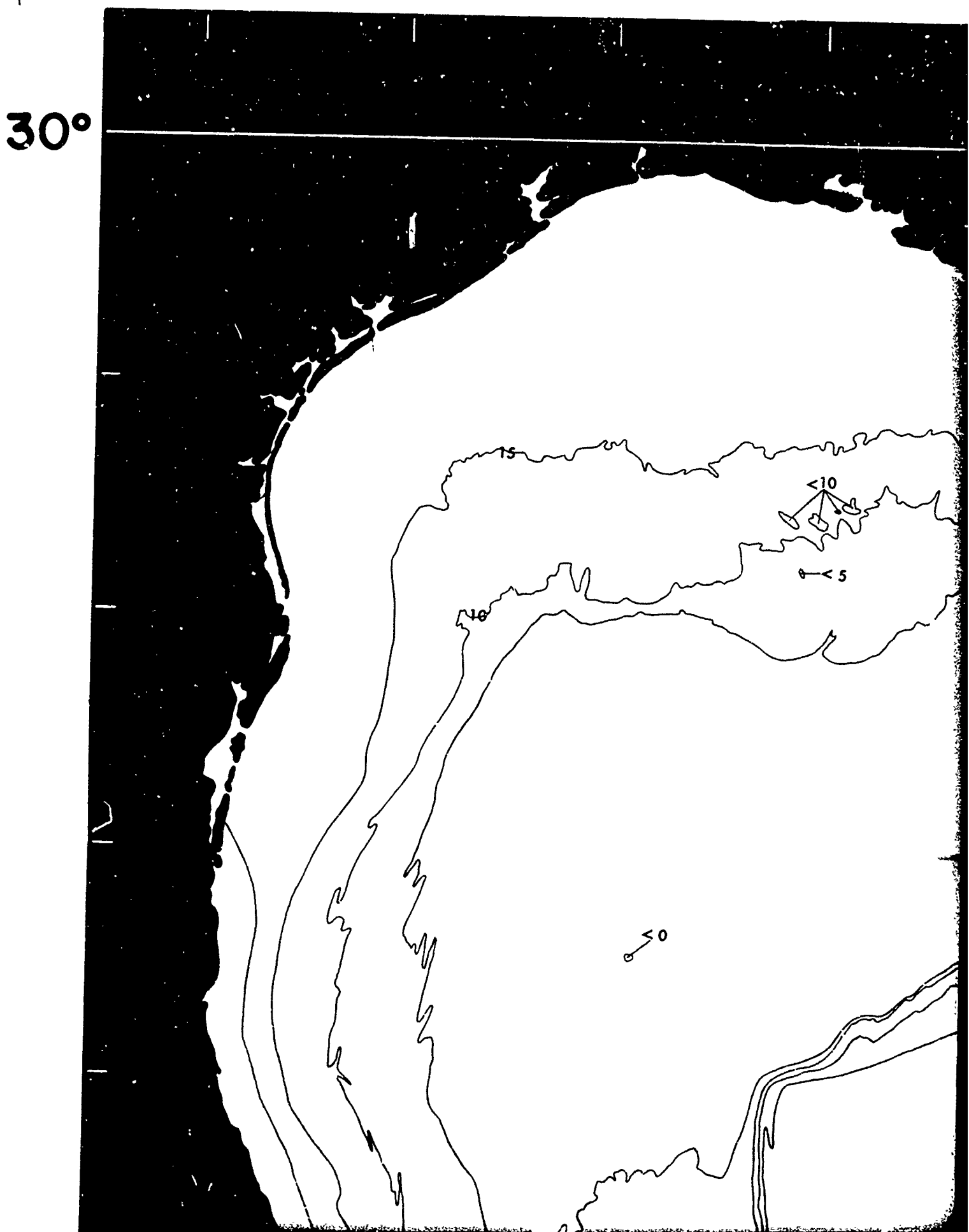
30°
15
<10
<5
10
<0

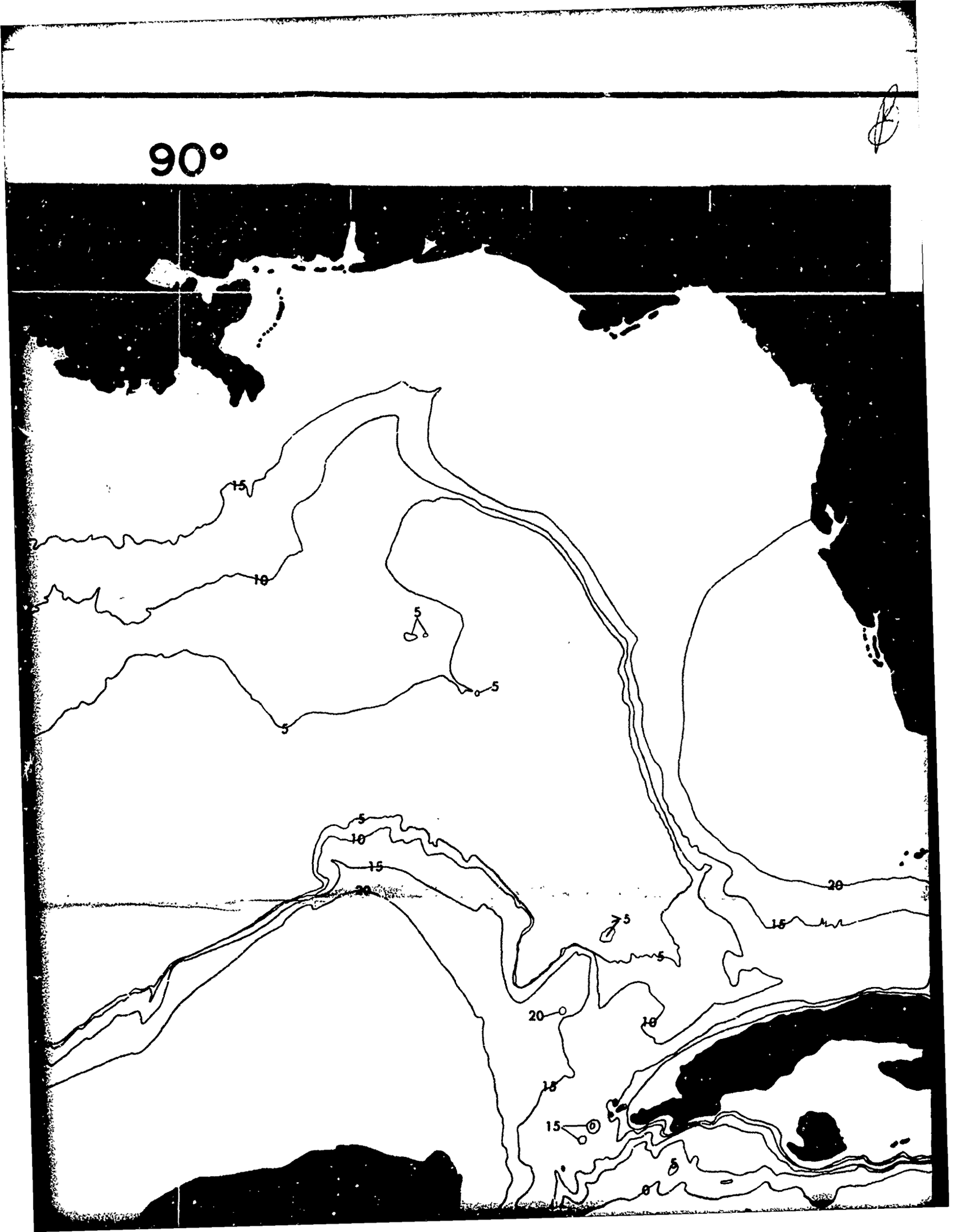
90°
15
10
5
5
5
5
10
15
20
5
15
20
5
20
10
10
15
5

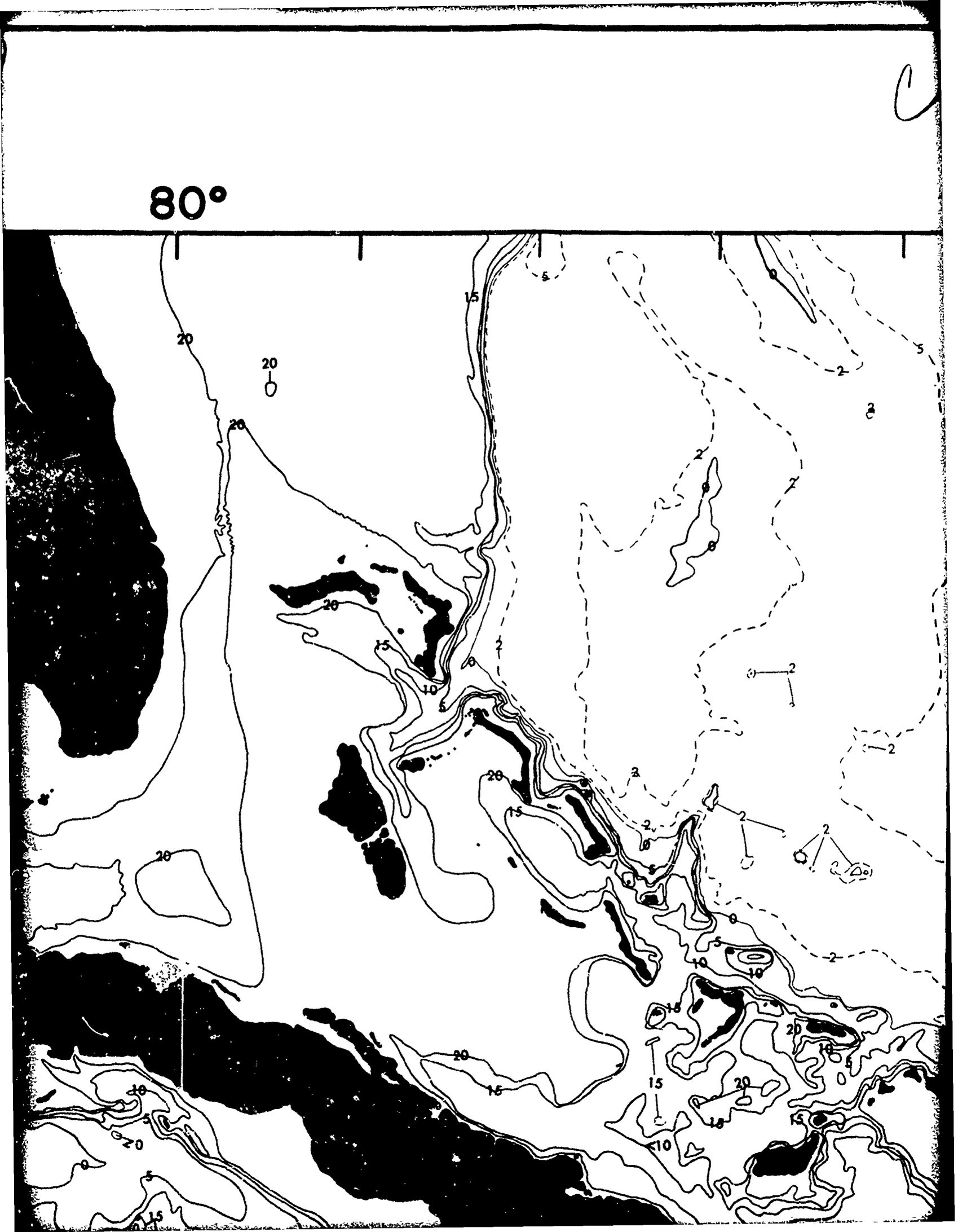
80°

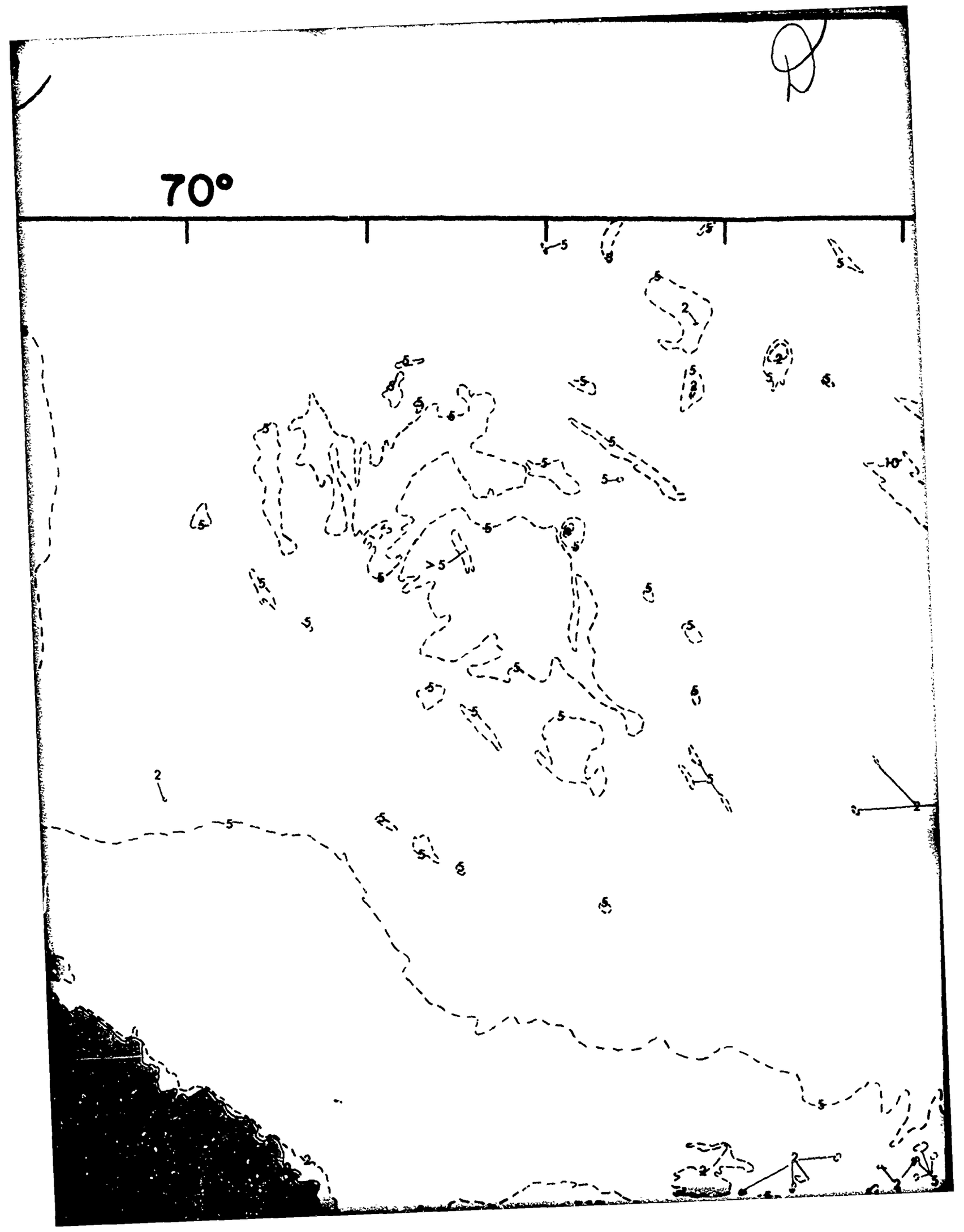
70°

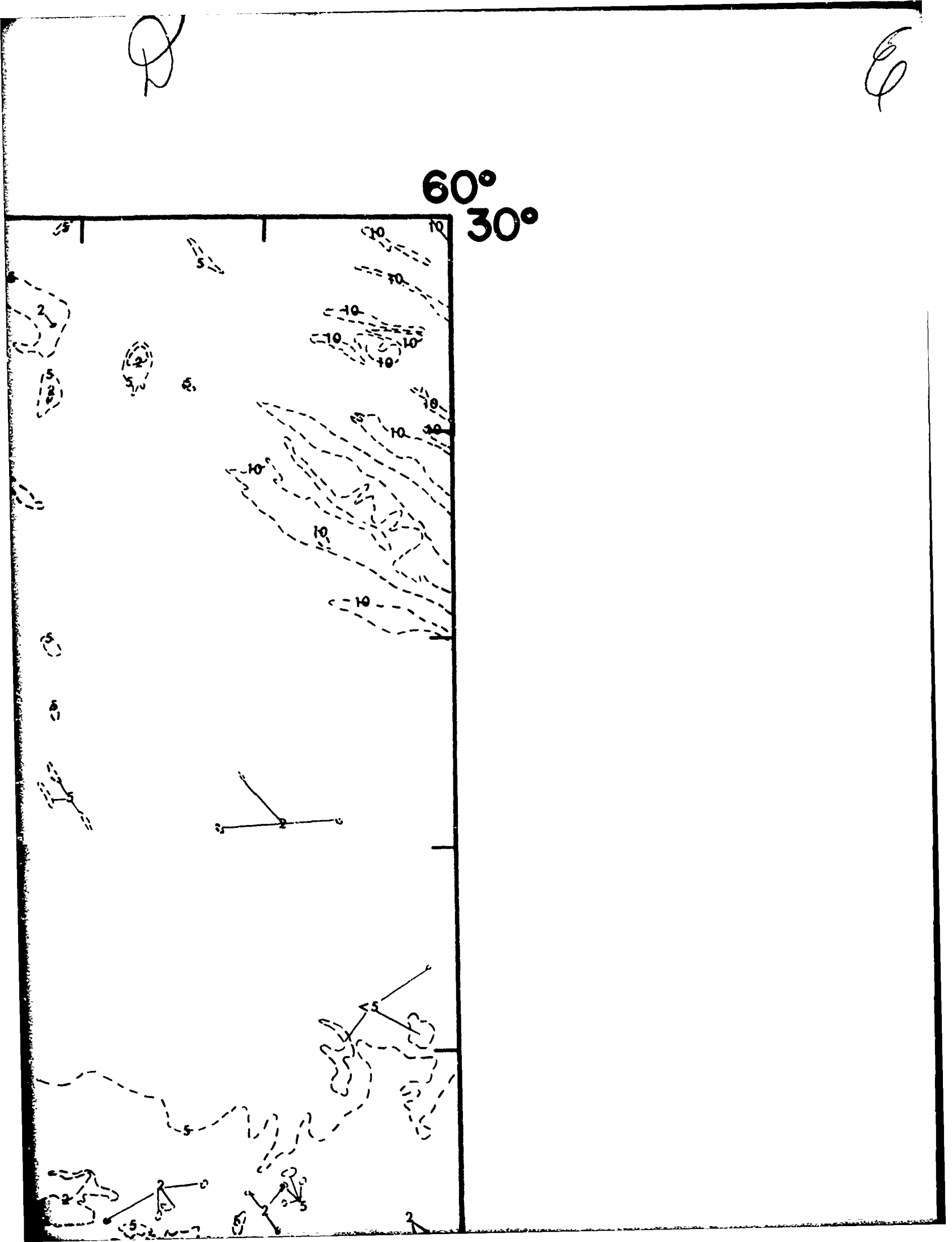
60°
30°

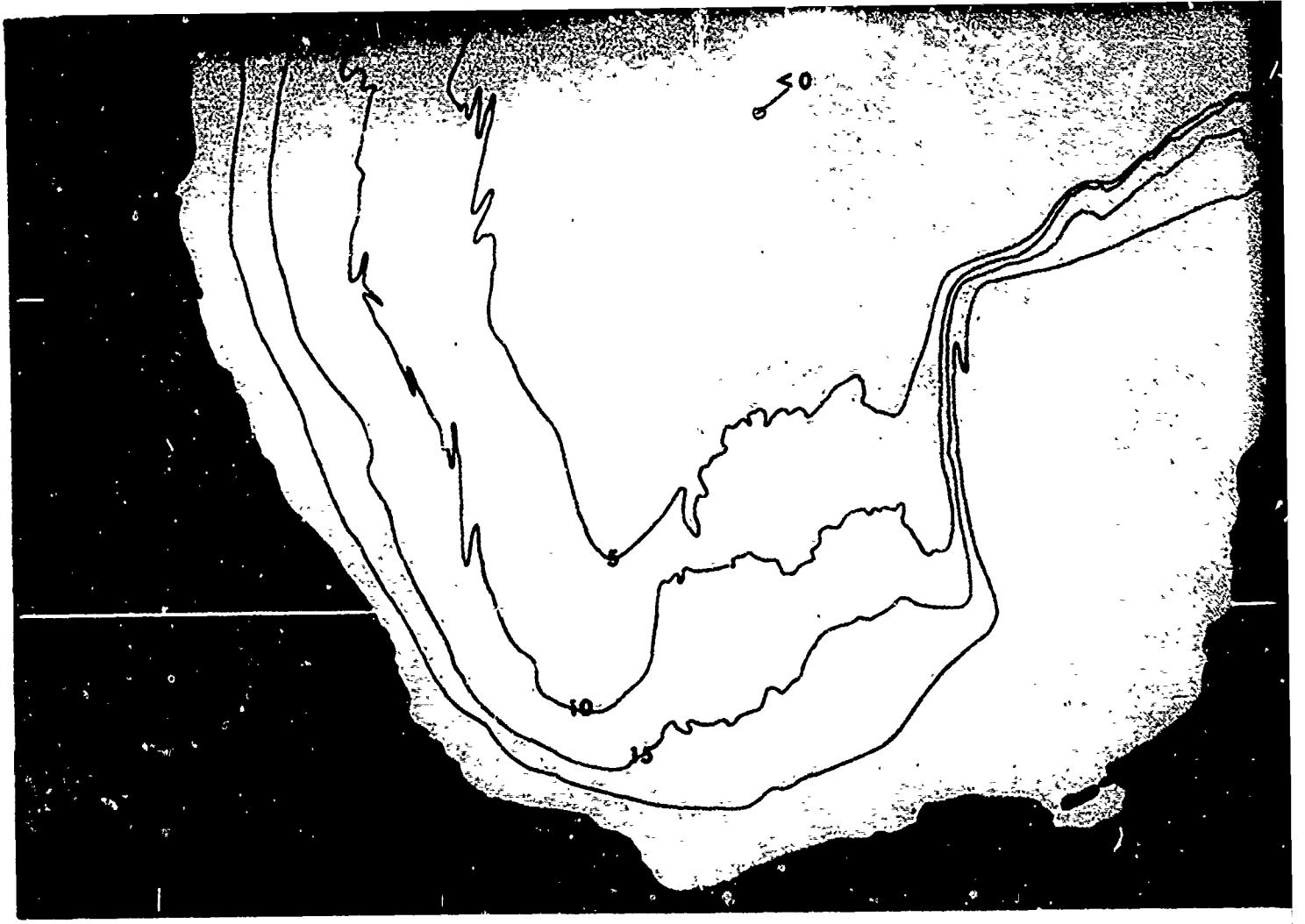

LEGEND

TOPOGRAPHY SHOALER THAN CRITICAL DEPTH (DEPTH DIFFERENCE)

TOPOGRAPHY EXCEEDING CRITICAL DEPTH TO 200 FATHOMS (DEPTH EXCESS)

TOPOGRAPHY EXCEEDING CRITICAL DEPTH MORE THAN 200 FATHOMS (DEPTH EXCESS)


20
10
15
<15
<0
5
0
10
20
15
5
2
-5
-10
-15
-20

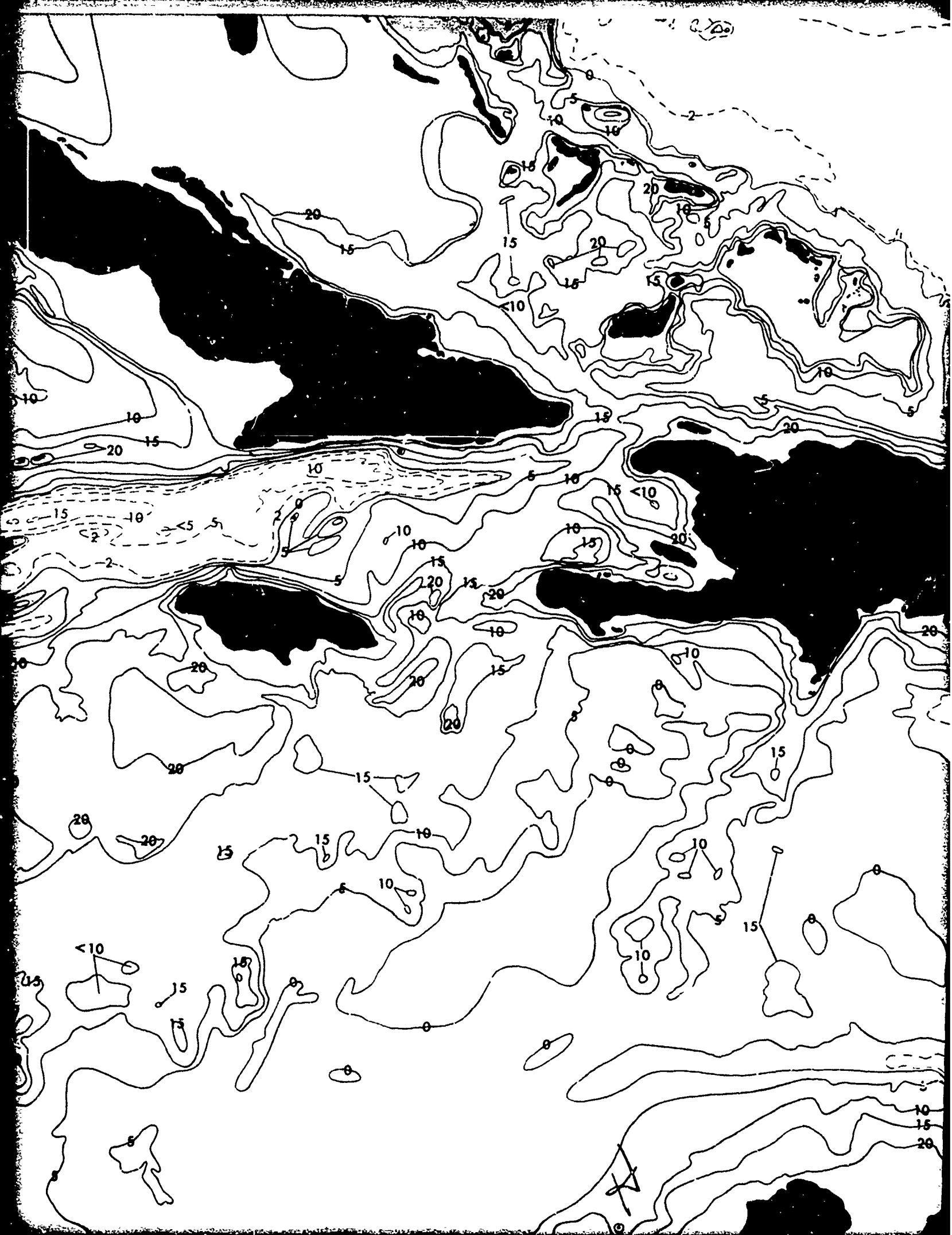

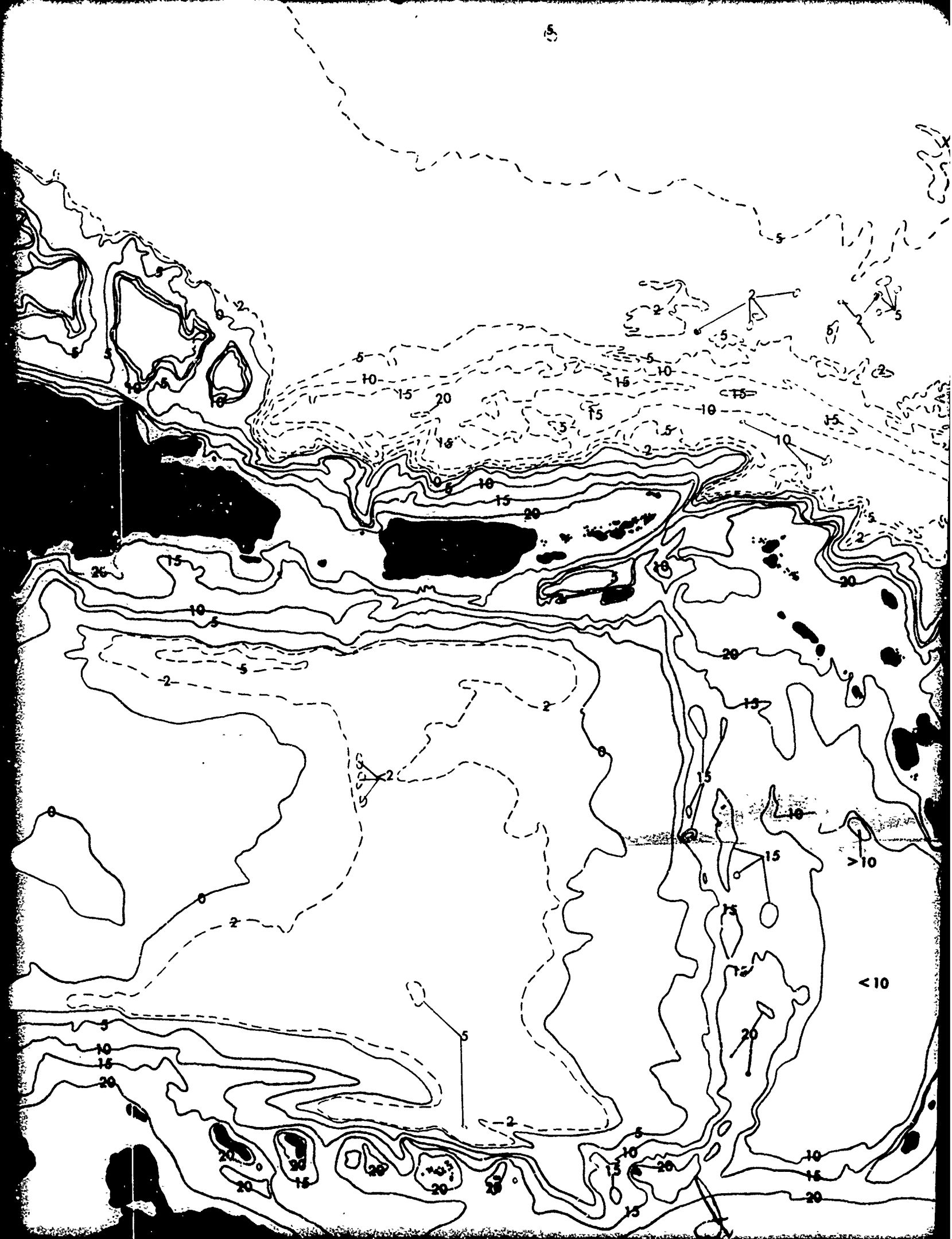
>10
<10

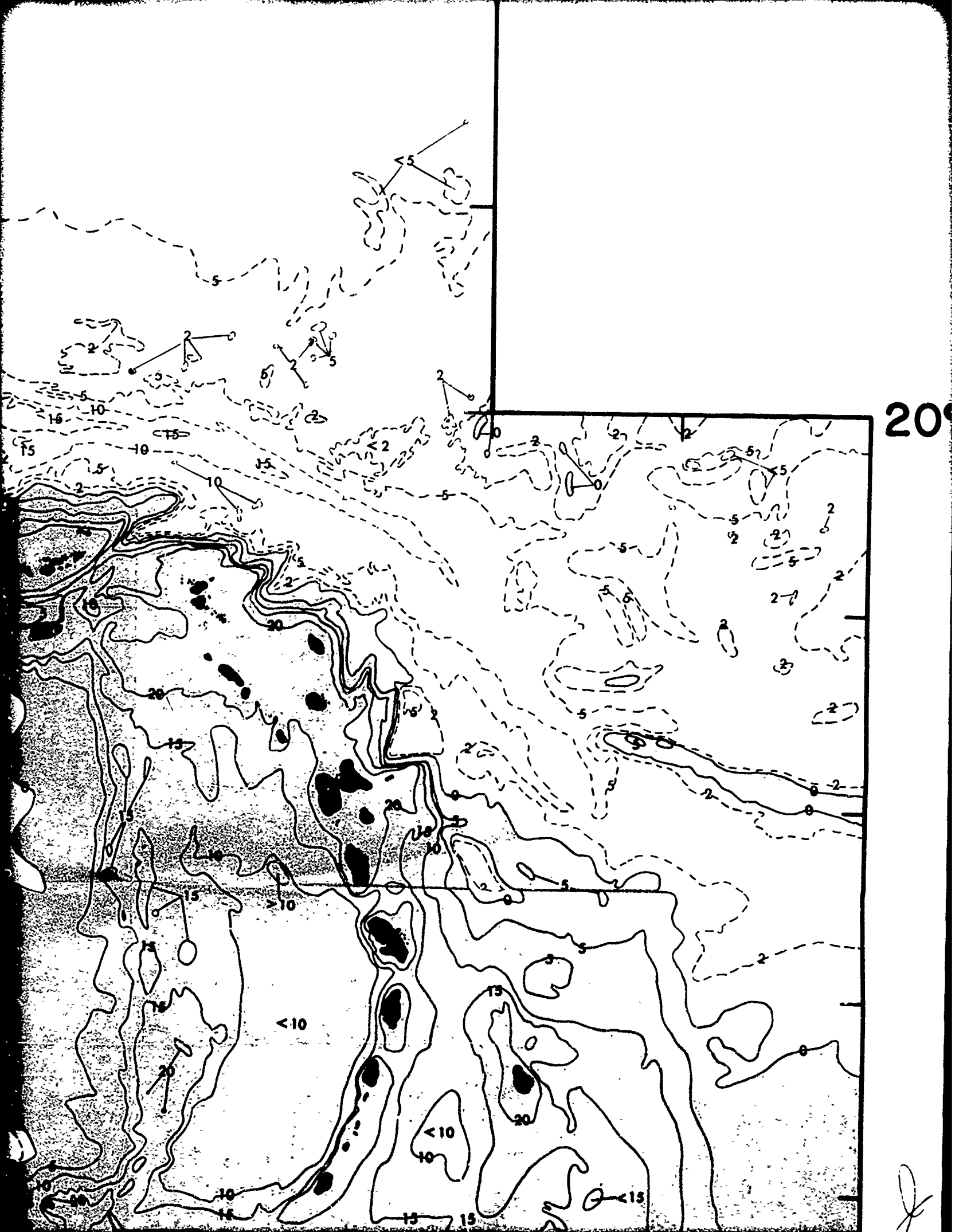
209
<10
>10
<10
<10
<15

LEGEND

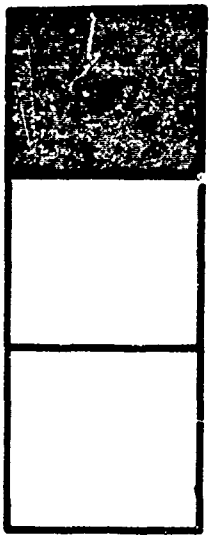

TOPOGRAPHY SHOALER THAN CRITICAL DEPTH (DEPTH DIFFERENCE)

TOPOGRAPHY EXCEEDING CRITICAL DEPTH TO 200 FATHOMS (DEPTH EXCESS)

TOPOGRAPHY EXCEEDING CRITICAL DEPTH MORE THAN 200 FATHOMS (DEPTH EXCESS)

CONTOURS IN FATHOMS X100

10

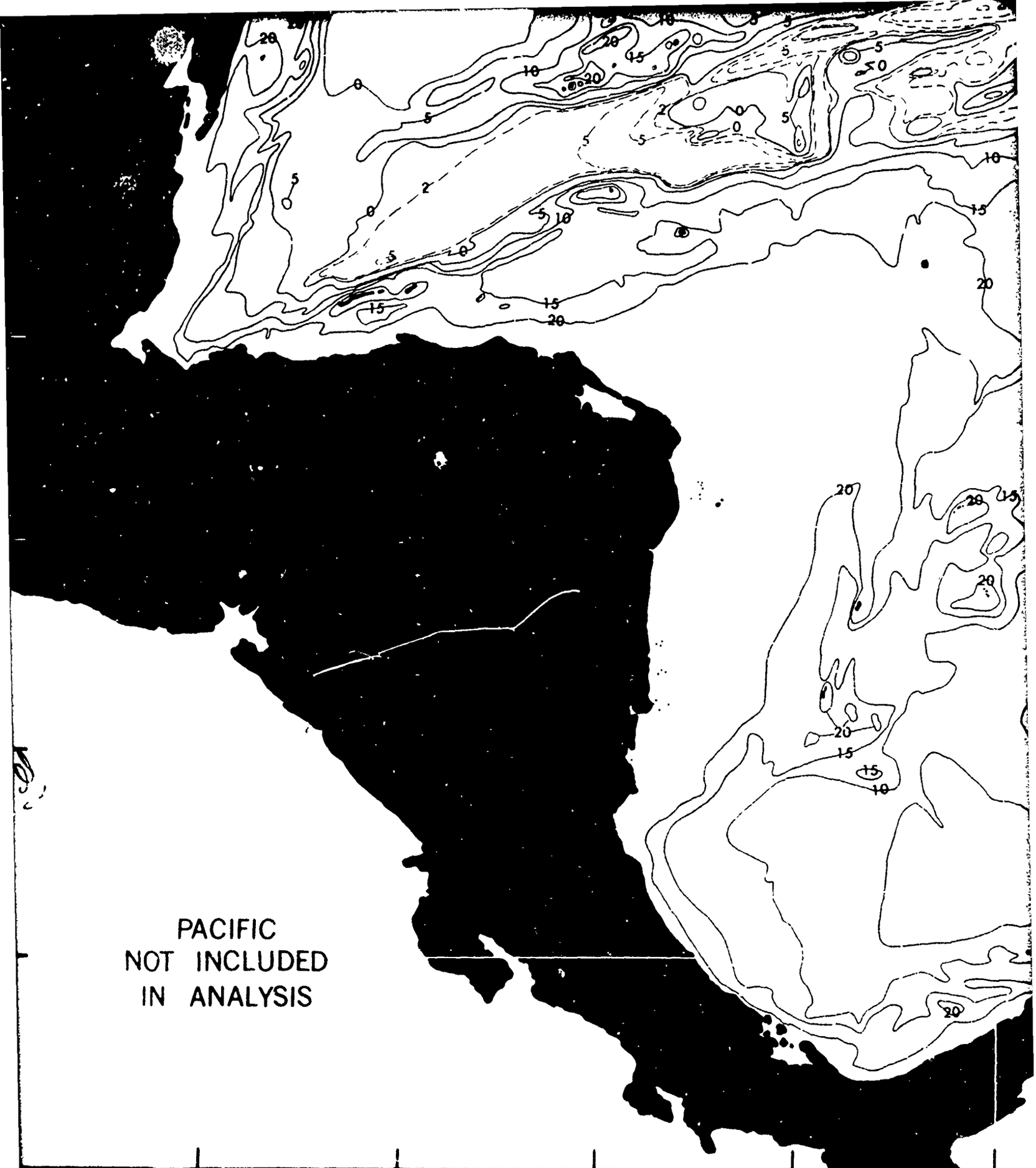

FIGURE 4-93 TOPOG

SHOALER AND DEEPER THAN CRITICAL DEPTH (WINTER)

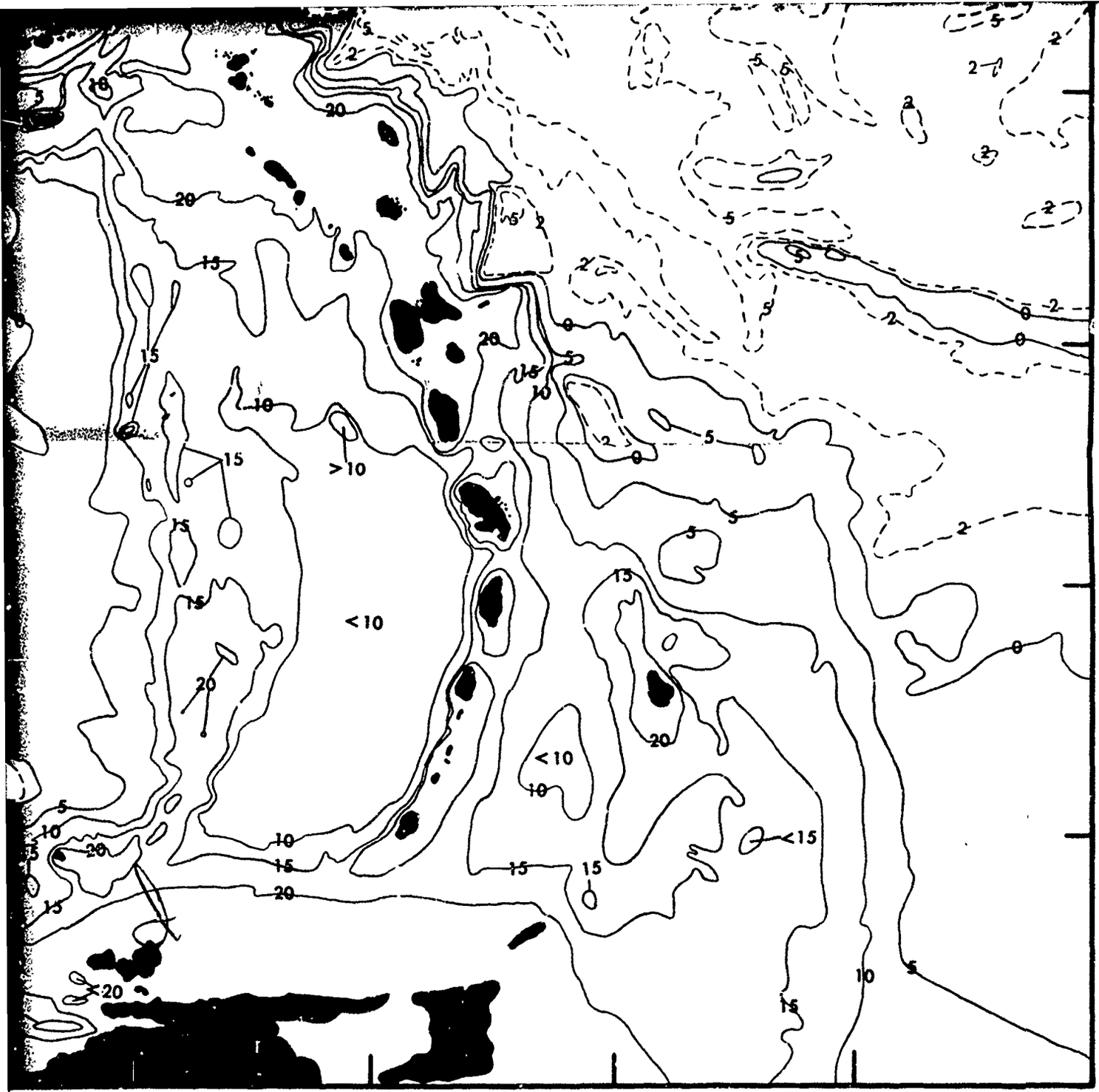
10°
60°

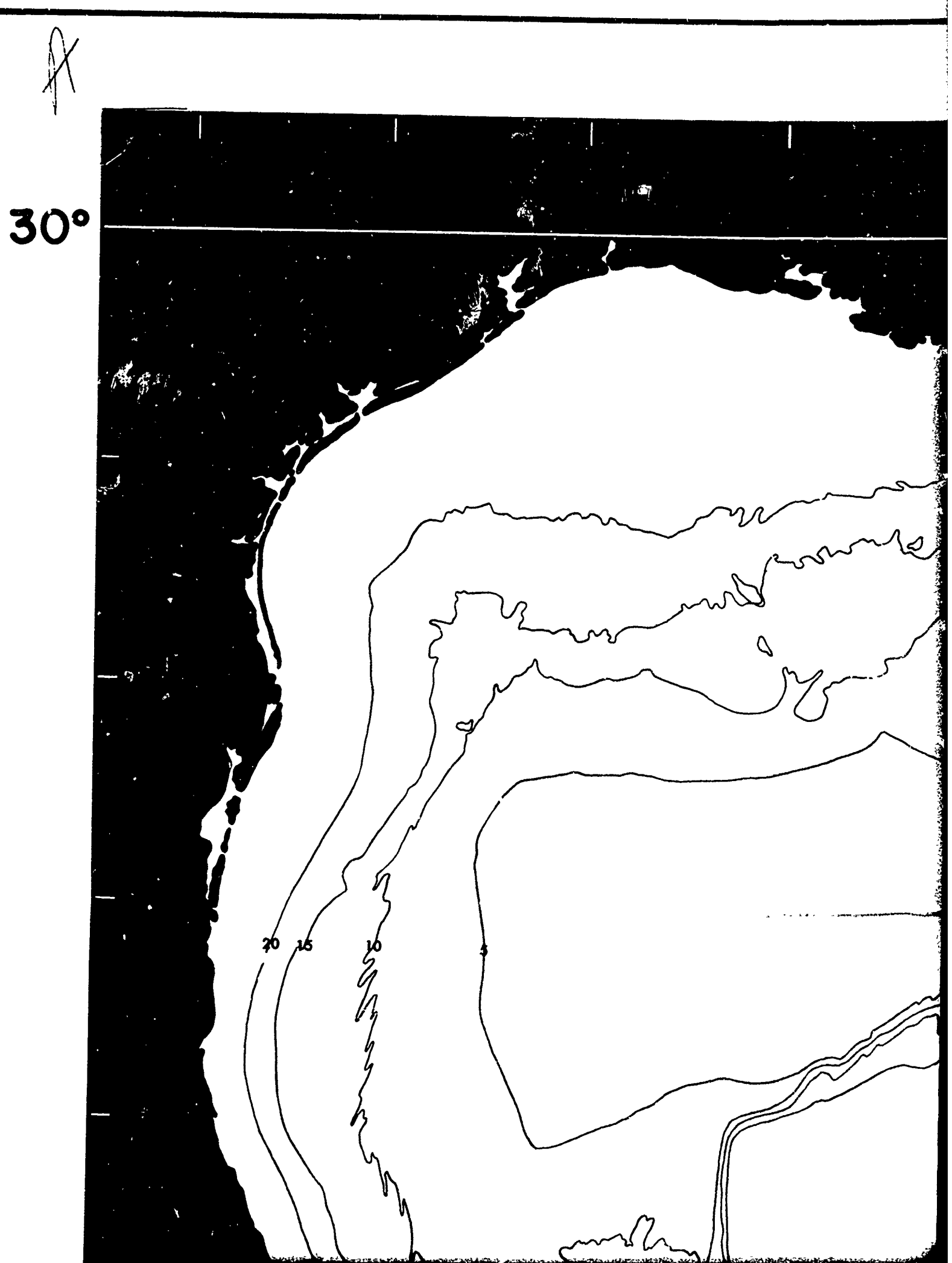
30°
20
15
10
5

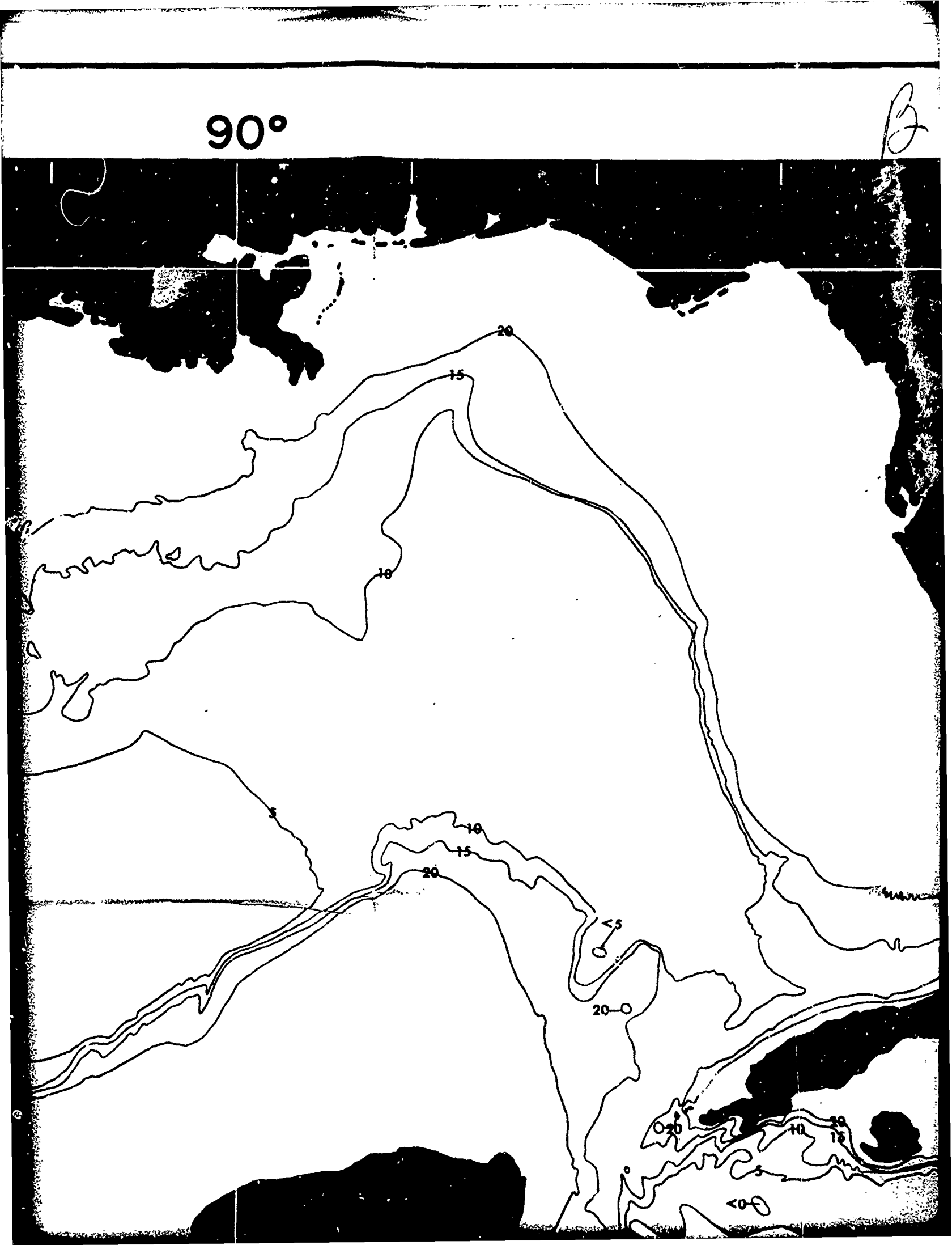
90°
20
15
10
5
10
15
20
<5
20
20
10
15
5
<0

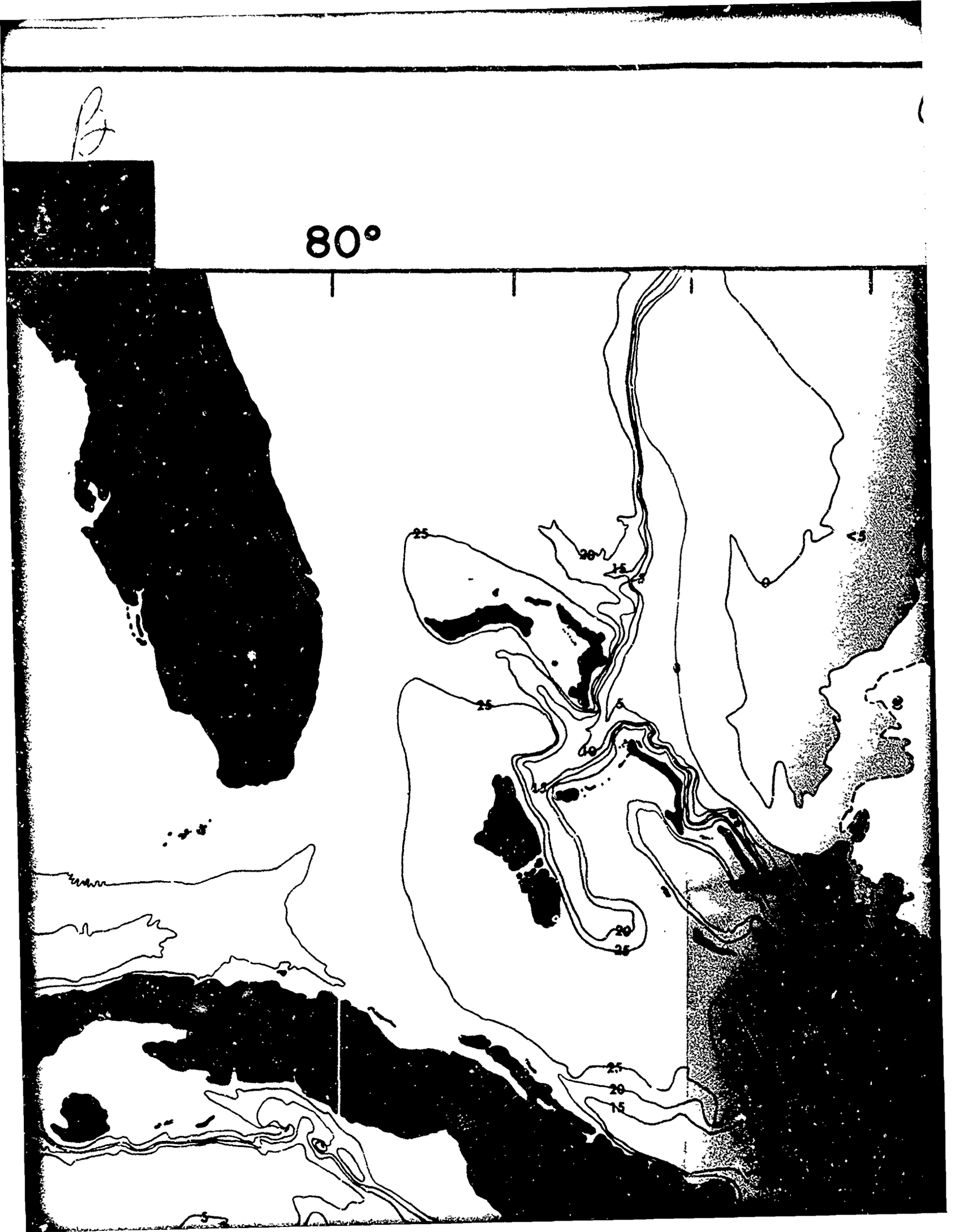
80°
25
20
15
5
0
25
5
20
25
25
20
15
5

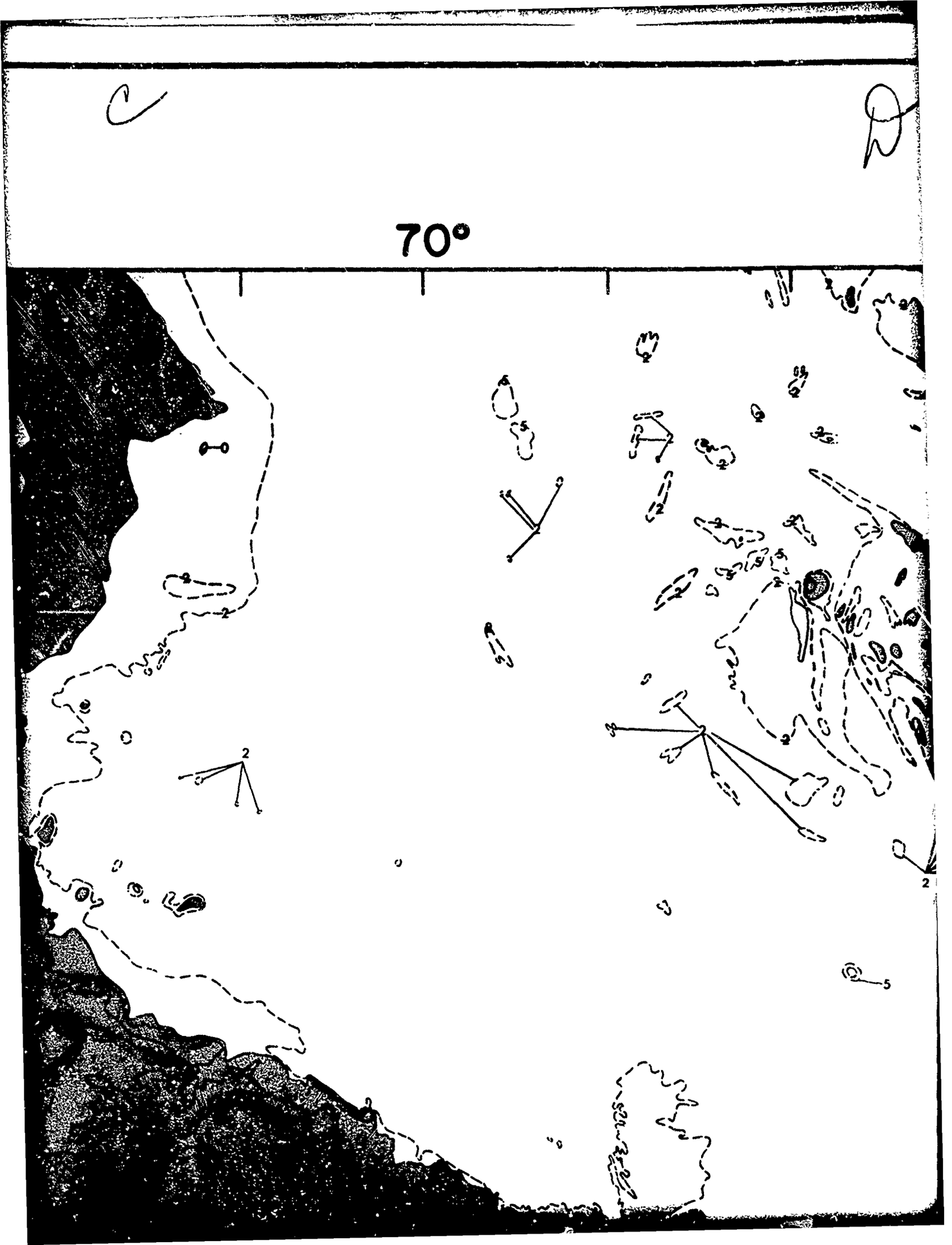
70°
2
2
5

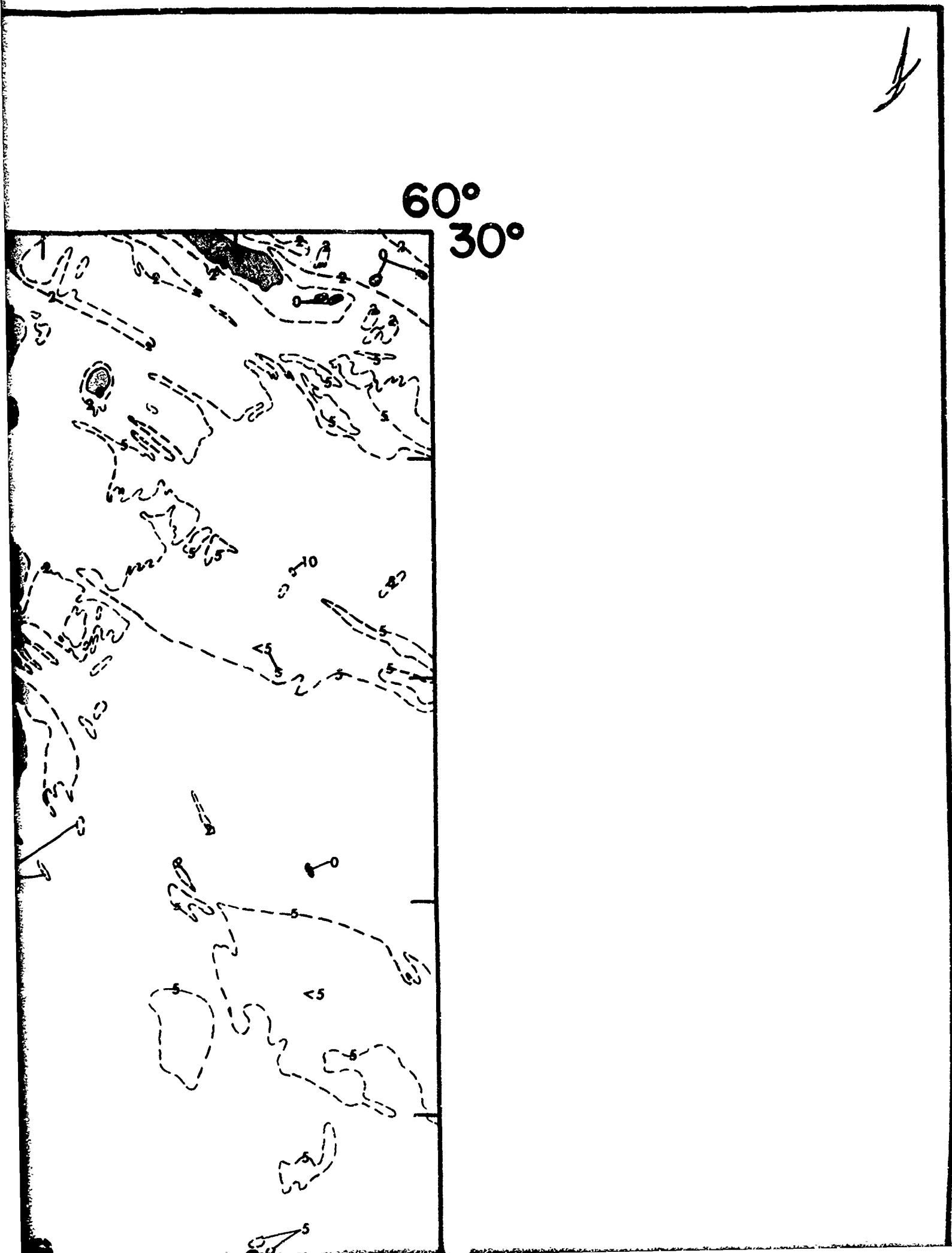
60°
30°
1
10
<5
0

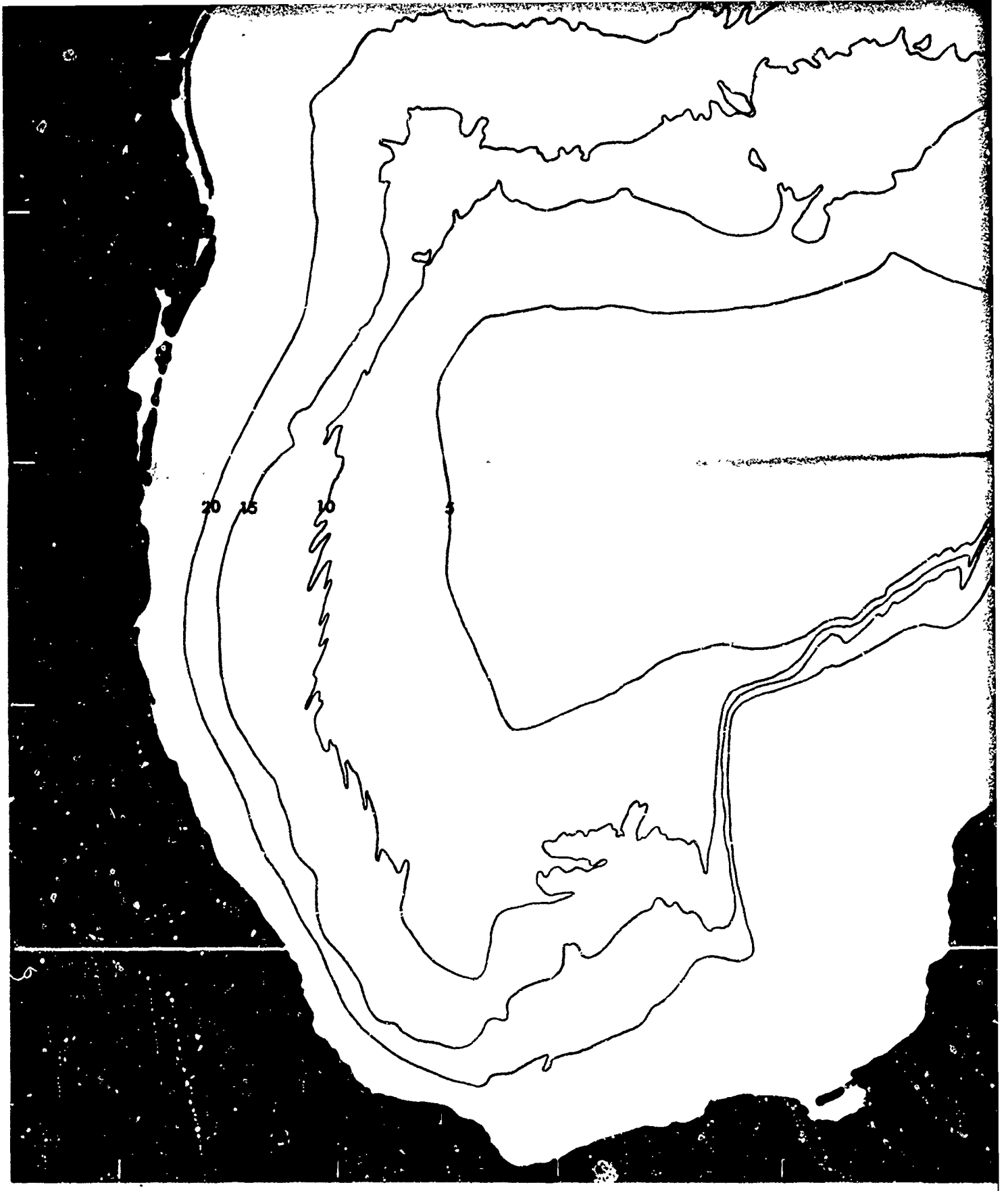
20
15
10
5
20°

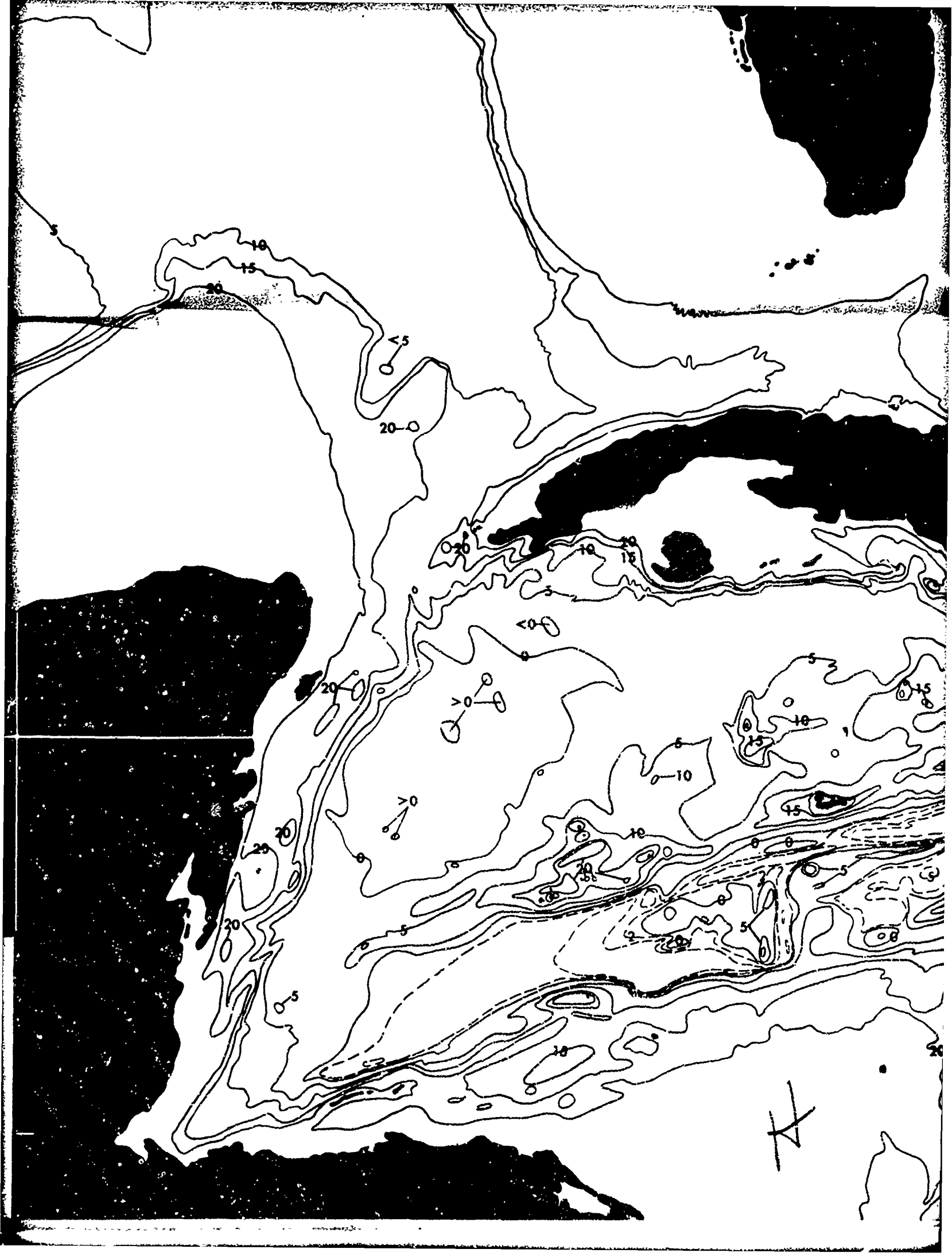
5
10
15
20
<5
20
20
10
15
<0
>0
5
15
10
10
15
>0
20
20
20
5
5
10
20


2
5
10
15
<15
<5
0

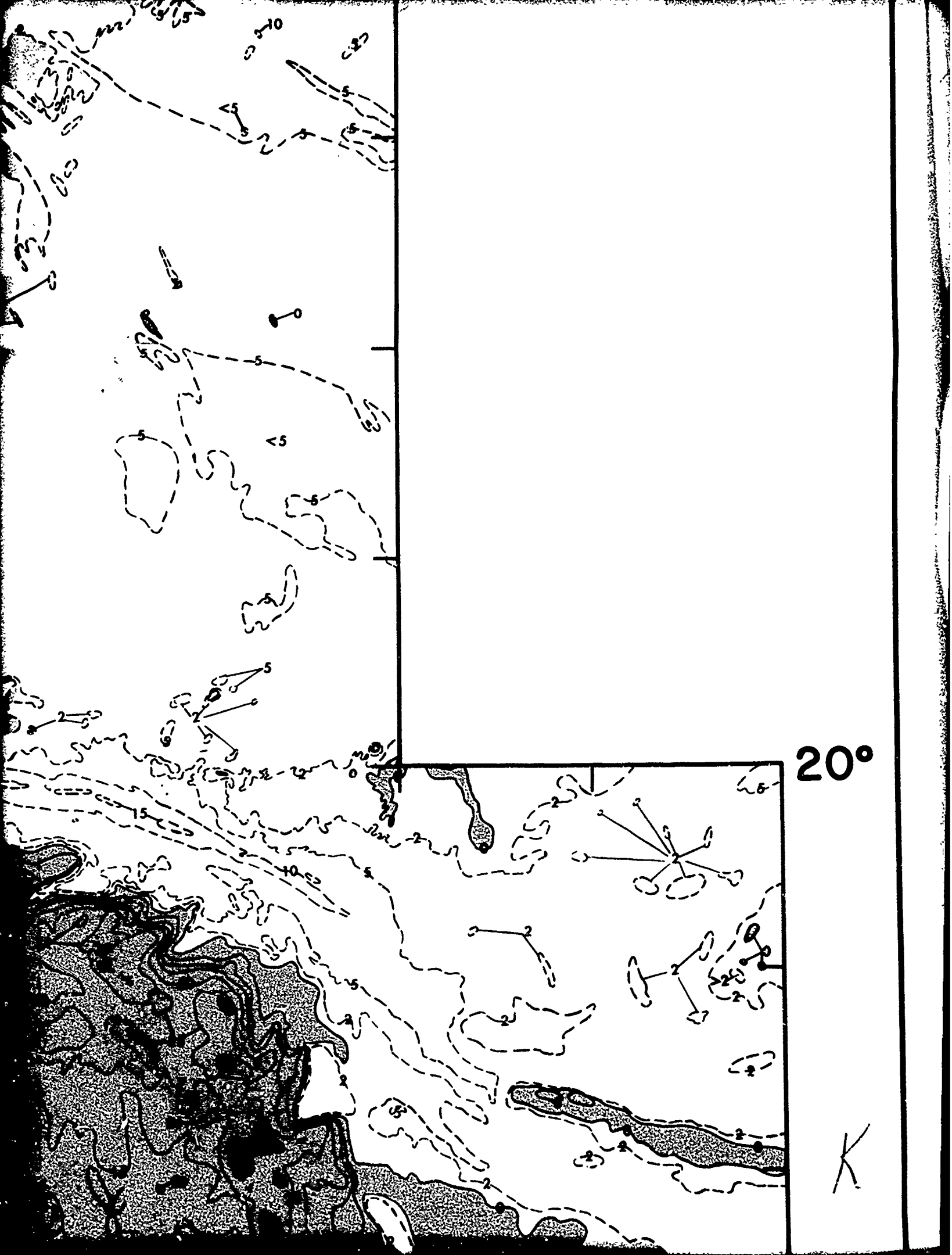
20°
K

LEGEND

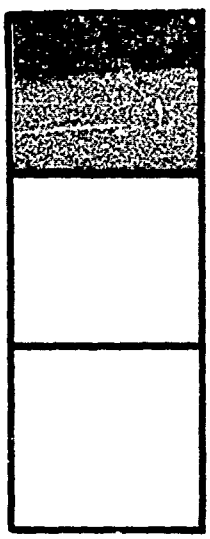

TOPOGRAPHY SHOALER THAN CRITICAL DEPTH (DEPTH DIFFERENCE)

TOPOGRAPHY EXCEEDING CRITICAL DEPTH TO 200 FATHOMS (DEPTH EXCESS)

TOPOGRAPHY EXCEEDING CRITICAL DEPTH MORE THAN 200 FATHOMS (DEPTH EXCESS)

CONTOURS IN FATHOMS X100

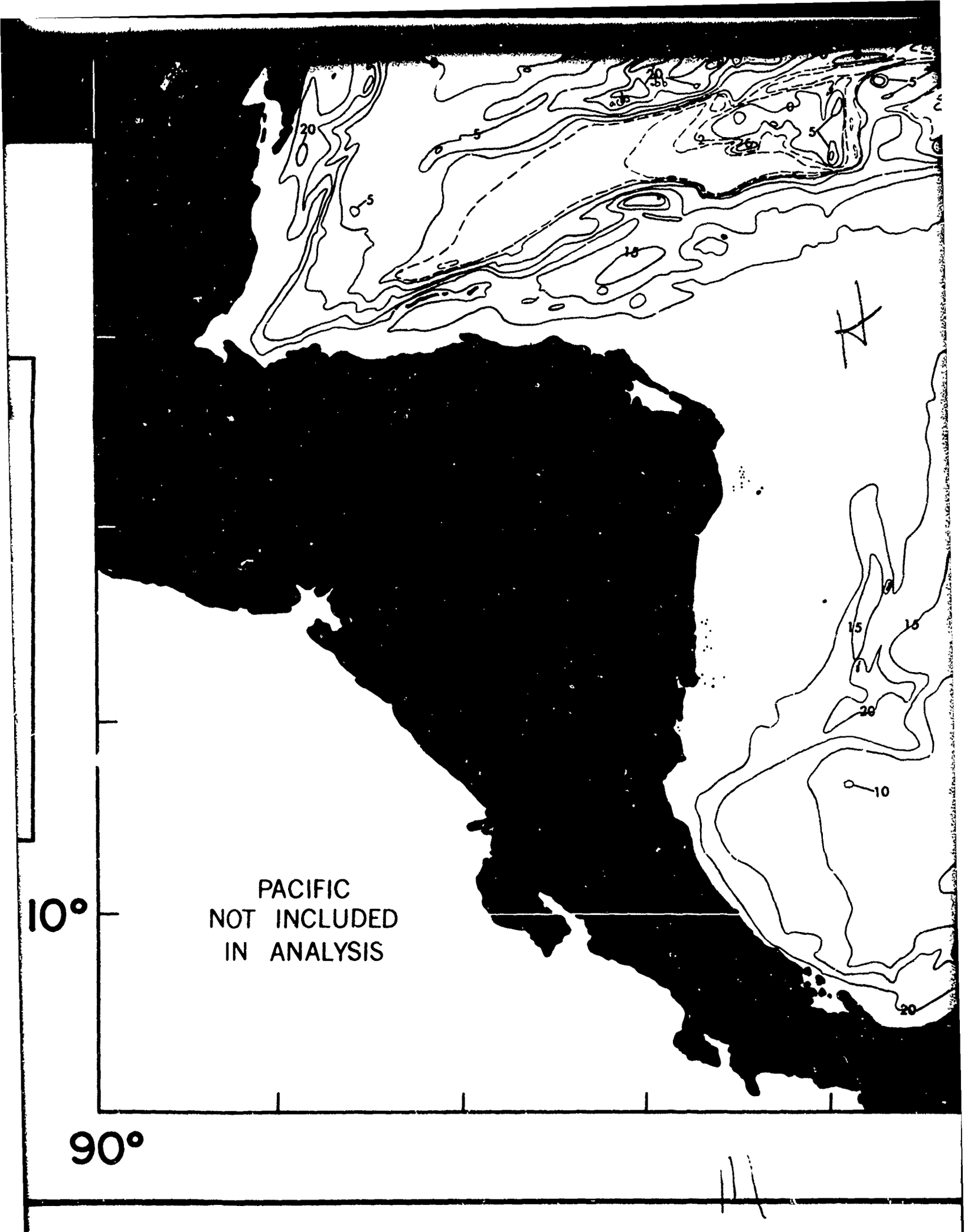

FIGURE 4

4 TOPOGRAPHY SHOALER AND DEEPER THAN CRITICAL DEPTH (SUMMER)

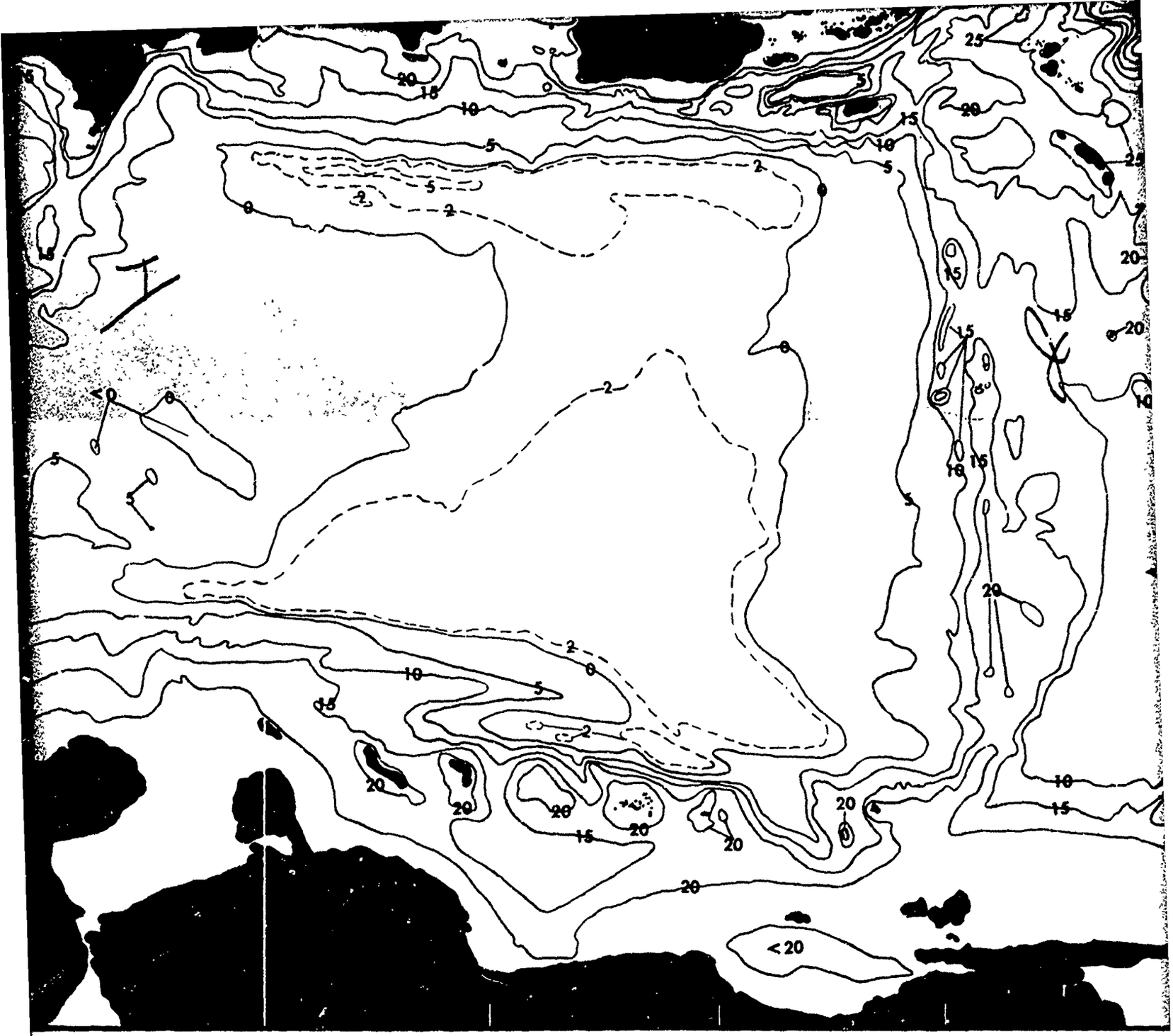
70°
< 20

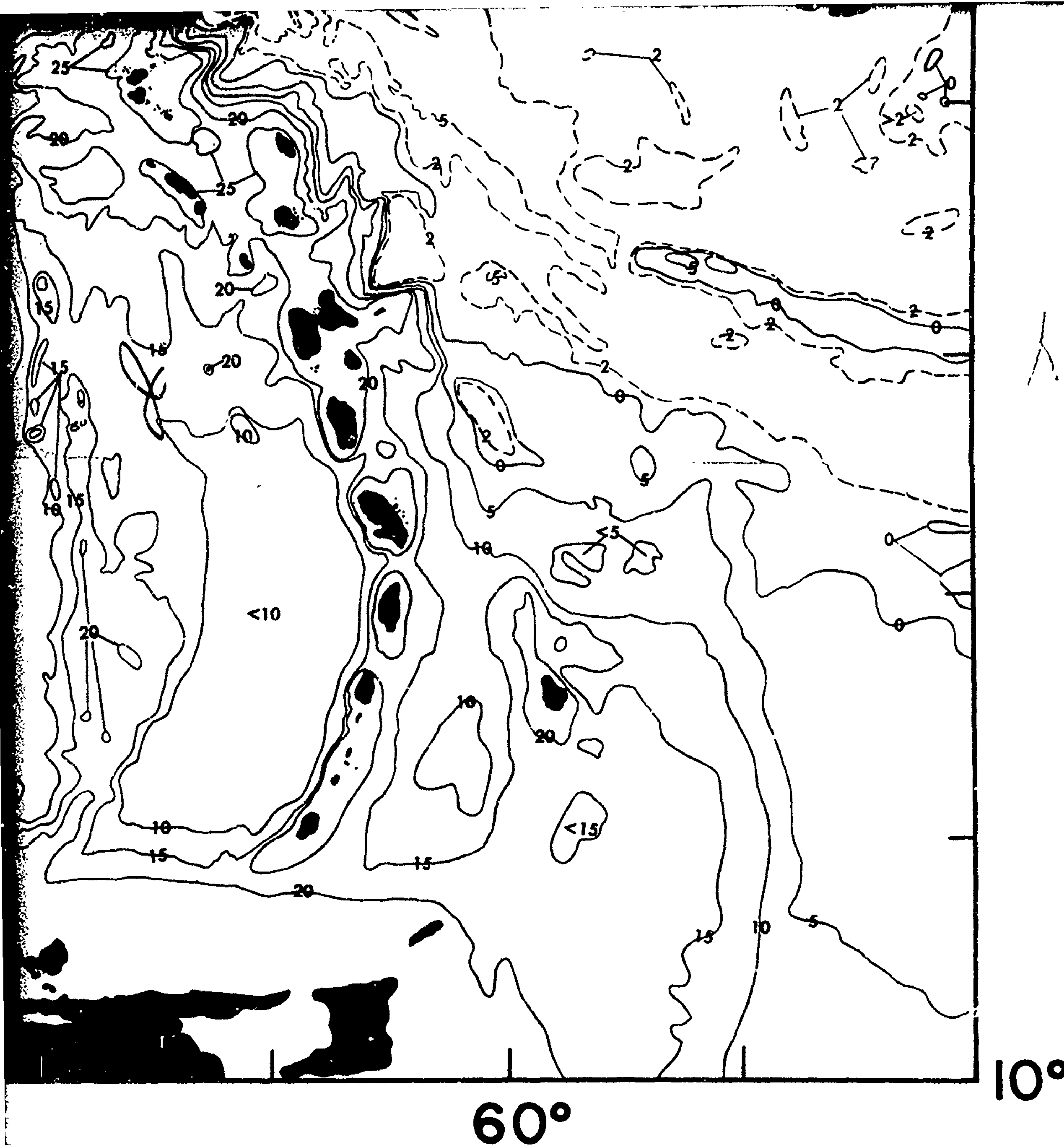

25
20
15
10
5
2
0
<10
<5
<15
>2
60°
10°

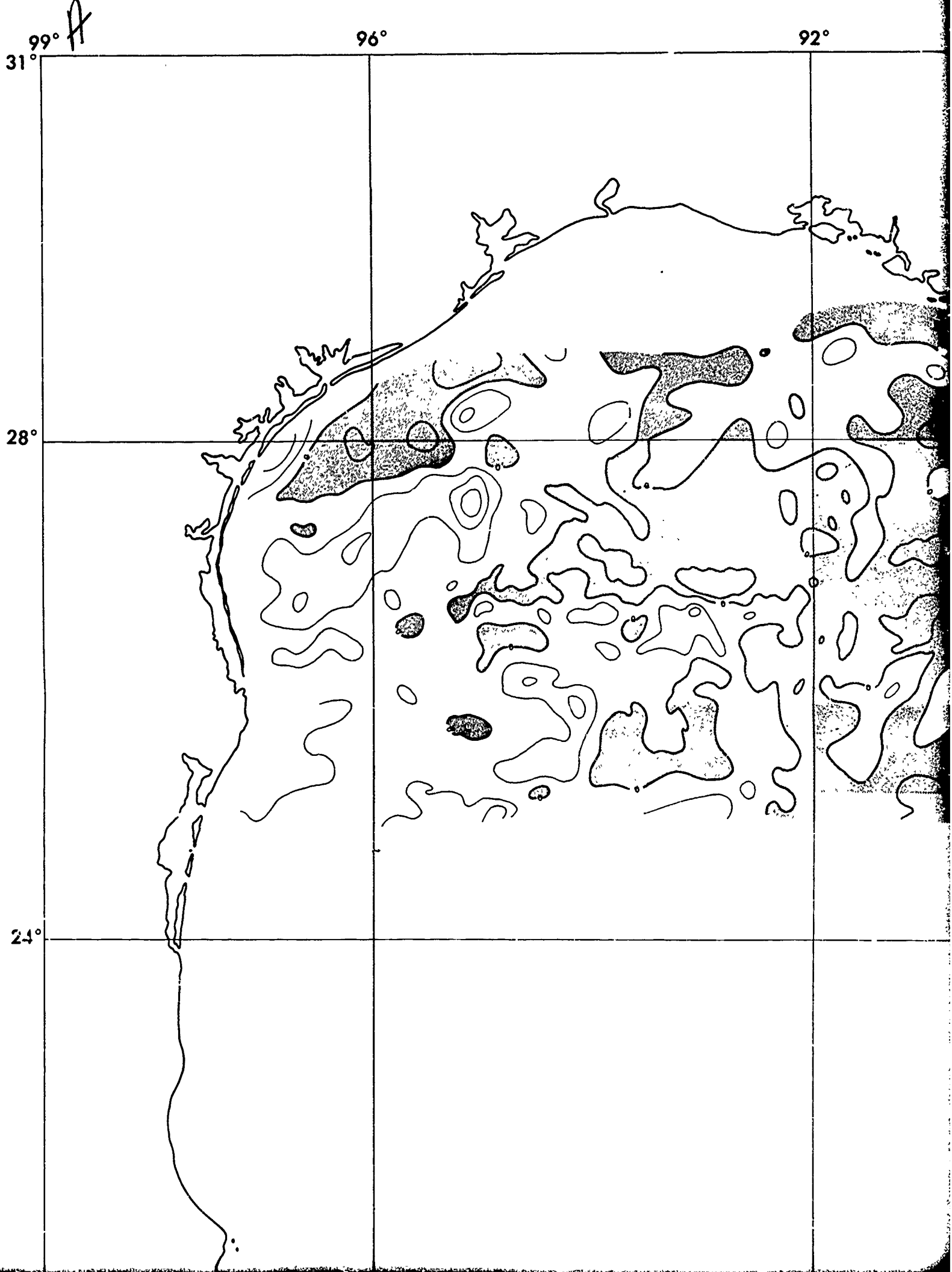
99°
96°
92°
31°
28°
24°

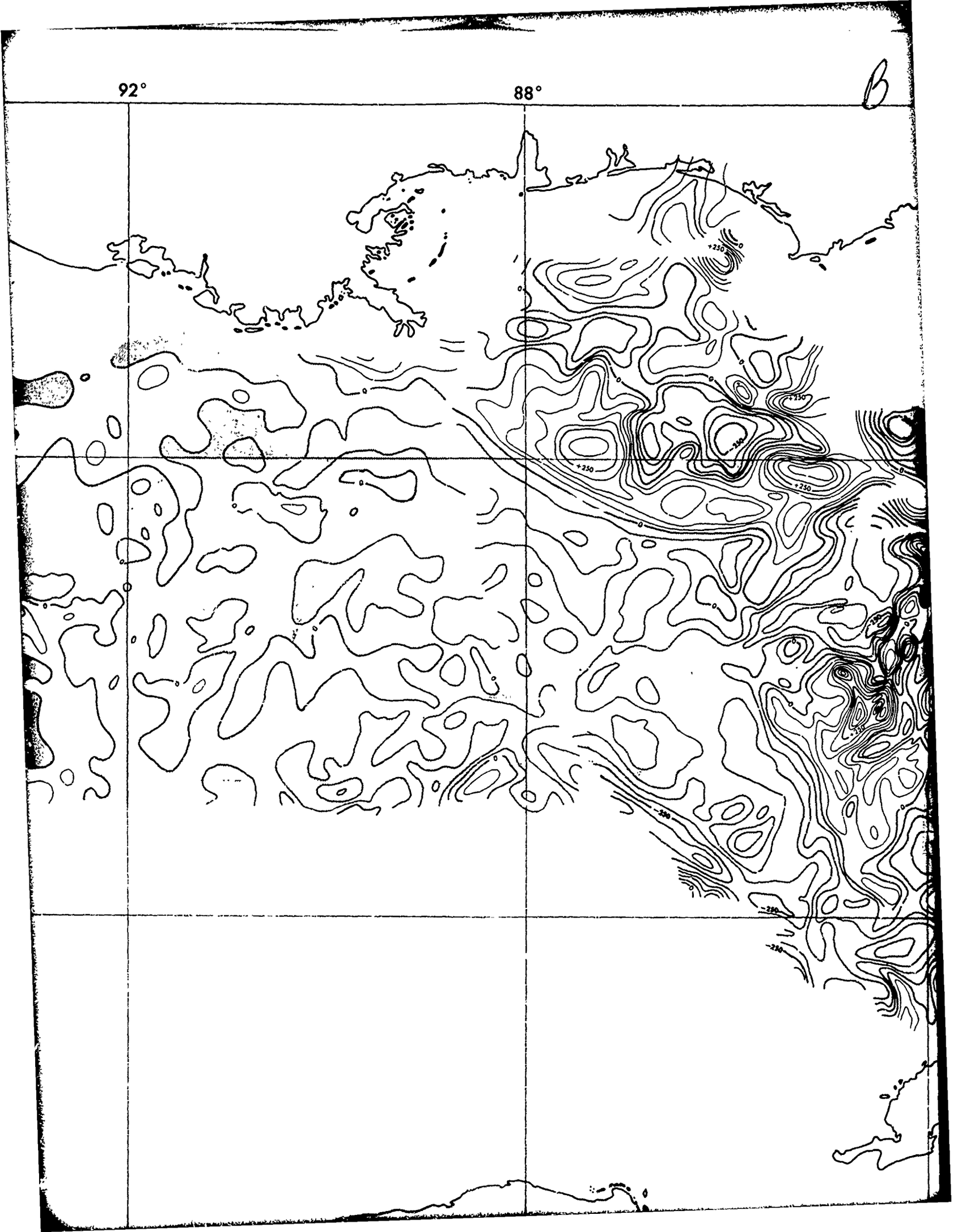
92°
88°
B
+250
0
-250

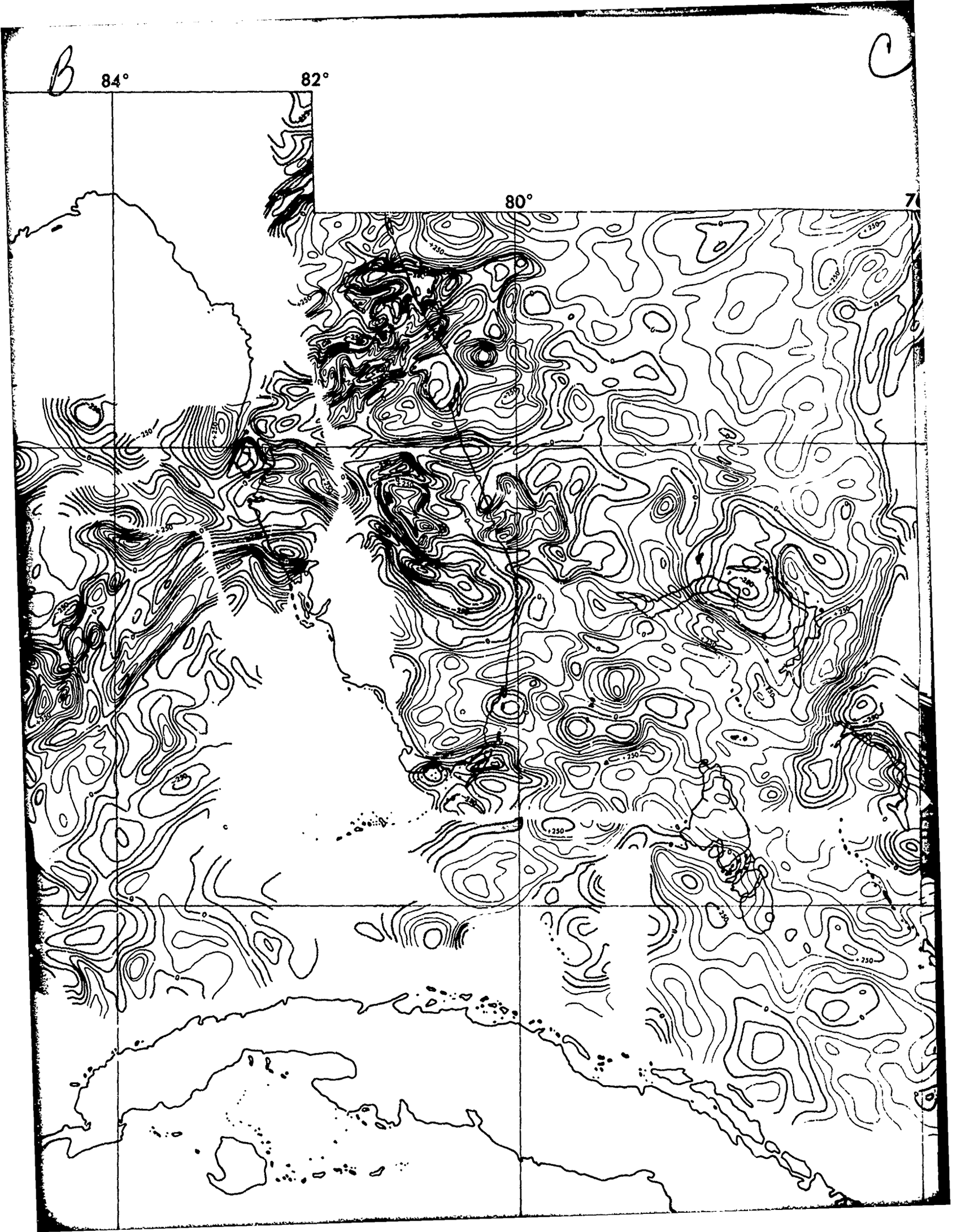
B
C
84°
82°
80°
7
+250
0
-250


72°
68°

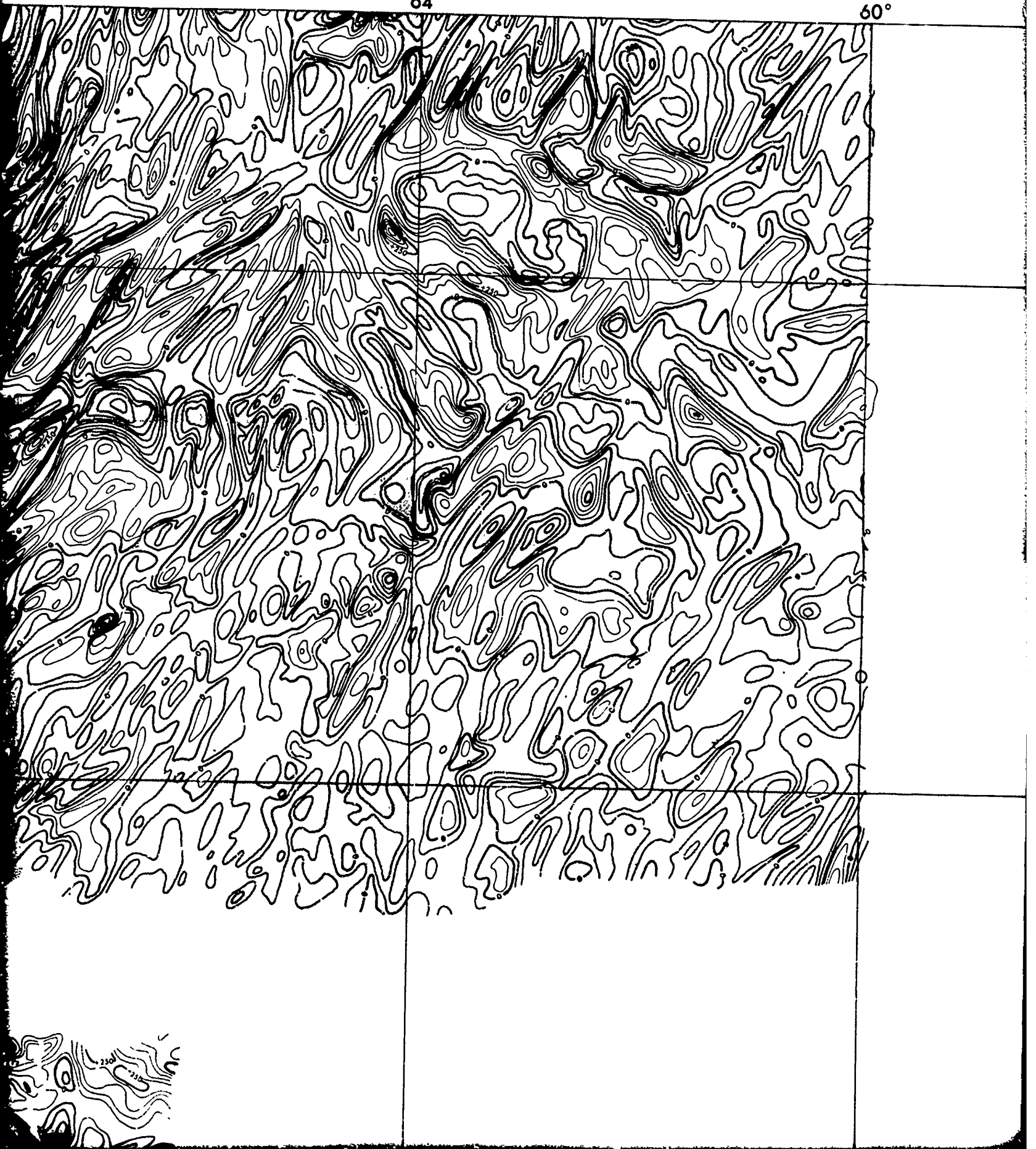
64°
60°

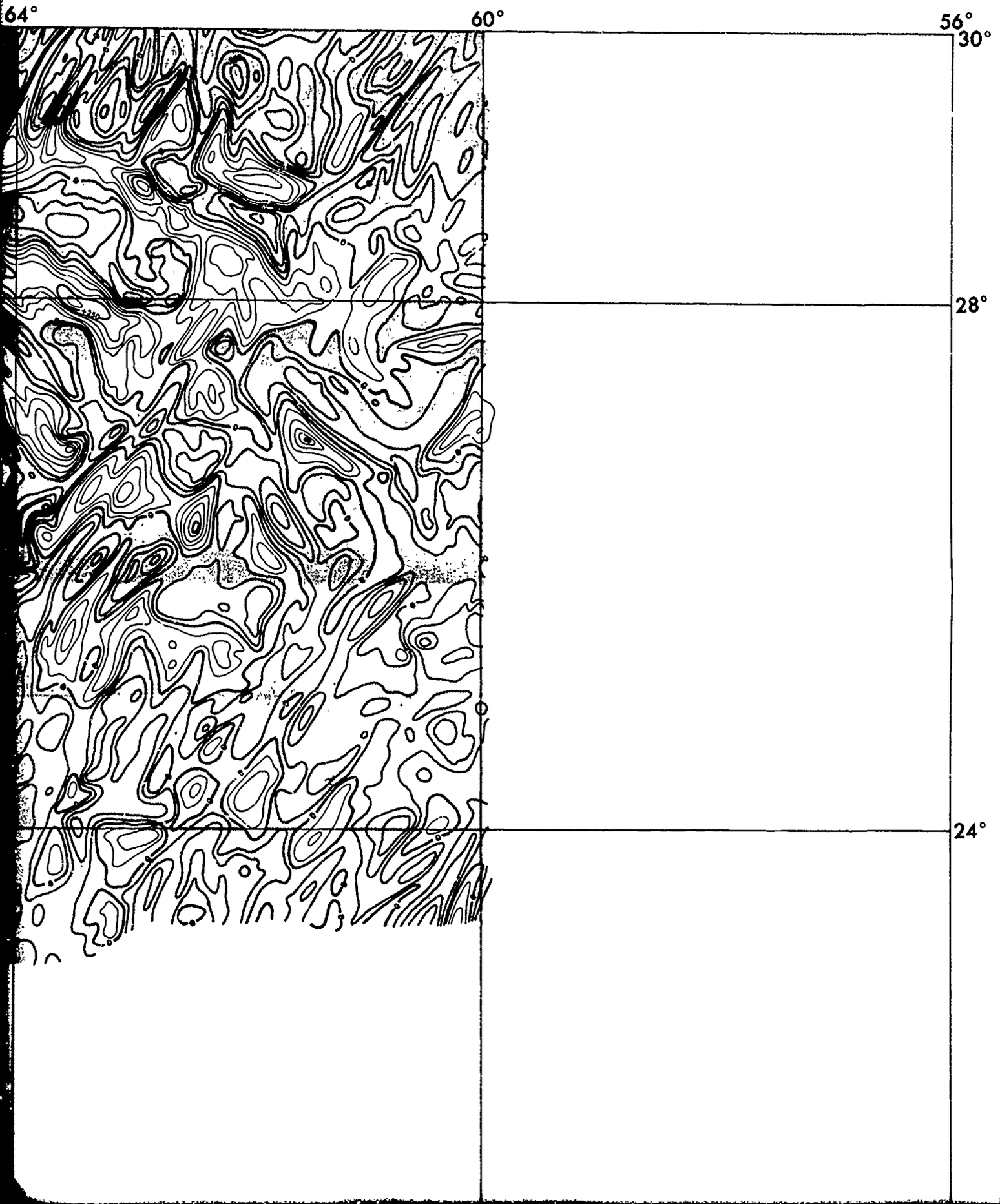
64°
60°
56°
30°
28°
24°

RESIDUAL MAGNETIC INTENSITY

PRELIMINARY CONTOUR CHART

GULF OF MEXICO — CARIBBEAN SEA — NORTH AMERICAN BA

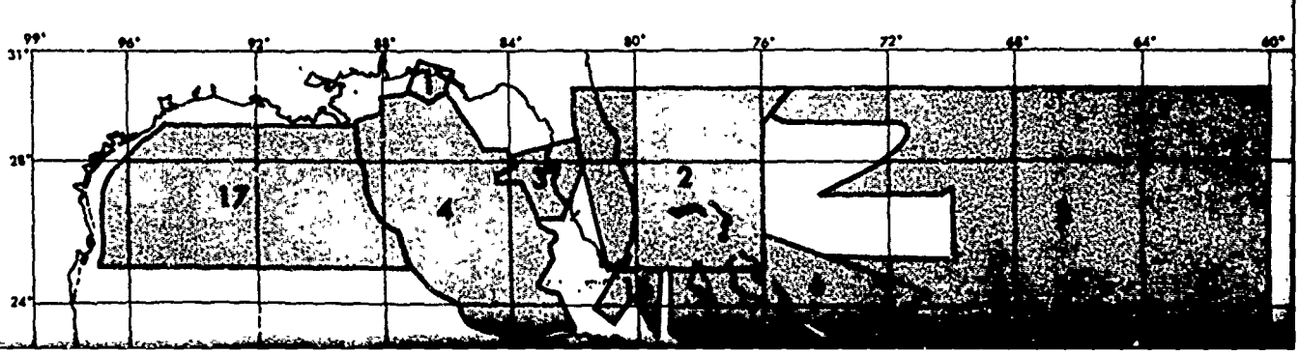

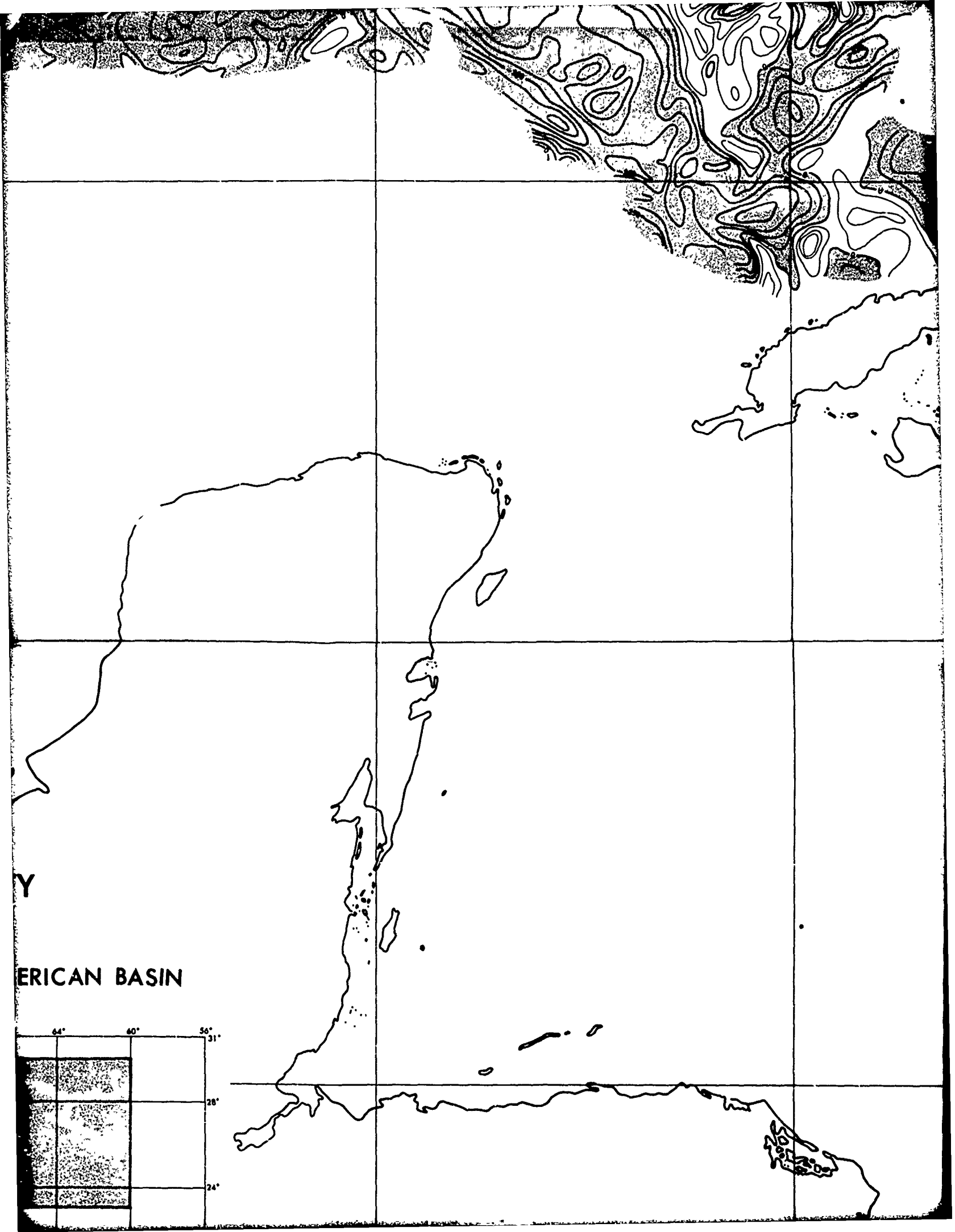
Y
ERICAN BASIN
64°
60°
56°
31°
28°
24°

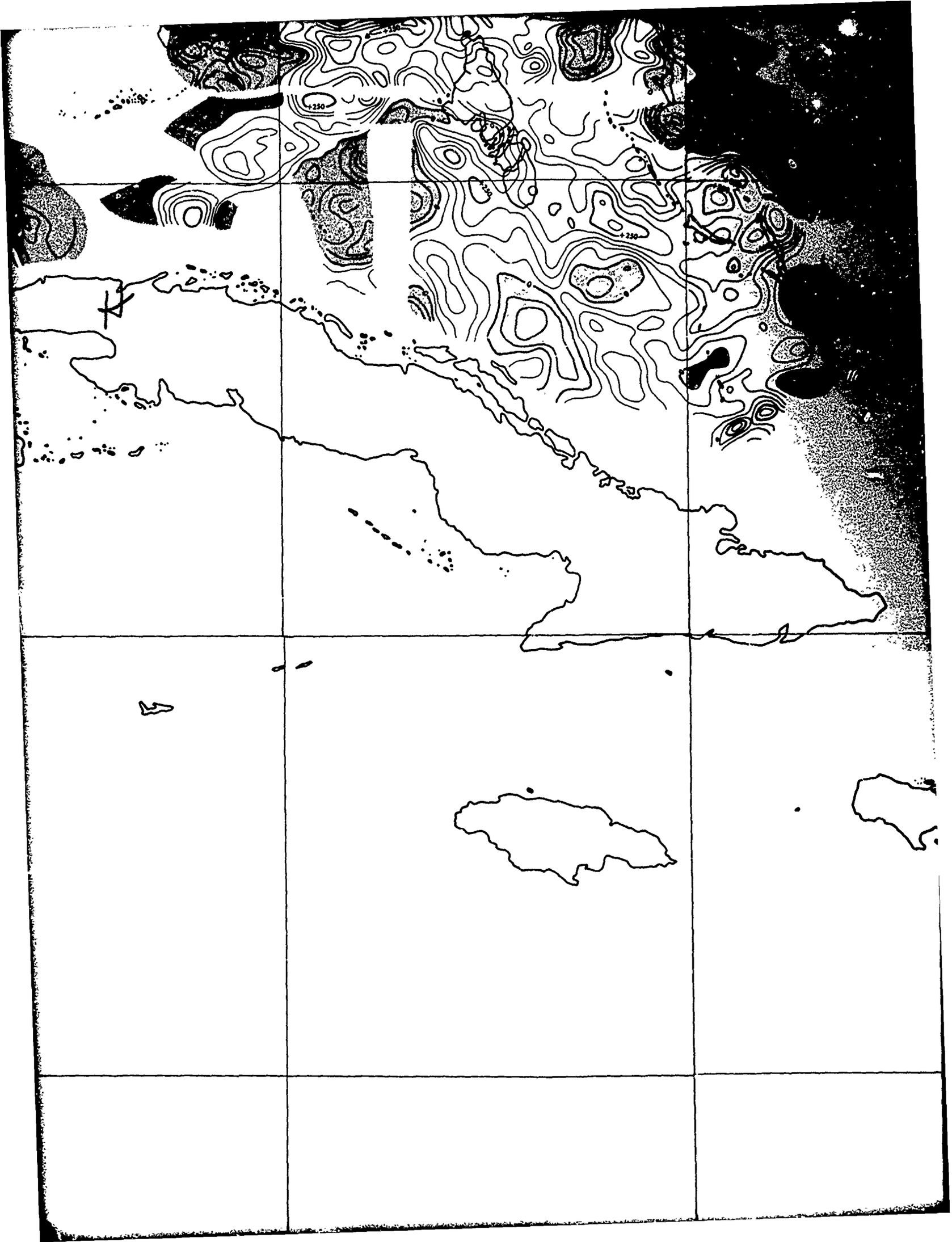
+250
+250
+250

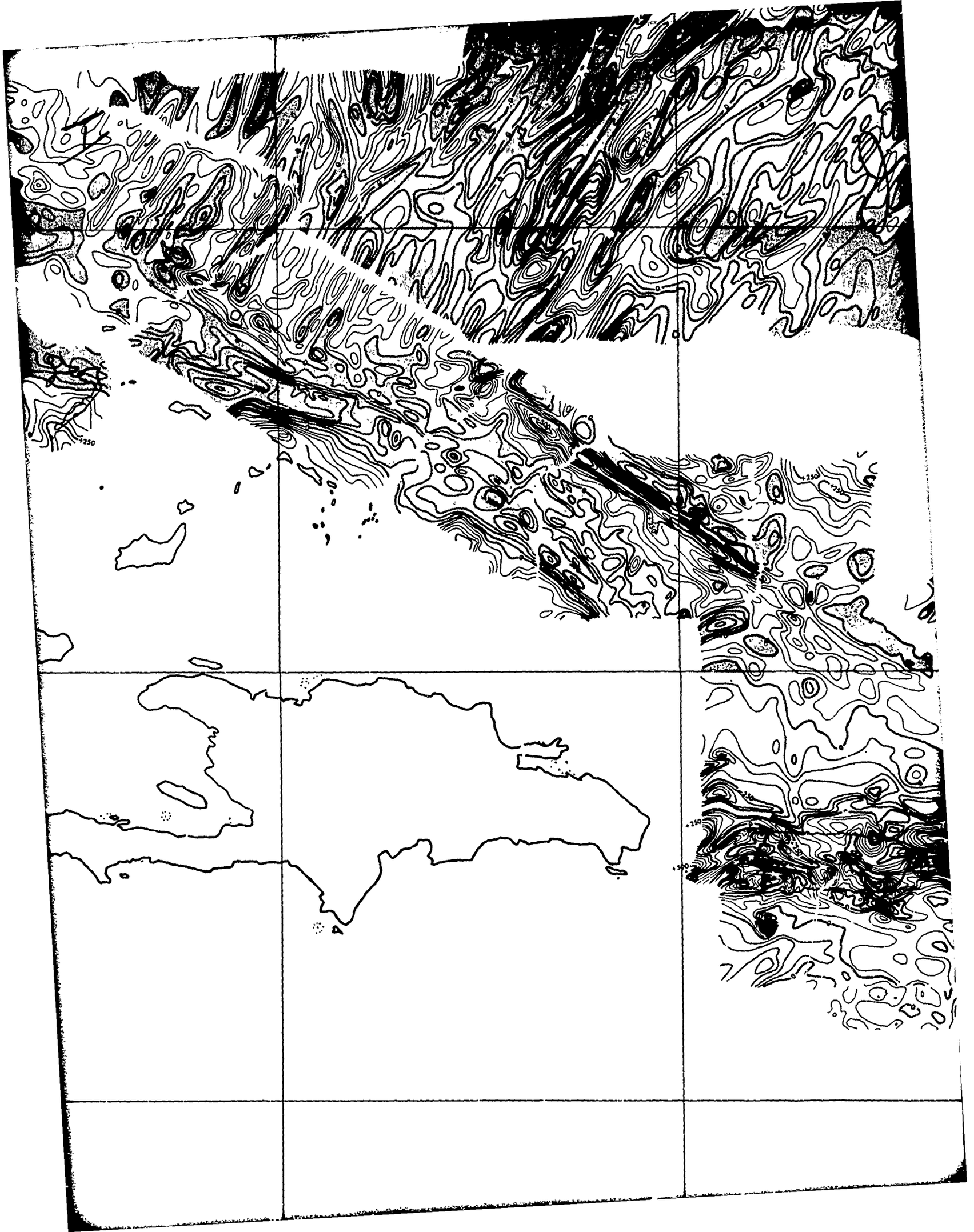
+250
+250
+250
+250
+250

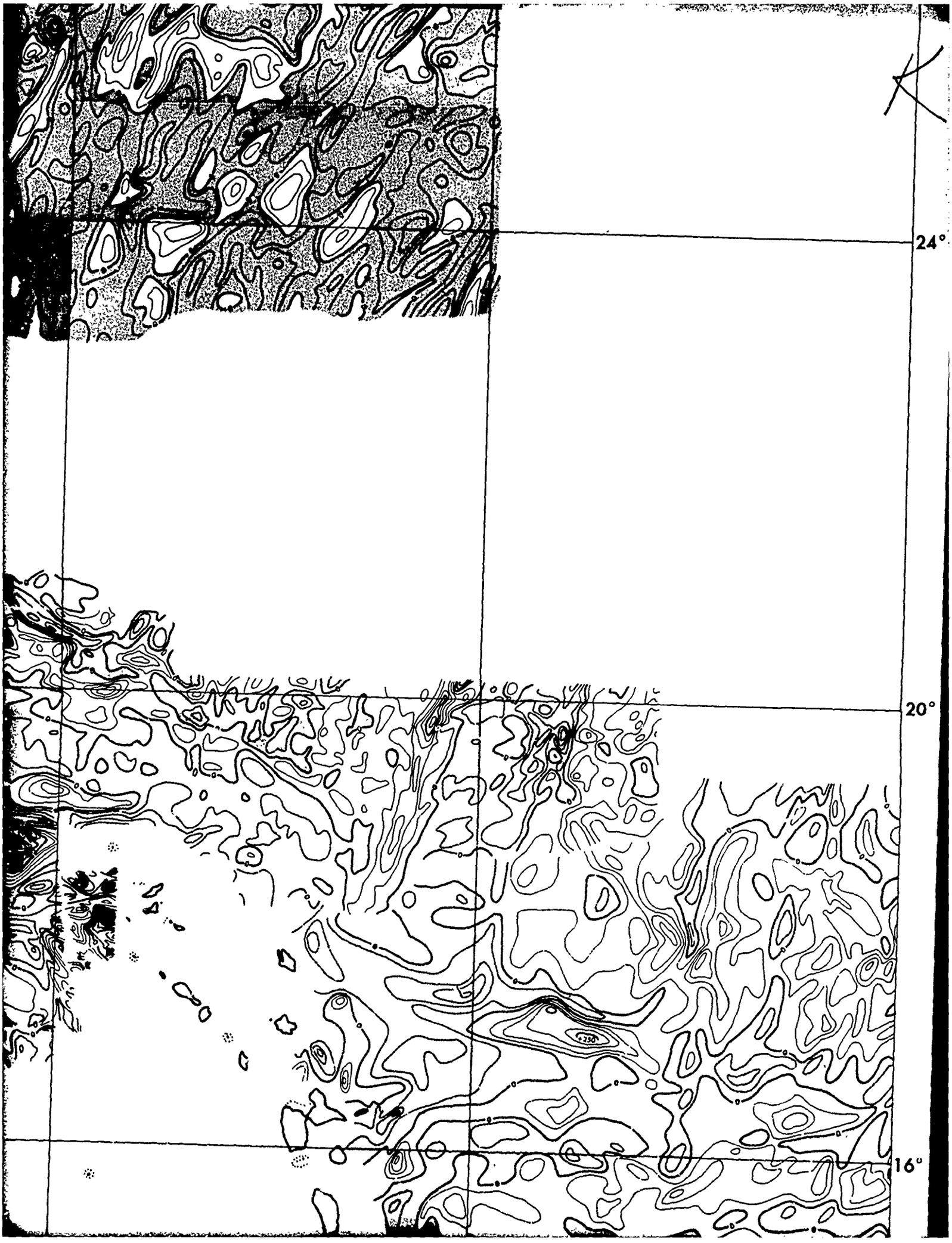
24°
20°
16°

RESIDUAL MAGNETIC INTENSITY

PRELIMINARY CONTOUR CHART

GULF OF MEXICO — CARIBBEAN SEA — NORTH AMERICAN

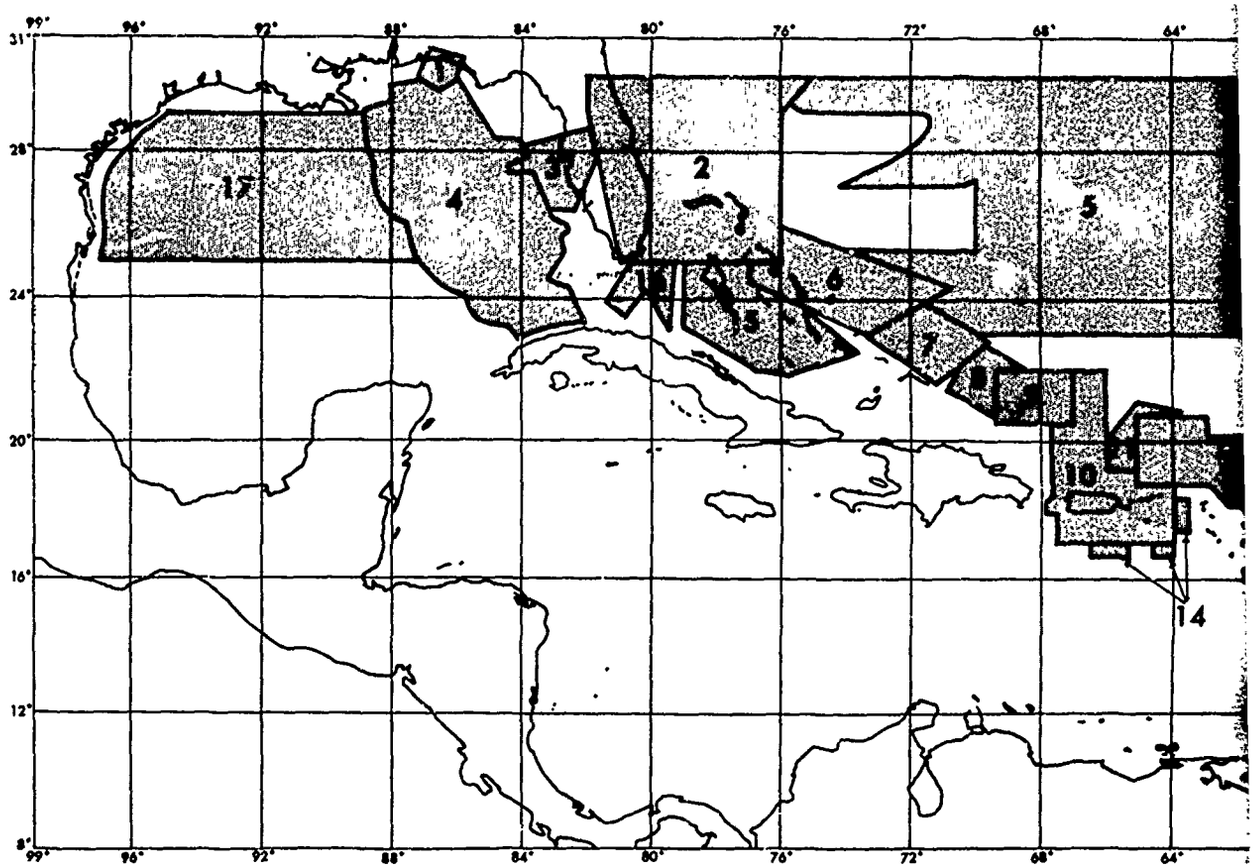

Area	Survey Altitude (feet)	Track Spacing (nm)	Track Orientation
1	20,000	2	N-S&E-W
2	500	5	NW-SE
3	1,000	5	SW-NE
4	0	15	E-W
5	0	20	E-W
6	500	5	NW-SE
7	0	5	NE-SW
8	600	5	NE-SW
9	0	3	E-W
10	1,000	10	N-S
11	0	5	NE-SW
12	0	3	N-S&E-W
13	1,000	10	E-W
14	0	5	N-S
15	1,500	5	NE-SW
16	0	10	EW-NS
17	0	10	E-W

CONTOUR INTERVAL

NEGATIVE RESIDUALS

VARIOUS REGIONALS

MERCATOR PROJECTI

SCALE 1° LONGITUDE

16°

12°

8°

99°

96°

92°

TIC INTENSITY

OUR CHART

EA – NORTH AMERICAN BASIN

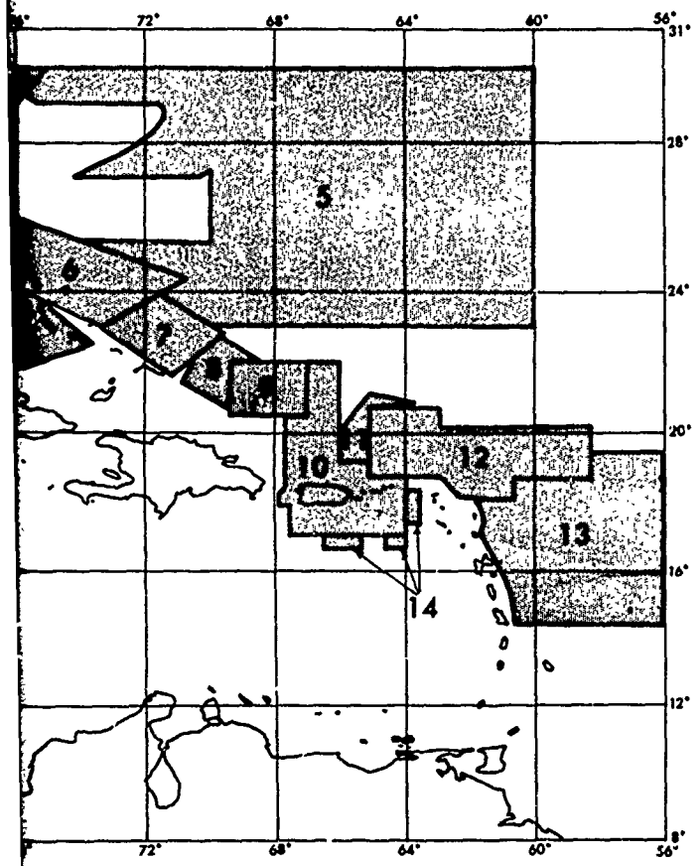

CONTOUR INTERVAL 50 GAMMAS

NEGATIVE RESIDUALS SHADED

VARIOUS REGIONALS REMOVED

MERCATOR PROJECTION

SCALE 1° LONGITUDE = 1 INCH

92°

88°

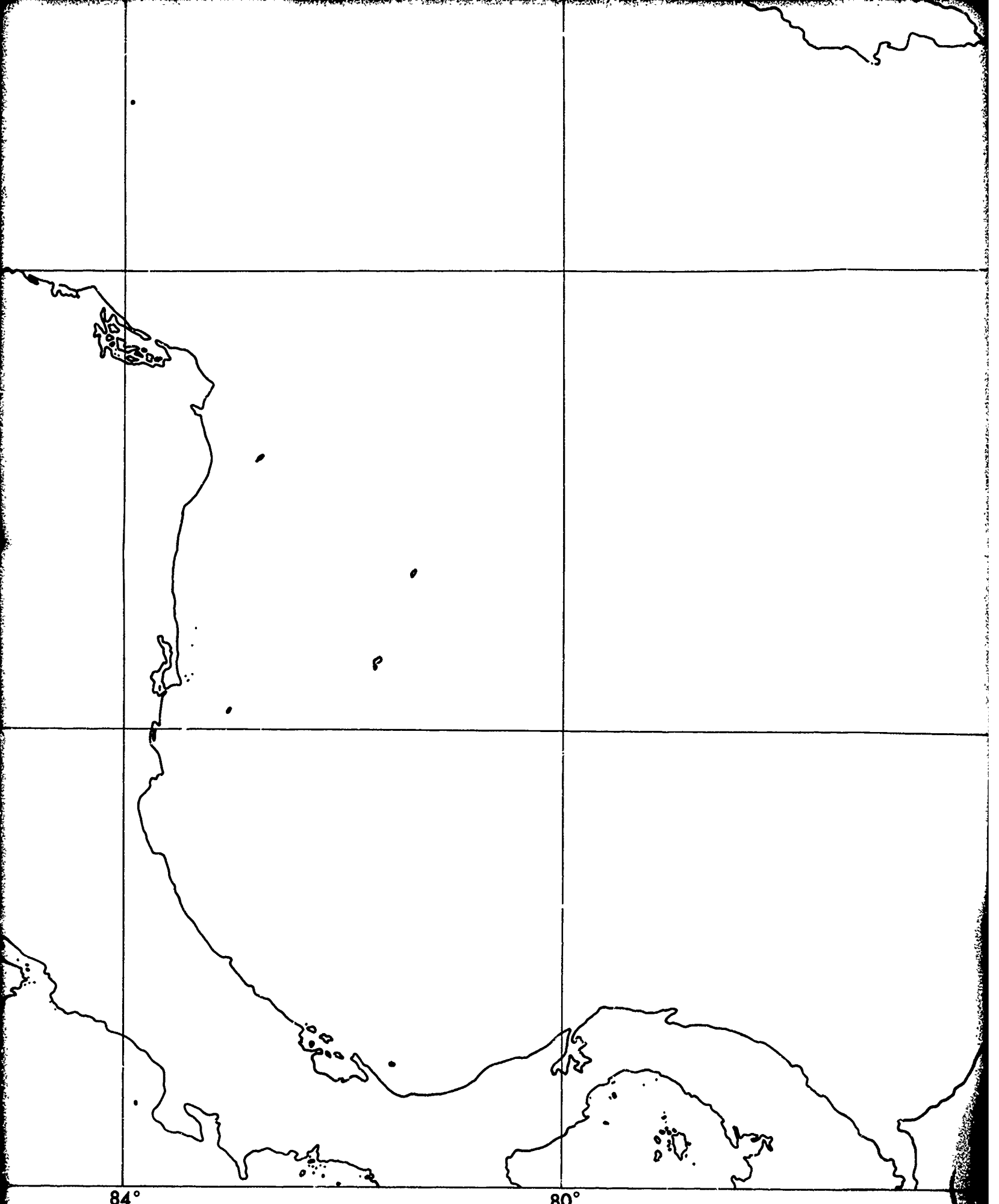

FIGURE 3-1 RESIDUAL MAGNETIC INTENSITY

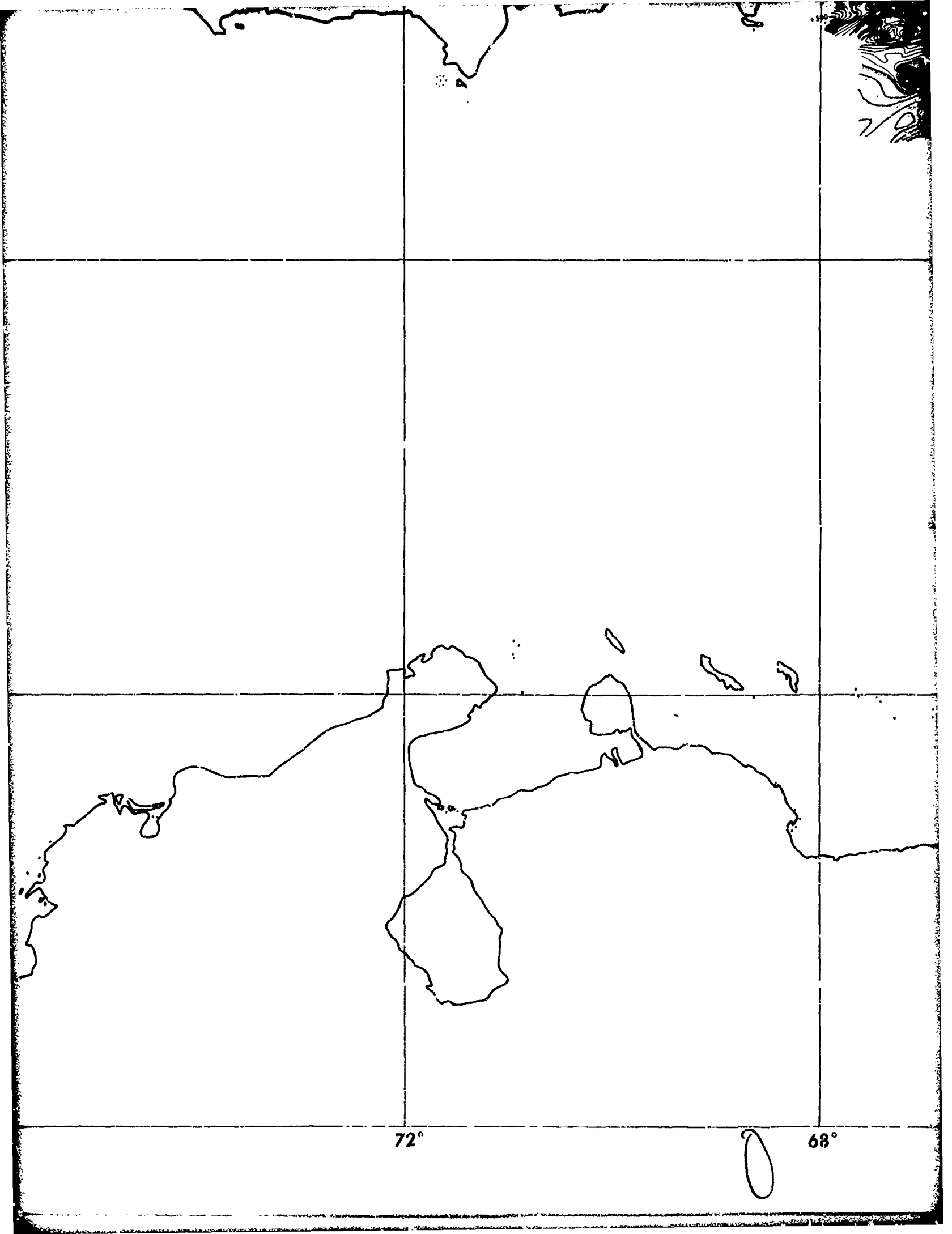
72°
68°

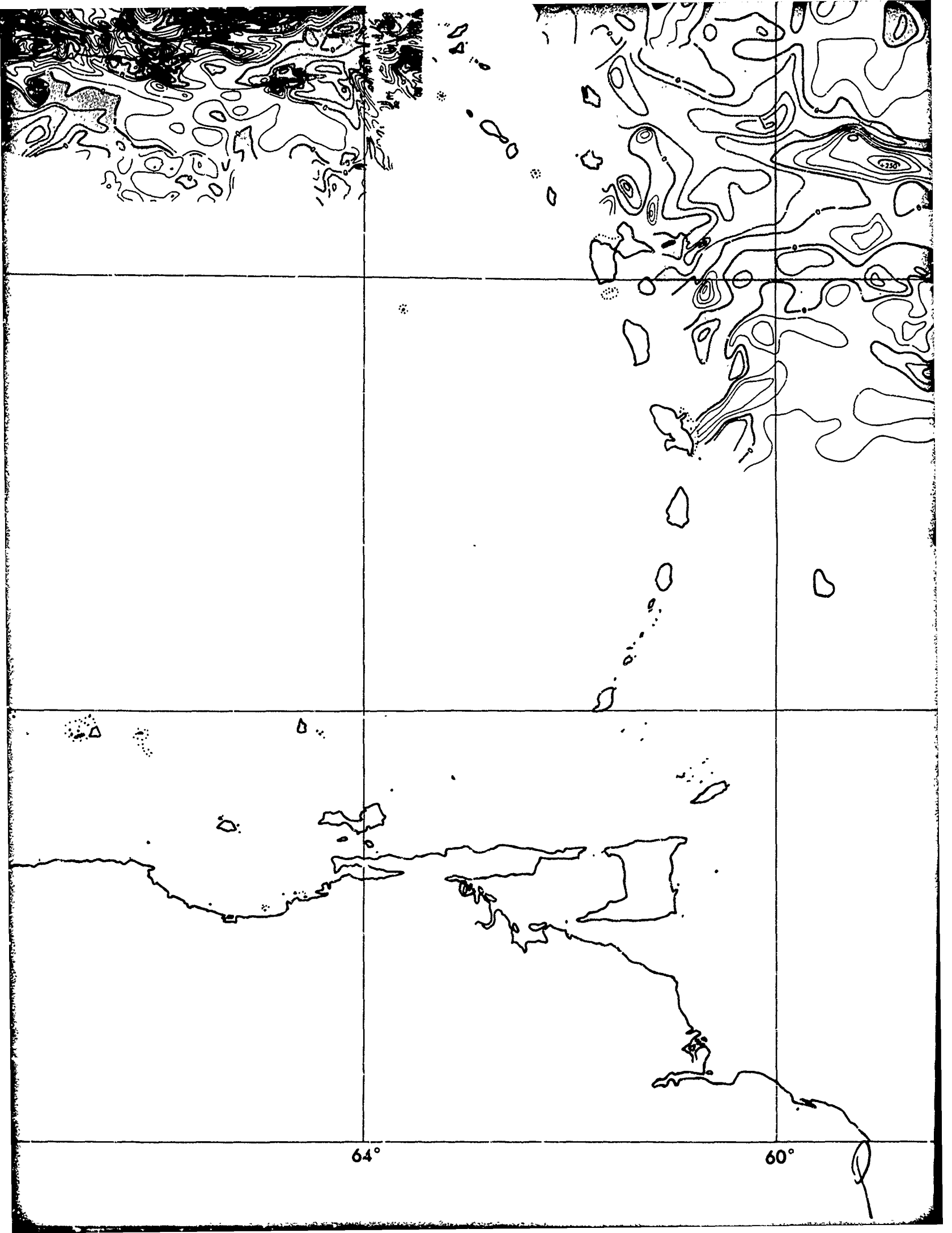
64°
60°

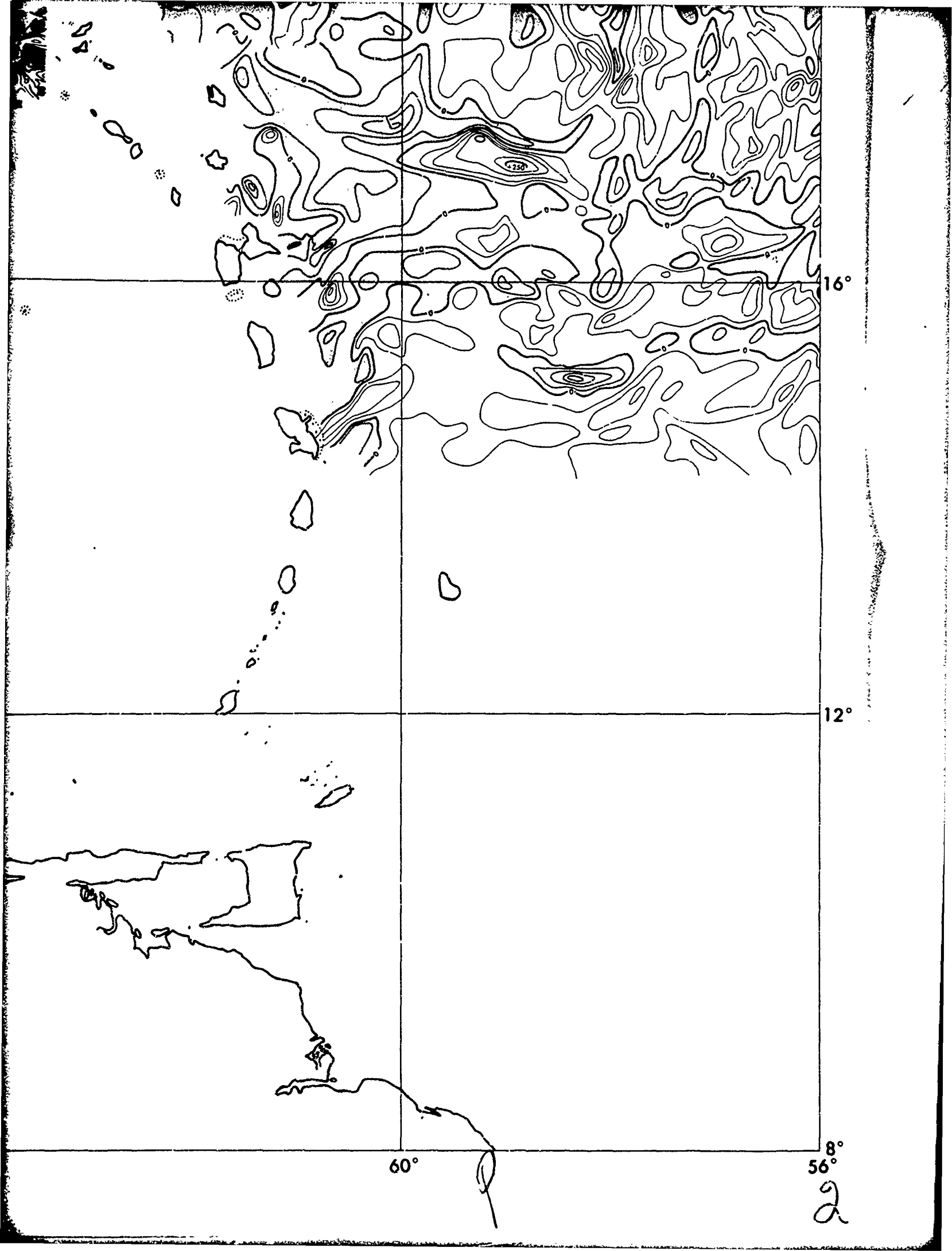
16°
12°
8°
60°
56°

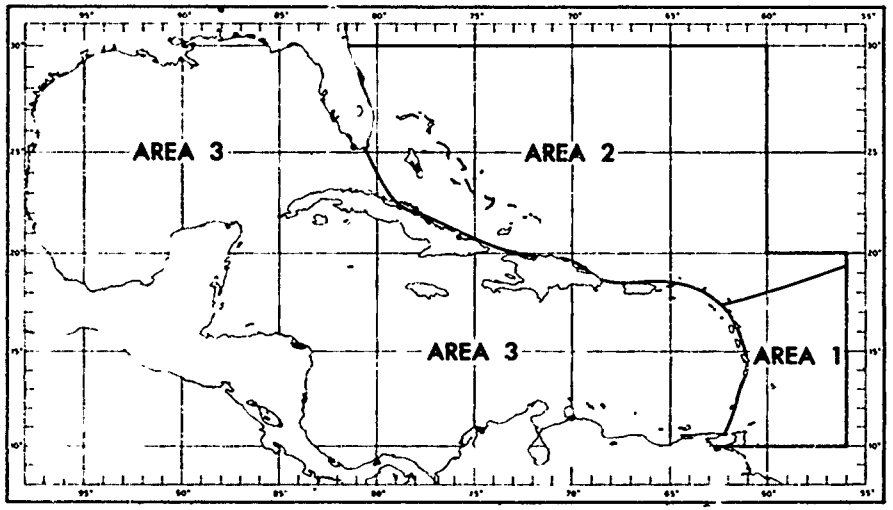

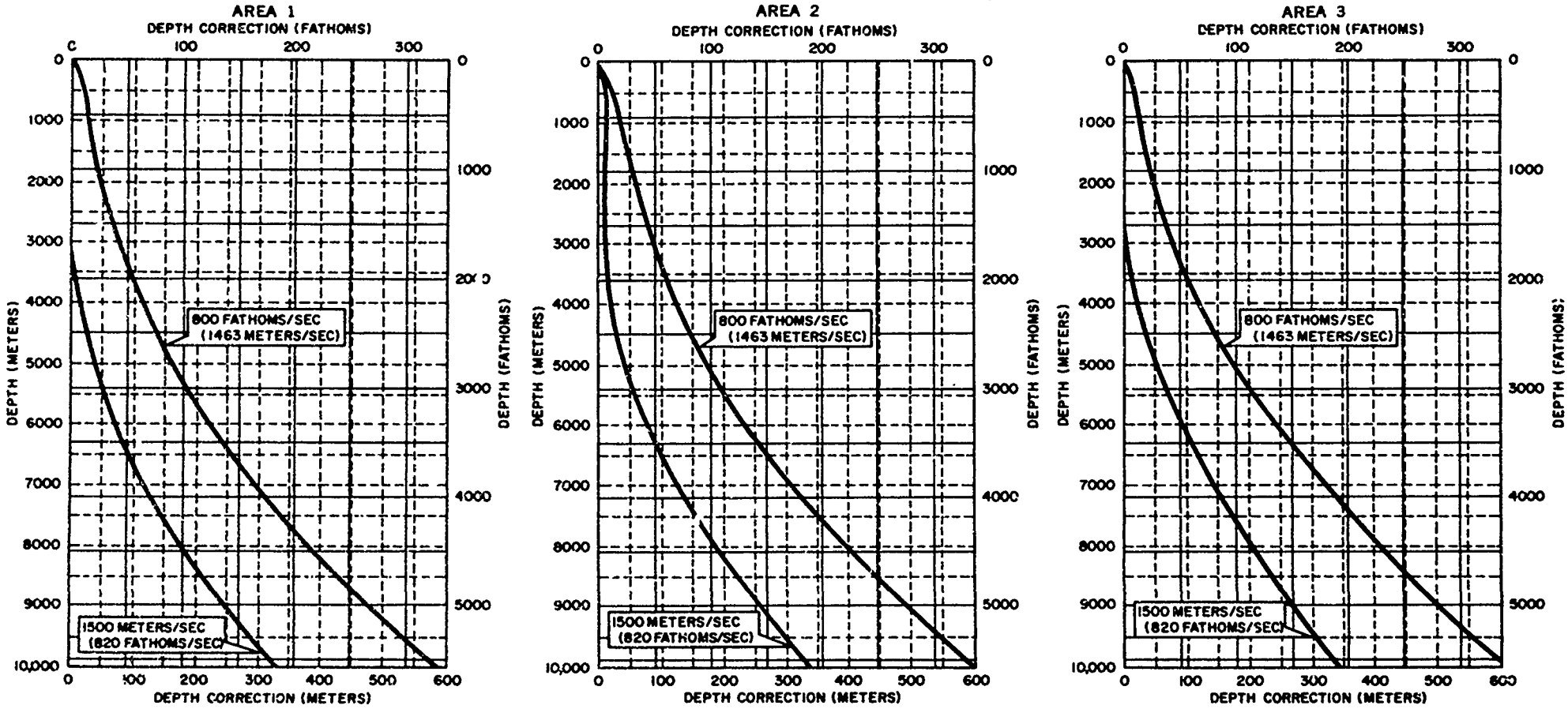

FIGURE 4-110 DEPTH CORRECTIONS FOR SOUND VELOCITY VARIATIONS

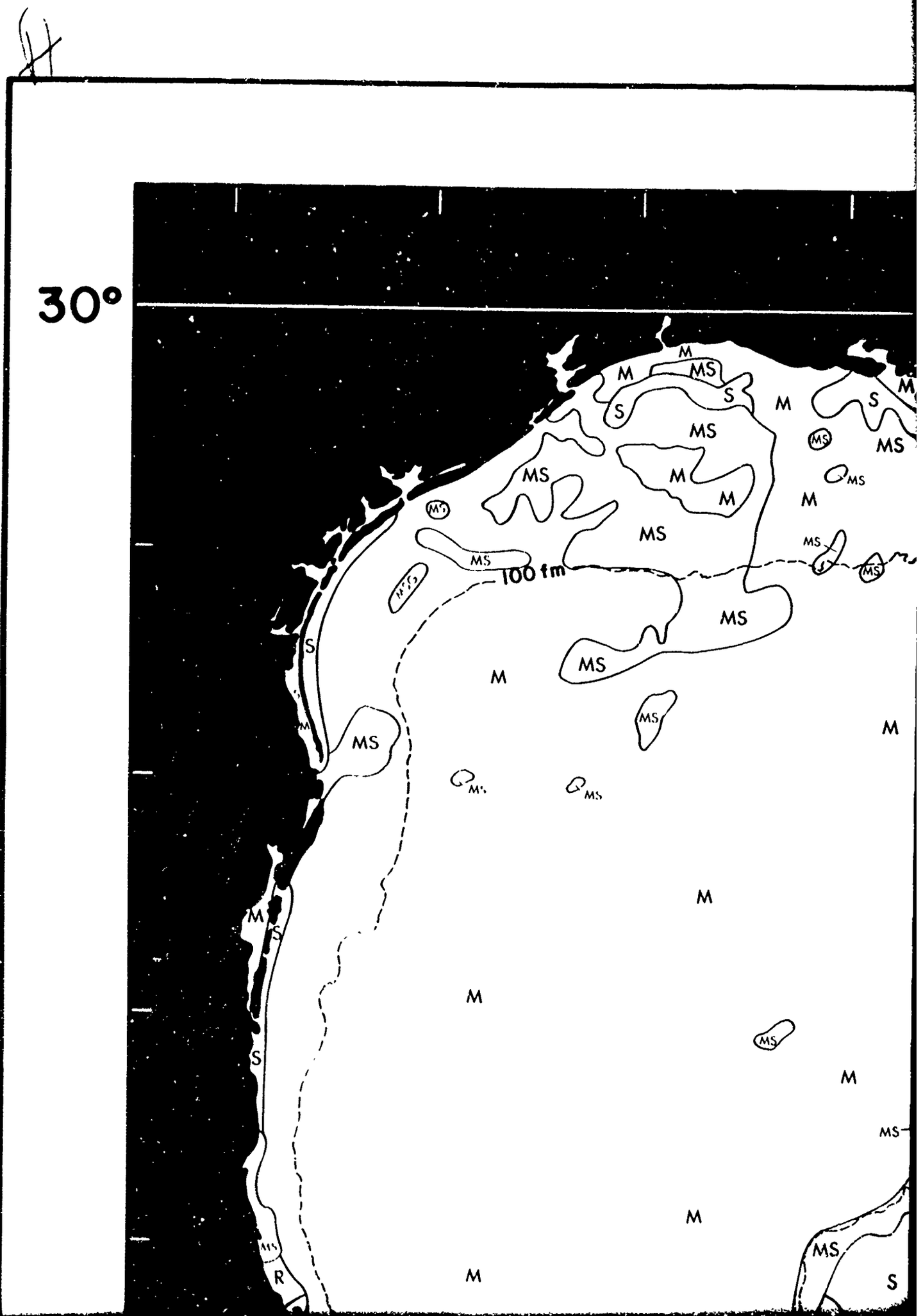
30°
100 fm

B

90°

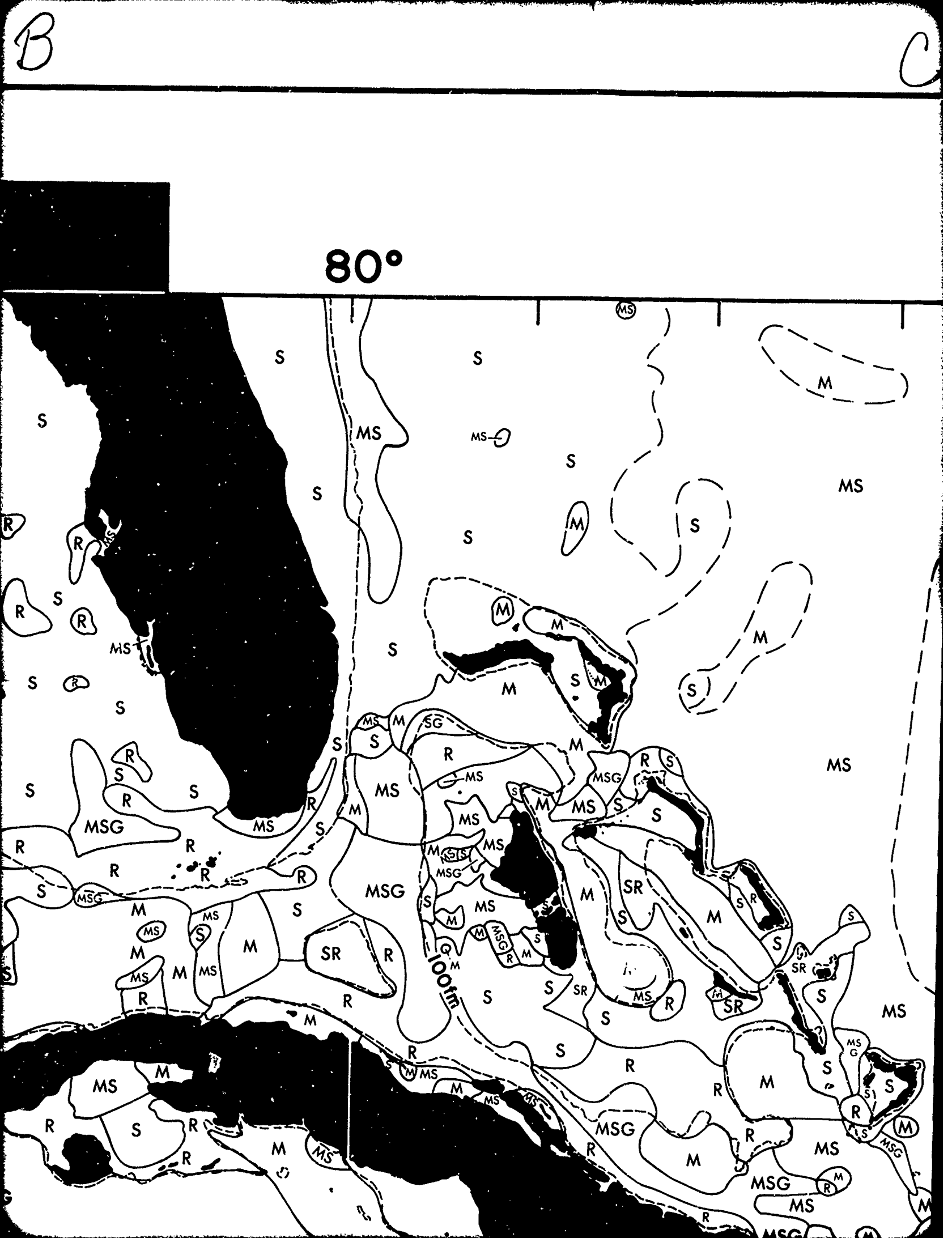
B
C
80°
100fm

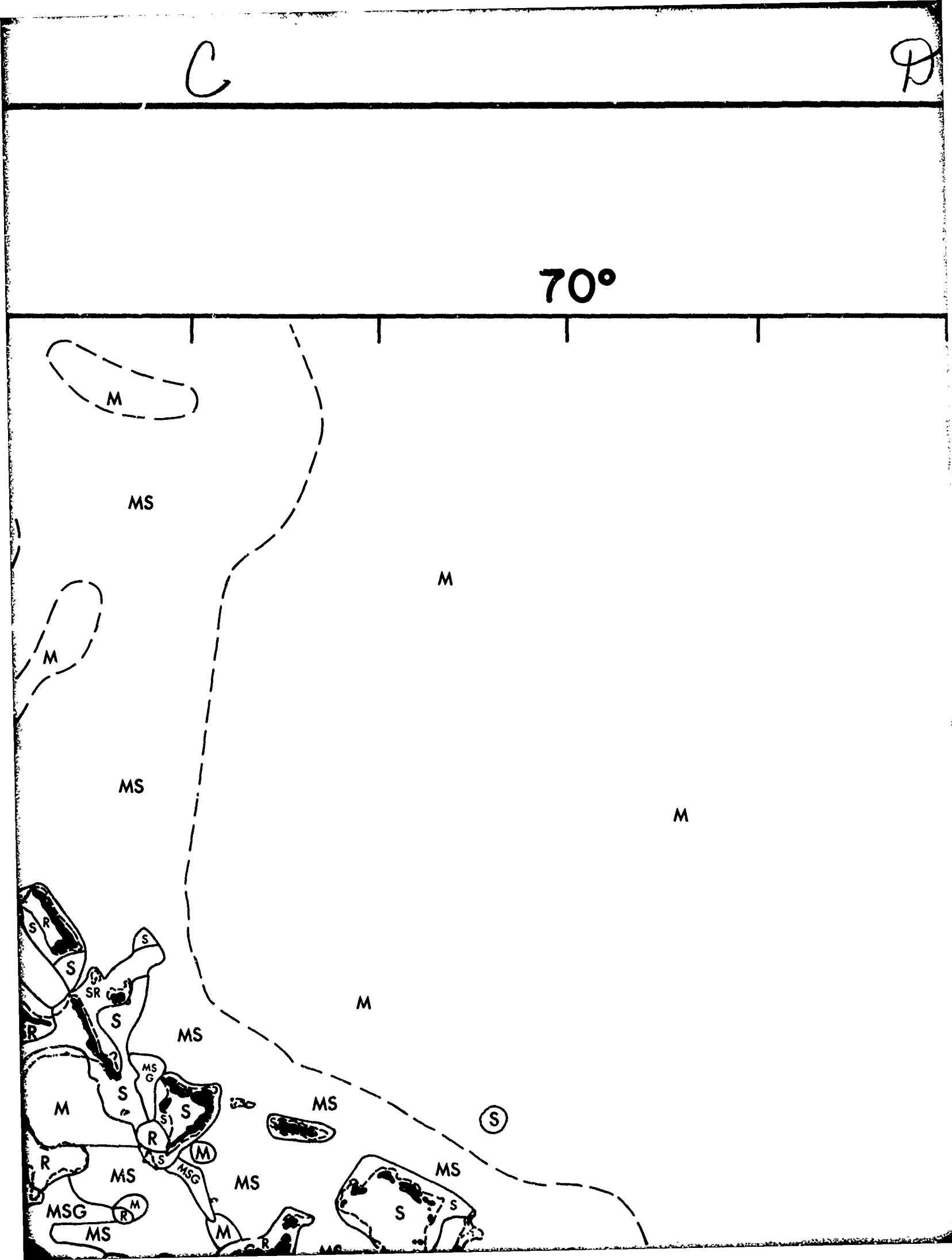
C
D
70°
M
MS
M
M
MS
M
S
R
S
S
SR
S
R
MS
G
S
M
S
S
MS
S
R
M
R
MS
MSG
MS
MSG
R
M
MS
M
R
MS
S
S
S

D

E

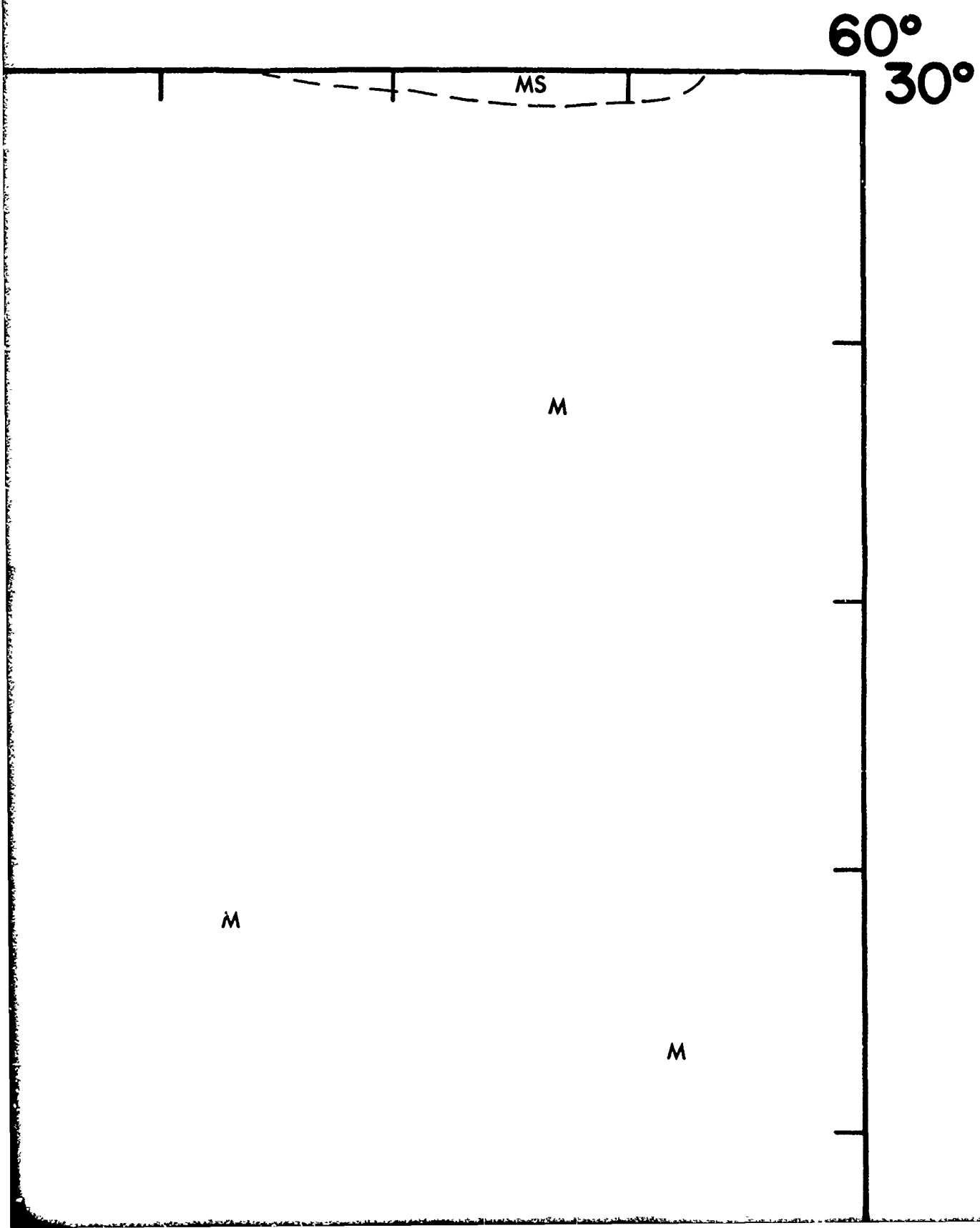

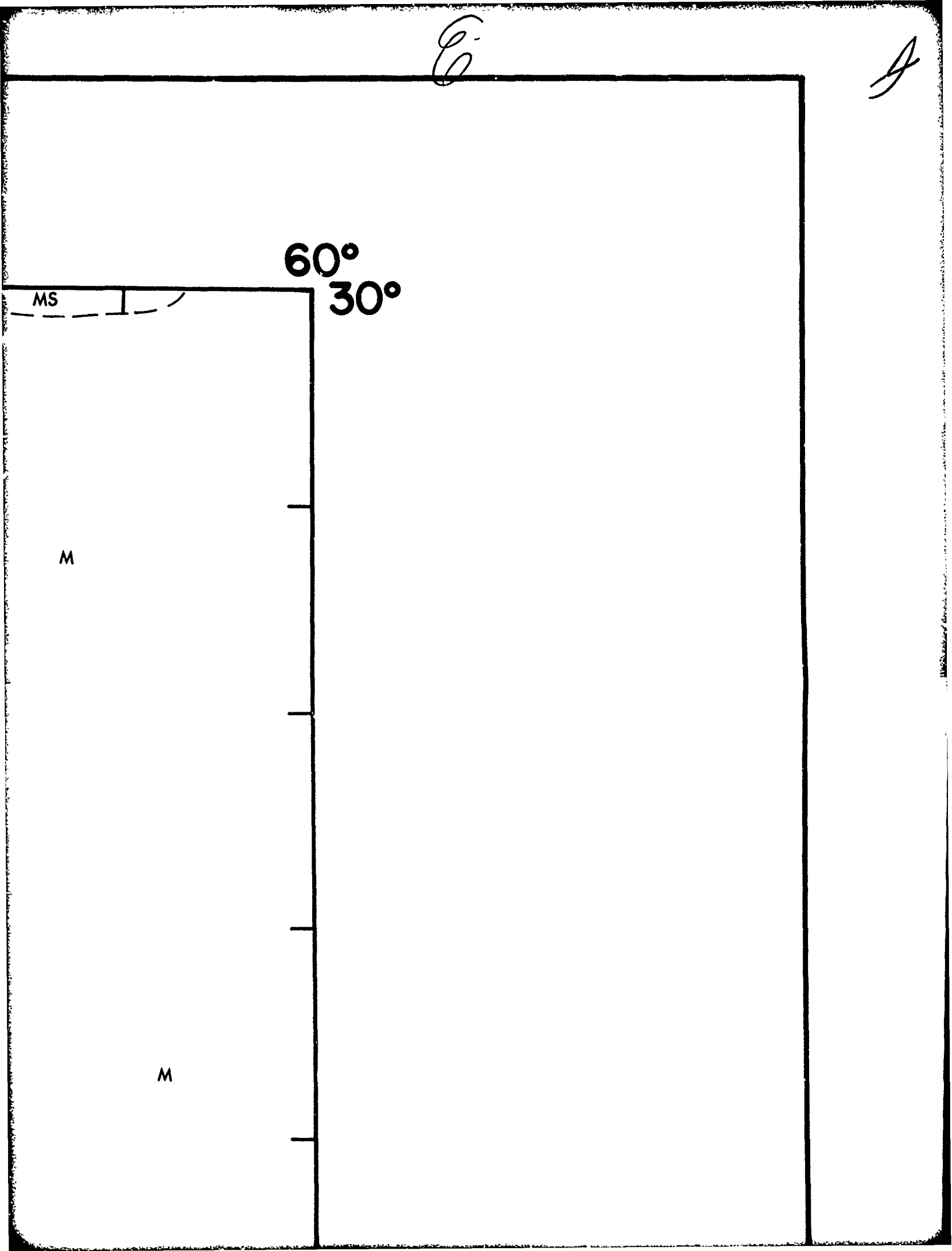
60°
30°
MS
M
M

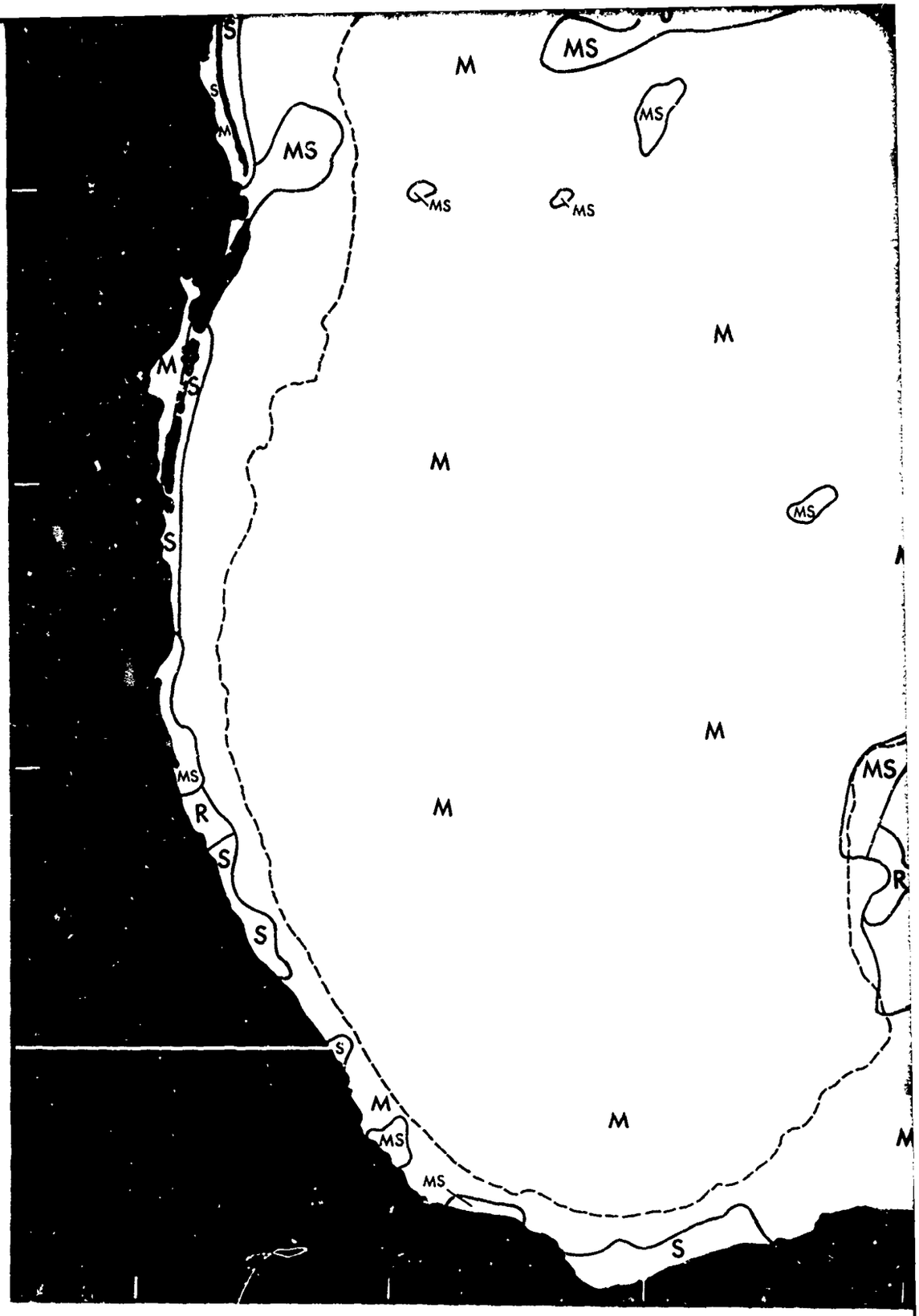
20°
MS
M
S
R
Q MS

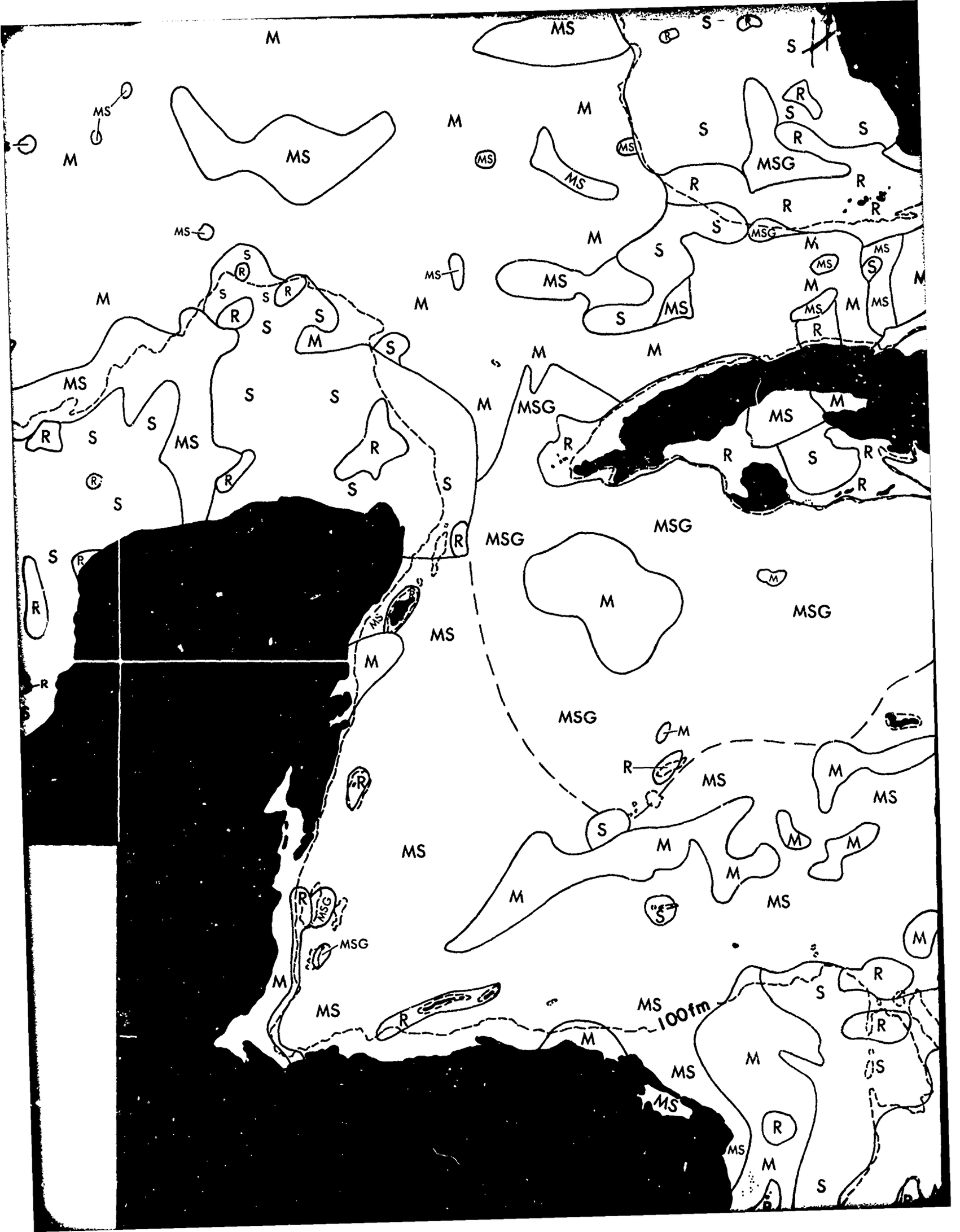
M
MS
S
R
MSG
100fm


100fm

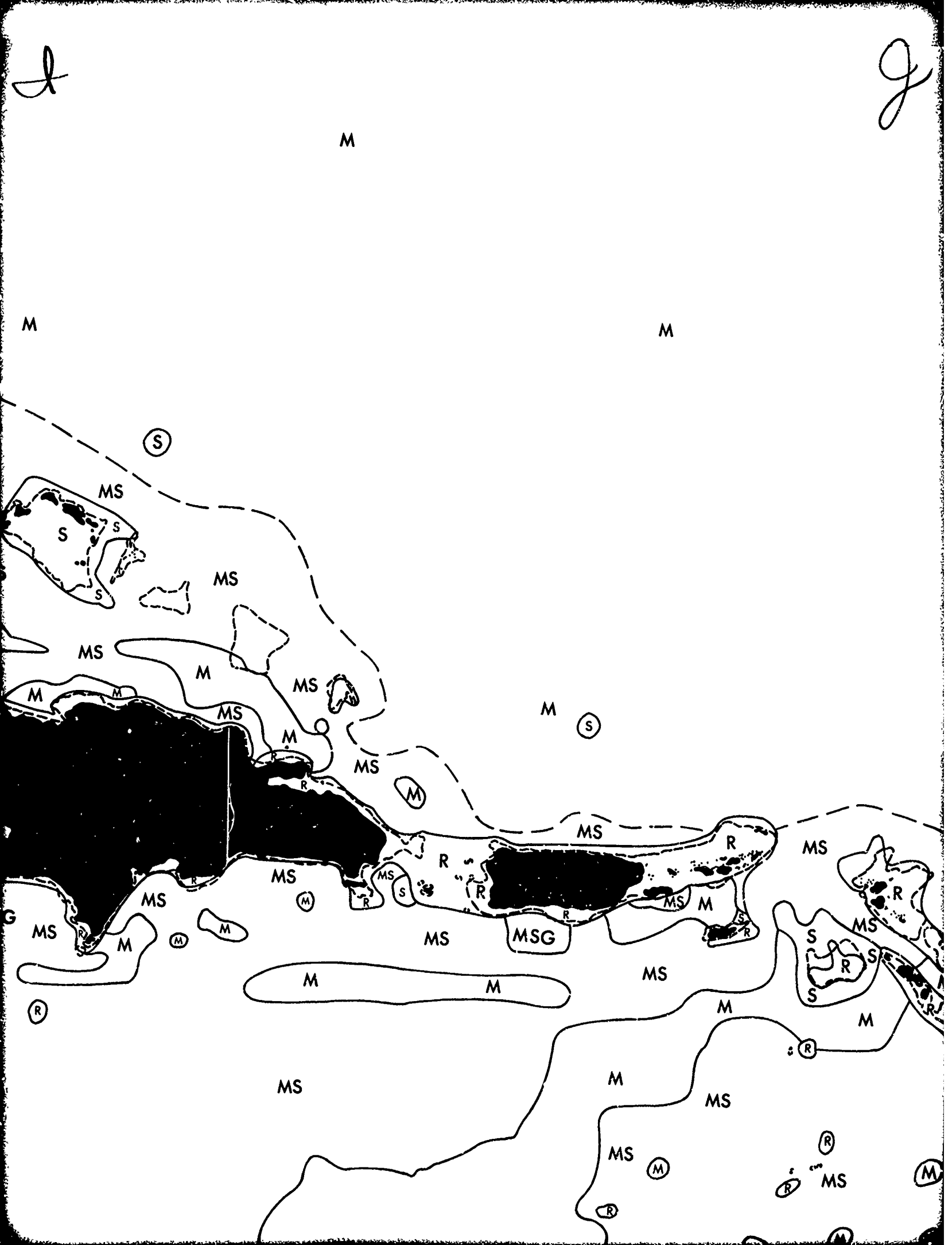
M
M
M
S
MS
S
S
S
MS
MS
M
M
M
MS
MS
M
M
S
MS
R
R
MS
MS
R
MS
MS
S
R
R
MS
M
MS
MS
M
M
MSG
MS
M
M
M
M
MS
M
MS
MS
M
MS
MS
M
MS
R

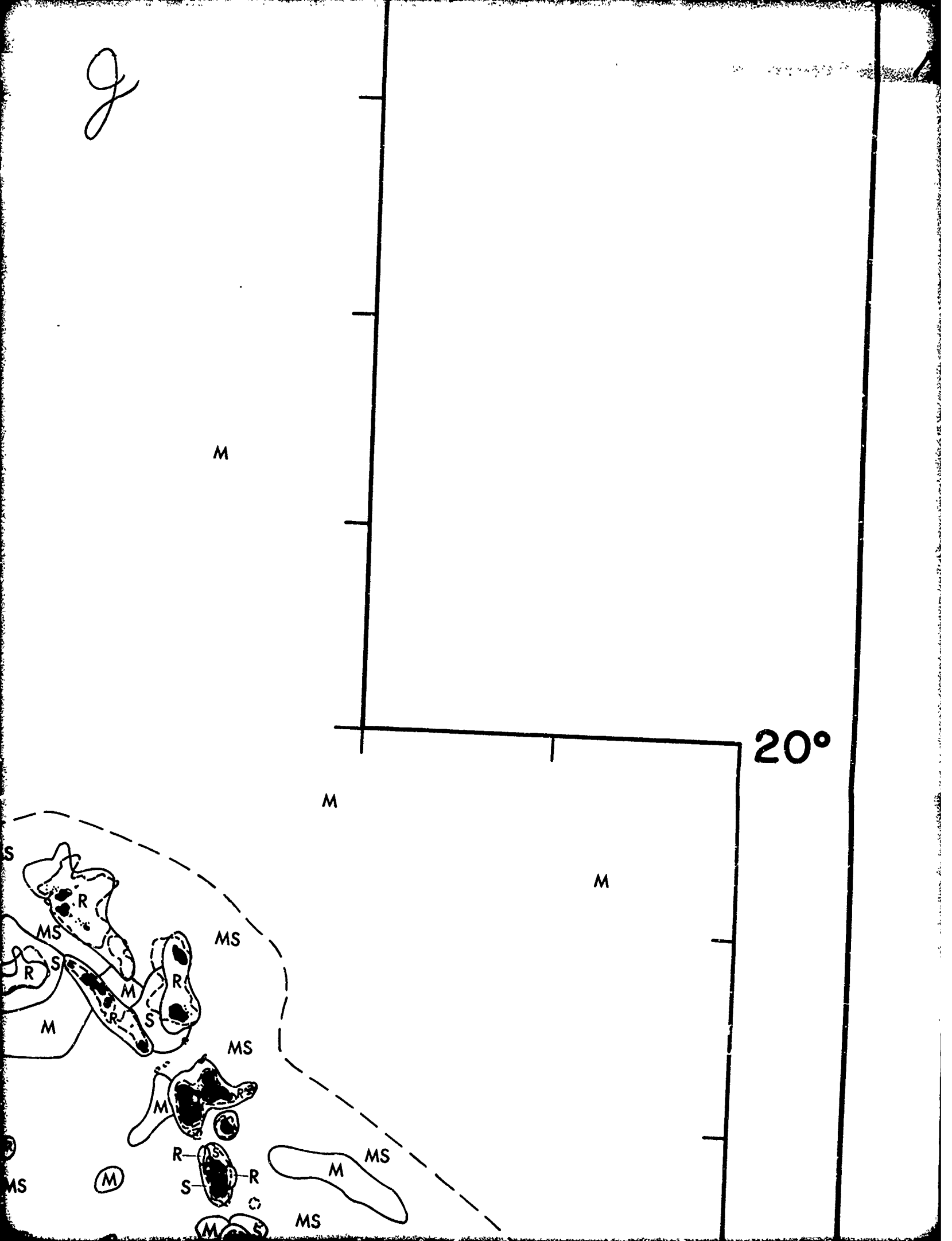
20°
M
M
M
MS
MS
MS
MS
MS
MS
R
S
R
S
R
S
R
S
R
S
R
S
M
M
M
M
M
M
M
M

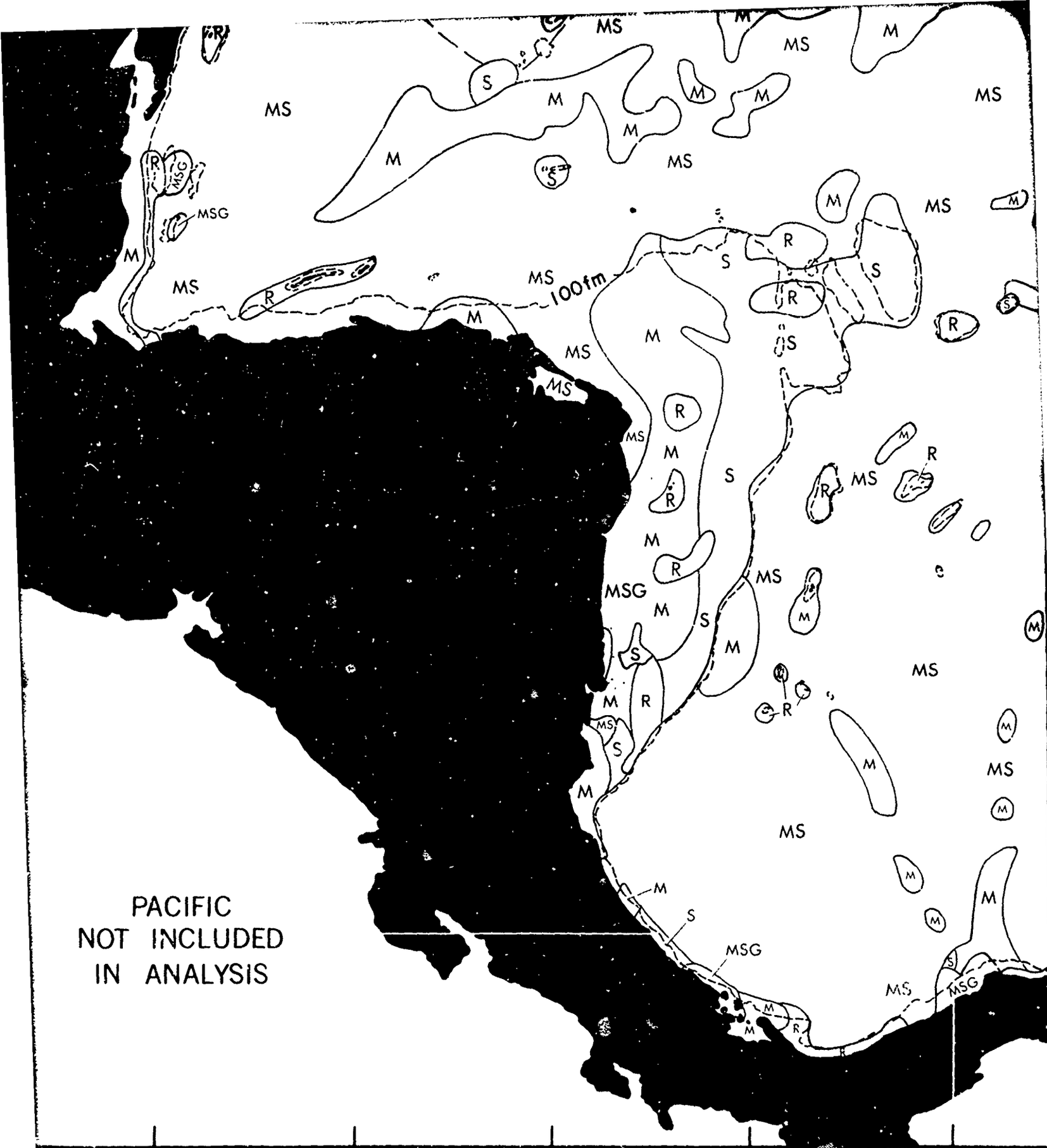
MS
M
S
R
MSG
100fm
PACIFIC
NOT INCLUDED
IN ANALYSIS
80°

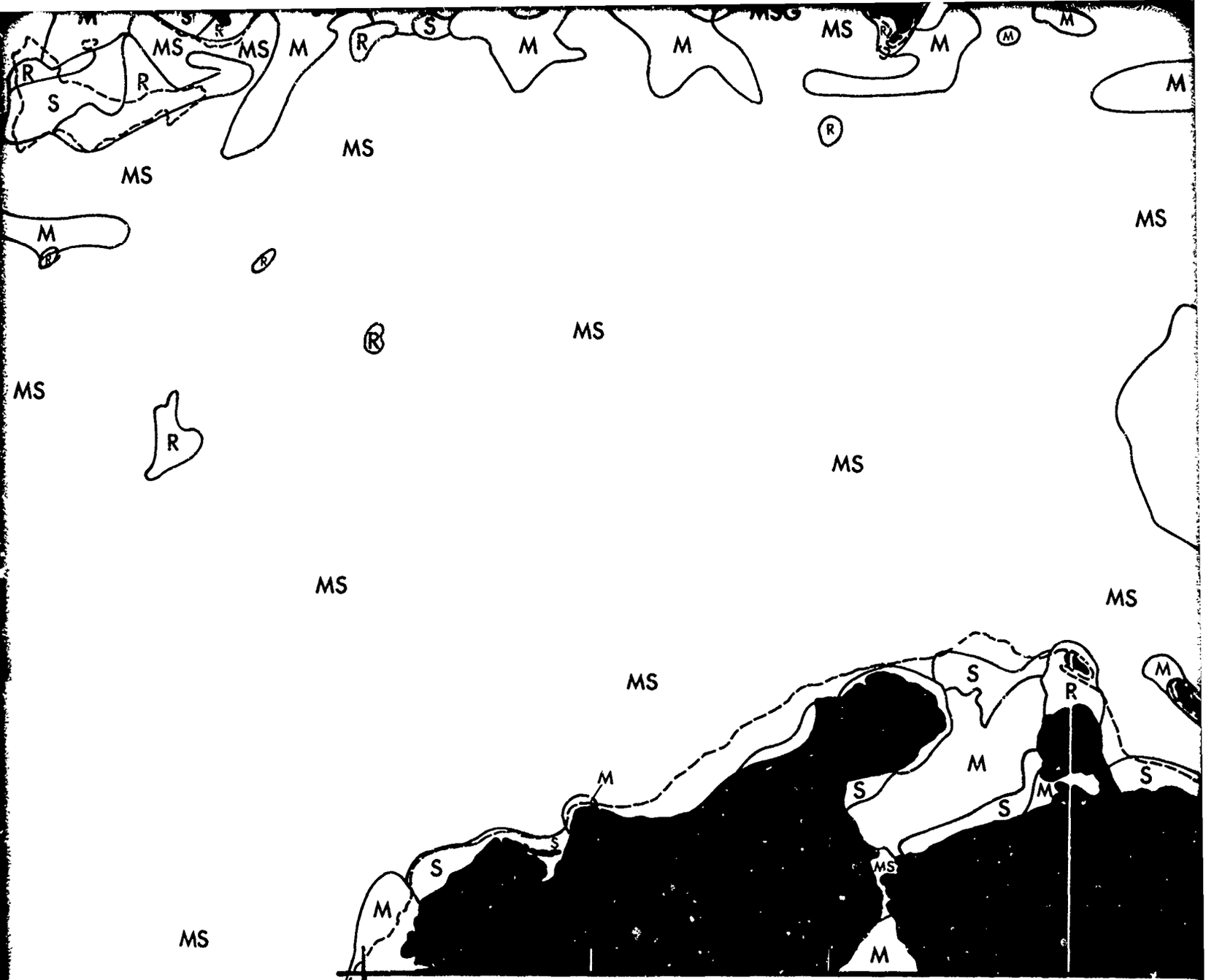

LEGEND

M	MUD (CLAY AND/OR SILT)
MS	MUD-SAND
S	SAND, SAND-GRAVEL AND/OR SHELL
MSG	MUD-SAND-GRAVEL AND/OR SHELL
R	COMBINATIONS OF BOTTOM TYPES DOMINATED BY GRAVEL AND ROCK (INCLUDES CORAL REEFS)

URE 4-111 BOTTOM SEDIMENTS


MS
M
R
S
MSG
100fm
60°

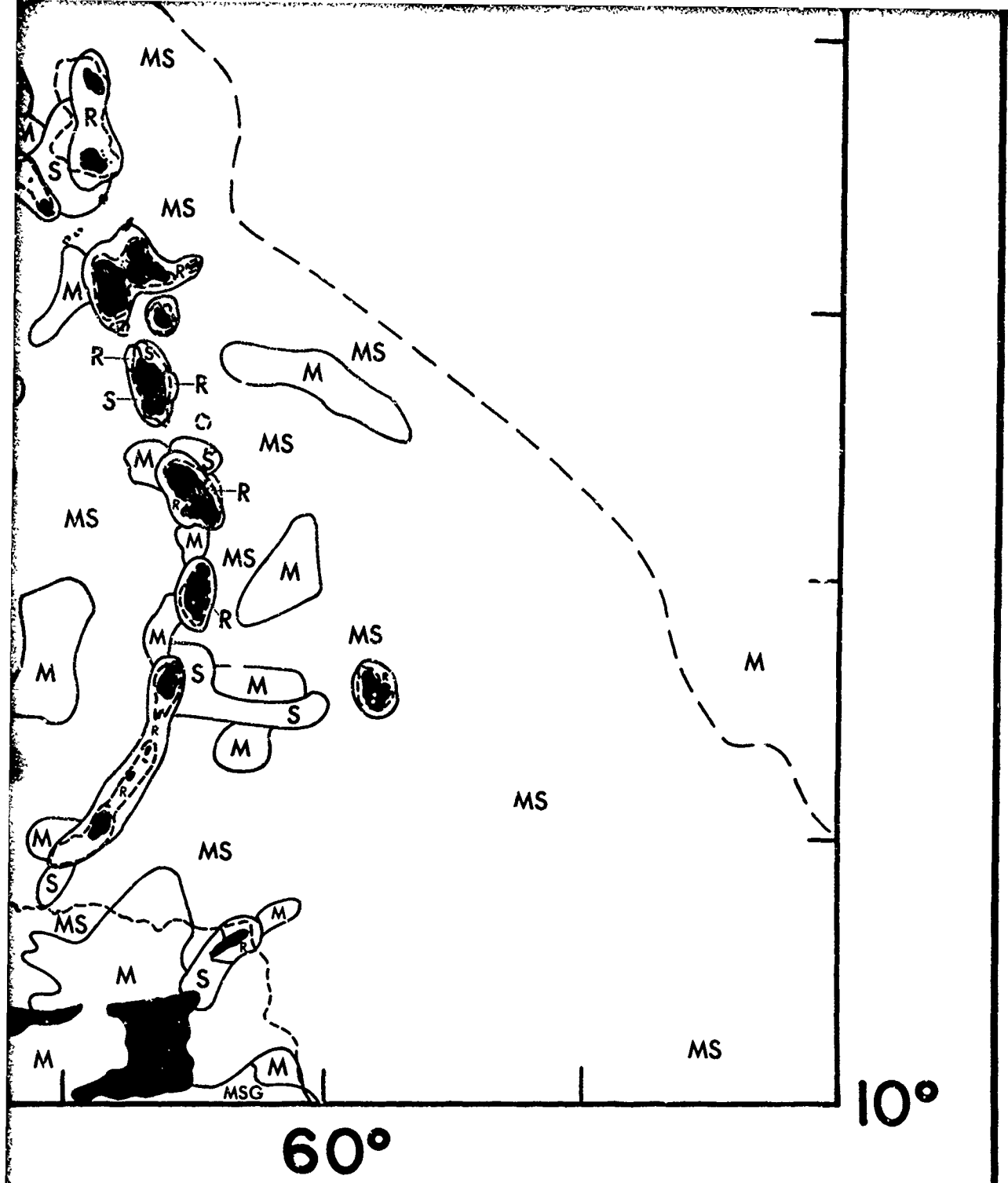
MS
R
S
M
MSG
60°
10°

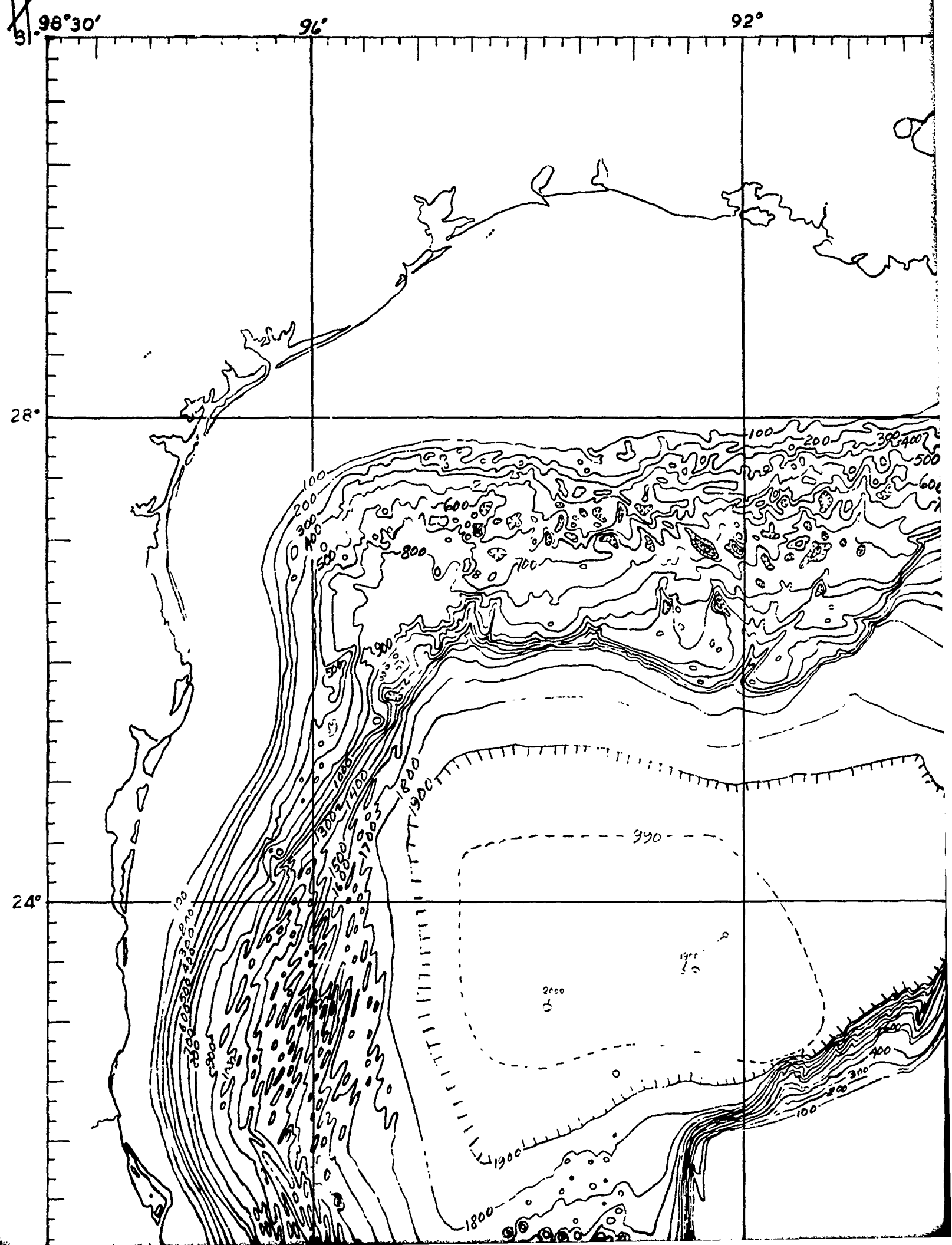
98°30'
96°
92°
28°
24°
100
200
300
400
500
600
700
800
900
1000
1100
1200
1300
1400
1500
1600
1700
1800
1900
2000

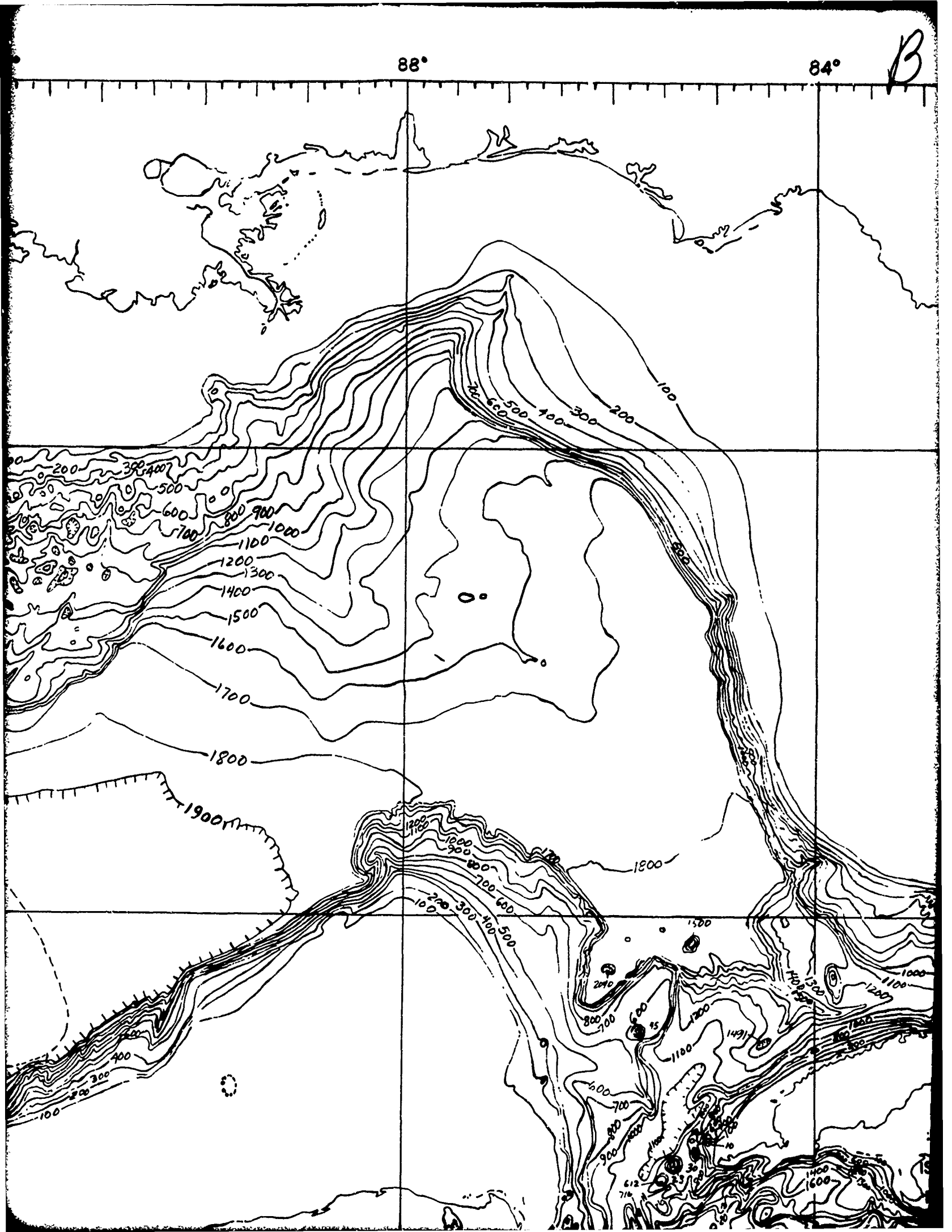
88°
84°
B

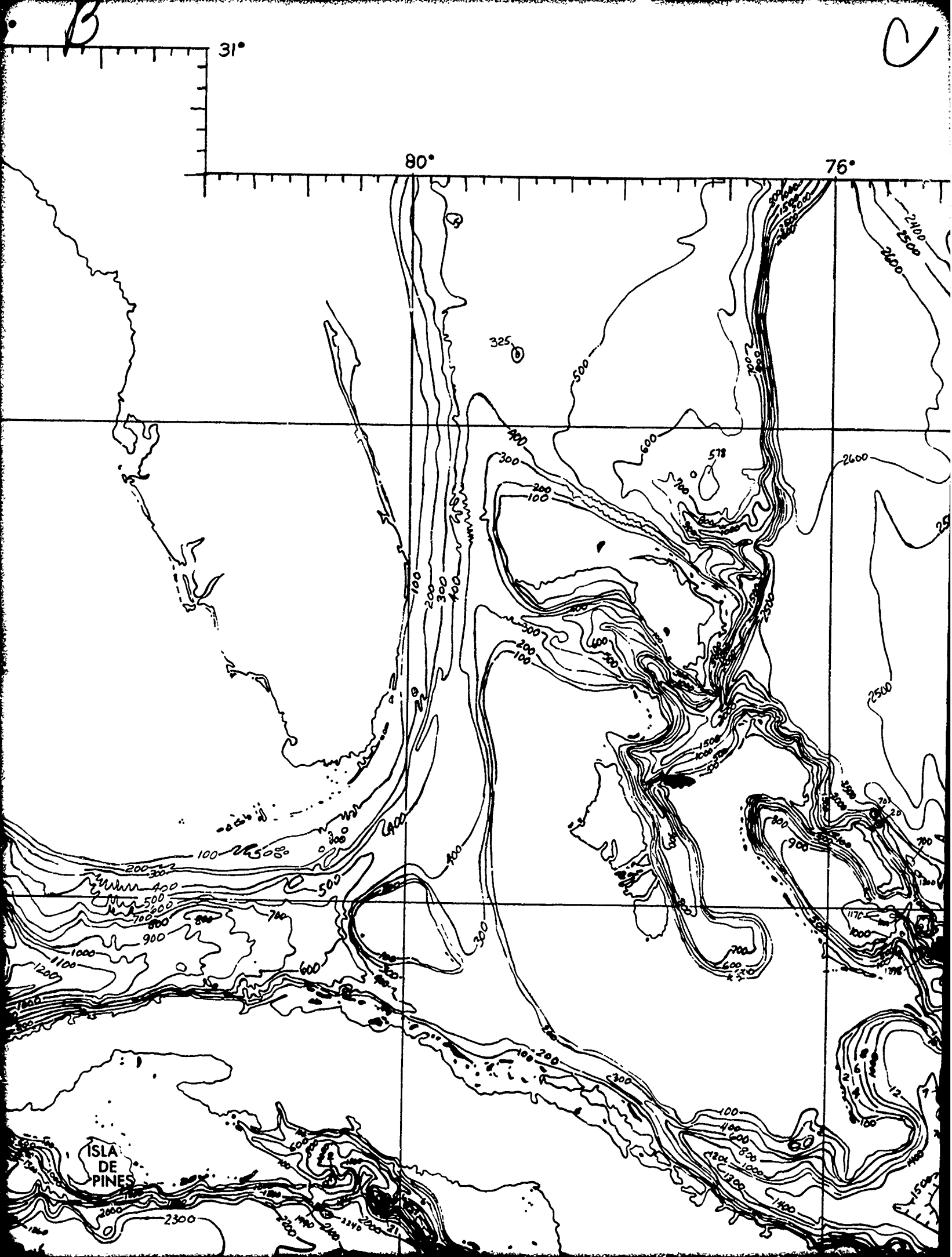
B
C
31°
80°
76°
ISLA
DE
PINES

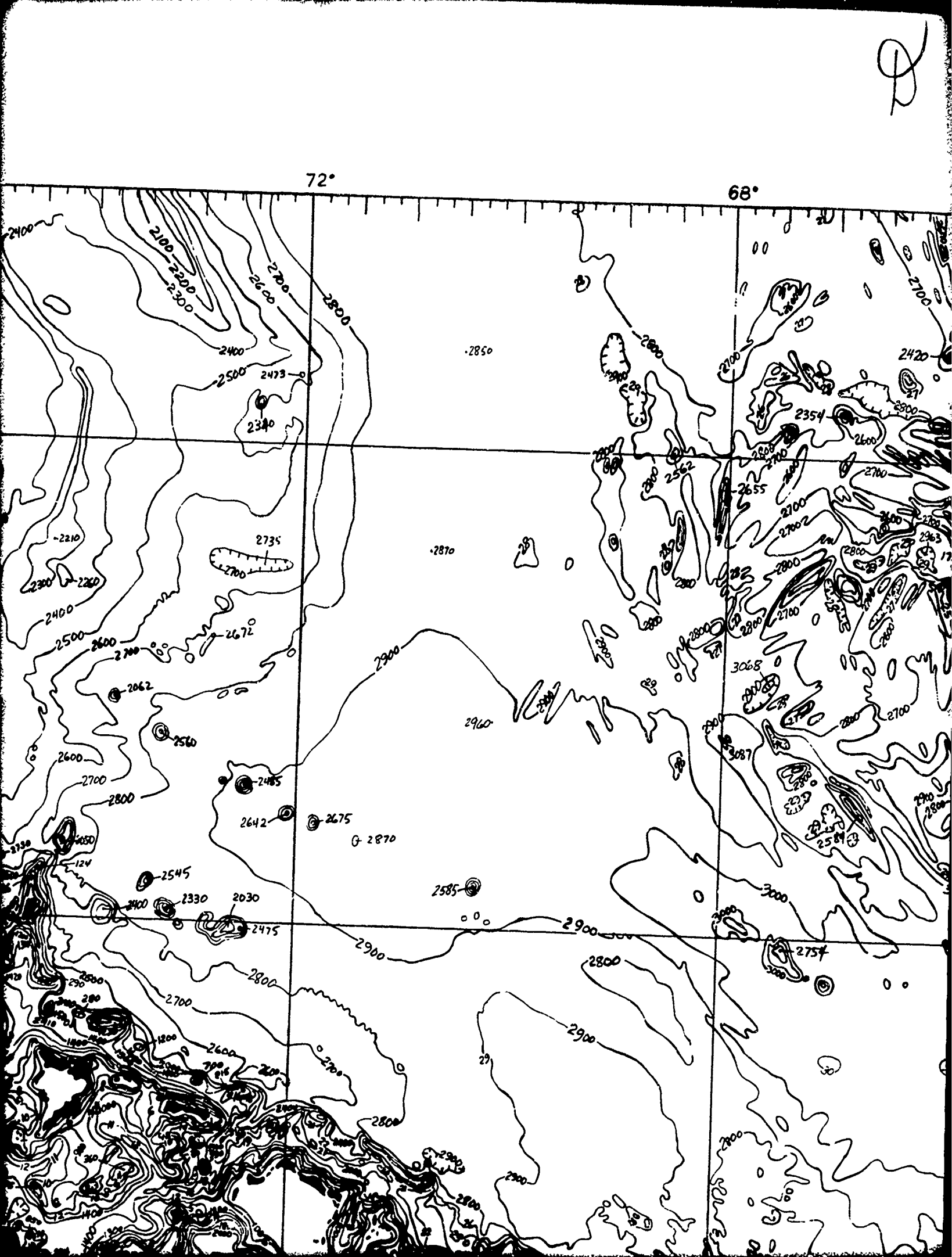
72°
68°
2400
2100
2200
2300
2600
2700
2800
2850
2473
2340
2735
2870
2210
2260
2672
2062
2560
2960
2485
2642
2675
2870
2545
2585
2330
2030
2475
3000
2754
2562
2655
2354
2420
2363
3068
3087
2584
2900

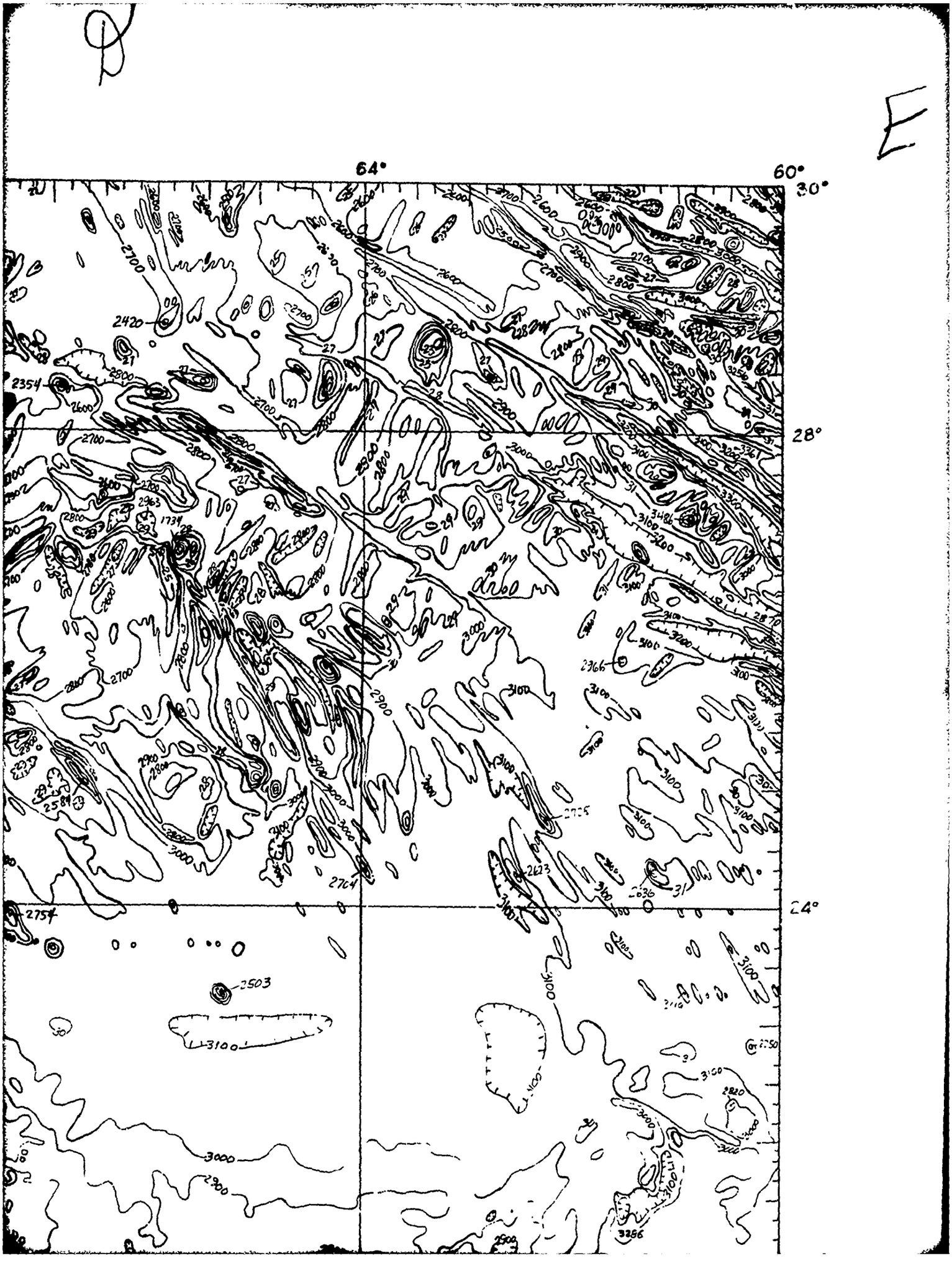
64°
60°
30°
28°
24°
2420
2354
2963
1739
2589
2754
2503
3100
3000
2900
2800
2700
2600
3256

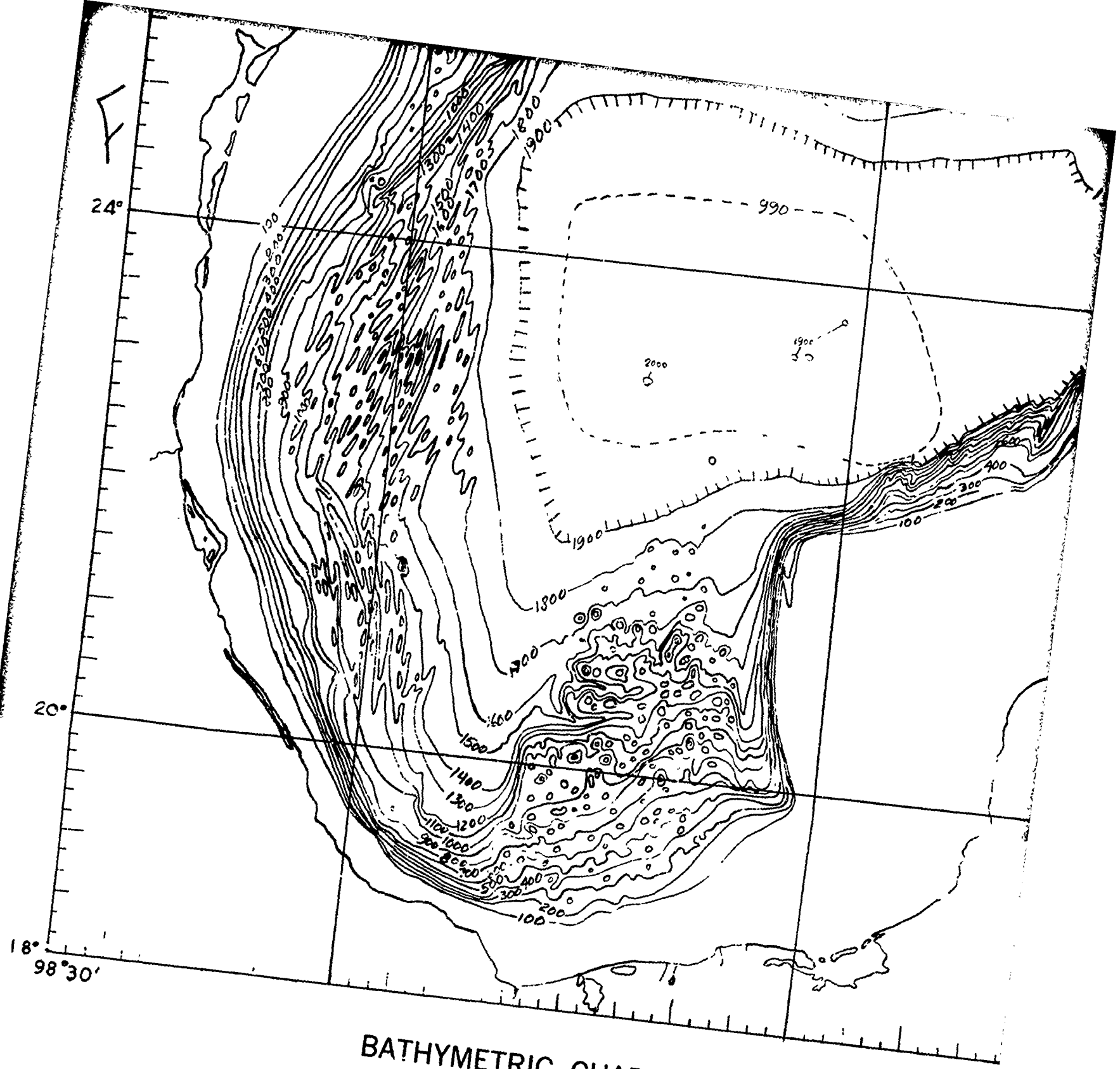

BATHYMETRIC CHART

Gulf of Mexico-Caribbean Sea-North American Basin

Scale: 1" = 1° longitude, $\frac{1}{(4,300,000)}$

Contour Interval: 100 fathoms* (Based on soundings uncorrected for variations in the velocity of sound in sea water.)

Compiled by Undersea Surveillance Oceanographic Project from the following sources:

1006 N	0906 N	0806 N	0706 N	0606 N
1005 N	0905 N	0805 N	0705 N	0605 N
1004 N	0904 N	0804 N	0704 N	0604 N

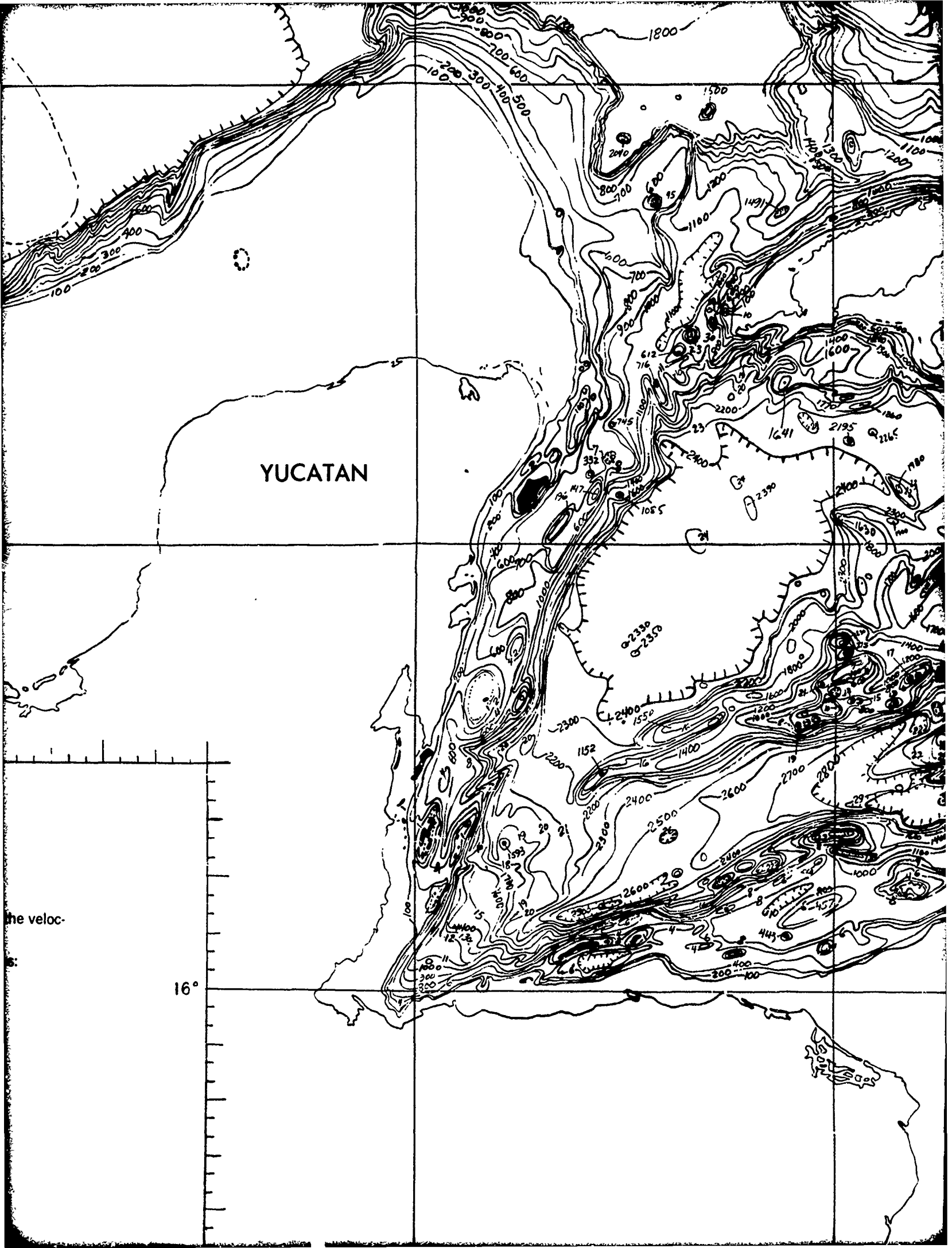

he veloc-

s:

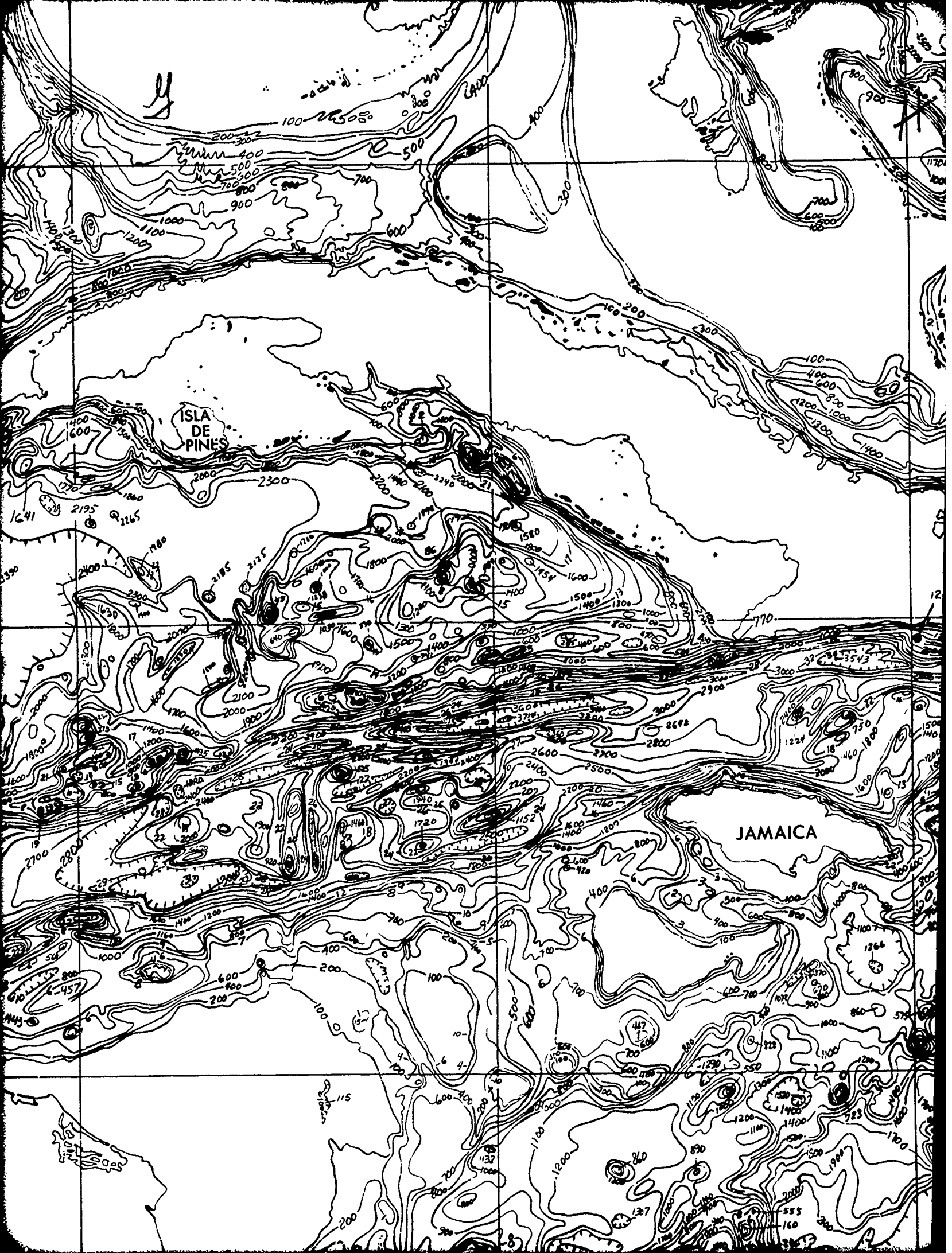
ISLA
DE
PINES
JAMAICA

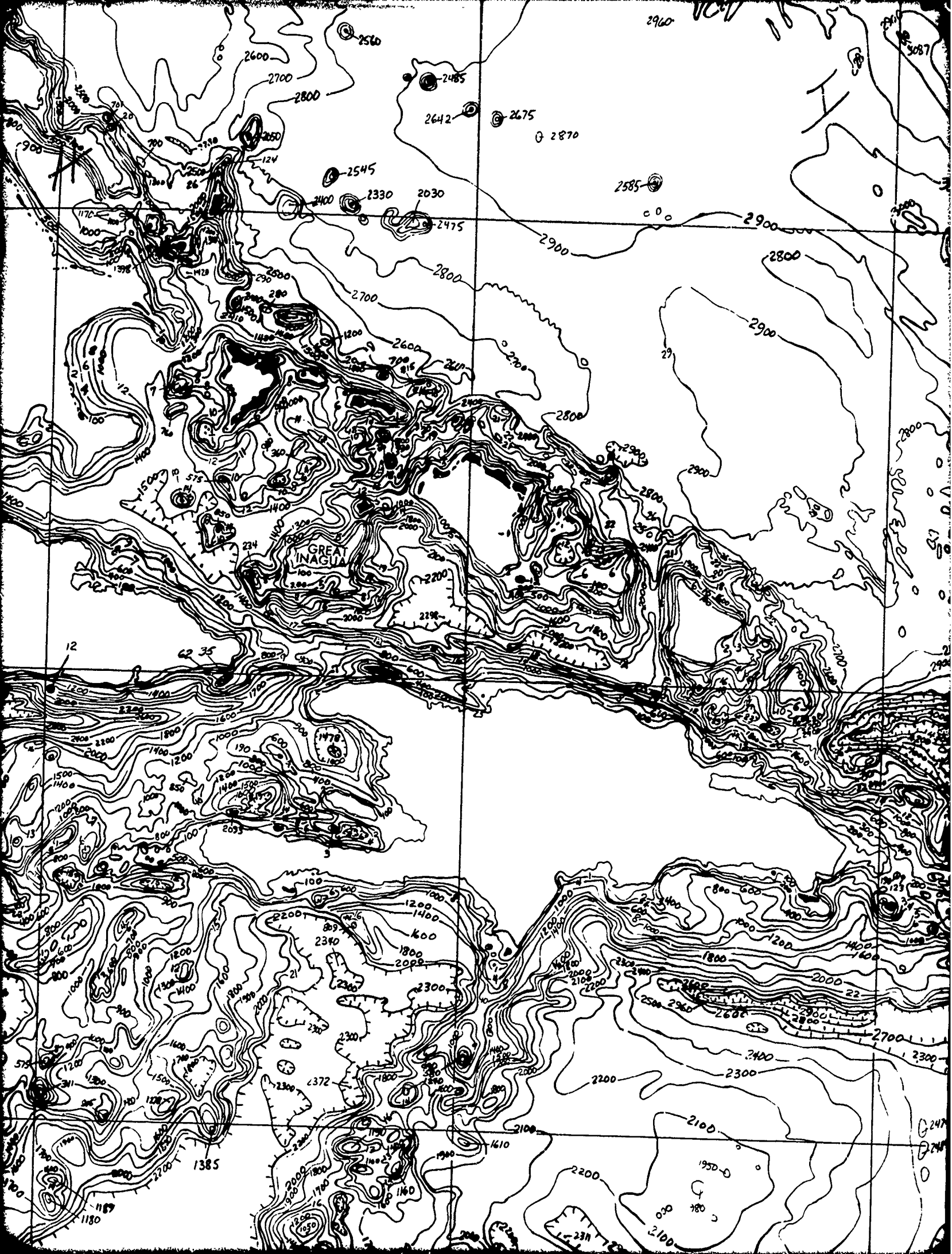
GREAT INAGUA

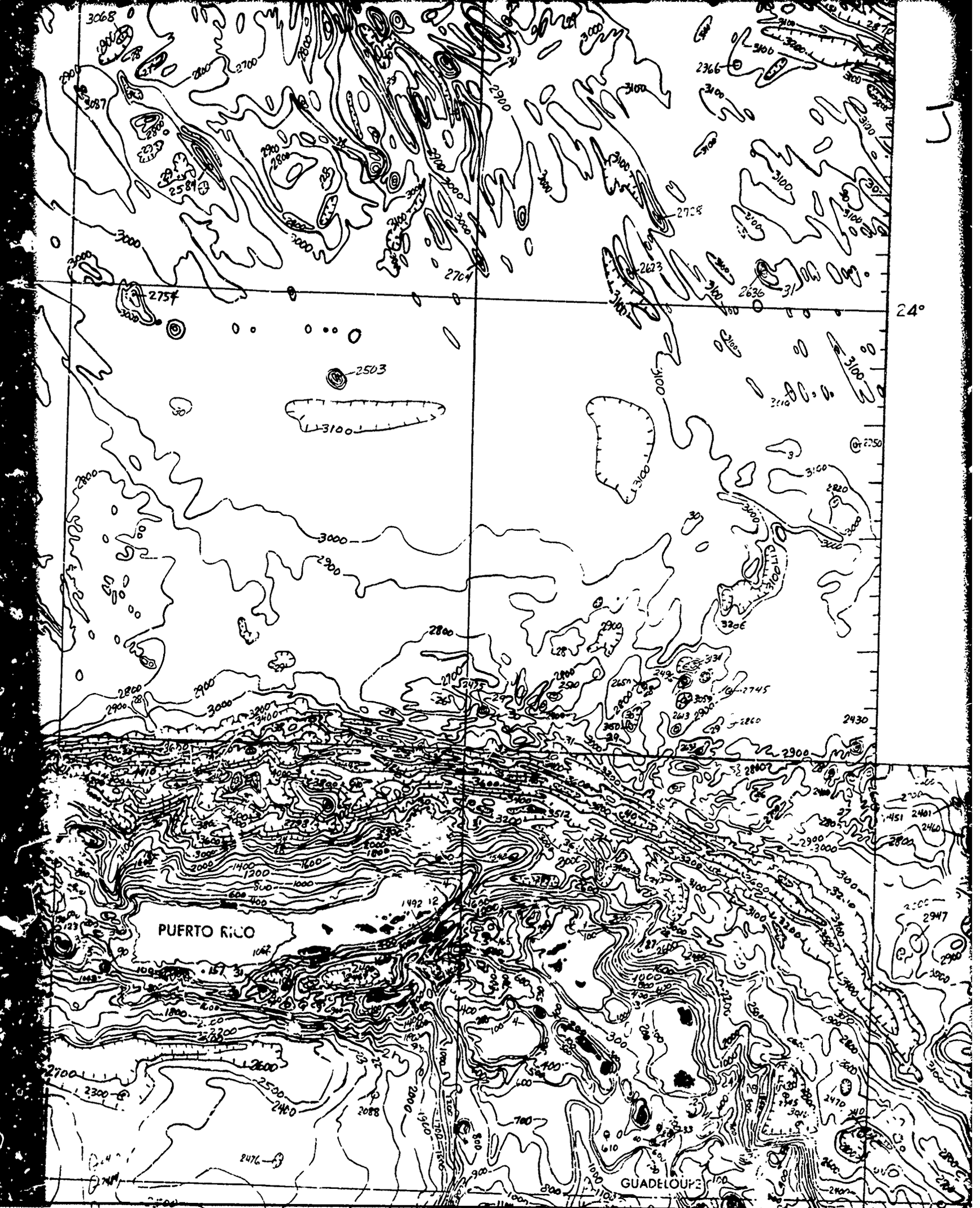
PUERTO RICO
GUADELOUPE
24°

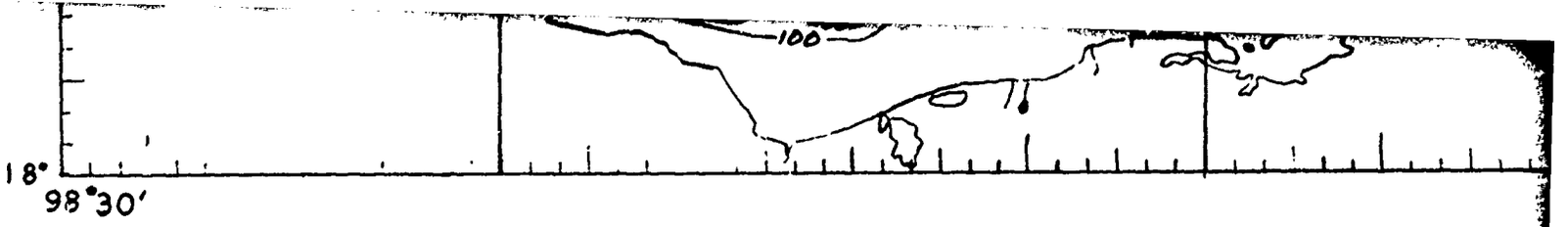

BATHYMETRIC CHART

Gulf of Mexico-Caribbean Sea-North American Basin

Scale: 1" = 1° longitude, (4,300,000)

Contour Interval: 100 fathoms* (Based on soundings uncorrected for variations in the velocity of sound in sea water.)

Compiled by Undersea Surveillance Oceanographic Project from the following sources:

1006 N	0906 N	0806 N	0706 N	0606 N
1005 N	0905 N	0805 N	0705 N	0605 N
1004 N	0904 N	0804 N	0704 N	0604 N
1003 N	0903 N	0803 N	0703 N	0603 N
1002 N	0902 N	0802 N	0702 N	0602 N

Data Index

1. BC 603N, 2nd., Nov., 1970 (Bathymetric data to Sept., 1965). GEBCO Data Sheet, 1969.
2. BC 604N, 1st ed., 1953, Revised June, 1966 (manuscript). GEBCO Data Sheet, 1969.
3. BC 703N, 1st Ed., 1953, Revised Sept., 1966 (manuscript). GEBCO Data Sheet, 1969. G. Peter (thesis), 1971, (Los Roques Basin).
4. BC 704N, 3rd Ed., June, 1970 (Bathymetric data to Dec., 1969). R. Perry, 1971, (Puerto Rico environs).
5. Area 705N: G. L. Johnson, 1970, (Code 7400, Ocean Floor Analysis).
6. BC 802N, 1st Ed., 1953, (Revised Feb., 1967). GEBCO Data Sheet, 1970.
7. BB 803N, 2nd Ed., Nov. 1969 (Bathymetric data to June, 1966).
8. BC 804N, 2nd Ed., March, 1968, (Bathymetric data to Oct., 1966).
9. BC 805N, 2nd Ed., 1970 (Bathymetric data to 1963).
10. BC 902N. GEBCO Data Sheet, 1968.
11. BC 903N, 2nd Ed., July, 1970 (Bathymetric data to Oct., 1964). GEBCO data sheet, 1969. USNS San Pablo cruise #939003, 1969. Bonacca Expedition, 1963 (AAPG Memoir #11, 1969).
12. BC 904N, 2nd Ed., Oct. 1962 (Bathymetric data to Oct. 1962). GEBCO data Sheet, 1967. USNS San Pablo cruise #939003, 1968. Bonacca Expedition, 1963 (AAPG Memoir #11, 1969).
13. Straits of Florida: R. J. Malloy and R. J. Hurley, 1970 (GSA Bull., v. 81, July, 1970).
14. Gulf of Mexico: R. N. Bergantino, 1970 (GSA Bull., v. 82, March, 1971), and E. Uchupi, 1967 (AAPG Bull., v 52, 1968).

*Space permitting

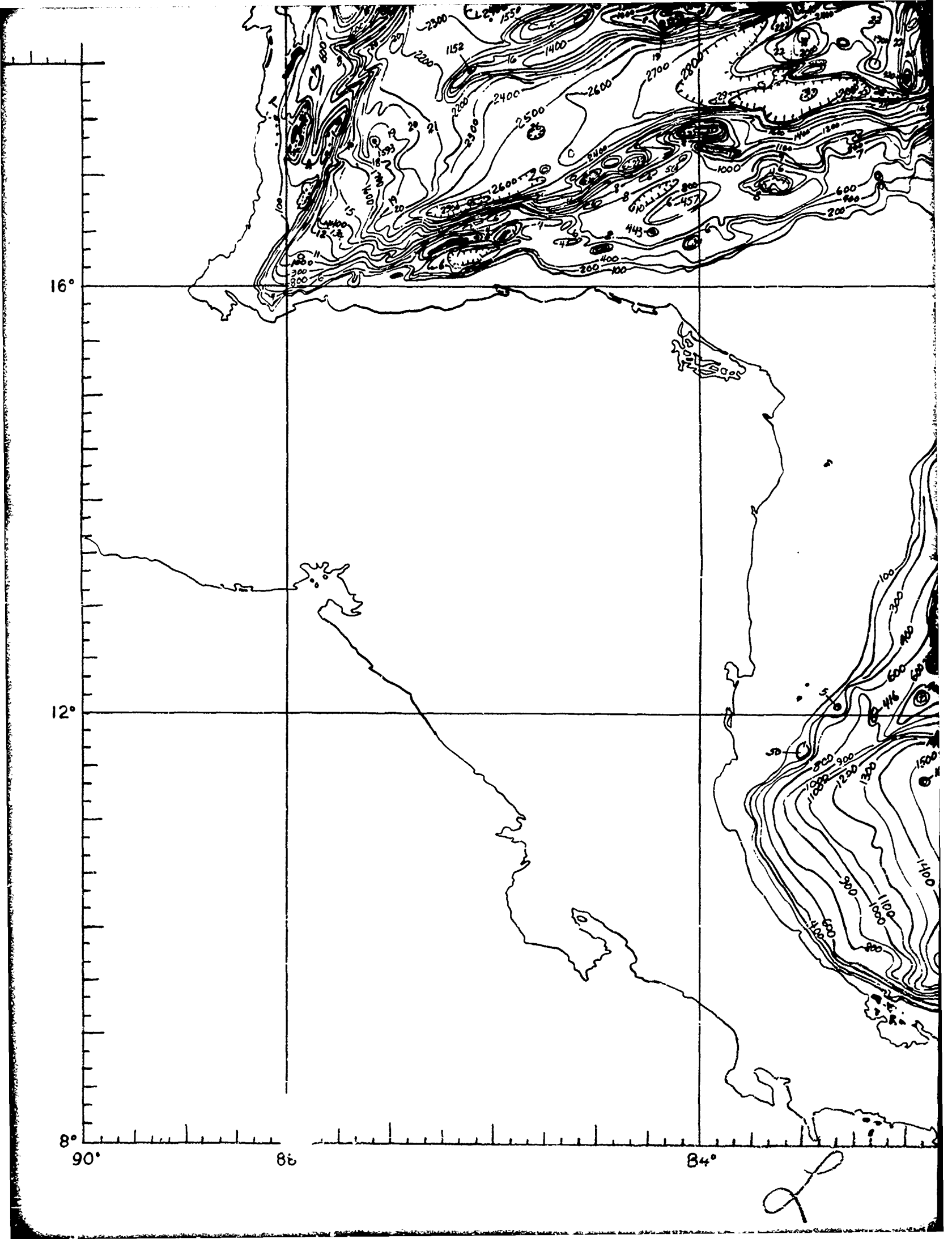
16°
12°
8°
90°
86
84°

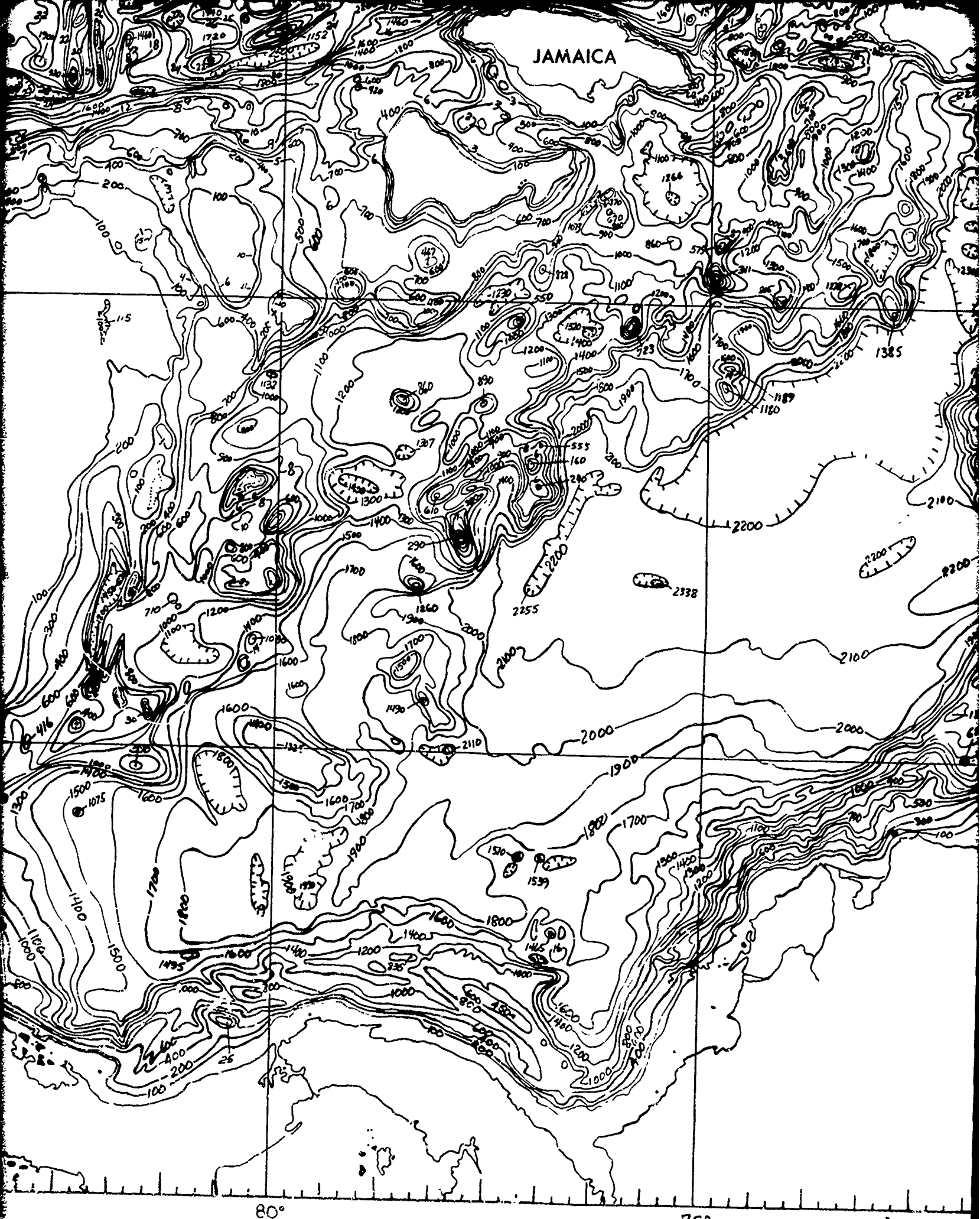

FIGURE 4-109 BATHYMETRY

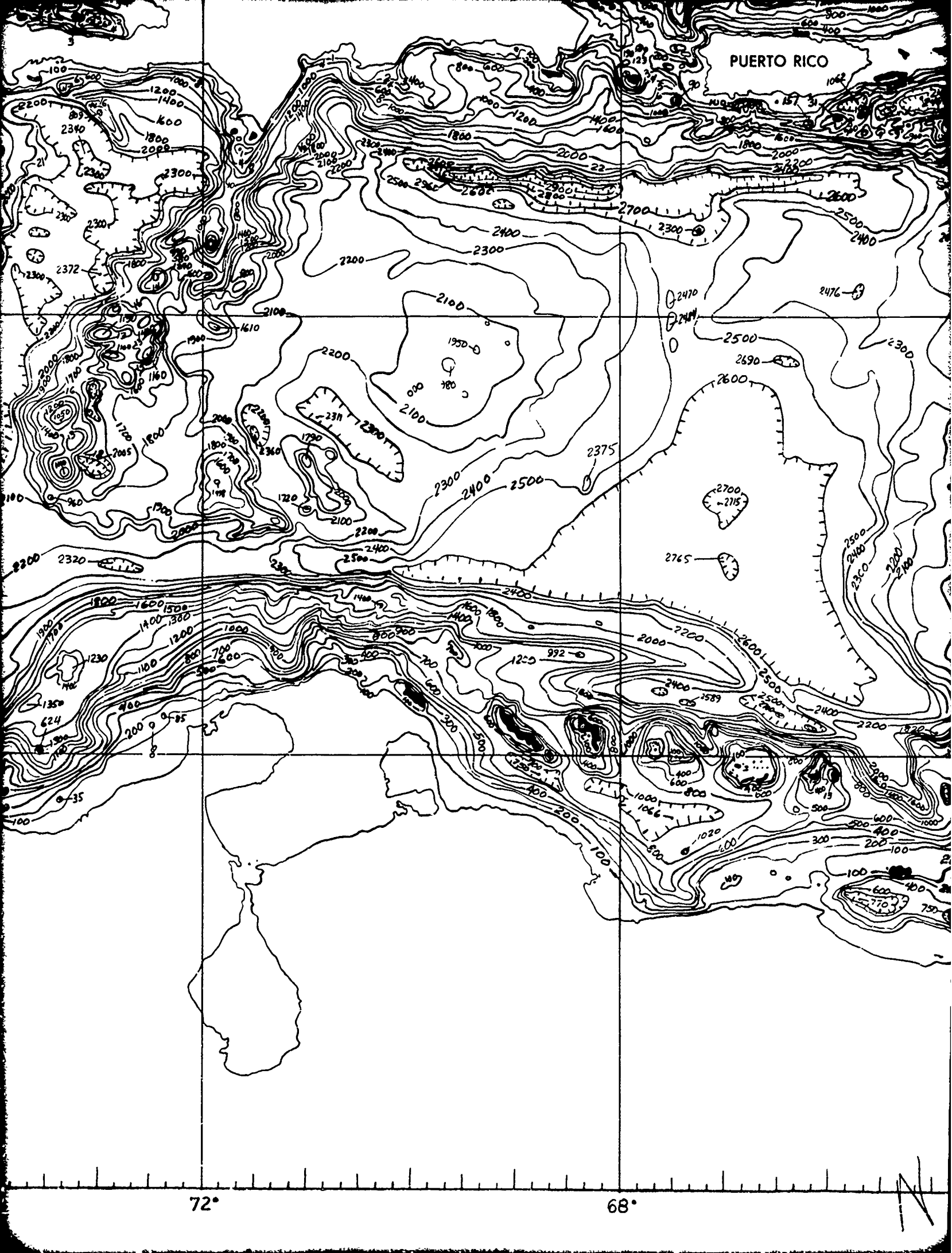
PUERTO RICO
72°
68°

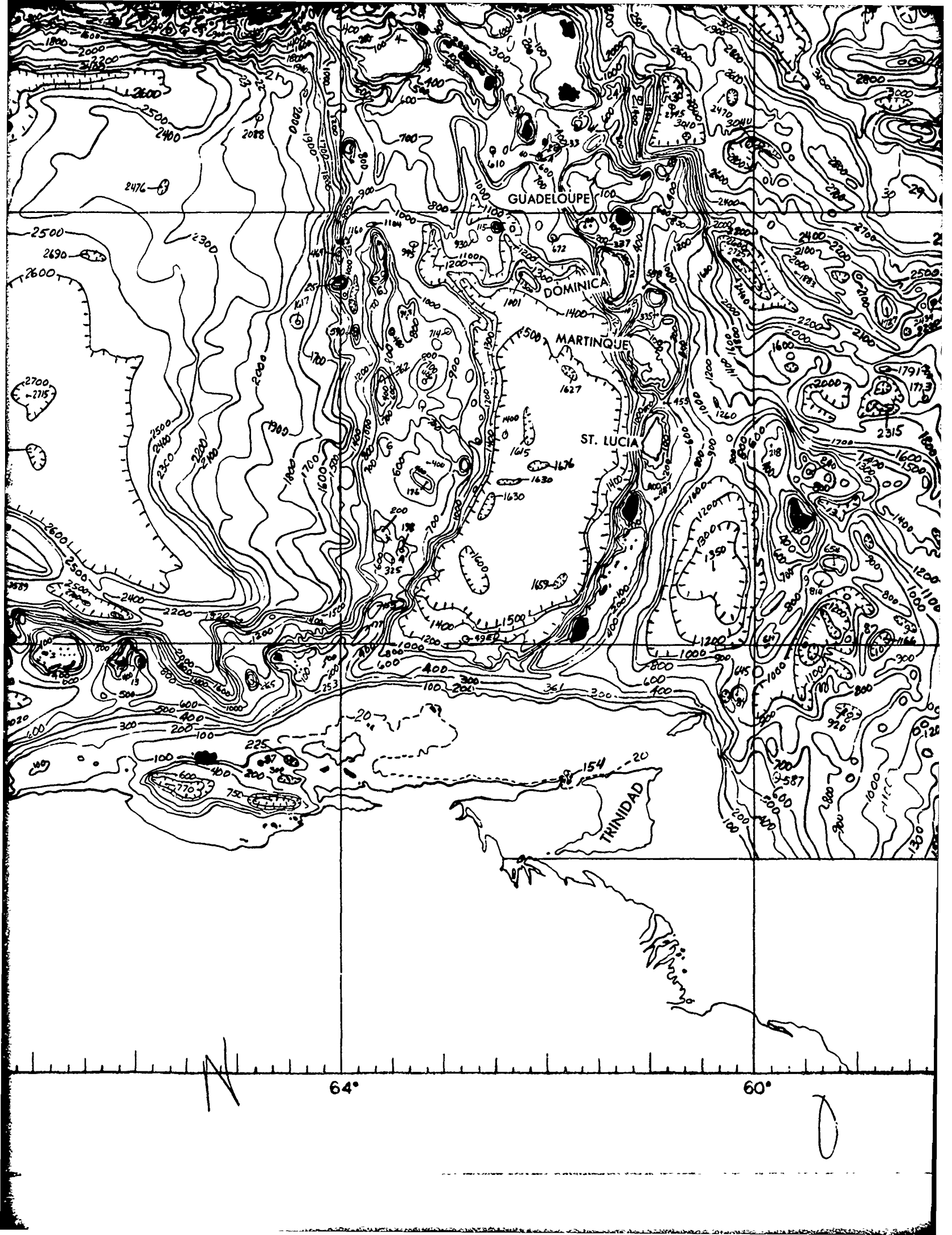
GUADELOUPE
DOMINICA
MARTINQUE
ST. LUCIA
TRINIDAD
64°
60°

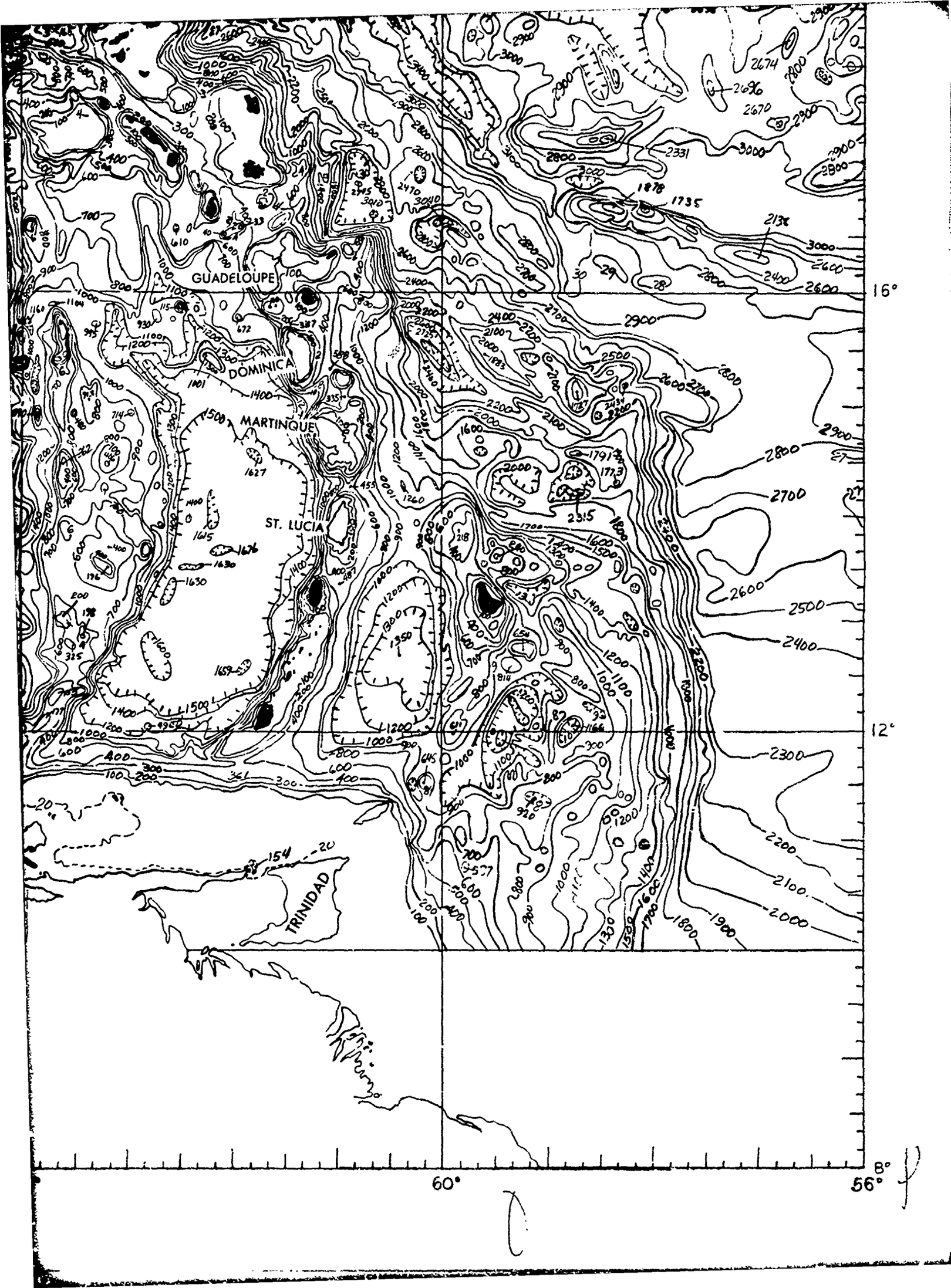
GUADELOUPE
DOMINICA
MARTINIQUE
ST. LUCIA
TRINIDAD
16°
12°
8°
60°
56°